COMMUNICATIONS
FROM THE
KONKOLY OBSERVATORY
OF THE
HUNGARIAN ACADEMY OF SCIENCES

MITTEILUNGEN
DER
STERNWARTE
DER UNGARISCHEN AKADEMIE
DER WISSENSCHAFTEN

BUDAPEST — SZABADSÁGHEGY

No. 80.

L. PATKÓS

UBV PHOTOMETRY OF SV CAM 1973—1980

BUDAPEST, 1982

ISBN 963 8361 15 8
HU ISSN 0324-2234
Felelős kiadó: Szeidl Béla

Hozott anyagról sokszorosítva

8213428 MTA KESZ Sokszorosító, Budapest. F. v.: dr. Héczey Lászlóné

UBV PHOTOMETRY OF SV Cam 1973-1980

A B S T R A C T

UBV observational material of the eclipsing binary SV Cam is presented and the existence of migrating distortion wave demonstrated. Observed light-up and connected period change indicate the appearance of gas streams in the system. Observed flare events may be connected with spotted region on the surface of the secondary component. Also presented 53 new photoelectric times of minima.

INTRODUCTION

The close binary system SV Cam (BD $+82^{\circ}174$; HD 4492) has been called a short period relative of the RS CVn group, showing irregular light curve variations, but no migration waves (*Hall* 1976). The present observational material proves, that the system shows migrating distortion waves, as well as some further interesting peculiarities.

The system ($P = 0^{d}.6$, m= 9.8-10.6, sp:G3V+K4V) was not found to be variable until 1929 (*Guthnick* 1929), but with the help of earlier Harvard plates, it was possible to follow its variability up to the last years of the 19th century. The first period, and the type of light variation was established by *Detre* (*Dunst* 1933). *Wood* (1946) was the first to report asymmetry in the light curve, and its variability. Extended observational material was published by *van Woerden* (1957) establishing the presence of irregular changes of the light curve and small random fluctuations of the period. *Hiltner* (1953) and *Hill* et al. (1975) published spectroscopic data. Further photoelectric observations were reported by *Nelson* (1963a,b) and by *Nelson* and *Duckworth* (1968). The first attempt to interpret the long-term variations in the O-C curve was made by *Sommer* (1956). He proposed a 57.5-years light-time effect for the system, but this result was incompatible with *van Woerden's* (1957) data. *Frieboes-Conde* and *Herczeg* (1973) tried to fit the O-C curve using another sine-wave with a period of 72.8 years. According to *Hilditch* et al.(1979) the system also contains a third body revolving around the eclipsing pair, but in an eccentric orbit and with a period of 64.1 years.

OBSERVATIONS

Extended photoelectric UBV photometry of the system SV Cam has been carried out at Konkoly Observatory since 1973. The following list contains the dates and Julian Dates of the observations presented in this paper:

J.D.			
2441695	12/13	Jan	1973
696	13/14	"	"
697	14/15	"	"
807	4/5	May	"
810	7/8	"	"
824	21/22	"	"
825	22/23	"	"
831	28/29	"	"
833	30/31	"	"
835	1/2	June	"
900	5/6	Aug	"
901	6/7	"	"
903	8/9	"	"
904	9/10	"	"
905	10/11	"	"
930	4/5	Sep	"
931	5/6	"	"
933	7/8	"	"
934	8/9	"	"
935	9/10	"	"
959	3/4	Oct	"
960	4/5	"	"
961	5/6	"	"
962	6/7	"	"
963	7/8	"	"
978	22/23	"	"
980	24/25	"	"
981	25/26	"	"
982	26/27	"	"
983	27/28	"	"
984	28/29	"	"
42019	2/3	Dec	"
022	5/6	"	"
066	18/19	Jan	1974

J.D. 2442106	27/28	Feb	1974
108	1/2	Mar	"
148	10/11	Apr	"
304	13/14	Sep	"
307	16/17	"	"
309	18/19	"	"
404	22/23	Dec	"
405	23/24	"	"
432	19/20	Jan	1975
460	16/17	Feb	"
461	17/18	"	"
465	21/22	"	"
466	22/23	"	"
522	19/20	Apr	"
523	20/21	"	"
545	12/13	May	"
603	9/10	July	"
634	9/10	Aug	"
829	20/21	Feb	1976
830	21/22	"	"
831	22/23	"	"
836	27/28	"	"
871	2/3	Apr	"
43061*	9/10	Oct	"
077*	25/26	"	"
078*	26/27	"	"
135*	22/23	Dec	"
192*	17/18	Feb	1977
198*	23/24	"	"
218*	15/16	Mar	1977
288*	24/25	May	"
344*	19/20	July	"
392*	5/6	Sep	"
393*	6/7	"	"
394*	7/8	"	"

Between Oct 1977 and July 1978 I observed SV Cam at Hoher List Observatory. These observations will be published later.

2443765*	13/14	Sep	1978
815	2/3	Nov	"

J.D. 2443849*	6/7	Dec	1978
878	4/5	Jan	1979
879	5/6	"	"
880	6/7	"	"
926	21/22	Feb	"
927	22/23	"	"
928	23/24	"	"
44048	23/24	June	"
049	24/25	"	"
081	26/27	July	"
103*	17/18	Aug	"
145	28/29	Sep	"
146	29/30	"	"
158	11/12	Oct	"
159	12/13	"	"
285	15/16	Feb	1980
345*	15/16	Apr	"
371	11/12	May	"
454	2/3	Aug	"
455	3/4	"	"
477	25/26	"	"
541	28/29	Oct	"
582	8/9	Dec	"

All these observations were obtained with two telescopes of Konkoly Observatory. Most of the observations were carried out at the Piszkéstető Mountain Station using the 50 cm Cassegrain reflector combined with a single channel integrating photometer equipped with an uncooled EMI 9058 QB type photomultiplier - before 10 October 1978 (J.D. 2443791) and an EMI 9502 S type photomultiplier since then. To realize the international UBV system we utilized the following Schott filters:

U = UG 2 (2 mm)
B = BG 12 (1 mm) + GG 13 (2 mm)
V = GG 11 (2 mm)

The other observations (denoted by an asterisk in the above list) were obtained using the 60 cm Newtonian reflector (Budapest, Szabadsághegy) combined with a single channel EMI 9502 B type photomultiplier and the following

filters:

$$U = UG\ 1\ (2\ mm)$$
$$B = BG\ 12\ (1\ mm) + GG\ 13\ (2\ mm)$$
$$U = GG\ 11\ (2\ mm)$$

In the case of the 50 cm Cassegrain telescope, the observing sequence was the following: comparison - sky - variable (several times) -comp... (all in the three colours). The integration time was 10 sec. Since the beginning of 1980 the measuring procedure has been controlled by a microprocessor, which also took over the filter change.

At the 60 cm Newtonian the observational sequence was: $comparison_{blue}$ - $comp_{yellow}$ - $variable_y$ - var_b - var_b - var_y - $comp_y$ - $comp_b$ - ... (each of these measurements lasted about 3 X 10 sec, and in all cases before and after the 10 sec measurement background was also measured). All these represent one yellow and one blue observational point in the light curve. (Ultraviolet observations for this star gave a too wide scatter because of the lights of Budapest).

The obtained data were transformed into the international UBV system in accordance with the following equations:

$$\Delta V = \Delta v + \varepsilon\mu\Delta(b-v)$$
$$\Delta B = \Delta b - (1 - \varepsilon\mu - \mu)\ \Delta(b-v)$$
$$\Delta U = \Delta u - (1 - \varepsilon\mu - \mu)\ \Delta(b-v) + (\phi - 1)\ \Delta(u-b)$$

The telescope constants used were:

60 cm Telescope	50 cm Telescope	
	before	after
	10. 10. 1978.	
$\varepsilon = -0.089$	$\varepsilon = 0.110$	$\varepsilon = -0.13$
$\mu = 1.095$	$\mu = 1.006$	$\mu = 1.26$
	$\phi = 1.421$	$\phi = 1$

As comparison star BD $+82^{\circ}168$ (HD 43883) was used with the check star BD $+82^{\circ}176$ (HD 45635). The comparison star was chosen (i) so as to be similar to the variable in colour and (ii) because of its proximity. The effect of differential atmospheric extinction was therefore neglected. No light variation of the comparison star was established.

PERIOD VARIATIONS

Investigations of the period variations were based on the data of the 1969 GENERAL CATALOGUE of VARIABLE STARS:

$$Min_I \text{ hel.} = 2433777.42453 + 0.5930718\ E$$

Figure 1 shows an O-C representation of the system in the last years (dots are the present observations, open circles represent the observations

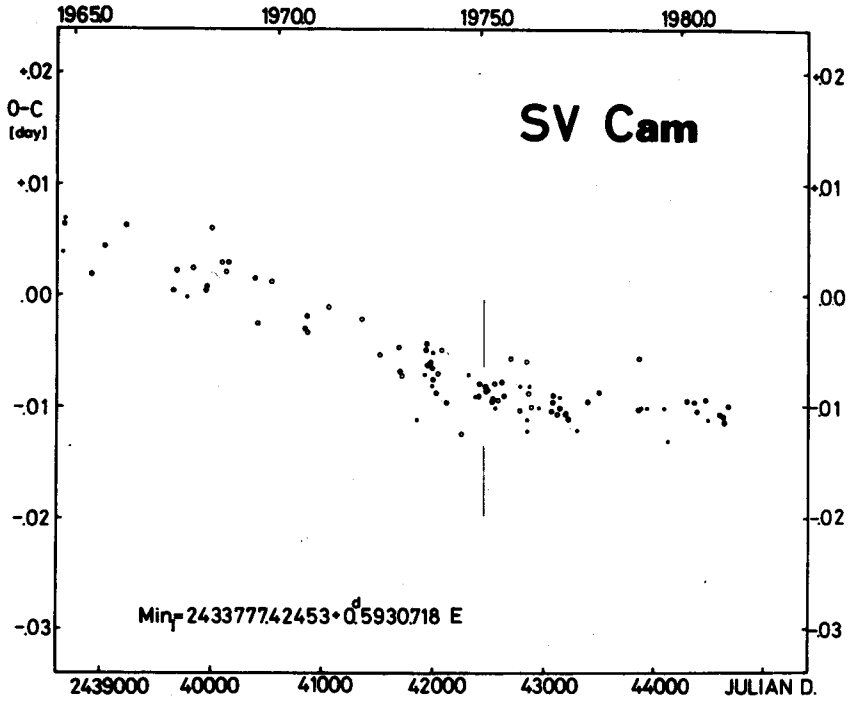

Figure 1

from the literature). Between J.D. 2442000 and 2443000 there is a break in the O-C. The direction of this break indicates a period increase which, it was thought, might have been caused by mass exchange between the components. This assumption was confirmed by the photometrically observed events at and after J.D. 2442460 (see later). Table 1 contains 53 heliocentric minima of SV Cam obtained at Konkoly Observatory:

Table 1

Min_I	O - C /GCVS 69/	Remarks
2441695.5194	-.0067	
697.298	-.007	
835.480	-.011	
905.467	-.007	
930.377	-.006	
931.5635	-.0052	Only V
933.3437	-.0042	
934.5278	-.0063	
959.437	-.006	Only V
960.623	-.006	
962.4024	-.0060	
978.416	-.005	
981.380	-.007	
982.5665	-.0064	
984.3449	-.0072	
42019.3347	-.0086	
106.5154	-.0095	
304.604	-.007	
405.4243	-.0088	
460.5805	-.0082	
465.3249	-.0084	
523.4453	-.0091	
545.388	-.010	
603.5100	-.0090	
634.3500	-.0088	
829.470	-.009	Only V
830.655	-.011	
836.585	-.011	Only V
871.578	-.010	
947.491	-.010	
43061.3603	-.0102	
077.3740	-.0094	
078.5608	-.0088	
135.4945	-.0100	
192.4293	-.0100	
198.3599	-.0102	
218.5236	-.0109	
288.505	-.012	
393.4808	-.0099	
849.5518	-.0111	
878.613	-.010	
880.393	-.010	
927.245	-.010	
928.430	-.011	
44049.4184	-.0097	
081.444	-.010	
103.385	-.013	
285.4614	-.0093	
345.3617	-.0092	
371.4559	-.0102	
454.4869	-.0092	
477.615	-.011	
582.5892	-.0104	

LIGHT-CURVE VARIATIONS

It is by no means easy to follow the nature of the light-curve variations of SV Cam since these variations need very closely observed full light-curves. Relatively rare observations are only able to provide additional results to the picture obtained in time intervals of frequent observations.

In order to be able to compare the different observed light-curves I referred them to a reference curve observed at J.D. 2442404/405. This reference curve is almost symmetrical and does not seem to be distorted. This light-curve (Fig. 15) could also be used to determine the system parameters.

I must draw attention to the fact that in the figures of this paper the B-V and U-B curves are drawn "upside down": this means that in the B-V curves relatively blue points are downwards; in the U-B curves relatively ultraviolet points are downwards (see, for example, the flares at J.D. 2444582 (Fig. 39)).

Like normal RS CVn systems SV Cam has a migrating distortion wave. Because this wave migrates very rapidly, it can be followed only in time intervals such as between J.D. 2441695-2442405 when observations are sufficiently close to each other:

J.D. 2441695 (Fig. 2)
696
The observational points nearly fit the reference curve but maxima are a little brighter. The secondary minimum is fainter.

J.D. 2441807 (Fig. 3)
810
824
825
831
833
835
Brightness decrease at and around primary minimum. Depth about 0.05 mag.

J.D. 2441900 (Fig. 4)
901
903
904
905
Brightness decreases at first maximum (the maximum following the primary minimum). Secondary minimum also touched. Maximum depth: about 0.1 mag. Primary minimum recovered, and there is even a small brightness increase relative to the reference curve: about 0.02 mag.

J.D. 2441931 (Fig. 5)
The second maximum (the maximum after the secondary minimum) fits the reference curve further on. The brightness increase at primary minimum continues, it is already about 0.06 mag over the reference curve.

J.D. 2441959 (Fig. 6)
960
961
Brightness decrease has migrated further with increasing orbital phase. Ascending branch to second maximum also touched. Decrease in first maximum and in secondary minimum almost 0.1 mag. Brightness at primary minimum about 0.05 mag over the reference curve.

J.D. 2441962 (Fig. 7)
963
These data confirm the observations obtained in the previous days. Note that the B - V and the U - B points show that where the distortion wave is present (in this case between phases 0.1 and 0.7) they are shifted to the visual and to the blue respectively. It shows that this light really originated from relatively low temperature regions. And to the contrary, B - V and U - B points originating from parts of the light curve uneffected by the distortion wave (in this case phases 0.8 - 0.9) are shifted relatively to the blue and to the ultraviolet respectively. This shows that they come from relatively hot regions of the system. The migration of the distortion wave can also be followed with the help of the B - V and U - B curves.

J.D. 2441978 (Fig. 8)
981
Brightness decrease at first maximum still present, descending branch of second maximum still untouched. There seems to exist a step at the bottom of the primary minimum, the second part of it is much deeper than the first part.

J.D. 2441982 (Fig. 9)
If one compares these data with those observed 20 days earlier the brightness decrease has migrated further, the peak of the second maximum is already lower than 20 days before. The decrease at the secondary minimum is already 0.1 mag. The step at the bottom of the primary minimum confirmed.

J.D. 2441983 (Fig. 10)
984
As this complete light curve shows, the migrating distortion wave is already situated at almost around phase 0.5. Depth at secondary minimum 0.1 mag. Asymmetric bottom of primary minimum confirmed again.

J.D. 2442019 (Fig. 11)
The distortion wave has migrated further, the first maximum has largely recovered. Brightness decrease at secondary minimum still 0.06 mag. The bottom of the primary minimum - especially its first part - has dropped below the reference level.

J.D. 2442066
Transition between the observations 2442019 and 2442106.

J.D. 2442106 (Fig. 12)
108
Distortion wave centred on the second maximum. Depth over 0.1 mag. First maximum wholly recovered.

J.D. 2442148 (Fig. 13)
Second maximum partly recovered.

J.D. 2442304 (Fig 14)
307
Second maximum wholly recovered. Bottom of primary minimum again over (0.05 mag) the reference level.

J.D. 2442404 (Fig. 15)
405
The reference curve itself. No distortion wave present. Almost symmetric shape. Upper envelope curve of the light curves with the distortion wave.

The migrating distortion wave is not the only peculiar light-curve change of SV Cam. The light-curve changes observed at and after J.D. 2442460 seem to be connected with the period increase between J.D. 2442000 and J.D. 2443000 (see Fig. 2)

J.D. 2442432 - 2442460 (Fig. 16)
461
At J.D. 2442432 the observed light-curve fits the reference curve. But yet a further month later a brightness increase of over 0.06 mag between the phases 0.25 and 0.65 appeared. At the same time the bottom of the primary minimum has dropped below the reference level.

J.D. 2442465 (Fig. 17)
466
This light-curve confirms wholly the observations of the previous days. The bottom of the primary minimum is clearly below the reference level. This and the light-up around phase 0.45 increase the amplitude of the light variations.

J.D. 2442522 (Fig. 18)
523
Two months later the light-up had almost disappeared but remains of it are still recognisable at secondary minimum.

In the time interval J.D. 2442523 - J.D. 2444454 details of the light-curve variations cannot be followed because the observations were relatively rare, and were concentrated to the primary minimum and its surroundings:

J.D. 2442545
The observed part of the light-curve fits the reference level.

J.D. 2442634 (Fig. 19)
The bottom of the primary minimum and the ascending branch of the first maximum shows a large brightness decrease, almost 0.1 mag. The new distortion wave begins to migrate.

J.D. 2442829 (Fig. 20)
830
831
836
Observations at and around primary minimum. Ascending branch (towards first maximum) lower. Overall brightness decrease?

J.D. 2443344 (Fig. 21)
First maximum 0.1 mag below the reference level.

J.D. 2443392 (Fig. 22)
393
394
Overall brightness decrease present. First maximum lower than the second.

J.D. 2443765 (Fig. 23)
Peculiar flat first maximum, with strong shoulder before secondary minimum.

J.D. 2443815 (Fig. 24)
Secondary minimum deeper than the surrounding parts of the light curve, and wider than usual.

J.D. 2443849 (Fig. 25)
Primary minimum, and ascending branch to first maximum observed. About 0.1 mag below the reference level.

J.D. 2443878 (Fig. 26)
879
880
Too wide scatter because of bad observational conditions. The whole light-curve about 0.1 mag below the reference level.

J.D. 2443926 (Fig. 27)
Too wide scatter because of bad conditions. Secondary minimum, second maximum, and primary minimum observed.

J.D. 2443927 (Fig. 28)
Phases 0.0 - 0.7 observed. First maximum 0.1 mag below the reference level.

J.D. 2443928 (Fig. 29)
Relatively flat maxima with strong shoulders before and after the primary minimum. Light-curve about 0.1 mag below the reference level.

J.D. 2444048 (Fig. 30)
049
Strong shoulder after the primary minimum has remained. Light-curve closer to the reference level than at J.D. 2443928.

J.D. 2444103 (Fig 31)
Primary minimum very deep. First maximum a little below the reference level.

J.D. 2444158 (Fig. 32)
159 (Fig. 33)
Observed part of the light-curve about 0.04 mag below the reference level.

J.D. 2444285 (Fig. 34)
First maximum about 0.1 mag, second maximum about 0.05 mag below the reference

level.

J.D. 2444371 (Fig. 35)
Light curve in the observed part (primary minimum) a little below the reference level.

J.D. 2444454 (Fig. 36)
455
Observed parts about 0.05 mag below the reference level. Especially at and around the secondary minimum.

J.D. 2444477 (Fig. 37)
The observed second maximum is about 0.09 mag below the reference level.

J.D. 2444541 (Fig. 38)
Distortion wave moving off the secondary minimum.

J.D. 2444582 (Fig. 39)
Distortion wave at primary minimum. Secondary minimum recovered. Flare events at phase 0.61 and at the bottom of the primary minimum. For further details, see *Patkós* (1981).

Budapest-Szabadsághegy, October 1, 1982

REFERENCES

Detre, L. (Dunst), 1933. *Astr. Nachr.*, *249*, *213*.

Frieboes-Conde, H. & Herczeg, T., 1973. *Astr. Astrophys. Suppl.*, *12*, *1*.

Guthnick, P., 1929. *Astr. Nachr.*, *235*, *83*.

Hall, D. S., 1976. in *Multiple Periodic Variable Stars*, IAU Coll. No 29. p. 287 ed. Fitch, W. S., D. Reidel, Dordrecht, Holland.

Hilditch, R. W., Harland, D. M., Mc Lean, B. J., 1979. *Mon. Not. R. astr. Soc.* *187*, *797*.

Hill, G., Hilditch, R. W., Younger, F. & Fisher, W. A., 1975. *Mem. R. astr. Soc.* *79*, *131*.

Hiltner, W. A., 1953. *Astrrophys J.*, *118*, *262*.

Nelson, B., 1963a. *Publs astr. Soc. Pacif.*, *75*, *18*.

Nelson, B., 1963b. *Publs astr. Soc. Pacif.*, *75*, *417*.

Nelson, B. & Duckworth, E., 1968. *Publs astr. Soc. Pacif.*, *80*, *562*.

Patkós, L., 1981. *Astrophys. Letters* *22*, *1*.

Sommer, R., 1956. *Astr. Nachr.*, *283*, *155*.

van Woerden, H., 1957. *Leiden Ann.*, *21*, *3*.

Wood, F. B., 1946. *Contr. Princeton Obs. No. 21, p. 40.*

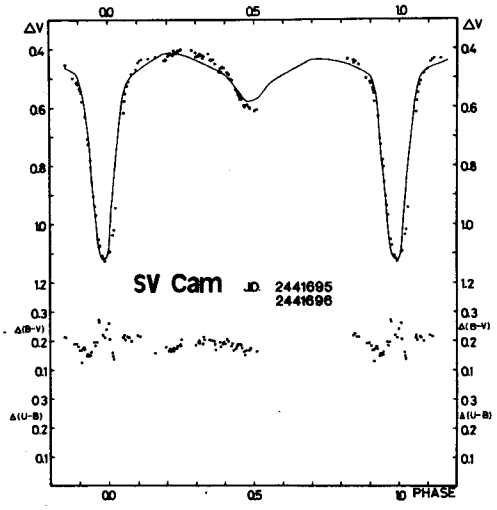

Figure 2.

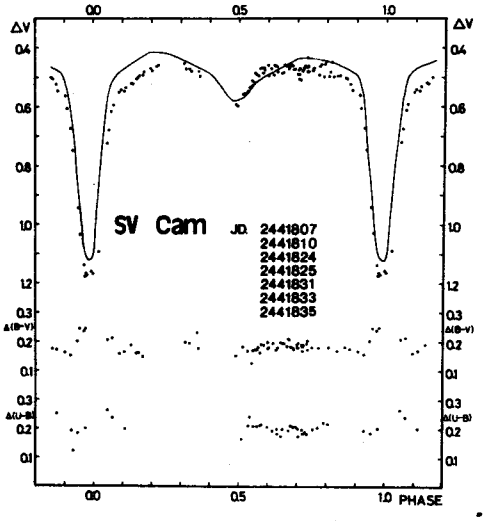

Figure 3.

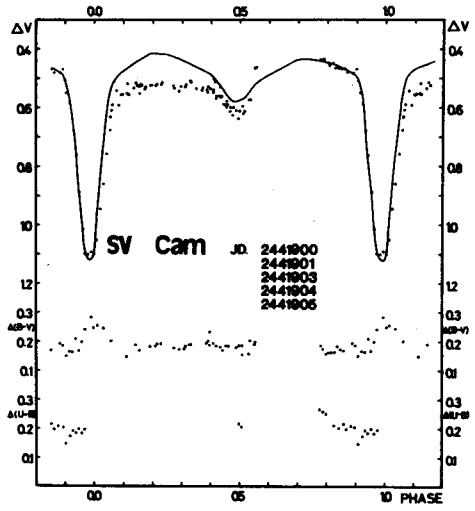

Figure 4.

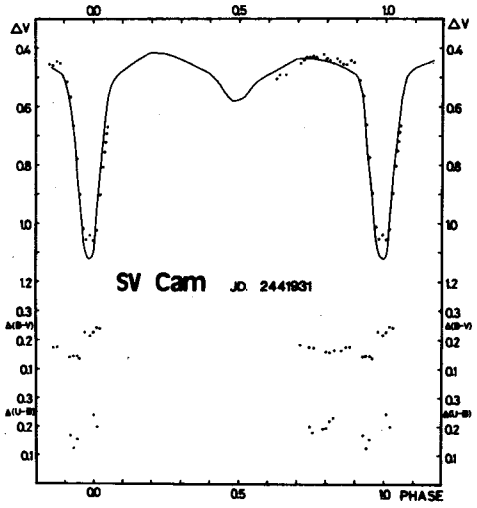

Figure 5.

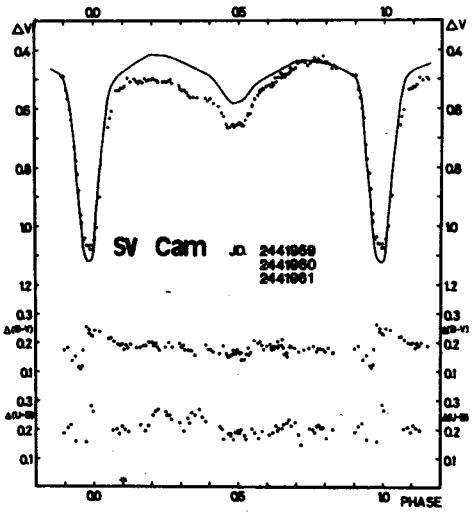

Figure 6.

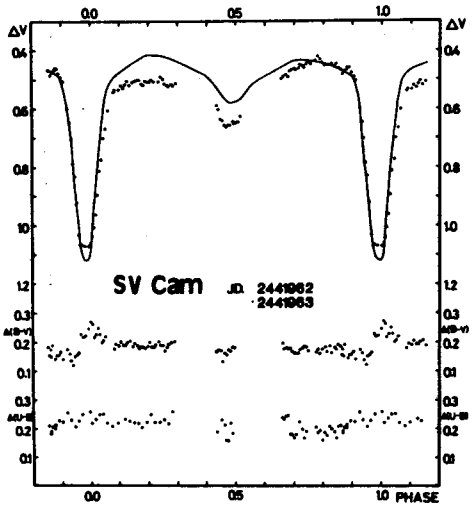

Figure 7.

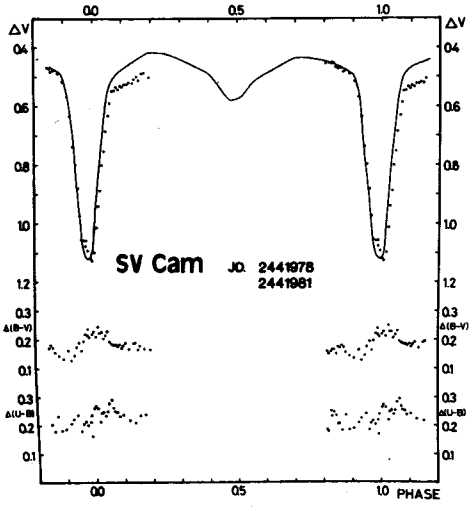

Figure 8.

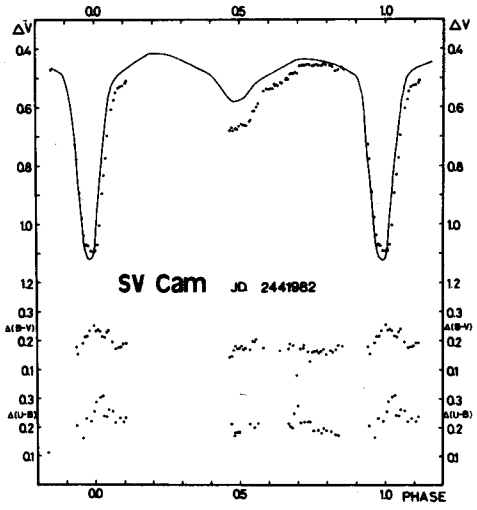

Figure 9.

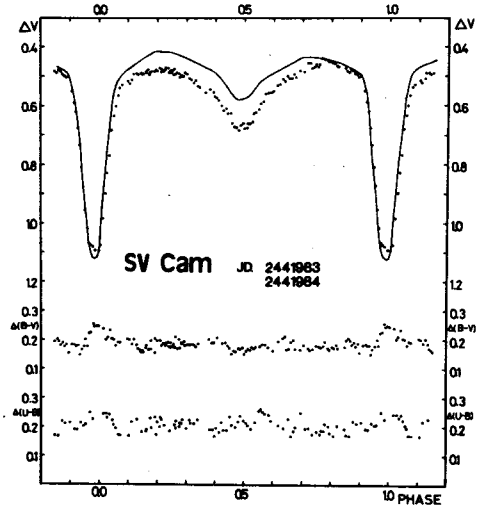

Figure 10.

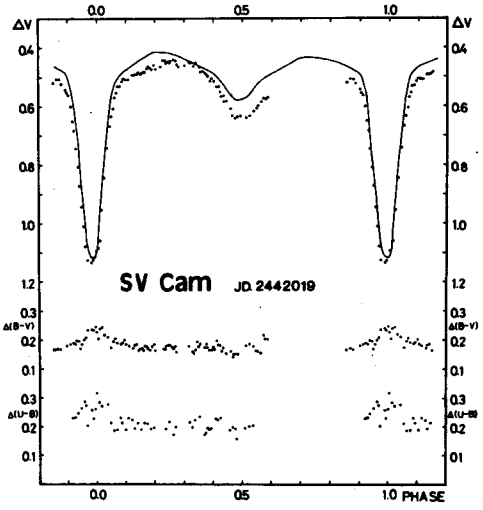

Figure 11.

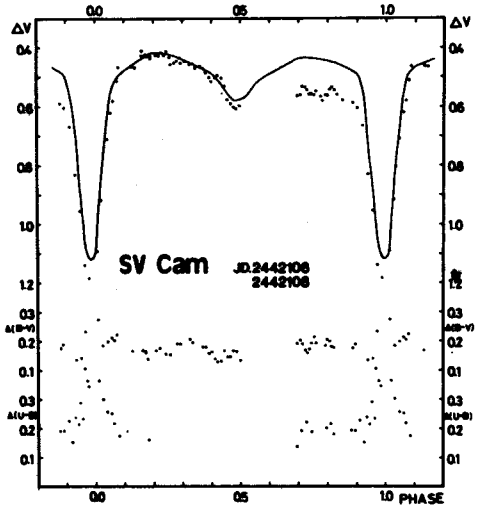

Figure 12.

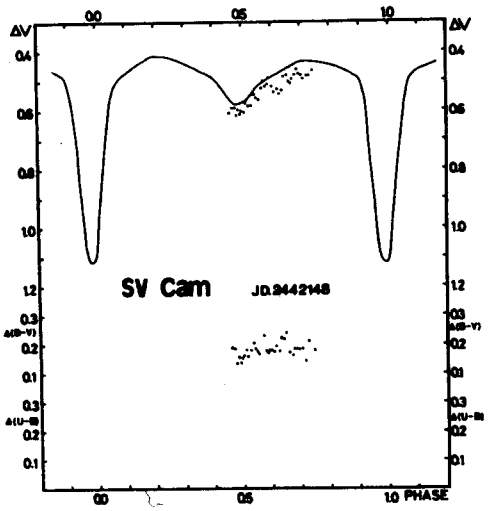

Figure 13.

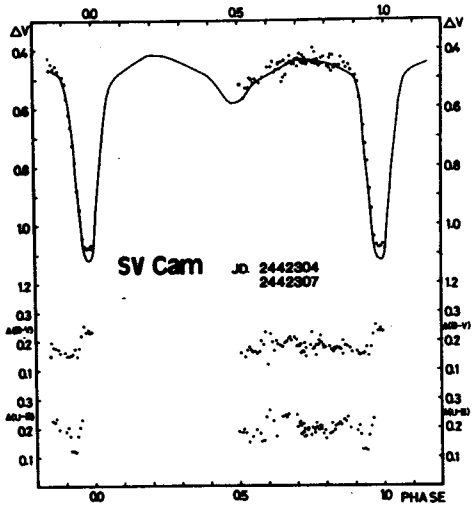

Figure 14.

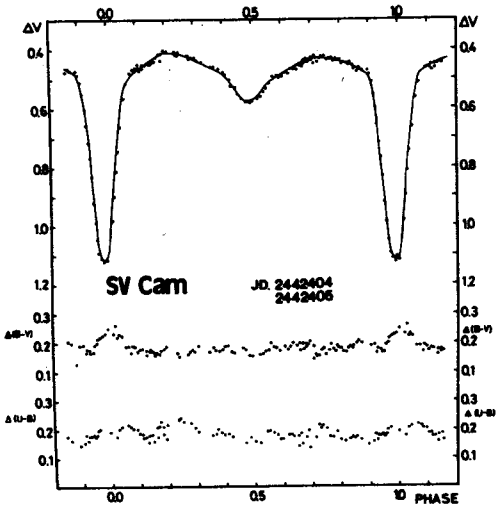

Figure 15.

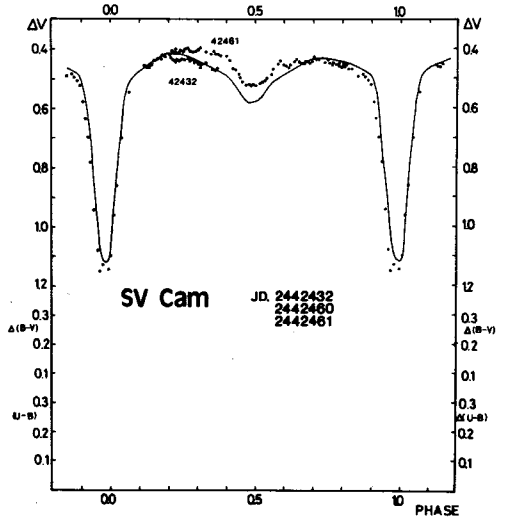

Figure 16.

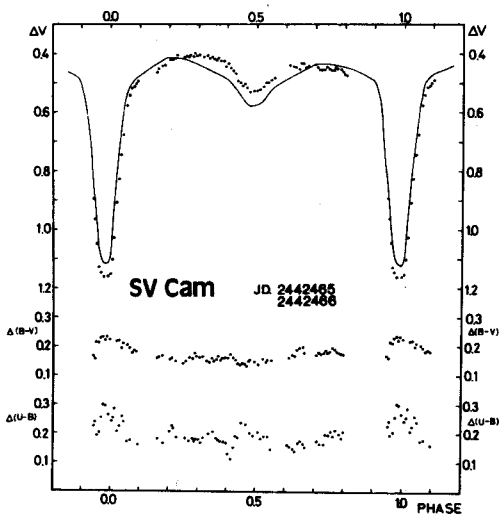

Figure 17.

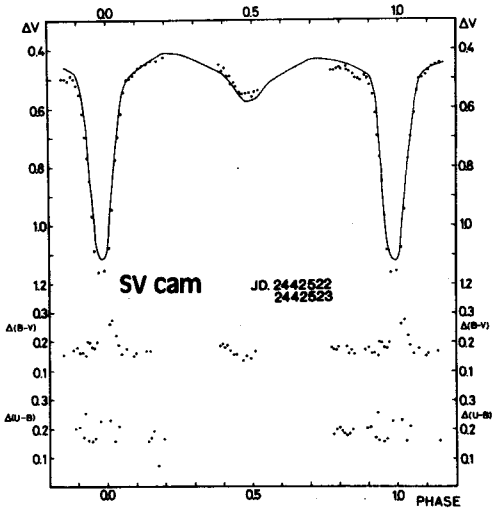

Figure 18.

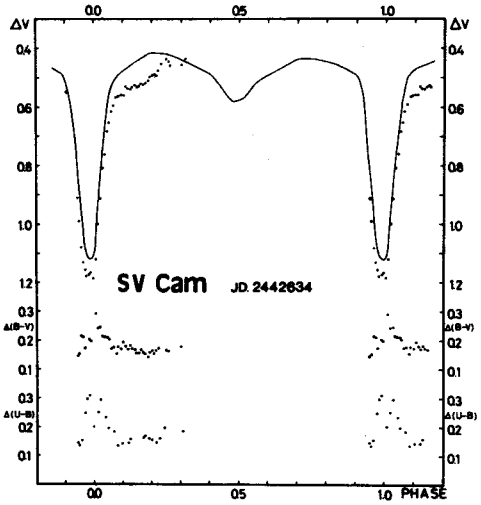

Figure 19.

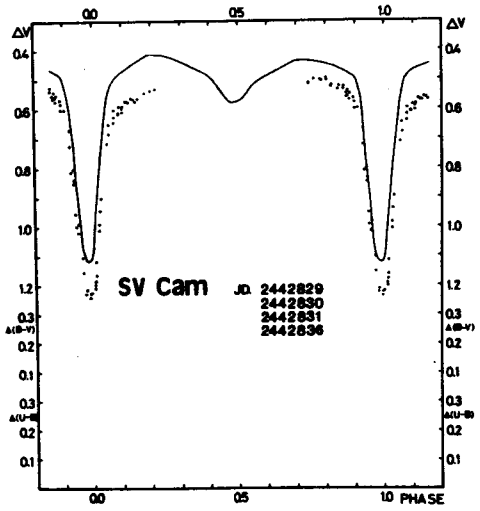

Figure 20.

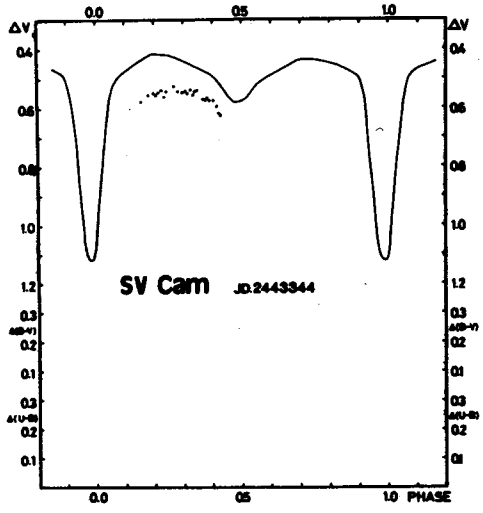

Figure 21.

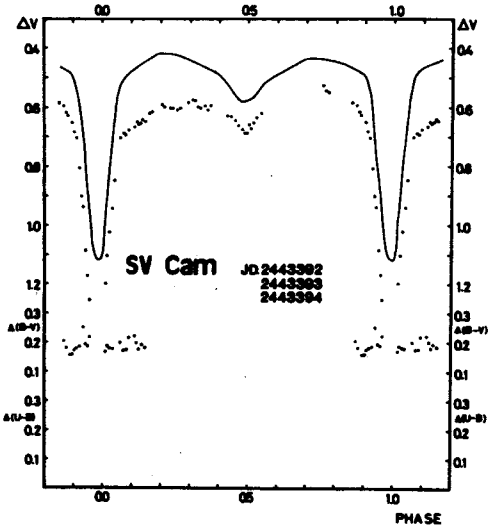

Figure 22.

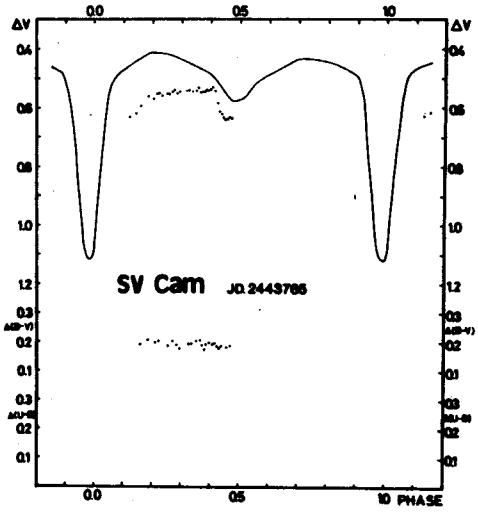

Figure 23.

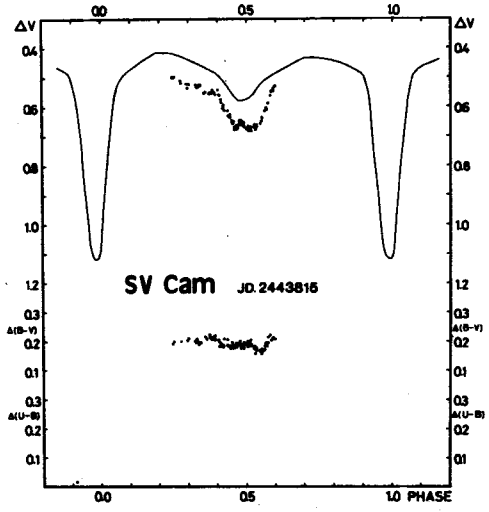

Figure 24.

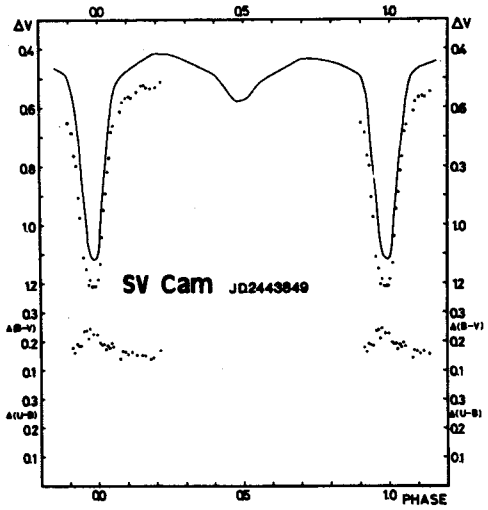

Figure 25.

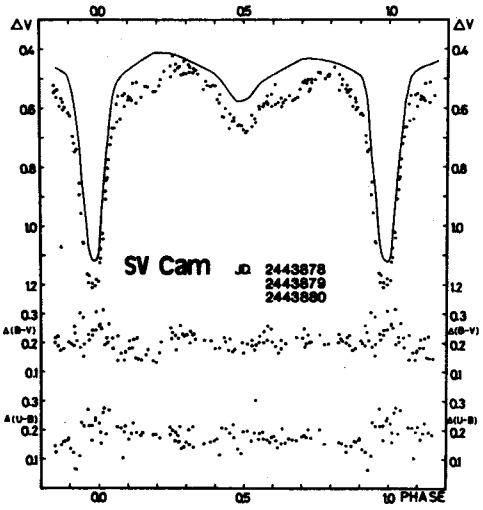

Figure 26.

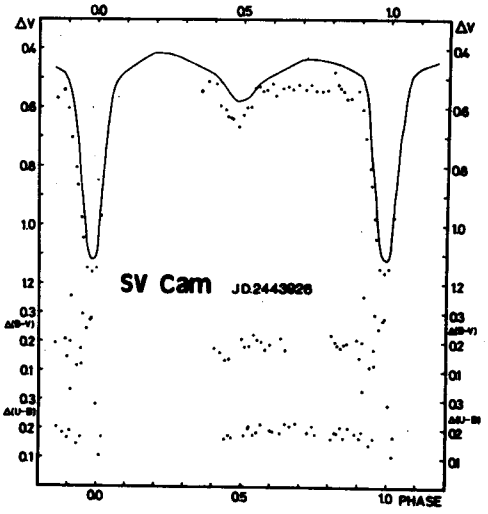

Figure 27.

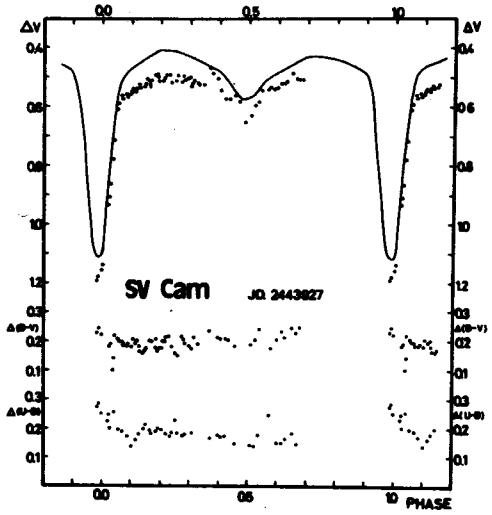

Figure 28.

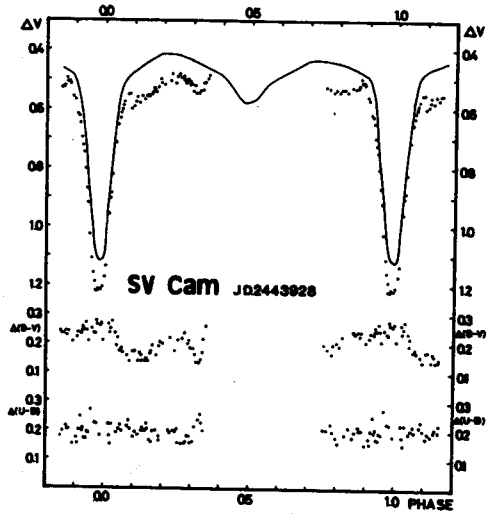

Figure 29.

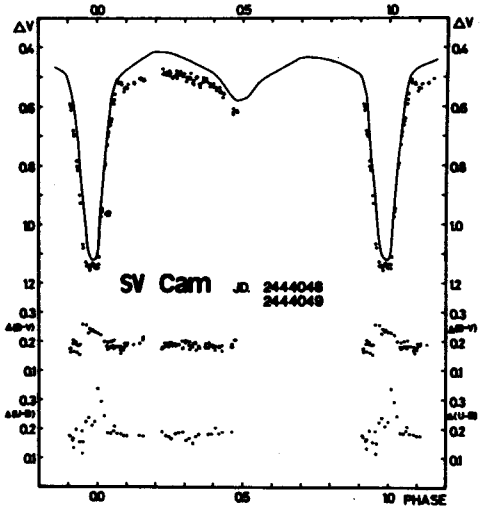

Figure 30.

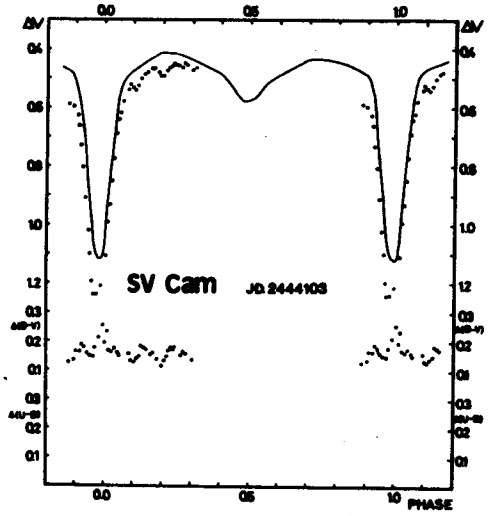

Figure 31.

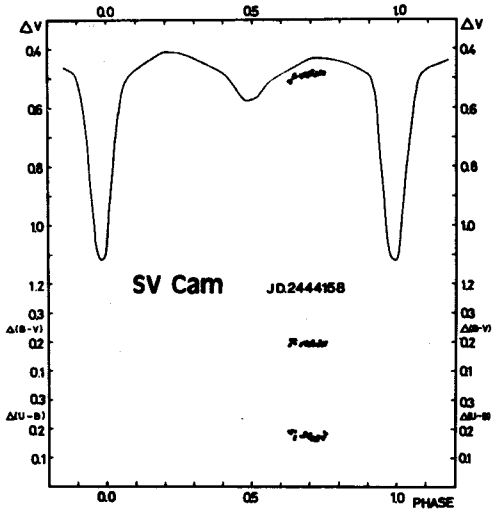

Figure 32.

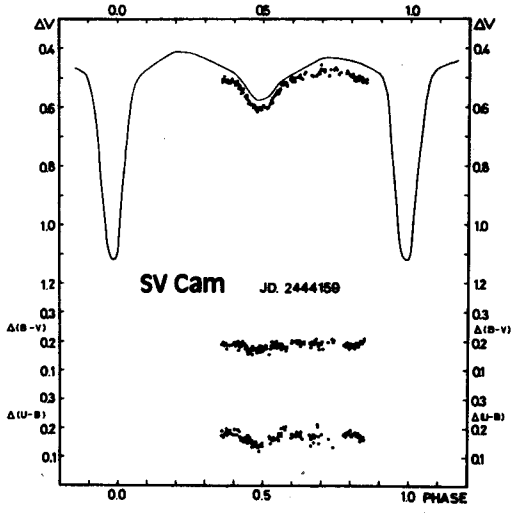

Figure 33.

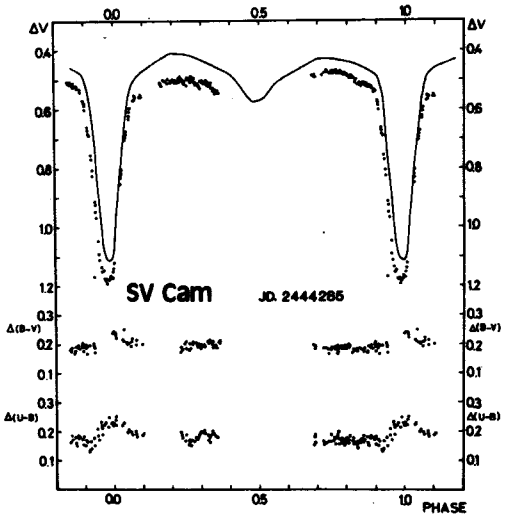

Figure 34.

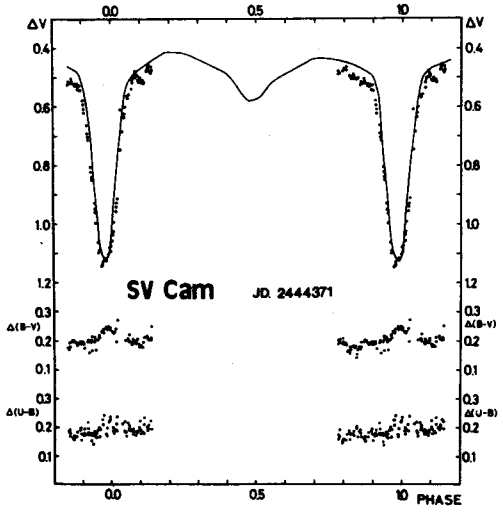

Figure 35.

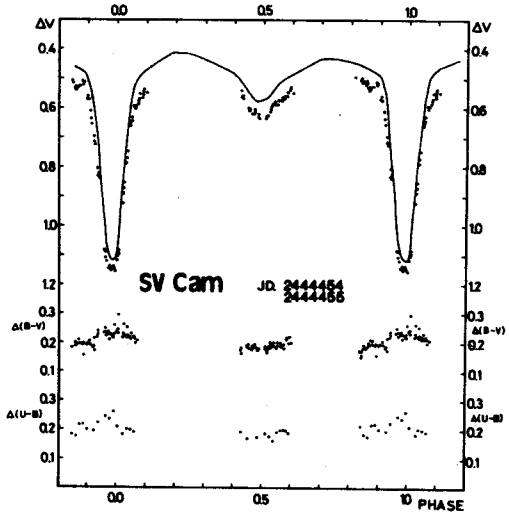

Figure 36.

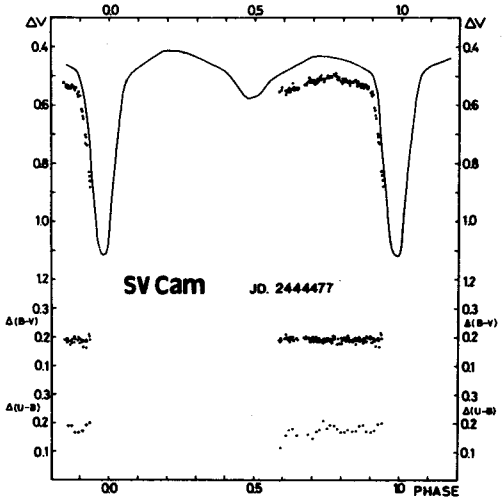

Figure 37.

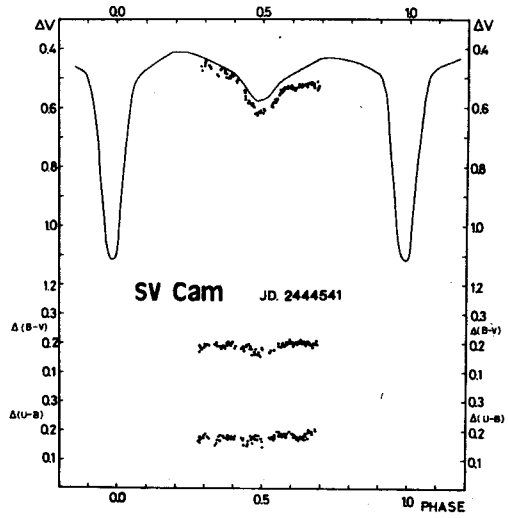

Figure 38.

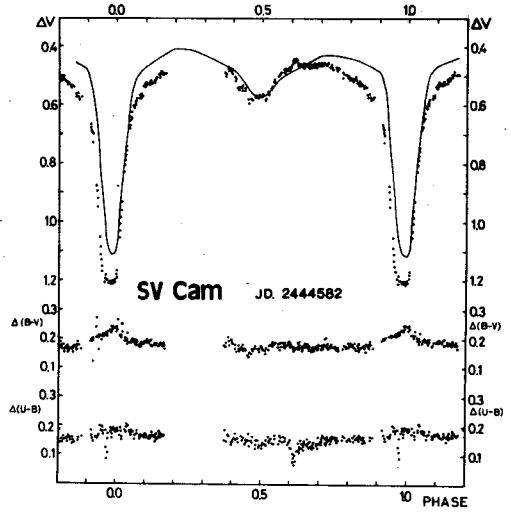

Figure 39.

Table 2

Photoelectric yellow observations of SV Cam

J.D.	ΔV	J.D.	ΔV	J.D.	ΔV
41695.4193	.437	41696.2591	.415	41697.3167	.975
41695.4303	.443	41696.2606	.410	41697.3201	.917
41695.4321	.450	41696.2653	.407	41697.3215	.884
41695.4341	.447	41696.2672	.405	41697.3223	.853
41695.4411	.458	41696.2888	.408	41697.3292	.751
41695.4560	.504	41696.2960	.417	41697.3311	.719
41695.4636	.518	41696.2974	.430	41697.3326	.694
41695.4654	.523	41696.3029	.427	41697.3359	.627
41695.4699	.538	41696.3045	.427	41697.3383	.619
41695.4713	.546	41696.3061	.422	41697.3399	.604
41695.4727	.556	41696.3100	.426	41697.3451	.552
41695.4731	.584	41696.3119	.435	41697.3469	.539
41695.4801	.633	41696.3133	.429	41697.3488	.520
41695.4843	.710	41696.3227	.422	41697.3523	.501
41695.4864	.730	41696.3267	.443	41697.3535	.497
41695.4911	.783	41696.3289	.443	41697.3556	.474
41695.4924	.807	41696.3324	.441	41697.3619	.476
41695.4940	.858	41696.3365	.455	41697.3638	.481
41695.4968	.906	41696.3444	.483	41697.3655	.473
41695.4998	.940	41696.3465	.472	41697.3702	.465
41695.5020	.971	41696.3480	.483	41697.3716	.476
41695.5076	1.054	41696.3510	.467	41697.3731	.474
41695.5094	1.075	41696.3528	.469	41697.3785	.472
41695.5150	1.109	41696.3543	.469	41697.3808	.483
41695.5165	1.119	41696.3607	.485	41697.3823	.485
41695.5201	1.129	41696.3623	.489	41697.3871	.460
41695.5270	1.099	41696.3638	.491	41697.3899	.459
41695.5295	1.095	41696.3674	.507	41697.3913	.471
41695.5360	1.038	41696.3694	.511	41697.4001	.453
41695.5380	1.021	41696.3715	.511	41697.4015	.462
41695.5420	.946	41696.3780	.545	41697.4090	.422
41695.5584	.621	41696.3807	.550	41697.4106	.420
41695.5603	.581	41696.3826	.561	41697.4121	.426
41695.5614	.555	41696.3858	.568	41697.4176	.425
41695.5656	.530	41696.3871	.576	41697.4190	.429
41695.5669	.515	41696.3887	.576	41697.4215	.420
41695.5733	.488	41696.3947	.597	41697.4253	.417
41695.5820	.473	41696.3967	.601	41697.4273	.414
41695.5869	.449	41696.3986	.597	41697.4298	.441
41695.5904	.442	41696.4019	.595	41697.4313	.414
41695.5937	.438	41696.4057	.605	41697.4361	.416
41695.6073	.437	41696.4071	.607	41697.4377	.420
41695.6222	.431	41696.4166	.615	41697.4392	.420
		41696.4208	.611	41697.4433	.417
				41697.4452	.413
41696.2332	.443	41697.2870	1.087	41697.4471	.423
41696.2356	.440	41697.2893	1.099	41697.4525	.430
41696.2369	.442	41697.2910	1.104		
41696.2422	.426	41697.2974	1.117	41807.3450	.513
41696.2438	.423	41697.2993	1.108	41807.3464	.530
41696.2454	.418	41697.3005	1.105	41807.3483	.519
41696.2505	.426	41697.3042	1.101	41807.3578	.498
41696.2526	.411	41697.3069	1.087	41807.3656	.489
41696.2539	.416	41697.3084	1.088	41807.3679	.470
41696.2569	.419	41697.3140	1.040	41807.3700	.478
		41697.3154	1.007		

Table 2 (cont.)

Photoelectric yellow observations of SV Cam

J.D.	ΔV	J.D.	ΔV	J.D.	ΔV
41807.3777	.497	41825.5098	.494	41900.3805	.518
41807.3887	.494	41825.5127	.484	41900.3908	.534
41807.3960	.484	41825.5256	.473	41900.4037	.582
41807.4053	.490	41825.5286	.479	41900.4154	.629
41807.4073	.487	41825.5392	.464	41900.4272	.642
41807.4183	.473	41825.5420	.462	41900.4381	.624
41807.4210	.463			41900.4495	.577
41807.4229	.461	41831.4588	.509	41900.4521	.577
41807.4280	.476	41831.4619	.511	41900.4616	.468
41807.4302	.475	41831.4749	.466	41900.4641	.466
41807.4382	.478	41831.4780	.464		
41807.4407	.473	41831.4870	.475	41901.3555	.636
41807.4461	.481	41831.5009	.466	41901.3581	.611
41807.4481	.475	41831.5043	.460	41901.3672	.546
41807.4571	.483	41831.5112	.459	41901.3778	.560
41807.4593	.483	41831.5146	.450	41901.3803	.558
41807.4667	.480	41831.5261	.453	41901.3884	.555
41807.4691	.474			41901.3917	.559
41807.4802	.495	41833.4079	.592	41901.4026	.538
41807.4890	.502	41833.4104	.599	41901.4147	.554
41807.5005	.500	41833.4217	.559	41901.4242	.541
41807.5023	.486	41833.4246	.558	41901.4266	.534
41807.5093	.503	41833.4311	.549	41901.4356	.527
		41833.4349	.536	41901.4385	.527
41810.4027	.493	41833.4457	.487	41901.4466	.527
41810.4049	.493	41833.4490	.493	41901.4494	.523
41810.4140	.470	41833.4560	.471	41901.4581	.524
41810.4161	.464	41833.4588	.470	41901.4606	.518
41810.4228	.436	41833.4715	.461	41901.4823	.529
		41833.4771	.474	41901.4852	.539
41824.4077	.455	41833.4857	.463	41901.4940	.547
41824.4123	.472	41833.4872	.465	41901.4972	.532
41824.4187	.474	41833.4896	.467	41901.5056	.533
41824.4227	.481	41833.5045	.462	41901.5081	.526
41824.4355	.482	41833.5087	.465	41901.5159	.513
41824.4386	.500	41833.5165	.456	41901.5188	.519
		41833.5215	.464	41901.5287	.538
41825.3931	1.176			41901.5395	.545
41825.3966	1.172	41835.3919	.498	41901.5419	.536
41825.4059	1.160	41835.3953	.498	41901.5503	.543
41825.4089	1.166	41835.4069	.505	41901.5529	.533
41825.4207	1.092	41835.4097	.509		
41825.4381	.724	41835.4168	.527	41903.3315	.553
41825.4409	.680	41835.4204	.548	41903.3366	.540
41825.4471	.617	41835.4350	.565	41903.3427	.553
41825.4502	.596	41835.4383	.609	41903.3483	.572
41825.4623	.554	41835.4457	.675	41903.3539	.563
41825.4658	.545	41835.4496	.751	41903.3592	.566
41825.4729	.550	41835.4612	.944	41903.3657	.594
41825.4757	.536	41835.4657	1.032	41903.3709	.594
41825.4871	.522	41835.4729	1.139	41903.3768	.602
41825.4904	.525	41835.4770	1.167	41903.3827	.602
41825.4977	.506			41903.3889	.612
41825.5006	.502	41900.3768	.505	41903.3950	.615
41825.5031	.497				

Table 2 (cont.)

Photoelectric yellow observations of SV Cam

J.D.	ΔV	J.D.	ΔV	J.D.	ΔV
41903.4014	.600	41930.4352	.537	41933.3562	1.039
41903.4071	.615	41930.4412	.536	41933.3621	.941
		41930.4473	.551	41933.3686	.822
41904.5288	.544	41930.4533	.531	41933.3745	.732
41904.5346	.565	41930.4597	.556		
41904.5432	.567	41930.4661	.535	41934.4464	.458
41904.5484	.591	41930.4720	.538	41934.4536	.460
41904.5549	.602			41934.4646	.470
41904.5608	.617	41931.3473	.505	41934.4728	.470
		41931.3531	.495	41934.4793	.520
41905.3396	.439	41931.3654	.492	41934.4857	.560
41905.3454	.440	41931.3951	.455	41934.4913	.633
41905.3520	.453	41931.4017	.444	41934.4974	.710
41905.3575	.462	41931.4077	.432	41934.5042	.837
41905.3634	.454	41931.4142	.432	41934.5111	.978
41905.3690	.469	41931.4204	.430	41934.5169	1.039
41905.3749	.471	41931.4269	.434	41934.5230	1.071
41905.3812	.473	41931.4416	.425	41934.5297	1.044
41905.3872	.473	41931.4478	.441	41934.5365	1.049
41905.3929	.485	41931.4550	.446	41934.5428	.999
41905.4049	.486	41931.4614	.457	41934.5496	.881
41905.4111	.473	41931.4683	.440	41934.5550	.795
41905.4142	.512	41931.4744	.450	41934.5622	.670
41905.4173	.552	41931.4812	.458	41934.5690	.604
41905.4240	.590	41931.4883	.459	41934.5744	.571
41905.4308	.682	41931.4958	.446	41934.5806	.524
41905.4373	.766	41931.5028	.453	41934.5870	.530
41905.4433	.892	41931.5158	.516	41934.5941	.493
41905.4502	1.018	41931.5230	.568	41934.6017	.507
41905.4552	1.100	41931.5292	.667	41934.6068	.512
41905.4616	1.104	41931.5367	.779		
41905.4682	1.094	41931.5417	.901	41935.5713	.486
41905.4737	1.102	41931.5495	1.017		
41905.4801	1.055	41931.5556	1.056	41959.4209	.989
41905.4864	.947	41931.5632	1.041	41959.4269	1.041
41905.4927	.863	41931.5697	1.060	41959.4334	1.066
41905.4995	.761	41931.5769	1.024	41959.4389	1.065
41905.5055	.680	41931.5833	.903	41959.4455	1.048
41905.5113	.593	41931.5893	.809	41959.4514	1.004
41905.5231	.569	41931.5928	.756	41959.4582	.902
41905.5410	.522	41931.5948	.724		
41905.5579	.520	41931.5968	.693	41960.3137	.667
41905.5611	.528	41931.5986	.670	41960.3202	.657
41905.5653	.530			41960.3266	.659
41905.5677	.525	41933.2959	.526	41960.3307	.655
41905.5700	.528	41933.3015	.588	41960.3356	.654
		41933.3074	.647	41960.3390	.662
41930.3353	.574	41933.3127	.732	41960.3508	.621
41930.3486	.765	41933.3190	.812	41960.3552	.621
41930.3567	.959	41933.3246	.939	41960.3587	.598
41930.4033	.820	41933.3308	1.017	41960.3629	.569
41930.4085	.712	41933.3370	1.056	41960.3705	.559
41930.4172	.592	41933.3429	1.068	41960.3741	.549
41930.4297	.532	41933.3493	1.053	41960.3785	.543

Table 2 (cont.)

Photoelectric yellow observations of SV Cam

J.D.	ΔV	J.D.	ΔV	J.D.	ΔV
41960.3820	.539	41961.2839	.533	41961.5885	.526
41960.3881	.529	41961.2875	.526	41961.5937	.515
41960.3943	.525	41961.2933	.501	41961.5986	.500
41960.4000	.517	41961.2992	.512	41961.6055	.500
41960.4058	.500	41961.3072	.503	41961.6097	.490
41960.4116	.499	41961.3110	.510	41961.6143	.489
41960.4174	.486	41961.3151	.517	41961.6181	.488
41960.4210	.495	41961.3188	.509	41961.6231	.467
41960.4256	.498	41961.3235	.515		
41960.4303	.489	41961.3278	.502	41962.3258	.407
41960.4357	.482	41961.3322	.507	41962.3291	.422
41960.4389	.474	41961.3360	.506	41962.3367	.445
41960.4430	.473	41961.3403	.505	41962.3370	.464
41960.4468	.466	41961.3441	.501	41962.3413	.463
41960.4516	.452	41961.3481	.505	41962.3449	.480
41960.4574	.448	41961.3517	.507	41962.3491	.494
41960.4621	.442	41961.3553	.513	41962.3530	.509
41960.4662	.450	41961.3645	.512	41962.3621	.603
41960.4720	.461	41961.3682	.512	41962.3667	.650
41960.4777	.449	41961.3722	.513	41962.3699	.706
41960.4821	.445	41961.3765	.509	41962.3744	.789
41960.4856	.434	41961.3802	.505	41962.3779	.834
41960.4901	.448	41961.3836	.518	41962.3823	.924
41960.4941	.438	41961.3967	.526	41962.3857	1.035
41960.4978	.443	41961.4001	.538	41962.3899	1.069
41960.5034	.426	41961.4044	.541	41962.3927	1.069
41960.5079	.447	41961.4084	.541	41962.3991	1.075
41960.5116	.447	41961.4127	.550	41962.4062	1.074
41960.5167	.455	41961.4167	.560	41962.4098	1.063
41960.5208	.471	41961.4208	.565	41962.4133	1.040
41960.5260	.459	41961.4273	.565	41962.4173	1.009
41960.5304	.470	41961.4345	.567	41962.4209	.965
41960.5653	.491	41961.4507	.567	41962.4247	.898
41960.5704	.493	41961.4555	.577	41962.4279	.816
41960.5752	.541	41961.4606	.569	41962.4321	.777
41960.5783	.569	41961.4675	.586	41962.4353	.703
41960.5825	.605	41961.4770	.597	41962.4396	.671
41960.5856	.638	41961.4829	.618	41962.4447	.608
41960.5924	.730	41961.4872	.629	41962.4572	.545
41960.5958	.778	41961.4917	.655	41962.4591	.539
41960.5993	.825	41961.4961	.666	41962.4670	.538
41960.6018	.879	41961.5045	.661	41962.4708	.524
41960.6060	.964	41961.5089	.666	41962.4761	.531
41960.6105	1.051	41961.5135	.661	41962.4801	.520
41960.6169	1.064	41961.5187	.651	41962.4842	.508
41960.6233	1.080	41961.5231	.655	41962.4892	.522
41960.6301	1.080	41961.5277	.662	41962.4949	.511
		41961.5317	.642	41962.4998	.507
41961.2537	.663	41961.5367	.627	41962.5044	.504
41961.2567	.634	41961.5454	.592	41962.5080	.505
41961.2611	.611	41961.5501	.573	41962.5122	.518
41961.2709	.542	41961.5613	.542	41962.5161	.522
41961.2764	.541	41961.5662	.537	41962.5199	.507
41961.2796	.535	41961.5847	.531	41962.5247	.510

Table 2 (cont.)

Photoelectric yellow observations of SV Cam

J.D.	ΔV	J.D.	ΔV	J.D.	ΔV
41962.5289	.510	41963.5169	.475	41981.3537	.796
41962.5329	.504	41963.5219	.470	41981.3589	.879
41962.5378	.510			41981.3628	.972
41962.5472	.511	41978.4104	1.076	41981.3672	1.054
41962.5515	.493	41978.4144	1.092	41981.3714	1.057
41962.5563	.503	41978.4195	1.119	41981.3763	1.057
41962.5599	.517	41978.4226	1.126		
41962.5648	.522	41978.4279	1.098	41982.2543	.682
41962.5682	.527	41978.4320	1.012	41982.2577	.671
41962.5730	.519	41978.4356	.939	41982.2619	.682
41962.5771	.524	41978.4388	.886	41982.2653	.673
41962.5820	.516	41978.4431	.800	41982.2697	.676
		41978.4469	.752	41982.2730	.663
41963.2572	.593	41978.4504	.685	41982.2774	.657
41963.2611	.606	41978.4552	.631	41982.2812	.662
41963.2657	.639	41978.4594	.588	41982.2856	.663
41963.2692	.644	41978.4632	.549	41982.2891	.665
41963.2738	.660	41978.4675	.546	41982.2934	.651
41963.2778	.666	41978.4716	.534	41982.2965	.644
41963.2815	.659	41978.4758	.542	41982.3007	.616
41963.2850	.659	41978.4794	.530	41982.3040	.615
41963.2903	.648	41978.4836	.533	41982.3080	.600
41963.2934	.654	41978.4875	.525	41982.3117	.587
41963.2978	.649	41978.4933	.524	41982.3223	.546
41963.3015	.646	41978.4976	.519	41982.3283	.538
41963.3060	.630	41978.5041	.521	41982.3343	.540
41963.3901	.498	41978.5078	.506	41982.3363	.537
41963.3937	.491	41978.5126	.500	41982.3409	.537
41963.3983	.487	41978.5162	.513	41982.3436	.521
41963.4022	.495	41978.5232	.488	41982.3472	.527
41963.4064	.473	41978.5278	.487	41982.3489	.525
41963.4098	.469	41978.5381	.502	41982.3522	.527
41963.4143	.466			41982.3570	.517
41963.4182	.469	41980.2836	.490	41982.3608	.518
41963.4227	.465	41980.2876	.494	41982.3679	.506
41963.4261	.452	41980.2926	.489	41982.3697	.501
41963.4307	.456	41980.2968	.479	41982.3729	.505
41963.4345	.463			41982.3761	.487
41963.4389	.452	41981.2713	.456	41982.3799	.485
41963.4439	.444	41981.2750	.454	41982.3832	.485
41963.4487	.452	41981.2797	.456	41982.3875	.483
41963.4588	.435	41981.2827	.452	41982.3906	.486
41963.4627	.424	41981.2854	.454	41982.3955	.461
41963.4668	.434	41981.2899	.467	41982.3987	.460
41963.4710	.446	41981.2944	.473	41982.4038	.460
41963.4763	.455	41981.2979	.469	41982.4074	.458
41963.4807	.455	41981.3014	.472	41982.4128	.457
41963.4855	.454	41981.3052	.484	41982.4161	.458
41963.4907	.450	41981.3092	.479	41982.4216	.461
41963.4960	.459	41981.3178	.490	41982.4260	.458
41963.4999	.451	41981.3269	.517	41982.4306	.456
41963.5043	.464	41981.3365	.568	41982.4348	.458
41963.5084	.470	41981.3421	.634	41982.4397	.460
41963.5130	.487	41981.3487	.736	41982.4440	.454

Table 2 (cont.)

Photoelectric yellow observations of SV Cam

J.D.	ΔV	J.D.	ΔV	J.D.	ΔV
41982.4501	.457	41983.3637	.516	41983.6271	.446
41982.4582	.460	41983.3688	.536	41983.6337	.452
41982.4625	.464	41983.3722	.539	41983.6372	.454
41982.4685	.477	41983.3836	.557	41983.6423	.457
41982.4742	.474	41983.3924	.547	41983.6457	.459
41982.4820	.467	41983.3986	.556	41983.6507	.467
41982.4858	.473	41983.4017	.569	41983.6541	.470
41982.5349	.728	41983.4058	.575		
41982.5384	.777	41983.4100	.585	41984.2609	.475
41982.5437	.890	41983.4159	.603	41984.2642	.484
41982.5487	.977	41983.4196	.618	41984.2683	.489
41982.5524	1.037	41983.4239	.612	41984.2717	.480
41982.5570	1.069	41983.4280	.629	41984.2761	.484
41982.5610	1.073	41983.4329	.628	41984.2797	.492
41982.5658	1.091	41983.4369	.662	41984.2835	.498
41982.5713	1.093	41983.4418	.674	41984.2871	.505
41982.5748	1.090	41983.4456	.677	41984.2915	.502
41982.5790	1.069	41983.4506	.686	41984.2988	.552
41982.5835	1.003	41983.4541	.669	41984.3033	.590
41982.5889	.895	41983.4586	.662	41984.3068	.623
41982.5924	.832	41983.4621	.679	41984.3114	.677
41982.5965	.774	41983.4666	.677	41984.3146	.735
41982.6000	.697	41983.4697	.662	41984.3187	.812
41982.6037	.606	41983.4738	.661	41984.3222	.871
41982.6132	.575	41983.4776	.656	41984.3266	.955
41982.6165	.548	41983.4824	.629	41984.3298	1.016
41982.6215	.533	41983.4855	.626	41984.3342	1.068
41982.6258	.528	41983.4914	.614	41984.3369	1.074
41982.6309	.526	41983.4953	.593	41984.3420	1.081
41982.6364	.518	41983.4997	.586	41984.3469	1.093
41982.6383	.509	41983.5046	.562	41984.3529	1.094
		41983.5108	.560	41984.3577	1.076
41983.2535	.491	41983.5158	.558	41984.3625	.984
41983.2574	.494	41983.5209	.553	41984.3677	.899
41983.2634	.485	41983.5295	.534	41984.3710	.830
41983.2675	.479	41983.5335	.529	41984.3759	.771
41983.2724	.487	41983.5402	.511	41984.3797	.683
41983.2804	.485	41983.5441	.519	41984.3841	.636
41983.2854	.484	41983.5493	.502	41984.3876	.603
41983.2907	.473	41983.5531	.508	41984.3923	.567
41983.2946	.486	41983.5580	.508	41984.3961	.542
41983.2990	.483	41983.5624	.496	41984.4008	.531
41983.3027	.472	41983.5664	.504	41984.4120	.517
41983.3095	.489	41983.5750	.483	41984.4157	.526
41983.3135	.488	41983.5831	.486	41984.4209	.512
41983.3199	.476	41983.5921	.458	41984.4249	.491
41983.3258	.489	41983.5957	.459	41984.4301	.491
41983.3313	.506	41983.6004	.474	41984.4333	.495
41983.3354	.502	41983.6038	.471	41984.4424	.495
41983.3419	.489	41983.6078	.461	41984.4500	.490
41983.3459	.495	41983.6113	.470	41984.4561	.494
41983.3509	.508	41983.6153	.463	41984.4596	.485
41983.3542	.515	41983.6186	.443	41984.4692	.482
41983.3600	.526	41983.6238	.445	41984.4801	.477

Table 2 (cont.)

Photoelectric yellow observations of SV Cam

J.D.	ΔV	J.D.	ΔV	J.D.	ΔV
41984.4882	.479	42019.4426	.482	42022.4644	.434
41984.4938	.474	42019.4462	.470	42022.4676	.439
41984.4977	.483	42019.4489	.463	42022.4712	.444
41984.5014	.482	42019.4523	.468	42022.4728	.452
41984.5064	.497	42019.4565	.473	42022.4800	.450
41984.5090	.492	42019.4602	.459	42022.4872	.446
41984.5159	.493	42019.4632	.472	42022.4910	.465
41984.5208	.499	42019.4731	.464	42022.4998	.463
41984.5256	.502	42019.4788	.442	42022.5055	.474
		42019.4824	.444	42022.5086	.477
42019.2572	.520	42019.4851	.452	42022.5122	.482
42019.2648	.507	42019.4895	.449	42022.5160	.478
42019.2699	.508	42019.4921	.450	42022.5194	.490
42019.2741	.523	42019.4938	.444	42022.5221	.465
42019.2825	.543	42019.4998	.440	42022.5306	.482
42019.2854	.554	42019.5037	.444	42022.5342	.485
42019.2887	.562	42019.5065	.457	42022.5417	.494
42019.2926	.601	42019.5105	.463	42022.5447	.498
42019.2965	.651	42019.5227	.460		
42019.2996	.683	42019.5303	.449	42066.3246	.456
42019.3034	.745	42019.5339	.452	42066.3330	.452
42019.3079	.808	42019.5404	.463	42066.3441	.459
42019.3111	.870	42019.5441	.451	42066.3530	.451
42019.3149	.944	42019.5475	.458	42066.3608	.455
42019.3188	1.010	42019.5512	.466	42066.3659	.470
42019.3224	1.078	42019.5545	.483	42066.3714	.459
42019.3261	1.125	42019.5580	.480	42066.3758	.471
42019.3343	1.134	42019.5629	.486	42066.3857	.477
42019.3374	1.125	42019.5662	.491	42066.3906	.485
42019.3415	1.114	42019.5688	.497	42066.3958	.474
42019.3442	1.093	42019.5735	.512	42066.4021	.473
42019.3480	1.084	42019.5762	.504	42066.4639	.610
42019.3509	1.058	42019.5813	.514	42066.4669	.611
42019.3546	.954	42019.5870	.533	42066.4710	.606
42019.3603	.844	42019.5905	.532	42066.4744	.612
42019.3663	.742	42019.5939	.549	42066.4822	.595
42019.3717	.667	42019.5967	.566	42066.4862	.599
42019.3748	.634	42019.6001	.564	42066.4909	.612
42019.3786	.607	42019.6026	.583	42066.4956	.627
42019.3816	.569	42019.6065	.583	42066.5011	.614
42019.3850	.552	42019.6155	.608	42066.5070	.589
42019.3876	.531	42019.6189	.634	42066.5132	.598
42019.3920	.529	42019.6245	.640	42066.5243	.568
42019.3960	.513	42019.6281	.636		
42019.3998	.504	42019.6352	.634	42106.3414	.564
42019.4041	.506	42019.6467	.638	42106.3473	.562
42019.4089	.507	42019.6536	.633	42106.3517	.531
42019.4176	.492	42019.6609	.617	42106.3567	.534
42019.4212	.491	42019.6671	.607	42106.3610	.545
42019.4253	.489	42019.6701	.597	42106.3658	.559
42019.4291	.483	42019.6762	.584	42106.3695	.558
42019.4333	.488	42019.6815	.573	42106.3752	.562
42019.4361	.485	42019.6857	.573	42106.3796	.549
42019.4395	.482	42019.6901	.569	42106.3879	.568

Table 2 (cont.)

Photoelectric yellow observations of SV Cam

J.D.	ΔV	J.D.	ΔV	J.D.	ΔV
42106.3920	.581	42108.5514	.494	42304.3451	.518
42106.3985	.561	42108.5585	.503	42304.3486	.502
42106.4023	.563	42108.5648	.531	42304.3538	.512
42106.4072	.542	42108.5718	.576	42304.3564	.517
42106.4110	.535	42108.5774	.591	42304.3637	.496
42106.4158	.545	42108.5832	.602	42304.3730	.462
42106.4224	.562	42108.5892	.610	42304.3796	.461
42106.4334	.580	42108.5966	.597	42304.3837	.445
42106.4537	.589			42304.3876	.480
42106.4627	.605	42148.3116	.612	42304.3910	.473
42106.4741	.667	42148.3175	.594	42304.3951	.453
42106.4853	.831	42148.3217	.594	42304.3984	.470
42106.4953	.956	42148.3254	.620	42304.4027	.513
42106.5044	1.140	42148.3286	.601	42304.4062	.497
42106.5133	1.183	42148.3327	.616	42304.4101	.488
42106.5294	1.091	42148.3356	.605	42304.4180	.425
42106.5379	.918	42148.3407	.609	42304.4223	.445
42106.5417	.805	42148.3437	.578	42304.4267	.447
42106.5488	.710	42148.3499	.586	42304.4303	.438
42106.5569	.619	42148.3554	.586	42304.4347	.435
42106.5619	.581	42148.3585	.548	42304.4383	.417
42106.5676	.513	42148.3629	.549	42304.4423	.448
42106.5727	.464	42148.3662	.560	42304.4456	.452
42106.6196	.410	42148.3704	.567	42304.4497	.446
42106.6270	.423	42148.3757	.527	42304.4526	.455
42106.6364	.427	42148.3807	.503	42304.4580	.444
		42148.3839	.521	42304.4614	.441
42108.3790	.464	42148.3882	.512	42304.4657	.397
42108.3845	.466	42148.3916	.492	42304.4695	.411
42108.3991	.426	42148.3966	.521	42304.4746	.438
42108.4040	.426	42148.4011	.541	42304.4782	.459
42108.4095	.428	42148.4076	.532	42304.4839	.432
42108.4161	.437	42148.4116	.547	42304.4879	.427
42108.4264	.425	42148.4175	.535	42304.4961	.461
42108.4322	.426	42148.4218	.488	42304.4997	.468
42108.4366	.416	42148.4269	.484	42304.5042	.479
42108.4431	.425	42148.4306	.505	42304.5080	.467
42108.4486	.411	42148.4352	.511	42304.5122	.458
42108.4538	.432	42148.4385	.496	42304.5164	.459
42108.4576	.456	42148.4434	.482	42304.5205	.458
42108.4632	.452	42148.4478	.464	42304.5247	.471
42108.4687	.446	42148.4526	.479	42304.5299	.449
42108.4742	.435	42148.4564	.484	42304.5337	.465
42108.4776	.451	42148.4605	.497	42304.5393	.456
42108.4842	.446	42148.4682	.485	42304.5428	.472
42108.4950	.455	42148.4724	.485	42304.5523	.494
42108.5007	.455	42148.4800	.468	42304.5571	.517
42108.5058	.468			42304.5602	.567
42108.5160	.462	42304.3172	.522	42304.5650	.622
42108.5227	.471	42304.3254	.568	42304.5685	.665
42108.5273	.486	42304.3298	.533	42304.5726	.727
42108.5341	.502	42304.3337	.532	42304.5768	.786
42108.5390	.516	42304.3375	.500	42304.5810	.882
42108.5460	.503	42304.3410	.506	42304.5860	.947

Table 2 (cont.)

Photoelectric yellow observations of SV Cam

J.D.	ΔV	J.D.	ΔV	J.D.	ΔV
42304.5904	1.044	42404.4402	.447	42405.3050	.435
42304.5956	1.073	42404.4511	.458	42405.3092	.440
42304.6004	1.080	42404.4599	.460	42405.3137	.440
42304.6035	1.079	42404.4655	.461	42405.3168	.452
42304.6075	1.069	42404.4754	.470	42405.3220	.448
42304.6111	1.084	42404.4843	.482	42405.3272	.450
		42404.4881	.490	42405.3300	.458
42307.3622	.449	42404.4954	.506	42405.3342	.448
42307.3662	.446	42404.5006	.524	42405.3383	.457
42307.3732	.440	42404.5082	.532	42405.3432	.468
42307.3795	.452	42404.5131	.555	42405.3477	.478
42307.3851	.445	42404.5214	.570	42405.3536	.468
42307.3905	.451	42404.5301	.579	42405.3585	.475
42307.3941	.453	42404.5336	.580	42405.3699	.475
42307.4003	.460	42404.5391	.583	42405.3730	.488
42307.4051	.439	42404.5429	.580	42405.3776	.513
42307.4103	.423	42404.5530	.571	42405.3814	.555
42307.4145	.433	42404.5606	.562	42405.3855	.603
42307.4211	.445	42404.5662	.546	42405.3887	.659
42307.4261	.443	42404.5711	.534	42405.3932	.717
42307.4315	.447	42404.5756	.515	42405.3967	.770
42307.4346	.442	42404.5841	.492	42405.4001	.834
42307.4374	.452	42404.5919	.492	42405.4036	.922
42307.4416	.453	42404.5971	.499	42405.4078	.989
42307.4450	.455	42404.6037	.492	42405.4109	1.048
42307.4522	.452	42404.6086	.480	42405.4147	1.095
42307.4659	.433	42404.6156	.485	42405.4195	1.112
42307.4683	.421	42404.6207	.468	42405.4251	1.124
42307.4721	.424	42404.6273	.470	42405.4322	1.119
42307.4888	.430	42404.6343	.471	42405.4421	.984
		42404.6405	.459	42405.4460	.901
		42404.6471	.440	42405.4501	.815
42309.3096	.674	42404.6520	.445	42405.4539	.747
42309.3141	.681	42404.6631	.439	42405.4588	.664
42309.3190	.827	42404.6683	.426	42405.4678	.567
42309.3218	1.277			42405.4725	.516
42309.3263	1.352			42405.4798	.479
42309.3381	1.079	42405.2203	.465	42405.4859	.469
42309.3416	1.084	42405.2262	.457	42405.4914	.466
		42405.2321	.453	42405.4960	.466
42404.3114	.455	42405.2362	.462	42405.5001	.474
42404.3209	.455	42405.2397	.451	42405.5069	.465
42404.3259	.452	42405.2442	.436	42405.5109	.453
42404.3308	.447	42405.2477	.446	42405.5154	.449
42404.3343	.446	42405.2557	.433	42405.5199	.451
42404.3395	.446	42405.2598	.452	42405.5258	.439
42404.3459	.444	42405.2640	.432	42405.5300	.443
42404.3584	.438	42405.2685	.446	42405.5342	.427
42404.3943	.411	42405.2730	.434	42405.5392	.419
42404.4079	.424	42405.2765	.429	42405.5453	.414
42404.4120	.422	42405.2814	.427	42405.5498	.405
42404.4169	.433	42405.2883	.437	42405.5560	.407
42404.4211	.431	42405.2925	.435	42405.5710	.410
42404.4259	.430	42405.2963	.432	42405.5751	.420
42404.4315	.439	42405.3008	.441	42405.5783	.419

Table 2 (cont.)

Photoelectric yellow observations of SV Cam

J.D.	ΔV	J.D.	ΔV	J.D.	ΔV
42432.2477	.434	42461.2798	.438	42461.5866	.448
42432.2512	.440	42461.2871	.437	42461.5900	.454
42432.2553	.445	42461.2917	.423	42461.5958	.446
42432.2595	.440	42461.2970	.429	42461.5998	.430
42432.2631	.442	42461.3052	.422	42461.6046	.440
42432.2685	.440	42461.3100	.409	42461.6093	.440
42432.2747	.439	42461.3155	.412	42461.6163	.436
42432.2820	.436	42461.3187	.402	42461.6220	.449
42432.2866	.443	42461.3236	.417	42461.6271	.445
42432.2910	.441	42461.3281	.407	42461.6317	.454
42432.2945	.448	42461.3330	.411	42461.6374	.458
42432.2991	.448	42461.3371	.403	42461.6513	.453
42432.3026	.456	42461.3421	.401	42461.6586	.453
42432.3067	.468	42461.3465	.412	42461.6635	.464
42432.3109	.454	42461.3531	.414		
42432.3173	.451	42461.3573	.412	42465.3014	.893
42432.3260	.464	42461.3636	.404	42465.3043	.963
42432.3327	.474	42461.3671	.400	42465.3083	1.047
42432.3366	.477	42461.3791	.414	42465.3118	1.127
42432.3405	.469	42461.3896	.420	42465.3160	1.145
		42461.3953	.413	42465.3220	1.160
42460.4515	.454	42461.3986	.419	42465.3302	1.160
42460.4596	.456	42461.4032	.421	42465.3356	1.151
42460.4640	.464	42461.4097	.427	42465.3396	1.101
42460.4697	.467	42461.4211	.427	42465.3429	1.026
42460.4740	.461	42461.4268	.445	42465.3483	.908
42460.4786	.461	42461.4336	.470	42465.3524	.826
42460.4835	.472	42461.4385	.476	42465.3574	.745
42460.4897	.474	42461.4448	.489	42465.3615	.675
42460.5023	.494	42461.4481	.502	42465.3690	.577
42460.5133	.490	42461.4527	.515	42465.3740	.541
42460.5176	.499	42461.4609	.525	42465.3799	.515
42460.5235	.510	42461.4664	.525	42465.3839	.510
42460.5294	.526	42461.4706	.526	42465.3882	.501
42460.5356	.581	42461.4738	.526	42465.3918	.491
42460.5395	.638	42461.4800	.526	42465.4285	.464
42460.5459	.701	42461.4889	.520	42465.4320	.450
42460.5516	.784	42461.4927	.517	42465.4413	.439
42460.5589	.945	42461.4984	.512	42465.4452	.438
42460.5656	1.081	42461.5031	.502	42465.4553	.421
42460.5707	1.154	42461.5120	.491	42465.4599	.420
42460.5763	1.131	42461.5152	.473	42465.4649	.415
42460.5884	1.147	42461.5253	.454	42465.4702	.406
42460.5937	1.101	42461.5305	.444	42465.4839	.410
42460.5994	.963	42461.5378	.459	42465.4879	.408
42460.6054	.862	42461.5416	.462	42465.4931	.407
42460.6158	.702	42461.5467	.468	42465.4957	.405
42460.6287	.550	42461.5503	.458	42465.5017	.408
		42461.5595	.446	42465.5056	.398
42461.2545	.460	42461.5634	.439	42465.5094	.406
42461.2580	.463	42461.5698	.447	42465.5153	.403
42461.2628	.465	42461.5736	.450	42465.5222	.410
42461.2687	.456	42461.5788	.452	42465.5306	.406
42461.2736	.444	42461.5821	.446	42465.5356	.415

Table 2 (cont.)

Photoelectric yellow observations of SV Cam

J.D.	ΔV	J.D.	ΔV	J.D.	ΔV
42465.5404	.413	42522.5180	.490	42545.3786	1.142
42465.5445	.417	42522.5219	.516	42545.3833	1.131
42465.5493	.420	42522.5270	.514	42545.3896	1.139
42465.5521	.415	42522.5313	.525	42545.3936	1.120
42465.5572	.423	42522.5394	.545	42545.3991	1.109
42465.5636	.427	42522.5443	.550	42545.4033	1.079
42465.5684	.443	42522.5517	.549	42545.4062	1.026
42465.5721	.437	42522.5577	.547	42545.4110	.894
42465.5774	.447	42522.5646	.559	42545.4140	.848
42465.5827	.457	42522.5695	.543	42545.4204	.723
42465.5879	.467	42522.5770	.539	42545.4267	.619
42465.5918	.490			42545.4422	.506
42465.5965	.497	42523.3173	.469	42545.4457	.500
42465.6014	.508	42523.3224	.469	42545.4607	.475
42465.6059	.503	42523.3287	.464	42545.4676	.460
42465.6097	.516	42523.3338	.462	42545.4736	.468
42465.6163	.528	42523.3376	.468	42545.4788	.458
42465.6236	.527	42523.3438	.459	42545.4850	.435
42465.6299	.525	42523.3492	.471	42545.4894	.441
42465.6361	.521	42523.3538	.475	42545.4929	.453
42465.6425	.512	42523.3607	.484		
42465.6490	.497	42523.3657	.499	42603.4588	.508
42465.6524	.498	42523.3723	.500	42603.4654	.565
42465.6588	.490	42523.3772	.506	42603.4682	.604
42465.6660	.481	42523.3847	.489	42603.4730	.662
		42523.3897	.499	42603.4759	.703
42466.2886	.439	42523.3945	.520	42603.4793	.737
42466.2969	.445	42523.4008	.553	42603.4832	.813
42466.3001	.448	42523.4065	.616	42603.4869	.913
42466.3067	.453	42523.4113	.694	42603.4902	.979
42466.3117	.434	42523.4163	.767	42603.4953	1.093
42466.3171	.435	42523.4204	.847	42603.4985	1.126
42466.3208	.450	42523.4255	.966	42603.5036	1.151
42466.3268	.443	42523.4308	1.084	42603.5067	1.160
42466.3400	.437	42523.4393	1.159	42603.5105	1.163
42466.3443	.447	42523.4509	1.153	42603.5134	1.145
42466.3490	.456	42523.4603	1.073	42603.5196	1.136
42466.3528	.456	42523.4663	.944	42603.5223	1.122
42466.3589	.455	42523.4731	.773	42603.5272	1.029
42466.3642	.446	42523.4783	.697	42603.5300	.971
42466.3683	.453	42523.4855	.618	42603.5338	.884
42466.3733	.457	42523.4902	.543	42603.5371	.834
42466.3776	.457	42523.4962	.501	42603.5404	.750
42466.3819	.450	42523.5014	.497	42603.5435	.690
42466.3851	.453	42523.5097	.487		
42466.3914	.456	42523.5147	.475	42634.3270	.911
42466.3950	.463	42523.5205	.462	42634.3297	.991
42466.3992	.471	42523.5282	.453	42634.3348	1.081
42466.4035	.476	42523.5367	.446	42634.3385	1.132
		42523.5462	.438	42634.3421	1.157
42522.4977	.452	42523.5572	.438	42634.3455	1.179
42522.5029	.474	42523.5703	.425	42634.3501	1.173
42522.5079	.462			42634.3537	1.167
42522.5129	.491	42545.3741	1.077	42634.3589	1.184

Table 2 (cont.)

Photoelectric yellow observations of SV Cam

J.D.	ΔV	J.D.	ΔV	J.D.	ΔV
42634.3634	1.121	42829.4639	1.229	42836.6395	.640
42634.3686	1.000	42829.4730	1.246	42836.6486	.610
42634.3728	.913	42829.4830	1.210	42836.6569	.601
42634.3782	.809	42829.4919	1.008		
42634.3829	.762	42829.5126	.660	42871.4899	.591
42634.3879	.683	42829.5231	.621	42871.5015	.584
42634.3912	.654	42829.5317	.609	42871.5108	.605
42634.3957	.615	42829.5394	.594	42871.5128	.591
42634.3998	.593	42829.5410	.586	42871.5204	.588
42634.4067	.566	42829.5505	.573	42871.5397	.717
42634.4092	.563	42829.5533	.575	42871.5418	.778
42634.4152	.559	42829.5626	.565	42871.5489	.897
42634.4202	.558	42829.5661	.572	42871.5509	.937
42634.4249	.530			42871.5614	1.093
42634.4292	.537	42830.5818	.527	42871.5709	1.164
42634.4345	.539	42830.5891	.542	42871.5742	1.177
42634.4381	.531	42830.5903	.562	42871.5820	1.178
42634.4435	.526	42830.5967	.552	42871.5898	1.157
42634.4470	.531	42830.6197	.719	42871.5922	1.137
42634.4518	.528	42830.6274	.850	42871.5995	.995
42634.4560	.520	42830.6370	.991	42871.6016	.966
42634.4609	.522	42830.6440	1.112		
42634.4645	.519	42830.6490	1.160	43061.3178	.690
42634.4702	.508	42830.6538	1.185	43061.3226	.741
42634.4738	.497	42830.6612	1.212	43061.3296	.850
42634.4787	.491	42830.6709	1.188	43061.3362	.947
42634.4825	.489			43061.3407	1.064
42634.4870	.493	42831.2455	1.321	43061.3459	1.175
42634.4912	.475	42831.2622	1.205	43061.3497	1.232
42634.4967	.453	42831.2716	1.020	43061.3591	1.230
42634.5070	.438	42831.2929	.681	43061.3639	1.232
42634.5116	.446	42831.3027	.601	43061.3702	1.231
42634.5161	.459	42831.3142	.589	43061.3747	1.203
42634.5379	.455	42831.3260	.570	43061.3792	1.091
42634.5464	.435	42831.3373	.560	43061.3837	.994
		42831.3513	.564	43061.3882	.922
42829.3237	.520	42831.3646	.546	43061.3928	.819
42829.3362	.504	42831.3763	.539	43061.3983	.729
42829.3493	.505	42831.3863	.533	43061.4032	.686
42829.3513	.507			43061.4080	.661
42829.3602	.501	42836.5170	.548	43061.4126	.627
42829.3620	.507	42836.5184	.558	43061.4167	.620
42829.3702	.527	42836.5340	.601		
42829.3720	.520	42836.5533	.818	43077.3249	.594
42829.3845	.530	42836.5613	.967	43077.3303	.635
42829.3953	.535	42836.5628	1.011	43077.3363	.710
42829.4060	.568	42836.5835	1.217	43077.3416	.787
42829.4145	.564	42836.5909	1.227	43077.3468	.859
42829.4161	.577	42836.5925	1.226	43077.3513	.991
42829.4229	.597	42836.6004	1.181	43077.3558	1.096
42829.4335	.669	42836.6021	1.120	43077.3607	1.173
42829.4405	.803	42836.6106	.943	43077.3645	1.178
42829.4419	.838	42836.6128	.900	43077.3683	1.196
42829.4493	1.020	42836.6262	.711	43077.3721	1.209

Table 2 (cont.)

Photoelectric yellow observations of SV Cam

J.D.	ΔV	J.D.	ΔV	J.D.	ΔV
43077.3758	1.225	43135.3883	.616	43192.5502	.577
43077.3801	1.238	43135.3932	.605	43192.5582	.581
43077.3843	1.225	43135.3994	.601	43192.5669	.554
43077.3881	1.151	43135.4046	.613		
43077.3922	1.083	43135.4098	.623	43198.3364	1.003
43077.4009	.911	43135.4147	.623	43198.3476	1.180
43077.4051	.813	43135.4210	.613	43198.3664	1.240
43077.4112	.748	43135.4333	.616	43198.3799	1.075
43077.4199	.642	43135.4415	.630	43198.3855	.929
		43135.4514	.696	43198.3924	.847
43078.5099	.580	43135.4595	.787	43198.4035	.710
43078.5141	.610	43135.4654	.892	43198.4107	.659
43078.5183	.642	43135.4717	1.023	43198.4177	.637
43078.5224	.706	43135.4755	1.068	43198.4271	.604
43078.5266	.750	43135.4793	1.146	43198.4320	.609
43078.5311	.853	43135.4835	1.171	43198.4365	.601
43078.5356	.938	43135.4873	1.228		
43078.5400	1.023	43135.4911	1.249	43218.4709	.629
43078.5440	1.096	43135.4953	1.239	43218.4733	.639
43078.5504	1.155	43135.5008	1.228	43218.4761	.655
43078.5572	1.203	43135.5072	1.177	43218.4792	.674
43078.5613	1.211	43135.5161	1.023	43218.4827	.719
43078.5651	1.173	43135.5251	.844	43218.4858	.754
43078.5693	1.147	43135.5317	.744	43218.4889	.799
43078.5773	1.087	43135.5366	.709	43218.4971	.937
43078.5811	1.008	43135.5414	.672	43218.5018	1.012
43078.5869	.906	43135.5453	.655	43218.5053	1.091
43078.5922	.825	43135.5494	.643	43218.5101	1.152
43078.5960	.762	43135.5592	.633	43218.5160	1.203
43078.5995	.714	43135.5637	.644	43218.5233	1.230
43078.6033	.651	43135.5682	.636	43218.5268	1.222
43078.6072	.627	43135.5737	.629	43218.5313	1.197
43078.6129	.591	43135.5793	.606	43218.5365	1.166
43078.6190	.593	43135.5842	.607	43218.5396	1.131
				43218.5449	1.017
43135.2498	.591	43192.3825	.699	43218.5494	.926
43135.2564	.606	43192.3961	.811	43218.5521	.903
43135.2630	.603	43192.4027	.953	43218.5553	.860
43135.2668	.598	43192.4082	1.084	43218.5587	.815
43135.2707	.602	43192.4141	1.205	43218.5638	.763
43135.2764	.576	43192.4193	1.254	43218.5695	.718
43135.2825	.575	43192.4297	1.302	43218.5740	.675
43135.2892	.580	43192.4363	1.299	43218.5792	.625
43135.2957	.594	43192.4438	1.197	43218.5843	.611
43135.3012	.598	43192.4544	.995	43218.5921	.602
43135.3073	.604	43192.4617	.849	43218.6138	.573
43135.3318	.600	43192.4672	.744	43218.6306	.575
43135.3394	.585	43192.4731	.702		
43135.3436	.601	43192.4783	.674	43288.3665	.565
43135.3477	.602	43192.4895	.641	43288.3703	.570
43135.3546	.585	43192.4954	.617	43288.3748	.569
43135.3616	.590	43192.5050	.622	43288.3783	.570
43135.3686	.587	43192.5165	.615	43288.3859	.565
43135.3821	.598	43192.5304	.592	43288.3894	.559

Table 2 (cont.)

Photoelectric yellow observations of SV Cam

J.D.	Δ V	J.D.	Δ V	J.D.	Δ V
43288.3964	.583	43392.5032	.603	43765.4749	.554
43288.4009	.589	43392.5122	.597	43765.4788	.553
43288.4089	.593	43392.5178	.610	43765.4846	.561
43288.4145	.596	43392.5233	.595	43765.4951	.554
43288.4233	.606			43765.4999	.557
43288.4374	.636	43393.4047	.586	43765.5048	.547
43288.4432	.636	43393.4133	.596	43765.5096	.543
43288.4474	.651	43393.4183	.617	43765.5152	.553
43288.4516	.663	43393.4224	.629	43765.5208	.547
43288.4557	.672	43393.4307	.653	43765.5346	.545
43288.4616	.692	43393.4349	.664	43765.5395	.544
43288.4698	.762	43393.4397	.705	43765.5468	.547
43288.4769	.902	43393.4453	.809	43765.5534	.547
43288.4804	.967	43393.4498	.903	43765.5576	.535
43288.4874	1.090	43393.4533	.939	43765.5624	.549
		43393.4583	1.087	43765.5666	.549
43344.3604	.576	43393.4623	1.171	43765.5708	.548
43344.3743	.555	43393.4665	1.255	43765.5742	.542
43344.3847	.549	43393.4984	1.200	43765.5784	.545
43344.3900	.556	43393.5023	1.105	43765.5833	.540
43344.3955	.545	43393.5067	1.024	43765.5874	.534
43344.4007	.539	43393.5126	.943	43765.5916	.546
43344.4063	.561	43393.5165	.849	43765.5965	.587
43344.4115	.542	43393.5283	.705	43765.6006	.617
43344.4257	.526	43393.5348	.690	43765.6048	.625
43344.4340	.543	43393.5394	.695	43765.6083	.637
43344.4434	.546	43393.5449	.677	43765.6124	.644
43344.4493	.542	43393.5564	.668	43765.6159	.641
43344.4538	.550	43393.5612	.650	43765.6201	.635
43344.4594	.537	43393.5651	.658	43765.6242	.640
43344.4639	.555	43393.5692	.654		
43344.4681	.543	43393.5734	.643	43815.3106	.499
43344.4722	.539	43393.5783	.649	43815.3127	.501
43344.4847	.571			43815.3147	.498
43344.4886	.573	43394.3376	.630	43815.3267	.510
43344.4927	.566	43394.3442	.633	43815.3283	.519
43344.4972	.574	43394.3536	.647	43815.3394	.521
43344.5051	.575	43394.3601	.663	43815.3410	.536
43344.5115	.595	43394.3673	.677	43815.3444	.522
43344.5160	.619	43394.3724	.689	43815.3563	.526
43344.5195	.625	43394.3765	.690	43815.3576	.525
		43394.3807	.661	43815.3577	.530
43392.4011	.621	43394.3852	.674	43815.3602	.533
43392.4066	.616	43394.3894	.653	43815.3637	.530
43392.4271	.592	43394.3956	.635	43815.3644	.525
43392.4316	.599	43394.4059	.621	43815.3674	.526
43392.4428	.604	43394.5308	.530	43815.3739	.553
43392.4476	.605	43394.5376	.547	43815.3764	.551
43392.4563	.610	43394.5422	.553	43815.3843	.555
43392.4632	.604			43815.3857	.551
43392.4792	.582	43765.4195	.633	43815.3890	.551
43392.4889	.576	43765.4319	.621	43815.3897	.553
43392.4934	.578	43765.4416	.596	43815.3905	.542
43392.4983	.599	43765.4565	.564	43815.3946	.550
		43765.4673	.571		

Table 2 (cont.)

Photoelectric yellow observations of SV Cam

J.D.	ΔV	J.D.	ΔV	J.D.	ΔV
43815.3953	.549	43815.4781	.677	43849.6534	.522
43815.3959	.557	43815.4789	.672	43849.6580	.520
43815.3966	.557	43815.4796	.661	43849.6621	.529
43815.4019	.542	43815.4803	.668	43849.6711	.534
43815.4045	.558	43815.4870	.656	43849.6809	.528
43815.4056	.561	43815.4878	.655	43849.6913	.510
43815.4079	.575	43815.4886	.647		
43815.4087	.565	43815.4898	.648	43878.3414	.665
43815.4119	.597	43815.4907	.636	43878.3475	.638
43815.4126	.606	43815.4914	.639	43878.3557	.596
43815.4133	.594	43815.4963	.613	43878.3648	.597
43815.4152	.612	43815.4971	.612	43878.3716	.582
43815.4214	.613	43815.4978	.611	43878.3746	.588
43815.4222	.613	43815.4988	.603	43878.3825	.597
43815.4228	.630	43815.4995	.603	43878.3897	.591
43815.4263	.626	43815.5001	.604	43878.3950	.584
43815.4271	.635	43815.5009	.608	43878.4017	.596
43815.4302	.647	43815.5019	.587	43878.4057	.583
43815.4311	.653	43815.5035	.587	43878.4246	.577
43815.4318	.656	43815.5074	.560	43878.4342	.566
43815.4325	.650	43815.5100	.548	43878.4453	.514
43815.4361	.668	43815.5134	.546	43878.4524	.519
43815.4369	.677	43815.5143	.536	43878.4554	.509
43815.3756	.679	43815.5173	.529	43878.4633	.505
43815.4385	.676	43815.5182	.529	43878.4772	.481
43815.4393	.663			43878.4969	.494
43815.4400	.665	43849.5031	.653	43878.4994	.490
43815.4410	.673	43849.5111	.686	43878.5095	.466
43815.4449	.659	43849.5159	.765	43878.5196	.490
43815.4458	.644	43849.5205	.798	43878.5261	.507
43815.4465	.648	43849.5250	.905	43878.5347	.525
43815.4472	.660	43849.5288	.974	43878.5387	.545
43815.4480	.653	43849.5350	1.109	43878.5416	.541
43815.4485	.645	43849.5399	1.150	43878.5505	.569
43815.4522	.654	43849.5441	1.204	43878.5531	.583
43815.4529	.661	43849.5475	1.187	43878.5561	.600
43815.4534	.652	43849.5524	1.211	43878.5629	.620
43815.4542	.651	43849.5559	1.210	43878.5674	.628
43815.4549	.667	43849.5597	1.210	43878.5748	.720
43815.4555	.666	43849.5635	1.186	43878.5776	.749
43815.4598	.675	43849.5680	1.132	43878.5849	.894
43815.4617	.677	43849.5722	1.039	43878.5882	.958
43815.4624	.674	43849.5760	.947	43878.5932	1.055
43815.4630	.670	43849.5798	.889	43878.6016	1.162
43815.4636	.665	43849.5836	.815	43878.6050	1.169
43815.4647	.681	43849.5871	.767	43878.6108	1.211
43815.4654	.671	43849.5916	.680	43878.6185	1.182
43815.4669	.671	43849.5951	.658	43878.6265	1.126
43815.4677	.679	43849.6090	.611	43878.6290	1.078
43815.4688	.668	43849.6135	.580	43878.6320	1.025
43815.4695	.681	43849.6208	.564	43878.6392	.910
43815.4749	.666	43849.6277	.560	43878.6413	.844
43815.4755	.661	43849.6323	.564	43878.6434	.804
43815.4775	.664	43849.6433	.545	43878.6493	.724

Table 2 (cont.)

Photoelectric yellow observations of SV Cam

J.D.	Δ V	J.D.	Δ V	J.D.	Δ V
43878.6537	.669	43880.3036	.525	43880.6779	.636
43878.6616	.588	43880.3117	.538	43880.6883	.660
43878.6647	.560	43880.3149	.550	43880.6937	.663
43878.6746	.559	43880.3198	.565	43880.7030	.685
43878.6786	.553	43880.3260	.596		
43878.6861	.563	43880.3328	.608	43926.2812	.544
43878.6943	.519	43880.3432	.619	43926.2939	.512
43878.7031	.516	43880.3527	.696	43926.3092	.521
		43880.3592	.743	43926.3191	.596
43879.3646	.497	43880.3656	.853	43926.3290	.609
43879.3740	.455	43880.3735	1.058	43926.3330	.631
43879.3828	.462	43880.3834	1.193	43926.3391	.636
43879.3901	.444	43880.3905	1.195	43926.3435	.640
43879.3935	.438	43880.3973	1.202	43926.3541	.666
43879.4005	.457	43880.4040	1.188	43926.3634	.628
43879.4034	.465	43880.4073	1.109	43926.3703	.602
43879.4112	.469	43880.4125	1.044	43926.3792	.598
43879.4151	.475	43880.4194	.879	43926.3884	.534
43879.4348	.513	43880.4221	.836	43926.3955	.530
43879.4451	.529	43880.4246	.774	43926.4036	.545
43879.4538	.529	43880.4315	.700	43926.4112	.541
43879.4621	.584	43880.4358	.669	43926.4212	.520
43879.4694	.631	43880.4421	.646	43926.4291	.561
43879.4725	.633	43880.4489	.639	43926.4431	.535
43879.4811	.674	43880.4569	.596	43926.4530	.528
43879.4888	.648	43880.4647	.574	43926.4629	.538
43879.4922	.647	43880.4697	.569	43926.4744	.523
43879.5002	.662	43880.4725	.576	43926.4881	.540
43879.5107	.675	43880.4818	.585	43926.4990	.523
43879.5188	.681	43880.4909	.564	43926.5111	.544
43879.5279	.626	43880.4995	.528	43926.5229	.545
43879.5360	.652	43880.5043	.531	43926.5332	.541
43879.5436	.604	43880.5150	.548	43926.5467	.479
43879.5520	.587	43880.5200	.547	43926.5545	.523
43879.5595	.562	43880.5267	.527	43926.5589	.535
43879.5670	.557	43880.5299	.506	43926.5658	.546
43879.5750	.523	43880.5369	.478	43926.5721	.571
43879.5871	.569	43880.5493	.461	43926.5814	.569
43879.5965	.574	43880.5537	.457	43926.5961	.543
43879.6040	.562	43880.5595	.476	43926.6046	.606
43879.6153	.572	43880.5657	.466	43926.6124	.705
43879.6256	.541	43880.5718	.490	43926.6204	.807
43879.6359	.509	43880.5765	.486	43926.6242	.865
43879.6442	.547	43880.5813	.466	43926.6317	.978
43879.6469	.539	43880.5886	.483	43926.6354	1.047
		43880.5968	.482	43926.6433	1.149
43880.2266	.517	43880.6054	.489	43926.6525	1.164
43880.2359	.506	43880.6172	.539	43926.6617	1.150
43880.2422	.516	43880.6256	.526	43926.6720	.973
43880.2498	.507	43880.6359	.526		
43880.2601	.484	43880.6499	.555	43927.2460	1.191
43880.2697	.504	43880.6541	.573	43927.2488	1.178
43880.2782	.497	43880.6618	.604	43927.2552	1.155
43880.2974	.544	43880.6701	.623	43927.2578	1.136

Table 2 (cont.)

Photoelectric yellow observations of SV Cam

J.D.	ΔV	J.D.	ΔV	J.D.	ΔV
43927.2687	.934	43927.5650	.594	43928.4534	.904
43927.2708	.907	43927.5722	.582	43928.4555	.886
43927.2726	.862	43927.5793	.542	43928.4582	.824
43927.2780	.778	43927.5908	.539	43928.4650	.715
43927.2802	.713	43927.5956	.534	43928.4690	.655
43927.2867	.610	43927.6042	.537	43928.4727	.631
43927.2898	.569	43927.6102	.534	43928.4744	.614
43927.2961	.561	43927.6165	.520	43928.4768	.601
43927.2982	.570	43927.6253	.518	43928.4791	.588
43927.3054	.556	43927.6293	.514	43928.4812	.575
43927.3078	.566	43927.6404	.486	43928.4885	.552
43927.3139	.555	43927.6492	.505	43928.4915	.551
43927.3158	.547	43927.6562	.507	43928.4954	.601
43927.3179	.539	43927.6631	.509	43928.5003	.591
43927.3240	.547			43928.5031	.577
43927.3267	.536	43928.2948	.525	43928.5054	.560
43927.3307	.527	43928.3013	.531	43928.5113	.579
43927.3326	.536	43928.3088	.543	43928.5156	.557
43927.3402	.531	43928.3144	.536	43928.5209	.569
43927.3428	.522	43928.3202	.545	43928.5255	.555
43927.3459	.505	43928.3259	.534	43928.5282	.554
43927.3542	.511	43928.3306	.535	43928.5306	.557
43927.3634	.491	43928.3369	.544	43928.5355	.549
43927.3660	.492	43928.3470	.528	43928.5377	.543
43927.3683	.497	43928.3536	.530	43928.5394	.530
43927.3707	.513	43928.3578	.528	43928.5416	.535
43927.3778	.513	43928.3597	.522	43928.5451	.543
43927.3819	.503	43928.3642	.497	43928.5482	.526
43927.3854	.491	43928.3666	.510	43928.5531	.498
43927.3927	.491	43928.3697	.511	43928.5553	.513
43927.3962	.518	43928.3714	.517	43928.5615	.518
43927.4039	.512	43928.3778	.559	43928.5732	.505
43927.4064	.493	43928.3807	.570	43928.5756	.480
43927.4103	.517	43928.3860	.619	43928.5835	.512
43927.4203	.496	43928.3885	.627	43928.5866	.491
43927.4230	.510	43928.3906	.649	43928.5911	.482
43927.4266	.504	43928.3942	.699	43928.5937	.493
43927.4323	.500	43928.3969	.726	43928.5991	.490
43927.4350	.530	43928.3995	.750	43928.6008	.501
43927.4373	.521	43928.4025	.805	43928.6030	.502
43927.4411	.509	43928.4057	.871	43928.6051	.511
43927.4454	.520	43928.4088	.921	43928.6074	.501
43927.4512	.525	43928.4110	1.027	43928.6120	.507
43927.4610	.525	43928.4163	1.111	43928.6143	.517
43927.4730	.466	43928.4194	1.160	43928.6161	.518
43927.4795	.488	43928.4222	1.190	43928.6182	.541
43927.4902	.508	43928.4239	1.221	43928.6223	.522
43927.4955	.545	43928.4263	1.222	43928.6247	.548
43927.5054	.572	43928.4291	1.215	43928.6297	.547
43927.5122	.574	43928.4338	1.219	43928.6331	.537
43927.5240	.562	43928.4369	1.208	43928.6379	.536
43927.5326	.561	43928.4415	1.172	43928.6401	.512
43927.5446	.650	43928.4444	1.136	43928.6432	.510
43927.5508	.629	43928.4516	.959	43928.6488	.498

Table 2 (cont.)

Photoelectric yellow observations of SV Cam

J.D.	Δ V	J.D.	Δ V	J.D.	Δ V
43926.6504	.485	44048.4920	.548	44049.4712	.511
		44048.4968	.555	44049.4722	.522
44048.3758	.473	44048.4978	.569	44049.4777	.523
44048.3768	.491	44048.4987	.558	44049.4786	.521
44048.3778	.490	44048.5165	.623	44049.4797	.527
44048.3827	.494	44048.5175	.627	44049.4843	.550
44048.3837	.486	44048.5185	.607	44049.4853	.540
44048.3847	.488	44048.5232	.615	44049.4863	.538
44048.3893	.480	44048.5243	.614	44049.4903	.540
44048.3903	.497	44048.5253	.620	44049.4914	.526
44048.3912	.487			44049.4923	.526
44048.3956	.505	44049.3752	.593	44049.5039	.522
44048.3965	.504	44049.3762	.602	44049.5049	.521
44048.3976	.500	44049.3772	.614	44049.5059	.525
44048.4028	.492	44049.3816	.682	44049.5162	.507
44048.4037	.481	44049.3826	.695	44049.5172	.509
44048.4048	.505	44049.3836	.701	44049.5182	.507
44048.4092	.492	44049.3881	.785	44049.5231	.513
44048.4103	.488	44049.3891	.803	44049.5241	.510
44048.4112	.483	44049.3901	.816	44049.5251	.512
44048.4170	.498	44049.3946	.902		
44048.4181	.492	44049.3956	.928	44081.4676	.897
44048.4191	.491	44049.4018	1.066	44081.4686	.880
44048.4235	.515	44049.4028	1.080	44081.4696	.846
44048.4245	.503	44049.4077	1.128	44081.4781	.742
44048.4255	.503	44049.4087	1.128	44081.4791	.721
44048.4304	.502	44049.4097	1.141	44081.4801	.704
44048.4314	.508	44049.4138	1.139	44081.4846	.646
44048.4324	.488	44049.4148	1.147	44081.4856	.623
44048.4367	.522	44049.4157	1.156	44081.4866	.610
44048.4377	.524	44049.4199	1.140	44081.4910	.570
44048.4387	.511	44049.4210	1.133	44081.4920	.574
44048.4432	.500	44049.4220	1.136	44081.4930	.570
44048.4442	.504	44049.4265	1.149	44081.4971	.534
44048.4452	.502	44049.4280	1.137	44081.4981	.536
44048.4499	.526	44049.4322	1.149	44081.4991	.538
44048.4509	.526	44049.4331	1.136	44081.5042	.541
44048.4518	.536	44049.4341	1.110	44081.5052	.543
44048.4563	.518	44049.4384	.973	44081.5062	.551
44048.4574	.504	44049.4394	.957	44081.5109	.525
44048.4584	.513	44049.4404	.948	44081.5119	.522
44048.4631	.506	44049.4446	.810	44081.5129	.526
44048.4641	.516	44049.4456	.798	44081.5174	.516
44048.4651	.516	44049.4466	.794	44081.5184	.516
44048.4698	.522	44049.4512	.730	44081.5194	.529
44048.4708	.532	44049.4522	.701		
44048.4718	.523	44049.4532	.688	44103.3250	.592
44048.4767	.530	44049.4573	.664	44103.3337	.600
44048.4777	.535	44049.4583	.651	44103.3424	.630
44048.4786	.524	44049.4593	.641	44103.3459	.660
44048.4833	.546	44049.4636	.592	44103.3504	.733
44048.4843	.538	44049.4646	.576	44103.3549	.807
44048.4900	.535	44049.4655	.558	44103.3594	.912
44048.4910	.552	44049.4702	.516	44103.3653	1.021

Table 2 (cont))

Photoelectric yellow observations of SV Cam

J.D.	ΔV	J.D.	ΔV	J.D.	ΔV
44103.3695	1.102	44145.3272	.468	44158.3843	.491
44103.3733	1.193	44145.3314	.444	44158.3853	.491
44103.3775	1.238	44145.3323	.439	44158.3863	.489
44103.3822	1.238	44145.3333	.453	44158.3873	.483
44103.3917	1.210			44158.3933	.487
44103.4014	1.108	44146.3434	.522	44158.3942	.478
44103.4056	.993	44146.3450	.535	44158.3953	.484
44103.4098	.932	44146.3464	.538	44158.3961	.481
44103.4143	.850	44146.3512	.566	44158.4008	.487
44103.4181	.775	44146.3522	.566	44158.4018	.482
44103.4223	.692	44146.3532	.568	44158.4027	.483
44103.4268	.643	44146.3542	.574	44158.4038	.483
44103.4303	.623	44146.3664	.587		
44103.4355	.581	44146.3674	.590	44159.3590	.516
44103.4462	.542	44146.3684	.584	44159.3600	.508
44103.4500	.525	44146.3694	.593	44159.3610	.496
44103.4552	.537	44146.3745	.608	44159.3619	.510
44103.4594	.545	44146.3755	.599	44159.3664	.517
44103.4653	.529	44146.3764	.607	44159.3674	.513
44103.4722	.504	44146.3808	.607	44159.3684	.519
44103.4796	.489	44146.3817	.602	44159.3693	.520
44103.4841	.483	44146.3827	.601	44159.3742	.518
44103.4941	.471	44146.3837	.608	44159.3752	.514
44103.4980	.471	44146.3879	.591	44159.3762	.508
44103.5063	.483	44146.3889	.602	44159.3772	.506
44103.5108	.495	44146.3898	.600	44159.3827	.520
44103.5160	.497	44146.3909	.604	44159.3846	.517
44103.5231	.479			44159.3846	.526
44103.5299	.467	44158.3313	.514	44159.3856	.520
44103.5344	.461	44158.3323	.512	44159.3899	.527
44103.5383	.455	44158.3333	.517	44159.3910	.529
44103.5438	.459	44158.3342	.510	44159.3919	.540
44103.5480	.461	44158.3387	.501	44159.3929	.537
44103.5542	.466	44158.3398	.501	44159.3970	.554
44103.5591	.454	44158.3407	.492	44159.3980	.545
44103.5643	.461	44158.3418	.489	44159.3990	.551
44103.5755	.476	44158.3536	.495	44159.4000	.542
44103.5823	.469	44158.3545	.492	44159.4041	.564
		44158.3555	.500	44159.4051	.563
44145.2927	.459	44158.3565	.499	44159.4061	.570
44145.2938	.464	44158.3609	.491	44159.4071	.574
44145.2946	.464	44158.3619	.489	44159.4112	.584
44145.2990	.445	44158.3629	.493	44159.4122	.592
44145.3000	.433	44158.3639	.486	44159.4132	.592
44145.3010	.446	44158.3680	.486	44159.4142	.594
44145.3062	.468	44158.3690	.492	44159.4188	.595
44145.3072	.462	44158.3700	.495	44159.4198	.600
44145.3082	.449	44158.3709	.491	44159.4207	.601
44145.3140	.472	44158.3752	.482	44159.4217	.597
44145.3210	.471	44158.3762	.488	44159.4258	.605
44145.3252	.469	44158.3772	.482	44159.4267	.611
44145.3261	.453	44158.3782	.478	44159.4278	.616
				44159.4287	.612

Table 2 (cont.)

Photoelectric yellow observations of SV Cam

J.D.	ΔV	J.D.	ΔV	J.D.	ΔV
44159.4333	.605	44159.5408	.498	44285.3069	.475
44159.4343	.605	44159.5458	.496	44285.3112	.469
44159.4353	.610	44159.5469	.497	44285.3121	.474
44159.4363	.606	44159.5479	.495	44285.3165	.479
44159.4405	.597	44159.5488	.491	44285.3174	.480
44159.4415	.600	44159.5535	.487	44285.3224	.473
44159.4425	.601	44159.5545	.480	44285.3234	.478
44159.4435	.604	44159.5555	.473	44285.3244	.473
44159.4480	.604	44159.5565	.458	44285.3253	.477
44159.4490	.605	44159.5607	.477	44285.3296	.470
44159.4500	.601	44159.5626	.479	44285.3307	.477
44159.4509	.601	44159.5636	.477	44285.3316	.476
44159.4563	.590	44159.5764	.474	44285.3326	.474
44159.4573	.581	44159.5840	.475	44285.3375	.478
44159.4583	.587	44159.5850	.472	44285.3385	.472
44159.4593	.571	44159.5860	.473	44285.3395	.478
44159.4640	.562	44159.5870	.476	44285.3445	.483
44159.4649	.561	44159.5831	.495	44285.3455	.482
44159.4660	.557	44159.5941	.489	44285.3465	.476
44159.4670	.558	44159.5951	.490	44285.3474	.482
44159.4712	.545	44159.5961	.486	44285.3524	.481
44159.4721	.555	44159.6088	.488	44285.3534	.489
44159.4731	.545	44159.6098	.479	44285.3544	.488
44159.4741	.542	44159.6108	.484	44285.3554	.493
44159.4786	.525	44159.6118	.485	44285.3603	.485
44159.4796	.525	44159.6164	.492	44285.3613	.495
44159.4806	.527	44159.6174	.495	44285.3622	.492
44159.4816	.523	44159.6184	.499	44285.3633	.495
44159.4860	.523	44159.6194	.492	44285.3678	.509
44159.4870	.521	44159.6243	.509	44285.3698	.501
44159.4879	.526	44159.6253	.500	44285.3708	.500
44159.4889	.530	44159.6263	.504	44285.3756	.517
44159.4949	.507	44159.6273	.509	44285.3766	.519
44159.4959	.505	44159.6317	.504	44285.3776	.510
44159.4969	.502	44159.6328	.501	44285.3786	.521
44159.5011	.512	44159.6337	.510	44285.3827	.511
44159.5021	.510	44159.6347	.509	44285.3838	.514
44159.5031	.506	44159.6390	.512	44285.3847	.517
44159.5041	.515	44159.6400	.505	44285.3857	.512
44159.5091	.501	44159.6410	.511	44285.3905	.520
44159.5101	.500	44159.6420	.517	44285.3915	.515
44159.5111	.500	44159.6463	.515	44285.3925	.521
44159.5121	.498	44159.6473	.517	44285.3935	.526
44159.5162	.505	44159.6482	.518	44285.3983	.522
44159.5172	.507	44159.6492	.511	44285.3993	.525
44159.5182	.504			44285.4002	.524
44159.5192	.508	44285.2821	.486	44285.4012	.530
44159.5233	.488	44285.2831	.486	44285.4060	.535
44159.5243	.484	44285.2841	.488	44285.4070	.543
44159.5253	.483	44285.2851	.486	44285.4080	.542
44159.5263	.483	44285.2861	.491	44285.4090	.543
44159.5378	.496	44285.3008	.485	44285.4132	.572
44159.5388	.498	44285.3018	.484	44285.4142	.579
44159.5398	.494	44285.3060	.478	44285.4152	.588

Table 2 (cont.)

Photoelectric yellow observations of SV Cam

J.D.	ΔV	J.D.	ΔV	J.D.	ΔV
44285.4162	.604	44285.5690	.517	44285.6758	.537
44285.4215	.665	44285.5700	.522	44285.6768	.535
44285.4225	.674	44285.5757	.501	44285.6778	.548
44285.4235	.686	44285.5766	.503	44285.6822	.544
44285.4245	.691	44285.5776	.504	44285.6832	.539
44285.4291	.756	44285.5819	.511	44285.6842	.548
44285.4301	.772	44285.5829	.512	44285.6852	.547
44285.4311	.808	44285.5839	.496		
44285.4321	.828	44285.5849	.499	44345.3235	.696
44285.4369	.915	44285.5899	.509	44345.3282	.736
44285.4379	.926	44285.5909	.505	44345.3326	.820
44285.4388	.950	44285.5919	.504	44345.3372	.903
44285.4398	.970	44285.5928	.502	44345.3419	1.005
44285.4441	1.049	44285.5983	.507	44345.3458	1.075
44285.4451	1.092	44285.5992	.501	44345.3510	1.104
44285.4461	1.093	44285.6002	.508	44345.3556	1.130
44285.4471	1.113	44285.6012	.510	44345.3604	1.156
44285.4512	1.138	44285.6056	.509	44345.3653	1.156
44285.4522	1.153	44285.6066	.495	44345.3691	1.157
44285.4532	1.149	44285.6076	.492	44345.3733	1.139
44285.4542	1.149	44285.6086	.499	44345.3782	1.073
44285.4584	1.178	44285.6131	.500	44345.3826	.975
44285.4594	1.183	44285.6141	.505	44345.3872	.863
44285.4604	1.178	44285.6151	.505	44345.3926	.763
44285.4614	1.194	44285.6161	.515	44345.3976	.684
44285.4657	1.181	44285.6216	.521	44345.4021	.648
44285.4367	1.170	44285.6226	.495	44345.4115	.564
44285.4677	1.177	44285.6236	.497	44345.4157	.573
44285.4687	1.167	44285.6246	.501	44345.4206	.550
44285.4730	1.173	44285.6288	.508	44345.4254	.555
44285.4740	1.153	44285.6298	.501	44345.4323	.546
44285.4749	1.143	44285.6308	.491	44345.4365	.542
44285.4759	1.123	44285.6318	.494	44345.4407	.542
44285.4882	.855	44285.6361	.506		
44285.4892	.833	44285.6370	.496	44371.3352	.478
44285.4902	.821	44285.6381	.510	44371.3361	.487
44285.4912	.805	44285.6391	.516	44371.3372	.485
44285.4971	.705	44285.6432	.516	44371.3382	.486
44285.4981	.698	44285.6442	.520	44371.3438	.478
44285.4991	.687	44285.6451	.524	44371.3448	.476
44285.5001	.675	44285.6461	.528	44371.3458	.469
44285.5045	.634	44285.6506	.504	44371.3468	.469
44285.5054	.624	44285.6516	.506	44371.3510	.465
44285.5065	.609	44285.6526	.504	44371.3520	.476
44285.5075	.595	44285.6536	.510	44371.3530	.474
44285.5143	.572	44285.6606	.516	44371.3539	.475
44285.5153	.569	44285.6616	.503	44371.3579	.495
44285.5163	.556	44285.6625	.520	44371.3589	.500
44285.5173	.560	44285.6635	.508	44371.3599	.500
44285.5276	.558	44285.6677	.520	44371.3609	.505
44285.5286	.551	44285.6686	.517	44371.3652	.491
44285.5296	.559	44285.6697	.512	44371.3662	.495
44285.5306	.559	44285.6707	.527	44371.3672	.504
44285.5680	.513	44285.6748	.531	44371.3682	.504

Table 2 (cont.)

Photoelectric yellow observations of SV Cam

J.D.	ΔV	J.D.	ΔV	J.D.	ΔV
44371.3722	.505	44371.4734	.993	44454.4287	.514
44371.3732	.505	44371.4779	.957	44454.4297	.524
44371.3742	.504	44371.4788	.941	44454.4312	.519
44371.3752	.502	44371.4798	.930	44454.4373	.574
44371.3796	.525	44371.4808	.912	44454.4383	.564
44371.3806	.523	44371.4871	.747	44454.4393	.577
44371.3815	.517	44371.4901	.685	44454.4444	.613
44371.3825	.520	44371.4945	.636	44454.4453	.640
44371.3874	.505	44371.4955	.623	44454.4464	.659
44371.3884	.513	44371.4965	.609	44454.4505	.700
44371.3894	.520	44371.4975	.600	44454.4515	.720
44371.3904	.520	44371.5019	.570	44454.4525	.730
44371.3949	.528	44371.5029	.561	44454.4535	.729
44371.3960	.525	44371.5038	.560	44454.4587	.809
44371.3969	.528	44371.5048	.558	44454.4597	.837
44371.3979	.525	44371.5101	.537	44454.4606	.827
44371.4029	.542	44371.5111	.517	44454.4616	.843
44371.4040	.527	44371.5120	.505	44454.4739	1.088
44371.4048	.544	44371.5130	.501	44454.4749	1.111
44371.4059	.545	44371.5173	.478	44454.4759	1.090
44371.4106	.578	44371.5183	.497	44454.4769	1.123
44371.4116	.593	44371.5193	.490	44454.4824	1.148
44371.4125	.608	44371.5203	.493	44454.4834	1.141
44371.4135	.622	44371.5247	.509	44454.4844	1.150
44371.4188	.663	44371.5256	.512	44454.4853	1.156
44371.4198	.691	44371.5267	.509	44454.4909	1.141
44371.4208	.703	44371.5276	.502	44454.4919	1.151
44371.4217	.714	44371.5318	.515	44454.4939	1.159
44371.4264	.806	44371.5328	.509	44454.4985	1.120
44371.4274	.822	44371.5338	.516	44454.4995	1.104
44371.4284	.840	44371.5348	.520	44454.5005	1.101
44371.4293	.850	44371.5409	.474	44454.5015	1.088
44371.4339	.930	44371.5419	.470	44454.5094	.928
44371.4349	.951	44371.5429	.462	44454.5104	.893
44371.4358	.961	44371.5438	.456	44454.5114	.876
44371.4368	.997	44371.5481	.479	44454.5124	.856
44371.4413	1.063	44371.5490	.484	44454.5171	.792
44371.4433	1.099	44371.5500	.462	44454.5180	.774
44371.4443	1.091	44371.5510	.475	44454.5190	.751
44371.4489	1.145			44454.5200	.745
44371.4499	1.143	44454.3862	.498	44454.5249	.666
44371.4508	1.138	44454.3982	.507	44454.5259	.654
44371.4517	1.130	44454.3993	.502	44454.5268	.649
44371.4559	1.121	44454.4002	.514	44454.5278	.634
44371.4570	1.119	44454.4012	.512	44454.5328	.597
44371.4579	1.126	44454.4056	.514	44454.5338	.608
44371.4589	1.126	44454.4066	.523	44454.5347	.598
44371.4632	1.102	44454.4076	.513	44454.5357	.598
44371.4642	1.081	44454.4085	.518	44454.5405	.589
44371.4651	1.096	44454.4129	.536	44454.5414	.580
44371.4661	1.075	44454.4139	.543	44454.5424	.574
44371.4705	1.058	44454.4149	.534	44454.5434	.554
44371.4715	1.036	44454.4159	.539	44454.5489	.568
44371.4724	1.026	44454.4215	.530	44454.5499	.559

Table 2 (cont.)

Photoelectric yellow observations of SV Cam

J.D.	Δ V	J.D.	Δ V	J.D.	Δ V
44454.5509	.547	44477.3904	.569	44477.4991	.509
44454.5519	.540	44477.3914	.568	44477.5001	.516
44454.5571	.553	44477.3923	.553	44477.5042	.523
44454.5581	.552	44477.3933	.555	44477.5052	.530
		44477.3980	.551	44477.5062	.513
44455.3412	.546	44477.3990	.548	44477.5072	.525
44455.3422	.567	44477.4000	.559	44477.5116	.524
44455.3431	.565	44477.4010	.552	44477.5126	.515
44455.3441	.572	44477.4054	.530	44477.5136	.519
44455.3550	.603	44477.4063	.548	44477.5146	.525
44455.3560	.612	44477.4073	.545	44477.5188	.524
44455.3570	.614	44477.4083	.553	44477.5197	.529
44455.3579	.607	44477.4138	.546	44477.5207	.522
44455.3634	.623	44477.4147	.550	44477.5217	.539
44455.3662	.623	44477.4157	.547	44477.5266	.528
44455.3672	.608	44477.4167	.546	44477.5275	.528
44455.3681	.615	44477.4303	.534	44477.5285	.522
44455.3691	.616	44477.4313	.531	44477.5295	.522
44455.3747	.624	44477.4322	.538	44477.5340	.518
44455.3757	.634	44477.4332	.531	44477.5350	.528
44455.3767	.638	44477.4380	.523	44477.5360	.540
44455.3776	.640	44477.4390	.508	44477.5370	.524
44455.3911	.637	44477.4400	.519	44477.5415	.533
44455.3920	.632	44477.4410	.526	44477.5424	.536
44455.3930	.630	44477.4459	.524	44477.5434	.543
44455.3940	.628	44477.4469	.522	44477.5444	.532
44455.3988	.616	44477.4479	.528	44477.5488	.544
44455.3998	.616	44477.4489	.532	44477.5497	.541
44455.4007	.609	44477.4529	.527	44477.5507	.537
44455.4017	.597	44477.4539	.521	44477.5517	.533
44455.4062	.589	44477.4549	.516	44477.5562	.539
44455.4072	.588	44477.4558	.520	44477.5572	.548
44455.4081	.583	44477.4602	.512	44477.5582	.541
44455.4091	.591	44477.4612	.508	44477.5592	.542
44455.4141	.591	44477.4622	.517	44477.5641	.562
44455.4151	.593	44477.4632	.502	44477.5651	.558
44455.4161	.577	44477.4678	.525	44477.5660	.572
44455.4171	.579	44477.4687	.514	44477.5670	.570
44455.4221	.578	44477.4697	.515	44477.5719	.616
44455.4231	.568	44477.4707	.513	44477.5729	.624
44455.4241	.569	44477.4757	.510	44477.5739	.641
44455.4287	.569	44477.4767	.507	44477.5749	.651
44455.4297	.567	44477.4777	.510	44477.5790	.704
44455.4342	.563	44477.4786	.511	44477.5800	.713
44455.4351	.550	44477.4828	.505	44477.5810	.735
44455.4399	.541	44477.4838	.505	44477.5820	.739
44455.4409	.533	44477.4848	.508	44477.5864	.831
44455.4464	.553	44477.4858	.508	44477.5874	.845
44455.4474	.551	44477.4899	.498	44477.5884	.862
		44477.4909	.500	44477.5894	.885
44477.3793	.556	44477.4919	.497		
44477.3803	.553	44477.4929	.503		
44477.3813	.551	44477.4972	.516	44541.2522	.461
44477.3823	.543	44477.4982	.515	44541.2531	.462

Table 2 (cont.)

Photoelectric yellow observations of SV Cam

J.D.	Δ V	J.D.	Δ V	J.D.	Δ V
44541.2541	.476	44541.3951	.589	44582.2347	.467
44541.2605	.459	44541.3961	.597	44582.2357	.474
44541.2614	.447	44541.3970	.585	44582.2367	.478
44541.2624	.442	44541.4016	.581	44582.2413	.484
44541.2691	.459	44541.4026	.572	44582.2423	.475
44541.2701	.462	44541.4036	.575	44582.2433	.490
44541.2716	.471	44541.4046	.571	44582.2479	.500
44541.2843	.490	44541.4097	.557	44582.2489	.513
44541.2853	.495	44541.4107	.552	44582.2499	.505
44541.2863	.494	44541.4117	.539	44582.2545	.536
44541.2923	.472	44541.4127	.550	44582.2555	.543
44541.2933	.471	44541.4171	.541	44582.2565	.535
44541.3943	.470	44541.4181	.534	44582.2614	.539
44541.2953	.465	44541.4191	.531	44582.2624	.546
44541.3003	.477	44541.4201	.533	44582.2634	.531
44541.3013	.484	44541.4246	.534	44582.2680	.540
44541.3022	.499	44541.4256	.531	44582.2690	.548
44541.3032	.486	44541.4265	.533	44582.2700	.548
44541.3076	.502	44541.4275	.532	44582.2750	.576
44541.3086	.500	44541.4320	.532	44582.2760	.591
44541.3096	.502	44541.4330	.527	44582.2770	.590
44541.3105	.492	44541.4340	.530	44582.2818	.577
44541.3149	.485	44541.4350	.535	44582.2828	.578
44541.3159	.494	44541.4399	.535	44582.2838	.580
44541.3169	.494	44541.4409	.542	44582.2886	.570
44541.3176	.492	44541.4418	.534	44582.2895	.571
44541.3225	.512	44541.4428	.536	44582.2906	.566
44541.3234	.517	44541.4475	.529	44582.2955	.571
44541.3245	.509	44541.4485	.526	44582.2965	.571
44541.3254	.507	44541.4495	.521	44582.2975	.562
44541.3389	.543	44541.4505	.523	44582.3026	.569
44541.3399	.550	44541.4550	.527	44582.3036	.565
44541.3409	.563	44541.4559	.522	44582.3046	.560
44541.3419	.572	44541.4569	.519	44582.3093	.583
44541.3469	.585	44541.4579	.524	44582.3103	.581
44541.3478	.579	44541.4634	.520	44582.3113	.575
44541.3488	.586	44541.4643	.525	44582.3157	.557
44541.3498	.585	44541.4653	.529	44582.3166	.559
44541.3546	.593	44541.4663	.521	44582.3176	.547
44541.3556	.587	44541.4709	.518	44582.3221	.537
44541.3566	.595	44541.4719	.520	44582.3231	.533
44541.3576	.598	44541.4728	.517	44582.3241	.533
44541.3627	.621	44541.4738	.515	44582.3284	.514
44541.3642	.621	44541.4791	.518	44582.3294	.509
44541.3651	.626	44541.4800	.528	44582.3304	.517
44541.3695	.614	44541.4810	.531	44582.3365	.496
44541.3705	.613	44541.4866	.512	44582.3375	.491
44541.3715	.610	44541.4876	.537	44582.3384	.491
44541.3724	.613	44541.4886	.533	44582.3397	.484
44541.3769	.618	44541.4896	.529	44582.3407	.484
44541.3779	.606			44582.3417	.485
44541.3789	.611	44582.2283	.488	44582.3464	.474
44541.3799	.610	44582.2293	.496	44582.3474	.484
44541.3941	.596	44582.2303	.491	44582.3484	.483

Table 2 (cont.)

Photoelectric observations of SV Cam

J.D.	ΔV	J.D.	ΔV	J.D.	ΔV
44582.3493	.489	44582.4347	.459	44582.5496	.674
44582.3503	.472	44582.4356	.453	44582.5506	.682
44582.3513	.479	44582.4366	.452	44582.5516	.692
44582.3561	.487	44582.4411	.466	44582.5526	.697
44582.3570	.474	44582.4421	.466	44582.5536	.724
44582.3580	.469	44582.4431	.460	44582.5622	.872
44582.3590	.472	44582.4441	.459	44582.5632	.891
44582.3600	.467	44582.4451	.468	44582.5642	.917
44582.3610	.463	44582.4460	.476	44582.5651	.945
44582.3662	.445	44582.4521	.468	44582.5700	1.049
44582.3672	.450	44582.4530	.472	44582.5710	1.082
44582.3682	.441	44582.4540	.477	44582.5720	1.107
44582.3692	.448	44582.4550	.471	44582.5730	1.126
44582.3701	.440	44582.4560	.471	44582.5739	1.147
44582.3711	.441	44582.4570	.474	44582.5749	1.165
44582.3753	.456	44582.4669	.481	44582.5796	1.205
44582.3764	.455	44582.4679	.484	44582.5806	1.190
44582.3773	.462	44582.4689	.488	44582.5816	1.177
44582.3783	.460	44582.4699	.488	44582.5825	1.179
44582.3793	.463	44582.4709	.490	44582.5835	1.196
44582.3803	.460	44582.4719	.490	44582.5845	1.196
44582.3845	.460	44582.4779	.498	44582.5891	1.204
44582.3855	.466	44582.4789	.501	44582.5900	1.201
44582.3865	.456	44582.4798	.501	44582.5910	1.206
44582.3875	.469	44582.4808	.509	44582.5920	1.202
44582.3885	.462	44582.4818	.504	44582.5930	1.201
44582.3895	.464	44582.4828	.503	44582.5940	1.208
44582.3936	.460	44582.4875	.507	44582.5989	1.205
44582.3946	.456	44582.4886	.514	44582.5999	1.196
44582.3956	.460	44582.4896	.514	44582.6009	1.197
44582.3966	.463	44582.4905	.506	44582.6019	1.192
44582.3975	.468	44582.4915	.501	44582.6029	1.178
44582.3986	.454	44582.4925	.510	44582.6039	1.163
44582.4035	.464	44582.4977	.518	44582.6089	1.051
44582.4045	.461	44582.4987	.516	44582.6098	1.023
44582.4055	.457	44582.4997	.520	44582.6109	1.004
44582.4065	.463	44582.5006	.527	44582.6118	.981
44582.4075	.458	44582.5017	.527	44582.6128	.958
44582.4084	.455	44582.5026	.522	44582.6133	.926
44582.4123	.465	44582.5078	.530	44582.6184	.827
44582.4138	.458	44582.5088	.536	44582.6195	.803
44582.4148	.460	44582.5098	.532	44582.6204	.788
44582.4158	.457	44582.5108	.534	44582.6214	.770
44582.4168	.457	44582.5117	.535	44582.6224	.752
44582.4177	.460	44582.5127	.536	44582.6234	.739
44582.4221	.459	44582.5190	.559	44582.6283	.677
44582.4231	.451	44582.5199	.569	44582.6293	.671
44582.4241	.457	44582.5209	.569	44582.6303	.652
44582.4251	.458	44582.5219	.557	44582.6312	.641
44582.4260	.455	44582.5229	.570	44582.6322	.644
44582.4270	.453	44582.5239	.579	44582.6332	.622
44582.4317	.455	44582.5287	.571	44582.6378	.609
44582.4327	.451	44582.5297	.569	44582.6388	.599
44582.4336	.459	44582.5486	.664	44582.6398	.597

Table 2 (cont.)

Photoelectric yellow observations of SV Cam

J.D.	ΔV	J.D.	ΔV	J.D.	ΔV
44582.6408	.590	44582.6623	.526	44582.6875	.501
44582.6418	.584	44582.6684	.527	44582.6885	.490
44582.6428	.579	44582.6694	.521	44582.6895	.491
44582.6487	.573	44582.6704	.519	44582.6905	.489
44582.6497	.564	44582.6714	.515	44582.6915	.486
44582.6507	.569	44582.6723	.522	44582.6925	.489
44582.6516	.562	44582.6733	.523	44582.6969	.491
44582.6526	.565	44582.6778	.520	44582.6978	.491
44582.6574	.532	44582.6787	.520	44582.6989	.489
44582.6584	.537	44582.6797	.514	44582.6998	.491
44582.6594	.525	44582.6807	.509	44582.7008	.490
44582.6604	.530	44582.6817	.510	44582.7018	.494
44582.6613	.522	44582.6826	.503		

Table 3

Photoelectric blue observations of SV Cam

J.D.	ΔB	J.D.	ΔB	J.D.	ΔB
41695.4216	.660	41696.2362	.617	41696.4816	.712
41695.4312	.663	41696.2434	.585	41696.4870	.715
41695.4335	.669	41696.2447	.587	41696.4885	.712
41695.4392	.664	41696.2464	.584	41696.4900	.719
41695.4411	.668	41696.2499	.592	41696.4946	.692
41695.4480	.676	41696.2519	.584	41696.4960	.702
41695.4501	.686	41696.2530	.576	41696.4974	.698
41695.4516	.686	41696.2585	.586	41696.5038	.700
41695.4580	.700	41696.2599	.588	41696.5069	.697
41695.4629	.707	41696.2611	.588	41696.5113	.699
41695.4666	.710	41696.2646	.591	41696.5128	.693
41695.4705	.712	41696.2662	.585	41696.5147	.692
41695.4719	.723	41696.2879	.586	41696.5200	.713
41695.4732	.734	41696.2954	.606	41696.5219	.714
41695.4768	.780	41696.2669	.608	41696.5339	.681
41695.4780	.785	41696.2980	.611	41696.5284	.695
41695.4794	.802	41696.3022	.620	41696.5300	.655
41695.4844	.867	41696.3039	.624	41696.5314	.682
41695.4857	.883	41696.3050	.613	41696.5383	.686
41695.4876	.904	41696.3111	.621	41696.5399	.680
41695.4906	.933	41696.3125	.640	41696.5419	.679
41695.4925	.993	41696.3143	.628	41696.5465	.673
41695.4987	1.117	41696.3254	.633	41696.5504	.701
41695.5011	1.137	41696.3282	.642	41696.5522	.716
41695.5033	1.206	41696.3339	.645	41696.5583	.702
41695.5070	1.324	41696.3361	.639	41696.5631	.686
41695.5082	1.327	41696.3374	.634	41696.5660	.659
41695.5156	1.333	41696.3457	.664	41696.5706	.648
41695.5194	1.339	41696.3471	.653	41696.5812	.593
41695.5227	1.352	41696.3522	.656	41696.5830	.584
41695.5277	1.355	41696.3537	.661	41696.5851	.556
41695.5290	1.299	41696.3556	.665	41696.5896	.546
41695.5348	1.224	41696.3598	.680	41696.5912	.568
41695.5360	1.184	41696.3629	.686	41696.5926	.607
41695.5375	1.157	41696.3686	.689	41696.6004	.784
41695.5492	.933	41696.3707	.698	41696.6029	.791
41695.5511	.905	41696.3728	.692		
41695.5531	.857	41696.3772	.715	41697.2876	1.332
41695.5577	.831	41696.3794	.726	41697.2904	1.345
41695.5592	.818	41696.3816	.741	41697.2920	1.347
41695.5608	.756	41696.3863	.761	41697.2959	1.338
41695.5668	.727	41696.3880	.757	41697.2985	1.343
41695.5691	.711	41696.3898	.759	41697.3001	1.337
41695.5738	.678	41696.3939	.758	41697.3062	1.336
41695.5862	.665	41696.3960	.748	41697.3077	1.323
41695.5914	.652	41696.3980	.761	41697.3091	1.317
41695.6006	.635	41696.4046	.767	41697.3131	1.286
41695.6086	.630	41696.4063	.775	41697.3147	1.240
41695.6108	.627	41696.4077	.783	41697.3160	1.196
41695.6167	.615	41696.4201	.773	41697.3207	1.096
41695.6184	.602	41696.4736	.731	41697.3221	1.065
41695.6216	.588	41696.4753	.718	41697.3236	1.042
		41696.4787	.716	41697.3282	.961
41696.2324	.621	41696.4801	.716	41697.3300	.924

Table 3 (cont.)

Photoelectric blue observations of SV Cam

J.D.	ΔB	J.D.	ΔB	J.D.	ΔB
41697.3319	.894	41807.4176	.658	41831.5155	.627
41697.3369	.813	41807.4205	.671	41831.5282	.653
41697.3391	.797	41807.4224	.668		
41697.3406	.780	41807.4288	.652	41833.4088	.746
41697.3439	.746	41807.4309	.649	41833.4119	.737
41697.3465	.729	41807.4374	.667	41833.4205	.740
41697.3481	.707	41807.4400	.666	41833.4236	.740
41697.3529	.679	41807.4468	.666	41833.4329	.711
41697.3548	.673	41807.4488	.647	41833.4357	.689
41697.3564	.669	41807.4564	.676	41833.4447	.655
41697.3599	.645	41807.4585	.655	41833.4480	.662
41697.3630	.648	41807.4674	.657	41833.4571	.634
41697.3653	.645	41807.4698	.655	41833.4597	.637
41697.3710	.643	41807.4780	.665	41833.4706	.647
41697.3721	.638	41807.4808	.677	41833.4738	.645
41697.3742	.644	41807.4904	.662	41833.4748	.648
41697.3778	.633	41807.4995	.670	41833.4907	.655
41697.3801	.644	41807.5018	.667	41833.5037	.656
41697.3816	.642			41833.5067	.656
41697.3886	.643	41810.4034	.672	41833.5192	.641
41697.3906	.633	41810.4055	.659	41833.5227	.645
41697.3924	.638	41810.4133	.653		
41697.3968	.626	41810.4154	.652	41835.3930	.666
41697.3995	.628	41810.4235	.639	41835.4088	.686
41697.4008	.627			41835.4179	.710
41697.4114	.595	41824.4068	.655	41835.4212	.714
41697.4128	.585	41824.4110	.662	41835.4355	.752
41697.4168	.596	41824.4194	.673	41835.4468	.868
41697.4183	.592	41824.4233	.688	41835.4506	.961
41697.4267	.588	41824.4347	.713	41835.4604	1.146
41697.4280	.590	41824.4375	.668	41835.4646	1.233
41697.4306	.597			41835.4739	1.391
41697.4354	.587	41825.4178	1.330	41835.4772	1.413
41697.4368	.588	41825.4218	1.250		
41697.4384	.583	41825.4371	.965	41900.3916	.700
41697.4445	.579	41825.4399	.910	41900.4047	.776
41697.4465	.581	41825.4484	.818	41900.4162	.781
41697.4478	.578	41825.4511	.789	41900.4279	.785
41697.4517	.583	41825.4632	.709	41900.4376	.778
41697.4536	.581	41825.4740	.711	41900.4403	.773
		41825.4768	.716	41900.4504	.733
41807.3457	.654	41825.4878	.712	41900.4531	.725
41807.3488	.677	41825.4987	.666	41900.4624	.655
41807.3561	.683	41825.5019	.663	41900.4648	.663
41807.3581	.674	41825.5108	.639		
41807.3649	.680	41825.5137	.642	41901.3577	.811
41807.3693	.667	41825.5239	.654	41901.3673	.742
41807.3772	.695	41825.5338	.642	41901.3697	.727
41807.3795	.689			41901.3897	.704
41807.3881	.688	41831.4600	.655	41901.3927	.703
41807.3956	.657	41831.4635	.655	41901.4036	.709
41807.3977	.666	41831.4730	.631	41901.4158	.716
41807.4046	.687	41831.4770	.632	41901.4380	.708
41807.4066	.682	41831.4861	.634	41901.4478	.707

Table 3 (cont.)

Photoelectric blue observations of SV Cam

J.D.	ΔB	J.D.	ΔB	J.D.	ΔB
41901.4505	.713	41905.4872	1.125	41933.3693	1.017
41901.4590	.712	41905.4939	1.056		
41901.4617	.704	41905.5120	.773	41934.4551	.622
41901.4849	.714	41905.5239	.744	41934.4660	.634
41901.4987	.703	41905.5418	.662	41934.4737	.664
41901.5064	.702	41905.5588	.712	41934.4801	.712
41901.5089	.700			41934.4867	.755
41901.5169	.703	41930.3362	.773	41934.4953	.903
41901.5196	.716	41930.3496	.980	41934.5049	1.038
41901.5297	.713	41930.4042	1.025	41934.5120	1.165
41901.5513	.731	41930.4094	.898	41934.5177	1.246
41901.5537	.733	41930.4181	.813	41934.5241	1.265
		41930.4247	.777	41934.5306	1.299
41903.3374	.726	41930.4306	.739	41934.5376	1.257
41903.3549	.740	41930.4362	.723	41934.5435	1.167
41903.3601	.752	41930.4541	.720	41934.5503	1.064
41903.3366	.770	41930.4729	.723	41934.5558	.991
41903.3746	.781			41934.5631	.870
41903.3902	.790	41931.3539	.685	41934.5689	.783
41903.3962	.791	41931.3667	.669	41934.5813	.732
41903.4023	.791	41931.3959	.630	41934.5955	.704
41903.4080	.791	41931.4056	.616	41934.6029	.691
		41931.4153	.605		
41904.5297	.746	41931.4246	.604	41935.5721	.693
41904.5357	.749	41931.4388	.600		
41904.5441	.757	41931.4488	.600	41959.4218	1.188
41904.5491	.764	41931.4561	.607	41959.4343	1.299
41904.5562	.793	41931.4657	.610	41959.4399	1.283
41904.5617	.793	41931.4790	.615	41959.4463	1.268
		41931.4892	.625	41959.4559	1.191
41905.3406	.625	41931.4966	.624	41959.4653	1.047
41905.3463	.618	41931.5102	.653		
41905.3529	.613	41931.5237	.758	41960.3145	.815
41905.3584	.618	41931.5300	.866	41960.3208	.830
41905.3643	.623	41931.5375	.983	41960.3296	.823
41905.3699	.632	41931.5427	1.093	41960.3366	.821
41905.3758	.654	41931.5537	1.261	41960.3396	.813
41905.3820	.644	41931.5640	1.264	41960.3514	.777
41905.3880	.646	41931.5707	1.267	41960.3557	.773
41905.3938	.657	41931.5777	1.205	41960.3634	.771
41905.4001	.674	41931.5839	1.095	41960.3710	.752
41905.4057	.671			41960.3747	.749
41905.4120	.677	41933.2966	.716	41960.3790	.728
41905.4181	.720	41933.3023	.773	41960.3825	.708
41905.4253	.800	41933.3081	.840	41960.3888	.713
41905.4316	.885	41933.3136	.927	41960.3950	.713
41905.4383	1.036	41933.3198	1.057	41960.3984	.702
41905.4441	1.122	41933.3258	1.162	41960.4029	.684
41905.4506	1.257	41933.3319	1.240	41960.4065	.682
41905.4562	1.343	41933.3378	1.274	41960.4109	.679
41905.4620	1.412	41933.3437	1.278	41960.4137	.680
41905.4689	1.380	41933.3501	1.264	41960.4184	.679
41905.4746	1.325	41933.3571	1.205	41960.4218	.676
41905.4810	1.255	41933.3629	1.162	41960.4287	.655

Table 3 (cont.)

Photoelectric blue observations of SV Cam

J.D.	ΔB	J.D.	ΔB	J.D.	ΔB
41960.4362	.660	41961.4153	.728	41962.4252	1.104
41960.4395	.657	41961.4214	.736	41962.4285	1.023
41960.4456	.647	41961.4286	.720	41962.4326	.937
41960.4550	.617	41961.4374	.744	41962.4359	.891
41960.4648	.619	41961.4431	.747	41962.4402	.856
41960.4757	.632	41961.4472	.758	41962.4454	.792
41960.4845	.624	41961.4514	.762	41962.4537	.746
41960.4908	.610	41961.4561	.748	41962.4576	.719
41960.4946	.616	41961.4611	.751	41962.4609	.731
41960.4985	.609	41961.4659	.744	41962.4675	.718
41960.5041	.610	41961.4776	.768	41962.4715	.729
41960.5084	.613	41961.4858	.812	41962.4771	.715
41960.5147	.629	41961.4924	.819	41962.4808	.703
41960.5240	.625	41961.4966	.813	41962.4849	.713
41960.5311	.626	41961.5047	.821	41962.4902	.719
41960.5686	.667	41961.5101	.824	41962.4959	.695
41960.5774	.738	41961.5142	.829	41962.5004	.701
41960.5863	.820	41961.5195	.814	41962.5049	.692
41960.5930	.906	41961.5237	.798	41962.5087	.689
41960.5998	.968	41961.5284	.792	41962.5128	.704
41960.6034	1.031	41961.5324	.792	41962.5168	.696
41960.6065	1.127	41961.5376	.789	41962.5206	.686
41960.6144	1.313	41961.5506	.740	41962.5254	.696
41960.6207	1.317	41961.5646	.728	41962.5295	.707
41960.6278	1.303	41961.5853	.702	41962.5335	.690
41960.6341	1.292	41961.5893	.706	41962.5384	.692
		41961.5969	.710	41962.5423	.702
41961.2543	.863	41961.6061	.704	41962.5488	.702
41961.2575	.839	41961.6103	.648	41962.5522	.688
41961.2637	.782	41961.6166	.637	41962.5567	.698
41961.2714	.736	41961.6237	.652	41962.5606	.689
41961.2769	.730			41962.5654	.707
41961.2801	.729	41962.3264	.568	41962.5687	.716
41961.2845	.706	41962.3298	.582	41962.5737	.719
41961.2881	.706	41962.3377	.604	41962.5802	.722
41961.2920	.696	41962.3417	.624		
41961.2977	.700	41962.3455	.642	41963.2578	.764
41961.3097	.689	41962.3497	.666	41963.2618	.793
41961.3175	.696	41962.3534	.696	41963.2663	.811
41961.3248	.698	41962.3627	.798	41963.2697	.783
41961.3285	.694	41962.3673	.837	41963.2741	.822
41961.3347	.708	41962.3704	.881	41963.2782	.817
41961.3409	.703	41962.3749	.931	41963.2821	.831
41961.3447	.692	41962.3785	1.028	41963.2857	.821
41961.3488	.704	41962.3829	1.135	41963.2909	.832
41961.3520	.695	41962.3864	1.214	41963.2939	.832
41961.3557	.685	41962.3905	1.296	41963.3909	.689
41961.3686	.698	41962.3943	1.289	41963.3942	.664
41961.3749	.710	41962.3997	1.296	41963.3988	.668
41961.3826	.696	41962.4065	1.312	41963.4028	.658
41961.3973	.729	41962.4105	1.320	41963.4068	.647
41961.4011	.723	41962.4138	1.285	41963.4103	.634
41961.4048	.731	41962.4177	1.202	41963.4151	.629
41961.4089	.720	41962.4214	1.157	41963.4188	.627

Table 3 (cont.)

Photoelectric blue observations of SV Cam

J.D.	ΔB	J.D.	ΔB	J.D.	ΔB
41963.4234	.618	41980.2975	.677	41982.4354	.616
41963.4267	.625			41982.4403	.620
41963.4313	.637	41981.2721	.618	41982.4448	.625
41963.4352	.640	41981.2755	.610	41982.4509	.612
41963.4393	.629	41981.2803	.616	41982.4587	.628
41963.4445	.616	41981.2832	.621	41982.4630	.630
41963.4491	.602	41981.2860	.630	41982.4696	.644
41963.4595	.593	41981.2904	.626	41982.4749	.654
41963.4631	.602	41981.2950	.650	41982.4827	.650
41963.4674	.599	41981.2984	.646	41982.5354	.930
41963.4717	.622	41981.3019	.662	41982.5391	.988
41963.4769	.635	41981.3058	.657	41982.5493	1.199
41963.4811	.619	41981.3105	.643	41982.5538	1.267
41963.4872	.637	41981.3185	.650	41982.5576	1.287
41963.4914	.615	41981.3275	.678	41982.5626	1.316
41963.4964	.633	41981.3375	.767	41982.5719	1.345
41963.5006	.631	41981.3427	.815	41982.5754	1.315
41963.5050	.656	41981.3495	.915	41982.5794	1.275
41963.5095	.661	41981.3541	1.015	41982.5840	1.183
41963.5138	.655	41981.3595	1.120	41982.5893	1.080
41963.5175	.660	41981.3636	1.178	41982.5930	1.016
41963.5228	.643	41981.3678	1.253	41982.5972	.965
		41981.3720	1.280	41982.6007	.890
41978.4111	1.303	41981.3770	1.298	41982.6091	.786
41978.4148	1.317	41981.3804	1.311	41982.6155	.736
41978.4201	1.345			41982.6222	.708
41978.4231	1.342	41982.2548	.820	41982.6264	.707
41978.4279	1.311	41982.2584	.822	41982.6316	.713
41978.4326	1.225	41982.2627	.845	41982.6369	.705
41978.4362	1.140	41982.2661	.857		
41978.4393	1.074	41982.2702	.842	41983.2540	.649
41978.4436	.984	41982.2737	.835	41983.2581	.646
41978.4475	.937	41982.2780	.841	41983.2640	.656
41978.4509	.889	41982.2819	.832	41983.2682	.650
41978.4558	.805	41982.2863	.839	41983.2738	.682
41978.4600	.758	41982.2955	.818	41983.2817	.686
41978.4638	.733	41982.3014	.813	41983.2864	.674
41978.4681	.725	41982.3047	.806	41983.2932	.676
41978.4722	.718	41982.3084	.800	41983.2995	.664
41978.4764	.723	41982.3122	.770	41983.3032	.660
41978.4798	.706	41982.3230	.720	41983.3102	.666
41978.4840	.713	41982.3576	.686	41983.3140	.673
41978.4881	.717	41982.3735	.670	41983.3206	.666
41978.4960	.692	41982.3768	.674	41983.3279	.666
41978.5049	.704	41982.3823	.669	41983.3320	.675
41978.5084	.696	41982.3900	.567	41983.3367	.681
41978.5132	.675	41982.3980	.631	41983.3426	.672
41978.5174	.682	41982.4043	.634	41983.3464	.684
41978.5262	.660	41982.4080	.643	41983.3516	.694
41978.5333	.696	41982.4132	.619	41983.3548	.703
41978.5389	.672	41982.4169	.589	41983.3606	.704
		41982.4223	.620	41983.3643	.701
41980.2843	.665	41982.4267	.620	41983.3693	.722
41980.2881	.666	41982.4312	.624	41983.3735	.737

Table 3 (cont.)

Photoelectric blue observations of SV Cam

J.D.	ΔB	J.D.	ΔB	J.D.	ΔB
41983.3929	.752	41984.2724	.678	42019.2578	.680
41983.3990	.752	41984.2767	.670	42019.2652	.677
41983.4021	.763	41984.2802	.686	42019.2706	.683
41983.4089	.785	41984.2840	.679	42019.2844	.729
41983.4184	.799	41984.2877	.689	42019.2911	.766
41983.4245	.809	41984.2922	.681	42019.2969	.857
41983.4290	.807	41984.2995	.753	42019.3004	.900
41983.4333	.815	41984.3039	.789	42019.3044	.975
41983.4374	.819	41984.3075	.828	42019.3083	1.035
41983.4423	.836	41984.3120	.886	42019.3115	1.076
41983.4461	.840	41984.3150	.922	42019.3153	1.162
41983.4513	.847	41984.3192	1.008	42019.3193	1.244
41983.4548	.834	41984.3228	1.090	42019.3227	1.311
41983.4591	.842	41984.3271	1.185	42019.3267	1.365
41983.4626	.829	41984.3303	1.220	42019.3351	1.368
41983.4668	.829	41984.3347	1.294	42019.3378	1.355
41983.4702	.827	41984.3374	1.303	42019.3420	1.350
41983.4745	.823	41984.3425	1.341	42019.3447	1.317
41983.4780	.816	41984.3457	1.332	42019.3484	1.276
41983.4828	.797	41984.3492	1.340	42019.3512	1.245
41983.4862	.794	41984.3533	1.330	42019.3551	1.144
41983.4942	.779	41984.3632	1.180	42019.3607	1.013
41983.5002	.758	41984.3681	1.065	42019.3670	.916
41983.5053	.742	41984.3716	1.010	42019.3738	.825
41983.5122	.731	41984.3762	.959	42019.3791	.785
41983.5214	.704	41984.3804	.863	42019.3819	.767
41983.5322	.724	41984.3846	.821	42019.3868	.722
41983.5408	.718	41984.3883	.764	42019.3926	.708
41983.5448	.720	41984.3930	.746	42019.3966	.701
41983.5499	.691	41984.3966	.727	42019.4007	.707
41983.5540	.676	41984.4014	.722	42019.4045	.693
41983.5588	.693	41984.4082	.719	42019.4100	.680
41983.5631	.698	41984.4124	.725	42019.4179	.663
41983.5671	.659	41984.4164	.720	42019.4217	.673
41983.5771	.650	41984.4214	.688	42019.4258	.672
41983.5852	.651	41984.4256	.692	42019.4298	.650
41983.5929	.627	41984.4307	.675	42019.4336	.657
41983.5962	.630	41984.4338	.664	42019.4366	.654
41983.6026	.640	41984.4383	.658	42019.4399	.648
41983.6101	.644	41984.4429	.654	42019.4429	.656
41983.6158	.628	41984.4501	.672	42019.4466	.644
41983.6193	.617	41984.4583	.657	42019.4494	.636
41983.6243	.624	41984.4676	.639	42019.4525	.636
41983.6278	.640	41984.4720	.641	42019.4569	.644
41983.6341	.623	41984.4814	.658	42019.4606	.644
41983.6377	.619	41984.4903	.665	42019.4635	.632
41983.6429	.631	41984.4945	.668	42019.4792	.612
41983.6462	.633	41984.4984	.657	42019.4830	.617
41983.6513	.649	41984.5021	.665	42019.4857	.630
41983.6547	.641	41984.5071	.668	42019.4899	.632
		41984.5096	.702	42019.4929	.631
41984.2616	.653	41984.5167	.699	42019.4971	.618
41984.2647	.683	41984.5215	.689	42019.5003	.613
41984.2692	.687	41984.5263	.695	42019.5040	.629

Table 3 (cont.)

Photoelectric blue observations of SV Cam

J.D.	ΔB	J.D.	ΔB	J.D.	ΔB
42019.5060	.619	42022.5421	.671	42106.5495	.863
42019.5107	.628	42022.5451	.682	42106.5575	.812
42019.5308	.629			42106.5626	.752
42019.5380	.615	42066.3128	.632	42106.5682	.712
42019.5407	.612	42066.3253	.641	42106.5734	.651
42019.5446	.620	42066.3336	.633	42106.5828	.649
42019.5477	.656	42066.3448	.627	42106.6172	.586
42019.5516	.652	42066.3511	.643	42106.6275	.587
42019.5550	.668	42066.3614	.634	42106.6374	.599
42019.5635	.663	42066.3666	.644		
42019.5665	.681	42066.3743	.645	42108.3796	.632
42019.5694	.678	42066.3862	.661	42108.4001	.594
42019.5739	.674	42066.3938	.646	42108.4047	.593
42019.5771	.675	42066.4660	.769	42108.4103	.572
42019.5803	.684	42066.4715	.782	42108.4170	.596
42019.5831	.692	42066.4750	.784	42108.4271	.593
42019.5874	.730	42066.4848	.760	42108.4351	.597
42019.5909	.724	42066.4913	.775	42108.4466	.573
42019.5942	.738	42066.4962	.770	42108.4562	.598
42019.5969	.727	42066.5018	.757	42108.4695	.632
42019.6004	.747	42066.5076	.742	42108.4765	.634
42019.6070	.748	42066.5139	.809	42108.4848	.627
42019.6158	.781	42066.5185	.793	42108.4956	.661
42019.6192	.778	42066.5248	.790	42108.5014	.656
42019.6219	.787	42066.5311	.768	42108.5063	.659
42019.6252	.789			42108.5147	.659
42019.6288	.787	42106.3418	.755	42108.5231	.659
42019.6357	.806	42106.3478	.749	42108.5280	.672
42019.6442	.816	42106.3519	.722	42108.5346	.667
42019.6473	.816	42106.3574	.708	42108.5396	.672
42019.6539	.811	42106.3616	.712	42108.5469	.636
42019.6614	.789	42106.3665	.731	42108.5524	.627
42019.6676	.765	42106.3701	.752	42108.5591	.649
42019.6706	.751	42106.3756	.769	42108.5654	.719
42019.6750	.745	42106.3802	.752	42108.5726	.729
42019.6820	.789	42106.3990	.745	42108.5781	.743
42019.6861	.777	42106.4028	.758	42108.5841	.773
42019.6905	.773	42106.4077	.737	42108.5899	.768
		42106.4116	.722	42108.5974	.731
42022.4665	.634	42106.4163	.731		
42022.4724	.637	42106.4231	.756	42148.3121	.789
42022.4804	.645	42106.4339	.735	42148.3182	.774
42022.4862	.638	42106.4500	.755	42148.3222	.740
42022.4888	.644	42106.4542	.772	42148.3261	.762
42022.4915	.652	42106.4594	.785	42148.3292	.742
42022.5004	.643	42106.4675	.804	42148.3333	.761
42022.5058	.656	42106.4723	.825	42148.3364	.765
42022.5091	.670	42106.4779	.928	42148.3412	.771
42022.5127	.659	42106.4860	1.029	42148.3443	.737
42022.5164	.656	42106.4959	1.189	42148.3506	.763
42022.5199	.662	42106.5050	1.395	42148.3560	.768
42022.5226	.645	42106.5139	1.435	42148.3593	.731
42022.5309	.672	42106.5305	1.279	42148.3636	.728
42022.5347	.675	42106.5403	1.045	42148.3669	.729

Table 3 (cont.)

Photoelectric blue observations of SV Cam

J.D.	ΔB	J.D.	ΔB	J.D.	ΔB
42148.3763	.742	42304.4983	.643	42404.3098	.626
42148.3813	.686	42304.5052	.633	42404.3141	.634
42148.3845	.685	42304.5084	.630	42404.3240	.611
42148.3889	.680	42304.5129	.633	42404.3311	.621
42148.3923	.684	42304.5168	.630	42404.3346	.616
42148.3972	.705	42304.5207	.632	42404.3398	.611
42148.4016	.728	42304.5254	.657	42404.3495	.625
42148.4082	.713	42304.5305	.639	42404.3537	.614
42148.4120	.761	42304.5341	.639	42404.3610	.608
42148.4180	.727	42304.5401	.636	42404.3690	.613
42148.4226	.721	42304.5432	.642	42404.3926	.589
42148.4295	.663	42304.5533	.668	42404.4006	.573
42148.4357	.663	42304.5576	.692	42404.4082	.584
42148.4392	.671	42304.5610	.743	42404.4124	.597
42148.4442	.654	42304.5656	.795	42404.4176	.608
42148.4484	.652	42304.5689	.852	42404.4214	.601
42148.4552	.664	42304.5730	.932	42404.4298	.624
42148.4610	.631	42304.5772	.980	42404.4409	.624
42148.4638	.693	42304.5817	1.091	42404.4522	.627
42148.4805	.646	42304.5865	1.215	42404.4610	.644
		42304.5914	1.310	42404.4662	.640
42304.3135	.726	42304.5962	1.308	42404.4731	.638
42304.3185	.701	42304.6011	1.319	42404.4794	.654
42304.3258	.694	42304.6041	1.305	42404.4849	.673
42304.3307	.700	42304.6080	1.308	42404.4891	.687
42304.3340	.692	42304.6115	1.310	42404.4957	.685
42304.3378	.670			42404.5013	.693
42304.3417	.672	42307.3629	.612	42404.5200	.742
42304.3457	.671	42307.3666	.608	42404.5249	.749
42304.3493	.661	42307.3721	.622	42404.5327	.736
42304.3540	.675	42307.3749	.626	42404.5395	.737
42304.3574	.705	42307.3788	.636	42404.5443	.746
42304.3620	.692	42307.3812	.640	42404.5535	.725
42304.3664	.708	42307.3842	.630	42404.5613	.717
42304.3709	.596	42307.3909	.640	42404.5669	.711
42304.3761	.684	42307.3948	.632	42404.5718	.699
42304.3802	.647	42307.4010	.614	42404.5763	.701
42304.3842	.627	42307.4034	.617	42404.5836	.689
42304.3881	.675	42307.4075	.589	42404.5877	.675
42304.3916	.650	42307.4107	.587	42404.5956	.668
42304.4307	.615	42307.4154	.574	42404.6044	.672
42304.4352	.606	42307.4305	.600	42404.6099	.659
42304.4388	.588	42307.4367	.612	42404.6165	.664
42304.4429	.610	42307.4423	.629	42404.6214	.669
42304.4462	.639	42307.4457	.622	42404.6290	.662
42304.4501	.624	42307.4526	.603	42404.6353	.662
42304.4585	.627	42307.4675	.596	42404.6412	.646
42304.4617	.647	42307.4728	.601	42404.6478	.626
42304.4661	.576	42307.4906	.581	42404.6527	.612
42304.4701	.574			42404.6641	.578
42304.4749	.633	42309.3117	.824	42404.6690	.577
42304.4786	.660	42309.3145	.864		
42304.4845	.611	42309.3193	1.055	42405.2225	.650
42304.4886	.618			42405.2289	.628

Table 3 (cont.)

Photoelectric blue observations of SV Cam

J.D.	ΔB	J.D.	ΔB	J.D.	ΔB
42405.2369	.635	42405.4967	.646	42460.5719	1.408
42405.2401	.640	42405.5008	.646	42460.5769	1.373
42405.2446	.635	42405.5099	.633	42460.5891	1.377
42405.2487	.644	42405.5168	.618	42460.5937	1.301
42405.2564	.630	42405.5203	.615	42460.6002	1.158
42405.2602	.602	42405.5265	.601	42460.6061	1.030
42405.2647	.595	42405.5303	.599	42460.6165	.850
42405.2689	.597	42405.5348	.583	42460.6294	.709
42405.2737	.606	42405.5397	.590		
42405.2772	.608	42405.5463	.588	42461.2553	.624
42405.2817	.590	42405.5501	.592	42461.2584	.614
42405.2888	.610	42405.5564	.590	42461.2692	.618
42405.2928	.629	42405.5714	.579	42461.2764	.613
42405.2970	.614	42405.5758	.572	42461.2840	.598
42405.3015	.607	42405.5789	.565	42461.2921	.596
42405.3057	.625			42461.2975	.601
42405.3098	.623	42432.2484	.624	42461.3010	.592
42405.3142	.627	42432.2519	.613	42461.3057	.573
42405.3189	.618	42432.2560	.617	42461.3104	.576
42405.3223	.617	42432.2598	.619	42461.3159	.558
42405.3279	.634	42432.2638	.627	42461.3191	.563
42405.3310	.639	42432.2692	.617	42461.3243	.578
42405.3348	.631	42432.2768	.614	42461.3285	.573
42405.3390	.652	42432.2824	.606	42461.3355	.566
42405.3439	.669	42432.2873	.596	42461.3427	.548
42405.3484	.678	42432.2933	.610	42461.3470	.568
42405.3546	.670	42432.2994	.626	42461.3537	.583
42405.3651	.668	42432.3029	.628	42461.3578	.572
42405.3722	.670	42432.3074	.642	42461.3642	.567
42405.3801	.725	42432.3117	.647	42461.3677	.565
42405.3862	.797	42432.3157	.641	42461.3774	.563
42405.3890	.865	42432.3198	.639	42461.3819	.559
42405.3935	.917	42432.3244	.653	42461.3882	.568
42405.3970	.969	42432.3285	.641	42461.3956	.566
42405.4008	1.046	42432.3351	.645	42461.3991	.579
42405.4043	1.148	42432.3410	.638	42461.4038	.582
42405.4081	1.217	42432.3449	.646	42461.4100	.579
42405.4112	1.286			42461.4218	.599
42405.4154	1.323	42460.4502	.631	42461.4274	.612
42405.4204	1.343	42460.4544	.631	42461.4367	.646
42405.4258	1.352	42460.4608	.628	42461.4451	.661
42405.4310	1.370	42460.4648	.637	42461.4484	.663
42405.4348	1.395	42460.4724	.641	42461.4532	.661
42405.4425	1.173	42460.4816	.658	42461.4591	.674
42405.4467	1.118	42460.4931	.688	42461.4638	.668
42405.4505	1.003	42460.5048	.694	42461.4671	.676
42405.4545	.935	42460.5160	.690	42461.4711	.685
42405.4591	.838	42460.5245	.691	42461.4741	.680
42405.4690	.729	42460.5301	.698	42461.4788	.673
42405.4734	.685	42460.5364	.769	42461.4824	.681
42405.4786	.664	42460.5402	.812	42461.4895	.688
42405.4824	.664	42460.5497	.953	42461.4930	.671
42405.4869	.652	42460.5596	1.173	42461.4989	.659
42405.4919	.637	42460.5669	1.316	42461.5036	.649

Table 3 (cont.)

Photoelectric blue observations of SV Cam

J.D.	ΔB	J.D.	ΔB	J.D.	ΔB
42461.5123	.651	42465.4706	.560	42466.3782	.650
42461.5157	.647	42465.4842	.553	42466.3825	.641
42461.5286	.634	42465.4883	.556	42466.3858	.636
42461.5382	.638	42465.4954	.567	42466.3917	.637
42461.5423	.627	42465.5022	.562	42466.3956	.641
42461.5510	.627	42465.5059	.578	42466.3997	.645
42461.5600	.622	42465.5099	.570	42466.4040	.655
42461.5642	.618	42465.5158	.571		
42461.5703	.606	42465.5228	.573	42522.4985	.651
42461.5741	.607	42465.5311	.561	42522.5035	.662
42461.5792	.622	42465.5368	.560	42522.5086	.660
42461.5824	.627	42465.5410	.575	42522.5137	.681
42461.5871	.618	42465.5449	.566	42522.5206	.675
42461.5906	.611	42465.5497	.572	42522.5276	.679
42461.5963	.605	42465.5529	.586	42522.5325	.694
42461.6003	.601	42465.5578	.578	42522.5455	.688
42461.6052	.613	42465.5640	.597	42522.5528	.703
42461.6097	.623	42465.5690	.601	42522.5619	.699
42461.6170	.610	42465.5726	.601	42522.5704	.711
42461.6225	.612	42465.5779	.625	42522.5778	.704
42461.6275	.635	42465.5833	.622		
42461.6323	.623	42465.5883	.631	42523.3181	.651
42461.6378	.625	42465.5924	.634	42523.3231	.643
42461.6520	.649	42465.5972	.639	42523.3294	.638
42461.6593	.635	42465.6021	.647	42523.3345	.651
		42465.6064	.649	42523.3399	.645
42465.3017	1.098	42465.6104	.653	42523.3446	.653
42465.3047	1.166	42465.6147	.672	42523.3499	.660
42465.3087	1.303	42465.6189	.681	42523.3544	.642
42465.3125	1.350	42465.6261	.674	42523.3607	.658
42465.3167	1.384	42465.6348	.661	42523.3666	.659
42465.3202	1.386	42465.6430	.661	42523.3880	.669
42465.3247	1.383	42465.6495	.645	42523.3955	.720
42465.3285	1.394	42465.6529	.648	42523.4015	.749
42465.3344	1.380	42465.6613	.639	42523.4072	.819
42465.3399	1.323	42465.6667	.633	42523.4139	.886
42465.3432	1.249	42465.6708	.601	42523.4171	1.009
42465.3488	1.086			42523.4211	1.105
42465.3528	1.005	42466.2858	.616	42523.4261	1.208
42465.3579	.908	42466.2893	.603	42523.4317	1.303
42465.3620	.837	42466.2974	.617	42523.4373	1.323
42465.3695	.764	42466.3008	.619	42523.4426	1.362
42465.3746	.722	42466.3071	.633	42523.4496	1.384
42465.3806	.694	42466.3122	.630	42523.4611	1.273
42465.3842	.690	42466.3178	.639	42523.4670	1.137
42465.3888	.679	42466.3212	.626	42523.4745	.959
42465.3924	.681	42466.3275	.623	42523.4790	.847
42465.4288	.619	42466.3449	.623	42523.4855	.779
42465.4325	.609	42466.3494	.632	42523.4968	.678
42465.4420	.608	42466.3533	.628	42523.5105	.634
42465.4457	.599	42466.3593	.628	42523.5156	.632
42465.4560	.577	42466.3646	.637	42523.5352	.620
42465.4603	.575	42466.3688	.634	42523.5445	.613
42465.4674	.559	42466.3737	.641	42523.5522	.616

Table 3 (cont.)

Photoelectric blue observations of SV Cam

J.D.	ΔB	J.D.	ΔB	J.D.	ΔB
42523.5688	.607	42634.3693	1.199	42829.4636	1.439
42523.5733	.595	42634.3735	1.107	42829.4651	1.446
		42634.3788	1.000	42829.4726	1.484
42545.3745	1.310	42634.3835	.936	42829.4742	1.489
42545.3773	1.370	42634.3884	.880	42829.4842	1.466
42545.3809	1.369	42634.3919	.838	42829.4916	1.408
42545.3862	1.376	42634.3963	.776	42829.4931	1.381
42545.3931	1.372	42634.4008	.756	42829.5122	.949
42545.3996	1.346	42634.4066	.734	42829.5140	.910
42545.4036	1.277	42634.4100	.739	42829.5229	.822
42545.4068	1.206	42634.4161	.730	42829.5407	.765
42545.4116	1.079	42634.4207	.738	42829.5518	.787
42545.4145	1.017	42634.4255	.714	42829.5631	.762
42545.4188	.937	42634.4303	.707		
42545.4234	.879	42634.4351	.717	42830.5815	.763
42545.4272	.820	42634.4384	.700	42830.5828	.752
42545.4445	.647	42634.4438	.697	42830.5895	.743
42545.4597	.637	42634.4478	.685	42830.5907	.770
42545.4625	.636	42634.4525	.681	42830.5969	.766
42545.4661	.633	42634.4568	.689	42830.5978	.773
42545.4700	.639	42634.4613	.680	42830.6046	.786
42545.4741	.632	42634.4652	.668	42830.6131	.790
42545.4822	.623	42634.4712	.645	42830.6194	.854
42545.4879	.617	42634.4744	.652	42830.6208	.896
		42634.4792	.655	42830.6367	1.239
42603.4591	.687	42634.4832	.645	42830.6382	1.273
42603.4661	.737	42634.4876	.651	42830.6453	1.426
42603.4734	.837	42634.4920	.637	42830.6528	1.500
42603.4781	.913	42634.4978	.629	42830.6542	1.503
42603.4838	1.029	42634.5025	.623	42830.6617	1.492
42603.4896	1.153	42634.5076	.609	42830.6702	1.424
42603.4963	1.317	42634.5121	.616		
42603.4991	1.351	42634.5166	.625	42831.2462	1.612
42603.5039	1.381	42634.5385	.625	42831.2627	1.492
42603.5076	1.405	42634.5470	.631	42831.2721	1.213
42603.5110	1.439			42831.2935	.853
42603.5145	1.410	42829.3243	.701	42831.3032	.783
42603.5199	1.372	42829.3253	.699	42831.3148	.782
42603.5230	1.331	42829.3374	.736	42831.3267	.758
42603.5276	1.227	42829.3502	.721	42831.3379	.743
42603.5307	1.137	42829.3570	.708	42831.3517	.752
42603.5345	1.056	42829.3629	.728	42831.3653	.762
42603.5376	1.007	42829.3707	.738	42831.3769	.746
42603.5409	.927	42829.3725	.716	42831.3875	.734
		42829.3910	.695		
42634.3196	.952	42829.3971	.719	42836.5346	.790
42634.3276	1.097	42829.4057	.711	42836.5538	1.076
42634.3304	1.189	42829.4150	.742	42836.5618	1.317
42634.3361	1.321	42829.4165	.730	42836.5632	1.346
42634.3389	1.356	42829.4244	.765	42836.5840	1.451
42634.3425	1.342	42829.4326	.843	42836.5914	1.437
42634.3508	1.374	42829.4339	.854	42836.5931	1.438
42634.3541	1.374	42829.4417	1.026	42836.6009	1.377
42634.3641	1.352	42829.4498	1.251	42836.6025	1.315

Table 3 (cont.)

Photoelectric blue observations of SV Cam

J.D.	ΔB	J.D.	ΔB	J.D.	ΔB
42836.6111	1.130	43077.3398	.930	43135.3248	.793
42836.6133	1.106	43077.3468	1.056	43135.3318	.782
42836.6268	.887	43077.3513	1.156	43135.3394	.795
42836.6390	.814	43077.3626	1.377	43135.3436	.786
42836.6407	.807	43077.3683	1.392	43135.3546	.773
42836.6497	.752	43077.3721	1.413	43135.3778	.774
42836.6568	.734	43077.3758	1.414	43135.3863	.791
		43077.3801	1.425	43135.3994	.798
42871.4896	.824	43077.3843	1.391	43135.4046	.807
42871.4915	.821	43077.3881	1.352	43135.4147	.794
42871.5009	.835	43077.3922	1.248	43135.4234	.814
42871.5033	.821	43077.3968	1.150	43135.4373	.806
42871.5114	.850	43077.4051	.999	43135.4435	.832
42871.5133	.841	43077.4112	.903	43135.4484	.874
42871.5201	.856	43077.4246	.777	43135.4543	.922
42871.5216	.844	43077.4346	.735	43135.4595	.981
42871.5313	.919			43135.4633	1.029
42871.5333	.928	43078.5099	.757	43135.4675	1.104
42871.5407	1.035	43078.5141	.761	43135.4717	1.186
42871.5424	1.057	43078.5183	.801	43135.4755	1.282
42871.5504	1.202	43078.5224	.860	43135.4793	1.354
42871.5618	1.371	43078.5266	.922	43135.4835	1.399
42871.5714	1.536	43078.5311	1.000	43135.4873	1.413
42871.5746	1.559	43078.5356	1.101	43135.4932	1.440
42871.5814	1.542	43078.5400	1.223	43135.5027	1.410
42871.5829	1.551	43078.5440	1.293	43135.5119	1.304
42871.5907	1.437	43078.5485	1.351	43135.5206	1.139
42871.5921	1.412	43078.5523	1.397	43135.5272	1.037
42871.6004	1.223	43078.5572	1.412	43135.5317	.957
42871.6014	1.188	43078.5632	1.407	43135.5400	.877
		43078.5693	1.380	43135.5453	.806
43061.3178	.875	43078.5773	1.266	43135.5494	.800
43061.3226	.935	43078.5811	1.180	43135.5550	.812
43061.3317	1.052	43078.5849	1.130	43135.5592	.817
43061.3433	1.306	43078.5888	1.067	43135.5637	.796
43061.3497	1.411	43078.5922	1.012	43135.5682	.764
43061.3546	1.412	43078.5978	.909	43135.5737	.766
43061.3702	1.402	43078.6033	.847	43135.5793	.802
43061.3747	1.371	43078.6091	.803	43135.5842	.790
43061.3792	1.242	43078.6148	.797	43135.5883	.791
43061.3837	1.165			43135.5935	.744
43061.3882	1.064	43135.2498	.813		
43061.3928	.984	43135.2543	.804	43192.3825	.898
43061.3983	.928	43135.2585	.812	43192.3961	1.028
43061.4032	.898	43135.2649	.808	43192.4027	1.131
43061.4080	.855	43135.2707	.793	43192.4082	1.243
43061.4126	.801	43135.2745	.786	43192.4141	1.356
43061.4167	.779	43135.2783	.781	43192.4245	1.452
43061.4230	.779	43135.2825	.794	43192.4297	1.459
		43135.2873	.780	43192.4386	1.412
43077.3249	.743	43135.2934	.786	43192.4494	1.265
43077.3280	.754	43135.3092	.786	43192.4593	1.085
43077.3325	.824	43135.3151	.780	43192.4702	.936
43077.3363	.874	43135.3214	.784	43192.4783	.861

Table 3 (cont.)

Photoelectric blue observations of SV Cam

J.D.	ΔB	J.D.	ΔB	J.D.	ΔB
43192.4843	.827	43218.6171	.740	43393.4583	1.280
43192.4895	.817	43218.6257	.750	43393.4623	1.358
43192.4987	.788	43218.6306	.743	43393.4665	1.474
43192.5122	.775			43393.4942	1.453
43192.5237	.776	43288.3684	.739	43393.4984	1.368
43192.5349	.752	43288.3766	.743	43393.5023	1.291
43192.5502	.728	43288.3821	.747	43393.5067	1.204
43192.5610	.719	43288.3894	.743	43393.5126	1.122
		43288.3925	.752	43393.5283	.904
43198.3334	1.142	43288.3987	.750	43393.5348	.863
43198.3393	1.275	43288.4047	.758	43393.5394	.870
43198.3438	1.359	43288.4089	.763	43393.5449	.893
43198.3514	1.422	43288.4127	.775	43393.5498	.888
43198.3573	1.460	43288.4181	.787	43393.5564	.888
43198.3632	1.476	43288.4310	.790	43393.5612	.849
43198.3695	1.438	43288.4412	.809	43393.5651	.834
43198.3743	1.353	43288.4474	.825	43393.5713	.839
43198.3799	1.267	43288.4557	.845	43393.5783	.831
43198.3855	1.106	43288.4641	.891		
43198.3924	.994	43288.4750	1.037		
43198.4035	.872	43288.4804	1.150	43765.4195	.810
43198.4084	.853	43288.4849	1.236	43765.4416	.766
43198.4153	.827	43288.4898	1.339	43765.4565	.769
43198.4226	.808			43765.4645	.755
43198.4271	.779	43344.3604	.742	43765.4725	.760
43198.4343	.783	43344.3743	.720	43765.4788	.754
		43344.3847	.741	43765.4975	.742
43218.4721	.807	43344.3900	.724	43765.5072	.746
43218.4792	.860	43344.3981	.701	43765.5152	.742
43218.4858	.935	43344.4088	.720	43765.5208	.724
43218.4921	1.028	43344.4257	.711	43765.5326	.744
43218.5003	1.159	43344.4313	.712	43765.5395	.735
43218.5053	1.268	43344.4368	.710	43765.5444	.737
43218.5080	1.314	43344.4434	.716	43765.5555	.742
43218.5122	1.372	43344.4493	.714	43765.5624	.752
43218.5195	1.437	43344.4538	.714	43765.5666	.736
43218.5233	1.462	43344.4594	.712	43765.5708	.719
43218.5282	1.455	43344.4639	.718	43765.5742	.731
43218.5330	1.419	43344.4701	.721	43765.5809	.737
43218.5365	1.351	43344.4866	.739	43765.5874	.725
43218.5396	1.323	43344.4949	.741	43765.5916	.739
43218.5431	1.258	43344.5051	.762	43765.5965	.770
43218.5466	1.182	43344.5137	.787	43765.6006	.794
43218.5508	1.114	43344.5195	.811	43765.6048	.808
43218.5553	1.009			43765.6159	.820
43218.5587	.962	43393.4047	.795	43765.6222	.822
43218.5653	.881	43393.4133	.800		
43218.5711	.827	43393.4183	.797	43815.3112	.694
43218.5754	.806	43393.4267	.797	43815.3139	.700
43218.5792	.792	43393.4307	.811	43815.3154	.702
43218.5827	.766	43393.4349	.856	43815.3273	.716
43218.5921	.749	43393.4397	.884	43815.3265	.707
43218.6032	.733	43393.4453	.994	43815.3312	.700
43218.6105	.740	43393.4533	1.188	43815.3397	.733

Table 3 (cont.)
Photoelectric blue observations of SV Cam

J.D.	ΔB	J.D.	ΔB	J.D.	ΔB
43615.3435	.746	43615.4545	.835	43649.5722	1.229
43615.3473	.712	43615.4552	.855	43649.5760	1.139
43615.3566	.727	43615.4615	.870	43649.5798	1.062
43615.3574	.725	43615.4620	.861	43649.5836	1.002
43615.3596	.741	43615.4627	.863	43649.5871	.946
43615.3605	.733	43615.4634	.869	43649.5916	.874
43615.3641	.716	43615.4641	.856	43649.5951	.840
43615.3647	.720	43615.4651	.866	43849.6090	.752
43615.3675	.736	43615.4665	.870	43849.6135	.748
43615.3756	.766	43615.4674	.861	43849.6184	.737
43615.3779	.762	43615.4684	.879	43849.6254	.716
43615.3853	.778	43615.4692	.864	43849.6323	.729
43615.3861	.767	43615.4700	.866	43849.6433	.699
43615.3893	.764	43615.4752	.839	43849.6534	.676
43615.3900	.756	43615.4764	.847	43849.6601	.676
43615.3909	.766	43615.4779	.830	43849.6711	.673
43615.3950	.762	43615.4793	.840	43849.6764	.675
43615.3956	.770	43615.4800	.833	43849.6854	.669
43615.3963	.762	43615.4807	.839	43849.6913	.680
43615.3970	.770	43615.4874	.822		
43615.4035	.755	43615.4882	.820	43878.3417	.800
43615.4046	.743	43615.4890	.814	43878.3476	.794
43615.4059	.767	43615.4903	.795	43878.3563	.799
43615.4083	.773	43615.4911	.804	43878.3651	.790
43615.4090	.776	43615.4918	.798	43878.3736	.795
43615.4123	.769	43615.4967	.786	43878.3831	.798
43615.4130	.783	43615.4974	.796	43878.3899	.781
43615.4149	.814	43615.4982	.795	43878.3966	.755
43615.4156	.822	43615.4991	.796	43878.4023	.771
43615.4216	.821	43615.4998	.791	43878.4082	.760
43615.4225	.810	43615.5006	.794	43878.4241	.788
43615.4239	.813	43615.5014	.783	43878.4340	.790
43615.4266	.816	43615.5031	.782	43878.4457	.733
43615.4275	.817	43615.5038	.789	43878.4546	.711
43615.4306	.847	43615.5078	.776	43878.4640	.711
43615.4315	.841	43615.5104	.751	43878.4985	.690
43615.4321	.840	43615.5140	.753	43878.5099	.697
43615.4353	.837	43615.5146	.741	43878.5201	.727
43615.4365	.859	43615.5178	.737	43878.5267	.723
43615.4372	.856	43615.5187	.741	43878.5367	.753
43615.4379	.855			43878.5413	.768
43615.4389	.862	43849.5031	.801	43878.5536	.773
43615.4396	.845	43849.5111	.864	43878.5635	.829
43615.4403	.855	43849.5159	.927	43878.5682	.872
43615.4417	.860	43849.5205	.990	43878.5746	.931
43615.4455	.839	43849.5250	1.092	43878.5776	.969
43615.4462	.839	43849.5288	1.160	43878.5876	1.111
43615.4469	.855	43849.5350	1.346	43878.5936	1.263
43615.4476	.845	43849.5399	1.368	43878.6037	1.395
43615.4483	.826	43849.5441	1.415	43878.6114	1.440
43615.4489	.838	43849.5475	1.432	43878.6191	1.462
43615.4526	.840	43849.5542	1.437	43878.6271	1.366
43615.4531	.841	43849.5616	1.424	43878.6305	1.361
43615.4539	.848	43849.5680	1.329	43878.6364	1.161

Table 3 (cont.)

Photoelectric blue observations of SV Cam

J.D.	ΔB	J.D.	ΔB	J.D.	ΔB
43878.6425	1.026	43880.3540	.767	43926.2938	.725
43878.6528	.879	43880.3427	.802	43926.3099	.735
43878.6636	.799	43880.3534	.910	43926.3204	.765
43878.6746	.754	43880.3597	1.007	43926.3316	.755
43878.6790	.727	43880.3654	1.101	43926.3395	.779
43878.6869	.749	43880.3723	1.244	43926.3438	.815
43878.6951	.730	43880.3755	1.322	43926.3530	.824
43878.7024	.736	43880.3838	1.405	43926.3643	.825
		43880.3908	1.425	43926.3706	.781
43879.3651	.691	43880.3976	1.440	43926.3800	.751
43879.3738	.653	43880.4059	1.409	43926.3868	.756
43879.3831	.712	43880.4129	1.276	43926.3959	.745
43879.3922	.665	43880.4204	1.077	43926.4040	.742
43879.4025	.661	43880.4222	1.021	43926.4117	.702
43879.4091	.696	43880.4249	1.004	43926.4218	.730
43879.4144	.686	43880.4319	.902	43926.4310	.721
43879.4352	.744	43880.4363	.819	43926.4437	.744
43879.4456	.737	43880.4425	.784	43926.4534	.705
43879.4543	.738	43880.4493	.783	43926.4631	.695
43879.4626	.791	43880.4549	.759	43926.4715	.714
43879.4718	.850	43880.4566	.757	43926.4773	.700
43879.4819	.835	43880.4652	.755	43926.4885	.705
43879.4893	.819	43880.4712	.756	43926.4996	.725
43879.4934	.832	43880.4791	.729	43926.5088	.731
43879.5006	.807	43880.4834	.720	43926.5147	.727
43879.5111	.845	43880.4912	.669	43926.5233	.697
43879.5199	.850	43880.4998	.689	43926.5353	.735
43879.5284	.829	43880.5039	.707	43926.5473	.725
43879.5364	.823	43880.5151	.688	43926.5548	.728
43879.5441	.816	43880.5207	.671	43926.5593	.727
43879.5525	.813	43880.5273	.683	43926.5661	.735
43879.5601	.818	43880.5306	.695	43926.5725	.760
43879.5675	.788	43880.5388	.689	43926.5790	.764
43879.5762	.787	43880.5499	.697	43926.5846	.774
43879.5876	.779	43880.5540	.668	43926.5949	.787
43879.5966	.768	43880.5596	.696	43926.5990	.782
43879.6055	.747	43880.5663	.695	43926.6050	.801
43879.6159	.732	43880.5747	.720	43926.6095	.855
43879.6260	.736	43880.5827	.714	43926.6127	.890
43879.6370	.715	43880.5897	.721	43926.6195	.965
43879.6461	.744	43880.5973	.716	43926.6119	1.011
		43880.6056	.752	43926.6246	1.034
43880.2280	.760	43880.6180	.741	43926.6322	1.186
43880.2360	.738	43880.6262	.739	43926.6352	1.306
43880.2425	.716	43880.6447	.764	43926.6438	1.401
43880.2502	.736	43880.6534	.767	43926.6510	1.430
43880.2605	.723	43880.6622	.819	43926.6536	1.437
43880.2701	.697	43880.6700	.827	43926.6622	1.389
43880.2790	.713	43880.6786	.849	43926.6713	1.231
43880.2978	.736	43880.6871	.858	43926.6741	1.158
43880.3035	.747	43880.6940	.875		
43880.3146	.746	43880.7035	.852	43927.2463	1.416
43880.3204	.772			43927.2492	1.413
43880.3265	.777	43926.2816	.738	43927.2550	1.390

Table 3 (cont.)

Photoelectric blue observations of SV Cam

J.D.	ΔB	J.D.	ΔB	J.D.	ΔB
43927.2582	1.363	43927.5654	.795	43928.4695	.662
43927.2685	1.135	43927.5725	.805	43928.4749	.761
43927.2712	1.069	43927.5811	.743	43928.4767	.776
43927.2736	1.011	43927.5912	.596	43928.4817	.732
43927.2777	.921	43927.5971	.713	43928.4901	.708
43927.2795	.890	43927.6096	.744	43928.4946	.712
43927.2811	.862	43927.6189	.752	43928.5011	.755
43927.2864	.808	43927.6256	.730	43928.5044	.741
43927.2911	.775	43927.6297	.725	43928.5117	.707
43927.2964	.762	43927.6410	.743	43928.5150	.734
43927.2985	.751	43927.6496	.735	43928.5179	.721
43927.3057	.747	43927.6565	.758	43928.5206	.700
43927.3076	.752	43927.6634	.710	43928.5260	.693
43927.3149	.734			43928.5285	.703
43927.3186	.752	43928.2957	.723	43928.5309	.691
43927.3244	.738	43928.3019	.716	43928.5358	.712
43927.3271	.734	43928.3096	.704	43928.5380	.709
43927.3312	.716	43928.3142	.736	43928.5406	.726
43927.3330	.700	43928.3206	.742	43928.5480	.694
43927.3393	.699	43928.3256	.730	43928.5535	.695
43927.3425	.697	43928.3312	.763	43928.5557	.720
43927.3456	.692	43928.3380	.745	43928.5609	.714
43927.3533	.711	43928.3463	.746	43928.5729	.711
43927.3568	.702	43928.3540	.771	43928.5760	.715
43927.3637	.699	43928.3569	.765	43928.5855	.675
43927.3664	.673	43928.3595	.758	43928.5926	.696
43927.3687	.675	43928.3646	.745	43928.6009	.718
43927.3711	.689	43928.3677	.737	43928.6057	.742
43927.3764	.691	43928.3711	.754	43928.6124	.710
43927.3790	.710	43928.3794	.769	43928.6147	.726
43927.3817	.709	43928.3871	.643	43928.6175	.714
43927.3844	.712	43928.3895	.874	43928.6227	.717
43927.3918	.709	43928.3960	.944	43928.6265	.708
43927.3972	.698	43928.3980	.981	43928.6301	.676
43927.4041	.712	43928.3999	1.033	43928.6334	.670
43927.4068	.697	43928.4030	1.083	43928.6384	.667
43927.4173	.725	43928.4062	1.164	43928.6412	.679
43927.4215	.710	43928.4089	1.217	43928.6437	.716
43927.4240	.701	43928.4116	1.277	43928.6496	.751
43927.4315	.667	43928.4182	1.384		
43927.4364	.701	43928.4313	1.437	44048.3760	.655
43927.4415	.729	43928.4232	1.440	44048.3771	.669
43927.4497	.715	43928.4249	1.453	44048.3780	.669
43927.4621	.705	43928.4273	1.494	44048.3829	.685
43927.4736	.715	43928.4295	1.481	44048.3840	.671
43927.4801	.729	43928.4343	1.473	44048.3850	.678
43927.4907	.741	43928.4372	1.457	44048.3896	.670
43927.4959	.769	43928.4412	1.399	44048.3906	.677
43927.5053	.769	43928.4520	1.197	44048.3915	.692
43927.5117	.779	43928.4538	1.130	44048.3959	.701
43927.5244	.756	43928.4560	1.106	44048.3969	.694
43927.5335	.747	43928.4586	1.044	44048.3979	.681
43927.5451	.795	43928.4655	.920	44048.4031	.678
43927.5572	.803	43928.4674	.876	44048.4041	.677

Table 3 (cont.)

Photoelectric blue observations of SV Cam

J.D.	ΔB	J.D.	ΔB	J.D.	ΔB
44048.4051	.688	44049.3904	1.022	44081.5132	.731
44048.4097	.680	44049.3949	1.102	44081.5177	.718
44048.4106	.673	44049.3959	1.152	44081.5187	.711
44048.4116	.679	44049.3969	1.187	44081.5197	.731
44048.4174	.697	44049.4021	1.332		
44048.4184	.666	44049.4095	1.390	44103.3273	.725
44048.4194	.680	44049.4140	1.372	44103.3379	.753
44048.4239	.705	44049.4156	1.395	44103.3424	.799
44048.4248	.705	44049.4208	1.373	44103.3504	.901
44048.4258	.703	44049.4223	1.381	44103.3549	.999
44048.4307	.692	44049.4269	1.376	44103.3594	1.094
44048.4317	.698	44049.4329	1.372	44103.3653	1.185
44048.4326	.678	44049.4392	1.187	44103.3714	1.301
44048.4371	.709	44049.4459	.996	44103.3775	1.389
44048.4379	.699	44049.4515	.897	44103.3813	1.419
44048.4390	.697	44049.4525	.869	44103.3896	1.438
44048.4435	.698	44049.4535	.873	44103.3962	1.416
44048.4444	.698	44049.4576	.838	44103.4014	1.307
44048.4455	.684	44049.4586	.829	44103.4056	1.230
44048.4501	.710	44049.4595	.817	44103.4098	1.103
44048.4512	.712	44049.4639	.768	44103.4143	1.017
44048.4521	.703	44049.4649	.744	44103.4202	.910
44048.4634	.693	44049.4659	.742	44103.4268	.806
44048.4644	.694	44049.4705	.697	44103.4305	.777
44048.4654	.711	44049.4715	.699	44103.4378	.722
44048.4701	.704	44049.4725	.705	44103.4500	.686
44048.4711	.723	44049.4780	.705	44103.4552	.673
44048.4721	.710	44049.4790	.694	44103.4594	.678
44048.4770	.720	44049.4800	.698	44103.4653	.673
44048.4779	.718	44049.4846	.716	44103.4696	.667
44048.4790	.717	44049.4856	.719	44103.4747	.683
44048.4836	.712	44049.4866	.731	44103.4796	.669
44048.4846	.718	44049.4907	.720	44103.4841	.658
44048.4856	.719	44049.4922	.720	44103.4941	.629
44048.4913	.733	44049.5051	.712	44103.4986	.632
44048.4923	.732	44049.5175	.702	44103.5063	.624
44048.4972	.747	44049.5234	.717	44103.5106	.614
44048.4982	.733	44049.5243	.725	44103.5209	.624
44048.4991	.746	44049.5254	.724	44103.5254	.624
44048.5169	.807			44103.5299	.637
44048.5179	.807	44081.4679	1.087	44103.5344	.638
44048.5187	.792	44081.4701	1.049	44103.5389	.635
44048.5237	.821	44081.4784	.914	44103.5404	.638
44048.5247	.823	44081.4794	.895	44103.5542	.622
44048.5257	.818	44081.4804	.887	44103.5591	.619
		44081.4849	.815	44103.5643	.621
44049.3756	.772	44081.4864	.800	44103.5733	.607
44049.3766	.784	44081.4914	.757	44103.5778	.612
44049.3775	.812	44081.4984	.721		
44049.3819	.880	44081.5046	.727	44145.2931	.657
44049.3829	.903	44081.5056	.720	44145.2951	.652
44049.3839	.908	44081.5066	.729	44145.2993	.616
44049.3884	.992	44081.5112	.717	44145.3013	.630
44049.3894	.998	44081.5122	.731	44145.3065	.648

Table 3 (cont.)

Photoelectric blue observations of SV Cam

J.D.	ΔB	J.D.	ΔB	J.D.	ΔB
44145.3085	.625	44158.3713	.680	44159.4219	.764
44145.3144	.642	44158.3756	.674	44159.4261	.780
44145.3153	.628	44158.3765	.682	44159.4281	.782
44145.3213	.653	44158.3775	.679	44159.4291	.769
44145.3256	.644	44158.3784	.672	44159.4336	.781
44145.3265	.645	44158.3846	.680	44159.4346	.776
44145.3275	.642	44158.3856	.678	44159.4356	.773
44145.3317	.631	44158.3866	.674	44159.4365	.786
44145.3327	.622	44158.3876	.671	44159.4409	.765
44145.3337	.626	44158.3936	.684	44159.4419	.782
		44158.3946	.673	44159.4428	.774
44146.3438	.711	44158.3956	.674	44159.4438	.784
44146.3453	.716	44158.3966	.669	44159.4483	.791
44146.3467	.717	44158.4012	.678	44159.4503	.779
44146.3515	.747	44158.4022	.669	44159.4556	.753
44146.3525	.748	44158.4032	.677	44159.4576	.761
44146.3535	.741	44158.4041	.678	44159.4586	.764
44146.3545	.747			44159.4596	.770
44146.3667	.759	44159.3593	.703	44159.4643	.739
44146.3677	.761	44159.3603	.694	44159.4653	.748
44146.3692	.761	44159.3613	.698	44159.4663	.753
44146.3738	.783	44159.3623	.704	44159.4673	.751
44146.3748	.784	44159.3666	.709	44159.4715	.738
44146.3758	.773	44159.3677	.705	44159.4725	.730
44146.3768	.781	44159.3687	.694	44159.4735	.735
44146.3810	.769	44159.3697	.708	44159.4745	.716
44146.3821	.777	44159.3745	.704	44159.4789	.716
44146.3830	.786	44159.3754	.699	44159.4799	.702
44146.3840	.776	44159.3755	.699	44159.4809	.705
44146.3882	.770	44159.3775	.701	44159.4819	.704
44146.3892	.767	44159.3830	.710	44159.4863	.702
44146.3902	.772	44159.3839	.715	44159.4873	.700
44146.3912	.763	44159.3850	.713	44159.4883	.697
		44159.3859	.710	44159.4893	.699
44158.3316	.701	44159.3903	.716	44159.5014	.708
44158.3325	.705	44159.3913	.734	44159.5024	.708
44158.3336	.720	44159.3923	.731	44159.5034	.711
44158.3346	.713	44159.3933	.718	44159.5044	.710
44158.3392	.705	44159.3974	.735	44159.5094	.701
44158.3401	.697	44159.3983	.739	44159.5104	.697
44158.3411	.694	44159.3993	.737	44159.5113	.703
44158.3421	.685	44159.4003	.757	44159.5124	.704
44158.3538	.687	44159.4045	.755	44159.5165	.709
44158.3548	.685	44159.4055	.744	44159.5175	.696
44158.3558	.691	44159.4065	.758	44159.5185	.691
44158.3568	.687	44159.4074	.761	44159.5195	.692
44158.3612	.685	44159.4115	.755	44159.5246	.677
44158.3621	.680	44159.4126	.750	44159.5256	.686
44158.3632	.678	44159.4135	.755	44159.5266	.674
44158.3642	.683	44159.4145	.768	44159.5382	.696
44158.3683	.679	44159.4191	.750	44159.5391	.675
44158.3692	.678	44159.4200	.778	44159.5401	.682
44158.3703	.685	44159.4211	.772	44159.5411	.698

Table 3 (cont.)

Photoelectric blue observations of SV Cam

J.D.	ΔB	J.D.	ΔB	J.D.	ΔB
44159.5462	.698	44285.3227	.664	44285.2854	.680
44159.5472	.687	44285.3237	.666	44285.2864	.684
44159.5482	.689	44285.3247	.660	44285.3011	.673
44159.5492	.697	44285.3257	.666	44285.3021	.671
44159.5538	.668	44285.3300	.655	44285.3063	.665
44159.5548	.658	44285.3310	.647	44285.3073	.660
44159.5558	.660	44285.3320	.648	44285.3115	.655
44159.5568	.642	44285.3330	.663	44285.3125	.644
44159.5610	.672	44285.3378	.668	44285.3168	.661
44159.5620	.678	44285.3388	.659	44285.3178	.664
44159.5630	.654	44285.3398	.667	44285.3227	.664
44159.5640	.661	44285.3407	.673	44285.3237	.666
44159.5767	.675	44285.3448	.669	44285.3247	.660
44159.5844	.683	44285.3458	.676	44285.3257	.666
44159.5852	.671	44285.3468	.664	44285.3300	.655
44159.5863	.677	44285.3478	.673	44285.3310	.647
44159.5873	.677	44285.3528	.684	44285.3320	.648
44159.6092	.671	44285.3538	.678	44285.3330	.663
44159.6102	.667	44285.3548	.681	44285.3378	.668
44159.6111	.676	44285.3557	.684	44285.3388	.659
44159.6121	.682	44285.3607	.660	44285.3398	.667
44159.6168	.671	44285.3626	.676	44285.3407	.673
44159.6178	.683	44285.3636	.679	44285.3448	.669
44159.6187	.688	44285.3701	.686	44285.3458	.676
44159.6197	.686	44285.3712	.685	44285.3468	.664
44159.6246	.688	44285.3759	.705	44285.3478	.673
44159.6256	.691	44285.3770	.699	44285.3528	.684
44159.6266	.694	44285.3779	.702	44285.3538	.678
44159.6276	.683	44285.3789	.699	44285.3548	.681
44159.6321	.697	44285.3831	.694	44285.3557	.684
44159.6331	.692	44285.3841	.690	44285.3607	.660
44159.6341	.692	44285.3851	.690	44285.3626	.676
44159.6351	.691	44285.3861	.704	44285.3636	.679
44159.6394	.701	44285.3908	.688	44285.3701	.686
44159.6404	.711	44285.3918	.694	44285.3712	.685
44159.6413	.706	44285.3928	.701	44285.3759	.705
44159.6423	.708	44285.3938	.718	44285.3770	.699
44159.6466	.719	44285.3986	.721	44285.3779	.702
44159.6476	.718	44285.3995	.714	44285.3789	.699
44159.6486	.725	44285.4006	.717	44285.3831	.694
		44285.4015	.719	44285.3841	.690
44285.2824	.682	44285.4064	.738	44285.3851	.690
44285.2834	.683	44285.4074	.750	44285.3861	.704
44285.2844	.672	44285.4083	.736	44285.3908	.688
44285.2854	.680	44285.4093	.735	44285.3918	.694
44285.2864	.684	44285.4135	.764	44285.3928	.701
44285.3011	.673	44285.4145	.782	44285.3938	.718
44285.3021	.671	44285.4155	.792	44285.3986	.721
44285.3063	.665	44285.4165	.803	44285.3995	.714
44285.3073	.660	44285.4219	.867	44285.4006	.717
44285.3115	.655	44285.4295	.968	44285.4015	.719
44285.3125	.644	44285.2824	.683	44285.4064	.738
44285.3168	.661	44285.2834	.683	44285.4074	.750
44285.3178	.664	44285.2844	.672	44285.4083	.736

Table 3 (cont.)

Photoelectric blue observations of SV Cam

J.D.	ΔB	J.D.	ΔB	J.D.	ΔB
44285.4093	.735	44285.5673	.719	44285.6835	.747
44285.4135	.764	44285.5683	.703	44285.6845	.758
44285.4145	.782	44285.5693	.721	44285.6855	.765
44285.4155	.792	44285.5703	.724		
44285.4165	.803	44285.5750	.699	44345.3233	.869
44285.4219	.867	44285.5760	.687	44345.3282	.917
44285.4295	.968	44285.5770	.697	44345.3326	.971
44285.4304	.988	44285.5780	.712	44345.3372	1.064
44285.4314	1.010	44285.5822	.693	44345.3417	1.196
44285.4324	1.044	44285.5842	.688	44345.3456	1.293
44285.4371	1.106	44285.5852	.685	44345.3510	1.330
44285.4382	1.145	44285.5902	.689	44345.3556	1.393
44285.4392	1.169	44285.5912	.687	44345.3604	1.382
44285.4402	1.176	44285.5922	.683	44345.3653	1.392
44285.4444	1.274	44285.5996	.677	44345.3691	1.389
44285.4454	1.306	44285.6006	.682	44345.3733	1.372
44285.4464	1.333	44285.6015	.672	44345.3782	1.267
44285.4473	1.344	44285.6059	.676	44345.3672	1.037
44285.4516	1.401	44285.6069	.684	44345.3928	.949
44285.4526	1.387	44285.6089	.681	44345.3976	.881
44285.4535	1.398	44285.6135	.703	44345.4069	.776
44285.4545	1.402	44285.6154	.718	44345.4115	.751
44285.4588	1.434	44285.6164	.702	44345.4157	.747
44285.4597	1.438	44285.6219	.686	44345.4205	.699
44285.4608	1.441	44285.6239	.702	44345.4254	.712
44285.4617	1.431	44285.6249	.689	44345.4323	.705
44285.4660	1.420	44285.6291	.706	44345.4365	.714
44285.4670	1.413	44285.6301	.703	44345.4407	.710
44285.4680	1.412	44285.6311	.695		
44285.4690	1.412	44285.6321	.706	44371.3355	.671
44285.4733	1.403	44285.6364	.705	44371.3365	.687
44285.4743	1.381	44285.6374	.704	44371.3375	.679
44285.4752	1.355	44285.6384	.710	44371.3385	.684
44285.4763	1.329	44285.6394	.704	44371.3441	.667
44285.4885	1.052	44285.6435	.717	44371.3451	.665
44285.4895	1.042	44285.6445	.716	44371.3461	.678
44285.4905	1.024	44285.6455	.711	44371.3470	.656
44285.4915	1.006	44285.6464	.712	44371.3513	.658
44285.4974	.909	44285.6509	.699	44371.3523	.659
44285.4984	.897	44285.6519	.703	44371.3533	.658
44285.4994	.887	44285.6529	.703	44371.3542	.647
44285.5004	.861	44285.6539	.706	44371.3583	.664
44285.5048	.824	44285.6609	.721	44371.3592	.655
44285.5058	.826	44285.6619	.714	44371.3602	.681
44285.5068	.813	44285.6639	.728	44371.3612	.666
44285.5078	.807	44285.6680	.728	44371.3655	.675
44285.5147	.768	44285.6690	.713	44371.3665	.679
44285.5156	.760	44285.6700	.730	44371.3675	.679
44285.5166	.774	44285.6710	.719	44371.3684	.685
44285.5176	.774	44285.6752	.724	44371.3726	.676
44285.5279	.756	44285.6762	.734	44371.3735	.688
44285.5289	.746	44285.6771	.730	44371.3745	.697
44285.5299	.743	44285.6781	.733	44371.3755	.683
44285.5309	.748	44285.6825	.749	44371.3799	.700

Table 3 (cont.)

Photoelectric blue observations of SV Cam

J.D.	ΔB	J.D.	ΔB	J.D.	ΔB
44371.3809	.692	44371.4904	.895	44454.4396	.788
44371.3819	.696	44371.4948	.802	44454.4447	.830
44371.3829	.705	44371.4956	.796	44454.4457	.840
44371.3878	.705	44371.4968	.785	44454.4508	.890
44371.3887	.715	44371.4978	.787	44454.4518	.908
44371.3897	.721	44371.5022	.770	44454.4528	.941
44371.3907	.721	44371.5032	.761	44454.4538	.939
44371.3953	.721	44371.5042	.757	44454.4590	1.039
44371.3963	.719	44371.5051	.770	44454.4600	1.068
44371.3973	.717	44371.5104	.716	44454.4610	1.060
44371.3983	.718	44371.5114	.706	44454.4620	1.097
44371.4033	.728	44371.5123	.709	44454.4743	1.331
44371.4043	.727	44371.5133	.688	44454.4752	1.348
44371.4053	.741	44371.5176	.680	44454.4762	1.339
44371.4062	.749	44371.5186	.685	44454.4772	1.356
44371.4109	.781	44371.5196	.691	44454.4827	1.377
44371.4119	.789	44371.5206	.707	44454.4837	1.373
44371.4129	.805	44371.5250	.697	44454.4847	1.362
44371.4138	.815	44371.5260	.690	44454.4857	1.374
44371.4191	.872	44371.5270	.688	44454.4912	1.365
44371.4201	.892	44371.5279	.689	44454.4922	1.370
44371.4211	.910	44371.5322	.689	44454.4932	1.380
44371.4221	.916	44371.5331	.708	44454.4942	1.397
44371.4267	1.010	44371.5341	.712	44454.4989	1.349
44371.4277	1.031	44371.5351	.709	44454.4998	1.344
44371.4287	1.060	44371.5412	.688	44454.5008	1.324
44371.4297	1.055	44371.5422	.672	44454.5018	1.300
44371.4342	1.152	44371.5432	.666	44454.5097	1.126
44371.4352	1.153	44371.5442	.670	44454.5107	1.113
44371.4362	1.181	44371.5484	.684	44454.5117	1.095
44371.4372	1.197	44371.5494	.684	44454.5127	1.084
44371.4417	1.285	44371.5503	.719	44454.5174	1.002
44371.4437	1.314	44371.5513	.722	44454.5183	.977
44371.4447	1.329			44454.5193	.972
44371.4492	1.375	44454.3865	.672	44454.5203	.958
44371.4502	1.373	44454.3986	.675	44454.5252	.876
44371.4512	1.361	44454.3996	.656	44454.5261	.862
44371.4522	1.365	44454.4006	.666	44454.5272	.851
44371.4563	1.373	44454.4016	.683	44454.5281	.844
44371.4573	1.371	44454.4059	.697	44454.5331	.819
44371.4583	1.376	44454.4069	.708	44454.5341	.815
44371.4593	1.353	44454.4078	.697	44454.5350	.793
44371.4635	1.340	44454.4089	.707	44454.5360	.788
44371.4645	1.334	44454.4142	.725	44454.5408	.790
44371.4655	1.324	44454.4152	.732	44454.5418	.781
44371.4665	1.309	44454.4162	.724	44454.5428	.763
44371.4708	1.276	44454.4213	.741	44454.5437	.758
44371.4718	1.256	44454.4223	.728	44454.5492	.757
44371.4728	1.235	44454.4243	.715	44454.5502	.744
44371.4737	1.204	44454.4290	.709	44454.5512	.737
44371.4782	1.189	44454.4300	.714	44454.5522	.744
44371.4792	1.119	44454.4315	.699	44454.5575	.733
44371.4801	1.117	44454.4377	.760	44454.5585	.739
44371.4811	1.101	44454.4386	.761	44454.5648	.725

Table 3 (cont.)

Photoelectric blue observations of SV Cam

J.D.	ΔB	J.D.	ΔB	J.D.	ΔB
44454.5667	.725	44477.3983	.743	44477.5065	.702
		44477.3993	.740	44477.5075	.700
44455.3415	.729	44477.4003	.735	44477.5120	.713
44455.3425	.743	44477.4013	.738	44477.5129	.703
44455.3434	.728	44477.4057	.735	44477.5139	.704
44455.3444	.730	44477.4067	.733	44477.5149	.715
44455.3552	.794	44477.4076	.732	44477.5191	.725
44455.3563	.797	44477.4086	.733	44477.5201	.721
44455.3573	.802	44477.4141	.738	44477.5211	.716
44455.3583	.796	44477.4150	.739	44477.5220	.715
44455.3637	.798	44477.4160	.734	44477.5269	.707
44455.3665	.797	44477.4170	.749	44477.5278	.709
44455.3674	.798	44477.4306	.726	44477.5288	.707
44455.3684	.802	44477.4316	.727	44477.5298	.704
44455.3694	.810	44477.4326	.729	44477.5343	.715
44455.3750	.807	44477.4336	.726	44477.5353	.705
44455.3760	.808	44477.4384	.710	44477.5363	.716
44455.3770	.816	44477.4394	.709	44477.5373	.719
44455.3780	.807	44477.4403	.710	44477.5418	.728
44455.3914	.819	44477.4413	.703	44477.5428	.728
44455.3923	.806	44477.4463	.714	44477.5437	.722
44455.3933	.801	44477.4472	.721	44477.5447	.724
44455.3943	.787	44477.4482	.715	44477.5491	.717
44455.3991	.795	44477.4492	.711	44477.5501	.726
44455.4001	.798	44477.4532	.715	44477.5510	.725
44455.4011	.784	44477.4542	.716	44477.5520	.716
44455.4020	.792	44477.4552	.704	44477.5566	.725
44455.4064	.779	44477.4562	.695	44477.5575	.744
44455.4075	.781	44477.4606	.703	44477.5585	.736
44455.4084	.782	44477.4616	.694	44477.5595	.746
44455.4094	.777	44477.4625	.693	44477.5644	.750
44455.4144	.772	44477.4635	.696	44477.5654	.764
44455.4154	.769	44477.4681	.701	44477.5664	.766
44455.4164	.776	44477.4691	.705	44477.5673	.771
44455.4174	.775	44477.4700	.697	44477.5722	.810
44455.4224	.768	44477.4710	.698	44477.5732	.816
44455.4234	.753	44477.4760	.690	44477.5742	.833
44455.4244	.760	44477.4770	.699	44477.5752	.842
44455.4290	.760	44477.4780	.701	44477.5793	.896
44455.4300	.742	44477.4790	.699	44477.5803	.914
44455.4345	.764	44477.4831	.688	44477.5812	.922
44455.4355	.759	44477.4841	.695	44477.5823	.947
44455.4402	.753	44477.4851	.692	44477.5867	1.048
44455.4412	.738	44477.4861	.680	44477.5877	1.058
44455.4467	.748	44477.4903	.700	44477.5887	1.064
		44477.4912	.697	44477.5897	1.091
44477.3797	.739	44477.4922	.689		
44477.3807	.731	44477.4932	.707	44541.2515	.653
44477.3816	.738	44477.4975	.688	44541.2525	.652
44477.3826	.740	44477.4985	.705	44541.2535	.652
44477.3907	.761	44477.4995	.705	44541.2544	.645
44477.3917	.753	44477.5005	.693	44541.2608	.639
44477.3927	.760	44477.5046	.698	44541.2617	.639
44477.3936	.748	44477.5055	.715	44541.2627	.639

Table 3 (cont.)

Photoelectric blue observations of SV Cam

J.D.	ΔB	J.D.	ΔB	J.D.	ΔB
44541.2694	.654	44541.4048	.757	44582.2492	.681
44541.2709	.658	44541.4100	.739	44582.2502	.685
44541.2724	.664	44541.4110	.749	44582.2549	.725
44541.2846	.686	44541.4120	.743	44582.2559	.704
44541.2856	.687	44541.4130	.736	44582.2569	.708
44541.2866	.684	44541.4180	.728	44582.2618	.717
44541.2876	.673	44541.4194	.724	44582.2628	.719
44541.2926	.659	44541.4204	.733	44582.2638	.719
44541.2941	.657	44541.4249	.723	44582.2683	.715
44541.2955	.653	44541.4259	.727	44582.2693	.721
44541.3006	.670	44541.4269	.734	44582.2703	.733
44541.3025	.677	44541.4278	.730	44582.2753	.734
44541.3035	.673	44541.4323	.732	44582.2763	.737
44541.3079	.691	44541.4333	.739	44582.2773	.745
44541.3089	.702	44541.4343	.739	44582.2821	.736
44541.3099	.700	44541.4353	.735	44582.2831	.753
44541.3109	.685	44541.4402	.729	44582.2841	.744
44541.3152	.680	44541.4412	.738	44582.2889	.748
44541.3162	.685	44541.4421	.731	44582.2899	.753
44541.3172	.693	44541.4431	.728	44582.2909	.752
44541.3182	.705	44541.4478	.728	44582.2958	.745
44541.3228	.698	44541.4488	.720	44582.2968	.728
44541.3238	.696	44541.4496	.723	44582.2978	.740
44541.3248	.696	44541.4508	.723	44582.3029	.752
44541.3259	.688	44541.4553	.722	44582.3039	.739
44541.3392	.729	44541.4562	.729	44582.3049	.741
44541.3402	.741	44541.4572	.727	44582.3096	.751
44541.3412	.744	44541.4582	.723	44582.3106	.734
44541.3422	.747	44541.4637	.727	44582.3116	.742
44541.3472	.771	44541.4647	.727	44582.3160	.728
44541.3481	.775	44541.4657	.720	44582.3169	.723
44541.3491	.779	44541.4666	.718	44582.3179	.725
44541.3501	.781	44541.4712	.724	44582.3224	.720
44541.3549	.775	44541.4722	.720	44582.3234	.714
44541.3559	.771	44541.4732	.712	44582.3244	.721
44541.3569	.776	44541.4742	.711	44582.3287	.704
44541.3579	.768	44541.4794	.716	44582.3297	.707
44541.3635	.789	44541.4804	.716	44582.3307	.702
44541.3645	.783	44541.4814	.719	44582.3371	.685
44541.3654	.797	44541.4869	.721	44582.3381	.673
44541.3698	.772	44541.4879	.740	44582.3390	.666
44541.3708	.778	44541.4889	.726	44582.3400	.680
44541.3718	.769	44541.4899	.729	44582.3410	.671
44541.3728	.771			44582.3420	.676
44541.3783	.792	44582.2286	.677	44582.3467	.673
44541.3792	.790	44582.2296	.674	44582.3477	.667
44541.3802	.795	44582.2306	.673	44582.3486	.665
44541.3944	.762	44582.2350	.685	44582.3496	.670
44541.3954	.765	44582.2360	.679	44582.3506	.670
44541.3964	.767	44582.2370	.669	44582.3516	.671
44541.3974	.757	44582.2416	.683	44582.3564	.676
44541.4019	.753	44582.2426	.680	44582.3574	.670
44541.4029	.758	44582.2436	.689	44582.3583	.667
44541.4039	.761	44582.2483	.695	44582.3593	.657

Table 3 (cont.)

Photoelectric blue observations of SV Cam

J.D.	ΔB	J.D.	ΔB	J.D.	ΔB
44582.3603	.651	44582.4463	.650	44582.5635	1.124
44582.3613	.641	44582.4524	.650	44582.5645	1.148
44582.3665	.621	44582.4533	.650	44582.5655	1.168
44582.3675	.625	44582.4544	.645	44582.5704	1.286
44582.3685	.615	44582.4553	.641	44582.5714	1.299
44582.3695	.616	44582.4563	.651	44582.5723	1.337
44582.3705	.613	44582.4573	.654	44582.5733	1.356
44582.3714	.623	44582.4672	.666	44582.5743	1.381
44582.3757	.636	44582.4682	.657	44582.5753	1.404
44582.3767	.653	44582.4692	.670	44582.5799	1.426
44582.3776	.635	44582.4702	.671	44582.5809	1.406
44582.3786	.659	44582.4712	.670	44582.5819	1.398
44582.3796	.637	44582.4721	.669	44582.5829	1.411
44582.3806	.645	44582.4782	.680	44582.5839	1.429
44582.3848	.633	44582.4792	.692	44582.5848	1.434
44582.3858	.636	44582.4802	.693	44582.5894	1.440
44582.3868	.644	44582.4811	.695	44582.5904	1.434
44582.3878	.648	44582.4821	.694	44582.5914	1.440
44582.3888	.643	44582.4831	.689	44582.5923	1.452
44582.3897	.654	44582.4879	.701	44582.5933	1.445
44582.3940	.644	44582.4889	.705	44582.5943	1.457
44582.3949	.647	44582.4899	.690	44582.5993	1.448
44582.3959	.638	44582.4909	.696	44582.6003	1.447
44582.3969	.635	44582.4919	.684	44582.6013	1.430
44582.3979	.643	44582.4929	.682	44582.6022	1.418
44582.3989	.641	44582.4980	.700	44582.6032	1.411
44582.4039	.627	44582.4990	.697	44582.6042	1.381
44582.4048	.632	44582.5000	.712	44582.6092	1.260
44582.4058	.637	44582.5010	.696	44582.6102	1.235
44582.4068	.628	44582.5020	.699	44582.6112	1.206
44582.4078	.631	44582.5030	.703	44582.6121	1.188
44582.4088	.639	44582.5081	.712	44582.6131	1.176
44582.4132	.641	44582.5091	.709	44582.6141	1.136
44582.4142	.641	44582.5101	.709	44582.6188	1.018
44582.4151	.630	44582.5111	.717	44582.6198	1.006
44582.4161	.635	44582.5121	.720	44582.6207	.987
44582.4171	.643	44582.5131	.711	44582.6217	.963
44582.4224	.632	44582.5193	.745	44582.6227	.937
44582.4234	.638	44582.5203	.744	44582.6237	.935
44582.4244	.638	44582.5212	.751	44582.6286	.868
44582.4254	.641	44582.5222	.752	44582.6296	.855
44582.4264	.632	44582.5232	.762	44582.6305	.848
44582.4273	.638	44582.5242	.763	44582.6315	.845
44582.4320	.637	44582.5290	.745	44582.6325	.831
44582.4330	.641	44582.5300	.765	44582.6335	.824
44582.4340	.643	44582.5490	.871	44582.6382	.810
44582.4350	.633	44582.5499	.881	44582.6392	.796
44582.4360	.642	44582.5509	.895	44582.6401	.783
44582.4370	.631	44582.5519	.898	44582.6411	.776
44582.4414	.644	44582.5529	.920	44582.6421	.786
44582.4424	.647	44582.5539	.931	44582.6431	.773
44582.4434	.649	44582.5605	1.048	44582.6480	.760
44582.4444	.652	44582.5615	1.080	44582.6490	.751
44582.4453	.649	44582.5625	1.099	44582.6500	.755

Table 3 (cont.)

Photoelectric blue observations of SV Cam

J.D.	ΔB	J.D.	ΔB	J.D.	ΔB
44582.6510	.751	44582.6716	.719	44582.6899	.680
44582.6520	.757	44582.6726	.709	44582.6908	.681
44582.6577	.728	44582.6736	.706	44582.6918	.679
44582.6587	.728	44582.6781	.708	44582.6928	.678
44582.6597	.724	44582.6791	.709	44582.6972	.676
44582.6606	.721	44582.6800	.700	44582.6982	.683
44582.6616	.724	44582.6810	.701	44582.6992	.677
44582.6626	.730	44582.6820	.697	44582.7001	.664
44582.6687	.720	44582.6830	.693	44582.7011	.672
44582.6697	.719	44582.6879	.681	44582.7021	.663
44582.6707	.717	44582.6889	.676		

Table 4

Photoelectric ultraviolet observations of SV Cam

J.D.	ΔU	J.D.	ΔU	J.D.	ΔU
41807.3564	.889	41835.3939	.854	41931.3496	.904
41807.3652	.889	41835.4078	.898	41931.3549	.897
41807.3875	.885	41835.4189	.966	41931.3680	.862
41807.3963	.862	41835.4344	.974	41931.3969	.820
41807.3983	.861	41835.4483	1.110	41931.4036	.814
41807.4050	.860	41835.4516	1.177	41931.4167	.804
41807.4200	.866	41835.4611	1.375	41931.4222	.784
41807.4295	.859	41835.4766	1.615	41931.4286	.803
41807.4341	.867			41931.4359	.806
41807.4392	.868	41903.3332	.955	41931.4435	.790
41807.4474	.854	41903.3383	.966	41931.4497	.797
41807.4495	.846	41903.3447	.994	41931.4571	.826
41807.4566	.848	41903.3499	.999	41931.4633	.837
41807.4693	.854	41903.3674	1.011	41931.4702	.840
41807.4785	.875	41903.3727	1.009	41931.4762	.775
41807.4910	.887	41903.3809	1.012	41931.4840	.698
41807.5001	.886	41903.3972	1.006	41931.5047	.805
41807.5134	.894	41903.4034	.995	41931.5175	.880
				41931.5245	.981
41810.4052	.834	41905.3413	.886	41931.5310	1.048
41810.4189	.834	41905.3473	.873	41931.5384	1.192
		41905.3538	.864	41931.5443	1.336
41825.4192	1.588	41905.3707	.852	41931.5512	1.518
41825.4237	1.458	41905.3801	.851	41931.5583	1.584
41825.4362	1.236	41905.3889	.866	41931.5651	1.554
41825.4390	1.201	41905.3949	.862	41931.5717	1.476
41825.4493	1.044	41905.4038	.879	41931.5790	1.348
41825.4520	1.012	41905.4132	.903	41931.5849	1.281
41825.4606	.964	41905.4188	.907		
41825.4639	.936	41905.4277	1.014	41933.3002	.987
41825.4748	.915	41905.4327	1.153	41933.3120	1.156
41825.4777	.910	41905.4391	1.263	41933.3238	1.324
41825.5187	.859	41905.4452	1.386	41933.3327	1.434
		41905.4515	1.483	41933.3477	1.482
41831.4646	.849	41905.4576	1.572	41933.3545	1.385
41831.4717	.843	41905.4754	1.664	41933.3703	1.201
41831.5001	.849	41905.4822	1.534		
41831.5149	.849	41905.5013	1.188	41934.4559	.795
41831.5254	.853	41905.5127	.979	41934.4670	.800
		41905.5597	.905	41934.4744	.826
41833.4211	.906			41934.4904	1.019
41833.4338	.913	41930.3373	1.019	41934.5025	1.235
41833.4368	.915	41930.3431	1.146	41934.5127	1.378
41833.4453	.867	41930.3514	1.300	41934.5315	1.574
41833.4578	.849	41930.4050	1.380	41934.5390	1.500
41833.4604	.839	41930.4104	1.447	41934.5447	1.373
41833.4693	.857	41930.4192	.994	41934.5639	1.133
41833.4728	.854	41930.4254	.970	41934.5696	1.003
41833.4884	.857	41930.4370	.972	41934.5795	.942
41833.4919	.865	41930.4432	.981	41934.5966	.917
41833.5034	.857	41930.4493	.990	41934.6037	.896
41833.5204	.856	41930.4554	.982	41934.6092	.891
41833.5239	.847	41930.4708	.974		
		41930.4832	.970	41935.5730	.866

Table 4 (cont.)

Photoelectric ultraviolet observations of SV Cam

J.D.	ΔU	J.D.	ΔU	J.D.	ΔU
41959.4227	1.224	41961.3273	.891	41962.4885	.941
41959.4381	1.538	41961.3352	.918	41962.4988	.919
41959.4503	1.486	41961.3434	.946	41962.5074	.909
41959.4633	1.307	41961.3493	.962	41962.5136	.903
		41961.3543	.957	41962.5235	.914
41960.3155	1.007	41961.3693	.965	41962.5321	.946
41960.3214	.991	41961.3733	.953	41962.5410	.920
41960.3302	1.016	41961.3772	.952	41962.5511	.917
41960.3369	1.015	41961.3812	.936	41962.5593	.924
41960.3401	1.020	41961.3979	.949	41962.5675	.928
41960.3484	.991	41961.4055	.919	41962.5765	.980
41960.3582	.972	41961.4140	.961	41962.5834	.948
41960.3640	.947	41961.4176	.953		
41960.3718	.919	41961.4218	.984	41963.2604	.966
41960.3793	.910	41961.4290	.981	41963.2685	1.024
41960.3934	.892	41961.4379	1.012	41963.2750	1.031
41960.4013	.880	41961.4436	.994	41963.2786	.983
41960.4069	.890	41961.4519	.982	41963.2826	.984
41960.4127	.881	41961.4665	.982	41963.2864	1.045
41960.4206	.882	41961.4764	.985	41963.2916	1.016
41960.4294	.879	41961.4798	.997	41963.2944	1.002
41960.4384	.868	41961.4844	.989	41963.2993	.978
41960.4462	.854	41961.4882	.981	41963.3029	.978
41960.4529	.812	41961.4971	1.001	41963.3911	.915
41960.4585	.763	41961.5020	.994	41963.3949	.899
41960.4655	.818	41961.5107	1.016	41963.3998	.905
41960.4764	.829	41961.5152	1.008	41963.4034	.897
41960.4833	.824	41961.5200	.993	41963.4074	.822
41960.4868	.804	41961.5291	.970	41963.4109	.809
41960.4914	.823	41961.5330	.955	41963.4154	.794
41960.4952	.824	41961.5473	.917	41963.4193	.801
41960.4998	.810	41961.5654	.910	41963.4256	.844
41960.5047	.814	41961.5975	.900	41963.4318	.836
41960.5109	.788	41961.6088	.892	41963.4357	.800
41960.5248	.822	41961.6198	.876	41963.4411	.812
41960.5318	.829			41963.4499	.789
41960.5691	.890	41962.3287	.766	41963.4600	.801
41960.5766	.945	41962.3369	.805	41963.4635	.785
41960.5836	.996	41962.3443	.859	41963.4681	.803
41960.5933	1.099	41962.3523	.904	41963.4734	.787
41960.6147	1.471	41962.3617	1.003	41963.4775	.813
41960.6241	1.591	41962.3693	1.088	41963.4816	.803
41960.6287	1.560	41962.3773	1.186	41963.4880	.832
41960.6351	1.494	41962.3852	1.401	41963.4921	.822
		41962.3929	1.542	41963.4968	.819
41961.2626	1.009	41962.4073	1.573	41963.5010	.810
41961.2703	.962	41962.4127	1.522	41963.5054	.864
41961.2754	.919	41962.4202	1.413	41963.5102	.868
41961.2807	.928	41962.4274	1.311	41963.5144	.841
41961.2868	.906	41962.4348	1.164	41963.5182	.856
41961.2942	.891	41962.4434	1.044	41963.5234	.856
41961.3000	.907	41962.4540	.940		
41961.3083	.926	41962.4649	.944	41978.4155	1.570
41961.3181	.913	41962.4793	.942	41978.4205	1.607

Table 4 (cont.)

Photoelectric ultraviolet observations of SV Cam

J.D.	ΔU	J.D.	ΔU	J.D.	ΔU
41978.4237	1.597	41982.3986	.850	41983.4119	.972
41978.4284	1.531	41982.4068	.849	41983.4171	1.005
41978.4332	1.399	41982.4137	.823	41983.4208	.991
41978.4368	1.354	41982.4174	.823	41983.4272	.995
41978.4398	1.281	41982.4251	.808	41983.4338	1.049
41978.4442	1.198	41982.4340	.809	41983.4382	1.033
41978.4480	1.166	41982.4409	.802	41983.4448	1.035
41978.4513	1.127	41982.4454	.812	41983.4519	1.057
41978.4564	1.073	41982.4514	.808	41983.4553	1.073
41978.4605	1.012	41982.4613	.814	41983.4615	1.055
41978.4641	.982	41982.4705	.822	41983.4671	1.039
41978.4686	.971	41982.4756	.823	41983.4706	1.028
41978.4727	.957	41982.4852	.835	41983.4768	1.012
41978.4803	.950	41982.5378	1.163	41983.4850	1.009
41978.4927	.926	41982.5461	1.324	41983.4929	1.040
41978.5054	.914	41982.5498	1.397	41983.4965	1.027
41978.5158	.916	41982.5562	1.508	41983.5008	1.000
41978.5268	.920	41982.5658	1.551	41983.5059	.980
		41982.5724	1.584	41983.5128	.957
41981.2727	.800	41982.5760	1.582	41983.5167	.937
41981.2760	.793	41982.5846	1.436	41983.5218	.927
41981.2808	.871	41982.5899	1.358	41983.5326	.926
41981.2837	.859	41982.5935	1.231	41983.5433	.914
41981.2865	.875	41982.5977	1.165	41983.5524	.898
41981.2910	.873	41982.6016	1.099	41983.5583	.860
41981.2956	.855	41982.6097	1.017	41983.5635	.863
41981.2989	.861	41982.6160	.941	41983.5675	.853
41981.3043	.843	41982.6244	.938	41983.5783	.898
41981.3110	.882	41982.6321	.928	41983.5877	.832
41981.3190	.849	41982.6376	.939	41983.5952	.822
41981.3281	.912			41983.6031	.816
41981.3384	1.001	41983.2566	.829	41983.6105	.818
41981.3433	1.090	41983.2645	.836	41983.6164	.795
41981.3527	1.205	41983.2648	.837	41983.6198	.806
41981.3600	1.333	41983.2743	.880	41983.6249	.817
41981.3643	1.424	41983.2847	.853	41983.6283	.842
41981.3684	1.482	41983.2918	.875	41983.6346	.823
41981.3727	1.493	41983.2957	.893	41983.6384	.802
41981.3781	1.521	41983.3019	.864	41983.6451	.801
41981.3810	1.477	41983.3126	.855	41983.6535	.849
		41983.3248	.885		
41982.2570	1.031	41983.3325	.891	41984.2620	.860
41982.2635	1.021	41983.3373	.900	41984.2651	.856
41982.2663	1.030	41983.3451	.872	41984.2713	.851
41982.2708	1.020	41983.3520	.921	41984.2791	.896
41982.2743	1.021	41983.3553	.915	41984.2863	.895
41982.2961	1.027	41983.3625	.912	41984.2963	.931
41982.3037	1.008	41983.3698	.952	41984.3045	1.000
41982.3112	.997	41983.3741	.964	41984.3103	1.047
41982.3739	.884	41983.3853	.970	41984.3175	1.177
41982.3773	.874	41983.3934	.942	41984.3232	1.341
41982.3812	.869	41983.3995	.946	41984.3276	1.411
41982.3843	.864	41983.4027	.941	41984.3354	1.548
41982.3922	.873	41983.4067	.969	41984.3424	1.567

Table 4 (cont.)

Photoelectric ultraviolet observations of SV Cam

J.D.	ΔU	J.D.	ΔU	J.D.	ΔU
41984.3541	1.556	42019.4781	.856	42106.4705	1.040
41984.3636	1.366	42019.4847	.815	42106.4785	1.130
41984.3684	1.282	42019.4919	.848	42106.4834	1.217
41984.3721	1.216	42019.5006	.793	42106.4898	1.323
41984.3767	1.152	42019.5059	.824	42106.4939	1.398
41984.3810	1.064	42019.5113	.837	42106.4994	1.525
41984.3852	.998	42019.5181	.855	42106.5031	1.697
41984.3888	.950	42019.5224	.845	42106.5080	1.777
41984.3935	.908	42019.5330	.837	42106.5118	1.758
41984.3972	.894	42019.5398	.811	42106.5170	1.758
41984.4149	.889	42019.5449	.861	42106.5214	1.710
41984.4240	.904	42019.5536	.894	42106.5292	1.594
41984.4327	.894	42019.5638	.843	42106.5332	1.525
41984.4507	.854	42019.5670	.859	42106.5410	1.255
41984.4588	.877	42019.5700	.871	42106.5501	1.093
41984.4683	.873	42019.5744	.865	42106.5581	1.033
41984.4729	.866	42019.5773	.873	42106.5632	.948
41984.4796	.881	42019.5881	.953	42106.5714	.854
41984.5075	.892	42019.5914	.955	42106.5835	.809
41984.5100	.896	42019.5960	.963	42106.6209	.723
41984.5175	.894	42019.6164	.966	42106.6258	.726
41984.5222	.902	42019.6210	.979	42106.6329	.754
		42019.6257	.980	42106.6405	.787
42019.2684	.793	42019.6293	.955		
42019.2915	.977	42019.6462	1.010	42304.3139	.899
42019.2974	1.107	42019.6544	1.001	42304.3190	.881
42019.3008	1.170	42019.6617	.981	42304.3230	.890
42019.3070	1.251			42304.3265	.877
42019.3139	1.382	42022.4669	.833	42304.3329	.844
42019.3201	1.564	42022.4728	.823	42304.3405	.839
42019.3231	1.612	42022.4808	.839	42304.3481	.858
42019.3271	1.570	42022.4867	.831	42304.3545	.869
42019.3355	1.618	42022.4921	.860	42304.3580	.849
42019.3384	1.582	42022.4994	.845	42304.3625	.854
42019.3424	1.595	42022.5079	.845	42304.3675	.887
42019.3450	1.612	42022.5167	.859	42304.3740	.900
42019.3503	1.545	42022.5203	.845	42304.3826	.859
42019.3554	1.350	42022.5288	.861	42304.3886	.832
42019.3675	1.147	42022.5314	.849	42304.3922	.858
42019.3744	1.017	42022.5426	.856	42304.4315	.811
42019.3810	.963	42022.5456	.845	42304.4360	.816
42019.3872	.904			42304.4394	.774
42019.3932	.935	42106.3423	.889	42304.4435	.808
42019.3969	.917	42106.3505	.926	42304.4466	.800
42019.4033	.889	42106.3602	.929	42304.4526	.822
42019.4106	.902	42106.3725	.948	42304.4591	.811
42019.4183	.892	42106.3807	.976	42304.4625	.810
42019.4220	.866	42106.4016	.952	42304.4666	.755
42019.4283	.874	42106.4101	.943	42304.4705	.805
42019.4356	.846	42106.4167	.925	42304.4755	.839
42019.4417	.865	42106.4235	.933	42304.4796	.829
42019.4483	.851	42106.4346	.926	42304.4851	.792
42019.4550	.833	42106.4528	.955	42304.4893	.792
42019.4624	.836	42106.4599	.986	42304.4988	.816

Table 4 (cont.)

Photoelectric ultraviolet observations of SV Cam

J.D.	ΔU	J.D.	ΔU	J.D.	ΔU
42304.5056	.853	42404.3244	.771	42405.3352	.812
42304.5091	.835	42404.3356	.772	42405.3397	.831
42304.5136	.841	42404.3426	.791	42405.3442	.849
42304.5173	.847	42404.3553	.796	42405.3527	.838
42304.5219	.855	42404.3617	.777	42405.3592	.822
42304.5271	.875	42404.3697	.779	42405.3689	.813
42304.5310	.859	42404.3976	.809	42405.3744	.808
42304.5347	.873	42404.4107	.814	42405.3787	.852
42304.5404	.836	42404.4202	.811	42405.3824	.942
42304.5440	.833	42404.4273	.804	42405.3866	.992
42304.5539	.869	42404.4336	.822	42405.3901	1.068
42304.5580	.921	42404.4471	.818	42405.3939	1.121
42304.5617	.944	42404.4551	.815	42405.3973	1.186
42304.5660	.946	42404.4617	.826	42405.4012	1.274
42304.5695	1.014	42404.4665	.841	42405.4046	1.363
42304.5735	1.076	42404.4745	.835	42405.4085	1.449
42304.5776	1.209	42404.4797	.846	42405.4119	1.506
42304.5824	1.357	42404.4876	.863	42405.4157	1.568
42304.5869	1.491	42404.4968	.863	42405.4189	1.672
42304.5918	1.603	42404.5093	.883	42405.4313	1.574
42304.5966	1.689	42404.5232	.898	42405.4449	1.322
42304.6014	1.735	42404.5332	.910	42405.4512	1.172
42304.6046	1.724	42404.5425	.900	42405.4557	1.096
42304.6087	1.637	42404.5520	.887	42405.4598	1.060
42304.6122	1.542	42404.5676	.899	42405.4696	.922
		42404.5721	.896	42405.4744	.885
42307.3673	.819	42404.5808	.884	42405.4789	.867
42307.3728	.823	42404.5884	.850	42405.4873	.845
42307.3756	.818	42404.5940	.839	42405.4925	.827
42307.3791	.826	42404.5985	.837	42405.4970	.829
42307.3955	.824	42404.6106	.843	42405.5052	.814
42307.4013	.797	42404.6172	.848	42405.5126	.807
42307.4038	.788	42404.6221	.839	42405.5189	.800
42307.4082	.792	42404.6301	.839	42405.5291	.809
42307.4114	.776	42404.6360	.841	42405.5310	.802
42307.4138	.751	42404.6507	.815	42405.5352	.813
42307.4180	.772	42404.6619	.805	42405.5404	.799
42307.4309	.774	42404.6697	.783	42405.5491	.806
42307.4353	.795			42405.5571	.785
42307.4433	.785	42405.2249	.780	42405.5661	.799
42307.4460	.784	42405.2315	.781	42405.5720	.809
42307.4529	.769	42405.2389	.809	42405.5762	.811
42307.4678	.763	42405.2472	.775	42405.5793	.807
42307.4731	.772	42405.2588	.786		
		42405.2654	.811	42432.2506	.810
42309.3121	.925	42405.2696	.805	42432.2567	.816
42309.3148	.999	42405.2741	.818	42432.2602	.814
42309.3197	1.302	42405.2821	.803	42432.2697	.802
42309.3232	1.692	42405.2894	.794	42432.2755	.777
42309.3277	1.263	42405.2954	.795	42432.2789	.772
42309.3391	1.661	42405.3040	.809	42432.2831	.774
42309.3423	1.771	42405.3126	.790	42432.2876	.764
		42405.3213	.777	42432.2921	.780
42404.3129	.802	42405.3298	.801	42432.2956	.819

Table 4 (cont.)

Photoelectric ultraviolet observations of SV Cam

J.D.	ΔU	J.D.	ΔU	J.D.	ΔU
42432.2998	.824	42461.4347	.806	42465.6000	.881
42432.3033	.817	42461.4395	.823	42465.6091	.883
42432.3077	.833	42461.4473	.853	42465.6174	.880
42432.3123	.835	42461.4538	.860	42465.6247	.870
42432.3164	.847	42461.4595	.875	42465.6335	.873
42432.3200	.842	42461.4660	.876	42465.6394	.843
42432.3269	.837	42461.4716	.889	42465.6477	.843
42432.3356	.861			42465.6535	.832
42432.3415	.845	42465.3022	1.358	42465.6598	.790
42432.3453	.845	42465.3052	1.476		
		42465.3092	1.522	42466.2862	.769
42460.4499	.807	42465.3136	1.573	42466.2899	.765
42460.4547	.817	42465.3172	1.642	42466.2978	.765
42460.4634	.828	42465.3208	1.685	42466.3012	.766
42460.4729	.840	42465.3250	1.685	42466.3075	.800
42460.4849	.843	42465.3313	1.654	42466.3129	.809
42460.4967	.853	42465.3367	1.594	42466.3181	.797
42460.5057	.858	42465.3404	1.542	42466.3217	.777
42460.5167	.882	42465.3438	1.454	42466.3283	.778
42460.5252	.872	42465.3493	1.254	42466.3411	.801
42460.5308	.893	42465.3535	1.182	42466.3456	.801
42460.5445	1.077	42465.3583	1.132	42466.3518	.794
42460.5568	1.335	42465.3625	1.042	42466.3597	.794
42460.5673	1.476	42465.3702	.918	42466.3650	.832
42460.5725	1.662	42465.3752	.886	42466.3693	.832
42460.5781	1.727	42465.3806	.862	42466.3742	.854
42460.5898	1.688	42465.3912	.841	42466.3786	.836
42460.5950	1.546	42465.4310	.797	42466.3849	.851
42460.6010	1.439	42465.4424	.773	42466.3921	.837
42460.6065	1.241	42465.4487	.779	42466.3962	.827
42460.6170	1.037	42465.4564	.785	42466.4004	.856
		42465.4606	.793	42466.4046	.861
42461.2667	.780	42465.4625	.785		
42461.2809	.791	42465.4694	.748	42523.3239	.826
42461.2905	.764	42465.4868	.739	42523.3301	.846
42461.2979	.776	42465.4959	.740	42523.3352	.855
42461.3040	.779	42465.5028	.753	42523.3407	.846
42461.3136	.759	42465.5063	.747	42523.3454	.842
42461.3195	.771	42465.5104	.751	42523.3506	.833
42461.3250	.784	42465.5139	.750	42523.3549	.835
42461.3292	.765	42465.5184	.742	42523.3616	.859
42461.3361	.745	42465.5232	.752	42523.3672	.870
42461.3435	.734	42465.5344	.760	42523.3749	.892
42461.3475	.734	42465.5436	.776	42523.3804	.886
42461.3540	.738	42465.5500	.765	42523.3859	.883
42461.3583	.734	42465.5535	.761	42523.3912	.899
42461.3666	.708	42465.5585	.761	42523.3992	.942
42461.3777	.703	42465.5646	.770	42523.4079	1.026
42461.3847	.737	42465.5696	.768	42523.4125	1.109
42461.3934	.733	42465.5731	.742	42523.4177	1.220
42461.4045	.771	42465.5785	.734	42523.4268	1.415
42461.4107	.766	42465.5840	.777	42523.4324	1.483
42461.4225	.786	42465.5889	.824	42523.4373	1.538
42461.4281	.800	42465.5927	.824	42523.4433	1.602

Table 4 (cont.)

Photoelectric ultraviolet observations of SV Cam

J.D.	ΔU	J.D.	ΔU	J.D.	ΔU
42523.4528	1.571	42634.3697	1.404	42836.5838	1.627
42523.4621	1.437	42634.3741	1.348	42836.5851	1.624
42523.4715	1.208	42634.3845	1.141	42836.5919	1.634
42523.4797	1.025	42634.3907	1.055	42836.5937	1.637
42523.4863	.895	42634.4014	.928	42836.6013	1.549
42523.4918	.859	42634.4088	.869	42836.6129	1.322
42523.4976	.816	42634.4190	.876	42836.6263	1.062
42523.5040	.802	42634.4308	.854	42836.6288	1.034
42523.5190	.810	42634.4356	.866	42836.6399	.962
42523.5298	.791	42634.4618	.836	42836.6411	.945
42523.5391	.777	42634.4659	.825	42836.6495	.911
42523.5452	.787	42634.4734	.807	42836.6563	.920
42523.5503	.811	42634.4801	.803		
42523.5558	.794	42634.4882	.788	43676.3426	.992
42523.5718	.769	42634.4957	.793	43676.3460	.986
		42634.5056	.812	43676.3567	.964
42545.3778	1.408	42634.5172	.807	43676.3649	.986
42545.3777	1.487	42634.5435	.812	43676.3743	.963
42545.3814	1.518			43676.3634	.967
42545.3843	1.562	42829.3329	.931	43676.3905	.933
42545.3887	1.585	42829.3507	.932	43676.3952	.911
42545.3924	1.578	42829.3538	.922	43676.4047	.974
42545.3967	1.518	42829.3614	.919	43676.4247	.957
42545.4001	1.462	42829.3637	.916	43676.4338	.953
42545.4040	1.392	42829.3712	.915	43676.4456	.902
42545.4072	1.287	42829.3794	.897	43676.4544	.889
42545.4118	1.250	42829.3869	.879	43676.4644	.908
42545.4194	1.157	42829.3961	.893	43676.4778	.914
42545.4238	1.095	42829.3976	.883	43676.4990	.859
42545.4278	1.005	42829.4070	.905	43676.5105	.831
42545.4450	.848	42829.4163	.917	43676.5213	.863
42545.4602	.823	42829.4250	1.005	43676.5276	.893
42545.4628	.820	42829.4330	1.058	43676.5368	.887
42545.4665	.817	42829.4344	1.095	43676.5417	.890
42545.4726	.788	42829.4413	1.213	43676.5524	.936
42545.4784	.784	42829.4429	1.235	43676.5570	.963
42545.4826	.806			43676.5639	1.024
42545.4902	.775	42831.2632	1.747	43676.5665	1.038
		42831.2725	1.472	43676.5773	1.150
42603.5206	1.498	42831.2941	1.052	43676.5868	1.332
42603.5237	1.431	42831.3037	1.017	43676.5904	1.414
42603.5280	1.392	42831.3154	1.044	43676.5941	1.470
42603.5310	1.297	42831.3273	1.020	43676.6029	1.613
42603.5348	1.251	42831.3386	1.003	43676.6059	1.633
42603.5380	1.151	42831.3527	1.033	43676.6118	1.667
42603.5414	1.091	42831.3657	1.013	43676.6195	1.657
		42831.3778	.983	43676.6299	1.490
42634.3280	1.287	42831.3865	.992	43676.6307	1.371
42634.3311	1.389			43676.6415	1.281
42634.3364	1.491	42836.5187	.927	43676.6443	1.223
42634.3429	1.606	42836.5265	.973	43676.6532	1.079
42634.3471	1.654	42836.5350	1.024	43676.6618	1.007
42634.3515	1.682	42836.5549	1.419	43676.6649	.947
42634.3624	1.564	42836.5630	1.636	43676.6773	.935

Table 4 (cont.)

Photoelectric ultraviolet observations of SV Cam

J.D.	ΔU	J.D.	ΔU	J.D.	ΔU
43878.6955	.957	43880.3742	1.457	43926.3534	1.009
43878.7033	.943	43880.3835	1.637	43926.3642	.984
		43880.3912	1.599	43926.3711	.943
43879.3654	.859	43880.3980	1.659	43926.3793	.967
43879.3742	.849	43880.4052	1.649	43926.3815	.961
43879.3835	.900	43880.4086	1.536	43926.3891	.930
43879.3925	.876	43880.4133	1.437	43926.3962	.931
43879.4026	.882	43880.4209	1.308	43926.4043	.937
43879.4111	.905	43880.4255	1.222	43926.4120	.918
43879.4155	.915	43880.4323	1.079	43926.4206	.922
43879.4356	.912	43880.4366	1.042	43926.4234	.920
43879.4461	.897	43880.4429	.996	43926.4293	.916
43879.4547	.929	43880.4496	.979	43926.4341	.915
43879.4632	.937	43880.4594	.968	43926.4441	.911
43879.4719	.964	43880.4655	.923	43926.4537	.917
43879.4815	1.004	43880.4717	.934	43926.4641	.913
43879.4919	1.045	43880.4817	.917	43926.4756	.925
43879.5011	1.010	43880.4897	.887	43926.4866	.911
43879.5115	1.043	43880.4936	.881	43926.4919	.903
43879.5203	1.037	43880.5043	.913	43926.5001	.916
43879.5284	1.028	43880.5160	.886	43926.5092	.938
43879.5369	1.024	43880.5208	.864	43926.5153	.893
43879.5448	1.006	43880.5295	.863	43926.5236	.873
43879.5529	.987	43880.5393	.864	43926.5359	.886
43879.5605	.971	43880.5503	.902	43926.5478	.892
43879.5666	.962	43880.5545	.894	43926.5552	.915
43879.5741	.967	43880.5603	.888	43926.5597	.917
43879.5794	.959	43880.5650	.878	43926.5664	.952
43879.5869	.929	43880.5682	.869	43926.5729	.930
43879.5972	.913	43880.5731	.846	43926.5828	.973
43879.6042	.925	43880.5774	.860	43926.5953	.968
43879.6162	.913	43880.5831	.877	43926.6054	.996
43879.6267	.936	43880.5901	.869	43926.6099	1.062
43879.6365	.941	43880.5977	.876	43926.6134	1.091
43879.6465	.925	43880.6063	.899	43926.6116	1.203
		43880.6185	.892	43926.6250	1.254
43880.2284	.933	43880.6267	.897	43926.6326	1.413
43880.2366	.930	43880.6369	.925	43926.6361	1.505
43880.2429	.900	43880.6451	.937	43926.6443	1.626
43880.2506	.902	43880.6546	1.002	43926.6834	1.665
43880.2608	.913	43880.6626	1.029	43926.6625	1.592
43880.2706	.858	43880.6709	1.028	43926.6711	1.415
43880.2792	.870	43880.6790	1.028	43926.6739	1.365
43880.2969	.903	43880.6875	1.003		
43880.3046	.905	43880.6943	.984	43927.2466	1.689
43880.3110	.898	43880.7039	1.019	43927.2496	1.688
43880.3157	.906			43927.2561	1.630
43880.3274	.930	43926.2822	.895	43927.2595	1.574
43880.3331	.944	43926.2941	.904	43927.2689	1.329
43880.3419	.962	43926.3095	.901	43927.2717	1.290
43880.3469	.995	43926.3194	.933	43927.2733	1.243
43880.3540	1.062	43926.3322	.931	43927.2798	1.141
43880.3600	1.118	43926.3399	.973	43927.2890	.990
43880.3663	1.285	43926.3459	.988	43927.2977	.948

Table 4 (cont.)

Photoelectric ultraviolet observations of SV Cam

J.D.	ΔU	J.D.	ΔU	J.D.	ΔU
43927.3067	.923	43928.3312	.914	43928.5741	.913
43927.3160	.883	43928.3383	.932	43928.5770	.885
43927.3247	.898	43928.3458	.956	43928.5846	.893
43927.3315	.890	43928.3545	.946	43928.5876	.881
43927.3403	.898	43928.3586	.957	43928.5920	.890
43927.3446	.909	43928.3662	.954	43928.5945	.884
43927.3531	.897	43928.3693	.947	43928.6013	.883
43927.3565	.890	43928.3723	.964	43928.6062	.880
43927.3655	.876	43928.3796	.957	43928.6084	.886
43927.3703	.883	43928.3875	1.032	43928.6129	.898
43927.3779	.898	43928.3898	1.063	43928.6151	.899
43927.3852	.894	43928.3916	1.110	43928.6178	.871
43927.3933	.880	43928.3956	1.156	43928.6231	.873
43927.3970	.890	43928.3984	1.202	43928.6275	.905
43927.4045	.890	43928.4010	1.263	43928.6338	.905
43927.4092	.875	43928.4038	1.294	43928.6386	.926
43927.4204	.896	43928.4066	1.359	43928.6415	.923
43927.4239	.887	43928.4096	1.440	43928.6441	.933
43927.4925	.895	43928.4120	1.520	43928.6497	.922
43927.4364	.901	43928.4172	1.602		
43927.4502	.915	43928.4203	1.630	44048.3774	.860
43927.4626	.893	43928.4230	1.671	44048.3842	.854
43927.4752	.890	43928.4259	1.698	44048.3909	.859
43927.4814	.913	43928.4293	1.709	44048.3962	.865
43927.4911	.932	43928.4363	1.647	44048.4044	.867
43927.4963	.943	43928.4416	1.612	44048.4109	.864
43927.5056	.948	43928.4442	1.575	44048.4187	.863
43927.5124	.949	43928.4524	1.384	44048.4257	.867
43927.5189	.934	43928.4543	1.297	44048.4321	.856
43927.5247	.900	43928.4565	1.226	44048.4389	.851
43927.5339	.905	43928.4590	1.201	44048.4448	.865
43927.5444	.962	43928.4679	1.060	44048.4515	.889
43927.5576	.940	43928.4726	1.025	44048.4715	.901
43927.5657	.941	43928.4762	.995	44048.4773	.903
43927.5729	.953	43928.4793	.951	44048.4854	.924
43927.5816	.899	43928.4821	.950	44048.4916	.918
43927.5865	.920	43928.4898	.934	44048.4990	.928
43927.5939	.903	43928.4931	.942	44048.5182	.992
43927.5975	.894	43928.4955	.937		
43927.6037	.920	43928.5023	.924	44049.3759	.956
43927.6103	.898	43928.5064	.917	44049.3769	.972
43927.6192	.892	43928.5121	.904	44049.3822	1.054
43927.6282	.895	43928.5184	.908	44049.3832	1.072
43927.6414	.925	43928.5210	.904	44049.3842	1.085
43927.6499	.894	43928.5264	.896	44049.3898	1.208
43927.6569	.920	43928.5289	.918	44049.3962	1.326
43927.6638	.942	43928.5312	.905	44049.4015	1.453
		43928.5361	.876	44049.4025	1.479
43928.2960	.923	43928.5385	.876	44049.4035	1.515
43928.3024	.913	43928.5412	.905	44049.4093	1.587
43928.3100	.942	43928.5481	.892	44049.4154	1.622
43928.3146	.935	43928.5538	.885	44049.4216	1.589
43928.3211	.912	43928.5560	.880	44049.4277	1.601
43928.3253	.893	43928.5612	.882	44049.4338	1.617

Table 4 (cont.)

Photoelectric ultraviolet observations of SV Cam

J.D.	ΔU	J.D.	ΔU	J.D.	ΔU
44049.4401	1.386	44158.3625	.865	44159.4204	.910
44049.4462	1.192	44158.3635	.861	44159.4214	.937
44049.4528	1.059	44158.3644	.856	44159.4224	.921
44049.4589	1.010	44158.3686	.852	44159.4263	.924
44049.4642	.951	44158.3696	.853	44159.4274	.923
44049.4662	.928	44158.3706	.863	44159.4289	.933
44049.4719	.887	44158.3715	.844	44159.4339	.916
44049.4793	.878	44158.3759	.840	44159.4349	.913
44049.4859	.902	44158.3769	.845	44159.4359	.901
44049.4920	.898	44158.3779	.843	44159.4369	.916
44049.5056	.893	44158.3789	.836	44159.4412	.913
44049.5178	.888	44158.3849	.846	44159.4422	.923
44049.5247	.901	44158.3859	.840	44159.4570	.930
		44158.3869	.846	44159.4580	.930
44081.4692	1.280	44158.3878	.848	44159.4590	.917
44081.4797	1.084	44158.3949	.842	44159.4646	.911
44081.4862	1.004	44158.3959	.834	44159.4656	.914
44081.4917	.961	44158.3969	.838	44159.4671	.915
44081.4988	.889	44158.4015	.847	44159.4671	.915
44081.5059	.908	44158.4024	.860	44159.4718	.898
44081.5125	.897	44158.4035	.862	44159.4728	.893
44081.5190	.901	44158.4045	.850	44159.4738	.899
				44159.4748	.898
44145.2954	.813	44159.3596	.879	44159.4793	.887
44145.3069	.776	44159.3615	.876	44159.4802	.887
44145.3137	.821	44159.3626	.878	44159.4812	.889
44145.3217	.810	44159.3670	.891	44159.4822	.908
44145.3269	.812	44159.3680	.889	44159.4866	.907
44145.3335	.793	44159.3690	.902	44159.4876	.895
		44159.3700	.886	44159.4886	.905
44146.3451	.887	44159.3748	.891	44159.4955	.870
44146.3533	.898	44159.3758	.887	44159.4965	.857
44146.3671	.945	44159.3768	.895	44159.4975	.860
44146.3685	.935	44159.3778	.890	44159.5017	.878
44146.3751	.947	44159.3833	.903	44159.5027	.890
44146.3814	.936	44159.3853	.911	44159.5037	.885
44146.3824	.936	44159.3863	.892	44159.5047	.883
44146.3839	.939	44159.3906	.904	44159.5097	.874
44146.3885	.916	44159.3916	.913	44159.5107	.880
44146.3895	.926	44159.3926	.919	44159.5117	.890
44146.3905	.921	44159.3936	.917	44159.5127	.890
44146.3915	.931	44159.3975	.908	44159.5168	.878
		44159.3987	.908	44159.5178	.873
44158.3319	.892	44159.3997	.910	44159.5188	.880
44158.3329	.899	44159.4006	.922	44159.5198	.857
44158.3348	.901	44159.4048	.912	44159.5239	.850
44158.3395	.863	44159.4058	.911	44159.5249	.846
44158.3404	.866	44159.4068	.926	44159.5259	.846
44158.3415	.879	44159.4078	.918	44159.5269	.837
44158.3424	.857	44159.4119	.927	44159.5385	.865
44158.3542	.856	44159.4129	.907	44159.5395	.855
44158.3551	.860	44159.4139	.918	44159.5405	.852
44158.3570	.859	44159.4149	.928	44159.5415	.840
44158.3615	.859	44159.4194	.914	44159.5465	.845

Table 4 (cont.)

Photoelectric ultraviolet observations of SV Cam

J.D.	ΔU	J.D.	ΔU	J.D.	ΔU
44159.5475	.867	44285.3260	.818	44285.4385	1.344
44159.5485	.863	44285.3303	.829	44285.4395	1.360
44159.5495	.859	44285.3313	.837	44285.4405	1.396
44159.5541	.828	44285.3323	.855	44285.4447	1.524
44159.5551	.817	44285.3333	.823	44285.4457	1.541
44159.5561	.825	44285.3381	.838	44285.4467	1.551
44159.5571	.807	44285.3391	.821	44285.4477	1.562
44159.5623	.846	44285.3401	.830	44285.4524	1.618
44159.5633	.836	44285.3411	.838	44285.4544	1.630
44159.5643	.819	44285.3452	.824	44285.4591	1.651
44159.5771	.844	44285.3462	.832	44285.4621	1.675
44159.5852	.833	44285.3471	.840	44285.4668	1.642
44159.5867	.815	44285.3481	.854	44285.4683	1.634
44159.5877	.824	44285.3531	.842	44285.4693	1.637
44159.5948	.836	44285.3540	.850	44285.4736	1.614
44159.5958	.836	44285.3551	.855	44285.4746	1.610
44159.5968	.825	44285.3560	.857	44285.4756	1.595
44159.6100	.850	44285.3610	.836	44285.4766	1.552
44159.6115	.856	44285.3620	.834	44285.4894	1.270
44159.6124	.862	44285.3630	.856	44285.4913	1.245
44159.6171	.866	44285.3639	.840	44285.4983	1.102
44159.6186	.868	44285.3695	.846	44285.5002	1.080
44159.6201	.880	44285.3705	.841	44285.5056	1.024
44159.6259	.870	44285.3715	.839	44285.5076	.999
44159.6279	.872	44285.3763	.870	44285.5149	.966
44159.6324	.880	44285.3773	.862	44285.5160	.959
44159.6334	.869	44285.3783	.869	44285.5170	.957
44159.6344	.874	44285.3793	.869	44285.5179	.966
44159.6354	.881	44285.3834	.856	44285.5237	.940
44159.6397	.880	44285.3844	.877	44285.5302	.939
44159.6407	.863	44285.3854	.883	44285.5677	.909
44159.6417	.869	44285.3864	.868	44285.5687	.904
44159.6427	.892	44285.3911	.882	44285.5701	.907
44159.6469	.879	44285.3921	.879	44285.5753	.894
44159.6479	.892	44285.3931	.870	44285.5763	.894
44159.6489	.871	44285.3941	.872	44285.5775	.904
44159.6499	.895	44285.3989	.896	44285.5782	.885
		44285.3999	.900	44285.5830	.877
44285.2827	.837	44285.4009	.901	44285.5846	.873
44285.2837	.859	44285.4019	.910	44285.5855	.883
44285.2847	.864	44285.4067	.916	44285.5905	.897
44285.2857	.845	44285.4087	.917	44285.5915	.867
44285.2867	.850	44285.4097	.905	44285.5925	.883
44285.3015	.840	44285.4138	.924	44285.5983	.876
44285.3024	.821	44285.4148	.958	44285.5999	.892
44285.3066	.824	44285.4163	.963	44285.6009	.895
44285.3076	.818	44285.4222	1.050	44285.5019	.887
44285.3118	.816	44285.4231	1.056	44285.6052	.879
44285.3128	.819	44285.4242	1.058	44285.6072	.872
44285.3171	.852	44285.4251	1.084	44285.6082	.871
44285.3181	.832	44285.4302	1.163	44285.6092	.869
44285.3231	.834	44285.4317	1.207	44285.6148	.879
44285.3240	.834	44285.4327	1.226	44285.6157	.883
44285.3250	.843	44285.4375	1.334	44285.6222	.850

Table 4 (cont.)

Photoelectric ultraviolet observations of SV Cam

J.D.	ΔU	J.D.	ΔU	J.D.	ΔU
44285.6232	.865	44371.3831	.874	44371.4951	1.018
44285.6242	.860	44371.3881	.871	44371.4961	.977
44285.6252	.850	44371.3891	.876	44371.4971	.968
44285.6295	.874	44371.3900	.874	44371.4981	.948
44285.6304	.868	44371.3910	.890	44371.5025	.981
44285.6324	.872	44371.3956	.886	44371.5035	.952
44285.6367	.883	44371.3966	.884	44371.5045	.962
44285.6377	.884	44371.3976	.901	44371.5055	.949
44285.6387	.883	44371.4036	.916	44371.5107	.900
44285.6397	.889	44371.4046	.929	44371.5117	.900
44285.6433	.907	44371.4056	.922	44371.5127	.874
44285.6448	.908	44371.4066	.920	44371.5136	.871
44285.6468	.905	44371.4112	.956	44371.5180	.855
44285.6513	.899	44371.4122	.976	44371.5189	.859
44285.6523	.906	44371.4132	1.002	44371.5199	.882
44285.6532	.907	44371.4142	1.017	44371.5209	.889
44285.6542	.908	44371.4194	1.099	44371.5253	.893
44285.6612	.889	44371.4204	1.081	44371.5264	.912
44285.6621	.910	44371.4214	1.108	44371.5273	.882
44285.6632	.902	44371.4224	1.138	44371.5283	.868
44285.6642	.891	44371.4270	1.198	44371.5325	.882
44285.6683	.911	44371.4280	1.197	44371.5335	.891
44285.6693	.924	44371.4290	1.229	44371.5344	.921
44285.6713	.913	44371.4300	1.242	44371.5354	.933
44285.6750	,913	44371.4345	1.335	44371.5415	.879
44285.6785	.923	44371.4355	1.335	44371.5425	.861
		44371.4365	1.367	44371.5435	.865
44371.3358	.839	44371.4375	1.404	44371.5445	.886
44371.3368	.856	44371.4420	1.490	44371.5487	.909
44371.3378	.850	44371.4430	1.501	44371.5497	.924
44371.3388	.867	44371.4440	1.512	44371.5507	.915
44371.3445	.812	44371.4450	1.519	44371.5516	.927
44371.3454	.824	44371.4495	1.600		
44371.3464	.825	44371.4505	1.577	44454.3868	.881
44371.3474	.815	44371.4515	1.601	44454.4004	.871
44371.3516	.815	44371.4525	1.610	44454.4077	.884
44371.3526	.814	44371.4566	1.553	44454.4150	.903
44371.3536	.829	44371.4576	1.548	44454.4231	.937
44371.3546	.832	44371.4586	1.533	44454.4308	.923
44371.3586	.849	44371.4596	1.543	44454.4384	.958
44371.3596	.848	44371.4638	1.558	44454.4526	1.117
44371.3605	.831	44371.4648	1.553	44454.4608	1.285
44371.3615	.847	44371.4658	1.552	44454.4760	1.587
44371.3659	.855	44371.4668	1.528	44454.4845	1.602
44371.3668	.850	44371.4711	1.453	44454.4930	1.634
44371.3678	.853	44371.4721	1.444	44454.5007	1.542
44371.3688	.869	44371.4731	1.397	44454.5116	1.285
44371.3729	.881	44371.4741	1.389	44454.5192	1.175
44371.3739	.870	44371.4785	1.366	44454.5270	1.053
44371.3748	.875	44371.4795	1.307	44454.5349	.993
44371.3758	.859	44371.4805	1.347	44454.5426	.953
44371.3802	.882	44371.4814	1.307	44454.5510	.930
44371.3812	.883	44371.4897	1.066	44454.5583	.946
44371.3822	.880	44371.4907	1.061		

Table 4 (cont.)

Photoelectric ultraviolet observations of SV Cam

J.D.	ΔU	J.D.	ΔU	J.D.	ΔU
44455.3433	.924	44541.2939	.822	44541.4282	.917
44455.3571	.966	44541.2949	.838	44541.4356	.928
44455.3674	.969	44541.3014	.851	44541.4405	.922
44455.3768	.983	44541.3033	.850	44541.4420	.911
44455.3932	.987	44541.3083	.868	44541.4434	.913
44455.4009	.964	44541.3092	.878	44541.4482	.903
44455.4083	.940	44541.3102	.874	44541.4491	.892
44455.4162	.961	44541.3112	.852	44541.4501	.899
44455.4238	.951	44541.3156	.856	44541.4511	.891
44455.4299	.947	44541.3165	.860	44541.4561	.904
44455.4348	.955	44541.3175	.878	44541.4581	.898
44455.4410	.931	44541.3184	.870	44541.4640	.907
44455.4475	.918	44541.3231	.864	44541.4650	.892
		44541.3241	.875	44541.4660	.906
44477.3815	.845	44541.3251	.875	44541.4669	.904
44477.3925	.910	44541.3260	.868	44541.4715	.893
44477.4002	.912	44541.3396	.906	44541.4725	.909
44477.4072	.910	44541.3406	.909	44541.4735	.910
44477.4159	.891	44541.3415	.916	44541.4745	.909
44477.4401	.866	44541.3425	.907	44541.4797	.910
44477.4481	.862	44541.3485	.922	44541.4807	.903
44477.4550	.878	44541.3494	.930	44541.4873	.935
44477.4624	.869	44541.3504	.939	44541.4887	.933
44477.4699	.906	44541.3553	.952	44541.4902	.941
44477.4778	.879	44541.3562	.941		
44477.4849	.884	44541.3572	.944	44582.2209	.834
44477.4921	.880	44541.3582	.933	44582.2299	.870
44477.4993	.880	44541.3628	.957	44582.2309	.836
44477.5064	.873	44541.3643	.955	44582.2353	.861
44477.5138	.870	44541.3658	.966	44582.2363	.849
44477.5209	.895	44541.3702	.941	44582.2373	.853
44477.5287	.876	44541.3721	.951	44582.2419	.825
44477.5361	.880	44541.3776	.953	44582.2429	.836
44477.5431	.914	44541.3786	.952	44582.2439	.846
44477.5509	.915	44541.3796	.935	44582.2486	.855
44477.5583	.908	44541.3805	.941	44582.2495	.865
44477.5662	.931	44541.3952	.937	44582.2505	.866
44477.5740	.997	44541.3967	.933	44582.2553	.883
44477.5811	1.110	44541.3977	.931	44582.2562	.861
44477.5885	1.260	44541.4022	.922	44582.2572	.865
		44541.4032	.932	44582.2621	.891
44541.2516	.814	44541.4042	.932	44582.2631	.875
44541.2528	.812	44541.4052	.933	44582.2641	.884
44541.2537	.815	44541.4103	.941	44582.2687	.864
44541.2547	.817	44541.4114	.937	44582.2697	.885
44541.2611	.815	44541.4123	.920	44582.2706	.883
44541.2620	.822	44541.4133	.927	44582.2756	.917
44541.2630	.832	44541.4178	.914	44582.2766	.901
44541.2702	.832	44541.4187	.913	44582.2776	.882
44541.2722	.833	44541.4197	.910	44582.2824	.901
44541.2854	.838	44541.4207	.909	44582.2834	.900
44541.2869	.834	44541.4252	.912	44582.2844	.919
44541.2879	.833	44541.4262	.909	44582.2892	.880
44541.2929	.837	44541.4272	.916	44582.2902	.898

Table 4 (cont.)

Photoelectric ultraviolet observations of SV Cam

J.D.	ΔU	J.D.	ΔU	J.D.	ΔU
44582.2912	.907	44582.3943	.790	44582.4902	.861
44582.2962	.894	44582.3952	.782	44582.4912	.864
44582.2972	.870	44582.3963	.802	44582.4922	.845
44582.2981	.887	44582.3972	.794	44582.4932	.854
44582.3033	.875	44582.3982	.776	44582.4984	.866
44582.3043	.883	44582.3992	.766	44582.4994	.871
44582.3052	.890	44582.4042	.770	44582.5003	.873
44582.3099	.887	44582.4051	.775	44582.5013	.856
44582.3109	.879	44582.4061	.775	44582.5023	.876
44582.3119	.894	44582.4071	.763	44582.5033	.876
44582.3163	.898	44582.4081	.784	44582.5084	.872
44582.3173	.875	44582.4091	.777	44582.5094	.879
44582.3183	.880	44582.4145	.778	44582.5104	.863
44582.3227	.881	44582.4154	.781	44582.5114	.878
44582.3237	.866	44582.4164	.770	44582.5124	.868
44582.3247	.861	44582.4174	.807	44582.5134	.888
44582.3291	.852	44582.4184	.784	44582.5196	.887
44582.3300	.869	44582.4228	.781	44582.5215	.919
44582.3310	.870	44582.4236	.791	44582.5225	.904
44582.3374	.828	44582.4247	.795	44582.5235	.923
44582.3394	.832	44582.4257	.803	44582.5245	.923
44582.3404	.851	44582.4267	.810	44582.5293	.947
44582.3413	.844	44582.4276	.808	44582.5303	.940
44582.3423	.846	44582.4323	.789	44582.5493	1.071
44582.3470	.826	44582.4333	.785	44582.5502	1.063
44582.3480	.837	44582.4343	.805	44582.5512	1.072
44582.3490	.823	44582.4353	.808	44582.5522	1.076
44582.3500	.827	44582.4363	.790	44582.5532	1.081
44582.3510	.837	44582.4373	.801	44582.5542	1.120
44582.3519	.836	44582.4418	.806	44582.5609	1.236
44582.3567	.818	44582.4428	.813	44582.5628	1.280
44582.3577	.821	44582.4437	.798	44582.5638	1.311
44582.3587	.815	44582.4447	.810	44582.5648	1.338
44582.3596	.811	44582.4457	.813	44582.5658	1.369
44582.3606	.779	44582.4467	.826	44582.5707	1.502
44582.3616	.760	44582.4527	.819	44582.5717	1.542
44582.3669	.735	44582.4537	.816	44582.5727	1.541
44582.3679	.718	44582.4547	.805	44582.5736	1.574
44582.3688	.699	44582.4557	.814	44582.5746	1.585
44582.3698	.689	44582.4566	.803	44582.5756	1.599
44582.3706	.703	44582.4576	.815	44582.5802	1.610
44582.3717	.736	44582.4676	.820	44582.5812	1.539
44582.3760	.765	44582.4686	.835	44582.5822	1.498
44582.3770	.791	44582.4695	.820	44582.5832	1.538
44582.3780	.766	44582.4705	.834	44582.5842	1.597
44582.3789	.773	44582.4725	.842	44582.5852	1.622
44582.3799	.778	44582.4785	.844	44582.5897	1.639
44582.3809	.797	44582.4795	.852	44582.5907	1.631
44582.3852	.768	44582.4805	.856	44582.5917	1.616
44582.3861	.786	44582.4815	.856	44582.5926	1.632
44582.3871	.771	44582.4824	.849	44582.5936	1.647
44582.3881	.786	44582.4834	.852	44582.5946	1.653
44582.3891	.796	44582.4882	.860	44582.5996	1.644
44582.3901	.805	44582.4892	.865	44582.6006	1.627

Table 4 (cont.)

Photoelectric ultraviolet observations of SV Cam

J.D.	ΔU	J.D.	ΔU	J.D.	ΔU
44582.6015	1.614	44582.6339	1.006	44582.6730	.893
44582.6025	1.614	44582.6385	.967	44582.6739	.881
44582.6035	1.590	44582.6395	.968	44582.6784	.865
44582.6045	1.584	44582.6405	.958	44582.6794	.870
44582.6095	1.427	44582.6414	.963	44582.6794	.870
44582.6105	1.424	44582.6424	.960	44582.6804	.870
44582.6115	1.388	44582.6434	.959	44582.6814	.865
44582.6125	1.345	44582.6494	.919	44582.6823	.858
44582.6134	1.329	44582.6503	.906	44582.6833	.870
44582.6144	1.301	44582.6513	.931	44582.6882	.847
44582.6191	1.207	44582.6523	.922	44582.6892	.867
44582.6201	1.191	44582.6533	.919	44582.6901	.867
44582.6211	1.162	44582.6580	.905	44582.6911	.857
44582.6220	1.165	44582.6590	.901	44582.6921	.849
44582.6230	1.144	44582.6600	.906	44582.6931	.856
44582.6240	1.112	44582.6610	.900	44582.6975	.853
44582.6269	1.052	44582.6620	.904	44582.6985	.858
44582.6299	1.036	44582.6630	.896	44582.6995	.848
44582.6309	1.037	44582.6690	.886	44582.7005	.846
44582.6319	1.017	44582.6710	.887	44582.7014	.821
44582.6329	1.007	44582.6720	.888	44582.7024	.837

COMMUNICATIONS
FROM THE
KONKOLY OBSERVATORY
OF THE
HUNGARIAN ACADEMY OF SCIENCES

MITTEILUNGEN
DER
STERNWARTE
DER UNGARISCHEN AKADEMIE
DER WISSENSCHAFTEN

BUDAPEST — SZABADSÁGHEGY

No. 81.

M. PAPARÓ

STRUCTURE OF NGC 2420

BUDAPEST, 1982

ISBN 963 8361 16 6
HU ISSN 0324 - 2234
Felelős kiadó: Szeidl Béla

Hozott anyagról sokszorosítva

8213429 MTA KESZ Sokszorosító, Budapest. F. v.: dr. Héczey Lászlóné

STRUCTURE OF NGC 2420

ABSTRACT

A new examination of the structure of NGC 2420 has been made according to Kholopov's method. 1890 stars were measured between the circles of about 6′ and 25′ radius centred on the cluster, for which photographic B,V magnitudes and positions were obtained down to the limiting magnitude of plates ($17^{m}.8$ in V) but in constructing the density distributions stars down to $17^{m}.5$ were chosen. A literature determination of the proper motion of stars in a circle of 12′ radius was used to define the place and shape of the C-M diagram. Around this diagram bands of $0^{m}.1$, $0^{m}.2$ and $0^{m}.3$ width in B-V were drawn to select the members of the cluster. The stars were separated into four groups and surface density distributions were made for the whole cluster and for each subgroup. The distributions of the stars reveal two different parts of the cluster: the core has a radius of 5.1 pc, whereas the halo extends as far as 12.7 pc. The brighter stars belong to the core and many of fainter ones to the halo - as might be expected from the theory. The whole halo seems to be steady against the irregular forces of background stars but the outer part of the halo from 8.2 pc radius is not stable against the tidal force.

INTRODUCTION

As early as at the beginning of this century *Shapley* (1916) pointed out that outside an inner dense part in M 67 the density is ten times higher than the density of the background typical in this galactic latitude. According to Shapley the well-defined part with 6′.5 radius in M 67 is only the core of a more extensive cluster. In 1922 Trumpler obtained similar result for Pleiades, Praesepe, h Persei, M 11 and M 37.This phenomenon has been investigated fairly accurately by *Kholopov* (1953, 1968) and *Artuhina* (1966) since 1953. They have studied about twelve clusters, both open and globular ones and have found that each cluster consists of two main parts: core and halo.

A preliminary examination of the open cluster NGC 2420 was made by the author (1977, hereinafter Paper I) in accordance with Cannon's photometry. The area of 12′ radius centred on the cluster measured by Cannon proved too small to demonstrate the halo of the cluster which seems to extend further than 12′. The aim of present work is to investigate a larger area around the cluster following Kholopov's method described in Paper I and to define the radius of the halo.

OBSERVATIONAL MATERIAL

From the observational point of view, the open cluster NGC 2420 is highly appropriate. Its galactic coordinates are: $l^{II}=198^{o}$, $b^{II}=+20^{o}$. Because of the high galactic latitude the interstellar reddening has only a small value and the density of the background stars is considerably smaller than in the galactic plane. The observations were carried out with the 60/90/180 cm Schmidt telescope of Konkoly Observatory's mountain station in the period 1976-1977. B,V colours were derived for 1890 stars brighter than $17^{m}.8$ photographic magnitude. The photometry is based on five plates taken in each colour. The emulsion types, filters and exposure times used are given below:

	plate	filter	exposure time
B	Kodak 103a-O	Schott GG_{13} 2mm	30^{m}
V	Kodak 103a-D	Schott GG_{14} 2mm	30^{m}

The international system is connected with the instrumental system by the equations:

$$V_{instr} = V - 0.112(B-V) + 0.074$$

$$(B-V)_{instr} = 0.933(B-V) + 0.029$$

The plates were measured with Konkoly Observatory's Cuffey-type iris photometer using 15 photoelectric standards taken from *West*'s article (1967). The mean errors of the photographically determined colours are $\pm\ 0^{m}.06$ in both B and V. The scale of the Schmidt plates did not allow the measurement of the stars in the centre of the cluster. The stars were measured between the circles of about 6' and 25' radius centred on the cluster, as identified on the chart shown in Fig. 6 a,b,c,d. The magnitudes and positions are listed in the Table.

The inner part of the cluster was studied by the photometry of *West* (1967), *Cannon* and *Lloyd* (1970) and *McClure et al.* (1974). There are overlaps between these works and the area measured by the author. Stars in the overlapping areas were used to transform

the magnitudes into a common system. The magnitudes were not corrected for interstellar reddening because its values are negligible. According to *McClure et al.* (1974) $E(B-V) = 0^m.02$ and $E(U-B) = 0^m.02$.

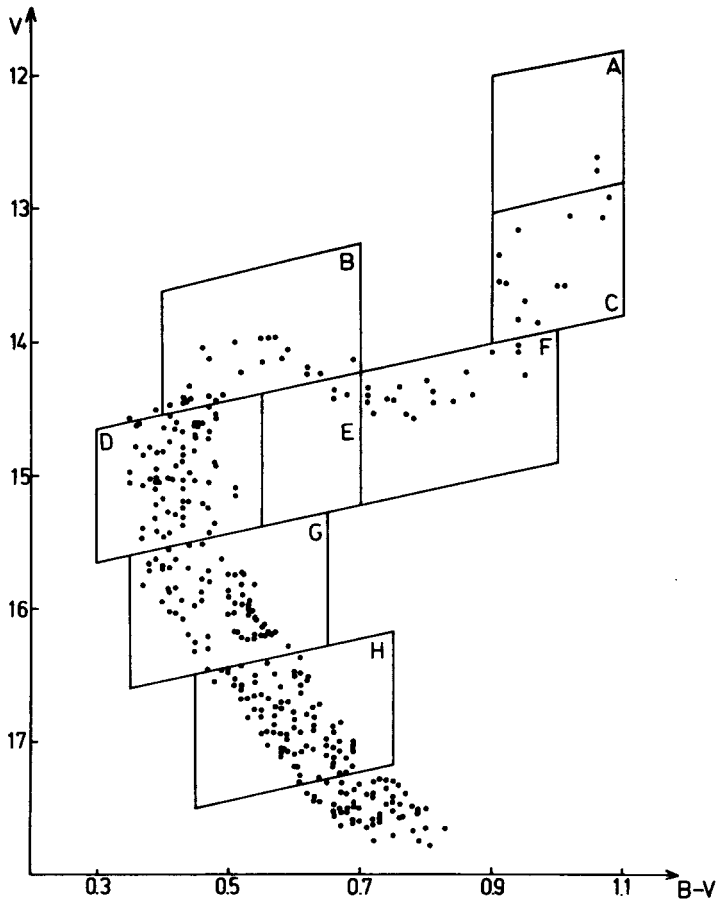

Fig. 1 The C-M diagram of NGC 2420

SURFACE DENSITY DISTRIBUTION

When studying the structure of open clusters according to density distribution we have to pay great attention to the construction of density distribution curves. In the early fifties *Kholopov* (1953) began to deal with this problem and discussed in detail which parts of the examination need special care.

a. Since in the clusters there are stars of different mass and they play a different role in the dynamic evolution of clusters, it is very useful to separate them into different subsystems. For this purpose the cluster was divided into subsystems by boxes according to Cannon's article on the C-M diagram (Fig.1). The size of the boxes also depends on the number of stars belonging to the box. The boxes marked A,B, C,E and F were treated together because of the small number of stars in each box. The stars in these boxes all are giants, so they play a similar role in the dynamic evolution of clusters. Density distributions were made for the whole cluster and the following subgroups:

   A+B+C+E+F group - containing the brightest stars ($m \sim 1.2\ M_\odot$)
   D group - containing the turn-off point of the cluster ($m \sim 1.2\ M_\odot$)
   G group - where $m \sim 1.0\ M_\odot$
   H group - where $m \sim 0.8\ M_\odot$

b. *Cannon* and *Lloyd* (1970) determined the proper motion of stars in NGC 2420 in a circle of 12′ radius. *McClure et al.* (1974) using their own photometry and Cannon's proper motions, made the C-M diagram of the cluster for which they fitted a theoretical diagram. Around this diagram, bands of $0^m.1$, $0^m.2$ and $0^m.3$ width in B-V were drawn to investigate that particular width in which the ratio of member stars to non member stars is suitable. This means that most of the member stars of the cluster belong to the band but the number of non member stars is as small as possible. In Fig.2 a,b,c the cumulative frequency distribution can be seen for different width versus distance measured from the centre. The number of the stars in a circle of r radius (N(r)) comes from the

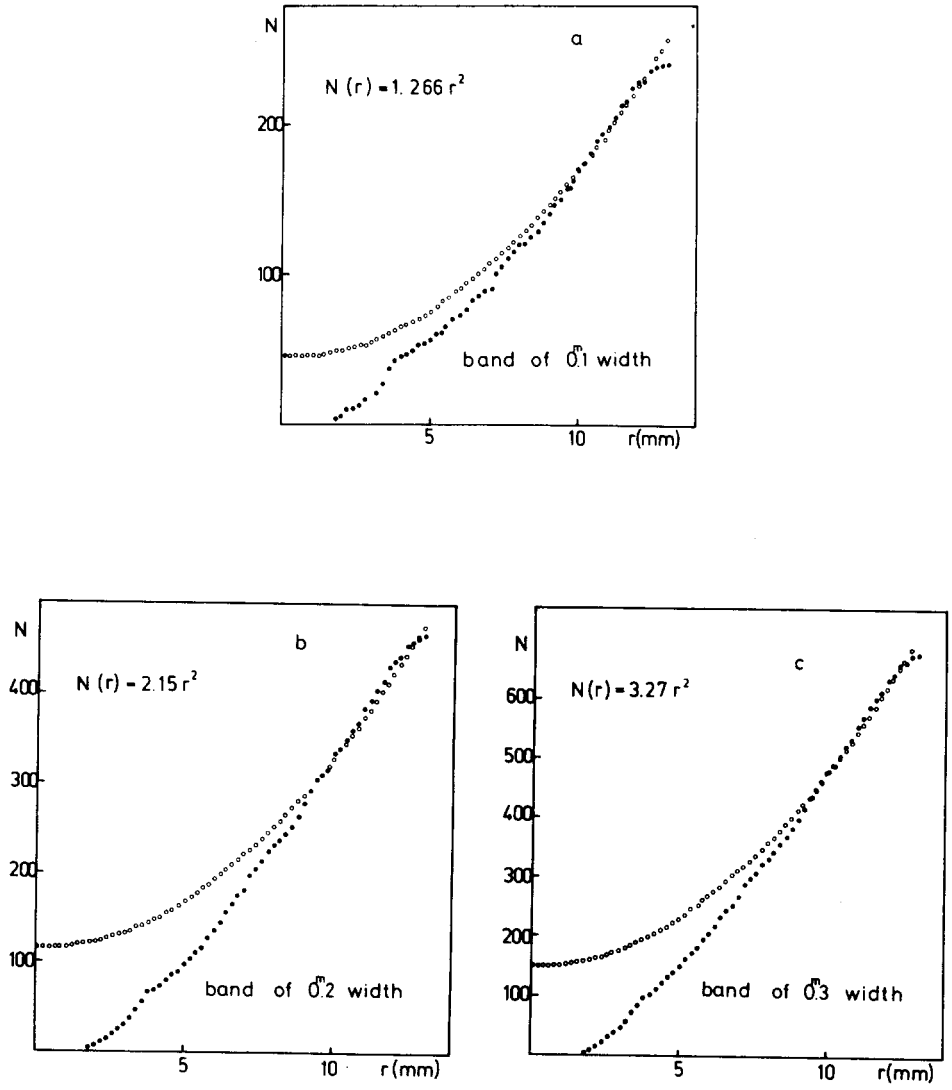

Fig. 2 a,b,c The cumulative frequency distributions for bands of $0^m.1$, $0^m.2$ and $0^m.3$ width in B-V.

number of member stars and background stars. Supposing uniform distribution of background stars, a parabola can be fitted for the outer part of the cumulative frequency distribution. According to the investigation the right width is around $0^m.2$. Adopting Cannon's result that the natural width of the C-M diagram of NGC 2420 is less than $0^m.1$ and taking the error of BV photometry to $0^m.1$, the final width of the band was chosen to be $0^m.15$.

c. The position of the measured stars in the Cartesian coordinate system on the plate can be found in the Table. The zero

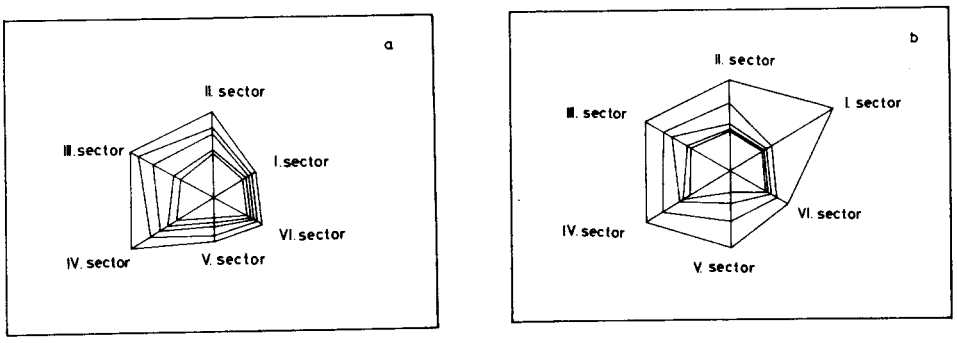

Fig. 3 a,b The equal density curves before the modification of the centre and after it.

point of the coordinate system is the star named II-1-20 by *West* (1967). As a first approximation this point was chosen for the centre of the cluster, but the equal density curves became asymmetrical. As a second approximation the arithmetical mean was used for the centre. After correction, the equal density curves are much more symmetrical (Fig. 3 a,b).

d. In accordance with Kholopov's method described in Paper I the surface density distribution was made for the whole cluster and for each subgroup. The curves concern the outermost part of the cluster (Fig. 4 a,b,c,d,e).

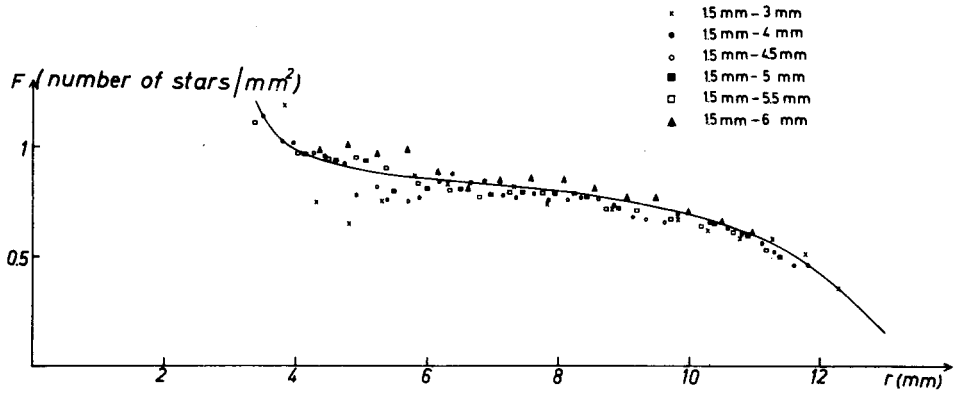

Fig. 4 a Density distribution curve for the whole cluster.

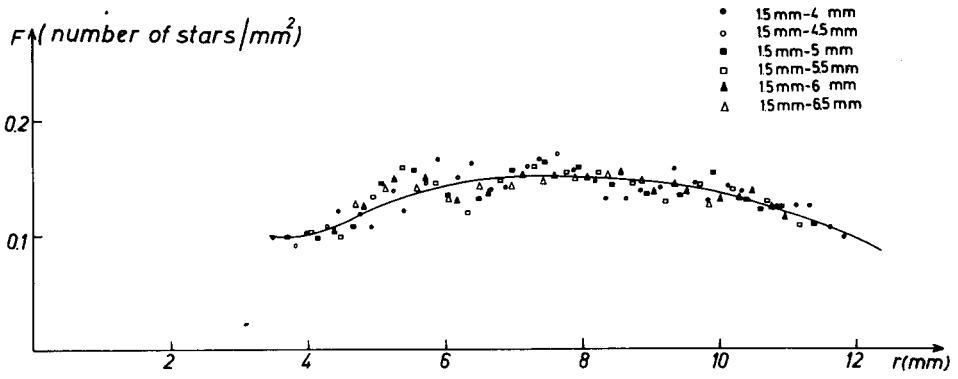

Fig. 4 b Density distribution curve for the A+B+C+E+F group.

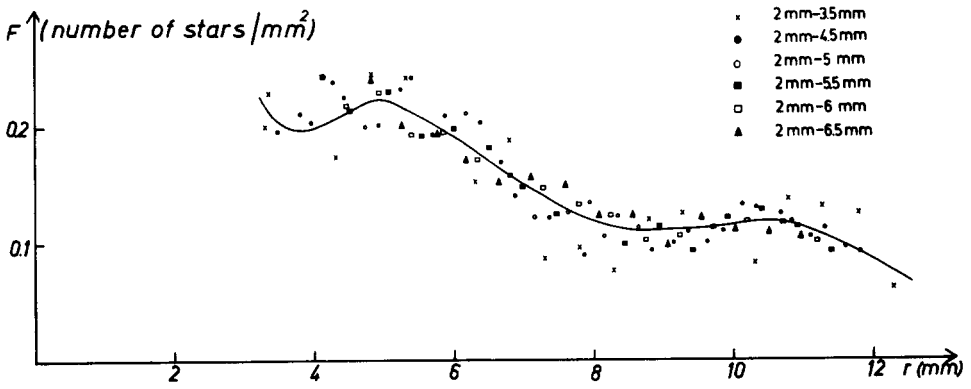

Fig. 4 c Density distribution curve for the G group.

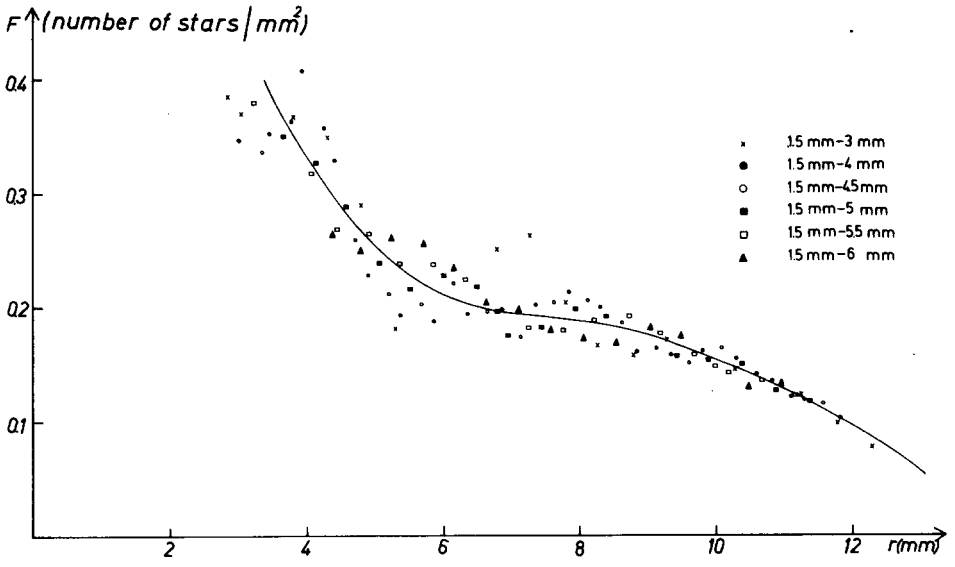

Fig. 4 d Density distribution curve for the H group.

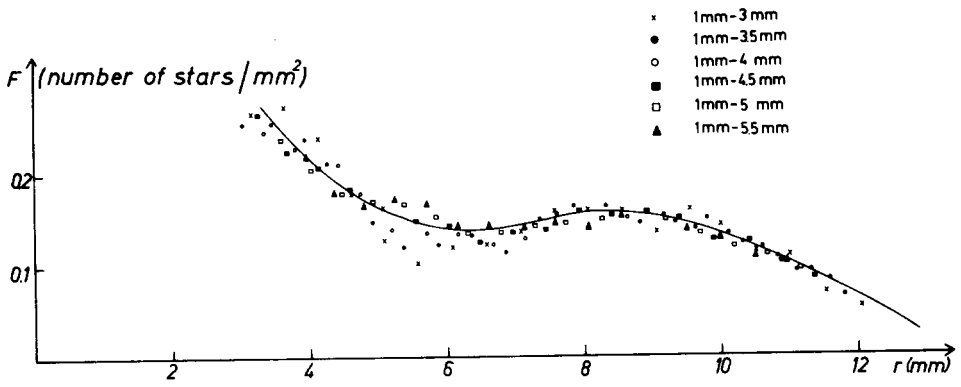

Fig. 4 e Density distribution curve for the D group.

DISCUSSION OF THE DENSITY DISTRIBUTIONS

In Paper I, selection of the members of the cluster was based on the proper motion of stars, but there are no proper motion measurements for the stars in the outer part of the cluster. To select the cluster members in the present case a band of suitable width was defined in B-V around the C-M diagram of the cluster. A comparison could be made between these two methods by deriving the densities for Cannon's stars selected by both criteria. The curves can be seen in Fig. 5. The curves made by two different methods are mostly the same within a σ error bar, but at that part where the density gradient is highest the curves are within two σ error bars. From these examinations the existence of the different density parts and the place of the inflexion point can be defined more or less exactly.

In Paper I the density distribution of stars in the centre of the cluster was discussed. Two different parts could be seen according to the change in the density gradient. The large negative density gradient of the inner dense part changes at a radius

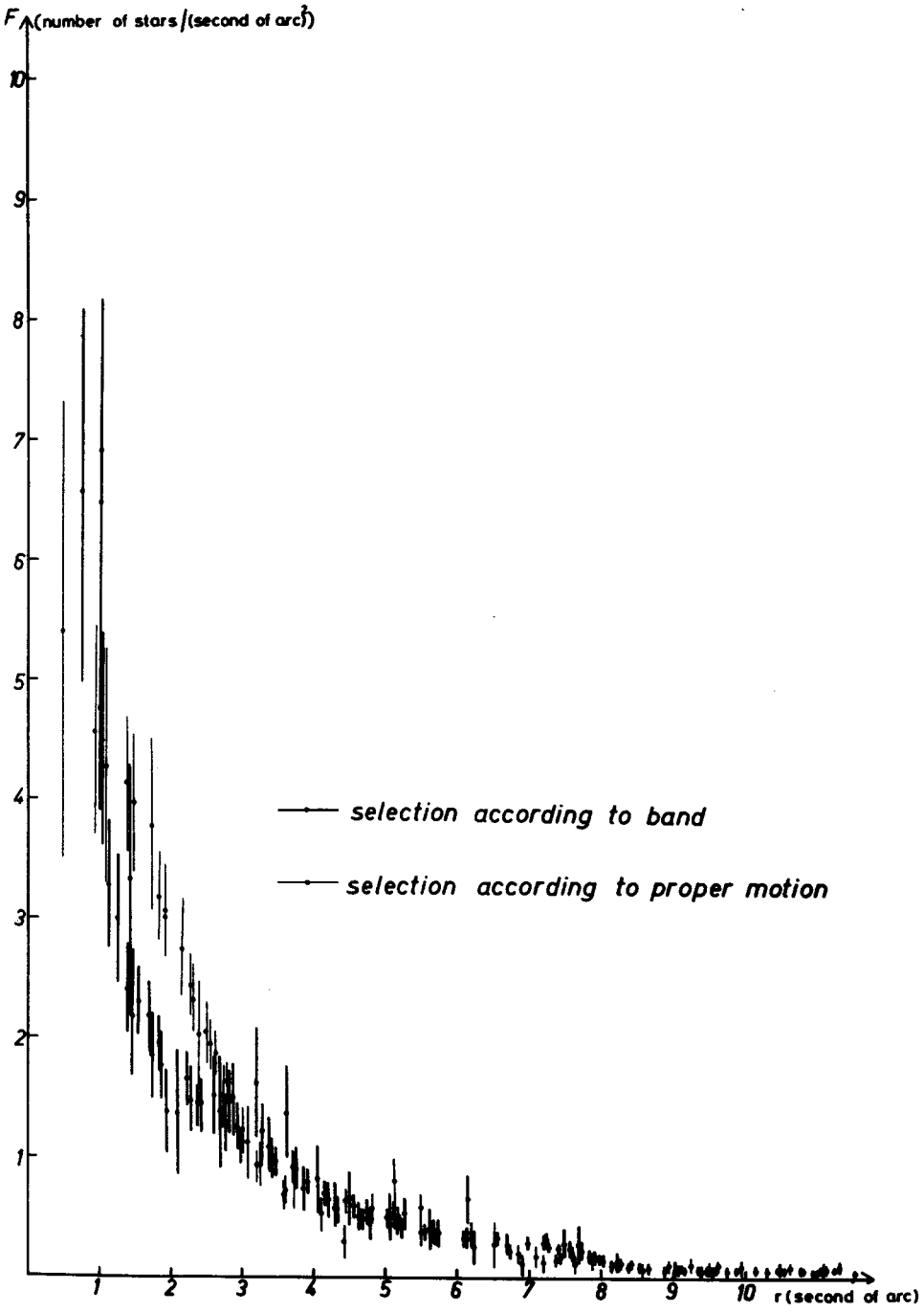

Fig. 5 Density distribution curves made by different methods.

of about 3!3 and continues with a less steep decline in the outer less dense part having a radius of 7!4.

The examination of density distribution is extended in this paper to 25′ from the centre using the band criteria for the selection. The density distribution of the whole cluster has a small but defined slope as far as about 18′. Around the central part of NGC 2420 can be seen the halo of very low density. At the A+B+C+E+F group of bright stars beyond about 7′ the cluster cannot be estimated. The curve for this group comes from the fluctuation of the background stars. The density distributions of the D,G and H groups have a defined slope except some lower local minimum. " Defined slope " means the existence of a halo of fainter stars. The inner part of greater density continues to 3.8 mm which is equal 7′17′′ taking into account the 115′′/mm scale of Schmidt plates. This result is almost the same as the value of the less dense part in Paper I. The border of the outer lower density part is 9.5 mm = 18′13′′. Using a distance of 2400 pc (*West*, 1967) for NGC 2420, the core of the cluster has a 5.1 pc radius, the halo of the cluster has 12.7 pc.

Salukvadze (1977) obtained a much higher value for the radius of the core and the halo but I believe it comes only from the fluctuation of the background stars.

A similar result has been obtained by *Archemashvili* (1979) for this cluster. For faint objects the mean radius of core is 5!5 (3.2 pc) and 15!5 (9 pc) for the halo. He got a 2!5 (1.4 pc) radius for the brightest stars: this value is consistent with our 3!3 (2.3 pc) data in Paper I. Taking into account the difference between the used distances the results are the same within 1 pc.

According to *Agekyan* and *Belozerova* (1979) the effective radius of the halo of the cluster is

$$R \sim 0.351\ N^{1/2} / D^{1/3}$$

Using N = 300 as the estimated number of member stars in NGC 2420 and D = 0.12/pc^3, the effective radius of the halo of NGC 2420 is R = 12.3 pc. D = 0.12/pc^3 is a general value. The density of the background stars at the present position of the cluster is considerably lower but during its lifetime this cluster crossed the galactic plane many times, where this effect was much stronger

than nowadays. The R = 12.3 pc effective radius means that the cluster seems to be stable against the irregular forces of its background stars.

The limiting radius of a cluster, because of the tidal force in the Galaxy, can be given by the following equation (*King*, 1962)

$$r_{lim} = R_p \ (M/3.5 \ M_g)^{1/3}$$

where M means the mass of the cluster, M_g the mass of Galaxy, and R_p the perigalactic distance of the cluster. Taking R_p = 8.6 kpc of "A" model from *Keenan* and *Innanen* (1974) and using N = 300 value for member of cluster as before and supposing 1 $M_\odot$ for each member star and 10^{11} $M_\odot$ for the mass of Galaxy, the limiting radius equal 8.2 pc for the NGC 2420 open cluster. Within this radius the cluster is stable whereas beyond it the stars evaporate because of the tidal force.

CONCLUSION

The NGC 2420 open cluster consists of a high density core with 5.1 pc radius and a lower density halo of 12.7 pc. Within the high density core there is a concentration of the brightest stars with 2.3 pc radius. The halo of the cluster seems to be stable against the irregular forces of the background stars and the inner part of halo from 5.1 pc to 8.2 pc is also stable against the tidal force. The outer part of the halo from 8.2 pc to 12.7 pc is not stable and is gradually destroyed by the tidal force.

ACKNOWLEDGEMENTS

I am indebted to Dr. B.A. Balázs for calling my attention to this problem and to Dr. L.G. Balázs for valuable discussions. I am grateful to Mrs. I. Kálmán and Mrs. I. Gál for their assistance in analysing the data.

Budapest - Szabadsághegy, September 7, 1982

REFERENCES

Agekyan,T.A., Belozerova,M.A. 1979, Astr.Zhu.56.9.
Archemashvili,V.M. 1979, Bull.Ac.Sci.Georg.93.No.2.333.
Artuhina,N.M.,Kholopov,P.N. 1966, Astr.Zhu.43.567.
Cannon,R.D.,Lloyd,C. 1970, M.N.R.A.S.150.279.
Keenan,D.W.,Innanen,K.A. 1974,Ap.J.189.205.
King,I. 1962, Astron.J.67.471.
Kholopov,P.N. 1953, Astr.Zhu.30.426.
Kholopov,P.N. 1968, Astr.Zhu.45.786.
McClure,R.D.,Forrester,W.T.,Gibson,J. 1974, Ap.J.189.409.
Paparó,M. 1977,Spatial structure of NGC 2420, in The role of star clusters in cosmogony and in the study of galactic structure, Ed.B.A.Balázs, Roland Eötvös Univ. p.47.
Salukvadze,G.N. 1977, Bull. Abastumansk.Astrofiz.Obs.48.135.
Shapley,H. 1916, Mt.W.Contr.117.
Trumpler,R.J. 1922, Allegheny Publ.,6.No.4.
West,F.R. 1967, Ap.J.Suppl.XIV.384,359.

Fig. 6 a Finding chart of the survey stars I.
East-northern part of the field

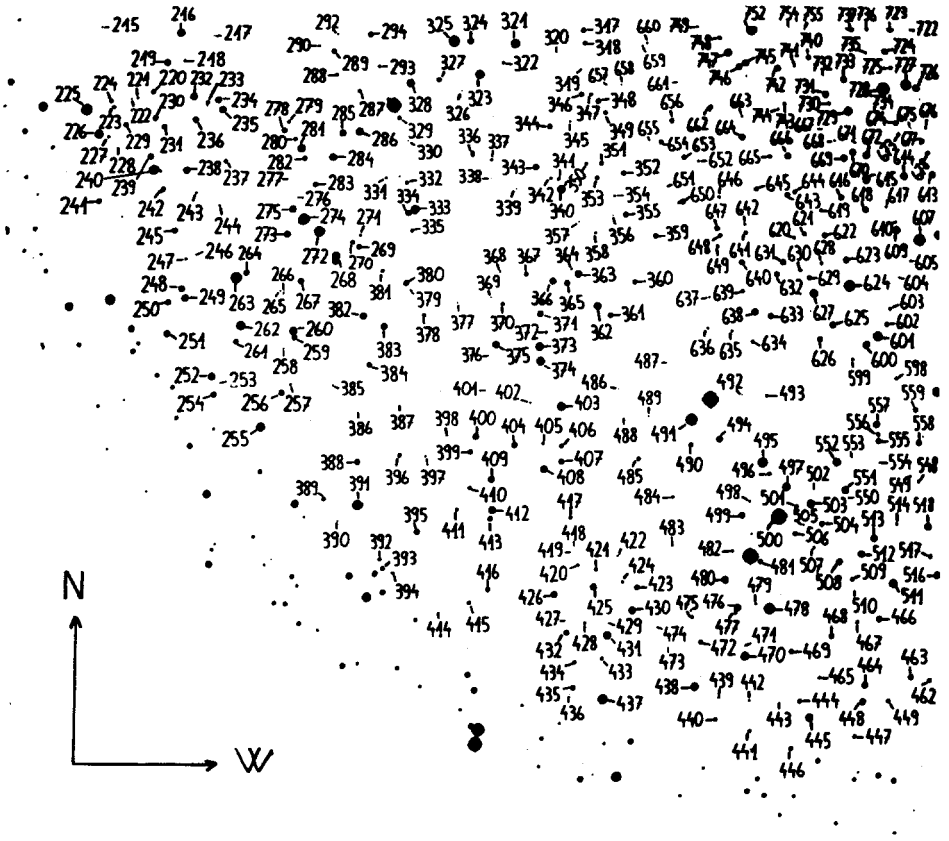

Fig. 6 b Finding chart of the survey stars II.
East-southern part of the field

Fig. 6 c Finding chart of the survey stars III.
South-western part of the field

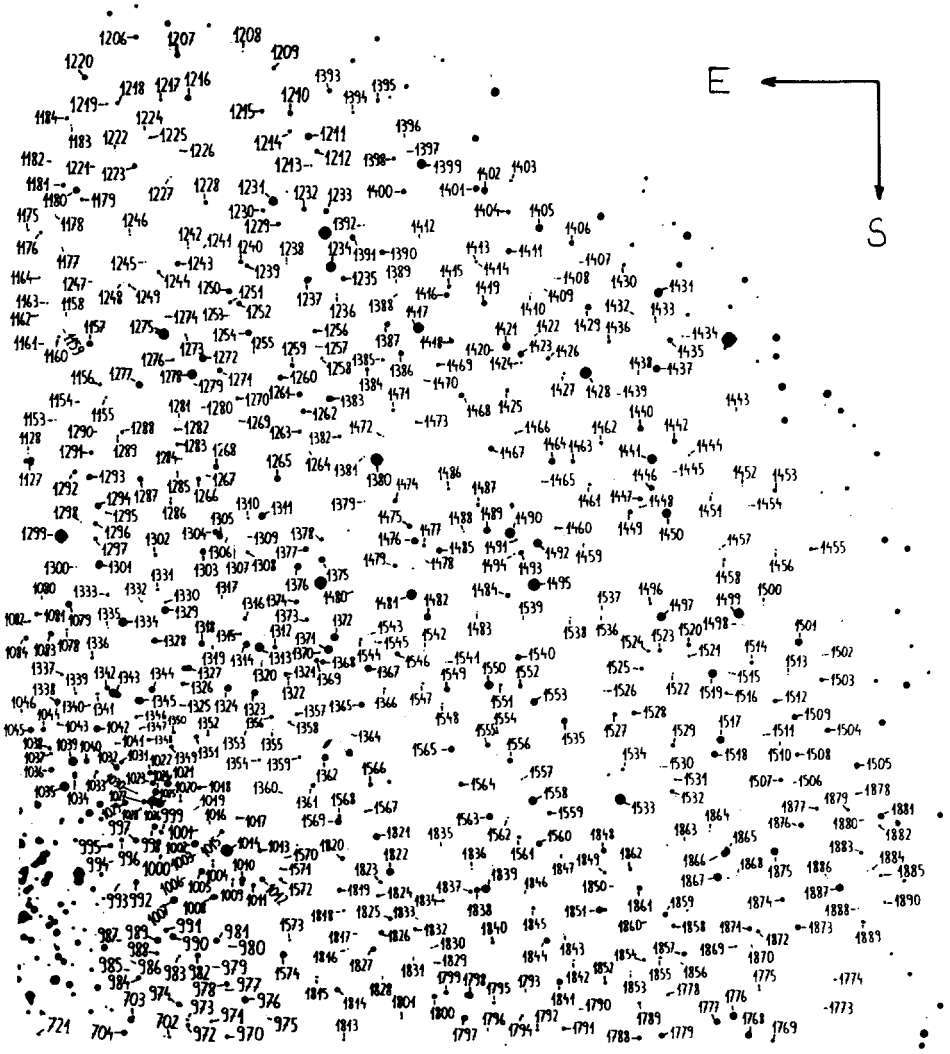

Fig. 6 d Finding chart of the survey stars IV.
West-northern part of the field

Table

No.	V	B-V	X	Y	No.	V	B-V	X	Y
1	17.54	0.31	-12.8	1.2	51	16.81	0.68	- 9.9	4.6
2	16.56	0.84	-12.4	1.2	52	14.26	0.70	-10.2	4.9
3	15.51	0.71	-12.1	1.2	53	16.21	1.18	-10.7	5.0
4	14.79	0.43	-12.0	0.9	54	16.36	0.88	-10.8	5.2
5	14.40	0.71	-11.5	0.8	55	17.43	0.89	-10.9	5.4
6	17.45	0.50	-10.9	0.6	56	15.17	0.98	-11.6	5.9
7	17.40	1.11	-10.8	0.4	57	15.71	1.00	-11.2	6.4
8	16.62	0.52	-10.4	0.5	58	14.98	0.44	-11.2	6.6
9	16.98	0.77	-10.2	0.6	59	17.07	0.30	-10.9	6.4
10	17.36	0.17	- 9.9	0.7	60	17.51	0.81	-10.6	6.4
11	15.28	0.25	-10.6	0.9	61*	16.20	0.22	-10.6	6.3
12	14.76	1.19	-10.8	1.0	62*	16.27	0.92	-10.5	6.4
13	13.86	0.58	-11.1	1.0	63	17.69	-	-10.1	5.5
14	15.17	0.87	-11.6	1.2	64	17.51	1.32	-10.0	5.9
15	16.83	0.43	-12.0	1.6	65	14.84	0.86	-10.0	6.1
16	14.90	0.83	-11.9	1.7	66	17.44	0.63	- 9.9	6.8
17	17.54	1.10	-11.5	1.6	67	16.85	0.39	-10.0	6.8
18	16.16	0.92	-11.5	1.4	68	16.79	0.45	-10.3	7.3
19	14.18	0.20	-11.3	1.6	69	17.60	-	- 9.8	8.1
20	17.06	0.76	-11.2	1.3	70	17.36	0.77	- 9.4	8.5
21	17.49	-	-10.5	1.1	71	16.73	0.64	- 9.3	7.6
22	17.51	0.67	-10.5	1.4	72	16.31	0.66	- 8.8	8.1
23	17.51	-	-10.8	1.3	73	14.90	0.64	- 8.8	8.6
24	16.53	0.45	-10.7	1.8	74	16.22	0.76	- 9.1	9.1
25	14.79	0.38	-11.0	2.0	75	13.44	0.80	- 8.9	9.3
26	15.55	0.67	-12.3	2.2	76	15.43	0.67	- 8.6	9.0
27	15.31	1.27	-12.5	2.3	77	15.91	0.62	- 8.6	9.3
28	14.25	0.59	-12.7	2.4	78	16.00	1.42	- 7.7	10.1
29	16.64	0.19	-11.1	2.5	79	15.48	0.90	- 7.1	10.4
30	14.56	0.51	-10.7	2.6	80	15.07	1.05	- 6.8	9.3
31	17.49	-	-10.2	3.0	81*	14.61	0.63	- 7.5	9.3
32	17.56	0.63	-10.4	3.1	82	16.51	0.60	- 7.8	9.3
33	14.15	0.81	-10.6	3.1	83	17.25	0.91	- 6.0	8.0
34	17.26	0.51	-10.9	3.1	84	14.71	0.45	- 6.3	7.8
35	17.36	1.17	-11.1	2.9	85	17.38	0.34	- 6.6	7.8
36	16.59	0.38	-11.3	2.9	86	16.01	0.53	- 7.1	7.4
37	17.13	-	-11.1	3.3	87	17.54	1.03	- 8.1	8.0
38	15.67	1.22	-10.9	3.6	88	14.35	0.71	- 8.0	7.8
39	17.18	0.88	-11.1	3.8	89	17.53	1.18	- 8.6	7.3
40	16.95	1.68	-11.1	4.0	90	17.42	1.25	- 8.8	7.3
41	17.11	0.78	-11.4	4.1	91	16.29	0.73	- 7.8	7.1
42	17.48	0.62	-11.7	3.9	92	12.30	0.39	- 6.1	7.1
43	15.02	0.41	-11.6	4.3	93	14.46	0.63	- 5.8	6.6
44	17.08	0.47	-12.0	4.5	94	14.87	0.55	- 5.8	6.3
45	15.99	0.28	-11.8	4.9	95	16.71	0.46	- 5.9	6.0
46	13.76	0.53	-11.2	4.8	96	15.52	0.65	- 6.6	5.9
47	17.47	1.13	-10.7	4.2	97	16.79	0.14	- 6.7	6.2
48	13.19	0.87	-10.6	3.8	98	11.97	0.45	- 8.0	6.7
49	17.61	0.69	-10.2	3.5	99	17.45	0.43	- 8.1	6.6
50	13.44	0.56	-10.1	3.9	100	15.90	0.80	- 8.3	6.6

Table (Cont.)

No.	V	B-V	X	Y	No.	V	B-V	X	Y
101*	16.40	0.77	- 9.3	6.6	151*	14.84	0.51	- 8.3	2.0
102	16.18	0.39	- 8.6	6.3	152*	11.84	0.87	- 8.0	2.1
103	13.29	0.32	- 8.5	6.2	153	17.27	0.80	- 7.5	2.5
104	16.00	0.87	- 8.5	5.9	154	14.23	0.52	- 7.5	2.7
105	17.22	1.12	- 9.2	5.9	155	15.53	0.80	- 6.2	3.1
106	15.31	0.78	- 9.6	5.8	156	11.16	0.15	- 5.2	3.1
107	17.65	0.83	- 9.4	5.8	157	17.50	0.62	- 5.0	2.9
108	15.13	0.57	- 9.0	5.5	158	14.62	0.26	- 5.0	2.8
109	17.00	0.67	- 9.3	5.1	159	12.97	0.33	- 5.4	2.3
110	17.63	0.67	- 9.4	4.6	160	17.20	0.56	- 6.3	2.4
111	17.57	0.43	- 9.1	4.6	161	15.33	1.29	- 6.3	2.1
112	15.44	0.62	- 8.8	4.5	162	16.71	0.42	- 6.1	2.1
113	17.49	0.88	- 8.7	4.7	163	15.71	0.69	- 5.9	2.1
114	17.36	0.59	- 8.6	5.2	164	16.17	0.51	- 5.4	2.0
115	11.60	0.42	- 8.3	4.9	165	17.09	0.26	- 5.6	1.8
116	16.08	0.98	- 8.3	4.6	166	16.82	0.53	- 6.4	1.4
117	15.95	0.33	- 8.4	4.2	167	17.73	-	- 6.8	1.2
118	16.80	0.62	- 8.1	4.2	168	16.91	1.71	- 7.2	1.4
119	17.67	-	- 8.2	4.3	169	15.82	1.01	- 7.8	1.4
120	17.42	0.11	- 7.8	4.6	170	15.19	0.54	- 8.3	1.1
121	17.30	0.85	- 7.0	5.5	171	16.66	0.67	- 8.8	1.5
122	14.54	0.72	- 6.5	5.4	172	17.06	0.63	- 9.0	1.5
123	14.24	0.62	- 5.5	5.4	173	16.48	0.76	- 9.0	1.3
124	17.05	0.58	- 5.4	5.1	174	17.33	0.55	- 9.3	1.4
125	16.07	0.54	- 5.5	4.8	175	16.86	0.38	- 9.5	1.4
126	17.77	0.81	- 5.6	4.7	176*	16.56	0.23	- 9.6	1.5
127	16.24	0.32	- 5.7	4.7	177*	16.82	0.19	- 9.6	1.6
128	16.47	0.60	- 6.0	4.9	178	16.04	0.83	- 9.1	0.9
129	16.19	0.70	- 6.0	5.0	179	17.30	1.01	- 9.3	0.3
130	15.11	0.76	- 6.9	4.8	180	12.41	0.48	- 9.0	0.0
131	16.38	1.20	- 6.8	4.7	181	16.42	0.36	- 8.4	0.7
132	17.46	0.34	- 6.5	4.8	182	17.55	0.66	- 8.3	0.9
133	17.70	0.75	- 6.4	4.4	183	16.08	0.71	- 7.6	0.9
134	17.24	1.49	- 5.7	4.1	184	13.72	0.49	- 6.7	0.2
135	17.22	0.50	- 5.3	3.5	185	16.70	0.59	- 6.6	0.5
136	17.51	0.79	- 5.7	3.5	186	16.47	0.32	- 5.7	0.5
137	15.96	0.72	- 6.3	3.8	187	17.61	1.10	- 5.4	0.7
138	17.34	0.47	- 6.6	3.5	188	15.11	0.74	- 5.2	0.4
139	17.49	0.92	- 7.0	4.1	189	13.85	1.31	- 5.0	- 0.1
140	16.79	1.31	- 7.2	3.9	190	12.81	1.14	- 5.3	- 0.4
141	15.94	0.74	- 7.9	3.7	191	17.76	0.61	- 5.5	- 0.1
142	17.30	0.11	- 8.1	3.8	192	15.17	0.79	- 5.9	- 0.7
143	16.18	0.56	- 8.6	3.9	193	13.67	0.52	- 6.6	- 0.4
144	17.49	0.69	- 8.6	3.5	194	15.95	0.74	- 6.7	- 0.2
145	14.54	0.67	- 9.1	3.8	195	17.47	0.66	- 7.0	- 0.1
146	16.75	0.58	- 9.7	3.7	196	17.56	0.63	- 7.1	- 0.1
147	16.81	0.39	- 9.6	3.5	197	16.71	0.94	- 7.2	- 0.1
148	15.70	0.33	- 9.6	3.1	198	15.41	0.63	- 7.0	- 0.4
149	16.22	0.52	- 9.3	2.3	199	17.57	0.76	- 6.8	- 0.8
150*	14.22	1.17	- 8.6	2.0	200	15.47	0.30	- 6.9	- 0.8

Table (Cont.)

No.	V	B-V	X	Y	No.	V	B-V	X	Y
201	15.90	0.52	- 7.6	- 0.6	251	14.98	0.53	-11.2	- 5.9
202	16.76	0.55	- 8.9	- 0.4	252	14.67	0.45	-10.5	- 6.5
203	15.18	0.75	- 9.9	- 0.9	253	17.50	1.43	-10.5	- 6.6
204	15.65	0.20	-10.0	- 1.1	254	15.55	0.81	-10.5	- 6.8
205	17.48	1.09	-10.1	- 1.3	255	13.06	1.02	- 9.9	- 7.2
206	16.66	0.54	-10.3	- 1.2	256	15.69	0.41	- 9.5	- 6.7
207	13.96	0.57	-10.5	- 1.1	257	17.57	0 29	- 9.4	- 6.6
208	17.01	0.09	-10.3	- 1.1	258	17.68	1.08	- 9.4	- 6.1
209	16.84	1.07	-10.6	- 1.0	259*	15.90	0.39	- 9.3	- 6.0
210	14.60	0.50	-11.6	- 0.8	260	14.00	0.51	- 9.3	- 5.9
211	17.30	0.51	-11.7	- 0.3	261	15.46	0.90	-10.2	- 6.0
212	15.91	1.53	-12.1	0.0	262	13.61	0.33	-10.1	- 5.8
213	16.58	0.80	-12.2	- 0.8	263	12.01	0.62	-10.1	- 5.1
214	17.49	0.60	-11.9	- 1.0	264	15.48	0.68	-10.0	- 5.0
215	17.39	1.29	-12.0	- 1.4	265	17.50	-	- 9.5	- 5.3
216	14.40	0.49	-10.8	- 1.5	266	17.24	0.67	- 9.4	- 5.3
217	17.61	0.58	-10.3	- 1.6	267	15.20	0.75	- 9.2	- 5.1
218	17.29	0.78	-10.8	- 2.0	268*	12.80	1.72	- 8.7	- 4.8
219	15.13	0.63	-11.0	- 2.0	269	15.13	1.20	- 8.4	- 4.7
220	16.14	0.55	-11.2	- 2.4	270	16.07	0.99	- 8.4	- 4.6
221	17.19	0.69	-11.5	- 2.5	271	16.57	1.64	- 8.3	- 4.5
222	17.68	0.78	-11.6	- 2.5	272	11.87	1.01	- 8.9	- 4.5
223	15.86	1.51	-11.8	- 2.6	273	15.03	0.50	- 9.4	- 4.5
224	15.65	1.15	-11.8	- 2.5	274	11.96	0.58	- 9.1	- 4.3
225	11.81	1.01	-12.2	- 2.6	275	14.39	0.68	- 9.3	- 4.1
226	13.75	0.75	-12.0	- 3.0	276	17.65	1.29	- 9.3	- 3.9
227	17.08	0.74	-11.9	- 3.0	277	17.54	1.16	- 9.3	- 3.7
228	17.13	0.45	-11.8	- 3.1	278	15.95	0.78	- 9.3	- 3.0
229	16.33	0.45	-11.7	- 2.8	279	17.07	0.59	- 9.3	- 2.8
230	15.94	0.40	-11.2	- 2.8	280	17.01	0.43	- 9.2	- 3.1
231	16.53	0.18	-11.1	- 2.9	281	13.96	0.56	- 9.1	- 3.2
232	14.68	0.51	-10.7	- 2.5	282	16.36	0.26	- 9.0	- 3.4
233	16.75	0.87	-10.4	- 2.6	283	16.20	0.33	- 8.9	- 3.8
234	15.07	0.57	-10.3	- 2.5	284	14.19	0.62	- 8.7	- 3.4
235	15.02	0.31	-10.2	- 2.7	285	14.78	0.70	- 8.5	- 3.1
236	15.60	0.52	-10.6	- 2.8	286	14.39	0.53	- 8.3	- 3.1
237	16.50	0.57	-10.2	- 3.4	287	16.84	0.72	- 8.2	- 2.5
238	14.89	0.43	-10.8	- 3.5	288	16.65	0.55	- 8.6	- 4.2
239	15.52	0.42	-11.3	- 3.3	289	15.99	0.60	- 8.6	- 1.9
240	13.01	0.54	-11.2	- 3.5	290	17.03	0.62	- 8.8	- 1.8
241	15.98	0.45	-12.1	- 3.9	291	16.76	0.50	- 9.3	- 1.3
242*	16.05	0.83	-11.1	- 3.8	292	17.60	-	- 8.5	- 1.7
243	17.49	0.17	-10.7	- 3.9	293	17.42	0.63	- 7.9	- 2.1
244	17.45	0.50	-10.3	- 4.1	294	15.86	0.36	- 8.0	- 1.7
245	15.30	0.84	-11.0	- 4.4	295	16.77	0.11	- 8.0	- 1.4
246	17.29	0.79	-10.8	- 4.7	296	17.66	0.33	- 8.1	- 1.2
247	17.10	0.65	-10.8	- 4.8	297	17.51	1.43	- 8.2	- 0.7
248	15.39	0.27	-10.9	- 5.2	298	17.02	1.18	- 7.7	- 1.3
249	14.54	0.48	-10.9	- 5.4	299	17.19	0.20	- 7.5	- 1.1
250	15.48	0.69	-11.1	- 5.4	300	13.86	0.48	- 7.3	- 1.4

Table (Cont.)

No.	V	B-V	X	Y	No.	V	B-V	X	Y
301	15.29	1.52	- 7.1	- 1.2	351	16.66	0.29	- 4.8	- 3.6
302	15.85	0.78	- 6.5	- 1.4	352	15.93	0.43	- 4.3	- 3.8
303	15.84	0.61	- 6.1	- 1.3	353	16.88	0.19	- 4.8	- 3.8
304	17.55	-	- 5.9	- 1.3	354	17.52	0.50	- 4.6	- 4.1
305	17.29	0.74	- 5.8	- 1.4	355	15.14	1.11	- 4.4	- 4.4
306	15.03	0.89	- 5.8	- 1.5	356	17.62	0.64	- 4.6	- 4.4
307	16.50	0.18	- 5.3	- 1.2	357	17.76	-0.01	- 5.2	- 4.4
308	16.16	0.16	- 5.3	- 0.8	358	17.43	0.41	- 4.9	- 4.6
309	15.23	0.71	- 5.1	- 0.8	359	16.24	0.18	- 4.0	- 4.7
310	17.30	1.42	- 4.9	- 0.9	360	16.71	0.14	- 4.3	- 5.3
311	17.55	1.06	- 4.7	- 0.4	361	16.15	0.42	- 4.7	- 5.8
312	16.91	-1.60:	- 4.5	- 0.7	362	14.34	0.44	- 4.9	- 5.7
313	13.55	0.91	- 4.3	- 1.0	363	14.60	0.46	- 5.1	- 5.2
314	17.54	0.51	- 5.0	- 1.2	364	17.70	0.56	- 5.2	- 5.1
315	15.87	0.29	- 4.5	- 1.5	365	15.63	0.42	- 5.3	- 5.3
316	17.39	0.67	- 4.9	- 1.6	366	15.20	0.62	- 5.5	- 5.3
317	16.20	0.55	- 5.0	- 1.8	367	16.56	0.41	- 5.9	- 5.2
318	16.76	0.46	- 4.9	- 2.0	368	17.62	0.50	- 6.3	- 5.1
319	17.27	1.13	- 4.9	- 2.3	369	17.55	0.90	- 6.4	- 5.4
320	17.60	1.11	- 5.3	- 2.1	370	17.12	0.22	- 6.3	- 5.6
321	14.06	-0.09	- 6.0	- 1.9	371	14.81	0.99	- 5.7	- 5.8
322	17.33	0.41	- 6.1	- 2.1	372	16.96	0.73	- 5.6	- 6.0
323	12.98	0.88	- 6.5	- 2.3	373	13.85	0.52	- 5.7	- 6.2
324	15.10	0.54	- 6.6	- 1.8	374	14.04	0.28	- 5.7	- 6.4
325	12.16	0.42	- 6.8	- 1.8	375	14.80	0.58	- 6.3	- 6.1
326	17.58	-	- 6.9	- 2.5	376	17.18	1.51	- 6.4	- 6.3
327	16.50	0.30	- 7.1	- 2.3	377	17.21	1.11	- 6.9	- 5.6
328	14.39	0.21	- 7.5	- 2.4	378	16.58	0.48	- 7.4	- 5.7
329	16.93	0.46	- 7.7	- 2.9	379	17.06	0.76	- 7.6	- 5.3
330	17.48	1.37	- 7.5	- 3.2	380	15.68	0.14	- 7.6	- 5.2
331	17.53	0.67	- 7.9	- 3.7	381	16.95	0.72	- 8.0	- 5.0
332	16.31	0.82	- 7.6	- 3.8	382	15.08	0.19	- 8.3	- 5.6
333*	12.92	1.12	- 7.5	- 4.2	383	15.05	0.47	- 8.0	- 5.9
334*	15.73	0.52	- 7.6	- 4.2	384	15.69	0.77	- 8.3	- 6.4
335	16.96	0.40	- 7.5	- 4.5	385	17.34	0.45	- 8.8	- 6.6
336	16.26	0.22	- 6.6	- 3.4	386	17.59	0.94	- 8.4	- 7.0
337	17.24	0.84	- 6.3	- 3.5	387	17.49	1.47	- 8.9	- 6.9
338	17.55	-	- 6.4	- 3.8	388	15.93	0.28	- 8.4	- 7.7
339	17.35	1.28	- 6.0	- 4.0	389	16.53	0.34	- 8.9	- 8.2
340	14.04	0.46	- 5.3	- 4.0	390	17.52	0.21	- 8.8	- 8.5
341	16.79	0.75	- 5.3	- 3.9	391	12.64	0.58	- 8.5	- 8.3
342	16.94	1.04	- 5.5	- 3.8	392	17.02	0.49	- 8.2	- 9.1
343	15.72	0.15	- 5.7	- 3.7	393	16.20	0.76	- 8.1	- 9.2
344	15.84	0.55	- 5.5	- 3.1	394	17.56	0.11	- 8.0	- 9.3
345	17.49	0.88	- 5.2	- 3.1	395	15.91	0.38	- 7.6	- 8.7
346	15.76	0.82	- 5.1	- 2.6	396	16.39	0.66	- 7.8	- 7.6
347	17.00	0.51	- 4.9	- 2.6	397	17.08	1.14	- 7.5	- 7.7
348	16.06	0.57	- 4.8	- 2.7	398	17.10	0.88	- 7.1	- 7.4
349	16.77	0.41	- 4.7	- 3.0	399	15.83	0.77	- 6.8	- 7.7
350	17.07	0.43	- 5.0	- 3.6	400	15.78	-0.27:	- 6.7	- 7.4

Table (Cont.)

No.	V	B-V	X	Y	No.	V	B-V	X	Y
401	17.68	0.93	- 6.5	- 6.8	451	17.16	0.40	0.3	-12.0
402*	17.69	0.52	- 5.9	- 7.0	452	17.82	0.58	0.9	-11.4
403	13.35	0.91	- 5.5	- 7.1	453	17.19	0.66	1.6	-11.4
404	15.56	0.41	- 6.1	- 7.6	454	16.61	0.81	1.8	-11.6
405	16.69	0.70	- 5.7	- 7.6	455	14.79	0.36	2.7	-10.8
406	16.16	0.29	- 5.5	- 7.6	456	17.54	0.24	2.4	-10.7
407	15.58	0.70	- 5.5	- 7.8	457	15.14	0.68	2.3	-11.0
408	14.67	0.47	- 5.7	- 7.9	458	11.49	0.12	1.6	-10.8
409	14.73	0.47	- 6.5	- 8.1	459	17.50	0.68	1.5	-10.5
410	16.47	0.82	- 6.8	- 8.1	460	17.62	0.28	0.3	-10.6
411	16.69	0.76	- 7.0	- 8.5	461	16.78	0.60	0.3	-10.8
412	14.47	0.65	- 6.5	- 8.5	462	16.88	-0.06	- 0.3	-11.1
413	16.06	0.75	- 6.6	- 8.6	463	15.91	0.50	- 0.6	-11.1
414	17.42	1.23	- 7.3	- 9.8	464	15.52	0.44	- 1.2	-11.1
415	16.78	0.21	- 6.9	- 9.8	465	17.03	0.94	- 1.9	-11.0
416	15.94	0.30	- 6.6	- 9.6	466	15.24	0.94	- 1.0	-10.2
417	16.02	1.54	- 5.3	- 8.6	467	16.66	0.87	- 1.3	-10.2
418	17.19	1.48	- 5.3	- 9.0	468	16.27	0.21	- 1.7	-10.4
419	17.50	0.93	- 5.3	- 9.1	469	16.31	0.78	- 2.3	-10.6
420	17.43	0.40	- 5.3	- 9.3	470	13.63	0.78	- 3.0	-10.7
421	16.39	0.85	- 5.0	- 9.3	471	17.57	0.88	- 3.0	-10.5
422	17.00	1.12	- 4.7	- 9.1	472	16.18	0.91	- 3.6	-10.4
423	16.04	0.50	- 4.4	- 9.6	473	17.51	-	- 3.9	-10.4
424	17.13	0.37	- 4.7	- 9.6	474	17.57	1.13	- 4.3	-10.1
425	15.10	0.39	- 5.1	- 9.6	475	17.06	0.12	- 3.8	-10.1
426	15.10	0.43	- 5.7	- 9.7	476	14.59	0.79	- 3.1	-10.0
427	17.29	0.93	- 5.5	-10.1	477*	16.57	0.67	- 3.1	-10.1
428	16.63	0.87	- 5.2	-10.1	478	12.27	0.56	- 2.6	-10.0
429	17.49	0.78	- 4.9	-10.1	479	17.09	1.40	- 2.8	-10.0
430	14.65	0.42	- 4.6	-10.0	480	14.40	0.87	- 3.2	- 9.5
431	13.69	0.95	- 4.9	-10.3	481*	14.97	2.02	- 2.7	- 9.3
432	16.09	0.22	- 5.5	-10.2	482	16.75	0.78	- 3.1	- 9.2
433	16.87	0.46	- 5.0	-10.6	483	17.31	0.67	- 4.0	- 9.1
434	16.62	0.65	- 5.4	-10.6	484	17.25	0.16	- 3.9	- 8.4
435	16.08	0.54	- 5.4	-11.0	485	16.72	0.29	- 4.4	- 7.8
436	17.59	-	- 5.5	-11.1	486	17.40	0.94	- 4.7	- 6.8
437	13.26	0.49	- 5.0	-11.2	487	17.61	0.66	- 4.0	- 6.6
438	13.62	1.02	- 3.7	-11.1	488	17.65	0.80	- 4.6	- 7.2
439	17.64	0.25	- 3.4	-11.3	489	17.11	0.94	- 4.2	- 7.2
440	17.07	0.38	- 3.4	-11.6	490	16.46	0.85	- 3.7	- 7.7
441	16.86	0.67	- 2.9	-11.7	491	11.93	0.58	- 3.6	- 7.3
442	17.88	-0.08	- 2.9	-11.3	492	17.62	0.39	- 2.8	- 7.0
443	17.85	-	- 2.4	-11.3	493	17.38	0.21	- 2.5	- 7.0
444	16.22	0.63	- 2.2	-11.3	494	15.49	0.58	- 3.2	- 7.6
445	14.49	0.64	- 2.0	-11.6	495	13.12	0.48	- 2.6	- 8.0
446	16.69	0.43	- 2.3	-12.0	496	16.88	0.72	- 2.5	- 8.1
447	16.53	0.87	- 1.4	-11.9	497	14.05	0.59	- 2.3	- 8.3
448	15.52	0.18	- 1.3	-11.3	498	17.46	0.20	- 2.8	- 8.5
449	17.04	0.30	- 0.9	-11.4	499	15.58	0.33	- 2.9	- 8.7
450	17.66	0.50	- 0.2	-11.2	500	11.95:	-1.25:	- 2.4	- 8.7

Table (Cont.)

No.	V	B-V	X	Y	No.	V	B-V	X	Y
501	16.41	0.95	- 2.1	- 8.6	551	14.07	1.16	- 1.4	- 8.4
502	17.65	0.36	- 1.9	- 8.4	552	13.55	1.23	- 1.6	- 8.0
503	14.15	0.55	- 2.0	- 8.6	553	17.47	0.92	- 1.3	- 8.0
504	16.41	0.30	- 1.8	- 8.9	554	17.49	0.87	- 0.9	- 8.1
505	17.43	0.80	- 2.0	- 8.9	555	15.48	0.79	- 0.9	- 7.7
506	16.38	0.89	- 2.2	- 9.0	556	16.82	0.55	- 1.0	- 7.6
507	17.36	-	- 1.8	- 9.2	557	15.29	0.42	- 1.0	- 7.4
508	14.76	-	- 1.6	- 9.4	558	15.82	0.37	- 0.3	- 7.7
509	17.23	0.05	- 1.3	- 9.6	559	16.30	0.84	- 0.3	- 7.2
510	17.57	-	- 1.5	- 9.8	560	13.16	0.94	- 0.1	- 7.1
511	13.85	0.97	- 0.8	- 9.7	561	17.49	-	0.1	- 6.9
512	15.29	0.61	- 1.3	- 9.3	562	15.95	0.56	0.0	- 6.7
513	14.64	0.78	- 1.0	- 9.1	563	17.71	0.62	0.5	- 6.5
514	17.33	0.45	- 0.7	- 8.9	564	14.44	0.75	0.9	- 6.3
515	17.45	0.82	- 0.2	- 9.8	565	17.25	1.13	1.2	- 6.3
516	15.38	0.13	- 0.1	- 9.6	566	16.95	0.59	2.0	- 6.3
517	17.07	0.39	- 0.2	- 9.3	567	14.07	0.94	2.5	- 6.4
518	14.84	0.43	- 0.2	- 9.0	568	16.46	0.49	2.9	- 6.9
519	15.05	0.39	0.0	- 8.7	569	14.52	0.49	3.1	- 6.5
520	17.56	0.76	0.0	-10.0	570	16.90	0.37	2.9	- 6.3
521	17.79	-	0.3	- 9.1	571	14.94	0.53	3.0	- 5.8
522	14.60	0.45	0.5	- 8.9	572	17.71	-	2.8	- 5.8
523	13.13	0.45	1.2	- 8.6	573	16.58	0.51	3.1	- 5.4
524	16.62	0.95	1.6	- 9.0	574	16.75	0.54	3.1	- 5.3
525	17.08	0.49	0.8	- 9.4	575	15.96	0.52	2.4	- 5.4
526	15.99	0.62	0.7	- 9.6	576	16.85	0.70	2.3	- 5.2
527	16.73	0.78	0.5	- 9.8	577	14.63	0.36	1.9	- 4.7
528	17.04	-0.02	0.5	-10.0	578	16.18	0.56	1.7	- 4.6
529	15.47	0.37	0.8	-10.1	579	16.93	0.32	1.7	- 5.0
530	17.13	0.66	1.3	- 9.8	580	17.27	0.34	1.9	- 5.1
531*	11.70	0.93	2.0	- 9.7	581	16.74	0.83	1.9	- 5.2
532	16.86	0.82	2.1	- 9.6	582	17.33	0.51	1.7	- 5.3
533	17.51	0.57	2.2	-10.0	583	12.60	0.65	1.8	- 5.8
534	17.17	0.81	2.9	-10.0	584	17.45	1.06	2.2	- 6.1
535	16.38	0.79	2.5	- 9.5	585	13.60	0.45	1.5	- 6.0
536	13.83	0.94	2.7	- 8.8	586	17.76	0.54	1.4	- 5.7
537	16.63	0.36	2.1	- 8.6	587	14.95	0.39	1.2	- 5.6
538	16.59	0.89	2.5	- 8.1	588	17.15	0.35	1.2	- 5.3
539	16.53	0.24	2.2	- 8.0	589	16.19	0.54	1.1	- 5.2
540	17.56	1.19	1.9	- 8.3	590	15.17	1.28	0.8	- 5.1
541	14.07	0.76	2.2	- 7.4	591	17.75	0.72	1.0	- 4.9
542	13.53	0.38	2.4	- 7.1	592	17.31	0.72	1.1	- 4.8
543	17.50	0.20	2.0	- 7.2	593	15.84	0.33	1.1	- 4.6
544	16.71	1.17	1.6	- 7.6	594	17.36	0.54	0.8	- 4.4
545	17.40	0.05	0.9	- 7.9	595	17.57	0.47	0.5	- 5.0
546	15.43	0.41	0.5	- 7.5	596	16.65	0.95	0.2	- 5.3
547	12.84	0.82	0.2	- 7.7	597	17.46	0.75	0.0	- 6.3
548	16.83	0.83	- 0.4	- 8.3	598	16.88	0.79	- 0.6	- 6.8
549	17.39	0.51	- 0.5	- 8.2	599	17.02	0.73	- 1.2	- 6.5
550	17.38	1.37	- 1.4	- 8.5	600	14.42	0.66	- 1.0	- 6.3

Table (Cont.)

No.	V	B-V	X	Y	No.	V	B-V	X	Y
601	13.01	0.78	- 0.8	- 6.2	651	17.50	-	- 3.9	- 4.0
602	16.54	0.19	- 0.7	- 6.0	652	17.23	0.68	- 4.3	- 3.6
603	16.92	0.78	- 0.7	- 5.8	653	16.31	0.84	- 3.5	- 3.5
604	17.56	1.17	- 0.5	- 5.3	654	16.62	0.10	- 3.8	- 3.3
605	17.60	-	- 0.2	- 5.1	655	17.52	-	- 4.0	- 3.3
606	13.10	0.88	0.1	- 4.8	656	15.87	0.74	- 3.7	- 3.0
607	12.07	0.52	- 0.2	- 4.9	657	17.75	0.79	- 4.6	- 2.5
608	-	-	-	-	658	17.47	0.87	- 4.4	- 2.5
609	14.59	0.22	- 0.5	- 4.7	659	17.37	0.98	- 4.1	- 2.0
610	16.81	1.48	- 0.5	- 4.6	660	17.25	0.78	- 4.0	- 1.9
611	17.42	1.15	0.2	- 4.1	661	17.48	1.09	- 3.6	- 2.4
612	16.45	0.50	0.2	- 4.0	662	15.50	0.74	- 3.1	- 2.9
613	15.05	0.58	0.1	- 3.9	663	17.46	1.02	- 2.7	- 3.0
614	14.62	0.63	- 0.4	- 4.0	664	15.02	0.71	- 2.7	- 3.2
615	13.63	1.04	- 0.9	- 4.0	665	16.97	0.52	- 2.3	- 3.6
616	15.66	0.54	- 1.3	- 4.2	666	15.22	0.39	- 2.0	- 3.6
617	17.60	0.45	- 0.7	- 4.3	667	17.47	0.86	- 1.5	- 3.2
618	15.17	0.70	- 0.9	- 4.4	668	17.40	0.71	- 1.3	- 3.3
619	17.19	0.49	- 1.6	- 4.4	669	15.24	0.02	- 1.2	- 3.6
620	17.37	0.30	- 2.0	- 4.8	670	15.34	0.25	- 1.1	- 3.6
621	16.73	0.89	- 1.9	- 4.7	671	17.20	1.23	- 1.0	- 3.4
622	15.98	0.58	- 1.6	- 4.7	672	14.61	0.45	- 0.9	- 3.6
623	14.98	0.75	- 1.2	- 5.1	673	17.09	0.38	- 0.4	- 3.3
624	11.80	0.90	- 1.2	- 5.5	674	16.13	0.33	- 0.5	- 3.2
625	15.07	0.37	- 1.5	- 6.1	675	17.14	0.42	- 0.2	- 3.3
626	15.87	0.46	- 1.7	- 6.3	676	17.11	0.58	0.0	- 3.2
627	13.57	1.00	- 1.7	- 5.5	677	14.99	0.05	- 0.1	- 3.4
628	17.47	-0.05	- 1.6	- 5.1	678	16.63	0.73	0.0	- 3.6
629	16.61	0.41	- 1.8	- 5.3	679	17.17	1.27	0.2	- 3.6
630	16.88	0.74	- 2.0	- 5.2	680	17.49	0.85	0.9	- 3.8
631	15.70	0.40	- 2.2	- 5.1	681	14.45	0.71	1.5	- 3.9
632	15.71	0.57	- 2.3	- 5.3	682	17.50	1.21	1.7	- 4.1
633	15.83	0.67	- 2.4	- 5.9	683	11.35	0.56	2.1	- 4.1
634	16.73	1.03	- 2.6	- 6.2	684	17.44	0.62	2.0	- 4.3
635	17.54	0.37	- 3.0	- 6.1	685	16.46	0.47	2.8	- 3.9
636	17.47	0.52	- 3.3	- 6.0	686	15.41	0.92	2.9	- 4.4
637	17.09	1.04	- 3.3	- 5.5	687	17.26	1.15	3.1	- 4.4
638	15.05	0.51	- 2.6	- 5.8	688	16.77	0.16	3.2	- 4.2
639	16.74	0.44	- 2.8	- 5.5	689	17.03	0.56	3.0	- 3.5
640	15.79	0.59	- 2.8	- 5.1	690	14.44	0.20	3.2	- 3.3
641	16.92	0.31	- 2.7	- 4.7	691	13.39	0.57	3.1	- 3.2
642	17.50	0.43	- 2.7	- 4.5	692	16.49	0.44	2.1	- 3.4
643	16.06	0.23	- 2.0	- 4.1	693	17.66	1.22	2.1	- 3.1
644	16.50	0.54	- 2.0	- 4.1	694	17.38	1.16	2.4	- 3.1
645	16.08	1.23	- 2.5	- 4.1	695	17.53	0.68	2.4	- 2.8
646	17.31	0.38	- 3.1	- 4.1	696	15.46	0.36	2.7	- 2.6
647	15.72	1.13	- 3.1	- 4.6	697	17.75	0.44	3.0	- 2.5
648	16.28	0.83	- 3.1	- 4.7	698	16.22	0.42	2.5	- 2.3
649	17.19	0.57	- 3.1	- 4.8	699	17.43	0.56	2.4	- 2.2
650	15.36	0.63	- 3.6	- 4.2	700*	13.84	1.09	2.5	- 2.0

Table (Cont.)

No.	V	B-V	X	Y	No.	V	B-V	X	Y
701*	15.83	1.46	2.6	- 2.1	751	16.67	0.37	- 3.0	- 1.5
702*	16.89	0.32	2.3	- 1.8	752	12.37	0.48	- 2.5	- 1.8
703	14.45	0.64	1.8	- 1.5	753	11.27	1.36	- 2.2	- 1.5
704	14.43	1.39	1.7	- 1.7	754	17.35	1.42	- 1.9	- 1.8
705	16.42	0.40	2.0	- 1.9	755	17.13	1.33	- 1.8	- 1.8
706	15.18	0.32	2.0	- 2.1	756*	15.17	0.90	- 1.9	- 1.2
707	14.55	0.48	2.0	- 2.2	757	17.08	0.85	- 1.9	- 1.0
708	14.67	0.53	1.6	- 2.6	758	17.35	1.08	- 2.9	- 1.0
709*	14.07	0.17	1.7	- 3.1	759	17.37	1.31	- 3.1	- 1.1
710*	15.12	0.73	1.5	- 3.1	760	15.32	1.56	- 3.3	- 0.9
711*	12.97	1.46	0.5	- 3.1	761	17.03	1.27	- 3.4	- 1.1
712*	14.82	0.67	0.4	- 3.1	762	16.85	0.84	- 3.9	- 1.0
713	15.13	0.57	0.8	- 2.9	763	16.80	0.45	- 3.5	- 0.6
714	16.71	0.70	0.9	- 2.9	764	17.48	0.74	- 3.5	- 0.4
715	17.29	1.15	0.5	- 2.8	765	16.70	0.50	- 3.4	- 0.4
716	14.77	0.33	0.5	- 2.5	766	17.27	0.79	- 3.3	- 0.5
717	13.47	0.45	0.3	- 2.3	767	17.59	1.23	- 2.7	- 0.3
718	15.94	0.46	0.6	- 2.0	768	16.38	0.92	- 3.2	- 0.1
719	16.92	0.42	1.0	- 2.0	769	16.93	0.66	- 3.6	- 0.1
720	16.40	0.63	1.3	- 1.9	770	16.67	0.56	- 3.9	- 0.1
721	16.58	0.52	0.5	- 1.7	771	17.42	0.85	- 4.2	- 0.4
722	15.02	0.41	- 0.3	- 2.0	772	17.28	0.92	- 4.2	- 0.2
723	15.17	0.40	- 0.5	- 1.9	773	17.06	0.96	- 4.4	- 0.1
724	15.87	0.84	- 0.6	- 2.1	774*	15.43	0.70	- 4.7	0.1
725	16.90	0.93	- 0.5	- 2.4	775	17.75	1.38	- 5.0	0.2
726	14.74	0.70	- 0.2	- 2.7	776	16.41	0.56	- 4.9	0.7
727	12.36	0.85	- 0.3	- 2.7	777*	15.52	0.56	- 4.9	0.9
728	11.05	0.90	- 0.6	- 2.7	778	16.42	1.19	- 4.9	1.1
729	13.77	0.49	- 1.1	- 3.0	779	14.53	0.54	- 5.0	1.5
730	17.29	0.20	- 1.4	- 2.9	780	15.82	1.24	- 4.9	1.4
731	14.69	0.85	- 1.5	- 2.7	781	15.74	0.65	- 4.8	1.3
732	17.01	1.24	- 1.5	- 2.5	782	15.89	-0.62:	- 4.7	1.0
733	15.03	0.43	- 1.2	- 2.5	783	17.43	1.29	- 4.4	0.8
734	17.58	1.28	- 0.9	- 2.6	784	16.01	0.91	- 4.5	0.6
735	17.38	1.08	- 0.8	- 2.2	785	17.07	0.61	- 4.6	0.4
736	15.96	0.28	- 0.8	- 1.8	786	17.08	0.90	- 4.3	0.2
737*	15.24	0.22	- 1.1	- 1.8	787	15.60	1.03	- 4.2	0.2
738*	12.93	0.84	- 1.1	- 1.8	788	16.19	0.60	- 3.8	0.1
739	14.42	1.26	- 1.3	- 1.7	789	17.53	0.37	- 3.6	0.9
740	16.17	0.84	- 1.7	- 2.2	790*	14.66	0.18	- 3.5	0.7
741*	16.35	0.89	- 1.9	- 2.2	791	17.23	0.87	- 3.5	0.4
742	15.36	0.31	- 2.1	- 2.3	792	15.84	0.42	- 3.2	0.4
743	17.21	0.19	- 2.0	- 2.9	793	16.87	0.63	- 2.7	0.2
744	17.02	1.14	- 2.1	- 2.9	794	15.93	0.58	- 2.6	0.4
745	14.84	0.54	- 2.6	- 2.2	795	17.02	1.20	- 2.5	0.4
746	14.92	0.84	- 2.8	- 2.3	796	16.81	0.07	- 2.6	0.6
747	14.46	0.43	- 2.8	- 2.1	797	16.71	0.31	- 2.8	0.7
748	16.10	1.28	- 3.0	- 1.9	798	16.64	0.43	- 2.9	0.9
749	17.28	0.64	- 3.3	- 1.7	799	17.31	1.44	- 2.9	1.0
750*	14.31	1.20	- 3.2	- 1.6	800	16.36	0.74	- 2.6	1.0

Table (Cont.)

No.	V	B-V	X	Y	No.	V	B-V	X	Y
801	16.43	0.86	- 2.9	1.1	851	17.43	0.99	- 4.5	4.9
802	16.89	0.60	- 3.1	1.0	852	16.98	0.73	- 4.8	5.0
803	16.23	0.53	- 3.3	1.0	853	13.59	0.56	- 4.9	5.8
804	15.02	0.39	- 3.3	1.2	854	17.54	1.43	- 4.7	5.6
805	17.05	0.48	- 3.5	1.2	855	17.32	0.61	- 4.6	5.8
806	17.10	0.56	- 4.1	1.0	856	17.46	0.79	- 3.7	6.0
807	16.39	1.09	- 4.2	1.3	857	15.91	0.35	- 3.6	6.0
808	16.88	1.12	- 4.4	1.4	858	16.02	0.41	- 3.1	5.6
809	16.74	0.69	- 4.1	1.8	859	16.56	0.92	- 3.1	5.5
810	16.76	0.77	- 3.3	1.8	860	17.25	1.40	- 2.5	5.3
811	16.67	0.52	- 2.9	1.4	861	17.20	0.78	- 2.9	5.8
812	16.46	0.37	- 2.7	1.4	862	17.59	1.02	- 3.0	6.2
813	16.92	0.61	- 2.9	2.5	863	17.60	0.99	- 2.9	6.2
814	17.26	0.81	- 3.2	2.3	864	14.73	0.60	- 2.6	6.7
815	17.00	1.06	- 3.8	2.1	865	12.21	0.54	- 2.7	6.8
816	17.58	0.53	- 3.8	2.3	866	14.39	0.36	- 3.5	6.9
817	16.80	0.69	- 3.9	2.2	867	14.44	0.48	- 3.2	6.6
818	17.37	-	- 4.1	2.3	868	16.28	0.59	- 3.0	6.5
819	14.42	0.51	- 4.6	2.4	869	15.70	0.54	- 3.1	6.4
820	17.01	0.26	- 3.9	2.6	870	12.30	0.99	- 3.3	6.4
821	17.22	0.41	- 3.6	2.9	871	17.53	0.98	- 3.4	6.3
822	17.28	1.69	- 3.9	3.0	872	15.33	0.24	- 3.6	6.6
823	17.41	0.61	- 4.2	2.8	873	16.73	0.08	- 4.0	6.5
824	16.19	0.44	- 4.5	2.9	874	15.64	1.90	- 4.3	6.4
825	17.62	0.91	- 4.6	3.2	875	16.98	0.65	- 4.3	6.7
826	16.52	0.45	- 4.3	3.0	876	17.28	1.12	- 3.9	7.0
827	15.63	1.52	- 4.0	3.2	877	17.39	0.06	- 4.5	7.1
828	16.65	1.19	- 2.7	3.1	878	15.71	0.38	- 5.4	7.3
829	11.85	1.04	- 2.3	3.3	879	17.10	0.40	- 5.3	7.3
830	17.50	0.85	- 2.4	3.5	880	15.03	1.01	- 4.7	7.3
831	17.66	0.66	- 2.5	3.6	881	17.01	0.88	- 4.1	7.4
832	15.85	1.02	- 2.7	3.9	882	12.78	0.63	- 3.6	7.7
833	17.59	-	- 2.5	4.0	883	14.62	0.93	- 3.4	7.4
834	15.24	0.64	- 2.9	4.0	884	17.34	1.61	- 3.1	7.7
835	17.04	1.21	- 2.9	4.1	885	16.75	1.70	- 3.1	7.5
836	12.89	0.84	- 3.1	4.1	886	16.74	0.43	- 2.8	7.4
837	15.04	0.32	- 4.0	3.9	887	16.88	0.57	- 2.5	7.9
838	16.08	0.43	- 4.5	4.1	888	16.71	1.32	- 2.8	7.9
839	14.98	0.35	- 5.0	3.9	889	15.21	0.46	- 2.8	8.3
840	17.31	-0.12:	- 5.1	3.9	890	13.78	1.16	- 2.8	8.9
841	17.10	0.55	- 4.2	4.5	891	17.45	-	- 2.6	9.1
842	15.81	0.52	- 3.9	4.7	892	17.22	0.87	- 2.2	9.4
843	11.59	0.45	- 3.6	4.7	893	17.63	1.35	- 2.0	9.7
844	17.36	0.04	- 3.3	4.7	894	13.25	0.89	- 2.3	9.5
845	16.70	0.74	- 3.5	5.0	895	17.18	1.07	- 2.8	9.3
846	13.66	0.40	- 3.6	5.2	896	16.83	0.87	- 3.1	9.2
847	17.42	1.22	- 3.8	5.4	897	14.38	0.45	- 3.4	9.1
848	16.19	0.66	- 3.9	5.1	898	17.36	1.94	- 3.3	9.0
849	14.60	0.17	- 4.1	4.9	899	17.56	1.70	- 3.4	8.8
850	17.65	0.33	- 4.3	5.0	900	17.35	0.88	- 3.5	8.5

Table (Cont.)

No.	V	B-V	X	Y	No.	V	B-V	X	Y
901	17.29	0.44	- 3.7	8.3	951	16.72	0.51	- 4.5	11.4
902*	14.85	0.62	- 4.0	7.9	952	15.87	1.01	- 4.6	11.2
903*	14.43	0.74	- 4.1	7.9	953	17.13	1.75	- 4.6	11.1
904*	12.55	0.45	- 4.2	7.8	954	17.47	-	- 3.0	11.4
905	17.44	2.03	- 4.6	7.7	955	16.00	0.69	- 3.0	11.3
906	15.76	0.60	- 4.5	8.2	956	17.13	0.39	- 2.9	11.0
907	17.47	0.96	- 3.9	8.4	957	17.66	-	- 2.5	10.4
908	17.41	1.35	- 3.9	8.7	958	17.61	-	- 2.3	10.4
909	17.36	0.82	- 4.1	8.8	959	17.30	0.77	- 2.0	10.4
910	16.46	0.78	- 4.1	9.3	960	17.24	-	- 1.7	10.5
911	13.92	0.45	- 3.9	9.3	961	17.38	-	- 1.5	10.7
912	17.43	-	- 3.7	9.7	962	17.41	0.84	- 2.3	11.6
913	16.24	0.81	- 3.3	10.5	963	16.49	0.61	- 2.6	12.3
914	17.58	1.34	- 3.7	10.9	964	17.50	1.05	- 2.4	12.4
915	17.38	0.60	- 4.5	10.4	965	15.27	0.79	- 2.2	11.9
916	17.13	-	- 4.3	10.4	966	16.25	1.41	- 1.8	11.7
917	14.73	0.53	- 4.5	10.6	967	17.24	0.82	- 1.8	11.9
918	17.43	0.81	- 4.7	10.3	968	17.49	1.31	- 1.7	12.1
919	17.47	1.69	- 4.8	9.8	969	17.67	-	- 1.8	12.3
920	17.36	0.56	- 4.9	9.6	970	16.48	0.42	3.2	- 1.8
921	16.39	0.72	- 4.7	9.4	971	16.81	0.63	3.0	- 1.6
922	15.96	0.61	- 4.8	9.1	972*	16.69	0.31	2.6	- 1.7
923	15.67	1.12	- 4.9	8.9	973*	17.19	0.60	2.6	- 1.6
924	15.33	0.39	- 5.4	8.3	974*	15.50	0.60	2.5	- 1.4
925	16.71	0.31	- 5.7	8.4	975	17.49	0.91	3.6	- 1.6
926	17.11	0.41	- 5.9	8.5	976	14.36	0.66	3.5	- 1.3
927	17.13	1.33	- 5.6	9.1	977	17.14	0.77	3.2	- 1.2
928	17.46	1.17	- 6.2	9.0	978	15.77	0.46	3.2	- 1.1
929	17.55	1.16	- 6.3	9.6	979	17.46	0.45	3.0	- 0.8
930*	14.02	-0.11	- 6.0	9.8	980	17.16	0.27	3.2	- 0.6
931*	12.60	0.17	- 5.9	9.7	981	15.20	0.43	3.2	- 0.6
932	16.82	0.40	- 5.5	9.9	982	15.40	0.87	2.8	- 0.7
933	17.22	1.16	- 5.3	10.0	983	17.03	0.69	2.5	- 0.7
934	14.94	0.75	- 5.4	10.0	984	16.20	0.35	2.0	- 1.0
935	14.45	0.81	- 5.9	10.3	985	17.60	0.61	1.8	- 0.9
936	17.41	1.71	- 6.3	10.9	986	17.60	0.70	1.8	- 0.7
937	17.70	0.36	- 6.3	11.0	987	16.77	1.43	1.7	- 0.4
938	16.99	0.47	- 6.0	10.9	988	15.99	1.08	2.2	- 0.6
939	15.92	0.79	- 5.9	10.9	989	14.36	0.81	2.2	- 0.4
940	17.00	1.08	- 5.6	10.7	990	14.71	0.51	2.4	- 0.3
941	17.68	0.45	- 5.2	10.4	991	15.86	0.59	2.3	- 0.2
942	16.39	1.32	- 5.3	10.7	992	15.39	0.54	1.9	0.5
943	17.10	-0.01	- 5.2	11.0	993	17.55	0.73	1.7	0.5
944	13.55	0.38	- 5.2	11.2	994	17.52	0.75	1.6	0.8
945	17.49	1.23	- 5.6	11.3	995	15.66	0.30	1.6	1.0
946	17.48	0.97	- 4.1	12.1	996	16.39	0.15	1.7	1.1
947	15.27	1.14	- 4.0	12.1	997	15.46	0.40	1.9	1.1
948	17.26	1.41	- 4.0	11.9	998	15.18	0.50	2.2	1.3
949	14.56	0.41	- 4.0	11.8	999	16.58	0.34	2.3	1.2
950	15.02	0.88	- 4.3	11.6	1000	17.45	-	2.2	0.9

Table (Cont.)

No.	V	B-V	X	Y	No.	V	B-V	X	Y
1001	16.97	1.20	2.8	1.2	1051	16.01	0.67	- 0.5	2.3
1002	14.52	0.39	2.8	1.0	1052	16.01	0.32	- 0.7	2.5
1003	17.47	1.25	2.8	0.9	1053	15.41	0.64	- 0.5	2.5
1004	17.12	0.68	3.0	0.8	1054*	12.09	1.05	- 0.3	2.5
1005	14.91	0.62	2.9	0.7	1055*	17.30	1.31	- 0.2	2.7
1006	17.27	-	2.6	0.5	1056*	17.58	-	- 0.1	2.8
1007	13.97	0.72	2.4	0.2	1057	17.30	0.96	- 0.3	2.8
1008*	14.51	1.06	3.0	0.2	1058	17.12	0.89	- 0.4	3.0
1009	17.55	0.29	3.3	0.5	1059	16.20	1.02	- 0.5	2.9
1010*	14.07	0.90	3.4	0.5	1060	17.36	0.69	- 0.4	2.8
1011	15.52	0.97	3.6	0.4	1061	17.51	0.40	- 0.5	2.7
1012	15.36	0.48	3.7	0.5	1062	17.59	1.12	- 0.7	2.8
1013	15.88	0.92	3.7	0.9	1063	15.27	0.23	- 0.8	2.8
1014	11.60	0.35	3.2	0.9	1064*	14.74	0.68	- 1.1	2.8
1015	16.15	0.64	3.1	1.2	1065	15.04	0.45	- 1.2	3.0
1016	17.72	-	3.0	1.3	1066	16.51	0.70	- 1.1	3.1
1017	16.69	1.03	3.4	1.4	1067	17.27	0.55	- 1.2	3.2
1018	16.92	0.30	2.9	1.9	1068	16.20	0.55	- 1.9	2.9
1019	17.22	0.82	2.8	1.5	1069	17.28	0.86	- 1.9	3.0
1020	16.79	0.47	2.6	1.7	1070	15.42	0.39	- 1.5	3.5
1021	14.60	0.42	2.4	1.9	1071	16.81	0.41	- 1.1	3.5
1022	16.68	0.10	2.2	2.0	1072	17.38	0.87	- 0.8	3.3
1023	15.77	0.26	2.2	1.9	1073	16.96	0.34	- 0.8	3.5
1024	14.83	0.50	2.2	1.8	1074	13.92	1.02	- 0.5	3.8
1025*	13.04	0.47	2.3	1.6	1075	15.25	0.76	- 0.2	3.7
1026*	12.26	0.87	2.2	1.7	1076	16.64	0.61	- 0.2	3.5
1027	16.20	0.27	2.1	1.6	1077	16.17	0.51	0.3	3.6
1028	17.30	0.45	2.0	1.5	1078	17.51	0.81	1.1	4.2
1029	15.65	0.33	1.8	1.6	1079	14.49	0.95	1.1	4.6
1030	17.36	0.74	2.0	1.8	1080	17.55	-	0.7	4.7
1031	17.17	-0.29:	1.8	2.2	1081	16.22	0.47	0.7	4.4
1032	14.61	0.99	1.7	2.1	1082	17.00	0.94	0.5	4.3
1033	16.94	0.47	1.4	2.1	1083	16.02	0.15	0.8	4.1
1034*	15.67	0.40	1.1	2.0	1084	16.04	0.42	0.5	4.1
1035	13.12	0.44	1.0	1.9	1085	16.55	0.30	0.1	4.1
1036	15.18	0.74	0.7	2.1	1086	17.36	0.99	0.0	4.3
1037	16.70	0.58	0.8	2.4	1087	16.73	0.63	- 0.1	4.2
1038	16.44	0.61	0.7	2.5	1088	14.07	1.03	- 0.4	4.3
1039	12.62	0.96	1.1	2.2	1089	15.99	0.83	- 0.7	4.2
1040	15.51	0.46	1.3	2.3	1090	13.35	0.73	- 0.8	4.6
1041	17.39	0.77	1.7	2.5	1091	16.79	0.46	- 1.1	4.4
1042	14.52	0.49	1.4	2.7	1092	16.26	0.31	- 1.1	4.1
1043	16.88	0.90	0.9	2.8	1093	17.07	0.25	- 1.4	4.1
1044	16.29	0.36	0.7	2.8	1094	16.91	0.46	- 1.6	4.1
1045	15.43	0.35	0.5	2.7	1095	16.87	0.76	- 1.6	4.4
1046	17.49	0.91	0.3	3.0	1096	17.60	-	- 1.4	4.6
1047	17.34	0.52	- 0.4	2.0	1097	15.85	0.24	- 2.2	4.5
1048	15.63	0.49	- 0.4	2.1	1098	17.60	0.96	- 2.5	4.4
1049	17.33	0.38	- 0.8	2.0	1099	14.72	0.70	- 2.3	4.7
1050	15.19	0.44	- 0.7	2.1	1100	17.74	-	- 2.3	5.0

Table (Cont.)

No.	V	B-V	X	Y	No.	V	B-V	X	Y
1101	15.90	0.64	- 2.1	4.6	1151	16.96	0.40	- 0.2	7.5
1102	13.54	0.34	- 1.1	4.9	1152	17.37	0.91	0.4	7.3
1103	14.82	0.50	- 0.1	4.7	1153	17.39	0.68	1.0	7.1
1104	15.78	1.09	0.1	4.8	1154	17.33	0.17	1.4	7.4
1105	17.60	0.65	0.1	4.9	1155	16.69	0.85	1.7	7.4
1106	16.31	0.90	0.2	5.0	1156	16.46	0.97	1.6	7.6
1107	17.66	-	0.1	5.3	1157	15.24	0.33	1.5	8.2
1108	17.41	0.30	0.2	5.5	1158	17.53	1.08	1.1	8.6
1109	17.45	0.55	0.2	5.7	1159	17.44	-	1.0	8.4
1110	17.35	1.11	0.1	5.7	1160	17.08	0.81	1.0	8.2
1111	16.37	0.35	0.0	5.5	1161	17.50	-	0.9	8.2
1112	14.64	0.40	- 0.2	5.5	1162	17.88	0.31	0.6	8.5
1113	15.23	0.58	- 0.6	5.0	1163	17.53	0.66	0.9	8.8
1114	16.33	1.27	- 1.1	5.2	1164	16.97	1.21	0.8	9.1
1115	17.14	0.73	- 1.2	5.3	1165	16.98	0.59	0.4	9.1
1116	17.55	0.94	- 1.8	5.5	1166	15.90	1.01	0.3	8.9
1117	17.47	-	- 2.1	6.3	1167	16.21	0.89	0.0	8.9
1118	17.60	0.27	- 2.1	6.2	1168	16.19	0.37	0.1	9.1
1119	16.74	0.57	- 1.8	6.0	1169	17.34	1.22	0.2	9.0
1120	17.35	1.32	- 1.6	6.0	1170	17.68	-	0.2	9.3
1121	16.84	0.96	- 1.4	5.8	1171	14.43	0.44	0.3	9.5
1122	16.50	0.65	- 1.3	5.7	1172	16.19	0.68	- 0.7	9.4
1123	15.93	0.72	- 1.1	5.7	1173	16.81	0.57	- 0.2	9.5
1124	17.10	-	- 0.9	5.9	1174	16.56	0.54	- 0.1	9.8
1125	16.55	0.48	- 0.4	5.9	1175	16.79	1.12	0.6	9.8
1126	17.65	0.71	- 0.1	6.2	1176	16.83	0.76	0.8	9.8
1127*	14.12	0.58	0.6	6.6	1177	17.24	-	1.1	9.6
1128	14.95:	3.07:	0.6	6.7	1178	17.33	1.28	1.0	10.0
1129	17.62	0.72	0.2	6.7	1179	16.58	0.87	1.4	10.2
1130	13.19	1.59	0.2	6.6	1180	14.34	0.76	1.3	10.3
1131	15.52	1.72	- 0.4	6.5	1181	16.31	0.62	1.1	10.4
1132	17.69	0.68	- 1.0	6.7	1182	17.50	-	0.9	10.7
1133	17.31	0.56	- 0.8	6.9	1183	17.36	0.93	1.2	11.2
1134	16.30	1.37	- 0.7	7.0	1184	16.59	0.37	1.2	11.3
1135	15.31	0.43	- 0.9	7.0	1185	17.47	0.92	0.6	11.2
1136	17.59	0.63	- 1.1	7.2	1186	17.45	0.79	0.4	10.9
1137	15.28	0.70	- 1.1	7.3	1187	16.92	1.69	0.5	11.9
1138	16.85	1.65	- 1.3	7.4	1188	16.30	0.71	0.2	11.8
1139	14.82	0.40	- 1.7	6.9	1189	16.60	0.69	- 0.1	11.4
1140	15.16	0.65	- 1.8	7.2	1190	17.61	-	0.0	11.2
1141	17.52	0.47	- 1.7	7.3	1191	16.85	1.83	0.1	11.1
1142	16.14	0.37	- 1.8	7.9	1192	17.19	1.02	0.2	10.6
1143	15.56	0.72	- 1.5	8.4	1193	17.47	1.10	0.2	10.7
1144	16.31	1.73	- 1.3	8.7	1194	15.86	0.67	0.1	10.4
1145*	17.14	1.00	- 1.1	8.7	1195	16.04	0.17	- 0.7	10.5
1146*	17.51	1.19	- 1.1	8.8	1196	14.66	0.96	- 0.8	10.5
1147	17.27	1.59	- 0.9	8.4	1197	17.33	1.02	- 0.8	10.8
1148	17.19	0.60	- 0.3	8.4	1198	16.42	0.52	- 1.1	11.0
1149*	16.38	1.81	0.0	7.8	1199	14.67	0.13	- 0.9	11.8
1150*	16.00	1.04	0.0	7.7	1200	16.25	0.45	- 1.2	12.7

Table (Cont.)

No.	V	B-V	X	Y	No.	V	B-V	X	Y
1201	17.60	0.73	- 0.8	12.9	1251	15.98	1.31	3.5	8.8
1202	17.43	1.14	- 0.3	12.7	1252	15.86	0.50	3.7	8.7
1203	14.72	0.72	- 0.2	12.2	1253	17.29	-	3.5	8.6
1204	16.26	0.39	0.1	12.4	1254	14.85	0.70	3.8	8.3
1205	15.62	1.67	0.6	12.6	1255	17.50	-	3.8	8.0
1206	15.80	0.77	2.3	12.4	1256	16.27	0.72	4.7	8.3
1207	15.16	1.09	2.8	12.1	1257	17.47	0.85	4.7	8.1
1208	17.45	0.95	3.9	12.2	1258	16.81	0.78	4.8	7.9
1209	16.14	0.74	4.2	11.9	1259	16.17	0.57	4.5	7.9
1210	15.46	0.66	4.4	11.3	1260	15.25	0.98	4.2	7.7
1211	14.35	0.70	4.7	11.0	1261	15.67	0.36	4.5	7.4
1212	16.43	0.44	4.8	10.8	1262	15.83	0.68	4.5	7.2
1213	17.35	0.77	4.7	10.6	1263	16.37	0.56	4.5	7.0
1214	16.61	0.43	4.4	11.0	1264	17.18	0.09	4.6	6.8
1215	16.86	0.03	4.0	11.3	1265	14.88	0.74	4.2	6.4
1216	15.06	0.74	3.0	11.5	1266	15.75	0.73	3.0	6.3
1217	17.11	0.74	2.5	11.5	1267	17.33	-	3.2	6.4
1218	16.78	0.40	2.0	11.5	1268	15.35	0.53	3.2	6.5
1219	17.39	0.62	1.8	11.5	1269	17.26	0.67	3.6	7.1
1220	15.64	0.53	1.5	11.9	1270	16.36	0.95	3.6	7.4
1221	17.47	1.37	1.7	10.6	1271	15.63	0.39	3.3	7.8
1222	17.56	-	1.9	10.8	1272	14.30	0.63	3.1	8.0
1223	15.30	0.98	2.2	10.7	1273	16.35	1.31	2.9	8.3
1224	17.58	-	2.2	11.1	1274	17.51	0.80	2.6	8.6
1225	17.05	0.36	2.4	11.0	1275	11.06	1.32	2.5	8.3
1226	16.71	1.71	2.9	10.8	1276	16.42	1.15	2.6	7.9
1227	17.20	1.66	2.6	10.5	1277	14.48	0.47	2.2	7.6
1228	16.09	0.71	3.2	10.1	1278*	12.42	1.03	2.9	7.7
1229	15.83	0.63	4.2	9.8	1279*	17.14	0.78	3.0	7.7
1230	15.92	1.06	4.0	10.0	1280	17.53	-	3.1	7.3
1231	13.30	0.39	4.2	10.1	1281	17.51	1.32	2.8	7.1
1232	15.88	0.41	4.6	10.0	1282	17.49	0.39	2.7	7.0
1233	14.94	1.09	4.9	10.0	1283	16.48	0.92	2.7	6.8
1234	11.96	1.01	5.0	9.2	1284	17.14	1.15	2.8	6.6
1235	15.74	0.93	5.2	9.0	1285	17.33	0.76	2.7	6.4
1236	17.32	0.54	5.0	8.9	1286	17.47	0.76	2.6	6.0
1237	14.43	0.62	4.6	9.0	1287	15.59	0.54	2.2	6.3
1238*	17.24	0.85	4.3	9.2	1288	16.11	1.03	2.0	6.9
1239*	15.45	1.27	3.8	9.2	1289	17.18	0.66	1.9	6.9
1240*	15.96	0.69	3.7	9.3	1290	17.29	-	1.4	7.0
1241	17.37	-	3.3	9.5	1291	16.21	0.93	1.5	6.7
1242	17.56	0.32	2.9	9.5	1292	16.03	0.89	1.2	6.4
1243	15.85	0.24	2.8	9.3	1293	14.93	0.84	1.5	6.4
1244	16.53	0.83	2.5	9.2	1294	14.93	0.48	1.6	5.9
1245	17.28	0.85	2.3	9.3	1295	16.88	1.18	1.7	5.9
1246	16.44	1.07	2.1	9.8	1296	16.47	0.36	1.6	5.7
1247	17.47	-	1.5	9.0	1297	16.54	0.62	1.5	5.5
1248	17.41	0.01	2.0	9.0	1298	17.38	0.93	1.3	5.7
1249	16.16	1.29	2.0	9.0	1299	11.11	0.47	1.0	5.5
1250	15.27	0.41	3.4	8.9	1300	17.22	1.34	1.3	5.1

Table (Cont.)

No.	V	B-V	X	Y	No.	V	B-V	X	Y
1301	14.15	0.38	1.6	5.1	1351	15.49	1.07	3.0	2.6
1302	16.55	0.74	2.4	5.3	1352	17.28	0.56	3.1	2.7
1303	15.03	0.63	3.1	5.3	1353	16.85	1.21	3.7	2.7
1304*	15.05	0.53	3.2	5.6	1354	17.02	0.77	3.9	2.3
1305*	14.92	0.77	3.3	5.5	1355	17.26	1.10	4.1	2.7
1306	17.41	0.41	3.5	5.6	1356	16.71	0.49	4.0	2.9
1307	16.94	1.26	3.5	5.3	1357	16.66	0.80	4.4	2.9
1308	17.39	0.06	3.8	5.3	1358	16.90	0.78	4.4	2.8
1309	17.29	0.90	3.7	5.5	1359	17.05	0.69	4.4	2.3
1310	16.94	0.75	3.7	5.8	1360	17.44	0.80	4.2	1.8
1311	14.56	0.31	4.0	5.8	1361	16.34	0.36	4.6	1.9
1312	16.18	0.61	4.1	3.9	1362	14.29	0.80	4.8	2.3
1313	13.19	0.31	3.9	3.9	1363	-	-	-	-
1314	14.73	0.57	3.7	3.9	1364	17.20	1.03	5.2	2.7
1315	16.84	0.93	3.6	4.1	1365	15.30	0.61	5.3	3.1
1316	16.05	0.73	3.7	4.3	1366	17.51	0.59	5.7	3.3
1317	17.32	1.35	3.3	4.6	1367	14.77	0.19	5.5	3.6
1318	15.04	0.63	3.0	3.9	1368*	16.04	0.53	4.8	3.7
1319	17.37	-	3.2	3.9	1369	16.55	0.33	4.6	3.7
1320	16.46	0.88	3.9	3.7	1370	17.66	0.50	4.8	3.9
1321*	15.89	1.10	4.2	3.5	1371	13.06	1.07	4.9	3.9
1322*	16.92	0.81	4.3	3.5	1372	14.13	0.47	5.0	4.0
1323	14.91	0.21	3.9	3.2	1373	16.72	0.38	4.6	4.3
1324	14.60	0.45	3.4	3.3	1374	15.05	1.66	4.4	4.6
1325	17.70	0.13	2.7	3.0	1375	14.74	0.54	4.8	5.2
1326	16.53	0.51	2.7	3.4	1376	14.81	0.45	4.4	5.0
1327*	14.73	0.98	2.8	3.6	1377	15.64	0.34	4.6	5.3
1328	14.37	1.44	2.4	4.0	1378	16.77	0.46	4.6	5.5
1329	13.57	1.23	2.5	4.4	1379*	17.52	1.04	5.4	6.0
1330	16.91	0.63	2.5	4.6	1380	11.51	0.31	5.6	6.5
1331	17.40	0.17	2.4	4.8	1381	17.53	0.95	5.4	6.6
1332	17.27	1.00	2.2	4.6	1382	16.99	0.83	5.1	6.9
1333	16.91	0.46	1.8	4.7	1383	14.48	0.50	5.0	7.4
1334	13.55	0.35	1.9	4.3	1384	16.45	0.80	5.5	7.8
1335	17.46	1.27	1.7	4.2	1385	17.08	0.58	5.7	7.9
1336	17.37	-0.16:	1.5	3.7	1386	15.79	0.30	6.0	8.0
1337	17.04	0.76	1.1	3.5	1387	15.72	0.57	5.8	8.4
1338	15.15	0.51	1.0	3.2	1388	17.48	-	4.9	8.9
1339	16.89	0.66	1.2	3.3	1389	17.30	-	5.8	8.9
1340	17.34	0.88	1.4	3.1	1390	15.68	0.56	5.7	9.5
1341	17.42	0.35	1.5	3.2	1391	15.18	0.59	5.2	9.7
1342	16.20	0.23	1.7	3.3	1392	17.50	0.70	5.4	9.9
1343*	13.10	0.71	1.8	3.3	1393	15.93	0.66	5.0	11.6
1344	14.49	0.94	2.2	3.3	1394	16.85	0.75	5.3	11.3
1345	13.96	0.28	2.1	3.1	1395	16.14	0.97	5.7	11.5
1346	17.06	0.42	2.1	2.9	1396	17.48	-	6.1	10.9
1347	17.40	0.61	2.2	2.7	1397	17.45	0.83	6.0	10.8
1348	16.87	0.37	2.2	2.6	1398	17.03	0.26	5.9	10.7
1349	16.49	0.41	2.6	2.5	1399	13.15	0.28	6.2	10.6
1350	17.01	0.42	2.6	2.7	1400	16.16	0.21	6.0	10.2

Table (Cont.)

No.	V	B-V	X	Y	No.	V	B-V	X	Y
1401	15.07	0.60	7.0	10.3	1451	16.50	1.50	10.4	6.0
1402	14.90	0.48	7.2	10.3	1452	17.37	1.07	10.9	6.1
1403	17.30	0.75	7.5	10.4	1453	16.20	0.61	11.3	6.0
1404	16.71	0.27	7.5	9.9	1454	17.59	0.44	11.0	5.9
1405	14.13	0.77	8.0	9.8	1455	16.32	0.74	11.9	5.2
1406	16.20	0.08	8.4	9.6	1456	17.37	0.60	11.2	5.2
1407	17.34:	-0.96:	8.4	9.3	1457	17.12	1.10	10.5	5.3
1408	17.36	1.27	8.2	9.0	1458	17.02	0.65	10.6	5.1
1409	17.07	-	8.0	8.9	1459	17.30	-	8.6	5.4
1410	17.15	1.10	7.8	8.9	1460	17.60	0.00	8.2	5.6
1411	15.73	0.14	7.5	9.5	1461	16.90	1.68	8.7	6.2
1412	17.31	-	6.2	9.7	1462	16.48	0.85	8.9	6.8
1413	17.07	0.69	7.0	9.3	1463	15.71	1.21	8.4	6.5
1414	17.38	-	7.1	9.2	1464	14.48	0.61	8.2	6.5
1415	16.28	0.84	6.6	8.9	1465	17.40	0.40	8.0	6.2
1416	16.09	0.23	6.6	8.8	1466	17.44	0.42	7.6	6.9
1417	12.22	0.32	6.2	8.4	1467	15.46	0.58	7.2	6.7
1418	16.02	0.51	6.7	8.2	1468	15.74	0.50	6.9	7.4
1419	15.70	0.44	7.2	8.7	1469	16.84	0.12	6.5	7.9
1420	17.53	0.89	7.3	8.0	1470	17.46	0.69	6.3	7.6
1421	14.08	0.35	7.5	8.1	1471	17.39	1.23	6.0	7.2
1422	17.53	0.79	7.9	8.2	1472	17.47	1.02	5.7	6.9
1423	15.07	0.71	7.7	7.9	1473	17.17	0.30	6.2	7.0
1424	17.06	0.76	7.7	7.8	1474	15.77	0.79	5.9	6.0
1425	16.68	0.53	7.5	7.4	1475	15.95	0.51	6.1	5.6
1426	15.96	1.12	8.1	7.9	1476	14.45	0.55	6.2	5.4
1427	17.33	0.45	8.3	7.7	1477	17.10	0.05	6.3	5.3
1428	11.32	0.98	8.7	7.7	1478	17.55	0.58	6.2	5.3
1429	15.24	0.43	8.7	8.7	1479	16.24	0.66	5.9	5.0
1430	17.24	0.22	9.2	9.2	1480	17.32	0.84	5.2	4.7
1431	13.38	0.56	9.7	8.8	1481	12.00	0.93	6.0	4.7
1432	17.37	1.06	9.3	8.5	1482	14.58	0.35	6.3	4.3
1433	17.39	0.58	9.6	8.4	1483	17.40	0.90	7.0	4.4
1434	16.76	1.51	10.1	8.2	1484	15.85	0.68	7.4	4.6
1435	15.70	0.27	9.9	8.1	1485	15.14	0.19	6.5	5.3
1436	16.79	0.42	9.0	8.1	1486	17.01	0.73	6.7	6.1
1437	14.12	0.69	9.7	7.7	1487	16.24	0.77	7.1	5.9
1438	17.48	1.09	9.4	7.7	1488	17.52	0.45	6.9	5.5
1439	17.32	-	9.0	7.3	1489	14.25	0.95	7.2	5.5
1440	14.87	0.84	9.4	6.9	1490	12.26	0.73	7.5	5.5
1441	12.71	0.56	9.6	6.5	1491	16.95	0.45	7.6	5.4
1442	15.49	0.73	9.9	6.8	1492	13.59	0.48	8.0	5.4
1443	17.27	-	10.7	7.1	1493	15.98	0.53	7.7	5.2
1444	17.05	0.91	10.1	6.6	1494	17.26	0.76	7.5	5.2
1445	17.43	-	9.8	6.3	1495	11.47	0.47	7.9	4.8
1446	15.17	0.98	9.6	6.1	1496	16.93	0.78	9.5	4.5
1447	15.78	0.77	9.4	5.9	1497	13.26	0.56	9.7	4.3
1448	17.12	0.86	9.4	5.8	1498	17.27	1.04	10.8	4.1
1449	15.85	0.72	9.2	5.8	1499	12.39	0.68	10.8	4.3
1450	12.61	1.06	9.8	5.8	1500	17.61	1.06	11.2	4.4

Table (Cont.)

No.	V	B-V	X	Y	No.	V	B-V	X	Y
1501	13.76	0.90	11.7	3.9	1551	16.57	0.61	7.4	3.3
1502	17.40	0.87	12.0	3.7	1552	15.94	0.82	7.6	3.3
1503	15.31	1.38	12.0	3.3	1553	14.48	0.41	7.9	3.1
1504	14.57	1.29	12.1	2.6	1554	17.25	0.61	7.2	2.7
1505	14.55	0.99	12.4	2.0	1555	15.28	1.05	7.1	2.5
1506	17.52	1.01	11.5	1.9	1556	15.33	0.81	7.5	2.1
1507	16.36	0.41	11.3	1.9	1557	16.94	0.58	7.6	1.9
1508*	16.02	0.63	11.6	2.3	1558	13.18	0.79	7.8	1.6
1509	15.42	0.58	11.6	2.8	1559	16.01	0.77	8.0	1.4
1510	17.40	0.85	11.4	2.5	1560	15.08	0.51	7.9	1.0
1511	17.55	0.47	11.2	2.5	1561	16.38	0.61	7.6	1.1
1512	16.13	0.79	11.3	3.0	1562	17.44	0.81	7.4	1.4
1513	17.37	1.06	11.5	3.4	1563	14.54	0.77	7.1	1.4
1514	16.19	0.64	11.0	3.6	1564	16.12	0.16	6.8	2.6
1515	17.25	1.00	10.7	3.5	1565	14.71	0.66	6.6	3.1
1516	16.90	0.43	10.6	3.2	1566	15.78	0.57	5.4	2.6
1517	13.93	0.44	10.5	2.5	1567	17.26	0.44	5.3	2.2
1518	14.45	0.84	10.4	2.2	1568*	17.24	0.52	5.0	2.1
1519	13.21	0.64	10.4	3.4	1569*	14.52	0.69	5.0	2.0
1520	15.35	1.30	10.1	3.9	1570	17.29	0.94	4.3	1.7
1521	16.88	0.99	10.1	3.7	1571	17.44	0.07	-	-
1522	17.38	0.89	9.9	3.4	1572	16.62	0.75	4.1	1.2
1523	15.88	0.66	9.7	3.8	1573	17.66	0.31	4.2	0.3
1524	16.85	0.78	9.5	3.8	1574	14.86	0.30	4.1	0.0
1525	16.59	0.58	9.4	3.5	1575	17.57	0.72	4.3	- 1.3
1526	17.72	0.63	8.9	3.2	1576	17.39	1.04	3.8	- 1.6
1527	16.01	0.98	9.0	2.9	1577	17.49	1.17	3.6	- 2.3
1528	16.13	0.58	9.2	2.9	1578	16.79	0.35	4.0	- 2.5
1529	15.98	0.78	9.8	2.4	1579	17.54	0.52	4.1	- 2.6
1530	17.40	0.37	9.6	2.1	1580	15.41	0.71	4.1	- 2.7
1531	17.17	0.88	9.8	1.9	1581	16.89	1.03	3.9	- 2.8
1532	15.91	0.88	9.8	1.7	1582	15.65	0.25	4.4	- 3.3
1533	11.06	1.50	9.1	1.6	1583	15.82	0.24	3.8	- 4.5
1534	16.93	0.57	9.1	2.0	1584	17.14	0.09	4.0	- 5.2
1535	15.05	0.35	8.3	2.8	1585	12.71	1.06	3.8	- 6.0
1536*	17.10	0.60	8.8	4.3	1586	16.17	1.71	3.8	- 6.2
1537*	17.69	0.36	8.8	4.4	1587	16.81	1.17	4.0	- 6.3
1538	17.45	0.64	8.4	4.3	1588	16.69	0.42	3.7	- 6.4
1539	17.40	-	7.7	4.2	1589	15.98	0.56	3.6	- 7.1
1540	14.86	0.83	7.6	3.7	1590	16.11	0.37	3.4	- 7.6
1541	17.46	0.57	6.6	3.7	1591	17.40	0.38	3.9	- 8.0
1542	16.27	0.81	6.2	3.9	1592	15.40	0.83	3.8	- 8.6
1543	17.38	1.01	5.5	4.1	1593	17.59	0.46	3.2	- 8.9
1544	16.50	1.43	5.3	4.0	1594	14.77	0.30	3.6	- 9.6
1545	17.21	1.00	5.6	3.9	1595	17.01	0.20	3.5	-10.3
1546	16.53	1.16	5.9	3.8	1596	14.40	0.47	3.2	-11.2
1547	17.53	0.36	6.2	3.4	1597	16.04	0.32	3.9	-11.0
1548	17.20	0.99	6.5	3.0	1598	16.94	0.42	3.9	-10.6
1549	15.24	0.58	6.6	3.3	1599	16.60	0.81	4.1	-10.6
1550	13.33	0.58	7.2	3.3	1600	15.45	0.66	4.2	-10.3

Table (Cont.)

No.	V	B-V	X	Y	No.	V	B-V	X	Y
1601	17.30	0.21	4.2	- 9.4	1651	14.18	1.13	6.4	- 7.0
1602	15.91	0.62	4.5	- 9.7	1652	17.45	0.63	7.0	- 7.3
1603	15.38	0.75	5.3	-10.3	1653	16.49	0.50	7.0	- 7.4
1604*	15.57	0.54	5.5	-10.3	1654	16.84	0.60	6.9	- 7.7
1605	17.52	0.59	5.9	-10.1	1655	17.43	0.59	7.6	- 8.1
1606	16.21	0.80	6.3	-10.0	1656	14.03	0.94	8.5	- 8.2
1607	13.56	0.27	6.5	- 9.9	1657	17.40	0.35	8.7	- 7.4
1608	17.31	0.65	6.7	- 9.7	1658	15.29	0.56	8.5	- 7.5
1609	15.40	0.37	6.2	- 9.9	1659	13.59	0.55	8.2	- 7.6
1610	16.81	1.23	6.0	-10.0	1660	16.98	0.41	7.9	- 7.6
1611	17.42	0.47	5.5	-10.0	1661	15.04	0.67	7.9	- 6.7
1612	15.76	0.30	5.2	- 9.8	1662	16.32	0.35	8.0	- 6.3
1613	16.18	0.40	5.5	- 9.5	1663	15.26	0.59	7.6	- 6.2
1614	15.28	0.56	5.4	- 9.3	1664	17.14	0.24	7.8	- 6.1
1615	15.09	0.91	5.2	- 9.2	1665	13.17	0.44	8.0	- 5.9
1616	15.58:	2.80:	3.9	- 9.1	1666	15.72	0.25	7.8	- 5.6
1617	17.41	0.55	4.0	- 9.0	1667	12.44	0.80	8.2	- 5.6
1618	17.60	0.94	4.2	- 8.7	1668	17.20	0.34	8.5	- 5.7
1619	15.81	0.20	4.6	- 8.3	1669	16.73	0.08	8.7	- 5.7
1620*	14.61	0.70	4.8	- 8.4	1670	14.71	0.96	9.2	- 6.2
1621	16.03	0.68	4.9	- 8.8	1671	17.55	-	9.9	- 7.3
1622	14.93	0.42	6.0	- 9.1	1672	17.33	0.92	9.8	- 6.7
1623	16.28	0.39	6.2	- 9.0	1673	15.74	0.51	10.1	- 6.1
1624*	11.08	0.88	6.9	- 9.1	1674	17.41	0.35	10.4	- 5.6
1625	16.00	0.36	7.0	- 8.6	1675	16.45	0.87	10.3	- 5.3
1626	16.30	0.47	6.8	- 8.3	1676	14.85	0.37	10.7	- 5.2
1627	15.69	0.12	6.5	- 8.6	1677	16.66	0.83	11.0	- 5.0
1628	16.46	1.09	6.4	- 8.9	1678	17.63	0.89	11.2	- 5.0
1629	17.35	0.32	6.3	- 8.3	1679	17.07	0.67	11.4	- 4.6
1630	16.77	0.41	5.7	- 8.2	1680	17.46	0.96	10.9	- 4.9
1631	16.31	0.41	6.2	- 7.9	1681	14.89	0.57	10.1	- 4.9
1632	16.60	0.36	5.7	- 7.6	1682	13.24	0.59	10.0	- 5.1
1633	11.13	0.95	4.8	- 7.5	1683	15.92	0.12	9.7	- 5.5
1634	17.56	0.73	4.3	- 7.4	1684	17.03	-0.22:	9.0	- 5.0
1635	14.83	0.39	4.5	- 7.1	1685	16.91	0.34	9.0	- 4.8
1636	13.44	0.38	3.2	- 7.0	1686	17.39	0.72	9.2	- 4.7
1637	14.61	1.07	4.1	- 6.6	1687	17.47	0.62	8.7	- 4.6
1638	14.68	0.43	5.2	- 5.8	1688	17.52	0.56	8.0	- 4.1
1639	15.48	-	5.6	- 6.0	1689	16.85	0.46	7.9	- 4.1
1640	15.33	0.76	5.2	- 6.2	1690	15.43	0.47	7.9	- 4.3
1641	15.09	0.32	5.2	- 6.8	1691	14.75	0.41	8.1	- 4.6
1642	15.68	0.05	5.5	- 6.3	1692	17.23	1.63	7.7	- 5.1
1643	14.01	0.30	5.7	- 6.3	1693	15.48	0.35	7.6	- 5.2
1644	16.63	0.30	5.9	- 6.0	1694	16.01	0.53	7.2	- 4.8
1645	13.92	0.44	6.1	- 6.1	1695	17.29	0.41	7.3	- 4.4
1646	17.13	0.74	6.5	- 6.2	1696	16.85	0.35	7.1	- 4.2
1647	16.77	0.36	6.7	- 6.4	1697	16.07	0.33	7.2	- 4.1
1648	17.51	1.37	6.1	- 6.3	1698	16.49	0.36	7.0	- 4.1
1649	17.47	0.18	5.9	- 6.7	1699	17.39	0.50	6.8	- 4.0
1650	16.14	0.91	6.1	- 6.7	1700	13.69	0.89	6.5	- 4.2

Table (Cont.)

No.	V	B-V	X	Y	No.	V	B-V	X	Y
1701	17.60	1.02	6.4	- 4.4	1751	16.74	0.41	9.5	- 3.0
1702	15.27	0.07	6.5	- 5.6	1752	16.15	0.66	9.3	- 2.8
1703	17.51	0.26	6.0	- 5.7	1753	16.21	0.54	9.7	- 2.4
1704*	12.04	0.61	6.3	- 4.7	1754	14.92	-1.54:	9.8	- 2.8
1705	12.71	0.65	6.2	- 4.8	1755	14.17	1.10	10.2	- 2.9
1706	15.83	0.66	6.2	- 4.3	1756	16.24	0.70	10.4	- 2.9
1707	16.76	0.24	5.9	- 4.2	1757	13.68	1.14	10.6	- 3.0
1708	15.87	0.79	5.7	- 4.3	1758	15.74	0.86	11.1	- 3.3
1709	15.23	0.66	5.6	- 4.9	1759	17.23	1.73	11.7	- 4.0
1710	17.82	0.52	5.3	- 4.9	1760	14.75	0.71	11.9	- 3.4
1711	17.51	0.94	4.9	- 5.0	1761	17.51	1.16	12.1	- 3.2
1712	17.42	1.05	4.7	- 3.2	1762	13.91	0.72	12.4	- 2.4
1713	17.05	1.08	4.8	- 3.6	1763	12.72	0.49	11.4	- 2.4
1714	15.79	0.47	5.0	- 3.6	1764	16.98	0.01	12.0	- 2.1
1715	17.51	0.53	5.5	- 3.5	1765	17.05	0.58	12.3	- 1.9
1716	15.81	0.76	6.1	- 3.6	1766	16.65	0.30	11.4	- 1.8
1717	17.27	1.19	6.3	- 3.3	1767	14.82	0.71	10.8	- 1.4
1718	15.30	0.35	6.1	- 3.4	1768	14.28	0.64	10.8	- 0.2
1719	16.13	0.55	5.9	- 3.4	1769	16.18	1.43	11.2	- 1.3
1720	17.59	0.54	5.8	- 3.3	1770	15.42	0.74	11.6	- 1.3
1721	16.50	0.35	5.7	- 3.0	1771	14.52	0.34	11.9	- 1.6
1722	16.34	0.82	5.1	- 3.0	1772	17.62	-	12.2	- 1.4
1723	17.60	0.69	5.3	- 2.7	1773	17.55	-	12.0	- 0.9
1724	17.36	-0.03	5.8	- 2.7	1774	17.59	-	12.1	- 0.4
1725	16.15	0.86	5.9	- 2.9	1775	16.76	1.05	11.0	- 0.6
1726	17.69	0.96	6.5	- 2.2	1776	13.55	0.92	10.6	- 1.0
1727	16.58	1.15	6.5	- 2.3	1777	14.57	0.78	10.3	- 1.1
1728	17.38	0.30	7.3	- 1.3	1778	16.52	0.62	9.7	- 0.6
1729	15.38	0.43	7.2	- 1.5	1779	15.36	0.73	9.6	- 1.2
1730	17.22	0.50	7.2	- 1.7	1780	15.96	0.33	9.3	- 1.8
1731	14.22	0.86	7.3	- 1.8	1781	16.03:	2.24:	9.2	- 2.1
1732	17.50	-	7.2	- 2.1	1782	14.56	0.59	9.1	- 2.1
1733	16.35:	2.37:	7.5	- 2.1	1783	17.30	1.65	8.9	- 2.7
1734	12.92	0.63	7.2	- 2.3	1784	15.72	0.52	8.7	- 2.4
1735	16.43	0.36	7.4	- 2.7	1785	15.05	0.39	8.4	- 2.1
1736	16.46	0.14	7.4	- 2.8	1786	16.32	0.80	8.7	- 1.8
1737	16.66	1.37	7.4	- 3.0	1787	16.64	0.72	9.1	- 1.4
1738	17.41	0.95	7.8	- 3.1	1788	16.37	0.34	9.2	- 1.2
1739	15.71	0.11	8.2	- 4.0	1789	16.93	0.56	9.2	- 0.7
1740	12.95	0.60	8.4	- 3.8	1790	17.43	0.75	8.3	- 0.8
1741	16.99	0.24	8.5	- 3.6	1791	15.91	0.98	8.2	- 1.1
1742	14.61	0.36	8.2	- 3.2	1792	16.80	0.99	7.8	- 1.1
1743	15.25	0.47	8.4	- 3.3	1793	17.61	0.53	7.7	- 0.6
1744	15.70	0.82	8.5	- 3.3	1794	17.41	0.37	7.5	- 0.9
1745	13.57	1.01	8.6	- 3.2	1795	17.31	0.70	7.2	- 0.7
1746	17.39	0.81	10.0	- 4.3	1796	17.53	-	7.1	- 1.1
1747	15.81	0.43	10.7	- 4.0	1797	14.87	0.83	6.8	- 0.9
1748	15.72	0.54	10.4	- 3.7	1798	14.04	0.37	6.8	- 0.6
1749	17.26	0.86	9.8	- 3.4	1799	15.72	0.84	6.5	- 0.5
1750	15.46	0.56	9.3	- 3.3	1800	16.15	0.36	6.3	- 0.6

Table (Cont.)

No.	V	B-V	X	Y	No.	V	B-V	X	Y
1801	17.54	0.11	5.8	- 0.9	1851*	14.44	0.43	8.7	0.8
1802	15.71	0.47	5.5	- 1.4	1852	16.74	0.38	8.8	- 0.4
1803	16.10	0.41	5.8	- 1.8	1853	17.42	0.72	9.1	- 0.2
1804	16.88	0.98	5.9	- 1.9	1854	16.43	0.63	9.3	0.0
1805	15.86	0.41	5.6	- 1.9	1855	17.00	0.69	9.6	0.0
1806	17.36	1.30	5.4	- 1.8	1856*	17.24	1.45	9.8	- 0.1
1807	16.23	0.92	4.9	- 2.1	1857*	15.50	0.82	9.9	0.0
1808	16.80	0.49	4.5	- 2.3	1858	16.46	-0.39:	9.8	0.4
1809	16.48	0.36	5.1	- 1.6	1859	15.28	0.79	9.6	0.6
1810	16.12	0.94	5.0	- 1.5	1860	17.02	-	9.3	0.6
1811	15.60	0.34	4.9	- 1.4	1861	15.62	0.34	9.2	1.0
1812	15.66	0.38	4.8	- 1.3	1862	16.83	0.37	9.1	1.3
1813	17.09	0.49	5.0	- 1.2	1863	17.59	0.88	9.9	1.6
1814	15.52	0.60	4.9	- 0.4	1864	17.28	1.17	10.3	1.9
1815	17.21	0.23	4.6	- 0.2	1865	13.37	0.47	10.6	1.5
1816	17.36	1.22	5.0	0.1	1866	13.56	-	10.4	1.3
1817	17.58	0.54	5.2	0.5	1867	13.75	0.32	10.3	1.1
1818	17.44	0.25	5.0	0.7	1868	17.77	0.62	10.7	1.2
1819	15.68	0.66	4.9	1.0	1869	17.25	0.46	10.6	0.1
1820	16.06	0.33	5.0	1.5	1870	17.56	0.89	10.8	0.2
1821	14.76	0.33	5.5	1.8	1871	15.52	1.00	10.8	0.4
1822	14.42	0.43	5.6	1.3	1872	16.68	0.08	11.0	0.3
1823	15.96	1.24	5.5	1.1	1873	15.19	0.59	11.6	0.4
1824	16.55	0.84	5.5	1.0	1874	15.94	0.53	11.3	0.8
1825	16.56	0.26	5.7	0.6	1875	13.98	0.55	11.2	1.5
1826	15.57	0.65	5.5	0.4	1876	15.59	0.57	11.7	1.9
1827	15.61	0.55	5.4	0.1	1877	16.75	0.30	11.9	2.1
1828	17.61	1.13	5.6	- 0.2	1878	17.22	1.13	12.4	2.3
1829	17.27	0.73	6.2	- 0.1	1879	16.44	0.89	12.3	2.1
1830	17.32	0.91	6.2	0.2	1880	17.33	1.07	12.6	1.9
1831	17.43	0.96	6.0	0.1	1881	14.00	1.29	12.8	2.0
1832	16.56	0.28	6.0	0.5	1882	16.94	1.31	12.8	1.9
1833	17.54	0.87	6.1	0.7	1883	16.60	0.35	12.5	1.5
1834	16.94	0.55	6.5	0.9	1884	17.11	0.44	12.6	1.3
1835	17.55	-	6.5	1.7	1885	16.96	0.09	12.7	1.1
1836	17.39	0.55	6.9	1.3	1886	17.62	1.00	12.0	1.1
1837	16.30	0.92	6.8	1.1	1887	14.03	0.44	12.1	1.0
1838	14.63	1.15	7.0	1.0	1888	16.41	1.92	12.4	0.7
1839	12.91	1.08	7.1	1.0	1889	15.83	1.16	12.5	0.5
1840	16.57	0.52	7.1	0.2	1890	17.05	0.66	12.6	0.7
1841	15.02	0.38	8.1	- 0.4					
1842	17.51	0.54	8.3	- 0.1					
1843	17.75	0.89	8.2	0.4					
1844	14.91	0.54	7.9	0.2					
1845	16.97	0.26	7.7	0.7					
1846	17.28	1.16	7.7	0.9					
1847	17.25	1.58	8.2	1.6					
1848	15.26	0.76	8.8	1.6					
1849	16.86	0.96	8.8	1.2					
1850	17.59	1.15	9.0	1.1					

NOTES TO THE TABLE

A * at the right upper side of the running number denotes that the photographic image of the measured star is distorted by a neighbouring star.

A colon beside the V and B-V colours denotes that the star is measured only on one or two plates or the measured magnitudes obtained from different plates have large dispersion.

COMMUNICATIONS
FROM THE
KONKOLY OBSERVATORY
OF THE
HUNGARIAN ACADEMY OF SCIENCES

MITTEILUNGEN
DER
STERNWARTE
DER UNGARISCHEN AKADEMIE
DER WISSENSCHAFTEN

BUDAPEST — SZABADSÁGHEGY

No. 82.

M. PAPARÓ and L. G. BALÁZS

DISTRIBUTION OF STARS OF SPECTRAL TYPES EARLIER THAN F7 AROUND IC 4665

BUDAPEST, 1982

ISBN 963 8361 17 4
HU ISSN 0324 - 2234
Felelős kiadó: Szeidl Béla

Hozott anyagról sokszorosítva

8213659 MTA KESZ Sokszorosító, Budapest. F. v.: dr. Héczey Lászlóné

DISTRIBUTION OF STARS OF SPECTRAL TYPES EARLIER THAN F7 AROUND IC 4665

ABSTRACT

A study was made of the spatial distribution of early type stars in a region of intermediate galactic latitude. Objective prism plates were used to survey an area of 19.5 $\square^{\circ}$ around the cluster IC 4665 for all stars of spectral types earlier than F7 down to $12^{m}5$ photographic magnitude. 427 stars were detected, for which spectral types and photographic UBV colours were obtained. Different amounts of interstellar reddening were derived for the $l<30^{\circ}$ and $l>30^{\circ}$ parts of the region. Separate absorption correction was made for each of the parts. The stars were divided into four groups: spectral type A1 and earlier, A2 - A7, A8 - F2 and F3 - F7, and the space densities were determined for each group. The shape of the space density curve of the A2 - A7 stars reveals the existence of two kinematic subgroups. The velocity dispersions characterizing these two subsystems have a ratio of 1:1.6. The interpretation of space density curves of stars earlier than A2 in terms of such subgroups faces difficulties because of the possible photometric distance scale error and the interference with the Gould belt.

INTRODUCTION

The logarithmic density of A type stars plotted against distance from the galactic plane displays an inflexion point. It is difficult to reconcile this point with a pure Gaussian velocity distribution assuming the stars to be distributed in plane parallel layers (*Woolley*, 1965). *Oort* (1932) wrote in his classical paper " that the velocity distribution is usually found to deviate somewhat from Gaussian distribution. However it can always be represented by a sum of two or three Gaussian components with different moduli. " Later *Van Rhijn* (1960) suggested that the dispersion in the linear velocity of A type stars increases with distance from the galactic plane. He claimed that two groups of A type stars with different dispersions can be found. Space density curves displaying these characteristics have been published, for instance, by *Kurochkin* (1958), *Upgren* (1962,1963), *Woolley* and *Steward* (1967), *Borzov* (1973) and *Balázs* (1975, hereafter referred to as Paper I). *Balázs* found that plotting the density ratios at z=0 of the two subsystems versus spectral type a jump can be seen on the curve at spectral type A0. He interpreted this

characteristic as a consequence of the discontinuous generation of stars and derived the time difference between the two birth events by the lifetime of stars at which the jump appeared on the curve. The possible cosmogonical significance of this jump on the curve needs further investigations using homogeneous stellar samples observed in different galactic directions to avoid misinterpretations of incomplete and inhomogeneous data.

The aim of the present work is to continue the investigation to get an overall picture about the spatial density distribution of stars with different spectral types around the Sun at intermediate galactic latitudes.

OBSERVATIONAL MATERIAL

An area of $19.5\square^{\circ}$ centred on $l^{II}=30^{\circ}.74$, $b^{II}=15^{\circ}.98$ ($\alpha=17^{h}48^{m}$, $\delta=5^{\circ}20'$) was investigated. The observations were carried out with the 60/90/180 cm Schmidt telescope of the mountain station of Konkoly Observatory. Spectral types and UBV colours were obtained for 427 stars brighter than $12^{m}.5$ photographic magnitude. The spectral types are based on three objective prism plates taken with a 5° UBK 7 (UV transmitting) prism that gives a dispersion of 580 Å/mm at H_{γ}. Kodak IIa-O emulsions were used and the widening was 18'', equivalent to 0.16 mm on the plate. The plates were made with double exposures of 6^{m} and 24^{m}, so that any systematic variations in the classification with photographic density could be estimated.

The UBV photometry is based on five plates in B and in U and on four plates in V. The emulsion types, filters and exposure times used are given in the following table:

	emulsion	filter	exp. time
U	Kodak 103a-O	Schott UG1 2mm	10^{m}
B	Kodak 103a-O	Schott GG13 2mm	5^{m}
V	Kodak 103a-D	Schott GG14 2mm	4^{m}

The relationships between the international system and the instrumental system are given by the following equations:

$$V_{instr} = V - 0.16(B-V) + 0.10$$

$$(B-V)_{instr} = 1.05(B-V) - 0.02$$

$$(U-B)_{instr} = 1.01(U-B) + 0.11(B-V) - 0.03$$

The plates were measured with Konkoly Observatory's Cuffey type iris photometer. The photoelectric sequence given by *Alcaino* (1965) was partly used and the four faintest stars were obtained with Konkoly Observatory's 50 cm Cassegrain telescope. The mean errors of the photographically determined colours are ± 0.07 ± 0.06 and ± 0.05 for U,B and V, respectively.

The spectral classification was based on the criteria given by *Stock* and *Slettebak* (1959), *Stock* (1971) and *Seitter* (1975). The classification using small scale spectra, however, is somewhat uncertain with late B and early A type stars because the hydrogen lines dominating the spectra of these stars reach their maximum strength and show little change with spectral type. Therefore an independent method, the Q method of *Becker* (1963) was used to determine the spectral types of stars earlier than A0.

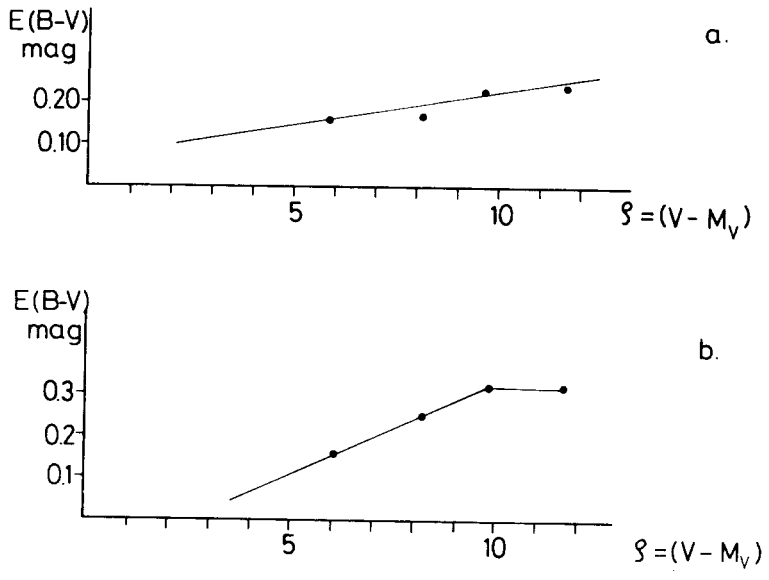

Fig. 1a-b The colour excesses (E_{B-V}) as functions of uncorrected distance moduli. (a: $l>30^{\circ}$, b: $l<30^{\circ}$)

After getting the colours of stars, Q = (U-B)- 0.72(B-V) values were calculated and spectral types were estimated. The differences between the spectral classes obtained by the two different methods were, except for a few cases, less than two subclasses. Finally the arithmetic mean of these two spectral classes was used.

INTERSTELLAR REDDENING

Adopting *Allen*'s (1973) relation between intrinsic colour index and spectral type, the E_{B-V} and E_{U-B} colour excesses were obtained. *Allen*'s relation between absolute magnitude and spectral type was used to compute the distance modulus for each star. The stars were divided into four groups according to their distance modulus: $<7^m$, 7^m-9^m, 9^m-11^m and $>11^m$. The mean distance modulus and the colour excesses were determined for each subgroup. The distribution of interstellar matter is inhomogeneous in this field. *FitzGerald* (1968) has shown that the $l^{II}<30^o$, $b=15^o$ and $l^{II}>30^o$, $b=15^o$ fields have different amounts of absorption. Up to 1500 pc for the former field he obtained $0.3 \leq E_y < 0.6$, for the latter one till 1000 pc the value $0.1 \leq E_y < 0.2$ is given. Adopting this result a line at $l^{II}=30^o$, parallel to the galactic axis was drawn on the plate and the absorption was determined separately on both sides of this line. The colour excesses determined by this method are plotted in Fig. 1/b for the $l^{II}<30^o$ side and Fig. 1/a for the $l^{II}>30^o$ side of the line, as a function of the distance modulus. It can be seen from this figure that a more dense absorbing material is situated on the $l^{II}<30^o$ side of the plate. The cluster IC 4665 has a distance modulus of $7^m.8$ according to *Alcaino* (1965). The $E_{B-V} = 0^m.17$ value at a distance modulus of $7^m.8$ obtained from Fig. 1/a is in good agreement with $E_{B-V} = 0^m.152$ given by *Alcaino* and with $E_{B-V} = 0^m.17$ given by *Hogg* and *Kron* (1955). Adopting E_{B-V} from Fig. 1/a and 1/b and a ratio of total to selective absorption equal to 3.0, the magnitudes were corrected for the absorption.

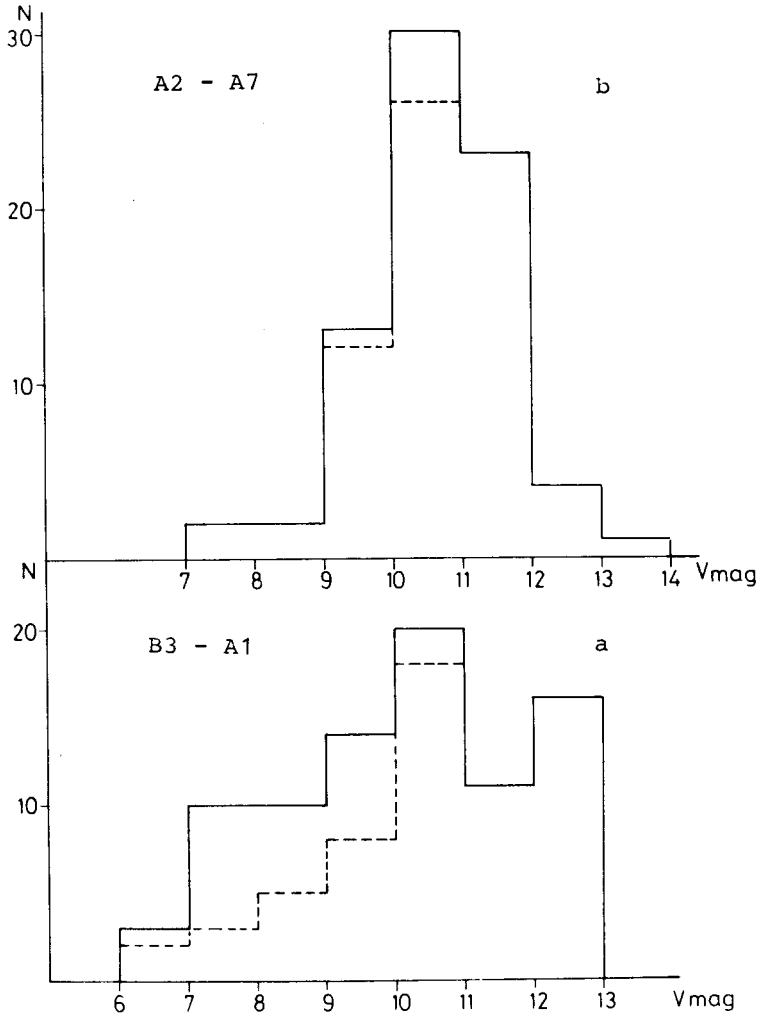

Fig. 2a-b The distributions of stars against the V magnitudes. Dashed lines indicate the corresponding distributions after excluding the cluster members of IC 4665.

THE SPACE DISTRIBUTION OF STARS

The limiting magnitude of our plates is generally $12^{m}.5$. Based on the sharpness of classificational criteria and on the number of stars in each subclass four subgroups were separated: stars earlier than A2, A2 - A7, A8 - F2 and F3 - F7. The distribution of stars against the V measured magnitude in the given subgroups is shown in Fig. 2a-d. Dashed lines indicate the cor-

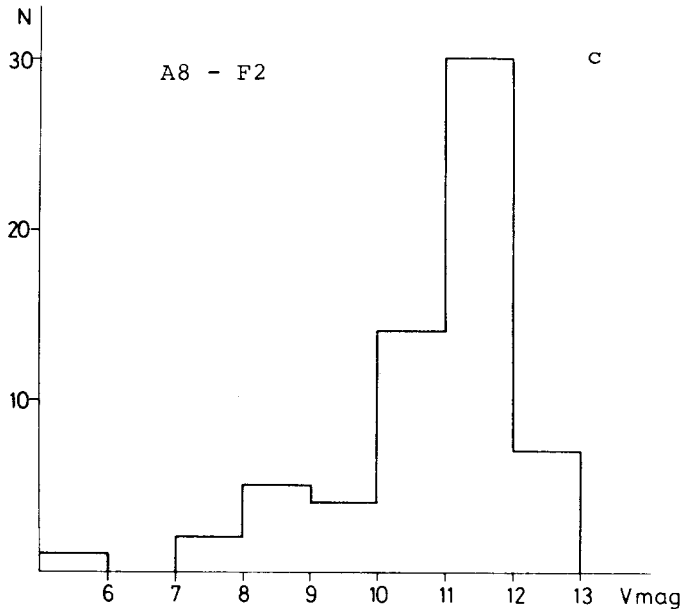

Fig. 2c The distribution of stars against the V magnitude.

responding distributions after excluding the cluster members of IC 4665 defined by *Alcaino* (1965). After correcting the magnitudes for interstellar absorption the basic convolution equation of stellar statistics

$$A(m) = \int_{-\infty}^{+\infty} D(y)\,\Phi(m-y)\,dy$$

can be solved separately for each subgroup. As usual, A(m) is the

number of stars in the apparent magnitude interval $(m-\delta m, m+\delta m)$; $D(y)$ is the number of stars between distance moduli $(y-\delta y, y+\delta y)$; and $\Phi(m-y)$ is the luminosity function of a given spectral and

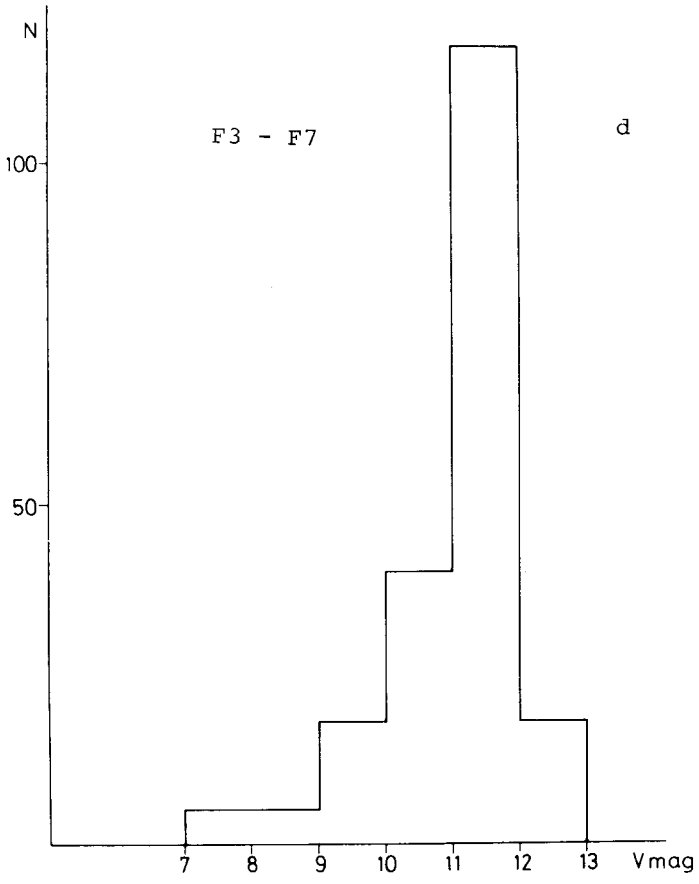

Fig. 2d The distribution of stars against the V magnitude.

luminosity class. Following *McCuskey* (1966) the form of Φ is a Gaussian function. Its mean absolute magnitude and standard deviation were taken from *Allen* (1973). To solve the equation the matrix method described by *Dolan* (1974) was used. The densities derived by this method are plotted in Fig. 3a-d. The dashed lines show the plate limit. Bars indicate the 1σ error bars obtained by *Dolan*'s method.

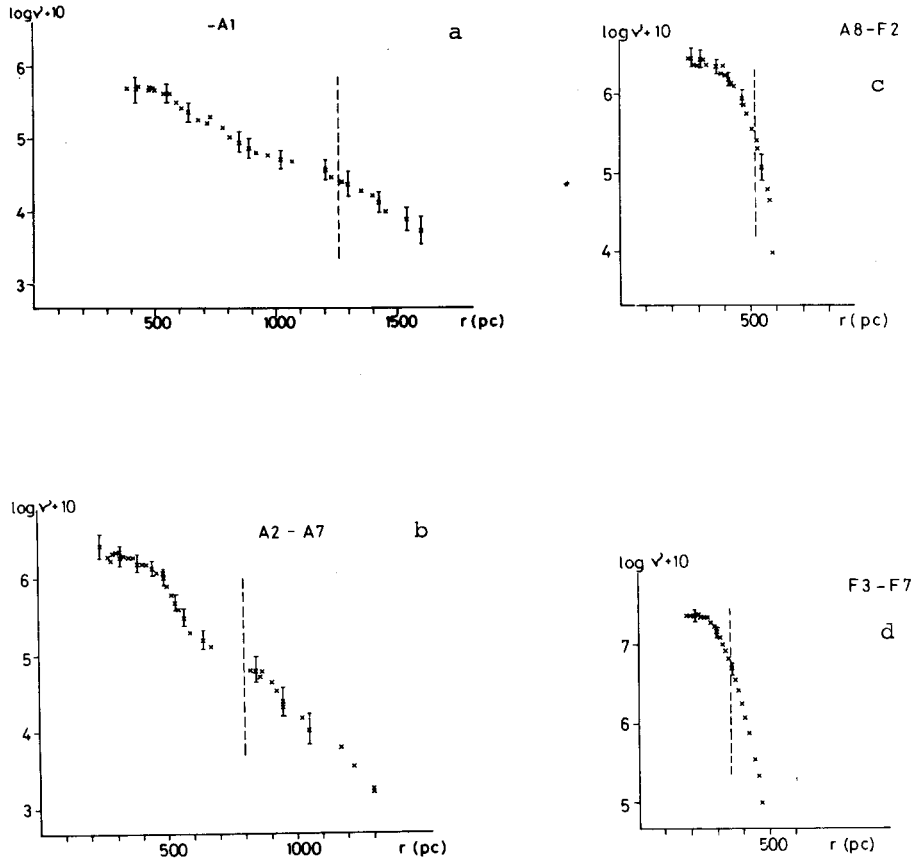

Fig. 3a-d The derived space densities of the different subgroups.
(The dashed lines show the plate limit.)

DISCUSSION OF THE SPACE DENSITIES

Except for the subgroup earlier than A2 the density gradients ($\partial\nu/\partial r$) are nearly the same up to 600 pc if the plate limit allows the determination of space densities up to this distance at all. At about 600 pc the density gradient of A2 - A7 stars changes and becomes smaller. The space density of stars earlier than A2 also displays similar characteristics, i.e. steeper gradient up to 900 pc and a change to a slower decrease afterwards. The gradient at the first part of the curve, however, is not so steep as in the case of A2 - A7 stars and it needs some further remarks. We shall return to this problem later.

As was pointed out previously (Paper I) the spatial distribution of the A stars near to the galactic poles shows a similar form to stars in some intermediate latitude galactic fields if the densities in line of sight were plotted against the corresponding z distances perpendicular to the galactic plane. The similarity between these distributions and those obtained by the present investigation therefore suggests that the density gradients are mainly due to the contributions of the gradients perpendicular to the galactic plane to the gradients in the line of sight. This result enables us to compute a relation connecting the spatial density, the standard deviation of the z velocity component and the gravitational potential, following the procedure outlined in Paper I. As a result we could get a curve for $(\sigma_z(z),z)$ plane characterizing the z dependence of σ_z.In the case of a Gaussian distribution of z velocities we should get a horizontal line in this diagram because in that case $\sigma_z(z)$ is independent of z. However, after computing the $\sigma_z(z)$ curve according to the procedure of Paper I we obtained the curve displayed in Fig. 4 for A2 - A7 stars. The curve can be characterized by a slowly decreasing part up to 140 pc in z and a nearly horizontal part from 170 pc in z. The two parts are connected by a steep increase. This form of the $\sigma_z(z)$ curve might possibly indicate the coexistence of two kinematically distinct subsystems with different characteristic velocity dispersions. The smaller dispersion component deviates somewhat from Gaussian distribution because the $\sigma_z(z)$ curve is not quite horizontal. The larger dispersion component, however, is fairly Gaussian because of the

nearly horizontal run of $\sigma_z(z)$ in that part of the diagram. The density and $\sigma_z(z)$ are dominated by the small dispersion component at $z<140$ pc because the small dispersion component has a 5.4 times higher density in the plane of the Galaxy. At $z>170$ pc, however, the larger dispersion subsystem dominates the curves because of its slower density decrease. $\sigma_z(0) = 7.0$ km/sec has been found in these computations. This value is close to that found in Paper I for a Lyra field. The run of $\sigma_z(z)$ at the small dispersion component deviates from pure Gaussian behavior. It might be interpreted by taking it into account that $\sigma_z(z)$ is based on the space density curve. Any systematic error in determining the space densities influences the shape of $\sigma_z(z)$. A very important source of systematic errors in determining the space densities by means of photometric parallaxes appears to be the lack of attention given to eliminate the effect of interstellar absorption from the photometric data. An overestimation of interstellar reddening causes a steeper and an underestimation a smaller density gradient than the true gradient in our case. As was

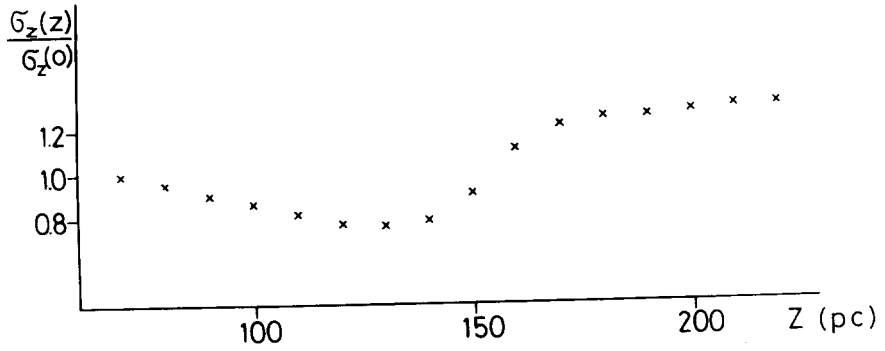

Fig. 4 The $\sigma_z(z)/\sigma_z(0)$ ratio computed from the density curve of A2 - A7 stars plotted against the hight (z) above the galactic plane.

mentioned earlier in this work the distribution of interstellar material is very patchy in this field and the western part contains more absorbing material than the eastern part. This was the

reason that the effect of interstellar absorption was evaluated for both parts separately. There was no way of determining the exact boundary between the lower and the higher absorbing region. We may expect, consequently, some over- or under-estimation in the absorption data. The absorbing material is concentrated at distance r<400 pc therefore that part of the space density curve could be distorted whereas at the remaining part only the distance scale is changed. The $0^m.24$ overestimation of the absorption corresponding to $0^m.08$ in E_{B-V} could account for the decreasing part of the $\sigma_z(z)$ curve. One could explain in this way the deflection of the $\sigma_z(z)$ curve from the pure Gaussian behaviour in the z<140 pc, region. The region z>140 pc, however, is little affected by absorption so it can be used to estimate the relative increase of σ_z between the two subsystems. The curve shows a 1:1.6 increase which is close to the value (1:1.8) was found in Paper I.

Let us now return to discuss the space density curve of stars younger than A2 in more detail. If one computed the $\sigma_z(z)$ plot in this case, following the procedure applied for A2 - A7 stars, one has $\sigma_z(0)$ = 10.2 km/sec - a value which is a factor of 1.5 - 2 higher than was measured by direct kinematical methods for early type stars. Moreover the percentage of the larger dispersion component is somewhat higher (13%) contradicting what is expected for these stars. It is worth while to discuss two points which might have some significance.

1. The uncertainties in determining the absolute magnitudes of early type stars is somewhat higher than in stars having spectral types later than A2 because of the lack of good classificational criteria on our small scale spectra. The photometric Q method was applied to remove this uncertainty but a systematic error of one subclass could still remain. One subclass error corresponds to about $0^m.5$ at late B type stars and could satisfactorily explain a 1.26 times higher scale.
2. The possible scaling error could not explain the higher percentage of larger velocity dispersion stars among our early type stars in the galactic plane as was obtained in our calculations. The relative density of the two subsystems, namely, is invariant to the scale changes. The

interpretation of density curves in terms of velocity dispersions perpendicular to the galactic plane was based on the assumption that the observed density gradients were mainly due to the contributions of z gradient related in the line of sight. This assumption seemed not to work in this area. *Stothers* and *Frogel* (1974) pointed out that the system of B type stars within 1000 pc from the Sun is composed of two subsystems: stars concentrating to the galactic plane and stars concentrating to a plane bending about $18^{\circ} \pm 1^{\circ}$ to the plane of our system. These latter stars form the Gould belt. The Gould belt passes the northern part of our area surveyed and could therefore influence the space distribution of stars earlier than A2. The space distribution of stars later than A2, however, shows no signs of such influence because their density curve fits well to the curves observed in other galactic directions not affected by the Gould belt.

CONCLUSIONS

The uneven distribution of interstellar material in our field causes difficulties in eliminating the effect of interstellar absorption on photometric data. The shape of the space density curve of the A2 - A7 type stars reveals the existence of two kinematically distinct subsystems with different dispersions perpendicular to the galactic plane. The main characteristics of these subsystems are close to the values found in previous works in other galactic directions. The interpretation of space density curve of stars earlier than A2, in terms of the subsystems mentioned above, is not a simple matter because of the possible photometric distance scale error and the interference by the Gould belt.

ACKNOWLEDGEMENTS

The authors are indebted to Dr.M. Kun for valuable advice in space density computations. They are grateful to Mrs.I. Kálmán, Mr.I. Tóth and Mr.L. Sturman for their assistance in photometric measurements and analysing the data.

Budapest-Szabadsághegy, 15 October 1982

REFERENCES

Alcaino, G., 1965, Bull. Lowell Obs.No.7.167.

Allen, C.W., 1973, Astrophysical Quantities 3rd.ed., Athlona Press, London.

Balázs, L.G., 1975, Mitt.Sternwarte Ung.Ak.Wiss.No.68.(Paper I)

Becker, W., 1963, Application of Multicolor Photometry in " Basic Astronomical Data ",ed.K.Aa.Strand, Univ. Chicago Press, p.241.

Borzov, G.G., 1973, Astr.Zhu.50. 1041.

Dolan, J.F., 1974, Astron. and Astrophys.35. 105.

FitzGerald, M.P., 1968, Astron.J.73.983.

Hogg, A.R. and Kron, G.E., 1955, Astron.J.60.365.

Kurochkin, N.E., 1958, Astr.Zhu.35.86.

McCuskey, S.W., 1966, Vistas in Astronomy 7. 141.

Oort, J.H., 1932, B.A.N. 6. 249.

Seitter, W.C., 1975, Atlas for Objective Prism Spectra; Bonner Spectral Atlas II. Ferd. Dümmler Verlag, Bonn.

Slettebak, A. and Stock, J. 1959, Astr. Abhandlungen der Hamburger Sternwarte Bd.V.Nr.5.

Stock, J., 1971, Application of Objective Prism Techniques in the Magellanic Clouds in " The Magellanic Clouds ", ed.A.B. Muller, D.Reidel Publishing Co.,p.181.

Stothers, R. and Frogel, J.A., 1974, Astron.J.79.456.

Upgren, A.R., 1962, Astron.J.67. 37.

Upgren, A.R., 1963, Astron.J.68. 194.

Van Rhijn, P.J., 1960, Pub.Kapteyn Astr.Lab.Groningen No.61.

Woolley, R., 1965, Motions of the Nearby Stars in " Galactic Structure ", ed.A.Blaauw and M.Schmidt, Univ. Chicago Press, p.85.

Woolley, R. and Steward, J.M., 1967, MN.136.329.

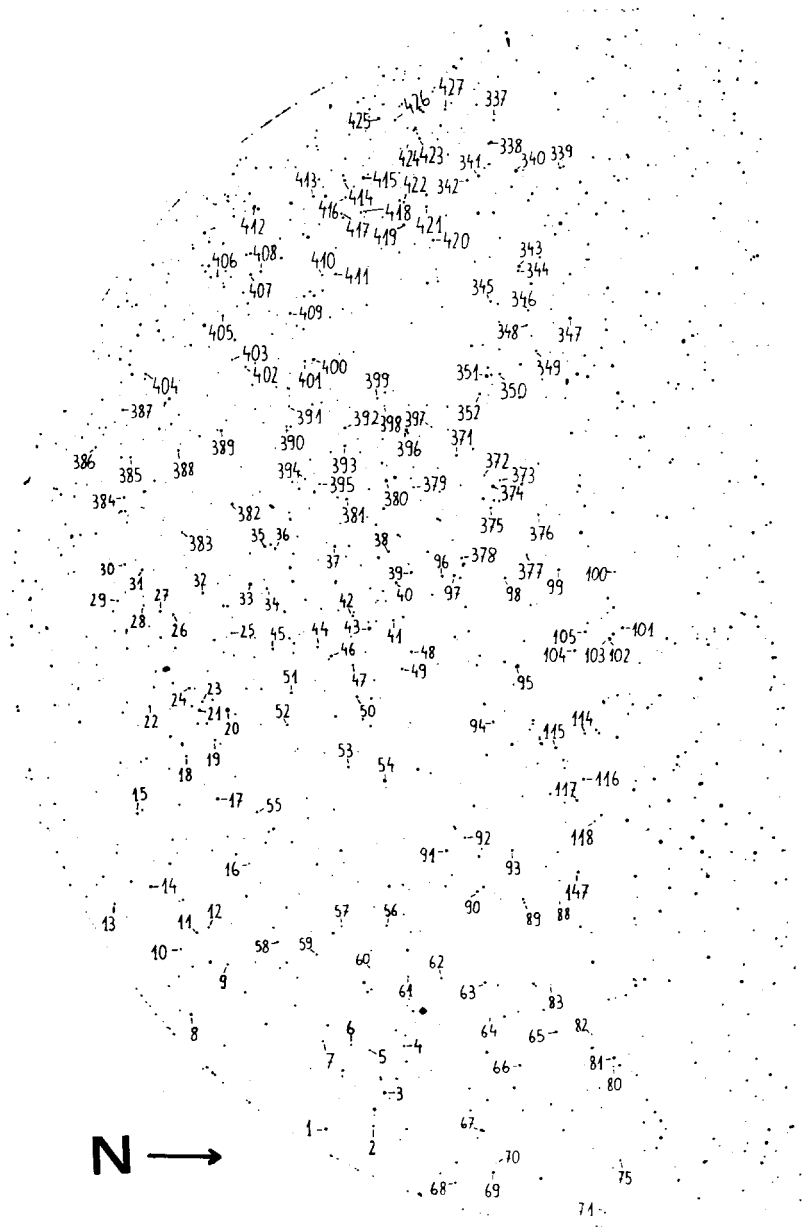

Finding chart of the survey stars

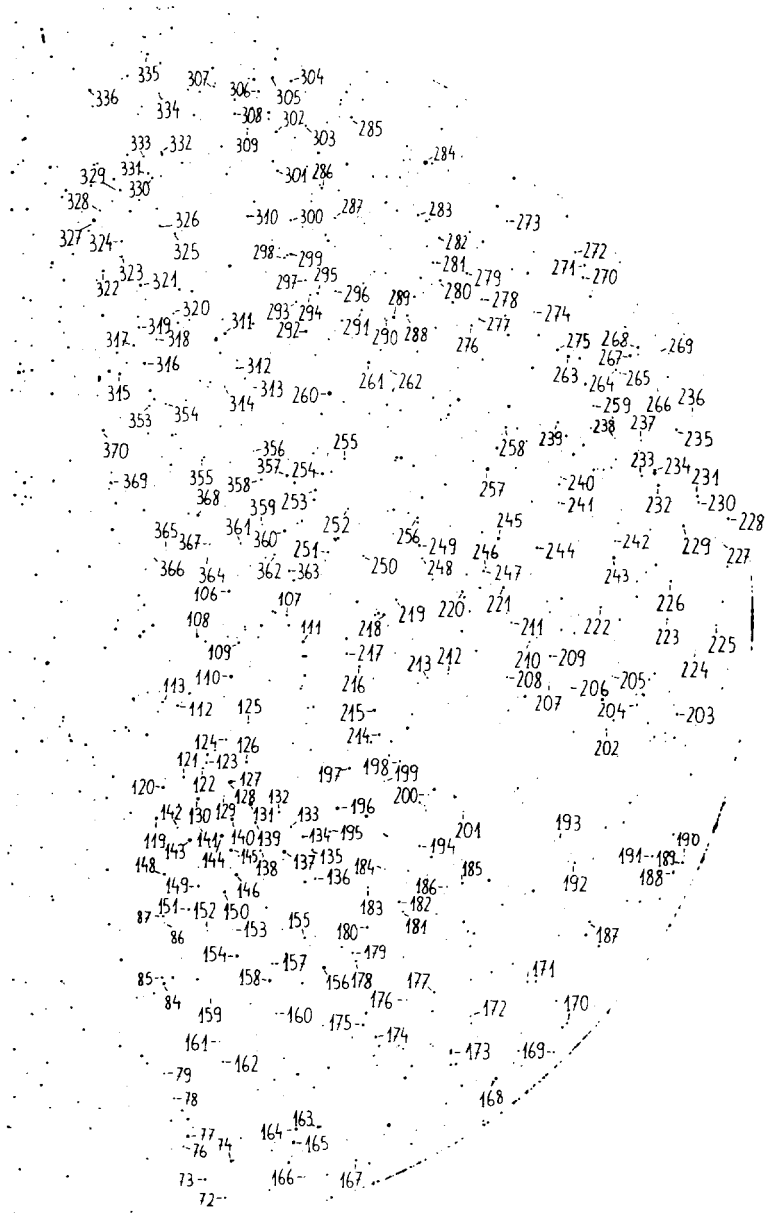

Finding chart of the survey stars

TABLE

Spectra and UBV data of survey stars

No.	Sp.	V	B-V	U-B	remarks
1	A3	8.45	0.42	0.07	BD +4°3481
2	A4	11.56	0.52	0.05	
3	F7	9.00	0.75	0.13	BD +4°3483
4	F4	11.94	0.79	-0.07	
5	A2	12.24	0.47	0.02	
6	F3	11.72	0.81	-0.02	
7	F2	11.62	0.70	0.19	
8	B6	9.92	0.33	-0.25	BD +3°3480
9	A2	11.87	0.65	0.15	
10	AO:	12.45	0.42	-0.10	
11	F5	11.72	0.64	0.14	
12	A8	12.06	0.68	0.09	
13	F7:	11.28	0.99	0.01	
14	A1	9.82	0.47	0.16	BD +3°3485
15	B8	11.45	0.21	-0.22	
16	F2:	12.39	0.64	-0.01	
17	F6	10.08	0.86	0.23	BD +3°3490, blend
18	F2:	11.51	0.92	-0.08	
19	F3:	11.50	0.91	-0.01	
20	B6	6.32	0.22	-0.10	BD +3°3493
21	F5	9.02	0.56	-0.03	BD +3°3492
22	F2	11.54	0.65	-0.15	
23	B9	12.07	0.29	-0.08	
24	A6	10.96	0.50	0.17	
25	F6	11.44	0.75	0.03	
26	F4:	11.96	0.69	-0.23	
27	A9	11.15	0.43	0.09	
28	F5:	11.92	0.67	-0.17	
29	F3	11.71	0.54	-0.16	
30	F3	11.03	0.60	-0.09	
31	A7	10.73	0.43	-0.03	BD +3°3506
32	F6	9.80	0.62	-0.15	BD +3°3504
33	A8	8.24	0.33	-0.07	BD +3°3505
34	F5	11.09	0.78	-0.02	
35	B6	10.68	0.10	-0.55	BD +3°3533, blend
36	F6	10.31	0.78	0.07	BD +4°3532
37	A3	10.41	0.39	-0.05	BD +4°3531
38	F6	11.15	0.65	-0.14	
39	F6	10.78	0.60	-0.26	
40	A5	10.64	0.31	-0.04	BD +4°3521
41	F3	10.83	0.76	-0.07	
42	A2	11.49	0.58	-0.14	
43	F3	7.41	0.44	-0.07	BD +4°3517
44	F3	11.95	0.41	0.04	blend
45	A1	11.67	0.39	-0.02	
46	A3	10.46	0.38	0.08	BD +4°3515
47	F4	11.20	0.68	0.02	
48	A6	10.33	0.34	0.12	BD +4°3516
49	A9	10.60	0.64	0.09	BD +4°3514
50	A4	11.25	0.65	0.04	BD +4°3513
51	F2	11.51	0.76	-0.13	

TABLE

/ Continued /

No.	Sp.	V	B-V	U-B	remarks
52	A1	11.74	0.62	0.07	
53	F5	11.07	0.85	0.10	
54	A9	7.94	0.45	-0.07	BD +4°3506
55	B9	11.51	0.61	0.06	
56	F3	11.47	0.84	0.03	
57	A2:	12.53	0.25	0.19	
58	F7:	11.44	0.88	0.01	
59	F0	11.40	0.71	0.18	
60	F2:	12.64	0.59	-0.08	
61	F7:	11.55	0.96	0.15	
62	F2	10.84	0.75	0.08	
63	F6	10.36	0.80	0.18	BD +4°3492
64	B6	12.29	0.74	-0.04	
65	F7	9.75	0.73	0.25	BD +5°3459
66	F5	10.99	0.71	-0.05	
67	A7	10.16	0.52	0.13	BD +4°3480
68	F4	10.66	0.54	0.14	BD +4°3475
69	A7	9.28	0.53	0.14	BD +4°3477
70	A1	12.33	0.20	0.08	
71	F6	10.44	0.38	0.14	BD +5°3445
72	F7	10.60	0.50	-0.05	
73	F7	9.63	0.48	0.22	BD +5°3446
74	A7	9.48	0.42	0.12	BD +5°3449
75	F6	11.48	0.63	0.18	
76	F2	11.90	0.52	-0.17	
77	B4	8.78	0.23	-0.53	BD +5°3450
78	F5	11.46	0.66	-0.10	
79	A1	11.54	0.54	-0.05	
80	A8	11.60	0.81	-0.12	
81	F0	9.22	0.46	-0.01	BD +5°3457
82	F4	11.44	0.67	0.23	
83	A6	11.77	0.70	0.02	
84	B6	8.77	0.07	-0.22	BD +5°3465
85	A1	10.38	0.29	0.10	
86	F6	11.32	0.69	0.02	
87	F4	10.74	0.59	0.08	
88	A1:	12.95	0.24	-0.42	
89	F6	11.06	0.74	0.13	
90	A7	11.27	0.51	0.13	
91	F6	9.45	0.72	0.24	BD +4°3502
92	F7:	11.88	0.73	0.05	
93	F7	11.24	0.79	0.17	
94	F2	11.10	0.59	-0.04	
95	F1	7.49	0.47	0.06	BD +5°3505, blend
96	F1	10.51	0.47	-0.08	BD +4°3523, blend
97	A1	10.33	0.27	0.12	BD +4°3524
98	F2	10.61	0.67	-0.07	BD +4°3525
99	B9	10.64	0.24	-0.04	
100	F5	11.61	0.58	-0.21	
101	A6	8.73	0.32	0.01	BD +5°3512
102	A4	10.48	0.56	-0.25	BD +5°3509

TABLE

/ Continued /

No.	Sp.	V	B-V	U-B	remarks
103	F7	10.43	0.38	0.01	
104	A2	10.84	0.34	-0.05	BD +5°3506
105°	A2	10.42	0.35	-0.17	
106	A1	9.91	0.09	0.02	BD +5°3518
107	A2	10.80	0.31	-0.05	
108	A6	9.20	0.42	-0.11	BD +5°3510
109	A1	10.30	0.33	0.01	BD +5°3507
110°	B7	7.66	0.01	-0.71	BD +5°3504
111	F5	9.97	0.42	-0.21	BD +6°3541
112	F2	10.69	0.49	0.08	BD +5°3502
113	F6	11.21	0.64	-0.17	
114	F5	11.72	0.61	0.02	
115	A0	10.38	0.19	0.10	BD +5°3499
116	A0	10.85	0.31	0.10	BD +5°3495
117	A1	10.76	0.55	0.29	BD +5°3492
118	F7:	11.88	0.76	-0.01	
119	F5	7.95	0.47	-0.10	BD +5°3488
120°	B7	9.05	0.06	-0.44	BD +5°3493
121	F6	9.84	0.65	0.10	BD +5°3496
122+	A4	10.93	0.41	0.14	
123	A2	10.96	0.39	0.14	
124	A8	11.76	0.34	0.07	
125	F1	12.11	0.23	-0.10	
126°	A1	9.97	0.14	0.06	BD +5°3497
127°	B9	10.33	0.24	0.16	
128°	B6	8.10	-0.02	-0.44	BD +5°3494
129	F0	11.62	0.47	0.11	
130+°	B7	8.23	0.10	-0.33	BD +5°3491
131°	B3	7.24	0.02	-0.64	BD +5°3490
132	F6	10.95	0.65	0.13	
133°	A7	10.67	0.42	0.23	BD +5°3485
134+°	A5	10.61	0.32	0.25	
135	F5:	11.68	0.61	0.26	
136+°	F5	11.58	0.53	0.00	
137	A0	7.57	0.11	0.07	BD +5°3481
138+°	F2	11.16	0.47	0.05	
139°	A2	10.52	0.28	0.17	BD +5°3486
140+°	B8	8.83	0.23	0.13	BD +5°3487
141	F3	11.67	0.44	0.11	
142	F2:	11.94	0.75	0.20	
143+°	B3	6.88	-0.01	-0.61	BD +5°3483
144°	B5	7.45	0.01	-0.60	BD +5°3484
145°	B4	7.69	0.02	-0.61	BD +5°3482
146°	B3	7.80	0.10	-0.61	BD +5°3478
147°	A1	9.95	0.39	0.08	BD +5°3480
148°	A1	9.18	0.24	0.00	BD +5°3479
149	A0	10.22	0.06	0.06	BD +5°3477
150+°	A1	9.10	0.17	0.03	BD +5°3476
151+°	A3	9.39	0.30	0.21	BD +5°3473
152	F6	11.22	0.52	0.08	
153	F5	11.79	0.41	-0.02	

TABLE

/ Continued /

No.	Sp.	V	B-V	U-B	remarks
154°	B7	8.38	0.07	-0.24	BD +5°3471
155	F5	10.92	0.53	0.22	
156	A6	7.42	0.40	0.15	BD +6°3514
157	A8	11.00	0.39	0.06	
158+o	B9	7.98	0.06	-0.19	BD +5°3466
159	F7:	11.76	0.54	0.10	
160	F7	11.22	0.45	0.10	
161	F7	11.28	0.60	0.10	
162	A0	10.82	0.12	0.19	BD +5°3456
163	A9	10.22	0.02	0.18	BD +6°3497
164	F7	9.30	0.53	0.09	BD +6°3496
165	A6	7.70	0.36	0.16	BD +6°3494
166	A9	11.84	0.14	-0.08	
167	F5	11.31	0.49	-0.11	
168	F5	9.19	0.53	-0.26	BD +6°3501
169	F6	10.32	0.56	-0.44	BD +7°3444, edge
170	F7	10.81	0.81	0.09	BD +7°3448
171	F3	11.23	0.48	0.08	BD +6°3513
172	F7:	11.80	0.72	-0.07	
173	F5	10.56	0.58	0.13	
174	F6	9.62	0.61	0.05	BD +6°3507
175	A2	10.12	0.17	0.14	BD +6°3508
176	F4:	12.40	0.36	-0.05	
177	A2	11.84	0.16	0.10	
178	F3	11.29	0.57	0.03	
179	A6	11.29	0.49	-0.04	
180	A1	10.72	0.17	0.22	BD +6°3516
181	F6	11.92	0.38	0.07	
182	F2	10.52	0.42	-0.04	BD +6°3518
183	F0	11.80	0.55	0.05	
184	F4:	11.99	0.51	-0.23	
185	A7	10.50	0.40	0.07	BD +6°3521
186	F5:	11.92	0.60	-0.25	
187	F7	10.80	0.61	0.10	
188	A2	10.76	0.44	0.00	BD +7°3459
189	F7	8.87	0.95	0.17	BD +7°3460
190	A1	11.89	0.29	-0.15	
191	F7	11.14	0.56	0.15	
192	F7:	12.38	0.65	0.23	
193	F7:	12.35	0.46	0.03	
194	F2	11.79	0.49	-0.09	
195°	F6	11.39	0.54	-0.04	BD +6°3523
196°	B6	7.88	0.01	-0.77	BD +6°3525
197	F6	10.35	0.63	-0.11	BD +6°3529
198	A1	11.59	0.25	0.14	
199	A0:	12.62	0.17	0.02	
200	A3:	12.88	0.06	0.09	blend
201	F7	11.89	0.60	-0.13	
202	A1	11.45	0.32	0.36	
203	F1	9.98	1.04	0.39	blend
204	F1	11.79	0.42	0.25	

TABLE

/ Continued /

No.	Sp.	V	B-V	U-B	remarks
205	B9:	12.20	0.30	0.03	
206	A0	12.76	0.03	0.03	
207	F3	11.87	0.47	0.00	
208	F5:	11.67	0.43	0.16	
209	A0	10.90	0.23	0.13	BD +7°3472
210	F6	11.31	0.58	0.13	
211	F7	11.40	0.57	0.30	
212	F4:	11.87	0.66	-0.10	
213	F7:	11.73	0.51	-0.10	
214	A6	10.87	0.37	0.03	
215°	A0	9.42	0.10	-0.07	BD +6°3533
216	F0	10.73	0.44	0.02	BD +6°3539
217	F5	11.45	0.54	-0.17	
218	F5	10.04	0.56	-0.14	BD +6°3546
219	F4	11.19	0.52	-0.05	
220	F5	10.23	0.47	0.08	BD +6°3548
221	F3	9.68	0.42	0.24	BD +6°3549
222	F1	11.13	0.37	0.26	
223	F5	11.07	0.55	0.22	
224	F4:	11.61	0.69	0.16	
225	F7	10.48	0.50	0.20	
226	A1	10.04	0.28	0.30	BD +7°3478
227	F5:	11.23	0.56	0.01	
228	F6	8.79	0.83	0.55	BD +7°3485, edge
229	A0	9.62	0.19	0.18	BD +7°3484
230	A2	10.53	0.41	0.08	
231	F6	9.20	0.61	0.33	BD +7°3486
232	F2	8.74	0.47	0.25	BD +7°3487
233	A0	11.20	0.38	0.06	
234	A0	10.27	0.11	0.11	
235	A5	9.87	0.36	0.28	BD +7°3494
236	F6	11.09	0.80	-0.06	
237	F6	11.24	0.59	0.18	blend
238	F2	11.66	0.51	0.00	
239	A6	11.01	0.39	0.10	
240	F4:	12.05	0.51	0.04	
241	F5:	11.79	0.53	0.22	
242	F7:	11.67	0.56	0.14	
243	F6	7.64	0.44	-0.02	BD +7°3481
244	F5	10.11	0.49	0.18	BD +6°3550
245	A0	8.74	0.15	0.13	BD +6°3553
246	F3	11.97	0.54	0.14	
247	F7	11.52	0.55	0.20	
248	F6	11.79	0.50	0.16	
249	F4	10.54	0.50	0.18	BD +6°3551
250	A0	12.18	0.31	0.09	
251	A8	11.63	0.28	0.00	
252	F0	12.04	0.28	-0.27	
253	A3	10.12	0.20	0.10	BD +6°3557
254	A5	10.15	0.40	0.24	BD +6°3559
255	F7	11.37	0.57	0.22	

TABLE

/ Continued /

No.	Sp.	V	B-V	U-B	remarks
256	F3	10.80	0.48	0.17	
257	F5	7.54	0.42	-0.01	BD +6°3560
258	F6	10.71	0.55	0.18	
259	F3	11.58	0.34	0.26	
260	F2	5.70	0.54	-0.10	BD +6°3566
261	A2	9.93	0.26	0.20	BD +6°3568
262	F5:	12.20	0.53	0.05	
263	F7	8.54	0.63	0.07	BD +7°3499
264	F6	11.49	0.71	0.07	
265	F4:	12.02	0.68	0.01	
266	F5:	11.84	0.66	0.19	
267	A4	9.28	0.32	0.20	BD +7°3490
268	A1	9.90	0.21	0.05	BD +7°3502
269	B7:	12.45	0.69	-0.05	
270	A8	10.58	0.56	0.28	BD +7°3504, blend
271	A1	10.14	0.36	0.32	BD +7°3505, edge
272	A5	11.48	0.71	0.11	
273	F7	11.48	0.69	0.15	
274	A1	12.01	0.45	0.23	
275	F0	9.61	0.44	0.28	BD +7°3501
276	F4	11.32	0.59	0.12	
277	A2	11.77	0.22	0.12	
278	A6	11.65	0.43	0.24	
279	F5	10.50	0.64	0.15	
280	A3	10.22	0.40	0.25	BD +6°3573
281	F7	11.12	0.59	0.16	
282	A3	10.94	0.37	0.12	
283	A6	10.98	0.47	0.17	
284	B4	6.19	0.19	-0.36	BD +6°3578
285	F2	11.05	0.57	0.27	BD +6°3580
286	A3	11.47	0.38	0.13	
287	F7:	11.54	0.72	0.24	
288	F5	11.65	0.56	0.20	
289	A3	9.75	0.30	0.17	BD +6°3570
290	F5:	12.55	0.31	0.07	
291	F6	11.03	0.82	0.16	
292	A4	9.56	0.43	0.22	BD +6°3569
293	F7:	11.69	0.71	0.30	blend
294	F4	11.44	0.60	0.08	
295	A0	10.37	0.23	0.10	BD +6°3572
296	F6	11.76	0.57	0.02	
297	F5:	11.65	0.62	0.11	
298	F3	11.32	0.65	-0.03	
299	A1	10.22	0.15	0.00	BD +5°3543
300	F6	11.33	0.73	-0.04	
301	F5	10.29	0.50	-0.08	BD +5°3548
302	A8	10.30	0.56	0.18	BD +5°3550
303	F4	11.68	0.55	0.11	
304	F5	9.12	0.63	0.07	BD +5°3553
305	F3	11.16	0.61	0.18	BD +5°3554
306	F6	10.93	0.71	0.18	

TABLE

/ Continued /

No.	Sp.	V	B-V	U-B	remarks
307	F7:	11.81	0.70	0.13	
308	F0	10.93	0.61	0.12	BD +5°3551
309	F6	11.98	0.62	0.10	
310	A3	11.02	0.32	0.28	
311	A3	9.38	0.38	0.17	BD +5°3535
312	F6	11.62	0.63	0.08	
313	F7:	14.53	-	-	
314	F5	12.12	0.49	-0.01	
315	F6	9.50	0.68	0.08	BD +5°3531
316	B9	9.03	0.23	0.07	BD +5°3533
317	F6	11.26	0.47	0.15	
318	F7:	11.84	0.69	0.03	
319	F6	10.84	0.68	0.11	
320	F6	11.72	0.53	0.13	
321	F4	9.53	0.62	-0.06	BD +5°3540
322	A9	10.95	0.43	0.18	
323	A2	12.07	0.27	0.12	
324	F6	11.11	0.77	0.07	
325	F5	10.68	0.71	0.16	
326	A2	11.91	0.27	0.14	
327	B3	7.47	0.05	-0.69	BD +5°3544
328	F5	11.60	0.48	0.10	
329	A3	10.63	0.39	0.11	BD +5°3545
330	F2	10.82	0.57	0.20	
331	F5	11.44	0.66	0.20	
332	F6	10.42	0.71	0.02	
333	F4	11.61	0.84	0.07	
334	F2	11.94	0.58	0.06	
335	A4:	10.90	0.30	0.48	BD +5°3559, edge
336	F2	8.85	0.58	0.02	BD +5°3552
337	F5	11.31	0.71	-0.03	
338	F7	8.65	0.69	0.04	BD +4°3558
339	F5	11.54	0.47	-0.05	
340	F5	7.55	0.52	-0.25	BD +5°3577
341	A1	9.25	-0.03	-0.62	BD +4°3557
342	A4	10.95	0.38	0.13	
343	F2:	8.87	0.55	0.02	BD +5°3541
344	F2	11.57	0.72	-0.05	
345	F6	11.39	0.54	0.04	BD +4°3547
346	F6	11.63	0.51	-0.01	
347	A1	8.89	0.15	-0.10	BD +5°3537
348	F7	11.51	0.80	-0.02	
349	F3	11.80	0.45	-0.05	
350	A1	10.91	0.49	0.00	
351	B4	7.88	0.03	-0.68	BD +4°3543
352	F6	10.97	0.67	-0.08	
353	F6	11.55	0.69	-0.03	
354	A1	12.35	0.35	0.16	
355	F2	11.38	0.59	0.22	
356	A1:	12.27	0.34	0.01	
357	A4	9.75	0.35	0.38	BD +5°3525, blend

TABLE

/ Continued /

No.	Sp.	V	B-V	U-B	remarks
358	F7	10.95	0.62	0.09	
359	A0:	12.15	0.35	-0.08	
360	F4	8.66	0.48	-0.11	BD +5°3520
361	F6	11.37	0.65	-0.05	
362	F6	11.33	0.51	-0.10	
363	F3	10.97	0.63	-0.13	BD +5°3519
364	F7:	12.12	0.65	-0.11	
365	F4:	12.36	0.53	-0.17	
366	A0	12.98	0.06	-0.10	
367	F7	11.84	0.60	-0.08	
368	A2	9.60	0.18	0.12	BD +5°3523
369	A2	11.65	0.31	0.19	
370	F7	9.98	0.71	0.33	BD +5°3527
371	A9	11.44	0.60	0.00	
372	F7:	12.10	0.67	-0.20	
373	F5:	12.15	0.72	-0.18	
374	A2	9.18	0.20	0.11	BD +4°3539
375	F1	11.63	0.50	-0.25	BD +4°3536
376	F4	11.20	0.57	-0.07	
377	A1	11.67	0.28	0.11	
378	F4	10.94	0.69	-0.20	
379	F7:	12.13	0.56	0.08	
380	B9	8.78	0.22	-0.12	BD +4°3541
381	F6	10.91	0.65	-0.06	
382	F7	10.00	0.59	-0.12	BD +3°3509
383	F3	11.89	0.55	-0.20	
384	F7:	11.55	0.83	-0.13	
385	F7:	12.04	0.59	-0.13	
386	F7:	11.06	0.92	-0.02	
387	F0	10.62	0.58	-0.13	
388	F5	10.84	0.68	-0.09	BD +3°3513
389	F4	9.70	0.63	-0.01	BD +3°3514
390	F7:	11.90	0.96	-0.09	
391	F2:	12.20	0.67	-0.32	
392	A6	11.48	0.30	-0.05	
393	F5	11.56	0.60	-0.12	
394	F5:	11.94	0.75	-0.04	
395	F2:	12.38	0.44	-0.21	
396	A9	8.97	0.37	-0.07	BD +4°3542
397	F7:	12.38	0.65	-0.27	
398	A2:	13.06	0.33	-0.27	
399	F5	12.31	0.54	-0.04	
400	F0	9.00	0.37	-0.07	BD +4°3545
401	A0	12.19	0.24	0.01	
402	F6	11.09	0.74	-0.11	
403	F5	11.85	0.69	-0.19	
404	A4	11.21	0.33	0.03	
405	F0	11.66	0.49	-0.10	
406	F2:	11.85	0.67	-0.01	
407	F4	10.79	0.59	-0.08	
408	A8	11.56	0.49	-0.23	

TABLE

/ Continued /

No.	Sp.	V	B-V	U-B	remarks
409	A0	11.37	0.07	-0.06	blend
410	F6	12.13	0.61	-0.18	
411	F6	11.42	0.60	0.08	
412	A5:	11.18	0.54	0.01	
413	A4	11.07	0.39	0.12	
414	A4	11.28	0.52	0.22	
415	B8	8.11	0.21	-0.12	BD +4°3556
416	F5:	11.65	0.56	0.03	
417	F7:	11.54	0.62	0.14	
418	F5:	11.80	0.58	0.09	
419	A8	9.54	0.40	0.17	BD +4°3551
420	A7	10.64	0.42	0.14	BD +4°3550
421	A1	10.98	0.12	-0.30	
422	F7:	11.69	0.69	-0.04	
423	F6	10.36	0.74	-0.01	BD +4°3559
424	F7:	12.72	1.67	0.61	blend
425	B7:	9.02	0.02	-0.47	BD +4°3560
426	A6	11.61	0.55	-0.05	
427	A3	11.60	0.44	-0.01	

Notes to the table:

A cross and a circle at the right upper side of the running number denotes photoelectrically measured colours and the member of the cluster according to Alcaino, respectively.

A colon beside the spectral types denotes that the star is classified from one plate.

Blend is remarked if the photographic image of the measured star is distorted by a neighbouring star.

Edge is remarked if the star is near the edge of the plate.

COMMUNICATIONS
FROM THE
KONKOLY OBSERVATORY
OF THE
HUNGARIAN ACADEMY OF SCIENCES

MITTEILUNGEN
DER
STERNWARTE
DER UNGARISCHEN AKADEMIE
DER WISSENSCHAFTEN

BUDAPEST — SZABADSÁGHEGY

No. 83.

MAGNETIC AND VARIABLE STARS

EDITED
BY
M. MARIK and L. SZABADOS

BUDAPEST, 1982

ISBN 963 8361 18 2
HU ISSN 0324-2234
Felelős kiadó: Szeidl Béla

Hozott anyagról sokszorosítva

8213660 MTA KESZ Sokszorosító, Budapest. F. v.: dr. Héczey Lászlóné

CONTENTS

PREFACE

The 5th conference of Subcommission No.4, "Magnetic Stars", and the 4th conference of Subcommission No.3, "Nonstationary Stars", of the multilateral cooperation "Stellar Physics and Evolution" was held as a joint symposium "Magnetic and Variable Stars" in Szombathely, Hungary, between 30 May and 3 June 1982. The symposium was organized by the Konkoly Observatory of the Hungarian Academy of Sciences, the Department of Astronomy of Eötvös Loránd University and the Eötvös Loránd Physical Society.

Fifty-four astronomers of seven countries participated in the symposium where 8 review papers and 31 contributed papers were read. The abstract or a short version of most of the papers presented is published in the present proceedings.

The editors wish to express their sincere appreciation to all who contributed to the success of the symposium. The financial support provided by the Hungarian Academy of Sciences and Eötvös Loránd University is gratefully acknowledged.

The Editors

Budapest-Szabadsághegy, 31 October 1982

Scientific Organizing Committee:
Co-chairmen: W. Schöneich and S. Kanyó; Secretary: L. Szabados
Members: V.L. Khokhlova, F. Krause, M. Marik, L.V. Mirzoyan, K.P. Panov, J. Smak, K. Stepien, B. Szeidl and W. Wenzel

Local Organizing Committee:
Chairman: M. Marik; Secretary: E. Vértes
Members: E. Rupp, L. Szabados, B. Szeidl, G. Tóth, M. Varga and I. Vincze

LIST OF PARTICIPANTS

Bulgaria

Kolev, D.Z.
Kovatchev, B.
Panov, K.P.
Popova, M.D.

Czechoslovakia

Hric, L.
Juza, K.
Mikulašek, Z.
Žižňovský, J.
Zverko, J.

Egypt

Soliman, M.A.

G.D.R.

Oetken, L.
Rädler, K.-H.
Richter, G.
Rössiger, S.
Rüdiger, G.
Schöneich, W.
Schult, R.

Poland

Gertner, J.
Jarzębowski, T.
Madej, J.
Muciek, M.
Opolski, A.
Smak, J.
Stępien, K.
Woszczyk, A.
Zaremba, D.

U.S.S.R.

Dolginov, A.Z.
Glagolevsky, Yu.V.
Khokhlova, V.L.
Mirzoyan, L.V.
Plachinda, S.I.

Hungary

Barcza, S.
Barlai, K.
Grandpierre, A.
Györgyey, J.
Kanyó, S.
Kovács, G.
Kun, M.
Láng, K.
Marik, M.
Oláh, K.
Pap, J.
Paparó, M.
Patkós, L.
Rupp, E.
Szabados, L.
Szeidl, B.
Tóth, G.
Vargha, M.
Vértes, E.
Vető, B
Vincze, I.
Virághalmy, G.
Zombori, O.

MAGNETIC Ap STARS — SURFACE CHEMICAL INHOMOGENEITIES AND METHODS OF SPECTROSCOPICAL ANALYSIS

V.L. Khokhlova
Astronomical Council of the U.S.S.R. Academy of Sciences
Pyatnitskaya 48, Moscow, SU-109017

Consideration was given to the difficulties arising when magnetic Ap stars with chemically inhomogeneous surfaces are analysed by traditional methods using the empirical or theoretical curve of growth. The result of abundance determination by the equivalent width of lines of an integrated spectrum depends on line intensity, and the determination of turbulent velocity leads to underestimation of this parameter. The discrepancies in abundance determinations made by the coincident statistics method (CSM) of Aikman and Cowley and by the theoretical curve of growth method are explained and it is pointed out that the CSM method seems to give more reliable results.

The necessity for determining local (coordinate-dependent) characteristics instead of integral characteristics (such as W or He) is pointed out. The result is shown of the mapping of some chemical elements over the surface of magnetic stars ε UMa, CU Vir, α^2 CVn, χ Ser and compared with the position of magnetic poles.

Hβ LINE VARIABILITY IN 73 DRACONIS

J. Madej
Warsaw University Observatory
Warsaw, Poland

A new photoelectric method for measurements of periodic Balmer line variations in magnetic Ap stars is proposed and tested in the case of the Hβ line in 73 Dra. The instrumentation consists of a standard one-channel photoelectric photometer and three double half wave (D.H.W.) interference filters of different half-widths, centred at Hβ. In this investigation the half-widths of the narrow, mean and wide filters are 30 Å, 75 Å and 144 Å, respectively. Variations of the index $\beta_3 = 2.5 \cdot \log(F_w/F_m)$, where F_w and F_m are the corresponding measured fluxes, represent the direct measure of the total Hβ equivalent width (W_λ) variations (in per cent) as both filters are sufficiently wide to cover the total $W_\lambda(H\beta)$ in Ap stars of any (T_{eff}, $\log g$) values. The Crawford index $\beta = 2.5 \cdot \log(F_w/F_m)$ variations give additional independent information on the character of the $W_\lambda(H\beta)$ phase curve.

This method applied to 73 Dra shows that this Ap star exhibits periodic variability of the Hβ line in the form of a single wave, and amplitude $\Delta W_\lambda/W_\lambda(max) \approx 7\%$. Moreover, the extremal values of $W_\lambda(H\beta)$ coincide in phase with extremal $H_{eff}(\varphi)$ values. Comparison with earlier spectroscopic observations shows that variable metallic lines near Hβ give rise to the β_3 variations of an order of magnitude less than Hβ itself. This result should be considered as verification of earlier photographic observations of Hγ and higher Balmer lines in 73 Dra, which previously gave particularly inconsistent results.

Comparison with measurements of standard stars shows that this method enables one to measure ΔW_λ variations with an error of only 2-3 %, which is superior to 10 % (or larger) and the sometimes subjective errors of W_λ measured on photographic spectrograms. Moreover, its high efficiency allows for future statistical investigation of Balmer line variations in Ap stars in a particularly homogeneous way.

PRELIMINARY RESULTS OF SPECTROPHOTOMETRIC STUDY OF THE Si-VARIABLE STAR θ Aur (HD 40312)

D. Kolev and E. Georgeva

Bulgarian Academy of Sciences, Section of Astronomy and National Astronomical Observatory, Sofia, ul. 7 Noemvri 1.

Spectrophotometric study of the Ap star θ Aur is carried out on 9 Å/mm and 4 Å/mm spectrograms. The variations of the equivalent widths of the Si II multiplets (1) and (3) are investigated for periods $1^d.3717$, $1^d.3735$ and $3^d.618$. The intensity of the lines varies more than twice. The best agreement between observations in the years 1981 and 1982 is achieved for $P \simeq 1^d.3717$. The following parameters were found according to the average Hγ profile of θ Aur: $T_e = 11500$ K, $\log g = 3.85$, Sp = B9 Vp.

The radius and the mass of the star are estimated as follows: $R = 2.5 R_\odot$ and $M = 3.5 M_\odot$. The projected rotational velocity is $v \cdot \sin i = 53.5 \pm 1.0$ km/s and the inclination angle has a value of 35° for the period $1^d.3717$.

ULTRAVIOLET OBSERVATIONS OF MAGNETIC CP STARS: A SHORT REVIEW

W. Schöneich
Zentralinstitut für Astrophysik
Potsdam, Telegrafenberg, DDR

Ultraviolet observations have proved to be very important for investigating magnetic stars. After the detailed review on Ap stars (Leckrone, 1975) new results have become available and it is now usual to discuss magnetic CP stars; these include the Helium variables in addition to the Ap stars. Ultraviolet observations of magnetic CP stars have been carried out with OAO-2, COPERNICUS, TD-1A, ANS and IUE. Photometric observations by Bernacca and Molnar (1972), Leckrone (1973), van Dijk et al. (1978) and Jamar et al. (1978) show that the relation between Balmer and Paschen continua for silicon stars is significantly different from that of normal stars, whereas for He-w stars and to some extent for Cr-Eu-Sr stars the disagreement is not so pronounced.

Time resolved photometric observations were made for a number of magnetic CP stars. In Table I those stars are collected for which light curves have been published.

Table I

star	experiment	reference
HD 15089	OAO-2	Molnar et al. (1976)
HD 112185	OAO-2	Molnar (1975)
HD 112413	OAO-2	Molnar (1973)
HD 124224	ANS	Molnar, Wu (1978)
HD 125823	OAO-2	Molnar (1974)
HD 140728	ANS	van Dijk et al. (1978)
HD 170000	TD-1A	Jamar (1977)
HD 215441	OAO-2	Leckrone (1974)

In the case of 21 other stars, variability on ultraviolet was noted (Table II).

Table II

reference	stars
Leckrone (1975)	HD 215038, 56 Ari, Chi Ser
van Dijk et al. (1978)	HD 22478, HD 25267, HD 32650, HD 56022, HD 118022, HD 122532, HD 125248, HD 133660, HD 151529, HD 173650, HD 193722, HD 196176, HD 196502, HD 203006
Jamar (1977, 1978)	56 Ari, HD 27309, HD 40312, HD 124224, HD 177410

For some other stars with known periods TD-1A observations made at different times are available. They are being investigated by Zelwanowa, Schöneich and Jamar. Preliminary results on Helium variables will be presented at this meeting (see the next paper on page 179).

The main results from UV light curves are:

- The UV light curves generally show the same character as those in the visible and can also be explained as rotational variability.
- The spots, bright in the visible, become dark in the UV. The dependence of the "null wavelength" on stellar temperature, suggested by Molnar et al. (1976), is doubtful as was noted by Jamar (1977).
- The large amplitudes in UV (≈0.5 mag in some cases) indicate that the dark spots should be very large (Jamar, 1978). The amplitude of 1.2 mag found by Leckrone (1975) at 1100 Å for α^2 CVn demands a minimum spot radius of 0.8 stellar radius. Such large radii are not in agreement with the shapes of the light curves. This can be explained if the limb darkening is very strong at this wavelength.
- The hotter Helium variable a Cen does not show a "null wavelength" in the observed spectral region (>1450 Å). This fact can give the key to the problem of the mechanism of light variability of magnetic CP stars.

Spectral observations of magnetic CP stars with high resolution in the ultraviolet were carried out with COPERNICUS and IUE. The results published till now are mainly of a qualitative character. Line identifications and the discovery of line variations are important especially for 4 He rich stars (HD 37017, σ Ori E, HD 37776, HD 64740). In these stars, the silicon lines vary in antiphase to the He lines, as in He weak and hot Ap stars, although the results of analysis (Hunger, 1975), that the He-r stars do not show silicon overabundances, has not been corrected till now. In Table III high resolution UV observations of magnetic CP stars are collected.

Table III

reference	stars
Barylak, Rakos (1981)	HD 219749
Castelli et al. (1981)	78 Vir
Fahey (1980)	HD 125823
Hunger, Heber (1981)	CPD-46° 3093
Leckrone (1980)	21 Per
Leckrone, Snijders (1979)	α^2 CVn
Lester (1979)	HD 64740
Mallama, Molnar (1977)	ε UMa
Rakos (1980)	HD 133029, HD 175362, HD 219749
Shore, Adelman (1981)	HD 37017, σ Ori E, HD 37776

Some papers, presented at the 2nd European IUE Conference, are not included because they were not available.

References:

Barylak, M., Rakos, K.D. 1981, In: Upper Main Sequence CP Stars, 23rd Liège Coll., p. 141.
Bernacca, P.L., Molnar, M.R. 1972, Ap.J., 178, 189.
Castelli, F., Faraggiana, R., Catalano, F.A., Maitzen, H.M. 1981, In: Upper Main Sequence CP Stars, 23rd Liège Coll., p. 135.
Fahey, R.P. 1980, NASA Conf. Publ. 2171, p. 177.
Hunger, K. 1975, In: Problems in Stellar Atmospheres and Envelopes, Ed.: Baschek, Kegel, Traving; Springer, Berlin, p. 57.
Hunger, K., Heber, U. 1981, Astron. Astrophys., 101, 269.
Jamar, C. 1977, Astron. Astrophys., 56, 413.
Jamar, C. 1978, Astron. Astrophys., 70, 379.
Jamar, C., Macau-Hercot, D., Praderie, F. 1978, Astron. Astrophys., 63, 155.
Lester, J.B. 1979, Ap.J., 233, 644.
Leckrone, D.S. 1973, Ap.J., 185, 577.
Leckrone, D.S. 1974, Ap.J., 190, 319.
Leckrone, D.S. 1975, IAU Coll. No. 32, Vienna, p. 465.
Leckrone, D.S. 1980, Highlights of Astronomy, 5, 277.
Leckrone, D.S., Snijders, M.A.J. 1979, Ap.J. Suppl., 39, 549.
Mallama, A.D., Molnar, M.R. 1977, Ap.J. Suppl., 33, 1.
Molnar, M.R. 1973, Ap.J., 179, 527.
Molnar, M.R. 1974, Ap.J., 187, 531.
Molnar, M.R. 1975, Astron. J., 80, 137.
Molnar, M.R., Mallama, A.D., Holm, A.V., Soskey, D.G. 1976, Ap.J., 209, 146.
Molnar, M.R., Wu, C.-C. 1978, Astron. Astrophys., 63, 335.
Rakos, K.D. 1980, NASA Conf. Publ. 2171, p. 167.
Shore, S.N., Adelman, S.J. 1981, In: Upper Main Sequence CP Stars, 23rd Liège Coll. p. 429.
van Dijk, W., Kerssies, A., Hammerschlag-Hensberge, G., Wesselius, P.R. 1978, Astron. Astrophys., 66, 187.

ULTRAVIOLET TD-1 OBSERVATIONS OF HD 170000 AND SIX HELIUM VARIABLES (PRELIMINARY RESULTS)

E. Zelwanowa and W. Schöneich
Zentralinstitut für Astrophysik, Potsdam, DDR

and

C. Jamar
Institut d'Astrophysique, Liège, Belgique

Observations are presented on the first seven magnetic CP stars with known periods and more than one available TD-1 (S2/68) observation.

The shape of the light curves of the silicon star HD 170000 (65 observations) varies strongly with the wavelength. There is evidence of two dark spots at phases 0.1 and 0.7 (light maximum in the visible is at phase 0.0). The second spot coincides with the positive magnetic pole.

The He-weak star HD 28843 (B9 IV Si) varies at λ 1440 in antiphase to λ 2740 and to the visible spectral region.

Similar behaviour but with smaller amplitude was found for HD 125823 and HD 175362.

For the He-rich star HD 64740 no significant variation was found.

For the stars HD 49333 (He-w) and HD 58260 (He-r) the periods are known only with low accuracy. It is impossible to derive the phases of the observations and therefore to derive conclusions on variability. Details are being prepared for publication.

HD 221568

K. Stepien
Warsaw University Observatory
Al. Ujazdowskie 4, Warsaw, Poland

A grid of model atmospheres with chemical compositions characteristic of the red and blue phases of HD 221568 was obtained by Dr. Mutham of Vienna Observatory. Theoretical energy distributions were fitted to spectrophotometric observations obtained by Kodaira, supplemented by UV observations obtained with the International Ultraviolet Explorer. A comparison of theoretical models at the same temperature but chemical abundances characteristic of blue and red phases shows that the differences due to a different chemical composition are very small which means that the large light variations observed for this star cannot be explained solely by the effect of differential blanketing. However, fits to observations show that the star has the same temperature (10300 ± 100 K) in both phases. It is suggested that the observed light variations can be explained by a difference in the effective radii of the star in both phases if the star is non-spherical. However, to explain the decrease of flux around band B of the UBV system in the red phase it seems to be necessary to assume that a part of the energy at the photospheric level occurs in a non-radiative way. The different possibilities of such a mode of transport are discussed.

MODEL OF φ DRACONIS

B. Musielok
Astronomical Institute of Wroclaw University
Wroclaw, Poland

A model of the surface brightness distribution was calculated for the Ap star φ Dra. The model is based on 49 photoelectric measurements in the Y band of the 10-colour system with some additional information taken from the ultraviolet photometry of Jamar (1977), the magnetic field measurements of Landstreet (1977) and spectroscopic measurements of the author. These data suggest that there are two spots on the surface of the star. The following parameters were determined: positions of the spots, their dimensions, contrasts to the remaining atmosphere and inclination of the rotational axis to the line of sight. Three of these parameters were compared with other measurements or theoretical presumptions.

PROBLEMS OF ESTIMATING THE ANGLE BETWEEN THE ROTATIONAL AND THE MAGNETIC AXES OF STARS — USING THE Ap STAR θ Aur (HD 40312) AS AN EXAMPLE

D.Z. Kolev
Bulgarian Academy of Sciences, Section of Astronomy and National Astronomical Observatory, Sofia, ul. 7 Noemvri 1, Bulgaria

Uncertainties in determining the obliquity (β) between the rotational axis of stars and the magnetic-dipole one are discussed. The Si-variable Ap star θ Aur is used as an example. Spectral observations of the variation in the Si II lines confirm the period $1^d.3717$; the magnetic measurements (1) give $P = 3^d.618$. The radius of the star is estimated to be $R = 2.5R_\odot$ and our measurements give $v \cdot \sin i = 53.5$ km/sec. New values for the parameters of the magnetic-dipole model for θ Aur are obtained using our data and measurements of the field from Borra and Landstreet (1). Namely, our measurements are: inclination angle $i = 35^o$, $\beta = 82^o$ and the polar field $B_p = 1670$ G; in contrast to the values in (1), viz. $i = 77^o$, $\beta = 51^o$ and $B_p = 1300$ G.

The general conclusion is that θ Aur is a rapid magnetic rotator with high obliquity.

Reference:
(1) Borra, E.F., Landstreet, J.D. 1980, Ap.J.Suppl., 42, 421.

PROPERTIES OF THE BOWEN PHASE-SHIFT COMPENSATOR

L. Oetken
Zentralinstitut für Astrophysik
Potsdam, Telegrafenberg, DDR

An observed unexpected stellar polarity reversal led to the re-discussion of instrumental phase shifts between rectangular light components, especially those introduced by the phase shift compensator constructed after a proposal of I.S. Bowen. Since this discussion may be of interest to other observers, the main results are summarized here. If such a compensator-device is made of two eighth-wave-retardation plates thus leading to a maximum phase shift of $\pi/2$ the direction of circulation of the light passing the compensator cannot be changed. Therefore no polarity reversal can be produced in all cases for which the telescope introduces effective phase shifts (retardances) smaller than $\pi/2$. However, if the instrument produces effective phase shifts larger than $\pi/2$ — under discussion for the 2 m Universal telescope at Tautenburg for stars near the pole — such an eighth-wave-plate compensator can produce circularly polarized light only without restoring the direction of circulation of the star light that may be misinterpreted as polarity reversal. If, on the other hand, the compensator is made of thicker retardation plates so that phase shifts larger than $\pi/2$ can be introduced by it, both possibilities exist, this means that the conservation of the direction of circulation as well as its change can generally be reached. Therefore, besides the usual calibration consisting of the reproduction of circular polarized light using an artificial circular polarized light source in the telescope tube, an additional test is necessary to decide what has happened.

DIRECT INTENSITY MICROPHOTOMETER

M. Minarovjech, M. Ribanský, J. Žižňovský, J. Zverko
Astronomical Institute, Slovak Academy of Sciences
Tatranská Lomnica, Czechoslovakia

A device for direct intensity recording of photographically recorded spectra is described. The principle of the device is based on an unusual expression of the characteristic curve enabling it to be approximated by a straight line through the whole range of optical densities usually used in photographic photometry. A special-purpose analog computer was then constructed utilizing modern elements. Examples of use as well as an estimate of errors are given.

FIRST OBSERVATIONS OF MAGNETIC STARS WITH THE NEW PHOTOELECTRIC PHOTOMETER OF THE NATIONAL ASTRONOMICAL OBSERVATORY

K.P. Panov
Department of Astronomy with National Astronomical Observatory,
Bulgarian Academy of Sciences
7 November str. 1, Sofia, Bulgaria

A new one-channel UBV photoelectric photometer was designed and built in the Department of Astronomy, Bulgarian Academy of Sciences, for the 60 cm telescope of the National Astronomical Observatory. Photon-counting mode is used. Details of the equipment are presented in another paper (Panov et al., 1982).

A programme of photoelectric observations of magnetic stars was started in 1981 with the 60 cm telescope of the National Astronomical Observatory in order to search for short-term light variations in these stars. Many reports have been published so far on this subject (e.g. Schöneich, 1978), but the problem is still unresolved.

Preliminary results were obtained for the stars HD 219749 (B9p) and 53 Cam (A2p). Most of the observations were carried out with an integration of 1 sec in all UBV colours quasi-simultaneously.

File observations of HD 219749 were obtained on 5 nights in September - October 1981. Short-term variation with a cycle of about 150 min is clearly seen in the run of 19/20.09.1981 in all UBV colours. The amplitudes are 0.01 mag in V, 0.01 mag in B and 0.02 mag in U. These short-term variations are also present in the runs of 20/21.09.1981 and 30/31.10.1981. Earlier results of Panov (1978) and Hildebrandt (1981) are thus confirmed by these new observations. It is not yet clear whether the short-term light variation of HD 219749 is related to the rotational period.

Rapid variability in the spectrum of 53 Cam was reported by Polosukhina et al. (1981) and by Kuvshinov and Plachinda (1980). File observations in UBV of the magnetic star 53 Cam were obtained during 3 nights of January 1982. The runs evaluated so far show complicated short-term variations. An increase of brightness is seen in the run of 21/22.01.1982 in all UBV colours: 0.01 mag in 1.5 hours. The observations of 27/28.01.1982 show short-term variations with rather different characteristics: quasi-periodic variation with a cycle of about 70 min and amplitude 0.008 mag is present in V.

During the same time irregular light variations with a decreasing amplitude are seen in B. The cycle length varies from 40 to 25 min. This is an indication that the short-term light variations of 53 Cam might have a complicated character.

References:

Hildebrandt, G. 1981, Commun. Special Astrophys. Obs., No. 32, 74.
Kuvshinov, V.M., Plachinda, S.I. 1980, Pisma v Astr. Zhu., 6, 368.
Panov, K.P. 1978, Publ. Astron. Inst. Czechosl. Acad. Sci., No. 54, 19.
Panov, K.P., Pamukchiev, I.Ch., Christov, P.P., Petkov, D.I., Notev, P.T., Kotsev, N.G. 1982, Comptes Rendus of the Bulgarian Acad. Sci. (in press).
Polosukhina, N.S., Chuvaev, K.K., Malanushenko, V.P., Tuominen, I., Kholsti, 1981, Commun. Special Astrophys. Obs., No. 32, 68.
Schöneich, W. 1978, Publ. Astron. Inst. Czechosl. Acad. Sci., No. 54, 16.

RESULTS OF NARROW-BAND PHOTOMETRY OF THE MAGNETIC STAR 53 Cam

V.I. Burnashev, N.S. Polosukhina, V.P. Malanushenko
Special Astrophysical Observatory, Zelenchuk, U.S.S.R.

During 16 nights between 20.02.80 and 15.03.81 using an SF-68 spectrophotometer, flux measurements of the magnetic star HD 65339 (53 Cam) were taken related to the comparison star HD 65301 in the spectral band $\Delta\lambda \simeq 30$Å, centred at $\lambda = 4187$ Å. The dispersion of measurements of relative fluxes $\Delta m_i = m_{53\ Cam} - m_{comp}$ for individual nights significantly exceeded the error of measurements and was ascribed to the real variations of 53 Cam flux for one night.

Our studies of the behaviour of this variation permitted us to draw the following conclusions:

1. There are periodic variations of complex character that may be described by a sum of three simple sinusoidal curves with the periods $P_1 = 20^m.14 \pm 0.0001$, $P_2 = 27^m.5828 \pm 0.0001$ and $P_3 = 79^m.2381 \pm 0.0001$, present during 1.5 year.
2. The amplitudes of variations change with the rotational phase of the star.
3. The exception to the typical behaviour stated above was the night of 15-16.12.1980 when the observed variations Δm can be described with the single period $P_1 = 47^m.02$.
4. On the basis of mean values of Δm the variation of the relative flux of radiation with the period of star rotation ($P = 8^d.0267$) was shown. These variations correlate well with the variations of the effective magnetic field of the star.

WORKING REPORT ON 8 Ap STARS

L. Hric and J. Zverko
Astronomical Institute of the Slovak Academy of Sciences
Tatranská Lomnica, Czechoslovakia

Eight doubtfully classified Ap stars were selected for detailed spectroscopic and photometric study. Locations in two-colour diagrams were found. All the stars studied are near the main sequence. Projected rotational velocities were determined from the Mg II 448.1 nm line. Remarkable differences of T_{eff} values derived from the UBV, uvbyβ, Hβ,γ,δ lines were found.

PHOTOMETRY OF AR Aur ECLIPSING Ap BINARY

K. Juza and J. Zverko
Astronomical Institute of the Slovak Academy of Sciences
Tatranská Lomnica, Czechoslovakia

The minima of a detached eclipsing system AR Aur were observed photoelectrically by a 0.6 m telescope at Skalnaté Pleso Observatory. Our data confirm that the orbital period is decreasing at the present time. The minima light curve shapes indicate possible total eclipses.

SEARCH FOR SHORT-PERIOD VARIATIONS IN Ap STARS

T. Jarzebowski
Wroclaw University Observatory
Kopernika 11, Wroclaw, Poland

Photoelectric observations of four peculiar stars — 21 Com, HD 71866, HD 224801 and HD 32633 — were made at San Pedro Martir Observatory (Baja California, Mexico).

21 Com was investigated on six nights. The observations do not confirm the 32 min period reported by Bahner and Mavridis and by Percy.

HD 71866 was investigated on three nights. The results do not exclude the possibility of some variations, but we did not find the 97 min oscillations quoted by Rakos.

The observations of HD 224801 and HD 32633 are shown in the figures (points and crosses refer to different comparison stars). Some light variations are possible, this can especially be seen in the case of HD 32633. The results do not confirm, however, the periods of 124 min and 106 min, reported by Rakos for HD 224801 and HD 32633, respectively.

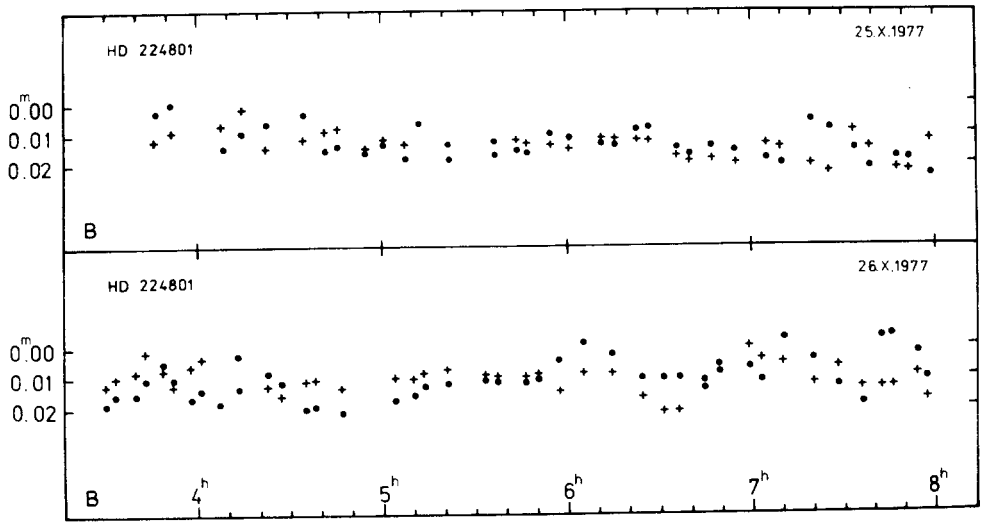

Figure 1

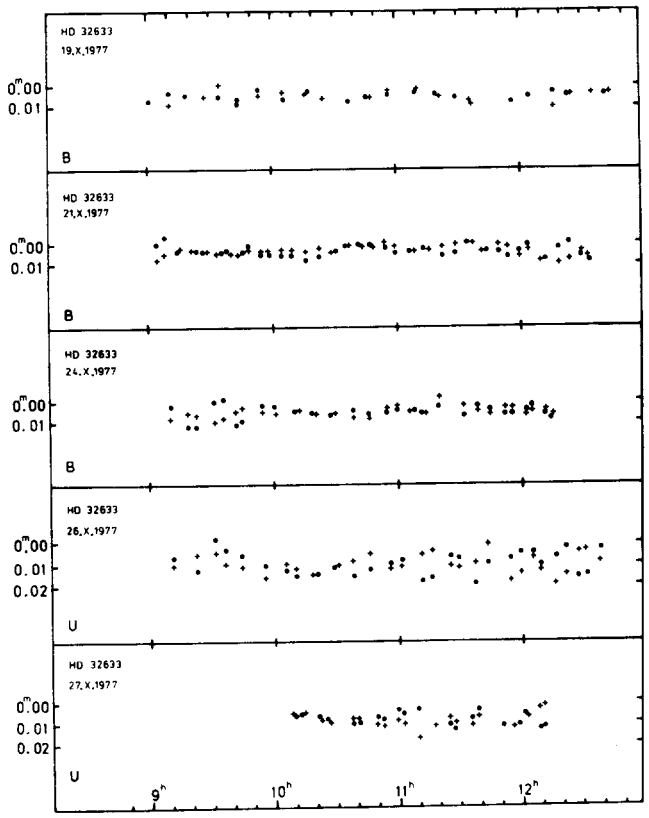

Figure 2

Taking into account all present observational data we see that short-period luminosity variations are definitely established only in two peculiar stars (investigated by Kurtz), viz. HD 24712 and HD 101065 . If, however, these variations were not associated with pulsation, one could conclude that there are no δ Scuti-type variables among peculiar stars.

SEARCH FOR RAPID LIGHT VARIABILITY OF HD 215441

J. Zverko
Astronomical Institute of the Slovak Academy of Sciences
Tatranská Lomnica, Czechoslovakia

and

K.P. Panov
Department of Astronomy with National Astronomical Observatory
Bulgarian Academy of Sciences, Sofia, Bulgaria

Photoelectric UBV and intermediate band observations were analysed for rapid light variability. The UBV observations were performed at the Bulgarian Academy of Sciences' Observatory, Rozhen, by a photoelectric photon counting photometer attached to a 0.6 m reflector. The observations were made with 1 or 10 sec integration time. The intermediate band observations were carried out at the Slovak Academy of Sciences' Observatory, Skalnaté Pleso, by a photometer arranged in a classic way equipped with a strip chart recorder. The filter used had a wavelength of $\lambda = 526$ nm and a HW = 19 nm. In both cases HD 215501 was the comparison star. The observations of the magnetic star were reduced in the usual way relative to the comparison. Moreover, the observations of the comparison were expressed in magnitudes. Thus two light curves were obtained, one for the magnetic star, the other for the comparison. The curves were always found to be similar to each other and variations on them strongly correlated to observation conditions. Scattering extends to 0.01 mag in the best conditions and this is so for the variable and the comparison as well. This is valid for both the UBV and intermediate band photometry. It is impossible to decide without a data frequency analysis whether there is an intrinsic rapid variability of less than 0.01 mag hidden in the HD 215441 light curve.

The rotational light curve was studied and an ephemeris JD(max. light) = 2 436 865.0 + $9^{d}.4875 \cdot E$ was derived.

γ Cyg — MAGNETIC PERIODIC STAR?

S.I. Plachinda, A.B. Severny, E.S. Dmitrienko
Crimean Astrophysical Observatory
Nauchny, Crimea, SU - 334413

The effective longitudinal magnetic fields of the supergiant γ Cyg were measured in 1977 and 1981 utilizing the photoelectric scanner-magnetometer of the Crimean Observatory's 2.6 m reflecting telescope. The star β CrB with the known variable magnetic field was used as a comparison star. We found good agreement of our observations of β CrB with the observations of other authors. The periodic variations, $8^{d}.2594$, of longitudinal magnetic field strength in the limits -40 gauss to +40 gauss were suspected for γ Cyg.

STELLAR ACTIVITY AND DYNAMO THEORY

G. RÜdiger
Zentralinstitut fÜr Astrophysik
Potsdam, Telegrafenberg, DDR

Skylab and EINSTEIN experiments revealed that (i) the solar corona is extremely inhomogeneous and (ii) stellar coronae exist along the whole main sequence. Both findings are incompatible with the standard theory of acoustic heating of a corona. There is little doubt that only magnetism is able to provide the observed large scale ("loop") structures and to ensure the frequent occurrence of stellar coronae. A new tool for the development of the dynamo theory has thus been provided.

The observations seem to confirm the newly established suggestion according to which the stellar activity may not decrease towards the lower end of the main sequence. Wilson found stars with cyclic chromospheric activity down to spectral type K5 and with periods of about 10 years. At least for G and K dwarfs the activity is thus due to a solar-like dynamo mechanism. In accordance with the dynamo theory the current observations have so far revealed no dependence of the cycle period on the spectral type. It has further been proved that (i) cyclic stars are weak emitters and (ii) weak emitters are old stars — so that the cyclic dynamo stars should be rather old.

The strong and the weak emitters are separated by a distinct gap which, however, disappears for stars later than (say) K3. In the latter region the weak emitters are missing rather than the old stars. We suggest that the rotation rate (t_{rot}) in its relation to the turnover time (t_{cor}) (taken in the bulk of the convection zone) determines the stellar magnetohydrodynamics: only slow rotators ($t_{rot} > t_{cor}$) can function as a cyclic dynamo. Since the turnover time of an M0 star is rather long (200 days), slow rotators of this type either do not yet exist or are very rare. This may be the reason for the non-existence of the Vaughan-Preston gap for the latest dwarfs.

Recent spectacular measurements of rotational periods via daily variations of H and K emission led to the conclusions that (i) all young stars possess one and the same period (about 7 days); (ii) the rotation rate increases with decreasing emission, i.e. with increasing age; (iii) among the stars with 40 days the K2 stars are cyclic and the K7 stars are eruptive. The key question is whether the last feature indicates the existence of a critical angular velocity which separates the cyclic and the non-cyclic emitters.

DWARF NOVAE

J. Smak
Copernicus Astronomical Center
Polish Academy of Sciences
Warsaw, Poland

During the last year major progress has been made in our understanding of the nature of dwarf novae and — in particular — of the mechanism responsible for the unstable character of accretion in those objects. In this paper I am not going to review the general field of cataclysmic binaries nor the previously existing accretion theories partly applicable to these objects: excellent reviews of this type can be found in the literature (cf. Robinson 1976, Pringle 1981). Instead I intend to concentrate on the most recent theoretical results concerning accretion in dwarf novae.

In the theory of thin, Keplerian accretion disks it is possible to treat separately the problem of radial structure (i.e. of radial flow or accretion) and the problem of vertical structure. Until very recently most authors concentrated on radial structure, bypassing the problem of the vertical structure through a crude averaging procedure. The new developments come from a detailed consideration of the vertical structure.

Let us consider the vertical structure at a distance r from the central mass M. After assembling all relevant equations for the vertical structure (basically of the same type as for the stellar interiors) one can see that one of the parameters involved must be independent, while all the others — after performing the integration in z — can be expressed as its functions. By analogy with stellar interiors (and the Vogt - Russell theorem) we can choose for this independent parameter the surface density Σ (i.e. the mass accumulated over 1 cm^2 of the equatorial plane). Since the accretion is responsible for the "energy generation" we can alternatively consider as the free parameter the local accretion rate $\dot{M}$ which — via simple proportionality — determines the local emerging flux or effective surface temperature: $F = \sigma T_e^4$. Two parameters are crucial for the vertical structure: the temperature gradient ∇ (as in stellar interiors) which depends on the mechanism of the energy transport in the vertical direction, and the coefficient of viscosity ν (per gram); note that viscosity is responsible for the outward flow of the

angular momentum necessary for the inward flow of mass (i.e. for the accretion) and hence for the local "energy generation" (more precisely for the dissipation of the mechanical energy). In the classical theory of α-disks (cf. Pringle 1981) the vertical structure is simply averaged under the assumption of radiative equilibrium (i.e. $\nabla = \nabla_r$). In addition, since the nature of viscosity remains unknown, one introduces an arbitrary, free parameter α defined by the relation: $\nu = \alpha \cdot v_s \cdot z_o$, where v_s is the velocity of sound and z_o is the thickness of the disk.

In the recent models of the vertical structure (Canizzo et al. 1982, Meyer and Meyer-Hofmeister 1981, 1982, Smak 1982a,c) the possibility of the convective transport of energy is explicitly included and the temperature gradient is calculated as $\nabla = min(\nabla_r, \nabla_c)$, again in full analogy with stellar interiors. With respect to α the three groups of papers differ significantly: the Meyers have used — essentially — the α-disk approach, i.e. have described viscosity via a single, free parameter α. Canizzo et al. use a lower value of α for the radiative regions and a higher value of α for the convective regions. In my models I assume that convection is the only source of turbulence responsible for viscosity and hence I put $\alpha = 0$ in the radiative regions; in the convective regions it is possible — in principle — to relate α to other convective parameters; however, since the mixing-length theory fails near $z = 0$, I have so far been unable to eliminate α in this way and it — essentially — remains a free parameter for the convective regions. These three different types of approach simply reflect our ignorance with respect to the true nature of viscosity. Very fortunately it turns out that most basic conclusions are — qualitatively — nearly the same. In what follows I will refer mostly to my own results but I wish to emphasize that the basic explanation of the nature of instability in the outer parts of disk in dwarf novae was first given by Meyer and Meyer-Hofmeister (1981).

Figure 1 shows the crucial $T_e - \Sigma$ relation resulting from the integration of the vertical structure. Although such a specific relation is obtained for a given distance r from the central star and with a specific value of α, it turns out that the shape of this relation is nearly universal. In particular, by going to other distances, or by changing α, we produce a shift only in the $\log \Sigma$ coordinate, while the critical points in $\log T_e$ (to be discussed below) remain almost unaffected. There is a simple explanation for the shape of this basic relation: the two "bends" BCD and DEF are related to the considerable decrease in the adiabatic gradient due to — respectively — partial ionization of hydrogen and formation of the molecular hydrogen. The crucial

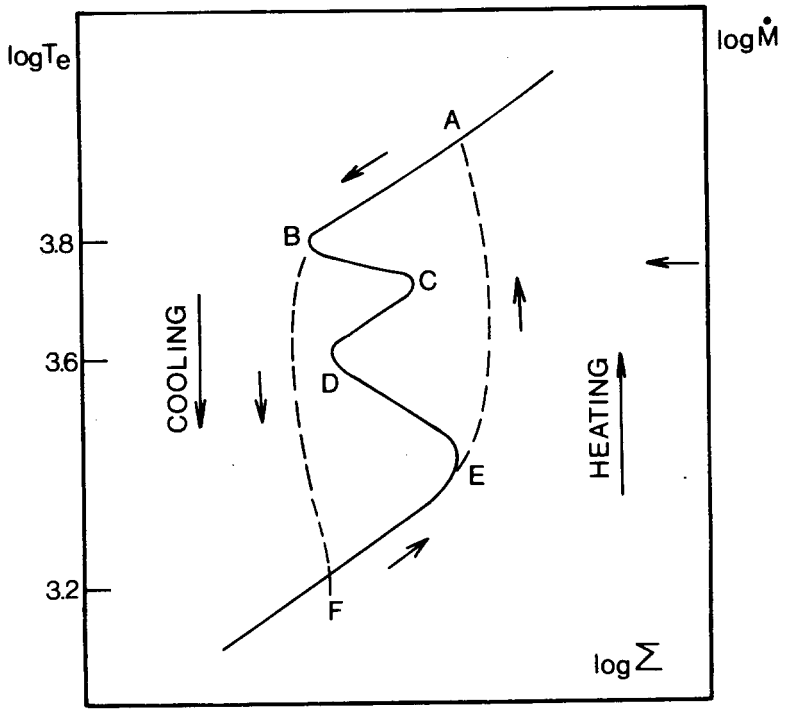

Figure 1 Schematic representation of the $\log T_e - \log \Sigma$ diagram. The $\log T_e$ values for points B, D, F marked on the left margin are only approximate and depend on the details of the vertical structure.

point is that branches BC and DE are unstable against perturbations in Σ (Meyer and Meyer-Hofmeister 1981, Smak 1982a); they are also unstable against thermal perturbations (Smak 1982c).

In the case of stationary accretion we have

$$F = \sigma T_e^4 \simeq \frac{3}{8\pi} \dot{M} \frac{GM}{r^3}$$

which shows that the lowest temperature will be at the outer edge of the disk and its value will be determined by the product $\dot{M}/r^3$. Critical analysis of the observational data (Smak 1982b) shows that in the case of novae and nova-like objects, i.e. in the case of disks with presumably stationary accretion, the temperatures of their outermost parts are higher than $\log T_e = 3.8$ (corresponding to the critical point B in Fig.1). In the case of dwarf novae, however, primarily due to lower accretion rates, the temperatures of the

outermost parts of their disks would — under stationary conditions — be below the critical value. Hence in this case we must expect instabilities.

So far I have discussed models in thermal equilibrium. Let us now consider possible deviations from the thermal equilibrium, i.e. models which include cooling or heating of the disk. Crude calculations show (Smak 1982c) that models with cooling are located to the left, while models with heating — to the right of the "standard" curve in the $T_e - \Sigma$ diagram. Suppose a local structure of the disk is represented by a point somewhere on the AB branch and we perturb such a model by moving it effectively to the left of the AB branch. It will fall into the "cooling" domain and hence will return to the "standard" curve: the AB branch is obviously stable against thermal perturbations! If we do the same to a point on the BC branch we will have the perturbed models also to the left but this time <u>below</u> the "standard" curve and "cooling" will mean moving down, i.e. further away from the initial location: the BC branch is thermally unstable!

What then is the nature and what are the consequences of instability in the outer parts of the disks of dwarf novae? Suppose the rate of mass-transfer from the secondary would require — under stationary conditions — that the temperature of the outermost parts of the disk be below the critical value of $\log T_e = 3.8$ (marked with an arrow in the right margin of Fig.1). Let us assume, for the sake of clarity, that the structure of these outer parts was described by a point somewhere on the BC branch. And suppose that due to a random perturbation it was forced to move up to the AB branch. (In fact it is irrelevant how we start. Due to the presence of instabilities we must end on the ABFE loop, as described below.) A model on the AB branch has a local accretion rate higher than the rate at which the material is supplied from the outside. This implies that Σ must decrease and our model will move down and to the left along the AB branch. At point B the tendency for decreasing Σ will still continue forcing our model to become thermally unstable: once in the "cooling" domain it will move down in a thermal time-scale; at the same time Σ will initially continue to decrease, but later will begin to increase. The thermal stability will return at point F where the local accretion rate is smaller than the mass-transfer rate. Hence Σ must increase and our model will move along the EF branch up and to the right. The loop is completed by a fast crossing of the "heating" domain from E to A, where the cycle begins again.

In this simplified picture the transition from F to E corresponds to the interval between the outbursts, when the material supplied from the second-

ary is mostly accumulated in the outer parts of the disk. The remaining part of the loop: EABF corresponds to an outburst and, in particular, the transition from A to B represents dumping of the previously accumulated material onto the central star. It can be roughly estimated that the time scale of the transition from A to B is about 10 times shorter than that from F to E.

It is clear that the unstable behaviour in the outermost parts, as described above, will affect the situation in the inner regions. Specifically, the local accretion rate in the outermost parts — which is variable — controls the rate of mass-transfer to the inner regions. It is therefore clear that a full, time-dependent model of the entire disk is necessary before a meaningful comparison with observations can be made.

To show that the picture presented above is consistent with the observational data one can mention spectral energy distributions of disks in dwarf novae (cf. Szkody 1981) which are generally inconsistent with predictions based on stationary accretion models. In particular, they suggest rather low temperatures being present somewhere; presumably in the outermost parts of these disks. For example, the infrared data for EX Hya (Sherrington et al. 1980) imply temperatures below 2000 K! This is consistent with temperatures characteristic for the EF branch in Fig. 1. In particular, this evidence speaks in favour of the ABFE loop. Within uncertainties of the available models another alternative would be to consider the ABDC loop: should point D be located further to the left there would indeed be no necessity to involve the EF branch. But the temperatures on the CD branch are above 4000 K. Quite in general, however, we cannot exclude that in different systems we can have different situations: either the ABFE loop or the ABDC loop. And speculating still further, that the existence of these two possibilities may explain outbursts and super-outbursts in the SU UMa type systems.

Let me conclude with two remarks. First, it is rather surprising and very remarkable that in spite of our continuing ignorance with respect to the nature of viscosity it is possible to explain the nature of dwarf novae with good prospects for studying their behaviour in a more quantitative way. Second, that once we have detailed, time-dependent models for disks in those systems, by comparing them with the wealth of the observational constraints we should be able to say more about the nature of viscosity. Dwarf novae may help us to understand the accretion phenomena in many other objects.

References:

Canizzo, J.K., Ghosh, P., Wheeler, J.C. 1982, Ap.J. (in press).
Meyer, F., Meyer-Hofmeister, E. 1981, Astr.Ap., 104, L10.
Meyer, F., Meyer-Hofmeister, E. 1982, Astr.Ap., 106, 34.
Pringle, J.E. 1981, Ann. Rev. Astr. Ap., 19, 137.
Robinson, E.L. 1976, Ann. Rev. Astr. Ap., 14, 119.
Sherrington, M.R., Lawson, P.A., King, A.R., Jameson, R.F. 1980, Mon. Not.R. astr. Soc., 191, 185.
Smak, J. 1982a, Acta Astr., 32 (in press).
Smak, J. 1982b, Acta Astr., 32 (in press).
Smak, J. 1982c, (in preparation).
Szkody, P. 1981, Ap.J., 247, 577.

SEPARATION OF WZ SAGITTAE STARS FROM FAST NOVAE BY A PURELY PHOTOMETRIC CRITERION

G.A. Richter
Zentralinstitut für Astrophysik
der Akademie der Wissenschaften der DDR
Sternwarte Sonneberg

WZ Sagittae stars are a small subgroup of dwarf novae with mean cycle lengths of several years and amplitudes with more than 7 mag. There are actually 4 members: WZ Sge, WX Cet, AL Com, UZ Boo. Their absolute magnitude during outburst amounts to $+2^M...+4^M$. Their eruption light curves are very similar to those of fast novae, which have absolute magnitudes of about -8^M. But their outburst spectra and physics of eruption are distinct. 20 to 30 days after the outbursts WZ Sge, AL Com and probably WX Cet have an abrupt brightness decrease of several magnitudes within about 1 day which is followed in some cases by a sudden return to the original value. If this should turn out to be a common property of all WZ Sge stars, it could be used as a means of separating WZ Sge stars from fast novae if no outburst spectra are available. Nova V 592 Her (1968) and the supposed supernova 1971 in M 31 would then have to be classified as WZ Sge stars.

PHOTOELECTRIC OBSERVATIONS AND PRELIMINARY ANALYSIS OF THE VARIABLE WHITE DWARF R 808

G. Kovács
Konkoly Observatory of the Hungarian Academy of Sciences
H-1525, Budapest, P.O. Box 67, Hungary

The photoelectric variability of R 808 was discovered by McGraw and Robinson (1976). From four nights of observation they concluded that the light variation was seemingly irregular with a quasiperiodicity at $\sim$1.2 mHz.

New photoelectric data of R 808 were obtained by the 100 cm telescope at Konkoly Observatory's mountain station in the spring of 1982. Altogether about 14 hours of data were accumulated on four not consecutive nights by the same photometer and data acquisition system as described earlier by Kovács (1981). We have used "white light" (no colour filter) and an integration time of 10 s for all our measurements. Because of computer dead-time and the printing of each item of data after integration, the sampling time was somewhat longer than 10 s, viz. $\sim$10.26 s. As the observations were made by a single-channel photometer, the data were seriously affected by atmospheric effects. Any possible long term variations of the data have been filtered out by use of polynomial fits to each run. The residuals have been analysed via FFT. One of our most reliable light curves and power spectra is shown in Fig. 1. Measured intensities have not been reduced to magnitude scale, but the total range of variation after the polynomial fit corresponds to about 0.3 mag. The light variation of $\sim$800 s with an amplitude of $\sim$0.15 mag is clearly seen at the second half of the light curve. The power spectrum exhibits this feature at $\sim$1.2 mHz. The origin of the other significant peak at $\sim$0.26 mHz is somewhat obscure because such a long term variation can also be caused by non-stellar phenomena (transparency changes, artificial effects of the polynomial fit).

Analysis of the other runs led to similar results. In each case a more or less stable frequency pattern was observed at around 0.26 , 1.2 mHz and (at a very low level) between 7 and 8 mHz.

It is clear that the light variation of R 808 cannot be represented by a simple frequency pattern. The question whether or not R 808 has a stable frequency spectrum can only be answered by further observations of low noise level.

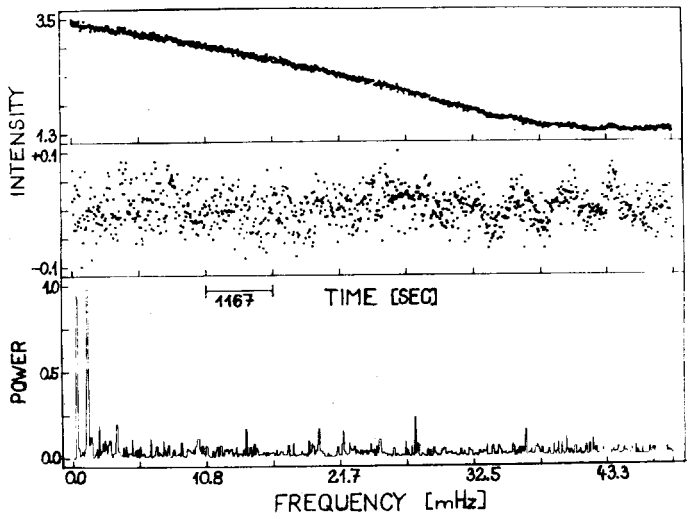

Figure 1. Photoelectric light curve and power spectrum of R 808 from 1st to 2nd April 1982. Uppermost part of the figure shows the original data obtained in unfiltered light. Applying a seventh order polynomial fit to these data gave the curve in the middle of the figure. Intensities (star+sky) are measured in the same (arbitrary) units for both curves. Starting time: $23^h 04^m00^s$ UTC; each point represents a 10 s integration; the number of points is 1024. The power spectrum was normalized to unity at its highest peak.

References:

Kovács, G. 1981, Acta Astr., 31, 207.

McGraw, J.T., Robinson, E.L. 1976, Astrophys. J., 205, L155.

PHYSICAL PROPERTIES OF STELLAR FLARES

L.V. Mirzoyan
Byurakan Astrophysical Observatory
Armenia, U.S.S.R.

The study of flare stars has two aspects: evolutionary and physical. Flare stars represent one of the earlier stages of stellar evolution and their observation from an evolutionary point of view has already been discussed (see, for example [1]). Here we are concerned with the physical properties of flare radiation.

Light curves. The light curves of flares obtained with high resolution in time are generally complex and can be presented as the superposition of the curves of two or more flares [2]. The time interval between the maximum and the second peak is less than 1 min in about 50% of cases and less than 5 min in 95% of cases. The probability of there being multipeaked light curves of flares increases with flare energy and becomes larger than 0.95 for the observed largest energies.

Colour indices. The mean colours U-B and B-V of flare radiation in maximum is practically the same for the UV Ceti type stars and the flare stars in stellar aggregates [4]. But they change significantly during flares indicating that the spectral composition of flare radiation changes in different phases of flares. A correlation between the colours of flare radiation in maximum and the increasing time of the corresponding flare is observed [3].

Spectra. The increasing of the flare light up to a maximum is always due to the continuous radiation. The line emission is a secondary factor and usually lasts longer than continuous flare radiation [5].

Mean frequencies. The mean frequency of flares for one single star increases rapidly to smaller flare energies and to shorter wavelengths. It increases also to low luminosities of stars [6]. In aggregates there exists a certain distribution function of mean frequencies for the flare stars. It can be determined from the observations using the chronologies of the first and the second flares of stars [7]. This distribution function is different for different aggregates [7,8].

"Fast" and "slow" flares. All flares can be divided into two groups: "fast" and "slow", according to the time of increase in luminosity [9]. These

two kinds of flares have quite different properties (time of increase in luminosity, mean frequency, colours). In fact the differences between them change continuously with time of increase in luminosity.

Problems. For the further physical study of stellar flares the following observations seem to be important:

1. Synchronous photoelectric observations of flares of UV Ceti type stars with very high resolution in time ($\sim$0.1 s) in few spectral bands, particularly with narrow filters.
2. Simultaneous spectral and photoelectric observations of flares of the UV Ceti type stars.
3. Far ultraviolet and X-ray observations of flare stars in minimum light.
4. Simultaneous photographic and radio observations of flares in stellar aggregates.

References:

[1] Ambartsumian, V.A., Mirzoyan, L.V.: In: New Directions and New Frontiers in Variable Star Research, IAU Coll. No. 15, Veröff. Bamberg, 9, No.100, 98, 1971.
[2] Mirzoyan, L.V.: In: Flare Stars, Fuors and Herbig-Haro Objects, ed.:Mirzoyan, L.V., Ac. Sci. Armenian SSR, Yerevan, 1980, p. 45.
[3] Mirzoyan, L.V., Melikian, N.D.: in preparation.
[4] Mirzoyan, L.V., Chavushian, H.S., Melikian, N.D., Natsvlishvili, R. Sh., Ohanian, G.B., Hambarian, V.V., Garibjanian, A.T.: Astrofizika, 17, 197, 1981.
[5] Moffett, T.J., Bopp, B.W.: Astrophys. J., Suppl., 31, 61, 1976.
[6] Mirzoyan, L.V.: In: Stellar Instability and Evolution, Ac. Sci. Armenian SSR, Yerevan, 1981.
[7] Ambartsumian, V.A.: Astrofizika, 14, 367, 1978.
[8] Parsamian, E.S.: Astrofizika, 16, 677, 1980.
[9] Haro, G.: In: Stars and Stellar Systems, Vol. 7, eds.: Middlehurst, B.A. and Aller, L.H., Univ. of Chicago Press, Chicago, 1968, p. 141.

FLARE STAR SEARCH IN THE PERIOD 1979-1982

M.K. Tsvetkov
Department of Astronomy and National Astronomical Observatory
Bulgarian Academy of Sciences

This work summarizes the main results about the monitoring observations and investigation of the flare stars which were obtained at the Department of Astronomy with National Astronomical Observatory (NAO) of the Bulgarian Academy of Sciences in the period 1979 - 1982.

The observations were made with the 50/70 cm Schmidt and the 60 cm Cassegrain telescopes at NAO - Rozhen. The aggregates Orion (M 42), Pleiades, Cygnus (NGC 7000 and γ Cygni) as well as other aggregates and the flare star EV Lac were included in the total observational programme. During about 450^h total effective time of observation at NAO - Rozhen, Byurakan Observatory and Konkoly Observatory 40 new flare stars were discovered (Table I). The data about the Rozhen monitoring observations are given in Table II.

Table I Monitoring observations in 1979 - 1982

Aggregate	T_{eff}	New flare stars	Flare-ups of known flare stars
NGC 7000	46^h40^m	4	2
γ Cygni	208 00	14	1
Pleiades	150 05	9	23
Orion (M42)	44 50	10	3
Field		3	
Total	$=449^h35^m$	40	29

Table II Monitoring observations at Rozhen in 1979 - 1982

Aggregate	T_{eff}	New flare stars	Flare-ups of known flare stars
γ Cygni	186^h00^m	11	1
Pleiades	110 45	5	14
Orion (M42)	44 50	10	3
Total	$= 341^h35^m$	26	18

The flare events of CE Orionis and the star Rozhen No.11 - Ori ($\Delta m_u \sim 8^m.0$) are of special interest, since CE Ori is a typical T Tauri star (IBVS Nos. 1889 and 2132). Table III and Figures 1 and 2 present some data about the flares of CE Ori and Rozhen No. 11 - Ori.

Table III Photometric data about the flare-up of CE Ori on 14.01.1980

No	U.T.	m_u	Δm_u
1	22^h16^m	($17^m.2$	
2	22 26.5	~16.9:	~$0^m.3$:
3	22 37	(17.2	
4	22 47.5	14.7	2.5
5	22 58	15.6	1.6
6	23 08.5	16.9	0.3

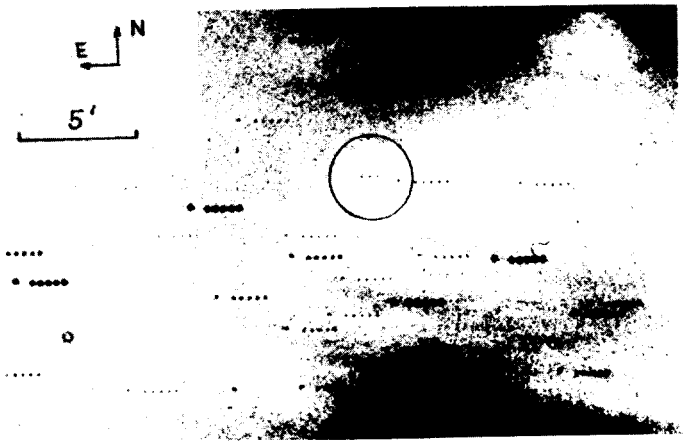

Figure 1 Flare-up of CE Ori (IBVS No. 1889)

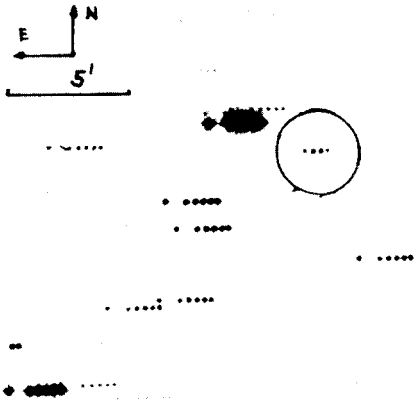

Figure 2 Flare-up of Rozhen No. 11 - Ori (IBVS No. 2132)

HIGH FLARE ACTIVITY OF THE STAR AD Leo IN 1982

K.P. Panov, M. Grigorova, A. Tsintsarova
Department of Astronomy with National Astronomical Observatory
Bulgarian Academy of Sciences, 7 November str. 1.
Sofia, Bulgaria

Photoelectric monitoring observations of the flare star AD Leo were carried out on 6 nights in February and March 1982 in the National Astronomical Observatory, using the 60 cm telescope and the photoelectric equipment. The one-channel UBV photoelectric photometer (Panov et al., 1982) operated in photon-counting mode. The observations were carried out in U colour with an integration of 1 sec. The standard deviation of random-noise fluctuations was 0.03 mag for all observations. During the total of 17^h57^m monitoring time 23 flares were observed. They are distributed over time as follows:

16/17.02.1982	5 flares in	3^h03^m monitoring time
18/19.02.1982	5 flares in	3^h04^m monitoring time
18/19.03.1982	1 flare in	2^h10^m monitoring time
25/26.03.1982	7 flares in	3^h45^m monitoring time
26/27.03.1982	3 flares in	3^h29^m monitoring time
27/28.03.1982	2 flares in	2^h26^m monitoring time

The observed flare frequency was thus 3 - 4 times higher than the same frequency obtained by others for AD Leo.

Reference:

Panov, K.P., Pamukchiev, I.Ch., Christov, P.P., Petkov, D.I., Notev, P.T., Kotsev, N.G. 1982, Comptes Rendus of the Bulgarian Academy of Sciences, in press.

BINARY STARS AMONG THE PHYSICAL VARIABLES

L. Szabados
Konkoly Observatory of the Hungarian Academy of Sciences
H-1525, Budapest, P.O. Box 67, Hungary

Abstract

This review summarizes our knowledge about the frequency of binaries among the various types of variables. Attention is drawn to some interesting phenomena observed in binary systems containing physical variables.

Introduction

In view of the known commonness of duplicity it is of interest to investigate to what extent the known types of variable stars are members in binary systems and how far binary nature affects their behaviour. Duplicity and its consequences were first reviewed by Larsson-Leander (1971). The review of Payne-Gaposchkin (1978) lists a large number of examples of binaries among physical variables. The last decade has demonstrated that the duplicity among variable stars deserves more attention. Although there are several types of variables (e.g. dwarf novae) where the duplicity is treated satisfactorily, this is not the case where the frequency of binaries is far from 100 per cent (e.g. pulsating variables).

Because of the presence of a close companion physical variability may be induced in an otherwise non-variable star and the behaviour of a physically variable star may be more or less influenced by the duplicity. Larsson-Leander (1971) lists three kinds of effects arising from the duplicity: gravitational effects, radiation effects and effects due to gaseous streams and mass transfer between the components. Gravitational effects may be important in pulsating variables where a sufficiently close companion produces tides that affect the physical conditions in the outer layers of the pulsating star, causing non-radial effects. Gaseous streams and mass transfer play an important role in cataclysmic variables.

One would expect that the frequency of binary stars among the physical variables does not differ significantly from the frequency observed in normal field stars. The discovery of the duplicity of several variables is not

a simple task. There are numerous methods to reveal the binary nature but their efficiency varies for different types of physical variables, and strong selection effects are present that work against the discovery of binaries.

The methods are as follows:

1. Visual discovery (e.g. Mira Ceti)
2. Eclipsing light variation
3. Radial velocity variation
4. Two components in the same spectrum (symbiotic stars)
5. Other spectral features (e.g. decreased ratio of emission/continuum in WR binaries, decreased IR masering in Miras)
6. Photometric evidences:
   - the reduced amplitude of the light curve
   - the general blueness (or redness) of the colour indices if the effective temperature of the companion is quite different from that of the variable (but interstellar reddening may mask the blueness)
   - the ratio of the amplitude in different photometric bands is different from the normal value
   - the "two-colour diagram" method (Madore, 1977)
   - the "phase shift" technique (Fernie, 1980)
7. Light-time effect in the O-C diagram (Coutts, 1971; Szabados, 1980 and 1981) which is especially useful when the colour of the companion does not differ considerably from that of the variable.

Pulsating variables

In addition to the light-time effect, there is another interesting phenomenon observed in the O-C diagrams of several binary Cepheids, viz. the "rejump" of the period (Szabados, 1977, 1980, 1981). The rejump of the period may occur suddenly, in this case the phenomenon can be interpreted as a phase shift in the phase of the maxima, but sometimes the return to the earlier pulsation period is slower, an intermediate period can be well determined. Rejump of the period was found at eight Cepheids in the northern sky and no single Cepheids show this phenomenon.

It is highly interesting that similar phenomenon can be observed in the O-C diagram for supermaxima of SU UMa type dwarf novae (Vogt, 1980). The rough constancy of the period of the supermaxima and its change may be caused by the rotating g-modes of the Roche-lobe filling secondary companion. As an

analogy, the rejump in the period of Cepheids may be caused by some non-radial effect since only binary Cepheids show rejumping period. However, the Cepheids are rather wide binaries and the non-radial effects due to the presence of the companion are expected not to be as pronounced as in dwarf novae.

In multiple periodic variable stars, e.g. in Delta Scuti and Beta Canis Majoris stars the ratio of periods can also be explained by non-radial pulsation.

Our knowledge about the duplicity of RR Lyrae variables is very limited. The only reliable binary system which contains RR Lyrae type variable is V 80 in the UMi dwarf galaxy. The ratio of its pulsation and orbital periods is very close to 1:4. Such a "synchronization" between pulsational and orbital motion has also been noticed in other binary systems containing a pulsating component (Frolov et al., 1980). This kind of resonance is very interesting and promising, but no firm conclusion can be drawn as to the frequency of its occurrence. It is worthy of notice that RR Leo may be another RR Lyrae star in a binary system if the wave in its O-C diagram proves to be periodic (Oláh and Szeidl, 1978).

Among the red giant variables we again find a small proportion of binaries, nevertheless there are very interesting binary systems among them. Both Mira Ceti and R Hydrae have faint visual companions. The period of R Hydrae decreased from 500 to 400 days in about two centuries. The companion of Mira Ceti is the faint blue variable star VZ Ceti whose eruptive behaviour is certainly affected and probably caused by material flowing from its red giant companion. R Aqr is an eclipsing binary. The duration of the eclipses is 8 years, and the eclipse itself is caused by a gas cloud around the blue secondary (Willson et al., 1981). Moreover, in 1885 a slow outburst was observed in this system.

One of the most interesting variables is the slow nova (or symbiotic variable) RR Telescopii. As the pre-outburst light curve shows, the red component became a Mira variable several years before the nova outburst (Robinson, 1975). The periodic light variation (P = 380 d) cannot be traced in visual light after the nova outburst, but can well be observed in the infrared. The period in the infrared is now the same as was in visible light prior to the outburst (Feast, 1979). It is obvious that there must have been a strong physical connection between the start of Mira type variation and the subsequent nova outburst.

The IR technique gave a new possibility to reveal Miras in binary systems (Feast, 1980). Several Miras with companions have unusually weak or ab-

sent OH/H_2O masering despite being bolometrically bright objects. In these cases (e.g. Mira Ceti), the projected distances of the companions from the Miras are in the range $10^{15} - 10^{17}$ cm whilst the radius of a typical masering circumstellar region is usually taken as 10^{16} cm. Evidently in these circumstances the companion can have a considerable influence on the masering gas.

Physical variability can be found among the Zeta Aurigae type eclipsing variables, too. The red supergiant component of the long period eclipsing binary VV Cephei shows semiregular variation with a period of 118 days (Mc Cook and Guinan, 1978).

Variable stars of lower luminosity

As is well known, the RS CVn stars are all binaries and at the same time physical variables, too, owing to the star-spots generated by the surface-activity.

In many of their optical characteristics the BY Draconis variables are similar to RS CVn binaries. A combination of both rapid rotation and extensive convection zones provides a necessary and sufficient condition for large scale stellar activity in late type stars. Since at least one of the BY Dra stars (AU Mic) is almost certainly single (Caillault, 1982), this suggests that rapid rotation and not duplicity is the determining factor in defining the level of stellar activity in such variables. Duplicity may only be relevant as a means of ensuring rapid rotation through synchronization.

The FK Comae stars form a new group of chromospherically active variable stars. According to a recent hypothesis (Bopp and Stencel, 1981), FK Comae stars are coalesced binaries, perhaps evolved W UMa stars.

It is a common opinion that the proportion of binaries among the pre-main sequence variables is quite high. In this case the presence of wide emission lines can easily be explained by the mass exchange between the components. Nevertheless, the only convincing example among the T Tauri stars is RY Tau.

The occurrence of binaries among flare stars is higher than that of binaries containing normal stars of late spectral type. Several cases are known where both components of the binary are flare stars (Mirzoyan, 1981).

Cataclysmic variables

Among the cataclysmic variables the occurrence of binaries is the highest among the variable stars, the outburst of these stars is closely connected with the duplicity.

We have observational evidence that about 60% of the total number of novae are binaries, however it is usually assumed that all novae are binary systems, just because there is no better explanation. The presence of several novae in globular clusters may be an argument against their overall duplicity (Webbink, 1980).

As to the recurrent novae, a very interesting observational fact should be mentioned. The recurrent nova T CrB has been observed to erupt four times with novae or flare-like events with peak amplitude of one magnitude or greater, and all these events occurred in nearly the same orbital phase (Palmer and Africano, 1982).

The dwarf novae are binaries without any exception. The intriguing property of the SU UMa subgroup was mentioned earlier in this paper. Similarly, the UX UMa stars are all binaries.

The symbiotic stars have been shown convincingly to be binaries. A recent review and their new classification is given by Allen (1979).

The AM Herculis type stars (polars) are magnetic binaries, in which a very strong magnetic field together with a high accretion rate is likely to lead to the steady burning with no outburst.

The X-ray binaries are binaries per definitionem. It is worth mentioning that besides the massive systems some other physical variables can also be placed among the X-ray binaries: e.g. several Be systems, the HZ Her type variables, the above-mentioned AM Her stars, several novae and RS CVn systems.

The Hubble-Sandage variables are the most luminous stars in external galaxies. Spectroscopically they closely resemble dwarf novae. Bath (1980) suggested that the close correspondence between the spectral appearance of the two classes combined with the difference in luminosity is well accounted for by a model of Hubble-Sandage variables in which the same physical processes occur but on a larger scale. According to this hypothesis H-S variables are binary systems and the accretion rates would be 10^{20}-10^{24} g/s, maximum disk temperatures are the same (10^4–$4\cdot10^4$ K) as quiescent dwarf novae with accretion rates 10^{14}–10^{17} g/s. The disk structure will be similar, simply larger radii. This larger disk has a luminosity $\sim10^{38}$ erg/s. According to Bath the closest related object Eta Carinae is also a massive interacting binary and its outburst in the 19th century was an accretion driven nova explosion.

Other physical variables

The observed slow rotation of Ap stars may well be caused by their mem-

bership in binary system, where a synchronization causes slow rotation. The observed frequency of binaries among the Ap stars seems to contradict this: various authors give 24–45 % for their occurrence (Jaschek and Jaschek, 1975). Another explanation for the slow rotation may be the magnetic braking. The problem with this latter mechanism is that it would result in circular orbit, but the observed orbits of Ap stars in spectroscopic binaries are eccentric.

The estimation of the occurrence of binaries among the Wolf–Rayet stars is rather uncertain. The concensus of opinion is that most WR stars are members in binary systems, and binary nature appears fundamental to the formation of WR stars except possibly for the more luminous WN7/WN8 subgroup (Moffat and Seggewiss, 1980).

Most central stars of planetary nebulae show a continuous spectrum, some have WR type spectra and others show Of type spectra with both absorption and emission lines. However, there are some peculiar cases where the central stars show late type spectra and yet the nebulae show high excitation lines. One possible explanation for this discrepancy is that these central stars are binary systems and the late type spectra refer to the companion stars of

Table I

Type of variability	Occurrence of binaries	Typical representatives
β CMa	∿25%	16 Lac, α Vir
Cepheids	∿25%	SU Cyg, CE Cas, BM Cas
δ Sct, Dwarf cepheids	∿25%	SZ Lyn, AB Cas
RR Lyr	probably low	V80 in UMi
Mira	probably low	o Cet, R Hyd, R Aqr
Semiregular	?	VV Cep
RS CVn	100%	RS CVn
BY Dra	not 100%	BY Dra
FK Com	100%	FK Com, UZ Lib
T Tau	30 - 50%	RY Tau
flare stars	>60%	Proxima Cen, UV Cet
Novae	⩽100%	DQ Her, RR Tel
Recurrent novae	∿100%	T CrB
Dwarf novae	100%	U Gem, SU UMa, Z Cam
UX UMa	100%	UX UMa
Symbiotic variables	100%	AG Peg
AM Her	100%	AM Her
Hubble-Sandage var., η Car	100% ?	η Car
Ap stars	24 - 45%	AR Aur
Wolf-Rayet stars	80%	V 444 Cyg
central stars of plan. neb.	not 0%	IC 2120, UU Sge
Fuors	100% ?	FU Ori

the hot blue stars of the PN.

Interestingly enough, a binary star model has been suggested for the fuors, too (Chochol and Tremko, 1980).

A short summary of the paper can be found in Table I. This review, however, does not give a complete listing of binary physical variables. There are several types of variables (e.g. W Vir and R CrB) which have not been treated in the literature from the point of view of duplicity.

The author wishes to thank Professor L.V. Mirzoyan for his valuable comments.

References:

Allen, D.A. 1979, In: Proc. I.A.U. Coll. No. 46, Ed.: Bateson et al., Univ. of Waikato, New Zealand, p. 125.
Bath, G.T. 1980, In: Close Binary Stars: Observations and Interpretation, Ed.: Plavec et al., Reidel, Dordrecht, p. 155.
Bopp, B.W., Stencel, R.E. 1981, Astrophys. J., 247, L131.
Caillault, J.-P. 1982, Astron. J., 87, 558.
Chochol, D., Tremko, J. 1980, In: Flare Stars, Fuors and Herbig-Haro Objects, Ed.: L.V. Mirzoyan, Erevan, p. 240.
Coutts, C.M. 1971, In: Proc. I.A.U. Coll. No. 15, Veröff. Remeis Sternwarte Bamberg, IX, Nr. 100, p. 238.
Feast, M.W. 1979, In: Proc. I.A.U. Coll. No. 46, Ed.: Bateson et al., Univ. of Waikato, New Zealand, p. 147.
Feast, M.W. 1980, In: Variability in Stars and Galaxies, Proc. Vth E.R.M.A., Institut d' Astrophysique, Liége, p. B.1.1.
Fernie, J.D. 1980, Astron. Astrophys., 87, 227.
Frolov, M.S., Pastukhova, E.N., Mironov, A.V., Moshkalev, V.G. 1980, Inf. Bull. var. Stars, No. 1894.
Jaschek, C., Jaschek, M. 1975, In: Physics of Ap Stars, Proc. I.A.U. Coll. No. 32, Ed.: Weiss et al., Univ. Sternw. Wien, Vienna, p. 219.
Larsson-Leander, G. 1971, In: Proc. I.A.U. Coll. No. 15, Veröff. Remeis Sternw. Bamberg, IX, Nr. 100, p. 185.
Madore, B.F. 1977, Mon. Not. R. astr. Soc., 178, 505.
McCook, G.P., Guinan, E.F. 1978, Inf. Bull. var. Stars, No. 1385.
Mirzoyan, L.V. 1981, Nestatsionarnost' i Evolutsiya Zvezd, Acad. Sci. Arm. S.S.R., Erevan, p. 145.
Moffat, A.F.J., Seggewiss, W. 1980, In: Close Binary Stars: Observations and Interpretation, Ed.: Plavec et al., Reidel, Dordrecht, p. 181.
Oláh, K., Szeidl, B. 1978, Mitt. Sternw. ung. Akad. Wiss., Nr. 71.
Palmer, L.H., Africano, J.L. 1982, Inf. Bull. var. Stars, No. 2069.
Payne-Gaposchkin, C. 1978, Ann. Rev. Astron. Astrophys., 16, 1.
Robinson, E.L. 1975, Astron. J., 80, 515.
Szabados, L. 1977, Mitt. Sternw. ung. Akad. Wiss., Budapest, Nr. 70.
Szabados, L. 1980, Mitt. Sternw. ung. Akad. Wiss., Budapest, Nr. 76.
Szabados, L. 1981, Commun. Konkoly Obs. Hung. Acad. Sci., No. 77.
Vogt, N. 1980, Astron. Astrophys., 88, 66.

Webbink, R.F. 1980, In: Close Binary Stars: Observations and Interpretation, Ed.: Plavec et al., Reidel, Dordrecht, p. 561.
Willson, L.A., Garnavich, P., Mattei, J.A. 1981, Inf. Bull. var. Stars, No. 1961.

V 1068 CYGNI — A LONG PERIOD RS CVn STAR?

S. Rössiger
Zentralinstitut für Astrophysik
Sternwarte Sonneberg, G.D.R.

Photoelectric UBV observations of the eclipsing binary V 1068 Cygni were obtained in the years 1979 - 1981. The depths of the minimum in the separate colours are: $\Delta V=0.30$, $\Delta B=0.58$, $\Delta U=0.93$ mag. Moreover there is an indication of a migrating wavelike distortion in the light curve, as it occurs in the RS CVn stars. With respect to the orbital period of 42.7 days the system would then be a member of the long-period RS CVn group.

Image tube spectra taken by P. Notni at the Tautenburg 2m telescope show that the components of the system have spectral types B5 - A5 and G8 II-III. The spectra do not reach the Ca II lines H and K. It is therefore impossible to decide on the presence of emission in those lines, which would be an important criterion of RS CVn stars and related objects. Further spectroscopic investigation is desirable.

SPOT ACTIVITY OF THE CLOSE BINARY SV Cam

L. Patkós
Konkoly Observatory of the Hungarian Academy of Sciences
H-1525, Budapest, P.O. Box 67, Hungary

Like other RS CVn systems, SV Cam has a migrating distortion wave. The amplitude of this wave is about 0.1 mag and it migrates towards increasing orbital phase. The wave is caused by dark spots on the surface of the secondary component. These spots migrate because of the differential rotation. The velocity of the migration is not constant, but its period must be about 400 days.

To explain the observed light curve changes, we also have to assume the existence of white spots — on the surface of the primary component. The one indication for this was given by the light-up which appeared between J.D. 2442432 and J.D. 2442461. This light-up may have been caused by a gas stream falling down on the surface of the primary component. The simultaneously observed period increase also indicates mass transfer from the smaller secondary component to the primary. Another indication for the existence of a white spot on the surface of the primary component comes from the observations J.D. 2441978 - 981. Three independent light curves were obtained and in each of them there is a step at the bottom of primary minimum. This phenomenon can be explained by the eclipse of a white spot on the surface of the primary component. The brightness of this spot is not enough to observe it in full light, but in the case of a transit eclipse even small brightness differences on the surface of the eclipsed component can be established. On the light curves observed two weeks earlier and one month later (and on other light curves of SV Cam) no step at the bottom of primary eclipse is present. This means that the assumed white spot also migrates for the same reason as dark spots on the surface of the secondary component.

My investigations suggest that the extended light curve variations in the system SV Cam are caused by both dark and white spots on the surface of the two components.

PHOTOELECTRIC MINIMA OF VW CEPHEI AND V 566 OPHIUCHI

H.A. Mahdy and M.A. Soliman
Helwan Institute of Astronomy and Geophysics
Helwan, Egypt

The eclipsing variables VW Cep and V 566 Oph were observed in B and V colours in Kottamia Observatory, Egypt, in 1981. The results of the photometry and the times of minima have been published in the Information Bulletin on Variable Stars, Nos. 2153 and 2154, respectively. The individual observations for both stars will be deposited in the Archives of Commission 27 of the IAU.

OBSERVATIONS OF A NEW MINIMUM IN OPTICAL RADIATION OF X-RAY SOURCE KR AURIGAE

M. Popova, A. Antov and V. Popov
Department of Astronomy, Bulgarian Academy of Sciences
72 Lenin Boulevard, 1184 Sofia, Bulgaria

KR Aurigae attracts the attention of astronomers due to its unusual properties. This variable was discovered by Popova (1960), who has also underlined its unique type of variability (Popova, 1965). The results of spectrophotometric study confirmed the unusual character of the object. The YY Ori type profile of Hβ showed a mean accretion velocity of about 3200 km/sec and a hypothesis of KR Aur being a possible black hole has been suggested (Popova and Vitrichenko, 1978). On the basis of observations from the American satellite HEAO-2, the star was recognized to be a source of soft X-ray radiation (Mufson et al., 1980).

In the National Astronomical Observatory of the Bulgarian Academy of Sciences at Roʃen, observations of KR Aurigae were carried out on 2 m RCC telescope and on a 500/700 mm Schmidt telescope. The results display a significant change in the brightness of the star. From December 1979 till March 1981 it remains at $13^m.5$ as during the preceding years. Variations of the order of some tenths of the magnitude are present. At the end of 1981 a dip occurred and the variable attained 17^m on 28 December 1981 (Popov, 1982).

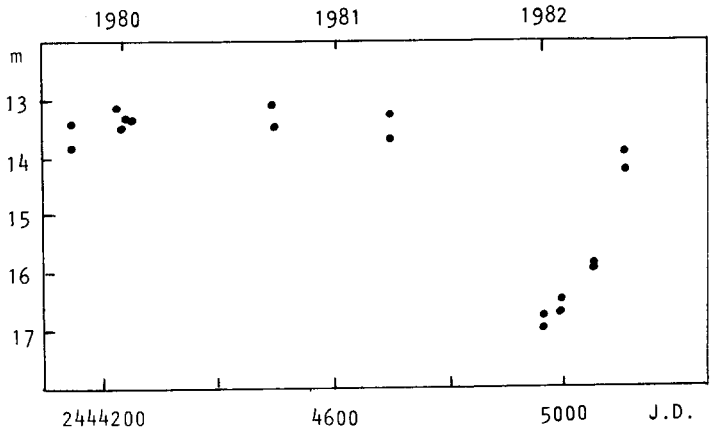

Figure 1

Observations over the next five months showed a gradual increase of brightness, reaching 14^m on 19 May 1982 (Figure 1).

The observed minimum is in agreement with the mean cycle of 7-9 years in light variations, suggested by Popova (1965).

Most of the photometric data on the variability of the star are obtained from Sonneberg, Moscow and Harvard plate collections (Popova, 1975; Liller, 1980). On these plates the star in minimum light is usually fainter than the limiting magnitude of the plates. Only a few observations in minimum light with more powerful telescopes are available. In order to fill the gaps in our observations during the last minimum, contributions from other observatories would be highly appreciated.

Since the photometric behaviour of KR Aurigae is very complicated, regular photometric and/or photoelectric patrol observations in different colours are very desirable.

References:

Liller, M.H. 1980, Astron. J., 85, 1092.
Mufson, S.L., Wisniewski, W.Z., McMillan, R.S. 1980, IAU Circ., No. 3471.
Popova, M.D. 1960, Mitt. veränderl. Sterne, Nr. 463.
Popova, M.D. 1965, Peremennye Zvezdy, 15, 534.
Popova, M.D. 1975, Astrophys. Investigations, Sofia, 1, 68.
Popova, M.D., Vitrichenko, E.A. 1978, Astr. Zhu., 55, 765.
Popov, V.N. 1982, Inf. Bull. var. Stars, No. 2095.

AQ LEONIS UPDATED

M. Jerzykiewicz
Wroclaw University Observatory, Poland

and

R.H. Schult and W. Wenzel
Central Institute for Astrophysics
Sonneberg Observatory, G.D.R.

All available photometric observations of the double-mode RR Lyrae variable AQ Leonis are examined. A mean B-V colour index is derived which places the star in the RR Lyrae gap at the transition line between the c- and a-type pulsators. The upper limit for the first-overtone to the fundamental switching rate is found to amount to between 5 and 10 per cent of the first-overtone amplitude over the last 20 years.

An abrupt change of the first-overtone period apparently occurred in the early seventies.

AN INTERESTING VARIABLE IN M 15

Katalin Barlai
Konkoly Observatory of the Hungarian Academy of Sciences
H-1525, Budapest, P.O. Box 67, Hungary

Among the RR Lyrae variables of the globular cluster M 15 there is one — V 15 — which calls our attention by its conspicuous O-C diagram (Fig. 1).

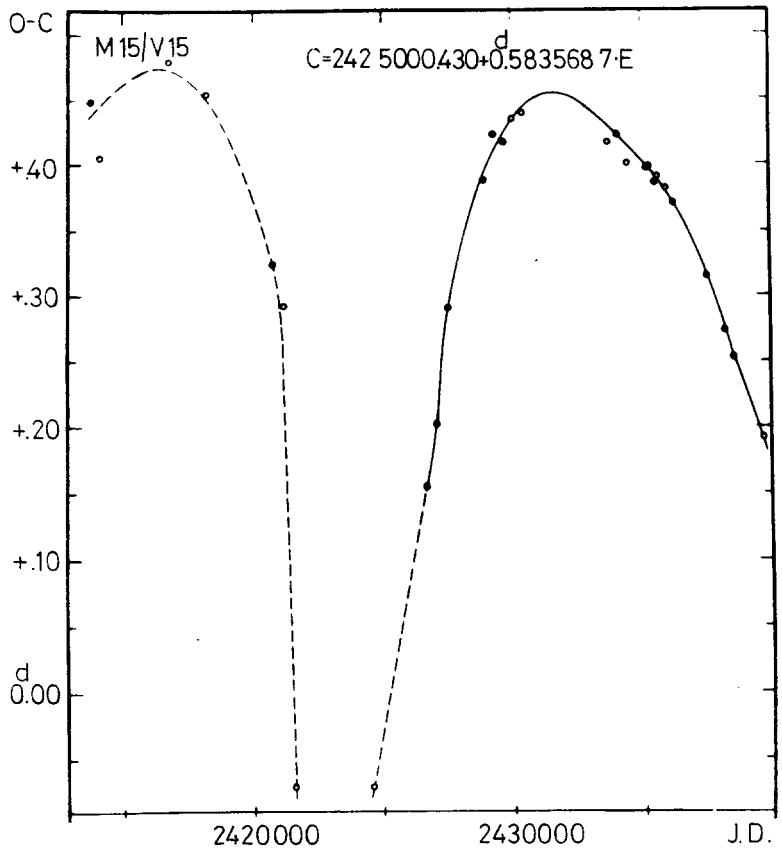

Figure 1

Smith and Wesselink (1977) claim: "This interesting variable has undergone so great a change in period during 74 years of observations that we cannot construct an unambiguous phase diagram." Smith and Sandage (1981)

write: "A simple abrupt period change and a simple linear period increase both can be excluded. Our phase diagram can be explained only if V 15 has undergone at least one period increase near J.D. 2427000 and one period decrease near J.D. 2438000." ... "We feel that the available observations do not permit an unambiguous description of the period behaviour of V 15 between J.D. 2421000 and 2427000."

The observational material obtained in Budapest during the past 45 years suggests the O-C diagram shown in Fig. 1. A large sudden change of the period is to be seen.

A model proposed by Sweigart and Renzini (1979) might offer a possibility to interpret (the unusual shape of) this O-C diagram. In accordance with their model the period changes of RR Lyrae stars can be explained by the development of a semiconvective zone around the core of the star. The composition redistribution in the convective core due to this zone results in a transfer of helium through this zone into the core by means of small random mixing events altering the pulsation period of the star. This process contributes substantially to the observed changes of the period in addition to the gradual change in the composition due to nuclear burning. Period changes of both signs can be produced by that process and the changes in the pulsation period are comparable with the typically observed ones.

A theoretical horizontal branch track in the HRD obtained by taking into account semiconvection describes two spikes. The evolutionary rate of change of the period (Figs. 2 and 3 of Sweigart and Renzini) shows large negative and positive changes of the period. According to the authors large period changes would occur in roughly several centuries as their reference model evolves through the spike.

Observations of RR Lyrae variables in globular clusters now cover about 80 years. Among the 120 variables of M15 we found one single O-C diagram showing large period changes within several years. Among the about 200 RR Lyrae variables of M3 we can also find one – V 58 – which shows similar behaviour in its O-C curve (Szeidl, 1965). This is not inconsistent with the abundances of sudden large period changes predicted by this model, so these unusual O-C diagrams are not to be discarded; they might be connected with the spike.

References:

Smith, H.A., Sandage, A. 1981, Astron. J., 86, 1870.
Smith, H.A., Wesselink, A.J. 1977, Astron. Astrophys., 56, 135.
Sweigart, A.V., Renzini, A. 1979, Astron. Astrophys., 71, 66.
Szeidl, B. 1965, Mitt. Sternw. ung. Akad. Wiss., Budapest-Szabadsâghegy, No.58.

MODEL OF FLUCTUATION OF PERIOD IN MULTIPLE PERIODIC VARIABLES

M. Marik
Department of Astronomy
Eötvös Loránd University, Budapest, Hungary

Let us suppose that the primary period of light variation (Π) is associated with the pulsation, and the secondary period (P) with the rotation of the star. The radius (R) of the star is:

$$R = R_o(1 + A\cdot\cos\frac{2\pi}{\Pi}t) \tag{1}$$

where R_o is the mean radius, A is the amplitude of the pulsation and t is the time. The angular velocity (ω) of the rotation is:

$$\omega = N(k\cdot M\cdot R^2)^{-1} \tag{2}$$

where N is the angular momentum, M the mass of the star and k is a constant of the order of magnitude 1. The mean angular velocity is:

$$\bar{\omega} = N(k\cdot M\cdot R_o^2)^{-1}\cdot(1 - A^2)^{-3/2} \tag{3}$$

Thus the period of rotation is

$$P = P_o\cdot(1 - A^2)^{3/2} \tag{4}$$

where P_o is the period of rotation for A = 0. Equation (4) means that if the amplitude of pulsation increases then the period of rotation decreases.

Let us suppose that the kinetic energy of the pulsation is constant. In this case we get:

$$A^2\cdot\Pi^{-2} = \text{constant}$$

and with Eq. (4):

$$P = P_o\cdot(1 - c\Pi^2) \tag{5}$$

Equation (5) enables us to explain the reflection of the O-C curves of the primary and secondary periods of RR Lyrae stars in some cases (Detre, 1969).

The angular displacement $\alpha(t)$ can be obtained from Eq. (2):

$$\alpha(t) = -\frac{P}{\Pi}\cdot\sqrt{1 - A^2}\left[\frac{A\cdot\sin\frac{2\pi}{\Pi}\cdot t}{1 + A\cdot\cos\frac{2\pi}{\Pi}\cdot t} - \frac{2}{\sqrt{1 - A^2}}\cdot\operatorname{arctg}\left(\frac{\sqrt{1 - A^2}}{1 + A}\cdot\operatorname{tg}\frac{\pi}{\Pi}t\right)\right] \tag{6}$$

The fluctuations of angular displacement at moments $t = P\cdot i$ $(i = 0,1,2,3,\ldots)$

are:

$$\Delta\alpha = 2\pi i - \alpha(P\cdot i) \tag{7}$$

The time differences Δt corresponding to $\Delta\alpha$ are:

$$\Delta t = O-C = \frac{P}{2\pi}\alpha(P\cdot i) - P\cdot i \tag{8}$$

If P/Π is an irrational number, we can get for the standard deviation of the secondary period:

$$\sigma_s^2 = A^2 \cdot \pi^{-1} \cdot \Pi^2 \tag{9}$$

or with Eq. (4):

$$\sigma_s = \Pi \cdot \pi^{-1} \sqrt{1 - \left(\frac{P}{P_O}\right)^{2/3}} \tag{10}$$

Equation (10) means that σ_s is proportional to Π and decreases with increasing P.

Our results are not in contradiction with the observations, but we have insufficient observations to assess the validity of our model (Marik, 1976).

References:

Detre, L. 1969, Non-periodic Phenomena in Variable Stars, Akadémiai Kiadó, Budapest, p. 3.
Marik, M. 1976, Az Eötvös Loránd Tudományegyetem Közleményei, No. 3.

PULSATION MODES AND PHOTOMETRIC MASSES OF CEPHEID VARIABLES

A. Opolski
Wroclaw University Observatory
Wroclaw, Poland

Abstract

On the basis of the Wesselink radii and colour indices $\langle B-V\rangle_o$ the relation $P_F - R - \langle B-V\rangle_o$ for fundamental periods P_F was established. This enabled separation of the first overtone pulsators: BG Cru, BF Oph, V 482 Sco, Y Sgr and U Aql. Transformation to the $P_F - M_{\langle V\rangle} - \langle B-V\rangle_o$ relation allows the statement that the calibration Cepheids are pulsating in the fundamental periods.

New photometric masses for Cepheids are proposed and the problem of the instability strip crossings discussed. A method is presented of determining the crossing numbers applying to about 60 stars. The consequences of stars being separated according to the crossings on the relations mass–period and mass–luminosity are discussed.

Introduction

Many papers have presented the relations or correlations for basic observational parameters of classical Cepheids. In most cases a larger or smaller group of these stars is regarded as a homogeneous body which should fulfil a unique relation of two or three parameters such as period P, radius R, colour index say $\langle B-V\rangle_o$, luminosity L or absolute magnitude M. These relations are generally known, e.g. the P–R relation or P–L–C relation. But from the theoretical considerations we know that Cepheids may be fundamental F or higher overtone H pulsators. In view of this it would be desirable to have the possibility to distinguish between corresponding periods P_F and P_H for individual stars and then to establish suitable relations such as $P_F - R$ and $P_H - R$.

A similar situation is that of the mass–luminosity relation M–L. According to the theory, the evolutionary tracks of yellow giants pass the instability strip several times. Therefore, on the $L - T_e$ plane the stars with different masses can be found at the same point, when they are on different crossings. So we should expect separate M–L relations for each crossing of

the instability strip.

It is generally assumed that all Cepheids are fundamental pulsators in the second crossing of the instability strip. This paper contains an attempt to verify this assumption and to separate Cepheids pulsating in different modes and being on different transits of the instability strip.

In our analysis we use the following observational data:

1. Mean and maximum Wesselink radii, R and R_{max}. These quantities were taken from three sources: $\log R_B$ — from Balona (1977), $\log R_{ST}$ — according to Sandage and Tammann, see Balona (1977) and $\log R_T$ — published by Thompson (1975). The relations $\log P - \log R$ resulting from these three series show systematic differences chiefly for the shortest and the longest periods. Therefore as the final values we adopted the mean of these three quantities:

$$\log R = \frac{1}{3}(\log R_B + \log R_{ST} + \log R_T)$$

Table I contains the $\log R$ values and the differences: $\Delta\log R_B = \log R_B - \log R$, $\Delta\log R_{ST} = \log R_{ST} - \log R$ and $\Delta\log R_T = \log R_T - \log R$. These differences, interpolated for a given period, were then applied to correct the individual values published in the above-mentioned papers to one system of $\log R$.

Table I

Mean $\log R$ values and differences for three systems

$\log P$	$\log R$	$\Delta\log R_B$	$\Delta\log R_{ST}$	$\Delta\log R_T$
0.40	1.428	+0.026	-0.013	-0.013
0.60	1.556	+ .018	- .009	- .009
0.80	1.685	+ .010	- .005	- .005
1.00	1.813	+ .002	- .001	- .001
1.20	1.941	- .006	+ .003	+ .003
1.40	2.070	- .013	+ .006	+ .007
1.60	2.203	- .027	+ .006	+ .021
1.80	2.341	-0.030	+0.014	+0.015

The mean R values have been changed to maximum radius R_{max}:

$$R_{max} = R + 0.5\,\Delta R$$

where ΔR is the amplitude of the displacement, acquired by means of the integration of velocity curves (Opolski, 1968)(Table II).

The $\log R_{max}$ values obtained in this manner are related to the periods:

$$\log R_{max} = 1.183 + 0.675 \cdot \log P \qquad (1)$$

Table II

Pulsation Modes and Observational Parameters of 66 Cepheids

	Puls. mode	$\log P$	$\log R$	$\log R_{max}$	$\langle B-V \rangle_o$	$\Delta \log P$	$M_{\langle V \rangle}$	M_{bol}	$\log T_e$
					m		m	m	
SU Cas	F	0.290	1.336	1.346	0.48	+0.013	-2.52	-2.43	3.800
RT Mus	F	.489	1.503	1.518	.50	- .003	-3.35	-3.27	.798
VZ CMa	F	.496	1.636	1.690	.31	- .093	-4.32	-4.17	.832
AZ Cen	F	.507	1.578	1.586	.51	- .071	-3.67	-3.59	.796
BG Cru	H	.524	1.661	1.668	.52	- .157	-4.04	-3.97	.795
R TrA	F	.530	1.534	1.554	.57	- .044	-3.41	-3.36	.788
UX Car	F	.566	1.534	1.564	.56	- .014	-3.50	-3.44	.789
RT Aur	F	.572	1.543	1.561	.58	+ .019	-2.62	-2.57	.787
AG Cru	F	.584	1.502	1.526	.53	+ .066	-3.34	-3.27	.793
BB Cen	F	.602	1.579	1.580	.57	- .002	-3.53	-3.48	.788
BF Oph	H	.609	1.684	1.706	.61	- .156	-4.11	-4.07	.783
AH Vel	F	.626	1.632	1.642	.54	- .035	-3.90	-3.83	.792
V Vel	F	.641	1.574	1.598	.56	+ .021	-3.65	-3.59	.789
T Vul	F	.647	1.594	1.617	.59	- .012	-3.70	-3.66	.785
FF Aql	F	.650	1.620	1.630	.59	- .025	-3.76	-3.72	.785
V482 Sco	H	.656	1.668	1.685	.67	- .129	-3.90	-3.90	.776
RY CMa	F	.670	1.555	1.589	.63	+ .021	-3.49	-3.46	.781
S Cru	F	.671	1.582	1.606	.61	+ .013	-3.61	-3.58	.783
AP Sgr	F	.704	1.552	1.566	.66	+ .066	-3.32	-3.31	.777
AP Pup	F	.706	1.674	1.695	.66	- .085	-3.97	-3.96	.777
δ Cep	F	.730	1.642	1.665	.61	+ .003	-3.89	-3.86	.783
V Cen	F	.740	1.672	1.698	.58	- .010	-4.12	-4.07	.787
V419 Cen	F	.741	1.657	1.667	.60	+ .017	-3.93	-3.89	.784
MY Pup	F	.755	1.662	1.670	.50	+ .083	-4.11	-4.03	.798
Y Sgr	H	.761	1.736	1.763	.70	- .133	-4.24	-4.25	.773
R Cru	F	.765	1.661	1.682	.63	+ .006	-3.95	-3.92	.781
T Ant	F	.771	1.691	1.714	.52	+ .036	-4.29	-4.22	.795
RV Sco	F	.783	1.636	1.665	.63	+ .079	-3.72	-3.69	.781
X Cru	F	.794	1.674	1.692	.69	- .010	-3.90	-3.90	.774
S TrA	F	.801	1.727	1.752	.68	- .068	-4.22	-4.22	.775
AW Per	F	.810	1.683	1.713	.65	+ .003	-4.06	-4.04	.779
BB Sgr	F	.822	1.733	1.753	.75	- .088	-4.11	-4.15	.767
AT Pup	F	.824	1.747	1.769	.59	- .015	-4.46	-4.42	.785
V Car	F	.826	1.683	1.717	.68	- .002	-4.05	-4.05	.775
T Cru	F	.828	1.776	1.797	.65	- .078	-4.50	-4.48	.779
U Sgr	F	.829	1.758	1.782	.71	- .093	-4.32	-4.34	.772
V636 Sco	F	.832	1.665	1.689	.72	+ .034	-3.84	-3.86	.771
V496 Aql	F	.833	1.718	1.726	.78	- .062	-3.92	-3.98	.764
BG Vel	F	.840	1.718	1.735	.73	- .019	-4.05	-4.08	.770
X Sgr	F	.846	1.792	1.811	.53	- .009	-4.76	-4.69	.793
U Aql	H	.847	1.802	1.825	.70	- .121	-4.55	-4.56	.773
η Aql	F	.856	1.776	1.800	.69	- .076	-4.44	-4.44	.774
R Mus	F	.876	1.709	1.737	.65	+ .041	-4.20	-4.18	.779
W Sgr	F	.881	1.751	1.778	.65	- .003	-4.46	-4.44	.779
ER Car	F	.887	1.662	1.691	.75	+ .050	-3.80	-3.84	.767
S Sge	F	.923	1.748	1.776	.74	- .009	-4.24	-4.27	.769
WX Pup	F	.951	1.763	1.790	.73	+ .008	-4.33	-4.35	.770
S Mus	F	.985	1.774	1.797	.57	+ .124	-4.63	-4.58	.788
S Nor	F	.989	1.725	1.756	.77	+ .664	-4.09	-4.14	.765
β Dor	F	0.993	1.838	1.864	0.73	- 0.037	-4.70	-4.73	3.770

Table II (cont.)

	Puls. mode	$\log P$	$\log R$	$\log R_{max}$	$\langle B-V\rangle_o$	$\Delta \log P$	$M_{\langle v\rangle}$	M_{bol}	$\log T_e$
XX Cen	F	1.040	1.765	1.801	$0^m.71$	+0.096	$-4^m.42$	$-4^m.44$	3.772
AD Pup	F	1.133	1.866	1.911	0.81	+0.002	-4.80	-4.88	3.760
Y Oph	F	1.233	2.002	2.019	0.66	+0.059	-5.44	-5.43	3.777
					$\langle B-V\rangle_o > 0.85$				
TT Aql	F	1.138	1.893	1.932	0.89	+0.001	-4.77	-4.89	3.750
SV Mon	F	.183	1.931	1.978	0.88	.000	-5.02	-5.14	.751
X Cyg	F	.215	1.965	2.021	0.98	- .062	-5.54	-5.72	.737
CD Cyg	F	.232	1.950	1.997	0.95	- .005	-4.99	-5.15	.742
SZ Aql	F	.234	1.931	1.994	0.94	+ .005	-4.99	-5.14	.743
VY Car	F	.278	2.011	2.058	0.93	- .017	-5.33	-5.47	.745
RZ Vel	F	.310	2.028	2.082	0.89	+ .007	-5.52	-5.64	.750
X Pup	F	.414	2.166	2.198	0.91	- .027	-6.02	-6.15	.747
T Mon	F	.432	2.090	2.122	1.07	.000	-5.57	-5.81	.723
l Car	F	.551	2.228	2.272	1.14	- .080	-5.85	-6.16	.712
U Car	F	.588	2.208	2.275	0.98	+ .029	-6.30	-6.48	.737
RS Pup	F	.617	2.290	2.347	0.98	- .022	-6.66	-6.84	.737
SV Vul	F	1.654	2.206	2.282	1.12	+0.022	-5.95	-6.24	3.715

The chief list of $\log R$ has been completed by the values taken from the paper of Sollazzo et al. (1981) and corrected to bring them to the same system $\log R_{max}$. Also, the results of Stobie and Balona (1979) have been used. Additionally, for stars RT Aur and SU Cas the data from Ivanov (1981) and from Joshi and Rautela (1980) were accepted.

2. Colour indices $\langle B-V\rangle_o$ are based on the values $\langle B-V\rangle$ from the catalogue by Schaltenbrand and Tammann (1971):

$$\langle B-V\rangle_o = \langle B-V\rangle - E(B-V) \qquad (2)$$

As colour excesses E(B-V) the values denoted as E_A in the paper by Dean et al. (1978) have been used. They have been supplemented by the reddenings derived by Pel (1978) and transferred to Dean's system. Also the $\langle B-V\rangle_o$ values published by Stobie and Balona (1979) were included (Table II).

Fundamental and first overtone pulsators

Instead of the generally used P–L–C relation we try to establish, as the first step, the P–R–$\langle B-V\rangle_o$ and P– R_{max} – $\langle B-V\rangle_o$ relations. They are based directly on the observational data gathered in Table II. For the shape of the relations we are seeking, we assume the simplest one:

$$\log P_F = a + b \cdot \log R + c \cdot \langle B-V \rangle_o \qquad (3)$$

where the values of a, b and c are to be determined by the least squares method. We hope to get such a relation for the fundamental periods, P_F, and then to identify the first overtone periods, P_H, as smaller by about 0.15 (see Cox and Hodson, 1978),

$$\log P_H = \log P_F - 0.15$$

for the same values of R and $\langle B-V \rangle_o$. Accordingly, as the criterion for the separation of P_H from P_F we use the difference $\Delta \log P$:

$$\Delta \log P = \log P - a - b \cdot \log R - c \cdot \langle B-V \rangle_o \qquad (4)$$

where P is the observed period. When $\Delta \log P = 0$ within the limits of the observational accuracy, the observed period is taken to be the fundamental one, $P = P_F$. When $\Delta \log P$ is about -0.15, then the star is pulsating in the first overtone, $P = P_H$. This method of selecting P_H from P_F requires suitable accuracy of the parameters R and $\langle B-V \rangle_o$ and small natural scatter in relation (3). Otherwise the standard deviation, s.d., of $\log P_F$ would be larger than the difference between $\log P_F$ and $\log P_H$.

After some trials it was found that the equation of the form (3) is realized with sufficient accuracy when the investigated stars are divided into two groups: $\langle B-V \rangle_o < 0.85$ and $\langle B-V \rangle_o > 0.85$. This division is similar to the usually used one, that is: $\log P < 1.00$ and $\log P > 1.00$.

In the first group, containing 53 stars, it was possible to identify 26 stars as typical fundamental pulsators. These stars were used to derive the basic equations for the present analysis:

for $\langle B-V \rangle_o < 0.85$

$$\log P_F = -1.584 + 1.1835 \cdot \log R_{max} + 0.560 \cdot \langle B - V \rangle_o \qquad (5a)$$
$$\text{s.d.} = 0.019$$

and

$$\Delta \log P = \log P + 1.584 - 1.1835 \cdot \log R_{max} - 0.560 \cdot \langle B - V \rangle_o \qquad (5b)$$

Similarly from 9 stars of the second group of 13 stars the following equations were found:

$\langle B - V \rangle_o > 0.85$

$$\log P_F = -1.423 + 1.1078 \cdot \log R_{max} + 0.471 \cdot \langle B - V \rangle_o \qquad (6a)$$
$$\text{s.d.} = 0.015$$

and

$$\Delta \log P = \log P + 1.423 - 1.1078 \cdot \log R_{max} - 0.471 \cdot \langle B - V \rangle_o \qquad (6b)$$

In both groups introducing $\log R_{max}$ instead of the normally used $\log R$ causes decreasing or the same values of the standard deviation for $\log P_F$. Therefore the equations with $\log R_{max}$ should be preferred and will be used in the following.

The $\log P$ values computed according to formulae (5b) and (6b) are also listed in Table II. Their frequency distribution is shown in Fig. 1. The distribution for the first group makes it possible to recognize 48 stars as fundamental pulsators with $-0.10 < \Delta\log P < +0.12$; and 5 stars as first overtone pulsators $-0.16 < \Delta\log P < -0.12$. These 5 Cepheids are: BG Cru, BF Oph, V 482 Sco, Y Sgr and U Aql. It may be noted that not a single one of these stars is listed by Cox (1979) as a candidate for the first overtone pulsators.

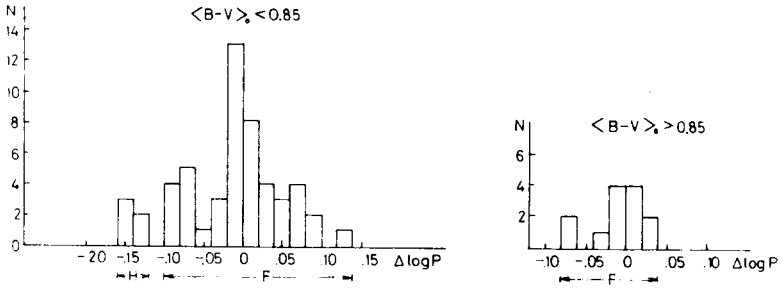

Figure 1. Frequency distribution of $\Delta\log P$ for groups of stars with $\langle B-V\rangle_o$ smaller and larger than 0.85 . The separation of fundamental F and first overtone H pulsators is shown.

Taking into consideration the estimated accuracy of the Wesselink radii, viz. 10% or $\log R \pm 0.04$, and the accuracy of $\langle B-V\rangle_o$, viz. ± 0.05 , the maximum error due to these factors amounts to ± 0.07 . The scatter of $\Delta\log P$ visible in Fig. 1 up to ± 0.10 for $\log P_F$ can be regarded as evidence that there is also a natural scatter of the investigated parameters in relation to formula (5a).

The frequency distribution of $\Delta\log P$ for the second group $\langle B-V\rangle_o > 0.85$ indicates a complete homogeneity with small dispersion $-0.08 < \Delta\log P < +0.04$.

In Fig. 2 the $\Delta\log P$ values are plotted as a function of $\log P$. For comparison the 11 double-mode Cepheids according to their $\log P_F$ and $\Delta\log P = \log P_H - \log P_F$ values are shown as a line with open circles from TU Cas ($\log P_F = 0.330$) to V 367 Sct ($\log P_F = 0.799$) (Stobie, 1977). Also a theoretical line, Cox and Hodson (1978), is added. This comparison makes it possible to conclude that the values of $\Delta\log P$ for 5 stars identified as the first overtone pulsa-

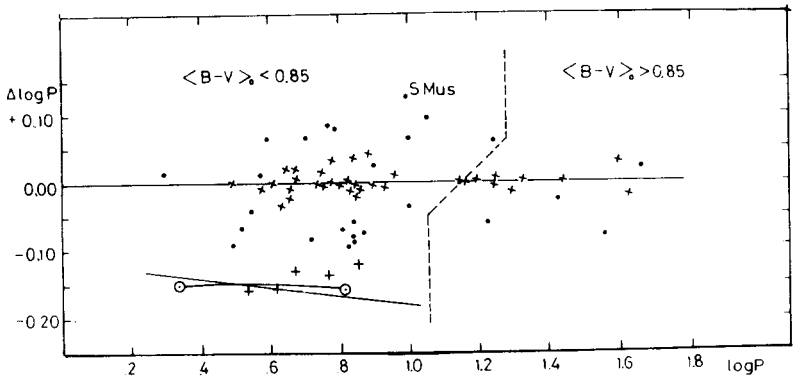

Figure 2. $\Delta \log P - \log P$ relation. The typical fundamental pulsators are indicated by small crosses (x) the remaining by points. The positions of 5 first overtone pulsators (BG Cru, BF Oph, V 482 Sco, Y Sgr and U Aql) are marked by + signs placed at about $\Delta \log P = -0.15$. In this region the line with open circles at the ends represents the double-mode Cepheids. The theoretical line (Cox and Hodson, 1978) is also shown.

tors are in accordance with other data and that all first overtone pulsators, single and double-mode Cepheids, occur in the similar ranges of periods, viz. $0.3 < \log P < 0.9$. This last conclusion is the reason we assume that 13 long period Cepheids of the second group are fundamental pulsators.

According to these results the stars in Table II are designated as fundamental F or first overtone H pulsators.

We may call attention to the fact that in our investigation the star SU Cas appears as a fundamental pulsator. This has been frequently regarded as doubtful, see Cox (1979). Moreover, S Mus, with the largest positive value of $\Delta \log P = +0.12$, is an unusual Cepheid and will be discussed in the last part of this paper.

The transformation of the above equations to the commonly used P–L–C relation is possible by replacing $\langle B-V \rangle_o$ by the surface brightness in the V band, S_v , and by calculating the absolute magnitudes M_v :

$$M_{<v>} = -5 \cdot \log R_{max} + S_v \tag{7}$$

This definition means that we assume as the representative state of the pulsating star the mean part of the descending branch of the light curve, when the radius passes through a flat maximum, the temperature is slowly decreasing and the photosphere is moving with a constant, downward acceleration. With the help of the next equation:

$$M_{bol} = -5 \cdot \log R_{max} - 10 \cdot \log T_e + 42.312 \tag{8}$$

we have

$$S_V = 42.312 - 10 \cdot \log T_e - B.C. \tag{9}$$

where

$$B.C. = M_{bol} - M_{<v>}$$

In other papers instead of S_V the surface brightness parameter, F_V is used:

$$F_V = \log T_e + 0.1 \cdot B.C. \tag{10}$$

and therefore

$$S_V = 42.312 - 10 \cdot F_V \tag{11}$$

According to Barnes (1980) the parameter F_V is related to the colour index $(V-R)_o$:

$$F_V = 3.957 - 0.360 \cdot (V-R)_o \tag{12}$$

This result is achieved by assuming that the slope

$$\frac{\Delta F_V}{\Delta (V-R)} = -0.360$$

derived from the pulsational changes of individual stars is valid also for the mean values of F_V and $(V-R)_o$ for all Cepheids. The zero point of equation (12) was adopted from the model atmosphere results. Replacing F_V by S_V

Table III

$<B-V>_o - S_V - \log T_e$ relation

$<B-V>_o$	$(V-R)_o$	S_V	B.C.	$\log T_e$
0.10	0.11	3.14	0.00	3.917
0.20	0.22	3.53	+ .13	.865
0.30	0.30	3.82	+ .14	.835
0.40	0.37	4.07	+ .11	.813
0.50	0.42	4.25	+ .08	.798
0.60	0.47	4.43	+ .04	.784
0.70	0.51	4.58	- .01	.774
0.80	0.56	4.76	- .07	.762
0.90	0.60	4.90	- .12	.749
1.00	0.66	5.12	- .19	.735
1.10	0.74	5.41	- .27	.717
1.20	0.81	5.66	- .37	.702
1.30	0.88	5.91	- .46	.686
1.40	0.96	6.20	- .60	.671
1.50	1.05	6.52	-0.75	3.654

we have:

$$S_V = 2.742 + 3.60 \cdot (V-R)_o \tag{13}$$

The next step is the transformation of $(V-R)_o$ to $\langle B-V\rangle_o$, which has been done with the aid of the results achieved for supergiants I by Johnson (1966). When we added the B.C.$-\langle B-V\rangle_o$ relation of Flower (1977) we got the complete set of data used in this investigation (Table III). The numerical quantities of this table can be approximated by the formulae:

for $0.4 < \langle B-V\rangle_o < 0.9$

$$\begin{aligned} S_V &= 3.41 + 1.660 \cdot \langle B-V\rangle_o \\ \log T_e &= 3.858 - 0.120 \cdot \langle B-V\rangle_o \end{aligned} \tag{14}$$

for $0.9 < \langle B-V\rangle_o < 1.2$

$$\begin{aligned} S_V &= 2.62 + 2.533 \cdot \langle B-V\rangle_o \\ \log T_e &= 3.892 - 0.158 \cdot \langle B-V\rangle_o \end{aligned} \tag{15}$$

The S_V-$\langle B-V\rangle_o$ relation can be tested by means of 6 calibration Cepheids, which are to be found in Table II and for which the M_V values were taken from van den Bergh (1977) and from Sandage and Tammann (1969) and corrected by -0.26 according to the new distance scale (Cox, 1979). For these stars the values of S_V result directly from formula (7), Table IV. In Fig. 3 we see that the individual points are scattered on both sides of the relation established above. The greatest deviation corresponds to SU Cas, $\Delta S_V = -0.55$, whereas for other stars ΔS_V is about ± 0.25. But SU Cas and RS Pup were not used by van den Bergh as they are unreliable.

Now it is possible to replace $\log R_{max}$ in formulae (5) and (6) by $M_{\langle V\rangle}$ and $\langle B-V\rangle_o$ with the aid of equations (7) and (14) or (15) to get the P–L–C relations:

for $0.4 < \langle B-V\rangle_o < 0.9$

$$\log P_F = -0.777 - 0.2367 \cdot M_{\langle V\rangle} + 0.953 \cdot \langle B-V\rangle_o \tag{16a}$$

$$\Delta\log P = \log P + 0.777 + 0.2367 \cdot M_{\langle V\rangle} - 0.953 \cdot \langle B-V\rangle_o \tag{16b}$$

for $0.9 < \langle B-V\rangle_o < 1.2$

$$\log P_F = -0.842 - 0.222 \cdot M_{\langle V\rangle} + 1.032 \cdot \langle B-V\rangle_o \tag{17a}$$

$$\Delta\log P = \log P + 0.842 + 0.222 \cdot M_{\langle V\rangle} - 1.032 \cdot \langle B-V\rangle_o \tag{17b}$$

With the aid of these formulae it is easy to calculate $\Delta\log P$ for the calibration of the Cepheids used by van den Bergh (1977) with the addition SZ Cas, RS Pup and S Vul. Colour indices are accepted as for other stars but

Table IV

Surface brightness for 6 calibration Cepheids

	$\log P_F$	$\langle B-V\rangle_o$	$M_{\langle v\rangle}$	$\log R_{max}$	S_v
U Sgr	0.829	0.57	-4.19	1.782	+4.72
S Nor	0.989	0.75	-4.29	1.756	+4.49
T Mon	1.432	0.98	-5.76	2.122	+4.85
SV Vul	1.654	1.08	-6.26	2.282	+5.15
SU Cas	0.290	0.48	-3.07	1.346	+3.66
RS Pup	1.617	0.98	-6.33	2.347	+5.40

Table IVb

Calibration Cepheids

	$\log P_F$	$\langle B-V\rangle_o$	$M_{\langle v\rangle}$	$\Delta \log P$
EV Sct	0.490	0.55	-2.88	+0.061
CEb Cas	0.651	.59	-3.46	.047
CF Cas	0.688	.68	-3.34	.026
CEa Cas	0.711	.66	-3.54	.021
CV Mon	0.731	.62	-3.61	.063
CS Vel	0.771	.68 ?	-3.31	.117
V367 Sct	0.799	.51 ?	-4.08	.124
U Sgr	0.829	.57	-4.19	.071
DL Cas	0.903	.71	-4.10	.034
S Nor	0.989	.75	-4.29	.036
TW Nor	1.033	.82 ?	-3.79	.132
SZ Cas	1.134	0.66	-5.06	+0.084
mean				+0.063
VY Car	1.277	0.94 ?	-5.23	+0.006
T Mon	1.432	0.98	-5.76	.002
RS Pup	1.617	0.98	-6.33	.061
SV Vul	1.654	1.08	-6.26	.017
S Vul	1.826	1.05	-6.89	+0.074
mean				+0.032

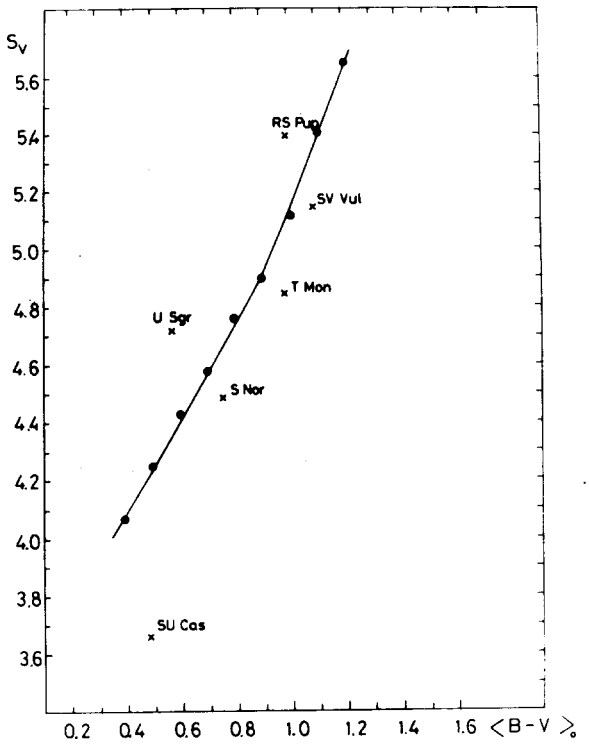

Figure 3. Surface brightness—colour index ($S_V - \langle B-V \rangle_o$) relation. The positions of 6 calibration Cepheids with known Wesselink radii are marked by x.

$M_{\langle V \rangle}$ has been diminished by 0.26, see Cox (1979), Table IVb.

From the $\Delta \log P$ values it is evident that all these stars are fundamental pulsators. But there is a systematic difference $\Delta \log P = +0.063$ for 12 stars of the first group and +0.032 for 5 stars of the second group. This may be removed, for example, by correction of $\log R_{max}$ by about +0.06 or +0.03 respectively. That would bring 3 calibration stars: S Nor, T Mon and SV Vul nearer to the line representing the $S_V - \langle B-V \rangle_o$ relation, Fig. 3.

Photometric masses and problem of instability strip crossings

The problem of Cepheid masses is still far from a final solution. From the discussion on this topic published by Cox (1979) it is evident that on the average discrepancies between masses determined by various methods are removed. But there is still a lack of relations between them and other parameters, e.g. mass—luminosity relation, which should exist according to the theory. These facts encourage one to search for an independent individual

mass determination and to verify the assumption that the observed Cepheids are all during the second crossing of the instability strip — the longest crossing time. In connection with this we may remark that according to the results of Becker et al. (1977) for certain masses and chemical compositions the lifetimes for the third crossing are longer than for the second one. So it seems worth trying to sort the Cepheids according to their crossings of the instability strip.

The possibility for such a test exists because of the results published by Pel (1978). On the basis of two colour indices of Walraven photometry he succeeded in establishing the effective gravity, g_e, for all the phases of 60 Cepheids. From his diagrams we estimated the values of $\log g_e$ for the phase of maximum radius R_{max}. The accuracy of this procedure is about ± 0.05, Table V. The actual gravity, g, and effective gravity, g_e, are connected with each other:

$$g = g_e - \ddot{r} \tag{18}$$

As the pulsation acceleration, $\ddot{r}$, we assume the value also for the phase of R_{max}. This may easily be estimated from the slope of the velocity curve, v_r, which in most cases is constant over the range of phases 0.3–0.6, when the radius reaches its maximum value. The pulsation acceleration is equal to:

$$\ddot{r} = -p\frac{dV_r}{dt} \qquad ; \qquad p = 1.31$$

The gravity g so derived is used to calculate the "photometric masses", M_{ph}:

$$g = g_\odot \frac{M_{ph}}{R^2_{max}}$$

where solar gravity $g_\odot = 2.74 \cdot 10^4$ cm·sec^{-2}, or

$$\log M_{ph} = \log g + 2 \cdot \log R_{max} - 4.438 \tag{19}$$

The photometric masses resulting from this relation should be related to the luminosities and effective temperatures. These two parameters have been replaced by the quantities $M_{<v>}$ and $<B-V>_o$ taken from Table II.

To begin with we start with the group of 29 stars for which the complete set of three observational data has been derived: $\log M_{ph}$, $M_{<v>}$ and $<B-V>_o$, Table V. We assume the relation

$$\log M_{ph} = a + b \cdot M_{<v>} + c \cdot <B-V>_o \qquad , \tag{20}$$

where the values a, b and c are to be calculated by the least squares method. We then proceed similarly to when selecting the first overtone pulsators.

We check the homogeneity of this group by investigating the frequency distribution of the quantity

$$\Delta \log M_{ph} = \log M_{ph} - a - b \cdot M_{<v>} - c \cdot <B-V>_o \qquad (21)$$

The solution of equation (20) for all 29 stars gives a large standard deviation, viz. s.d. = ±0.18 . But it was possible to select from this group 15 stars which satisfy the equation:

$$\log M_{ph2} = 0.042 - 0.354 \cdot M_{<v>} - 0.884 \cdot <B-V>_o \qquad (22a)$$

with s.d. = 0.046 . For these stars the values

$$\Delta \log M_{ph} = \log M_{ph2} - 0.042 + 0.354 \cdot M_{<v>} + 0.884 \cdot <B-V>_o \qquad (22b)$$

are in the range $-0.08 < \Delta \log M_{ph} < 0.12$. For the other 10 stars of the same group the $\log M_{ph}$ values are clustered near -0.17 , from -0.32 to -0.12 . In this way equation (22b) became the basis for dividing the 25 stars into two groups. This can be seen from Fig. 4, where the frequency distribution of $\Delta \log M_{ph}$ is displayed. Taking into account the passages of the evolutionary tracks of Cepheids across the instability strip, we suggest that these two groups include stars in the second and third crossing of the instability strip and that relation (22a) is valid for the second crossing $\log M_{ph2}$. Consequently, the remaining 4 stars may be classified as being in the first and fourth crossings, with 1 star added to the second crossing stars. As the limiting $\Delta \log M_{ph}$ values we accepted:

crossing number	$\Delta \log M_{ph}$ max.	min.
1	+0.38	+0.14
2	+0.14	-0.09
3	-0.09	-0.34
4	-0.34	-0.64

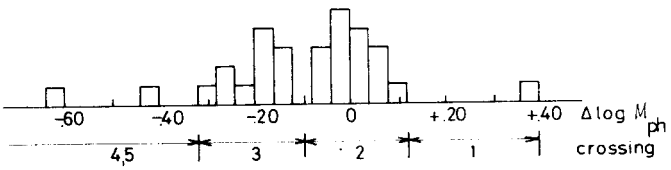

Figure 4. Frequency distribution of $\Delta \log M_{ph}$ for 29 stars. The separation of stars being in different crossings is indicated.

In order to increase the number of investigated stars we established the

Table V

Crossing Numbers and Photometric Masses of Cepheid Variables

	$\log P$	Mode & cross.	$\langle B-V\rangle_o$	$\log R_{max}$	$\log g_{eq}$	$\log g_e$	$\ddot{r}$	$\log g$	$\log M_{ph}$	$\Delta \log M_{ph}$	$M_{\langle v\rangle}$	M_{bol}	$\log T_e$
RT Mus	0.489	F2	0.50	1.518	2.62	2.12	-19.6	2.182	0.780	-0.004	$-3^m.35$	$-3^m.27$	3.798
AZ Cen	.507	F3	.51	1.586	2.05	1.91		1.99	0.72	- .16	-3.67	-3.59	.796
UZ Cen	.523	F,H2			2.28	2.08		2.14					
R TrA	.530	F2	.57	1.554	2.25	2.05	-29.1	2.149	0.819	+ .075	-3.41	-3.36	.788
Y Car	.561	F,H2			2.40	2.18		2.22					
SS Sct	.565	F3?	.61	1.53	2.01	1.83		1.92	0.54	- .10	-3.22	-3.19	.783
AX Vel	.565	F,H2			2.47	2.29		2.33					
UX Car	.566	F3?	.56	1.564	2.04	1.91		1.99	0.680	- .106	-3.50	-3.44	.789
AG Cru	.584	F3	.53	1.526	2.24	1.86	-22.9	1.982	0.596	- .159	-3.34	-3.27	.793
BF Oph	.609	H2	.61	1.706	2.01	1.83	-27.0	1.973	0.947	- .009	-4.11	-4.07	.783
AH Vel	.626	F4	.54	1.642	1.60	1.55	-10.4	1.663	0.509	- .435	-3.90	-3.83	.792
V Vel	.641	F1	.56	1.598	2.90!	2.38	-19.1	2.413	1.171	+ .334	-3.65	-3.59	.789
FF Aql	.650	F4	.59	1.630	1.20	1.15	-12.1	1.415	0.237	- .613	-3.76	-3.72	.785
V482 Sco	.656	H3	.67	1.685	1.73	1.53		1.69	0.62	- .21	-3.90	-3.90	.776
T Vel	.666	2			2.07	1.92		2.00					
RY CMa	.670	F3	.63	1.589	1.78	1.58	-22.7	1.785	0.525	- .180	-3.49	-3.46	.781
S Cru	.671	F2	.61	1.606	1.99	1.85		1.94	0.71	- .06	-3.61	-3.58	.783
SX Car	.687	2			2.11	1.96		2.03					
AP Sgr	.704	F4	.66	1.566	1.56	1.54	-10.5	1.566	0.260	- .374	-3.32	-3.31	.777
V381 Cen	.706	2	.60	1.66	2.03	1.93		2.01	0.90	+ .02	-3.87	-3.83	.784
AP Pup	.706	F2	.66	1.695	2.03	1.93		2.01	0.96	+ .10	-3.97	-3.96	.777
V Cen	.740	F2	.58	1.698	2.01	1.93	-14.7	2.000	0.958	- .028	-4.12	-4.07	.787
V419 Cen	.741	F3	.60	1.667	1.67	1.62		1.75	0.65	- .26	-3.93	-3.89	.784
UY Car	.744	2			2.02	1.92		1.99					
GH Car	.758	2			1.91	1.83		1.92					
Y Sgr	.761	H3	.70	1.763	1.53	1.51		1.67	0.76	- .16	-4.24	-4.25	.773
R Cru	.765	F2	.63	1.682	1.92	1.82	-12.2	1.892	0.818	- .064	-3.95	-3.92	.781
RV Sco	.783	F2	.63	1.636	1.97	1.89	-14.6	1.973	0.807	+ .007	-3.72	-3.69	.781
FM Aql	.786	1,2?			2.13	1.93		2.00					
X Cru	0.794	F3	0.69	1.692	1.57	1.57	-11.6	1.690	0.636	- .184	-3.90	-3.90	3.774

Table V (cont.)

	$\log P$	Mode & cross.	$\langle B-V \rangle_o$	$\log R_{max}$	$\log g_{eq}$	$\log g_e$	$\ddot{r}$	$\log g$	$\log M_{ph}$	$\Delta \log M_{ph}$	$M_{\langle V \rangle}$	M_{bol}	$\log T_e$
S TrA	0.801	F2	0.68	1.752	1.79	1.77	-12.6	1.857	0.923	- .010	-4.22	-4.22	3.775
BB Sgr	.822	F2	.75	1.753	1.67	1.62	-17.7	1.778	0.846	+ .014	-4.11	-4.15	.767
AT Pup	.824	F2	.59	1.769	1.98	1.88		1.96	1.06	- .04	-4.46	-4.42	.785
V Car	.826	F2	.68	1.717	1.91	1.81	-11.3	1.881	0.877	+ .004	-4.05	-4.05	.775
T Cru	.828	F2	.65	1.797	1.83	1.78	-14.1	1.869	1.025	- .033	-4.50	-4.48	.779
U Sgr	.829	F2	.71	1.782	1.75	1.65	-12.4	1.758	0.884	- .060	-4.32	-4.34	.772
V636 Sco	.832	F3	.72	1.689	1.61	1.56	- 9.3	1.653	0.593	- .170	-3.84	-3.86	.771
V496 Aql	.833	F3	.78	1.726	1.56	1.51	- 7.0	1.591	0.605	- .134	-3.92	-3.98	.764
BG Vel	.841	F1	.73	1.735	2.03	1.95		2.02	1.05	+ .32	-4.05	-4.08	.770
X Sgr	.846	F1	.53!	1.811	2.14	2.04		2.10	1.28	+ .20	-4.76	-4.69	.793
U Aql	.847	H3	.70	1.825	1.56	1.51	-14.2	1.663	0.875	- .159	-4.55	-4.56	.773
η Aql	.856	F3	.69	1.800	1.49	1.44	-12.4	1.602	0.764	- .245	-4.44	-4.44	.774
R Mus	.876	F3	.65	1.737	1.66	1.58		1.72	0.76	- .20	-4.20	-4.22	.779
IT Car	.877	2?	.77	1.72	1.59	1.51		1.67	0.67	- .07	-3.92	-3.97	.765
RS Ori	.879	2			1.60	1.55		1.70					
W Sgr	.880	F2	.65	1.79	1.82	1.77		1.87	1.01	- .05	-4.46	-4.44	.779
ER Car	.888	F2	.75	1.691	1.80	1.70		1.81	0.75	+ .03	-3.80	-3.84	.767
W Gem	.899	3	.71	1.77	1.46	1.31		1.56	0.66	- .26	-4.26	-4.27	.772
S Sge	.923	F3	.74	1.776	1.30	1.22	-17.1	1.531	0.645	- .243	-4.24	-4.27	.769
WX Pup	.951	F2	.73	1.790	1.88	1.80	- 9.3	1.857	0.999	+ .072	-4.33	-4.36	.770
GH Lup	.968	3,4?			1.18	1.13		1.46					
V500 Sco	.969	3			1.48	1.28		1.54					
FN Aql	.977	3	.774	1.82	1.50	1.25		1.52	0.72	- .25	-4.47	-4.50	.769
SX Vel	.980	3?	.61!	1.89	1.63	1.53		1.69	1.03	- .25	-5.02	-4.99	.783
YZ Sgr	.980	2	.75	1.82	1.61	1.56		1.71	0.91	- .04	-4.44	-4.48	.767
S Mus	.985	F?	.57!	1.797	2.82!	2.87!	- 7.6!	2.875!	2.031!	+ .856!	-4.63	-4.58	.788
S Nor	.989	F2	.77	1.756	1.56	1.46	-19.0	1.681	0.755	- .052	-4.09	-4.14	.765
AQ Car	.990	2			1.70	1.60		1.74					
β Dor	0.993	F2	.73	1.864	1.83	1.73	-15.6	1.845	1.135	+ .077	-4.70	-4.73	.770
XX Cen	1.040	F3	0.71	1.801	1.43	1.28	-12.8	1.505	0.669	- .308	-4.42	-4.44	3.772

relation of the difference ($\log g - \log g_e$) to $\log g_e$ for the investigated group of 29 stars:

$\log g_e$	$\log g - \log g_e$
1.20	0.30
1.40	0.20
1.60	0.13
1.80	0.10
2.00	0.07
2.20	0.05
2.40	0.03
2.60	0.02
2.80	0.01

This relation was used to change $\log g_e$ to $\log g$ when it was not possible to get the $\bar{r}$ value directly. Also, when $\langle B\text{-}V\rangle_o$ was not known, but $\log R_{max}$ was determined, equation (5a) was used to calculate the missing quantity. All these additional stars (Table V) have $\log R_{max}$, $\log M_{ph}$ to only two decimal figures, whereas the basic 29 stars have three figures in these quantities. This meant that it was possible to get, all in all, 47 values of $\Delta\log M_{ph}$. For these stars the crossing numbers have been estimated and given in Table V together with the designation of pulsation modes. For example, F2 means fundamental pulsator in the second crossing. The dependence of $\Delta\log M_{ph}$ on $\log M_{ph}$ can be seen from Fig. 5.

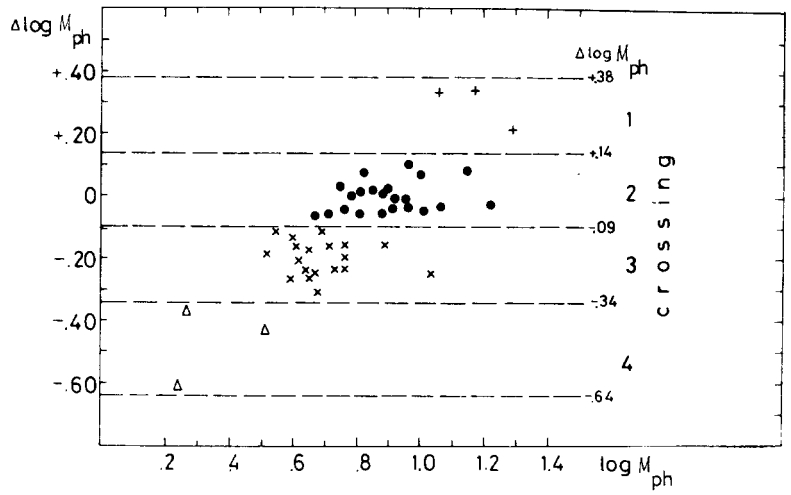

Figure 5. $\Delta\log M_{ph} - \log M_{ph}$ relation with division on crossings 1, 2, 3 and 4. The limiting values of $\Delta\log M_{ph}$ are shown. The stars in different crossings are denoted by the symbols which are also used in the all next Figures.

The separation of these stars according to their crossing number may al-

so be shown otherwise. By eliminating $\log M_{ph}$ and $M_{<v>}$ from formula (22a) with the aid of equations (7), (14) and (16) we have for the second crossing:

$$\log g + 1.4706 \cdot \langle B-V \rangle_o = 3.275 - 0.2325 \cdot \log R_{max} \qquad (23)$$

We may then introduce $\log P_F$ instead of $\log R_{max}$, (equation (5)), and we get the following relation of three parameters:

$$2.9634 - \log g = 1.3606 \cdot \langle B-V \rangle_o + 0.1964 \cdot \log P_F \qquad (24)$$

In both these formulae g denotes, as before, the gravity for the phase of R_{max} . On account of the small value of the coefficient by $\log P_F$ also $\log P_H$ may be used in formula (24), causing an error of 0.03 . Therefore in practice this formula may be used with every period P. The diagrams, Fig. 6 and Fig. 7, represent these two relations with the distinct separation of stars being in different crossings.

When we use the mean values of $\log g_{eq}$ given by Pel (1978) and $\log P_F$, then in the diagram of Fig. 8 it is possible to indicate the regions where the stars of different crossings are placed. So we may state that three double-mode Cepheids — UZ Cen, Y Car and AX Vel — for which $\log g_{eq}$ was also determined by Pel (1978), are in the second crossing. This diagram also allowed us to estimate the crossing numbers for the remaining stars, for which only P and g_{eq} are known. In this way we were able to complete the determination of the whole set of crossings amounting to 56 stars and 3 doubtful

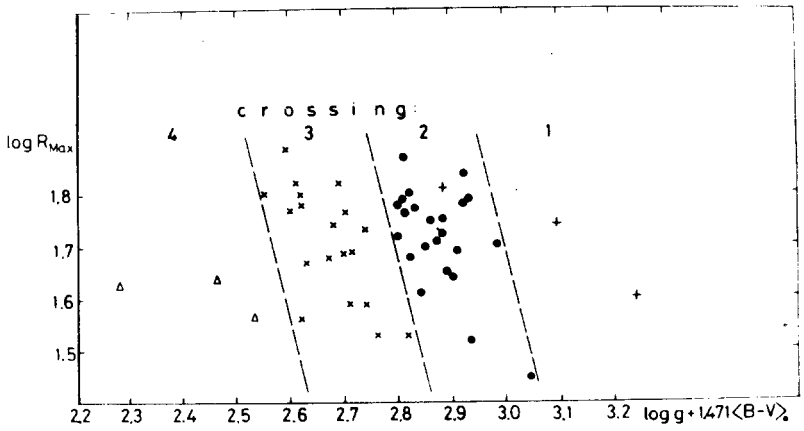

Figure 6. Separation of stars resulting from the formula (23) according to different crossings. Notation of stars as in Fig. 5. Only one first crossing star, X Sgr, is in the area of the second crossing stars.

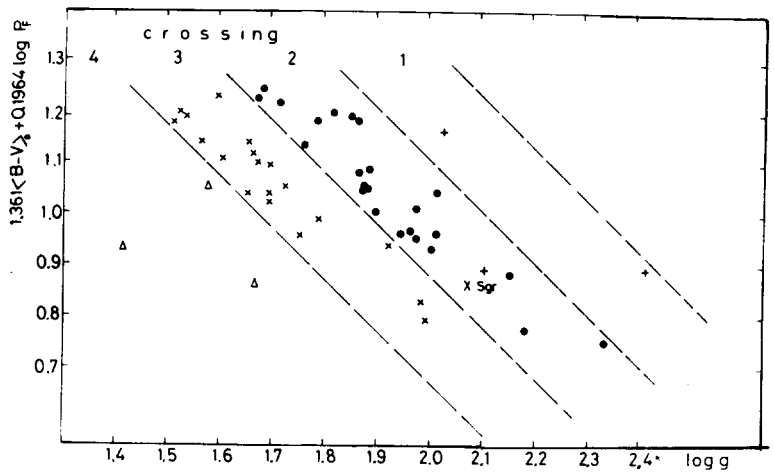

Figure 7. Separation of stars resulting from the formula (24) according to crossings. Notation of stars as in Fig. 5. X Sgr is in the area of the second crossing stars, as in Fig. 6.

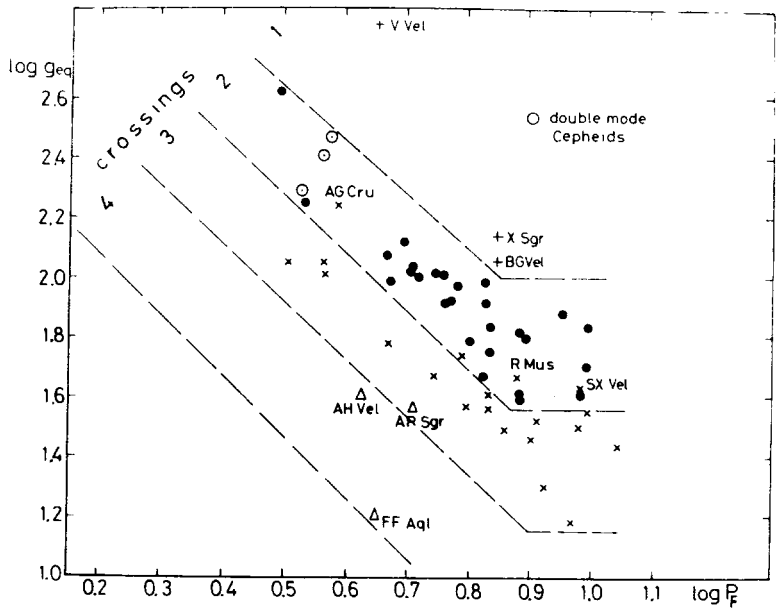

Figure 8. Stars in different crossings on the $\log g_{eq} - \log P_F$ plane. The separation is not so complete as in Figs. 6 and 7, but it is possible to indicate the limits between crossings sections.

cases:

crossing	$\Delta \log M_{ph}$			stars
	min.	mean	max.	
1	+0.14	+0.285	+0.38	3
2	-0.09	-0.005	+0.14	30
3	-0.34	-0.197	-0.09	20
4	-0.64	-0.474	-0.34	3

As the direct consequences of these results we present the following relations:

1. Mass – fundamental period relation. Three first overtone pulsators are plotted with periods increased by 0.15 . Unexpectedly for all crossings the smallest masses seem to occur near $\log P$ equals 0.675 (Fig. 9) though the separation of stars is not complete. For example, three second crossing stars are in the area of the third crossing.

2. Mass – luminosity relation (Fig. 10). Here the separation of stars is satisfactory. The relation indicates that the masses remain nearly constant up to $M_{bol} = -4.1$ and increase for greater luminosities.

3. H–R diagram, $M_{bol} - T_e$ relation (Fig. 11). The instability strip is well marked with the complete mixing of stars with different crossings. Only S Mus and XX Vel have too high temperatures.

4. Period – luminosity relation (Fig. 12) is quite normal. The width of the strip is about $0^m.85$ without separation of stars according to crossings. Here S Mus is in the centre of the strip, but X Sgr is outstanding.

Unfortunately Pel's data do not include long period Cepheids so that it is not possible to investigate the extension of these relations toward longer periods.

The star S Mus with normal P_F and M_{bol} has too high temperature and abnormally large gravity and mass. This star should be investigated with special attention.

It would be desirable to have an independent confirmation of the above results. Such a possibility may be offered by the secular changes of pulsation periods. From our formulae we can conclude that the evolution of Cepheids along the lines of constant masses should be accompanied by changes of their periods. During crossings 1, 3 and 5 – from the blue to red edge of the instability strip – the period should increase. By contrast, crossing numbers 2 and 4 should be accompanied by a decrease of the periods. The secular changes of periods have been investigated by Szabados (1977, 1980). A distinct result was obtained for η Aql: the period is increasing, which agrees with crossing number 3, as determined in the present paper.

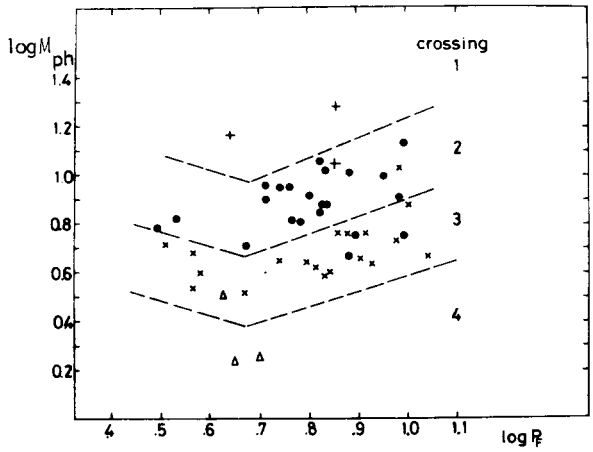

Figure 9. Mass — fundamental period relation. Periods of first overtone stars (BG Cru, BF Oph, V 482 Sco, Y Sgr, U Aql) are increased by 0.15 . Notation of stars as in Fig. 5. The smallest masses are near $\log P_F = 0.675$.

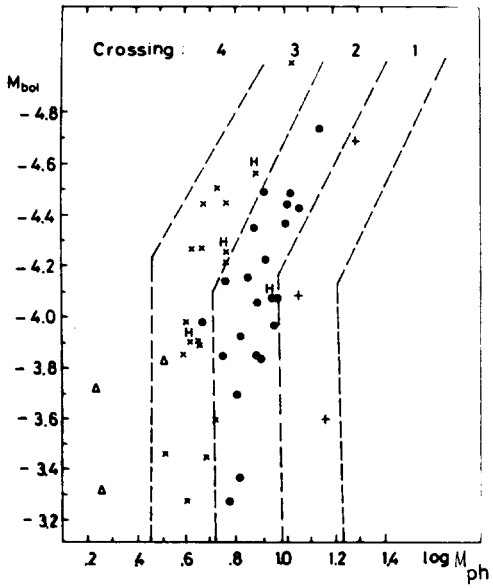

Figure 10. Mass — luminosity relation. In the range M_{bol} from -3.2 to -4.2 the masses seem to be constant. For greater luminosities the increase of masses is visible.

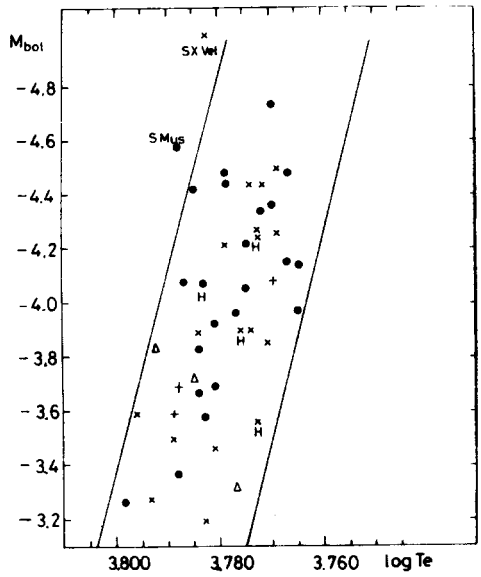

Figure 11. Theoretical H–R diagram. The complete mixing of different crossing stars in the instability strip is visible. Only S Mus and SX Vel have too high temperatures. The positions of the first overtone pulsators are indicated by H. Notation of stars as in Fig. 5.

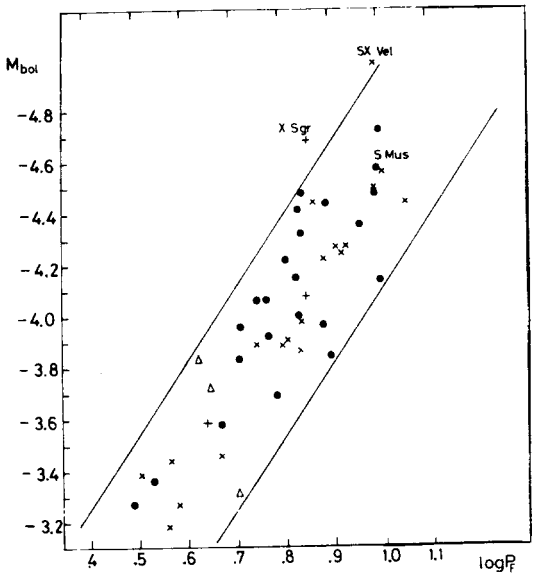

Figure 12. Luminosity – fundamental period relation. The first overtone pulsators are placed with periods increased by 0.15 . The stars of different crossings are mixed. The outstanding star is X Sgr but S Mus seems to be normal in this plane. Notation of stars as in Fig. 5.

References:

Balona, L.A. 1977, M.N.R.A.S., 178, 231.
Barnes, T.G. 1980, In: Current Problems in Stellar Pulsation Instabilities, NASA Tech. Memorandum 80625, p. 639.
Becker, S.A., Iben, I., Tuggle, R.S. 1977, Astrophys. J., 218, 212.
Cox, A.N., Hodson, S.W. 1978, I.A.U. Symposium, No. 80, p. 237.
Cox, A.N. 1978, Astrophys. J., 229, 212.
Dean, J.F., Warren, P.R., Cousins, A.W.J. 1978, M.N.R.A.S., 183, 569.
Flower, P.J. 1977, Astron. Astrophys., 54, 33.
Ivanov, G.R. 1981, Astrophys. Space Sci., 79, 107.
Johnson, H.L. 1966, Ann. Rev. Astron. Astrophys., 4, 193.
Joshi, S.C., Rautela, B.S. 1980, Astrophys. Space Sci., 70, 393.
Kraft, R.P. 1961, Astrophys. J., 134, 616.
Opolski, A. 1968, Acta Astron., 18, 515.
Pel, J.W. 1978, Astron. Astrophys., 62, 75.
Sollazzo, C., Russo, G., Onnembo, A., Caccin, B. 1981, Astron. Astrophys., 99, 66.
Sandage, A.R., Tammann, G.A. 1969, Astrophys. J., 157, 683.
Schaltenbrand, R., Tammann, G.A. 1971, Astron. Astrophys. Suppl. Ser., 4, 265.
Stobie, R.S. 1977, M.N.R.A.S., 180, 631.
Stobie, R.S., Balona, L.A. 1979, M.N.R.A.S., 189, 641.
Szabados, L. 1977, Mitt. Sternw. ung. Akad. Wiss., Budapest, Nr. 70.
Szabados, L. 1980, Mitt. Sternw. ung. Akad. Wiss., Budapest, Nr. 76.
Thompson, R.J. 1975, M.N.R.A.S., 172, 455.
van den Bergh, S. 1977, In: Proc. I.A.U. Coll. No. 37, Decalages vers le Rouge et Expansion de l'Univers, p. 13.

STANDSTILL OF SOME δ SCUTI STARS

B. Vetö
Institut for General Physics, Eötvös Loránd University
H-1088, Budapest, Muzeum krt. 6-8.
Hungary

There are a number of interesting variable stars which have been classified as δ Scuti variables on the basis of their amplitudes, periods and spectral type. Further observations suggested that these stars do not always show light variation. The contradictory observations on their variability have meant that these stars cannot be regarded as normal δ Scuti variables. The four best known of them show a great deal of similarity.

τ Cygni (HR 8130). Light variations of $0^m.02$ in yellow were announced by Pande (1960). Breger (1969) reported that this star did not vary. The last observations by Fesen (1973) during two nights in August 1972 indicated τ Cyg to be constant.

τ Pegasi (HR 8880). Breger (1969) found this star to be constant over four hours, but Millis and Thompson (1970) discovered a variation with a period of 80 minutes and an amplitude of $0^m.02$. Fesen (1973) has confirmed this variability. He determined the period and the amplitude from observations of two consecutive nights. These values were found to be 82.5 minutes and $0^m.015$ on the first and $0^m.025$ on the second night, and they were in good agreement with Millis' observations.

γ Bootis (HR 5435). Old measurements indicated a variability with a period of $0^d.29$ (Miczaika, 1952). Other observations showed no signs of variability (Millis, 1967). Sareyan et al. (1971) confirmed the old period and phase.

γ Coronae Borealis (HR 5849) is the most observed star of the four. It was classified as a δ Scuti star by Fernie (1969). Tippets and Wilcken (1970) reobserved the star and found no light variations during two nights. In the same year Percy (1970) examined the star and reported some variability with poorly defined period (about $0^d.03$). We have investigated this star (Vetö and Kovács, 1981) to determine the period of its light variation. The observations were made on four nights in May 1981. The star showed some signs of variations on one night only and on the other three nights it was constant.

The light curve on J.D. 2444706 is very similar to Percy's observations in yellow.

We calculated the power spectrum for all our data to determine the period of γ CrB and found a well separated peak at the frequency — similar to Percy — of 23.6 c/d, with an amplitude about $0^m.001$.

The radial velocity measurements on these stars suggested that the light variation is caused by pulsation. The dependence of the periods on the radius confirms it. These stars vary after a standstill with the old period. In the case of γ CrB we could find this period during the standstill but with an amplitude of less than $0^m.001$ only.

Unfortunately, the standstills of these stars can hardly be explained by a strong beat phenomenon because these standstills are too long. The similarity between these stars and the short periodic variability of Ap stars is easily apparent.

References:

Baglin, A., Breger, M., Chevalier, C., Hauck, B., leContel, J.M., Sareyan, J.P., Valtier, J.C. 1973, Astron. Astrophys., 23, 221.
Breger, M. 1969, Pub. A.S.P., 84, 443.
Breger, M. 1979, Pub. A.S.P., 91, 5.
Fernie, J.D. 1969, J.R.A.S. Canada, 63, 133.
Fesen, R.A. 1973, Pub. A.S.P., 85, 732.
Miczaika, G.R. 1952, Z. Astrophys., 30, 134.
Millis, R.L. 1967, Pub. A.S.P., 79, 262.
Millis, R.L., Thompson, D.T. 1970, Pub. A.S.P., 82, 352.
Pande, M. 1960, The Observatory, 80, 225.
Percy, J.R. 1970, Pub. A.S.P., 82, 126.
Sareyan, J.P., Zribi, G., Bijaoui, A. 1971, Inf. Bull. var. Stars, No. 531.
Tippets, R., Wilcken, S.K. 1970, Pub. A.S.P., 82, 1156.
Vetš, B., Kovács, G. 1981, Inf. Bull. var. Stars, No. 2030.

COMMUNICATIONS
FROM THE
KONKOLY OBSERVATORY
OF THE
HUNGARIAN ACADEMY OF SCIENCES

MITTEILUNGEN
DER
STERNWARTE
DER UNGARISCHEN AKADEMIE
DER WISSENSCHAFTEN

BUDAPEST – SZABADSÁGHEGY

No. 84.

B. SZEIDL

PERIOD CHANGES IN DWARF CEPHEIDS, III
SZ LYNCIS

BUDAPEST, 1983

ISBN 963 8361 08 5 összkiadás
ISBN 963 8361 20 4 III. rész

HU ISSN 0324 - 2234
Felelős kiadó: Szeidl Béla

Hozott anyagról sokszorosítva

8414710 MTA Sokszorosító, Budapest. F. v.: dr. Héczey Lászlóné

PERIOD CHANGES IN DWARF CEPHEIDS, III

SZ LYNCIS

ABSTRACT

2371 photoelectric UBV observations obtained between 1962 and 1979 and twelve radial velocity measurements made in 1971 are reported. The long-periodic variation in time of maximum light discovered by van Genderen has been confirmed and the values of its period (P_1 = 1170 days = 3.20 yr) and semiamplitude (A = 0.00540 day = 467 sec) were improved. A secular change in the pulsation period ($\beta = 10^{-12}$ day·cycle^{-1}) has been found. Small cycle-to-cycle variations are clearly seen but a search for periodic modulation failed. The photometric parameters of the light curves are discussed. The two-colour diagram of SZ Lyn suggests an interstellar reddening of E(B-V) = 0.04 magn. Our spectra do not show any feature of the presence of doubled lines. Our observations are compatible with the hypothesis that SZ Lyn is a single-lined spectroscopic binary with a period of 3.20 yr and a total velocity amplitude 18 km·s^{-1}.

INTRODUCTION

The light variability of SZ Lyncis (=BD+44°1718 = HD 67390 = AGK2 +44°795 = CSV 1220 = S4747) was discovered by *Hoffmeister* (1949a,b). The star was first investigated photographically and visually by *Soloviev* (1955) and *Tsesevich* (1956a, b) who considered it as an eclipsing variable of W UMa type with a period of 0.212 day, and later of 0.274 day. Using photoelectric observations *Schneller* (1961) and *Eggen* (1962) rejected the earlier classification and demonstrated the RRs character of the variable. *Gefferth* and *Szeidl* (1962) and *Notni* (1962) determined the correct period of its light variation: P = 0.12053 day. *Gefferth* and *Szeidl* (1962) noticed small changes in the light variation amplitude from cycle to cycle but failed to find periodic variations in the height of maximum. Later *van Genderen* (1963) and *Broglia* (1963) investigated the light curve of the variable and found no irregularities. *He Tien-jian* and *Xiong Da-run* (1964) found the period to be decreasing. *Joshi* and *Srivastava*'s (1967) observations showed sudden shifts in the time of occurrence of the star's light maximum. According to them the period of the variable and its light and colour curves undergo drastic changes. It was reported by *van Genderen* (1967) that there are small changes in the height of the maximum and in the form of

the light curve. He was the first to point out that the O-C's produced by a linear ephemeris appeared to follow a sine-curve relation with a period of 3.1 years. *Binnendijk* (1968), however, found no evidence for variation in the height of the maximum nor in the shape of the light curve. On the other hand, *Wisse* and *Wisse* (1969) found the changes in the height and shape to be roughly correlated, therefore they considered these variations as real. Moreover the epoch of maximum given by *Wisse* and *Wisse* (1969) considerably deviates from *van Genderen*'s nonlinear ephemeris. In an attempt to resolve the discrepancies, high speed UBV photometry was carried out by *Barnes* and *Moffett* (1974, 1975). The existence of irregularities in the height of maximum light having a total amplitude of about 0.04 magn was confirmed. *Barnes* and *Moffett* (1975) improved the parameters of the periodic variation from a linear element and interpreted this long periodic modulation as light travel time effect supposing that SZ Lyn is a member of a binary system. *Duerbeck* (1976) suggested that there was an increase in brightness of SZ Lyn. This effect, however, could not be confirmed by *Karetnikov* and *Medvedev* (1978). They were unable to find any correlation between high and sharp maxima, although they also pointed out the changes in the form of the light curve. *Garrido* et al. (1979) found that the variations in the height of the maximum did not exceed $\sim$0.03 magn and they confirmed that the residuals from a constant period fitted a sine-wave well. According to their study no other significant change in the period seemed to be present.

The observations of *Africano* (1978) and *Hopp* and *Witzigmann* (1979) showed, however, that the O-C values of the times of light maximum were definitely larger than the standard deviation in the determination of the non-linear ephemeris of *Barnes* and *Moffett* (1975). This fact suggests that a redetermination of the period should be done with new observations.

According to the studies of *Willis* (1972) and *Alania* (1972, 1974) the metal abundance of SZ Lyn is normal or the star is slightly metal deficient, since $\Delta S \simeq 1$ or 2 near minimum light.

The strongest support for the binary hypothesis may come from radial velocity measurements. First, *Woolley* and *Aly* (1966) investigated the radial velocity variation of SZ Lyn, but they did not remark on spectral duplicity. *McNamara* and *Feltz* (1976) secured a number of spectrograms of SZ Lyn with a dispersion of 40 $A \cdot mm^{-1}$; they did not comment upon doubled lines either. Their careful analysis showed that the velocity data were uncertain and too limited in scope for testing the binary hypothesis at that time. At any rate, the data available to them did not support the long-period velocity variation. Recently *Bardin* and *Imbert* (1981) measured the radial velocities of SZ Lyn at

high time resolution. The results fully confirmed the binary hypothesis and led to a coherent provisional orbit with a fairly large computed eccentricity.

We present our photometric and spectroscopic observations to enable a more rigorous period analysis and give further support to the hypothesis that SZ Lyn is a component of a binary system.

PHOTOMETRIC OBSERVATIONS

On 28 nights in the period 7 February 1962- 27 February 1979, 2371 three-colour photoelectric observations were obtained at Konkoly Observatory. Most of the observations were carried out with the 24 inch telescope equipped with an unrefrigerated photometer. This photometer employed an 1P21 photomultiplier tube in 1962 and an EMI 9502B tube in the years 1963-1979. The colour filters were nearly on the UBV system: in ultraviolet light 2 mm UG1, in blue light 1 mm BG12 plus 2 mm GG13, in yellow light 2 mm GG11 Schott-filters were used. On two nights (namely on J.D.2441679 and J.D.2443931) the 20 inch telescope at the mountain station of Konkoly Observatory was used. The photometer of this telescope contained an EMI 9058QB multiplier and the following Schott-filters: UG2 in U, BG12+GG13 in B, and GG11 in V.

A summary of photoelectric observations obtained at Konkoly Observatory in different years in UBV light by different observers is presented in Table 1.

All observations were made differentially with respect to the comparison star BD $+45^{\circ}1544$ chosen conveniently close to SZ Lyn. Additional observations were obtained during the observational period by checking the constancy of the comparison star. A second comparison star, BD $+44^{\circ}1716$, was selected for this purpose and the intercomparisons indicated that the main comparison star was sufficiently constant. The comparison stars were calibrated on the UBV system through reference to standard stars from the list of *Johnson* and *Morgan* (1953) and *Iriarte* et al. (1965). These observations were made on three good and uniform nights in 1964, 1967 and 1968, respectively. The magnitudes and colours of the comparison stars are given in Table 2. This table also lists the values of comparison stars of other observers.

The individual observations of SZ Lyn are presented in Table 9a,b,c.These observations have been converted to the standard UBV system. In the reduction of the observations to ΔU, ΔB and ΔV magnitudes, mean differential colour curves on the instrumental system were formed for each year and then these mean curves were used for the colour corrections in the transformation equa-

Table 1

Journal of observations

Date	J.D.	U	B	V	Observer
1962.02. 7/8	2437703.4007 - .4926	-	36	30	B. Szeidl
9/10	705.5297 - .5698	-	13	12	K. Gefferth
10/11	706.2517 - .3642	-	59	53	- " -
11/12	707.4157 - .6032	-	78	76	B. Szeidl
21/22	717.2963 - .3450	-	17	14	- " -
22/23	718.4326 - .5747	-	53	55	- " -
03. 2/3	726.4874 - .5291	-	22	16	- " -
20/21	744.3201 - .4112	-	28	22	- " -
1963.01.22/23	38052.3373 - .3868	18	16	-	K. Barlai
	.4266 - .5783	44	41	-	B. Szeidl
02.21/22	082.3243 - .5074	132	-	27	- " -
1964.02.13/14	38439.2701 - .5243	53	56	52	- " -
03. 2/3	457.3117 - .4575	40	41	42	- " -
1967.02. 5/6	39527.4781 - .5698	29	29	29	- " -
6/7	528.5788 - .6455	22	21	21	- " -
1968.02.18/19	39905.2832 - .3964	33	38	41	- " -
1969.01.21/22	40243.3204 - .4176	31	32	32	- " -
1971.01.28/29	40980.3980 - .4210	-	12	12	L. Büki
03.24/25	41035.3337 - .4386	-	55	55	- " -
31/04. 1	042.3650 - .4150	-	8	8	- " -
1971.12.26/27	41312.3880 - .4658	-	41	41	L. Vargha
1972.03.13/14	390.3182 - .4279	28	30	30	B. Szeidl
1972.12.27/28	41679.5672 - .7050	36	36	36	- " -
1974.02.27/28	42106.2898 - .4140	-	36	36	- " -
1975.02. 7/8	42451.3844 - .4872	-	40	40	K. Olah
10/11	454.3845 - .5092	-	45	45	B. Szeidl
1978.03.10/11	43578.3050 - .3880	-	31	29	- " -
1979.01. 5/6	43879.5399 - .5874	-	17	17	K. Olah
02.26/27	931.2953 - .4520	-	50	53	- " -
total number of observations		466	981	924	

Table 2

Comparison stars of SZ Lyn

Star	V	B-V	U-B	Reference
BD $+44^{o}1716$	8.48	+0.98	+0.79	Present paper (n=8)
$+44^{o}1719$	10.93	+0.78	+0.36	Eggen (1962)
$+45^{o}1540$	9.80	+0.49		Joshi, Srivastava (1967)
	9.88	+0.48		van Genderen (1967)
	9.974	+0.560		Karetnikov, Medvedev (1978)
$+45^{o}1544$	9.45	+0.48		Broglia (1963)
	9.48	+0.47		Joshi, Srivastava (1967)
	9.43	+0.46	+0.03	van Genderen (1967)
	9.556	+0.387		Karetnikov, Medvedev (1978)
	9.44	+0.45	+0.03	Present paper (n=8)

tions. As the comparison star was close to the variable, no correction has been made for differential extinction. The accuracy of the individual observations can be taken as about 0.01 magn.

THE PERIODS

The correct period of light variation of SZ Lyn was determined independently by *Gefferth* and *Szeidl* (1962) and by *Notni* (1962). *Gefferth* and *Szeidl* analysed their own photoelectric observations and combined them with those of *Schneller* (1961). They gave the ephemeris:

$$J.D.max = 2437718.5568 + 0^d.120\ 534\ 87 \cdot E. \qquad \text{Eq.1.}$$

Notni used *Soloviev*'s (1955) photographic, *Tsesevich*'s (1956a) visual and photographic, and *Schneller*'s (1961) photoelectric observations and he obtained:

$$J.D.max = 2437368.403 + 0^d.120\ 534\ 73 \cdot E. \qquad \text{Eq.2.}$$

First, *He Tian-jian* and *Xiong Da-run* (1967) concluded that the period was not constant. They computed an ephemeris with the quadratic term:

$$J.D.max = 2437780.0311 + 0^d.120\ 533\ 37 \cdot E - 5^d.728 \times 10^{-10} \cdot E^2. \qquad \text{Eq.3.}$$

Soon after this, a thorough investigation of the period of SZ Lyn was carried out by *van Genderen* (1967). From the photoelectrically observed times of maximum light available to him at that time, *van Genderen* came to the conclusion that the observations can adequately be represented by a periodic term:

$$J.D.max = T_o + P_o \cdot E - A \cdot \cos 2\pi \left(\frac{T_{max} - T_o}{P_1} - \Phi \right) \qquad \text{Eq.4.}$$

where $T_o = 2438124.39849$, $A = 0.00569$ day,
$P_o = 0.120\ 534\ 93$ day, $\Phi = -0.019$,
$P_1 = 1129$ days.

Later on this ephemeris was improved by *Barnes* and *Moffett* (1975) and by *Garrido* et al. (1979). The parameters of ephemerides derived by different authors are given in Table 3.

Recent observations suggested that a redetermination of the parameters of the ephemeris be carried out thereby enabling the periods to be greatly improved. Such a redetermination can, of course, be based only on photoelectric observations. The available times of light maxima observed photoelectrically

are collected in Table 4. The long series of visual and photographic maxima published by *Soloviev* (1955), *Tsesevich* (1956a, b, 1966), *Berdnikov* (1972, 1975, 1977), *Braune* et al. (1972, 1973, 1977, 1981) and *Busch* (1975, 1976) are not used here.

A small systematic phase lag between the blue and yellow light maxima have been found by some of the authors. For example, from the observations of *Karetnikov* and *Medvedev* (1977, 1978) a phase difference

$$\Delta T = T(\text{max. in B}) - T(\text{max. in V}) = -0.0006 \pm 0.0004$$

can be deduced. Since most of the authors determined the times of maximum brightness in B bandpass, we used the blue maxima (if available) as the zero phase in our period analysis. Some observers assumed that for every colour the maximum occurred at the same time and they published the average values of the time of blue and yellow light maxima. This discrepancy, however, does not give rise to serious problems in the period analysis. Usually the estimated accuracy of the determination of the time of the best observed maximum light is about 0.0007 day ≈ 1 minute. If we compare this value with

$$T(\text{max. in B}) - \frac{T(\text{max. in B}) + T(\text{max. in V})}{2} \approx -0^{d}.0003$$

it turns out immediately that the average values of times of maximum light in blue and yellow can also be used without any restriction in the period analysis.

It is clear that the O-C values for SZ Lyn produced by a linear ephemeris follow a sine-curve relation. Since previous investigations of the period changes of dwarf cepheids showed that the period of a star might be increasing or decreasing continuously, we tried to fit the epochs of maximum of SZ Lyn to the following relation:

$$J.D.max = T_o + P_o \cdot E + \frac{\beta}{2} \cdot E^2 - A \cdot \cos 2\pi \left(\frac{P_o}{P_1} \cdot E - \psi_o\right) \qquad \text{Eq.5.}$$

where T_o is the initial epoch of maximum corresponding to E=0; P_o is the pulsation period of SZ Lyn; P_1 is the period of the sinusoid; β is the secular change of the pulsation period during one cycle; A is the semiamplitude of the sine-curve; and ψ_o is the phase shift. Values for the six parameters were determined by the method of least squares giving the same weight to all observations:

T_o = 2438124.39801 ±.00012 | A = 0.00540 day, ±.00011

P_o = 0.120 534 934 day, ±18 | β = +0.010 x 10^{-10} day·cycle^{-1} ±.007

P_1 = 1170 days, ±3 | ψ = -0.015 ±.005.

For comparison with others' results these values are also given in Table 3. The observations used here cover almost $6P_1$ whereas the baseline of coverage was only $1.6P_1$ in *van Genderen*'s (1967), $3.8P_1$ in *Barnes* and *Moffett*'s (1975), and $5.0P_1$ in *Garrido* et al.'s (1979) discussions.

Four maxima have been excluded from the fit to Eq.5. Three (E=2919, 2977 and 18459) were already reported by *Joshi* and *Srivastava* (1967) and by *Wisse* and *Wisse* (1969) to deviate significantly from the non-linear ephemeris. The epoch (E=21073) published by *Popovici* (1971) deviates from our non-linear ephemeris by at least three times the acceptable timing uncertainties of photoelectric maxima ($\sim 0^d.0015$ = 2 minutes).

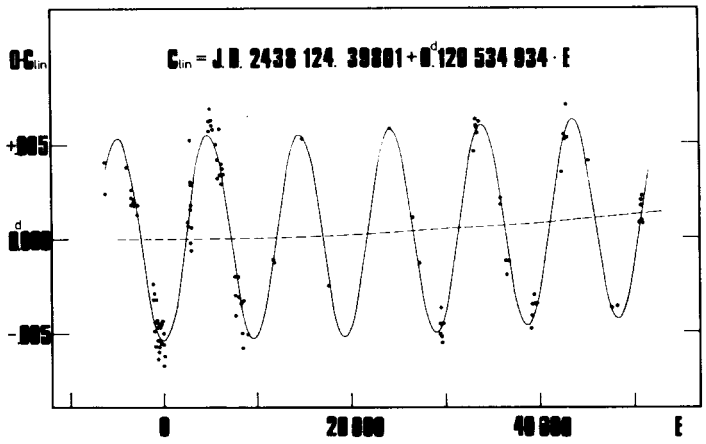

Figure 1: O-C_{lin} versus E. The solid line indicates the goodness of fit for the non-linear ephemeris Eq. 5. The dashed line shows the secular variation in the pulsation period.

In columns 4 and 5 of Table 4 the O-C_{lin} residuals from the linear portion of Eq.5, and the O-C residuals determined from Eq.5 are given. The phases of the sinusoid ψ are also given in Table 4 in column 6. Fig. 1 indicates the goodness of fit for the non-linear ephemeris. It shows the residuals from the linear part in Eq.5 versus epoch number E and the non-linear fit is drawn in.

Table 3

Parameters of ephemerides

T_o	P_o	P_1	A	φ	$10^{10} x\beta$	No. max	Reference
2433 946.493*	0.212 032 5	-	-	-	-	7*	Tsesevich (1956a)
33 946.523*	0.274 084 2	-	-	-	-	18*	Tsesevich (1956b)
37 718.5568	0.120 534 87	-	-	-	-	7	Gefferth, Szeidl (1962)
37 368.403	0.120 534 73	-	-	-	-	13	Notni (1962)
37 367.44321 ±.00087	0.120 533 34 ±.000 000 19	-	-	-	-	11	van Genderen (1963)
37 367.44186 26	0.120 533 486 52	-	-	-	-	11	Broglia (1963)
37 780.0311	0.120 533 37	-	-	-	-11.556	11	He Tian-jian, Xiong Da-run (1964)
38 124.39714 66	0.120 534 87 10	-	-	-	-	60	van Genderen (1967)
38 124.39849 21	0.120 534 93 05	1129 ±18	0.00569 ±.00018	-0.019 ±.011	-	48	van Genderen (1967)
39 121.7003	0.120 531 88	-	-	-	-	24	Binnendijk (1968)
38 124.39770 56	0.120 534 81 04	-	-	-	-	94	Barnes, Moffett (1975)
38 124.39828 17	0.120 534 906 20	1146 10	0.00572 19	-0.010 08	-	66	Barnes, Moffett (1975)
38 124.39824 17	0.120 534 920 13	1150 10	0.00573 20	-0.007 08	-	70	Garrido et al. (1979)
38 124.39801 12	0.120 534 934 18	1170 3	0.00540 11	-0.015 05	+0.010 ±. 07	116	Present study

*Minimum times and No. of minima are given

Table 4

Photoelectrically observed maxima

Epoch of maximum ($JD_\odot$)	Rem.	E	($O-C_{lin}$)	(O-C)	ϕ	B_{max}
2437367.441	Sc	- 6280	+0.0024	-0.0013	0.368	
368.407	Sc	- 6272	.0041	+0.0004	.369	
642.021	Eg	- 4002	.0038	-0.0005	.603	
706.2645	Pp	- 3469	.0022	-0.0008	.658	9.320
707.4695	Pp	- 3459	.0018	-0.0011	.659	9.334
.5908	Pp	- 3458	.0026	-0.0004	.659	9.312
718.5587	Pp	- 3367	.0018	-0.0009	.668	9.328
726.5141	Pp	- 3301	.0019	-0.0006	.675	9.341
744.3535	Pp	- 3153	.0021	+0.0002	.690	9.345
780.031	HX	- 2857	.0013	+0.0003	.721	
.152	HX	- 2856	+0.0018	+0.0008	.721	
977.343	HX	- 1220	-0.0024	+0.0018	.889	
997.351	HX	- 1054	.0032	+0.0013	.906	
38001.568	vG	- 1019	.0049	-0.0004	.910	
.689	vG	- 1018	.0044	+0.0001	.910	
003.378	HX	- 1004	.0029	+0.0017	.912	
021.576	vG	- 853	.0057	-0.0009	.927	
.699	vG	- 852	.0032	+0.0016	.927	
032.305	HX	- 764	.0043	+0.0007	.936	
052.4333	Pp	- 597	.0054	-0.0002	.953	9.340
.5545	Pp	- 596	.0047	+0.0005	.954	9.340
053.276	HX	- 590	.0064	-0.0012	.954	
055.205	HX	- 574	.0060	-0.0008	.956	
.3268	Br	- 573	.0047	+0.0005	.956	9.338
.4463	Br	- 572	.0057	-0.0005	.956	9.331
.5681	Br	- 571	.0045	+0.0007	.956	9.332
057.3752	Br	- 556	.0054	-0.0002	.958	9.335
.4964	Br	- 555	.0047	+0.0005	.958	9.349
.6172	Br	- 554	.0045	+0.0008	.958	9.329
082.4464	Pp	- 348	.0055	-0.0001	.979	
114.3880	Br	- 83	.0056	-0.0002	.006	9.354
118.367	vG	- 50	.0043	+0.0011	.010	9.340
.485	vG	- 49	.0068	-0.0014	.010	9.345
124.393	vG	0	.0050	+0.0004	.015	
140.423	Br	+ 133	-0.0062	-0.0009	.029	9.346
439.3565	Pp	2613	+0.0007	-0.0004	.284	9.331
.4772	Pp	2614	.0009	-0.0003	.284	9.333
457.3173	Pp	2762	.0018	+0.0002	.300	9.330
.4376	Pp	2763	.0016	-0.0001	.300	9.355
460.210	JS	2786	+0.0017	-0.0001	.302	
463.342	JS	2812	-0.0002	-0.0021	.305	
464.189	JS	2819	+0.0030	+0.0012	.305	
465.276	JS	2828	.0052	+0.0033	.306	
466.238	JS	2836	.0029	+0.0010	.307	
467.200	JS	2844	+0.0006	-0.0013	.308	
471.297	JS	2878	-0.0006	-0.0026	.311	
(476.249	JS	2919	+0.0095	+0.0074	.316)	
(483.241	JS	2977	.0105	+0.0081	.322)	
701.8866	Bi	4791	.0057	+0.0003	.509	
708.6377	vG	4847	.0069	+0.0015	.514	9.354
709.6014	vG	+ 4855	+0.0063	+0.0009	0.515	9.351

Table 4 (cont.)

Epoch of maximum ($JD_\odot$)	Rem.	E	$(O-C_{lin})$	(O-C)	ϕ	B_{max}
2438712.6148	vG	+ 4880	+0.0063	+0.0009	0.518	9.341
725.5117	vG	4987	.0060	+0.0007	.529	
752.5114	vG	5211	.0058	+0.0007	.552	9.354
788.5505	vG	5510	.0050	+0.0003	.583	9.359
809.4022	vG	5683	.0042	-0.0002	.600	9.339
830.4949	vG	5858	.0032	-0.0007	.618	9.340
834.234	JS	5889	.0058	+0.0018	.622	
844.4771	vG	5974	.0034	-0.0003	.630	9.354
849.5396	vG	6016	.0034	-0.0002	.635	9.344
850.3839	vG	6023	.0040	+0.0004	.635	9.338
.5034	vG	6024	.0029	-0.0006	.636	9.355
871.3567	vG	6197	+0.0037	+0.0006	.653	9.345
39052.5129	vG	7700	-0.0041	-0.0022	.808	9.336
.6355	vG	7701	.0020	-0.0001	.808	9.341
054.5631	vG	7717	.0030	-0.0010	.810	9.335
.6846	vG	7718	.0020	-0.0001	.810	9.340
092.7726	Bi	8034	.0031	-0.0001	.843	
121.7007	Bi	8274	.0034	+0.0003	.867	
130.4981	vG	8347	.0050	-0.0012	.875	9.316
145.4461	vG	8471	.0033	+0.0007	.888	9.334
.5642	vG	8472	.0058	-0.0017	.888	9.345
205.4706	vG	8969	.0052	-0.0003	.939	9.342
527.5441	Pp	11641	.0011	+0.0001	.214	9.337
528.6288	Pp	11650	.0012	-0.0001	.215	9.350
531.401	JS	11673	-0.0013	-0.0003	.218	
905.3070	Pp	14775	+0.0053	0.0000	.537	9.322
40243.3996	Pp	17580	-0.0025	-0.0002	.826	9.329
(349.3521	WW	18459	.0003	+0.0043	.917	9.386)
(664.4239	Po	21073	-0.0068	-0.0049	.186)	
41035.443	Pp	24151	+0.0058	+0.0001	.503	
312.4276	Pp	26449	+0.0011	+0.0004	.740	9.341
390.4113	Pp	27096	-0.0013	+0.0002	.806	9.352
678.8475	BM	29489	.0052	-0.0005	.053	
679.5714	Pp	29495	.0045	+0.0002	.054	9.315
.6913	Pp	29496	.0051	-0.0005	.054	9.320
683.7909	BM	29530	.0037	+0.0009	.057	9.292
.9096	BM	29531	.0055	-0.0009	.057	9.312
684.0312	BM	29532	-0.0045	+0.0001	.057	9.278
42106.3947	Pp	33036	+0.0046	-0.0007	.418	9.340
129.5391	KM	33228	.0063	+0.0008	.438	
136.2887	KM	33284	.0059	+0.0003	.444	
.4091	KM	33285	.0058	+0.0002	.444	
.5294	KM	33286	.0056	0.0000	.444	
162.4450	KM	33501	.0062	+0.0003	.466	
451.4834	Pp	35899	.0018	-0.0001	.713	9.340
454.4971	Pp	35924	+0.0021	+0.0003	.716	9.341
531.7560	Af	36565	-0.0019	-0.0015	.782	
532.7210	Af	36573	.0012	-0.0007	.783	
533.6852	Af	36581	.0012	-0.0008	.784	
837.3091	Du	39100	.0048	-0.0004	.043	9.280
841.2875	Du	39133	.0041	+0.0003	.047	9.270
871.4218	KM	39383	.0035	+0.0006	.072	
872.3861	KM	+39391	-0.0035	+0.0006	0.073	

Table 4 (cont.)

Epoch of maximum ($JD_\odot$)	Rem	E	($O-C_{lin}$)	(O-C)	ψ	B_{max}
2442874.3152	KM	+39407	-0.0030	+0.0011	0.075	
.4352	KM	39408	-0.0035	+0.0005	.075	
43232.4309	HW	42378	+0.0035	-0.0014	.381	
257.3835	GE	42585	.0053	0.0000	.402	
258.4685	GE	42594	.0055	+0.0002	.403	
287.3985	GE	42834	.0071	+0.0014	.428	
288.3600	GE	42842	.0043	-0.0014	.429	
578.3668	Pp	45248	+0.0041	+0.0007	.677	9.339
879.5758	Pp	47747	-0.0037	+0.0001	.934	9.341
931.4059	Pp	48177	-0.0036	+0.0006	.978	9.340
44222.3817	Ga	50591	+0.0008	+0.0003	.227	9.330
257.4574	Ga	50882	.0009	-0.0007	.257	9.316
261.3156	Ga	50914	.0020	+0.0003	.260	9.325
.4359	Ga	50915	.0017	+0.0001	.260	9.312
262.2787	Ga	50922	.0008	-0.0009	.261	9.315
269.2711	Ga	+50980	+0.0022	+0.0003	0.267	9.323

Remarks to Table 4: Sc = Schneller (1961); Eg = Eggen (1962); HX = He Tian-jian and Xiong Da-run (1964); vG = van Genderen (1963, 1967); Br = Broglia (1963); JS = Joshi and Srivastava (1967); Bi = Binnendijk (1968); WW = Wisse and Wisse (1969); Po = Popovici (1971); BM = Barnes and Moffett (1975); KM = Karetnikov and Medvedev (1977, 1978); Af = Africano (1978); Du = Duerbeck (1976); HW = Hopp and Witzigmann (1979); GE = Garrido et al. (1979); Ga = Garbusov (1980); Pp = Present paper

LIGHT AND COLOUR CURVES

Composite light curves in V are shown in Fig. 2 for different years. As can be seen in the figure the light curves are regular and typical of the class of variables to which SZ Lyn belongs. The small deviations in the light curves are caused by small cycle-to-cycle variations which do not exceed 0.04 in magnitude at maximum light in any bandpass. A part of the scatter on the light curves may be attributed to instrumental and extinction effects or observational errors.

Since some of the dwarf cepheids (e.g. RV Ari, VZ Cnc) show the beat phenomenon it is an obvious assumption that the cycle-to-cycle change can be explained by this phenomenon. A search for this effect in SZ Lyn was made but without success.

Changes in the height of maximum light with period P_1 have been claimed by some observers and denied by others. *Barnes* and *Moffett* (1975) found no significant variation in maximum with period P_1. On the other hand, *Garbusov* (1980) reported periodic brightness changes in maximum light. To see if this variation is real or not we also gave the blue (B) magnitude of our maxima in

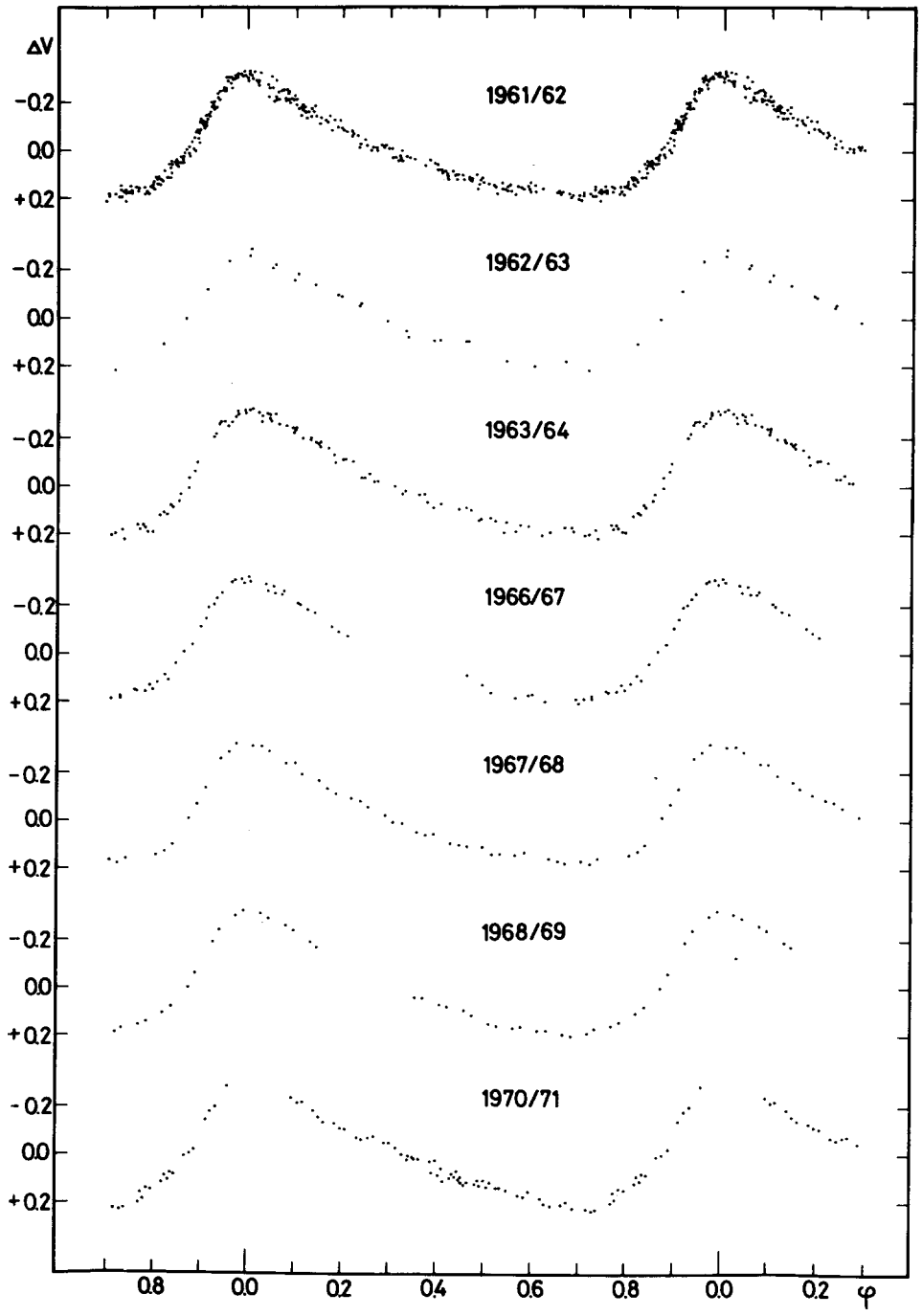
ΔV
-0.2
0.0
+0.2
1961/62
1962/63
1963/64
1966/67
1967/68
1968/69
1970/71
0.8
0.0
0.2
0.4
0.6
0.8
0.0
0.2
φ

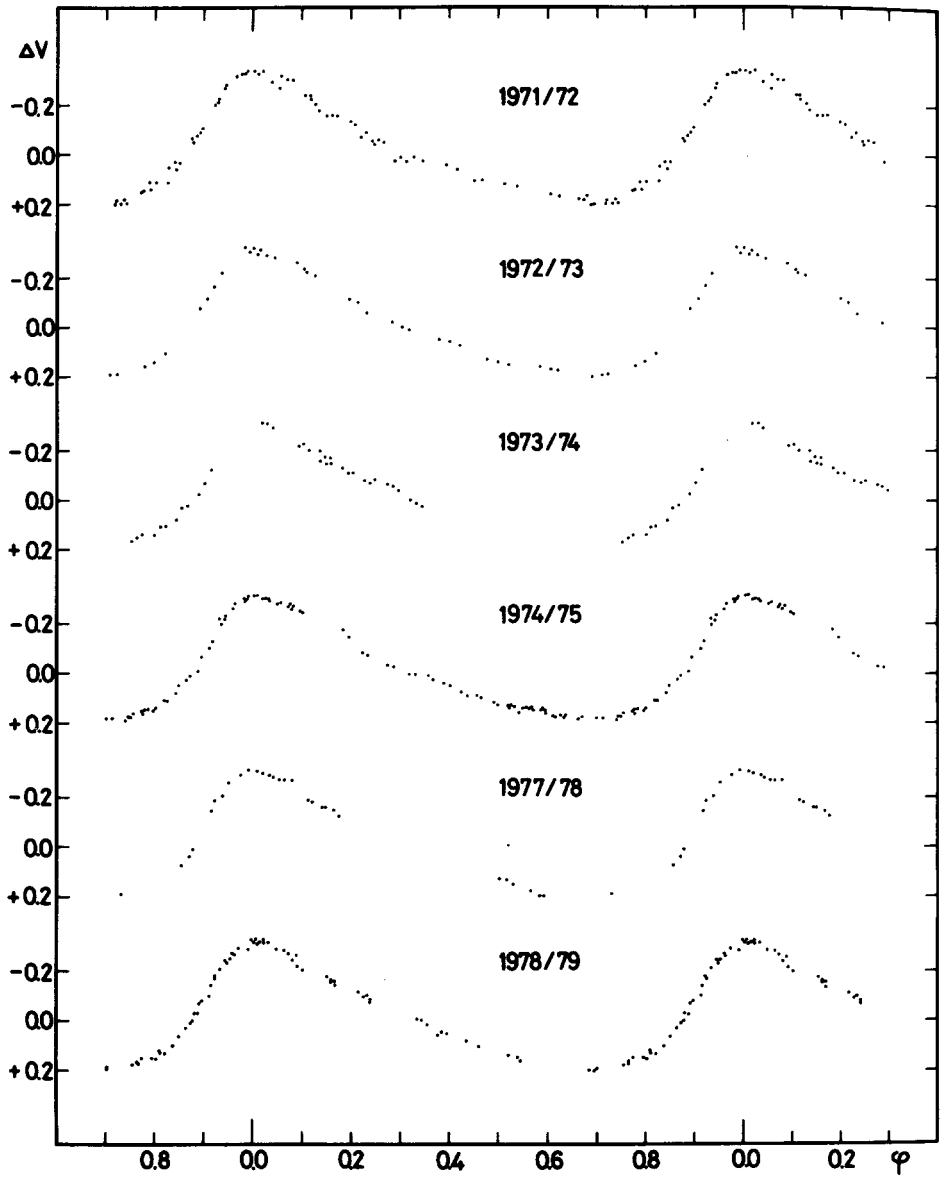

Figure 2: Composite light curves in V for different observational seasons

Table 4 and presented the B magnitude at maximum light versus phase in the P_1 = 1170-day cycle (Fig. 3). We found no evidence for periodic variation of brightness maximum. It is interesting to note that the B maxima of *Barnes* and *Moffett* and of *Duerbeck* lie above the average value.

The O-C values are also plotted against phase ψ in Fig. 3. No clear trend

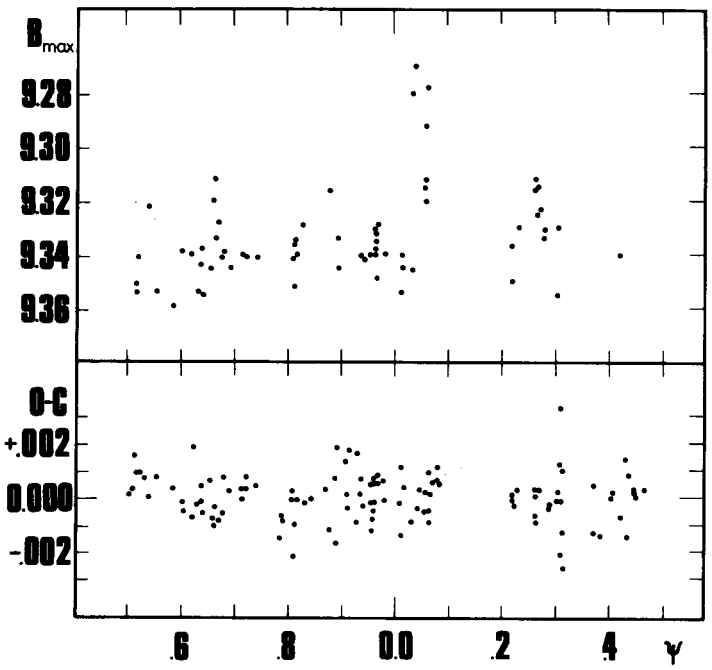

Figure 3: Maximum brightness in B light and variation in time of maximum versus phase of the 1170-day period.

seems to be present that would indicate a departure from the sinusoidal variation.

In order to investigate the light and colour curves, normal points were computed. First the individual observations were collected in phase using the ephemeris given by Eq. 5 and then they were averaged together into phase bins $0.02P_o$ wide. These values were then inter/extrapolated to the phases: φ = 0.01, 0.03,....,0.99. The normal points are given in Table 5. The most important characteristics of the light and colour curves were derived by using the normal points, and they are summarized in Table 6. The two-colour diagram for SZ Lyn during the mean cycle is shown in Fig. 4. The unusual feature in the colour loop during the phase interval 0.32-0.44 found by *Barnes* and *Moffett*

Table 5

Normal points of V, B-V and U-B observations

φ	V	B-V	U-B	φ	V	B-V	U-B
.01	9.129	+0.211	+0.147	.51	9.575	+0.361	+0.124
.03	9.146	.210	.150	.53	9.586	.355	.130
.05	9.166	.214	.147	.55	9.596	.355	.127
.07	9.183	.226	.141	.57	9.602	.365	.122
.09	9.206	.234	.144	.59	9.605	.374	.124
.11	9.235	.240	.146	.61	9.612	.374	.128
.13	9.259	.251	.136	.63	9.618	.372	.133
.15	9.281	.261	.133	.65	9.622	.375	.130
.17	9.302	.270	.138	.67	9.627	.376	.119
.19	9.322	.282	.136	.69	9.632	.371	.110
.21	9.345	.288	.130	.71	9.632	.368	.112
.23	9.368	.290	.124	.73	9.626	.369	.116
.25	9.388	.297	.124	.75	9.615	.372	.114
.27	9.407	.304	.130	.77	9.603	.370	.112
.29	9.426	.313	.128	.79	9.590	.362	.104
.31	9.445	.321	.120	.81	9.566	.353	.093
.33	9.458	.329	.117	.83	9.534	.340	.092
.35	9.468	.341	.114	.85	9.495	.323	.101
.37	9.482	.344	.115	.87	9.447	.306	.107
.39	9.499	.341	.123	.89	9.388	.285	.107
.41	9.516	.343	.123	.91	9.318	.267	.112
.43	9.531	.347	.119	.93	9.247	.253	.123
.45	9.541	.355	.116	.95	9.190	.236	.132
.47	9.550	.362	.113	.97	9.153	.221	.137
.49	9.563	+.363	+.116	.99	9.127	+.212	+.141

Table 6

Most important characteristics of the light and colour curves

$\langle V \rangle = 9.424$	$\langle B \rangle - \langle V \rangle = +0.303$	$\langle B-V \rangle = +0.312$
$\langle B \rangle = 9.727$	$\langle U \rangle - \langle B \rangle = +0.125$	$\langle U-B \rangle = +0.124$
$\langle U \rangle = 9.852$		
$V_{max} = 9.125$	$V_{min} = 9.633$ ($\varphi = .703$)	$A_V = 0.508$
$B_{max} = 9.336$	$B_{min} = 10.004$ ($\varphi = .684$)	$A_B = 0.668$
$U_{max} = 9.480$	$U_{min} = 10.127$ ($\varphi = .650$)	$A_U = 0.647$

(1975) is not seen in our diagram. The probable explanation for this is that our normal points are formed from the observations of different years and of different accuracy, and the fine details are smoothed out.

Although there is a slight difference between the forms of our two-colour diagram and that of *Barnes* and *Moffett* (1975), their results can be confirmed. An interstellar reddening of E(B-V) = 0.04 magn seems to be reasonable from our diagram.

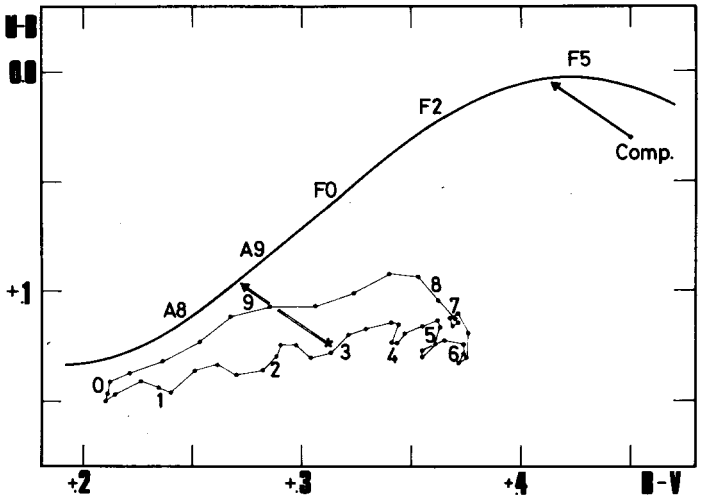

Figure 4: (U-B)-(B-V) diagram for SZ Lyn during the mean cycle. Phases are shown as numbers on the loop, with zero phase being that of maximum light. The mean position of SZ Lyn is also marked by an asterisk within the loop. The arrows point to the dereddened positions of SZ Lyn and its main comparison star in the two-colour diagram relative to the Hyades main sequence.

RADIAL VELOCITY MEASUREMENTS

Woolley and *Aly* (1966) were the first to measure the radial velocity of SZ Lyn. From 17 spectra they obtained a mean velocity of $+31.9 \pm 2.3$ km·s^{-1} and calculated a radial velocity amplitude of 23.7 ± 8.8 km·s^{-1}.

Later on *McNamara* and *Feltz* (1976) obtained spectrograms of SZ Lyn with the 100 inch telescope at Mount Wilson Observatory with a dispersion of 40 Amm^{-1}. From these measurements a mean velocity of $+22$ km·s^{-1} and a radial velocity amplitude of 44 km·s^{-1} were derived. The difference in the mean radial velocity values could be explained by the binary nature of SZ Lyn. *McNamara* and *Feltz* secured, however, a single-trail spectrogram of SZ Lyn as well, and obtained an average velocity 24.4 ± 2 km·s^{-1}. The binary phase of these observations was about the same as that of *Woolley* and *Aly*'s observations. Thus *McNamara* and *Feltz*'s results seem to be in contradiction with the binary hypothesis.

Bardin and *Imbert* (1981) observed SZ Lyn with the CORAVEL photoelectric spectrometer on two nights in 1979 and in 1980. They obtained very accurate and high time resolution radial velocity curves. Their results confirmed the

binary nature of SZ Lyn. They obtained for the average velocities 41.11 ± 0.14 $km \cdot s^{-1}$ on J.D. 2444206 and 43.36 ± 0.12 $km \cdot s^{-1}$ on J.D. 2444324. No significant amplitude variation was detected from cycle to cycle. The total variation of the radial velocity was 39.9 $km \cdot s^{-1}$. Using the available mean radial velocities an orbital eccentricity of e = 0.26 was computed which is fairly large. Here we should recall the fact that the O-C diagram of light maxima suggests nearly zero eccentricity.

As a contribution to settling this problem it seems to be worth publishing our radial velocity measurements. In 1971 twelve spectrograms (at a reciprocal dispersion of 60 Amm^{-1}) were secured with the Cassegrain spectrograph of the 72 inch telescope of the Dominion Astrophysical Observatory on baked IIa-O plates on three nights. The plates were measured on the DAO Arcturus measuring machine. Spectrograms of a number of standard velocity stars were also secured on the three nights and measured to check on possible systematic errors, but none were found. In Table 7 we list the plate number, the date and Julian Day of each spectrogram, the number of lines measured the radial velocity and the phase computed with Eq.5.

In Fig. 5 our individual radial velocity measurements are plotted against the phase of the pulsation period, and a free-hand velocity curve has been drawn through the observations. A mean velocity of about 32.8 $km \cdot s^{-1}$ was found from our velocity data (with an estimated error of 2.5 $km \cdot s^{-1}$). Relying only on our own data the maximum and minimum velocities of the SZ Lyn velocity curve have been fixed at about 53 $km \cdot s^{-1}$ and 14 $km \cdot s^{-1}$, respectively, which yield a velocity amplitude of 39 $km \cdot s^{-1}$.

Table 7

Radial velocities of SZ Lyn

Plate No.	Date	Heliocentric J.D. 24..	No. of lines	R.V. kms^{-1}	Phase
70887	1971.02.17	40999.8405	14	46.4 ± 4.2	0.6308
888		.8731	13	24.4 ± 4.9	.9012
889		.9037	4	19.1 ± 4.7	.1551
71017	1971.03.31	41041.7409	17	26.9 ± 2.0	.2505
018		.7638	15	36.9 ± 2.9	.4405
019		.7877	14	47.0 ± 4.1	.6388
020		.8162	13	32.3 ± 4.3	.8753
021		.8398	16	16.9 ± 3.2	.0710
063	1971.04.14	41055.7351	13	30.8 ± 3.0	.3516
064		.7695	4	50.9 ± 3.9	.6370
065		.8032	16	24.0 ± 3.5	.9166
066		.8348	15	20.4 ± 3.4	.1787

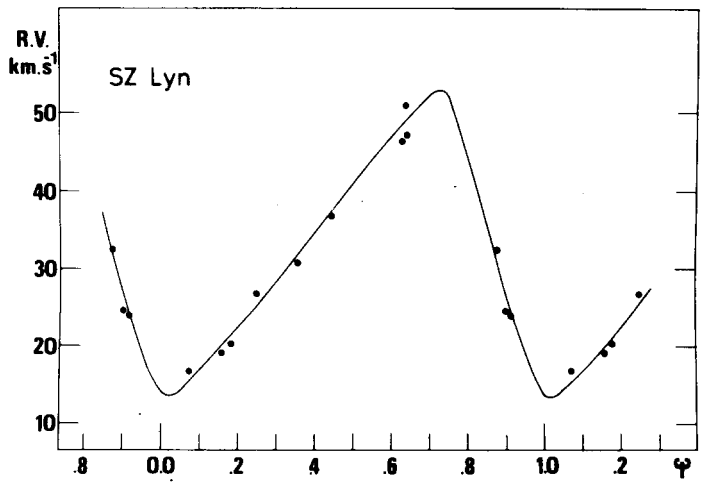

Figure 5: Radial velocity curve of SZ Lyn. A free-hand curve has been drawn through the observations.

BINARY MODEL

The 3.20-year periodicity in the time of maximum light found by *van Genderen* (1967) has been interpreted by *Barnes* and *Moffett* (1975) as a modulation of the phase of maximum light by binary motion. Since the O-C values can be fitted well with Eq.5 we have good reason to assume that the orbit of SZ Lyn in the binary system is nearly circular ($e \simeq 0$).

For a circular orbit of radius a and inclination i the variation in time of maximum light of a variable star attributed to the light travel time across the orbit in a binary system is given by

$$\Delta T_{max} = \frac{a \cdot \sin i}{c} \cos 2\pi \left(\frac{P_o}{P_1} \cdot E - \psi_o\right) \qquad \text{Eq.6.}$$

where P_o is the pulsation period, P_1 is the orbital period, c is the light velocity and ψ_o is the orbital phase at E = 0. Equation 6 is the last term in Eq.5:

$$a_{SZ} \sin i = cA = 0.93 \text{ AU},$$

$$K_{SZ} = cA \frac{2\pi}{P_1} = 8.69 \text{ km} \cdot \text{s}^{-1}$$

and the radial velocity variation is given by

$$\text{mean R.V.} = \gamma + K \cdot \sin 2\pi \left(\frac{P_o}{P_1} \cdot E - \psi_o\right) \qquad \text{Eq.7.}$$

where γ is the system velocity, relative to the Sun.

Equation 7 can be compared with the observations. In Table 8 the mean velocities of SZ Lyn taken from *Woolley* and *Aly* (1966), *McNamara* and *Feltz* and *Bardin* and *Imbert* (1981) are collected. Our measurement is also given. In Fig. 6 these data are plotted against orbital phase $\psi = (P_o/P_1)E - \psi_o$. If Eq.7 is fitted to the very accurate measurements of *Bardin* and *Imbert*, we obtain:

$\gamma = 34.00 \text{ km} \cdot \text{s}^{-1}$.

Figure 6 suggests that the orbit may be non-circular. Further precise radial velocity data are required to construct a reliable radial velocity curve

Table 8

Mean radial velocities of SZ Lyn

J.D. 24...	Mean velocity	Orbital phase (ψ)	Observers
38717	31.9	0.52	Woolley and Aly (1966)
41025	24.4 ± 2	2.49	McNamara and Feltz (1976)
41041	32.8 ± 2.5	2.51	Present paper
42474	22 ± 2	3.73	McNamara and Feltz (1976)
44206	41.11 ± 0.14	5.21	Bardin and Imbert (1981)
44324	43.36 ± 0.12	5.31	Bardin and Imbert (1981)

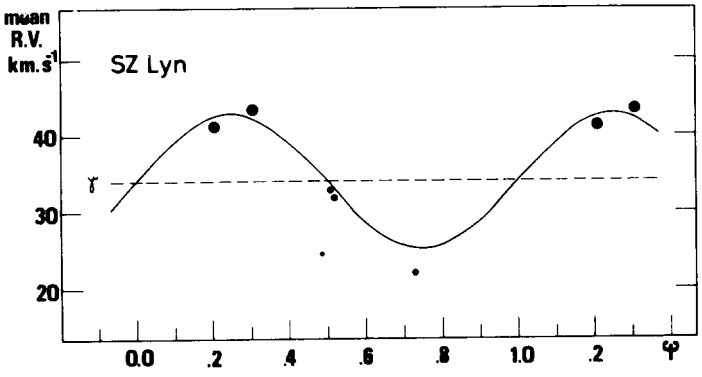

Figure 6: Mean radial velocities versus binary phase ψ. The solid line has been calculated from the variation in time of maximum light assuming a circular orbit (e=0). The curve was fitted to the observations of Bardin and Imbert (1981).

and to achieve the precision required for determining the eccentricity e of the binary orbit.

Since we failed to see any doubled lines in the spectra of SZ Lyn we have to assume that the variable is a single-lined spectroscopic binary. The mass function can easily be determined from the above derived data:

$$f(M_2) = \frac{M_2^3 \sin^3 i}{(M_{SZ}+M_2)^2} = 1.038 \times 10^{-7}(1-e^2)^{1.5} K^3 \cdot P_1$$

If we adopt e = 0

$$f(M_2) = 0.080\ M_\odot$$

where M_{SZ} is the mass of the pulsating component (dwarf cepheid SZ Lyn) of the system, and M_2 is the mass of the unseen companion.

The magnitude difference between SZ Lyn and the unseen companion should be, at least, 1.5 magn. Assuming that the unseen companion is a main sequence star, then the mass ratio of the components is

$$\frac{M_{SZ}}{M_2} \geq 1.43,$$

if the mass-luminosity function of *McCluskey* and *Kondo* (1972) is valid for both components. This result compared with the mass function of the binary system yields:

$$1 \geq \sin^3 i \geq \frac{0.47\ M_\odot}{M_2}\ .$$

Thus we obtain

$$0.70\ M_{SZ} \geq M_2 \geq 0.47\ M_\odot\ .$$

The unreddened mean colour index of SZ Lyn is $(B-V)_o = 0.27$. Hence, if it is on or near the main sequence, $M_V \simeq +2^m.6$, and $M_{SZ} \simeq 1.7\ M_\odot$, then $i \geq 50^\circ$.

It may also be natural to assume that the unseen companion is a white dwarf. Whatever the assumption the binary model describes and explains well the observed features: the variation in time of light maxima and mean radial velocities.

SUMMARY

Three-colour photoelectric observations obtained at Konkoly Observatory on 28 nights from 7 February 1962 through 27 February 1979 were used to define the photometric behaviour of SZ Lyn. Its light curves are typical of the class of variable to which SZ Lyn belongs, nevertheless small cycle-to-cycle variations are present in each bandpass. These variations, however, do not exceed 0.04 in magnitude at maximum light, and they are even smaller at minimum light. The search for both short and long periodic modulation in amplitude or in maximum brightness failed.

An interstellar reddening of E(B-V) = 0.04 magn has been deduced from our two-colour diagram. This value is slightly smaller than that given by *Barnes* and *Moffett* (1975).

All available light maxima observed photoelectrically were used to investigate the variation in the pulsation period. The long periodic variation in time of maximum light has been confirmed. The variation approximated by a sine-curve has a period of 1170 ± 3 days and a semiamplitude of 467 ± 10 sec. A secular change of $\beta = 10^{-12}$ day·cycle^{-1} in the pulsation period has been also found.

New radial velocity data of SZ Lyn obtained at Dominion Astrophysical Observatory with the Cassegrain spectrograph of the 72 inch telescope in 1971 have been given which provide a mean radial velocity of 32.8 km·s^{-1} at J.D. 2441041. All available radial velocity observations are discussed. It has been shown that both the photometric observations and the radial velocity measurements are compatible with the hypothesis proposed by *Barnes* and *Moffett* (1975) that SZ Lyn is a component of a binary system.

Acknowledgements

The author is grateful to his colleagues, Dr. Katalin Barlai, Dr. Katalin Oláh, Mr. L. Büki, Mr. K. Gefferth and Mr. L. Vargha for their help in the observations and reductions.

Budapest-Szabadsághegy, July 18, 1983

REFERENCES

Africano, J., 1978, Inf. Bull. Var. Stars No. 1408
Alania, I.F., 1972, Inf. Bull. Var. Stars No. 702
1974, Abastumani Bull. No. 45
Bardin, C. and Imbert, M., 1981, Astron. Astrophys. 98. 198
Barnes III, Th.G. and Moffett, Th.J., 1974, Bull. Am. Astr. Soc. 6. 466
1975, Astron. J. 80. 48
Berdnikov, L.N., 1972, Per. Zvezdy Suppl. 1. 387
1975, ibid. 2. 199
1977, ibid. 3. 329
Binnendijk, L., 1968, Astron. J. 73. 29
Braune, W., Hübscher, J. and Mundry, E., 1972, Astron. Nachr. 294. 123
1977, ibid. 298. 121
1981, ibid. 302. 53
Braune, W. and Mundry, E., 1973, Astron. Nachr. 294. 225
Broglia, P., 1963, Mem. Soc. astr. It. 34. 431
Busch, H., 1975, Mitteilungen Veränd. Sterne 7. 33
1976, ibid. 7. 150
Duerbeck, H.W., 1976, Inf. Bull. Var. Stars No. 1171
Eggen, O.J., 1962, Publ. Astron. Soc. Pacific 74. 159
Garbusov, G.A., 1980, Inf. Bull. Var. Stars No. 1854
Garrido, R., Alfaro, E.J., Quintana, J.M. and Saez, M., 1979, Astron. Astrophys. Suppl. 36. 51
Gefferth, K. and Szeidl, B., 1962, Inf. Bull. Var. Stars No. 7.1
He Tian-jian and Xiong Da-run, 1964, Acta Astr. Sinica 12. 57
Hoffmeister, C., 1949a, Erg.-H zu den Astron. Nachr. 12. Nr. 1.21
1949b, Mitteilungen Veränd. Sterne Nr. 314
Hopp, U. and Witzigmann, S., 1979, Inf. Bull. Var. Stars No. 1597
Iriarte, B., Johnson, H.L., Mitchell, R.I. and Wisniewski, W.K., 1965, Sky and Telescope 30. 21
Johnson H.L. and Morgan, W.W., 1953, Astrophys. J. 117. 313
Joshi, S.C. and Srivastava, H.N., 1967, Zeitschrift f. Astrophys. 67. 456
Karetnikov, V.G. and Medvedev, Yu.A., 1977, Inf. Bull. Var. Stars No. 1309
1978, Per. Zvezdy 21. 85
McCluskey, G.E. and Kondo, Y., 1972, Astrophys. Sp. Sci. 17. 134
McNamara, D.H. and Feltz, Jr., K.A., 1976, Publ. Astron. Soc. Pacific 88. 164
Notni, P., 1962, Inf. Bull. Var. Stars No. 7.2
Popovici, C., 1971, Inf. Bull. Var. Stars No. 508
Schneller, H., 1961, Astron. Nachr. 286. 102
Soloviev, A.V., 1955, Astr. Tsirk. No. 159.18
Tsesevich, V.P., 1956a, Astr. Tsirk. No. 170.16
1956b, ibid. No. 175.16
1966, RR Lyrae-Type Variable Stars (in Russian), Naukova Dumka, Kiev, p. 416
van Genderen, A.M., 1963, Bull. Astron. Inst. Neth. 17. 243
1967, ibid. 19. 74
Willis, R.B., 1972, Observatory 92. 14
Wisse, M. and Wisse, P.N.J., 1969, Bull. Astron. Inst. Neth. 20. 333
Woolley, R. and Aly, K., 1966, Roy. Obs. Bull. No. 114

Table 9a

Photoelectric yellow observations of SZ Lyn

J.D.	ΔV	J.D.	ΔV	J.D.	ΔV	J.D.	ΔV
2437703		2437706		2437707		2437707	
.4014	-0.047	.2572	-0.244	.4206	+0.171	.5308	+0.143
.4034	.015	.2583	.258	.4220	.169	.5356	.166
.4055	-0.020	.2593	.291	.4282	.170	.5377	.183
.4097	+0.043	.2604	.295	.4331	.184	.5686	.129
.4118	.026	.2630	.312	.4345	.178	.5707	.108
.4166	.059	.2651	.321	.4359	.178	.5743	+0.008
.4208	.095	.2670	.268	.4373	.163	.5755	-0.017
.4222	.118	.2695	.273	.4386	.166	.5768	.056
.4243	.119	.2707	.260	.4400	.164	.5782	.130
.4284	.116	.2717	.225	.4414	.151	.5796	.147
.4298	.163	.2741	.214	.4456	.128	.5810	.178
.4312	.135	.2753	.198	.4470	.108	.5824	.182
.4347	.180	.2764	.207	.4484	.083	.5852	.290
.4361	.136	.2791	.186	.4498	.056	.5866	.302
.4375	.148	.2815	.186	.4512	.046	.5880	.319
.4410	.153	.2843	.126	.4525	+0.024	.5893	.332
.4423	.151	.2857	.082	.4539	-0.007	.5907	.332
.4562	.208	.2871	.095	.4553	.046	.5921	.332
.4597	.193	.2885	.093	.4567	.083	.5935	.326
.4611	.209	.2913	.067	.4581	.119	.5963	.311
.4625	.175	.2927	.013	.4595	.132	.5991	.248
.4659	.153	.2944	.018	.4609	.191	.6005	.236
.4673	.148	.2989	-0.012	.4623	.238	.6018	.215
.4687	.110	.3003	+0.011	.4637	.254	.6032	-0.175
.4743	.051	.3031	.035	.4650	.310		
.4757	.033	.3121	.055	.4664	.301	2437717	
.4771	+0.012	.3135	.078	.4678	.319	.3047	+0.132
.4798	-0.076	.3149	.100	.4692	.311	.3061	.146
.4812	.106	.3163	.084	.4706	.310	.3082	.159
.4826	-0.160	.3177	.099	.4720	.253	.3116	.175
		.3211	.107	.4755	.258	.3130	.173
2437705		.3225	.097	.4775	.245	.3151	.195
.5297	-0.114	.3239	.112	.4789	.253	.3304	.111
.5311	.150	.3274	.151	.4803	.242	.3359	.070
.5517	.212	.3302	.161	.4817	.232	.3373	.028
.5524	.214	.3329	.146	.4831	.145	.3387	+0.024
.5534	.192	.3343	.162	.4866	.163	.3411	-0.048
.5543	.172	.3357	.160	.4907	.146	.3422	.123
.5564	.163	.3434	.171	.4921	.128	.3436	.139
.5573	.142	.3468	.188	.4935	.126	.3450	-0.181
.5615	.116	.3482	.204	.4949	.077		
.5656	.084	.3496	.178	.4963	.080	2437718	
.5677	.059	.3538	.175	.4977	.060	.4330	-0.305
.5698	-0.027	.3552	.165	.5027	.011	.4342	.300
		.3572	.156	.5048	.022	.4356	.303
2437706		.3607	.139	.5068	-0.007	.4384	.288
.2524	-0.091	.3628	.119	.5089	+0.002	.4412	.293
.2531	.091	.3642	+0.108	.5224	.100	.4456	.289
.2540	.119			.5245	.119	.4484	.254
.2549	.202	2437707		.5265	.118	.4525	.190
.2558	-0.201	.4157	+0.141	.5287	+0.119	.4546	-0.174

Table 9a (cont.)

Photoelectric yellow observations of SZ Lyn

J.D.	ΔV	J.D.	ΔV	J.D.	ΔV	J.D.	ΔV
2437718		2437726		2438082		2438439	
.4567	-0.112	.4950	+0.092	.4129	+0.216	.4639	-0.066
.4699	+0.002	.4964	.051	.4254	+0.104	.4701	.260
.4713	-0.003	.4978	+0.051	.4310	-0.002	.4722	.252
.4755	+0.032	.5006	-0.004	.4366	.120	.4764	.322
.4776	.043	.5020	.027	.4421	.243	.4785	.320
.4797	.030	.5034	.096	.4477	.261	.4826	.303
.4846	.043	.5055	.194	.4534	.213	.4847	.302
.4866	.057	.5068	.219	.4588	.159	.4889	.238
.4887	.084	.5082	.248	.4643	.143	.4958	.178
.4929	.100	.5103	.260	.4699	.094	.4979	.155
.4950	.117	.5221	.212	.4754	.053	.5021	.108
.4971	.137	.5277	.176	.4810	-0.012	.5042	.099
.5012	.145	.5291	-0.160	.4873	+0.049	.5083	.050
.5033	.159			.4941	.092	.5104	.019
.5054	.167	2437744		.5025	+0.094	.5146	-0.002
.5179	.181	.3208	+0.144			.5167	+0.035
.5200	.176	.3222	.168	2438439		.5208	.034
.5211	.205	.3236	.146	.2833	+0.091	.5229	+0.069
.5266	.189	.3278	.171	.2854	.073		
.5287	.167	.3291	.153	.2896	.094	2438457	
.5308	.170	.3305	.118	.2917	.091	.3131	-0.265
.5338	.182	.3340	.041	.2958	.134	.3145	.291
.5352	.162	.3354	.040	.2979	.132	.3180	.314
.5365	.144	.3368	.024	.3021	.151	.3200	.306
.5393	.073	.3403	+0.006	.3042	.192	.3235	.264
.5407	.063	.3416	-0.115	.3188	.187	.3256	.262
.5421	+0.050	.3659	.210	.3292	.180	.3291	.217
.5449	-0.037	.3673	.173	.3312	.191	.3312	.197
.5463	.084	.3708	.139	.3354	.110	.3346	.180
.5477	.104	.3722	.134	.3375	.090	.3395	.129
.5504	.175	.3736	-0.118	.3417	+0.006	.3464	.036
.5518	.210	.3909	+0.033	.3438	-0.100	.3506	-0.022
.5532	.257	.3923	.024	.3479	.205	.3575	+0.018
.5546	.279	.3937	.024	.3500	.265	.3624	.034
.5560	.306	.3958	.036	.3542	.313	.3742	.097
.5574	.308	.4018	.081	.3562	.303	.3763	.138
.5588	.304	.4039	+0.112	.3604	.266	.3805	.146
.5602	.294			.3625	.278	.3825	.194
.5615	.283	2438082		.3667	.251	.3867	.161
.5643	.223	.3275	-0.290	.3688	.237	.3888	.166
.5657	.205	.3333	.224	.3729	.192	.3923	.206
.5671	.212	.3391	.184	.3750	.175	.3944	.193
.5685	.210	.3504	.093	.3792	.096	.3978	.170
.5713	.189	.3553	-0.041	.3812	.113	.3999	.173
.5727	.186	.3616	+0.013	.3868	-0.036	.4041	.198
.5740	-0.134	.3671	.075	.4424	+0.205	.4062	.221
		.3754	.092	.4451	.182	.4096	.163
2437726		.3824	.095	.4507	.160	.4117	.175
.4881	+0.183	.3921	.177	.4528	.190	.4152	.118
.4902	.154	.3991	.201	.4576	.074	.4173	.114
.4916	+0.143	.4074	+0.178	.4597	+0.058	.4207	+0.027

Table 9a (cont.)

Photoelectric yellow observations of SZ Lyn

J.D.	ΔV	J.D.	ΔV	J.D.	ΔV	J.D.	ΔV
2438457		2439528		2439905		2440980	
.4228	-0.037	.6079	+0.092	.3839	+0.157	.4182	+0.110
.4298	.218	.6107	+0.040	.3860	.169	.4196	.109
.4319	.270	.6128	-0.009	.3881	.182	.4210	+0.114
.4353	.302	.6149	.039	.3922	.170		
.4374	.298	.6184	.146	.3943	.181	2441035	
.4416	.287	.6205	.206	.3964	+0.157	.3344	-0.238
.4437	.296	.6226	.253			.3358	.216
.4478	.248	.6260	.306	2440243		.3372	.217
.4499	.236	.6281	.293	.3218	+0.042	.3400	.185
.4541	.194	.6302	.298	.3239	.044	.3414	.155
.4563	-0.157	.6344	.258	.3281	.072	.3428	.146
		.6365	.251	.3301	.082	.3455	.132
2439527		.6386	.259	.3343	.095	.3469	.113
.4795	+0.087	.6427	-0.201	.3364	.120	.3483	.106
.4836	.133			.3406	.152	.3511	.067
.4857	.165	2439905		.3426	.163	.3525	.062
.4920	.185	.2839	+0.145	.3468	.168	.3539	.071
.4961	.170	.2860	.130	.3489	.165	.3553	.075
.5072	.191	.2881	+0.101	.3531	.183	.3580	.048
.5093	.187	.2922	-0.008	.3551	.180	.3594	.047
.5114	.177	.2943	.067	.3593	.196	.3608	-0.024
.5156	.160	.2964	.134	.3614	.200	.3643	+0.010
.5177	.160	.3005	.261	.3656	.187	.3657	.023
.5198	.149	.3026	.285	.3676	.171	.3671	.023
.5239	.112	.3047	.319	.3718	.157	.3699	.032
.5260	+0.038	.3089	.313	.3739	.145	.3713	.026
.5281	-0.008	.3110	.309	.3781	.107	.3727	.060
.5323	.111	.3131	.287	.3801	.081	.3754	.082
.5344	.196	.3172	.243	.3843	+0.003	.3768	.106
.5365	.233	.3193	.239	.3864	-0.062	.3782	.126
.5406	.300	.3214	.191	.3906	.189	.3810	.126
.5427	.312	.3255	.165	.3926	.242	.3824	.129
.5448	.314	.3276	.134	.3968	.302	.3838	.142
.5489	.293	.3297	.111	.3989	.321	.3865	.139
.5510	.283	.3339	.089	.4031	.308	.3879	.141
.5531	.245	.3360	.082	.4051	.291	.3893	.152
.5573	.212	.3381	.054	.4093	.262	.3921	.172
.5594	.179	.3422	-0.021	.4114	.243	.3935	.175
.5615	.170	.3443	+0.012	.4156	.190	.3949	.154
.5656	.111	.3464	.013	.4176	-0.165	.3976	.180
.5677	.087	.3505	.051			.3990	.208
.5698	-0.073	.3526	.057	2440980		.4004	.216
		.3547	.054	.3987	+0.001	.4032	.208
2439528		.3589	.094	.4001	.026	.4046	.198
.5802	+0.175	.3610	.103	.4015	.016	.4060	.225
.5844	.199	.3631	.108	.4064	.075	.4094	.228
.5927	.210	.3672	.112	.4078	.093	.4108	.235
.5962	.185	.3693	.140	.4092	.116	.4122	.229
.6004	.155	.3714	.141	.4126	.072	.4157	.205
.6038	.133	.3755	.145	.4140	.121	.4171	.188
.6059	+0.119	.3776	+0.135	.4154	+0.118	.4219	+0.122

Table 9a (cont.)

Photoelectric yellow observations of SZ Lyn

J.D.	ΔV	J.D.	ΔV	J.D.	ΔV	J.D.	ΔV
2441035		2441312		2441679		2442106	
.4233	+0.110	.4477	-0.158	.5950	-0.116	.3717	+0.107
.4247	.085	.4491	.158	.5971	.097	.3731	.104
.4275	.010	.4519	.134	.5990	.054	.3759	.080
.4289	+0.001	.4533	.123	.6055	-0.019	.3772	.028
.4303	-0.022	.4547	.071	.6078	+0.001	.3786	+0.023
.4330	.137	.4575	.056	.6096	.012	.3814	-0.026
.4344	.180	.4589	.060	.6168	.050	.3828	.069
.4358	.197	.4603	-0.053	.6195	.061	.3842	.125
.4386	-0.284	.4630	+0.024	.6220	.076	.3966	.313
		.4644	.007	.6287	.130	.3980	.307
2441042		.4658	+0.025	.6314	.139	.3994	.291
.3657	+0.101			.6340	.151	.4056	.221
.3671	.095	2441390		.6415	.162	.4070	.226
.3685	.095	.3189	-0.090	.6438	.172	.4084	.201
.4074	.162	.3210	-0.041	.6462	.175	.4112	.156
.4088	.146	.3307	+0.013	.6541	.202	.4126	.144
.4102	.148	.3328	.025	.6565	.196	.4140	-0.144
.4136	.092	.3383	.043	.6584	.191		
.4150	+0.082	.3411	.061	.6652	.156	2442451	
		.3453	.105	.6674	.138	.3851	-0.175
2441312		.3474	.103	.6702	+0.104	.3865	.144
.3887	+0.186	.3529	.117	.6787	-0.075	.3900	.083
.3901	.204	.3557	.131	.6805	.116	.3914	.071
.3915	.202	.3640	.157	.6823	.167	.3962	.030
.3943	.200	.3661	.168	.6841	.219	.3976	-0.025
.3957	.197	.3710	.179	.6911	.299	.4015	+0.006
.3971	.197	.3731	.165	.6931	.294	.4029	.004
.4012	.144	.3779	.186	.6953	.293	.4059	.013
.4026	.110	.3800	.179	.6974	.277	.4073	.027
.4040	.111	.3842	.147	.7050	-0.222	.4101	.041
.4074	.048	.3863	.146			.4115	.050
.4088	.028	.3904	.111	2442106		.4142	.074
.4102	+0.028	.3925	+0.058	.2905	-0.201	.4156	.096
.4130	-0.066	.3967	-0.050	.2917	.176	.4181	.090
.4144	.081	.3988	.092	.2931	.171	.4191	.097
.4158	.111	.4029	.214	.2959	.130	.4219	.118
.4185	.201	.4050	.285	.2973	.108	.4233	.127
.4199	.228	.4099	.329	.2987	.107	.4260	.139
.4213	.273	.4120	.337	.3015	.081	.4271	.136
.4241	.317	.4161	.295	.3029	.071	.4302	.137
.4255	.332	.4182	.265	.3042	.083	.4313	.140
.4269	.340	.4258	.223	.3070	.065	.4337	.151
.4296	.331	.4279	-0.179	.3084	.054	.4351	.164
.4310	.340			.3098	.037	.4385	.168
.4352	.319	2441679		.3126	-0.003	.4399	.170
.4366	.306	.5693	-0.323	.3140	+0.016	.4427	.187
.4380	.300	.5713	.323	.3154	.024	.4441	.175
.4408	.242	.5731	.313	.3647	.164	.4476	.180
.4422	.237	.5818	.259	.3661	.153	.4490	.179
.4436	.205	.5838	.235	.3675	.142	.4521	.189
.4463	-0.159	.5864	-0.207	.3703	+0.140	.4531	+0.176

Table 9a (cont.)

Photoelectric yellow observations of SZ Lyn

J.D.	ΔV	J.D.	ΔV	J.D.	ΔV	J.D.	ΔV
2442451		2442454		2443578		2443931	
.4566	+0.166	.4898	-0.214	.3807	-0.191	.3482	+0.138
.4576	+0.144	.4919	.258	.3818	.179	.3504	.148
.4754	-0.223	.4926	.283	.3842	.161	.3514	.166
.4768	.235	.4947	.301	.3849	.160	.3682	.201
.4813	.291	.4954	.301	.3870	.144	.3696	.204
.4823	.310	.4974	.316	.3880	-0.125	.3706	.189
.4858	.300	.4981	.315			.3779	.169
.4872	-0.297	.5002	.300	2443879		.3789	.148
		.5009	.292	.5406	+0.194	.3823	.155
2442454		.5030	.283	.5464	.178	.3833	.124
.3852	-0.272	.5037	.285	.5477	.175	.3845	.134
.3862	-0.269	.5058	.275	.5515	.147	.3896	.030
.4393	+0.132	.5065	.258	.5531	.133	.3908	+0.009
.4400	.128	.5085	.247	.5566	.102	.3918	-0.028
.4418	.157	.5092	-0.241	.5579	.063	.3928	.067
.4425	.140			.5613	+0.003	.3938	.079
.4446	.139	2443578		.5624	-0.028	.3960	.139
.4453	.149	.3071	+0.129	.5655	.102	.3970	.179
.4474	.144	.3092	.136	.5668	.170	.3982	.212
.4481	.150	.3106	.153	.5698	.227	.3996	.246
.4501	.175	.3149	.180	.5712	.271	.4008	.251
.4508	.180	.3169	.197	.5763	.316	.4018	.264
.4529	.182	.3182	.202	.5773	.311	.4029	.293
.4668	.176	.3349	.191	.5788	.312	.4050	.286
.4675	.161	.3495	.076	.5866	-0.260	.4060	.324
.4696	.153	.3516	.041			.4070	.327
.4703	.144	.3523	+0.007	2443931		.4080	.315
.4724	.151	.3571	-0.145	.2953	-0.239	.4090	.325
.4731	.142	.3578	.185	.2965	.215	.4100	.314
.4751	.109	.3599	.205	.2979	.198	.4120	.286
.4758	.112	.3613	.262	.3041	.175	.4140	.283
.4779	.079	.3641	.289	.3048	.159	.4150	.265
.4786	.049	.3662	.308	.3058	.154	.4254	.154
.4807	.024	.3682	.306	.3117	.110	.4265	.136
.4814	+0.007	.3696	.294	.3127	.088	.4342	.097
.4836	-0.007	.3714	.287	.3142	-0.067	.4352	.082
.4843	.066	.3721	.281	.3321	+0.048	.4465	-0.006
.4863	.099	.3738	.272	.3333	.056	.4476	+0.003
.4870	.132	.3748	.271	.3380	.085	.4490	.019
.4891	-0.195	.3766	-0.268	.3412	+0.103	.4514	+0.062

Table 9b

Photoelectric blue observations of SZ Lyn

J.D.	ΔB	J.D.	ΔB	J.D.	ΔB	J.D.	ΔB
2437703		2437703		2437703		2437703	
.4007	-0.210	.4090	-0.116	.4194	-0.020	.4278	+0.004
.4021	.185	.4111	.080	.4215	.016	.4291	.029
.4048	-0.135	.4132	-0.076	.4236	-0.015	.4305	+0.039

Table 9b (cont.)

Photoelectric blue observations of SZ Lyn

J.D.	ΔB	J.D.	ΔB	J.D.	ΔB	J.D.	ΔB
2437703		2437706		2437707		2437707	
.4340	+0.061	.2637	-0.563	.4164	+0.078	.5235	+0.034
.4354	.052	.2644	.582	.4213	.068	.5256	.036
.4368	.045	.2656	.551	.4234	.063	.5277	.011
.4403	.074	.2689	.567	.4248	.069	.5298	.046
.4416	.077	.2702	.562	.4262	.067	.5346	.038
.4430	.092	.2711	.529	.4275	.083	.5367	.047
.4465	.095	.2734	.477	.4289	.114	.5388	+0.069
.4479	.119	.2746	.453	.4338	.089	.5697	-0.009
.4493	.109	.2759	.431	.4352	.093	.5734	.050
.4528	.120	.2784	.428	.4366	.103	.5748	.091
.4541	.133	.2796	.383	.4380	.084	.5762	.177
.4555	.122	.2808	.372	.4393	.072	.5775	.263
.4590	.141	.2822	.336	.4407	.098	.5787	.311
.4604	.140	.2850	.293	.4421	.099	.5803	.336
.4618	.122	.2864	.296	.4463	.047	.5817	.366
.4652	.122	.2878	.301	.4477	+0.014	.5845	.475
.4666	.094	.2906	.246	.4491	-0.012	.5859	.548
.4680	+0.110	.2920	.231	.4505	.061	.5873	.559
.4736	-0.037	.2934	.213	.4518	.077	.5886	.578
.4750	.071	.2968	.174	.4532	.100	.5900	.571
.4764	.080	.2982	.179	.4546	.188	.5914	.588
.4791	.187	.2996	.135	.4560	.219	.5928	.583
.4805	.230	.3024	.126	.4574	.264	.5942	.579
.4819	-0.353	.3114	.055	.4588	.300	.5956	.550
		.3128	.025	.4602	.370	.5998	.439
2437705		.3142	.021	.4616	.409	.6012	.466
.5304	-0.265	.3156	.008	.4630	.452	.6025	-0.438
.5318	.306	.3170	-0.006	.4644	.485		
.5521	.442	.3204	+0.013	.4657	.532	2437717	
.5528	.412	.3218	.030	.4671	.542	.2963	+0.040
.5538	.395	.3232	.039	.4685	.556	.2984	.044
.5548	.372	.3267	.038	.4699	.555	.3005	.051
.5557	.351	.3281	.059	.4713	.547	.3040	.106
.5568	.364	.3295	.037	.4727	.532	.3054	.091
.5594	.305	.3322	.072	.4762	.505	.3075	.101
.5608	.346	.3336	.072	.4782	.500	.3109	.104
.5622	.326	.3350	.062	.4796	.489	.3123	.124
.5663	.255	.3378	.089	.4810	.450	.3137	.106
.5691	-0.211	.3392	.101	.4824	.398	.3311	.039
		.3427	.098	.4838	.402	.3324	+0.022
2437706		.3461	.107	.4873	.370	.3366	-0.096
.2517	-0.224	.3475	.127	.4914	.268	.3380	.111
.2527	.317	.3489	.113	.4928	.291	.3394	.180
.2535	.382	.3531	.116	.4942	.250	.3417	.255
.2545	.360	.3545	.114	.4956	.258	.3429	.295
.2554	.394	.3558	.093	.4970	.232	.3443	-0.345
.2565	.438	.3600	.065	.4984	.220		
.2576	.468	.3614	.044	.5037	.176	2437718	
.2588	.481	.3635	+0.010	.5058	.169	.4326	-0.468
.2598	.511			.5079	.152	.4335	.482
.2626	-0.565	2437707		.5100	-0.128	.4349	-0.521

Table 9b (cont.)

Photoelectric blue observations of SZ Lyn

J.D.	ΔB	J.D.	ΔB	J.D.	ΔB	J.D.	ΔB
2437718		2437726		2437744		2438052	
.4363	-0.523	.4874	+0.063	.4112	+0.068	.5554	-0.527
.4377	.518	.4895	.031			.5623	.508
.4391	.518	.4909	+0.028	2438052		.5651	.456
.4477	.440	.4943	-0.044	.3405	-0.259	.5665	.423
.4518	.408	.4957	.070	.3424	.198	.5679	.406
.4532	.396	.4971	.100	.3438	.164	.5706	.368
.4553	.323	.4999	.131	.3481	.137	.5720	.328
.4706	.206	.5013	.181	.3500	.102	.5734	.311
.4720	.170	.5048	.338	.3516	.077	.5762	-0.270
.4766	.111	.5062	.405	.3561	.070		
.4787	.128	.5075	.449	.3579	.064	2438439	
.4856	.064	.5096	.504	.3595	.050	.2708	-0.137
.4877	-0.031	.5110	.510	.3651	.018	.2729	.131
.4898	+0.003	.5124	.541	.3674	-0.008	.2826	.031
.4940	.042	.5145	.555	.3725	+0.044	.2847	.031
.4960	.039	.5159	.543	.3748	.074	.2889	-0.016
.4981	.051	.5173	.510	.3813	.093	.2910	+0.006
.5044	.087	.5214	.463	.3831	.110	.2951	.037
.5064	.092	.5228	.426	.3859	+0.108	.2972	.043
.5148	.113	.5256	.422	.4266	-0.460	.3014	.061
.5190	.089	.5270	.386	.4280	.487	.3035	.091
.5210	.116	.5284	-0.409	.4294	.515	.3125	.087
.5231	.127			.4403	.487	.3174	.120
.5276	.069	2437744		.4417	.475	.3285	.075
.5297	.076	.3201	+0.093	.4431	.468	.3306	.058
.5318	.102	.3215	.124	.4463	.413	.3347	+0.012
.5345	.072	.3229	.105	.4477	.410	.3368	-0.021
.5358	.062	.3271	.095	.4491	.388	.3410	.147
.5372	+0.005	.3284	.108	.4533	.333	.3431	.232
.5400	-0.047	.3298	+0.075	.4547	.326	.3472	.392
.5414	.096	.3333	-0.023	.4561	.296	.3493	.457
.5428	.142	.3347	.094	.4602	.261	.3535	.547
.5456	.260	.3361	.091	.4616	.228	.3556	.553
.5470	.275	.3396	.148	.4630	-0.213	.3597	.548
.5484	.375	.3410	.239	.5248	+0.080	.3618	.517
.5511	.425	.3423	.260	.5262	.087	.3660	.458
.5525	.471	.3458	.400	.5276	.085	.3682	.446
.5539	.530	.3562	.522	.5304	.040	.3722	.390
.5553	.577	.3604	.462	.5317	+0.018	.3743	.362
.5581	.574	.3652	.432	.5331	-0.003	.3785	.298
.5595	.567	.3666	.413	.5359	.060	.3806	.269
.5608	.564	.3701	.366	.5373	.088	.3847	-0.219
.5622	.556	.3715	.349	.5387	.146	.4431	+0.109
.5650	.519	.3729	.320	.5415	.231	.4458	.105
.5664	.484	.3902	.090	.5429	.278	.4514	.055
.5678	.467	.3916	.080	.5442	.316	.4535	+0.042
.5692	.447	.3951	.056	.5470	.435	.4583	-0.052
.5720	.421	.4008	.031	.5484	.470	.4604	.093
.5734	.376	.4029	-0.014	.5498	.485	.4646	.257
.5747	-0.367	.4050	+0.006	.5526	.552	.4667	.317
		.4091	+0.042	.5540	-0.553	.4708	-0.481

Table 9b (cont.)

Photoelectric blue observations of SZ Lyn

J.D.	ΔB	J.D.	ΔB	J.D.	ΔB	J.D.	ΔB
2438439		2438457		2439528		2440243	
.4729	-0.509	.4325	-0.512	.6121	-0.134	.3211	-0.094
.4771	.558	.4360	.523	.6142	.175	.3232	.070
.4792	.541	.4381	.519	.6177	.298	.3274	-0.031
.4833	.497	.4423	.511	.6198	.373	.3294	+0.007
.4854	.480	.4444	.504	.6219	.438	.3336	.014
.4896	.418	.4485	.437	.6253	.507	.3357	.017
.4965	.313	.4506	.429	.6274	.518	.3399	.044
.4986	.292	.4548	-0.370	.6337	.509	.3419	.044
.5028	.242			.6358	.479	.3461	.065
.5049	.228	2439527		.6379	.466	.3482	.079
.5090	.180	.4788	+0.013	.6420	-0.416	.3524	.090
.5111	.164	.4816	.034			.3544	.089
.5153	.124	.4850	.058	2439905		.3586	.105
.5174	.090	.4934	.100	.2832	+0.035	.3607	.106
.5215	.081	.4968	.090	.2853	+0.024	.3649	.106
.5236	-0.046	.5065	.112	.2874	-0.013	.3670	.095
		.5086	.128	.2915	.102	.3711	.090
2438457		.5107	.114	.2936	.226	.3732	+0.077
.3124	-0.493	.5149	.103	.2957	.303	.3774	-0.001
.3142	.538	.5170	.103	.2998	.464	.3794	.044
.3173	.568	.5191	+0.072	.3019	.533	.3836	.159
.3194	.540	.5232	-0.010	.3040	.565	.3857	.220
.3228	.522	.5253	.068	.3082	.556	.3899	.373
.3249	.509	.5274	.131	.3103	.559	.3920	.444
.3284	.422	.5316	.286	.3124	.539	.3961	.548
.3305	.409	.5337	.350	.3165	.475	.3982	.559
.3339	.362	.5358	.417	.3186	.439	.4024	.547
.3457	.211	.5399	.500	.3207	.390	.4044	.528
.3513	.157	.5420	.542	.3248	.352	.4086	.494
.3568	.112	.5441	.552	.3269	.318	.4107	.472
.3631	.068	.5482	.547	.3290	.273	.4149	.394
.3694	-0.028	.5503	.492	.3332	.246	.4170	-0.369
.3749	+0.012	.5524	.491	.3415	.159		
.3770	.013	.5566	.414	.3436	.122	2440980	
.3812	.069	.5587	.396	.3498	.072	.3980	-0.128
.3832	.070	.5608	.377	.3519	.067	.3994	.125
.3874	.097	.5649	.285	.3540	.052	.4008	.124
.3895	.091	.5670	.277	.3582	-0.041	.4057	.073
.3930	.103	.5691	-0.257	.3603	+0.002	.4071	.069
.3950	.132			.3624	-0.004	.4085	-0.033
.3985	.111	2439528		.3665	+0.030	.4119	+0.005
.4006	.105	.5795	+0.096	.3686	.050	.4133	.002
.4048	.103	.5837	.098	.3707	.066	.4147	.010
.4069	.120	.5878	.122	.3748	.082	.4175	.052
.4103	.093	.5920	.133	.3769	.097	.4189	.062
.4124	+0.071	.5955	.107	.3790	.082	.4203	+0.074
.4159	0.000	.5997	.107	.3832	.104		
.4180	-0.013	.6031	.064	.3853	.103	2441035	
.4214	.126	.6052	.056	.3874	.103	.3337	-0.448
.4235	.200	.6072	+0.004	.3915	.110	.3351	.447
.4305	-0.456	.6100	-0.075	.3936	+0.123	.3365	-0.413

Table 9b (cont.)

Photoelectric blue observations of SZ Lyn

J.D.	ΔB	J.D.	ΔB	J.D.	ΔB	J.D.	ΔB
2441035		2441035		2441312		2441679	
.3393	-0.379	.4379	-0.484	.4623	-0.152	.6212	-0.036
.3407	.369			.4637	.131	.6280	+0.033
.3421	.353	2441042		.4651	-0.122	.6305	.023
.3448	.303	.3650	+0.004			.6332	.043
.3462	.283	.3664	.008	2441390		.6408	.090
.3476	.279	.3678	.008	.3182	-0.240	.6429	.085
.3504	.243	.4067	.086	.3203	.211	.6454	.103
.3518	.231	.4081	.067	.3300	.117	.6531	.108
.3532	.215	.4095	.052	.3321	.081	.6559	.096
.3546	.181	.4129	+0.019	.3376	.046	.6577	.105
.3573	.160	.4143	-0.032	.3404	-0.049	.6646	.069
.3587	.158			.3446	+0.003	.6668	.066
.3601	.141	2441312		.3467	.018	.6692	+0.007
.3629	.113	.3880	+0.107	.3522	.052	.6780	-0.233
.3650	.082	.3894	.108	.3550	.072	.6799	.320
.3664	.083	.3908	.103	.3633	.109	.6817	.374
.3692	.086	.3936	.097	.3654	.119	.6835	.452
.3706	.085	.3950	.104	.3703	.127	.6906	.556
.3720	.061	.3964	.087	.3724	.119	.6924	.562
.3747	.030	.4005	.025	.3772	.113	.6944	.556
.3761	-0.016	.4019	.034	.3793	.096	.6968	.520
.3775	+0.016	.4033	.018	.3835	.074	.7042	-0.441
.3803	0.000	.4067	+0.010	.3856	+0.065		
.3817	+0.008	.4081	-0.025	.3897	-0.005	2442106	
.3831	.021	.4095	.085	.3918	.044	.2898	-0.361
.3858	.039	.4123	.139	.3960	.171	.2911	.355
.3872	.032	.4137	.153	.3981	.240	.2924	.346
.3886	.041	.4151	.230	.4022	.398	.2952	.313
.3914	.083	.4178	.359	.4043	.435	.2966	.300
.3928	.080	.4192	.376	.4092	.526	.2980	.294
.3942	.085	.4206	.412	.4113	.523	.3008	.243
.3969	.138	.4234	.510	.4154	.520	.3022	.239
.3983	.138	.4248	.531	.4175	.505	.3036	.239
.3997	.124	.4262	.546	.4251	.408	.3063	.207
.4025	.122	.4289	.541	.4272	-0.370	.3077	.185
.4039	.122	.4303	.534			.3091	.178
.4053	.119	.4345	.491	2441679		.3119	.132
.4087	.106	.4359	.453	.5682	-0.546	.3133	.134
.4101	.107	.4373	.465	.5707	.572	.3147	-0.113
.4115	.105	.4401	.453	.5726	.573	.3640	+0.089
.4150	.089	.4415	.412	.5804	.499	.3654	.075
.4164	.066	.4429	.395	.5832	.472	.3668	.057
.4212	+0.014	.4456	.332	.5855	.441	.3696	.063
.4226	-0.014	.4470	.314	.5944	.317	.3710	.052
.4240	.056	.4484	.312	.5964	.299	.3724	+0.022
.4268	.120	.4512	.251	.5983	.246	.3752	-0.019
.4282	.138	.4526	.251	.6046	.169	.3765	.069
.4296	.177	.4540	.220	.6071	.143	.3779	.101
.4323	.307	.4568	.195	.6091	.120	.3807	.163
.4337	.362	.4582	.201	.6161	.050	.3821	.203
.4351	-0.410	.4596	-0.197	.6185	-0.053	.3835	-0.253

Table 9b (cont.)

Photoelectric blue observations of SZ Lyn

J.D.	ΔB	J.D.	ΔB	J.D.	ΔB	J.D.	ΔB
2442106		2442454		2443578		2443931	
.3959	-0.545	.3845	-0.467	.3099	+0.043	.2970	-0.473
.3973	.539	.3859	-0.448	.3142	.048	.2984	.455
.3987	.524	.4390	+0.041	.3162	.073	.3045	.373
.4049	.453	.4397	.034	.3176	.077	.3053	.358
.4063	.434	.4414	.043	.3328	.120	.3065	.350
.4077	.426	.4421	.054	.3342	+0.117	.3122	.271
.4105	.386	.4442	.075	.3481	-0.031	.3137	.244
.4119	.337	.4449	.075	.3491	.085	.3147	.235
.4133	-0.329	.4470	.081	.3509	.120	.3328	.052
		.4477	.078	.3519	.139	.3338	.052
2442451		.4498	.100	.3564	.303	.3407	-0.009
.3844	-0.313	.4505	.098	.3575	.345	.3422	+0.012
.3854	.301	.4526	.107	.3592	.434	.3499	.040
.3893	.222	.4665	.102	.3606	.465	.3509	.038
.3907	.215	.4672	.096	.3634	.526	.3520	.044
.3955	.165	.4693	.098	.3655	.544	.3689	.098
.3969	.150	.4700	.078	.3675	.551	.3701	.096
.4008	.092	.4721	.059	.3689	.541	.3723	.087
.4022	.087	.4728	.043	.3710	.532	.3784	.071
.4049	.075	.4748	.023	.3717	.520	.3828	+0.037
.4066	.061	.4755	+0.019	.3731	.520	.3839	-0.012
.4094	.059	.4776	-0.026	.3745	.491	.3850	.054
.4108	.045	.4783	.052	.3762	.467	.3903	.157
.4135	.023	.4804	.110	.3800	.427	.3913	.180
.4149	-0.024	.4811	.137	.3835	.384	.3923	.223
.4177	+0.011	.4832	.176	.3846	.378	.3933	.250
.4184	.020	.4839	.228	.3863	.357	.3955	.314
.4212	.035	.4859	.288	.3877	-0.331	.3965	.360
.4226	.048	.4866	.309			.3977	.383
.4253	.056	.4887	.370	2443879		.3991	.427
.4267	.057	.4894	.418	.5399	+0.117	.4003	.474
.4295	.081	.4915	.458	.5457	.097	.4013	.495
.4309	.085	.4922	.473	.5470	.091	.4034	.531
.4330	.099	.4943	.515	.5507	.067	.4045	.548
.4344	.101	.4950	.534	.5522	.050	.4055	.554
.4378	.118	.4970	.544	.5559	+0.004	.4065	.534
.4392	.113	.4977	.546	.5573	-0.039	.4095	.537
.4420	.122	.4998	.544	.5606	.149	.4115	.519
.4434	.115	.5005	.541	.5617	.193	.4125	.521
.4469	.124	.5026	.518	.5647	.273	.4135	.502
.4483	.116	.5033	.513	.5661	.324	.4145	.492
.4514	.108	.5054	.496	.5691	.425	.4260	.327
.4524	.110	.5061	.485	.5704	.470	.4270	.307
.4559	.108	.5081	.450	.5757	.544	.4356	.217
.4573	+0.086	.5088	-0.440	.5767	.544	.4372	.195
.4747	-0.376			.5779	.542	.4470	.061
.4761	.416	2443578		.5874	-0.439	.4481	.053
.4806	.496	.3050	+0.011			.4497	.043
.4820	.535	.3064	.015	2443931		.4520	-0.035
.4851	.550	.3085	+0.026	.2959	-0.501		
.4865	-0.525						

Table 9c

Photoelectric ultraviolet observations of SZ Lyn

J.D.	ΔU	J.D.	ΔU	J.D.	ΔU	J.D.	ΔU
2438052		2438052		2438082		2438082	
.3373	-0.138	.5602	-0.451	.3936	+0.108	.4553	-0.334
.3415	.137	.5616	.440	.3941	.134	.4560	.340
.3431	.119	.5630	.398	.3948	.165	.4567	.332
.3442	.121	.5658	.365	.3956	.167	.4595	.274
.3491	.044	.5672	.329	.3998	.214	.4602	.263
.3507	.035	.5686	.304	.4004	.213	.4609	.263
.3526	.026	.5713	.277	.4011	.196	.4616	.259
.3570	-0.024	.5727	.250	.4018	.202	.4623	.257
.3588	+0.035	.5741	.241	.4025	.206	.4650	.248
.3602	.041	.5769	.175	.4080	.143	.4657	.236
.3641	.037	.5783	-0.187	.4087	.146	.4664	.236
.3660	.100			.4094	.152	.4671	.223
.3681	.084	2438082		.4102	.151	.4678	.221
.3718	.072	.3243	-0.446	.4109	.146	.4706	.202
.3762	.132	.3265	.403	.4136	.161	.4713	.199
.3780	.117	.3291	.417	.4143	.151	.4720	.195
.3822	.139	.3345	.360	.4150	.187	.4727	.189
.3868	+0.135	.3354	.368	.4157	.180	.4734	.181
.4273	-0.374	.3412	.289	.4164	.178	.4761	.127
.4287	.404	.3419	.282	.4199	.164	.4768	.132
.4301	.421	.3426	.254	.4206	.134	.4775	.087
.4410	.368	.3511	.132	.4213	.132	.4782	.082
.4424	.368	.3518	.146	.4220	.106	.4789	.094
.4438	.364	.3525	.135	.4227	.117	.4824	.092
.4470	.305	.3532	.157	.4261	.064	.4831	.081
.4484	.297	.3560	.130	.4268	.044	.4838	.069
.4498	.287	.3567	.100	.4275	.033	.4845	.057
.4540	.223	.3574	.125	.4282	.013	.4852	.054
.4554	.198	.3581	.105	.4289	+0.010	.4879	.003
.4567	.193	.3588	.095	.4317	-0.066	.4886	-0.004
.4609	.167	.3622	.082	.4324	.096	.4893	+0.017
.4623	.149	.3629	.087	.4331	.116	.4900	.011
.4637	-0.119	.3636	.053	.4338	.137	.4907	.008
.5255	+0.131	.3643	.055	.4345	.161	.4948	.087
.5269	.150	.3650	.058	.4373	.270	.4963	.112
.5283	.134	.3678	-0.018	.4379	.271	.4970	.112
.5311	.094	.3684	+0.001	.4386	.289	.4984	.120
.5324	.076	.3691	+0.010	.4393	.297	.4991	.105
.5338	+0.040	.3698	-0.006	.4400	.331	.5032	.144
.5366	-0.007	.3705	+0.010	.4428	.395	.5046	.142
.5380	.023	.3761	.047	.4435	.412	.5053	.151
.5394	.080	.3768	.056	.4442	.426	.5067	.168
.5422	.208	.3782	.067	.4449	.436	.5074	+0.162
.5436	.232	.3789	.047	.4456	.428		
.5449	.282	.3796	.066	.4484	.391	2438439	
.5477	.362	.3831	.070	.4491	.389	.2701	+0.003
.5491	.418	.3838	.085	.4498	.391	.2722	.002
.5505	.403	.3845	.075	.4504	.378	.2819	.047
.5533	.480	.3852	.093	.4511	.377	.2840	.068
.5547	.485	.3866	.100	.4539	.335	.2882	.049
.5561	-0.456	.3928	+0.107	.4546	-0.331	.2903	+0.096

Table 9c (cont.)

Photoelectric ultraviolet observations of SZ Lyn

J.D.	ΔU	J.D.	ΔU	J.D.	ΔU	J.D.	ΔU
2438439		2438457		2439527		2439905	
.2944	+0.117	.3166	-0.454	.5225	+0.050	.3075	-0.463
.3007	.176	.3187	.438	.5246	+0.010	.3096	.457
.3028	.179	.3221	.390	.5267	-0.010	.3117	.456
.3069	.201	.3242	.333	.5309	.138	.3158	.431
.3167	.230	.3277	.318	.5330	.182	.3179	.359
.3278	.198	.3298	.299	.5351	.324	.3200	.318
.3299	.199	.3332	.264	.5392	.418	.3241	.254
.3340	.117	.3450	.116	.5413	.451	.3262	.202
.3361	+0.043	.3520	-0.032	.5434	.474	.3325	.129
.3403	-0.035	.3562	+0.024	.5475	.451	.3367	.052
.3424	.125	.3638	.025	.5496	.470	.3408	-0.011
.3465	.275	.3687	.043	.5517	.408	.3450	+0.031
.3486	.275	.3756	.113	.5559	.344	.3596	.104
.3528	.402	.3777	.142	.5580	.301	.3617	.115
.3549	.442	.3819	.184	.5601	.311	.3658	.118
.3590	.419	.3839	.184	.5642	.195	.3679	.152
.3611	.408	.3881	.203	.5663	.161	.3700	.170
.3653	.329	.3902	.192	.5684	-0.142	.3741	.165
.3674	.306	.3937	.213			.3762	.195
.3778	.180	.3957	.222	2439528		.3783	.219
.3799	.162	.3992	.214	.5788	+0.150	.3825	.228
.3840	-0.137	.4013	.201	.5830	.153	.3846	.190
.4444	+0.226	.4055	.236	.5871	.191	.3867	.213
.4472	.185	.4075	.203	.5913	.161	.3908	.237
.4521	.139	.4113	.183	.5948	.167	.3929	.232
.4542	.132	.4131	+0.169	.5990	.170	.3950	+0.226
.4590	+0.006	.4221	-0.039	.6024	.149		
.4611	-0.032	.4242	.101	.6045	.123	2440243	
.4653	.185	.4313	.327	.6065	+0.091	.3204	-0.008
.4674	.223	.4332	.381	.6114	-0.027	.3225	+0.008
.4715	.389	.4367	.400	.6135	.031	.3267	.019
.4736	.432	.4388	.404	.6170	.181	.3288	.051
.4778	.421	.4430	.388	.6191	.265	.3329	.063
.4799	.416	.4450	.364	.6212	.321	.3350	.083
.4840	.361	.4492	.316	.6246	.447	.3392	.092
.4861	.337	.4513	.285	.6267	.428	.3412	.136
.4903	.274	.4555	.201	.6288	.417	.3454	.172
.4972	.195	.4575	-0.190	.6330	.411	.3475	.191
.4993	.162			.6351	.411	.3517	.211
.5035	.117	2439527		.6372	.381	.3538	.204
.5056	.094	.4781	+0.133	.6413	.349	.3579	.215
.5097	.080	.4809	.116	.6455	-0.300	.3600	.211
.5118	.044	.4843	.200			.3642	.215
.5160	.004	.4954	.156	2439905		.3663	.183
.5181	-0.009	.4975	.199	.2846	+0.010	.3704	.138
.5222	+0.042	.5058	.215	.2867	+0.002	.3767	.076
.5243	+0.047	.5079	.231	.2908	-0.084	.3788	+0.036
		.5100	.170	.2929	.192	.3829	-0.045
2438457		.5142	.195	.2950	.198	.3850	.105
.3117	-0.359	.5163	.179	.2991	.298	.3892	.297
.3138	-0.404	.5184	+0.153	.3033	-0.439	.3913	-0.368

Table 9c (cont.)

Photoelectric ultraviolet observations of SZ Lyn

J.D.	ΔU	J.D.	ΔU	J.D.	ΔU	J.D.	ΔU
2440243		2441390		2441679		2441679	
.3954	-0.450	.3647	+0.200	.5672	-0.405	.6401	+0.180
.3975	.459	.3696	.218	.5700	.440	.6423	.177
.4017	.440	.3717	.237	.5720	.448	.6446	.180
.4038	.435	.3765	.209	.5797	.375	.6524	.203
.4079	.390	.3786	.189	.5825	.347	.6552	.186
.4100	.377	.3828	.175	.5846	.311	.6571	.184
.4142	.312	.3849	.153	.5937	.178	.6639	.162
.4163	-0.290	.3890	.088	.5957	.177	.6662	.146
		.3911	+0.040	.5977	.144	.6683	+0.109
2441390		.3953	-0.067	.6039	.053	.6775	-0.115
.3293	-0.040	.3974	.101	.6064	.044	.6793	.178
.3314	0.000	.4015	.256	.6085	-0.019	.6811	.261
.3362	+0.023	.4036	.304	.6152	+0.045	.6829	.314
.3397	.051	.4085	.405	.6178	.040	.6900	.427
.3439	.065	.4106	.411	.6203	.050	.6918	.429
.3460	.128	.4147	.408	.6270	.119	.6938	.432
.3515	.120	.4168	.398	.6294	.118	.6961	.404
.3543	.154	.4244	.314	.6323	+0.129	.7034	-0.313
.3626	+0.207	.4265	-0.267				

COMMUNICATIONS
FROM THE
KONKOLY OBSERVATORY
OF THE
HUNGARIAN ACADEMY OF SCIENCES

MITTEILUNGEN
DER
STERNWARTE
DER UNGARISCHEN AKADEMIE
DER WISSENSCHAFTEN

BUDAPEST — SZABADSÁGHEGY

No. 85.

L. G. BALÁZS, M. PAPARÓ, I. TÓTH

DISTRIBUTION OF STARS OF SPECTRAL TYPES OF F7 AND EARLIER IN A FIELD AROUND NGC 7686

BUDAPEST, 1985

ISBN 963 8361 21 2
HU ISSN 0324 — 2[illegible]4

Felelős kiadó: Szeidl Béla

Hozott anyagról sokszorosítva

8616202 MTA Sokszorosító, Budapest. F. v.: dr. Héczey Lászlóné

DISTRIBUTION OF STARS OF SPECTRAL TYPES OF F7 AND EARLIER IN A FIELD AROUND NGC 7686

ABSTRACT

A statistical study was performed on 993 stars of spectral type F7 and earlier in 19.5 sq. deg. field centred on NGC 7686 down to a limiting magnitude of 12.5. The observational material was obtained with Konkoly Observatory's 60/90/180 cm Schmidt telescope. The stars were classified utilizing small scale spectra (580 Å/mm at Hγ) and photographic UBV colours were measured. The interstellar absorption in this area was determined to be A_v = 1.2 mag. and the space densities in the spectral groups of B8-A1, A2-A3, A4-A7, A8-F2 and F3-F7 were obtained using the matrix method of Dolan. Our empirical space distributions were compared with an exponential model, with Camm's models, with Bahcall's model and with that of Woolley and Stewart. The best fit was obtained by an isothermal model and this fitting enabled us to estimate the total mass density near the Sun resulting 0.104 $M_\odot/pc^3$ using the B8-A1 group and 0.159 $M_\odot/pc^3$ using the A type stars. These figures do not differ from the observed total mass density on the one sigma significance level.

INTRODUCTION

The present work is a continuation of the combined spectral and multicolour investigation of stars of spectral types of F7 and earlier at intermediate galactic latitudes. In two previous papers (*Balazs 1975, Paparo and Balazs 1982*,hereafter referred to as Paper I and Paper II, respectively) we found further evidence to those reported in the literature (see references in Paper I), that the space distribution of A type stars is composed of two kinematically different subsystems resulting in an inflexion point on the log-density curve at about 200 pc above the galactic plane. On combining the results of other authors with our own measurements, we found (see Paper I) that the density ratio at z=0 of the two subsystems depends on spectral type and displays a jump at about AO. We interpreted this jump as a consequence of discontinuous star formation in the region surveyed (r<1000 pc from the Sun). It is thought that this jump might result from the passage of the density wave through the solar neighbourhood. The life times of these stars at which the jump appeared enabled us to estimate the period between two

consecutive increases of star formation activity. It turned out to be of 1×10^8 years $< \tau < 6 \times 10^8$ years.

Discontinuous star formation followed by dynamic evolution could account for the shape of the spatial distribution of the stars perpendicular to the galactic plane. Recent investigations (*Wielen 1977, Wielen and Fuchs 1983, Villumsen 1984, Lacey 1984, Palous and Piskunov 1985*) have confirmed the result of *Spitzer and Schwarzschild (1953)* that the dynamic evolution of stellar spatial and kinematic distributions could proceed fast enough to be significant during the period mentioned above. Thus, in addition to discontinuous star formation, this is an important phenomenon in interpreting the spatial distribution of stars having life times in the order of 10^8 years, i.e. of the A type stars. The significance of the spatial distribution of A type stars in studying star formation periods and dynamic evolution has been emphasized by *Balazs (1977,1984)*.

It is important to prove that the space distribution of A type stars observed is really due to the processes mentioned above. To exclude the possibility that the observed characteristics represent a local phenomenon only, one should extend the investigations as far from the Sun as possible. Since the inflexion point appears at about 200 pc above the galactic plane, one has to make observations at intermediate or low galactic latitudes in order to extend the domain of investigations. This was an important motivation for selecting the galactic latitudes of our investigations in Papers I and II. The area presently surveyed has a somewhat lower latitude, of 11.63 degrees.

OBSERVATIONAL MATERIAL

We have investigated an area of 19.5 sq.deg. centred on l=109.52 deg. , b=11.63 deg. (alpha=$23^h27.8^m$, delta=$48^o51'$). The observations were carried out with the 60/90/180 cm Schmidt telescope of the mountain station of Konkoly Observatory. We obtained spectral types and UBV colours for 993 stars down to 12.5 photographic magnitude. For spectral classification we used

three objective prism plates taken with a 5 deg. UBK7 (UV transmitting) prism that gives a dispersion of 580 Å/mm at $H\gamma$. The widening and the exposures were the same as in Papers I and II as were the criteria for spectral classification.

The UBV photometry was based on five plates in U, two plates in B and four plates in V. The emulsion types, filters and exposure times were the same as previously.

The relationship between the international system and the instrumental system gives the following equations:

$$V = V_{instr} + 0.15(B-V)_{instr} - 0.14$$

$$B-V = 0.98(B-V)_{instr} + 0.01$$

$$U-B = 0.99(U-B)_{instr} - 0.13(B-V)_{instr} + 0.15$$

The plates were measured with Konkoly Observatory' s Cuffey-type iris photometer. We used the photoelectric sequence of *Hoag (1961)*. The mean errors of the photographically determined colours were 0.10, 0.08, 0.07 in U,B and V, respectively.

INTERSTELLAR REDDENING

Adopting *Allen's(1973)* relation between the intrinsic colour index and spectral type we have derived the E(B-V), E(U-B) colour excesses using Allen's relation between the absolute magnitude and spectral type and computing the apparent distance modulus for each star. The stars were divided into seven groups according to their distance modulus: <7, 7-8, 8-9, 9-10, 10-11, 11-12 and >12 mag. and the mean distance modulus and the colour excesses for each subgroup were determined. The colour excesses determined in this way are plotted in Fig.1 as a function of the distance modulus. According to *Svolopoulos (1961)* the distance modulus of the NGC 7686 cluster is 8.6 mag. and the mean reddening equals 0.17 mag. which is in good agreement with our value. Adopting E(B-V) from Fig.1 and a ratio of total to selective absorption equal to 3.0, we have corrected the magnitudes for the absorption.

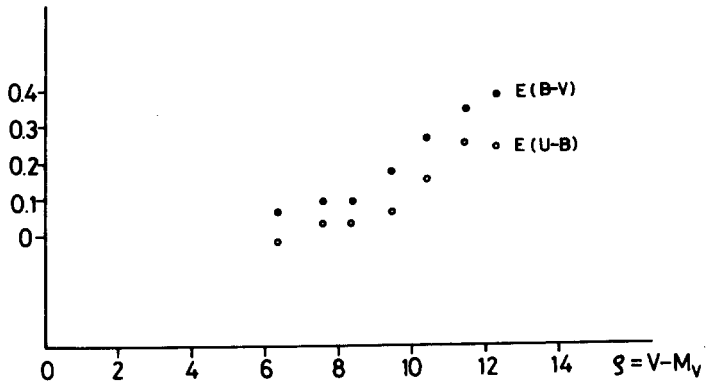

Fig.1 Colour excesses as functions of the apparent distance moduli of the stars.

SPACE DISTRIBUTION OF STARS

Preparing the input data for computation:

After removing the effect of interstellar absorption from the apparent magnitudes of the stars we determined the space densities of the stars in our sample by solving the basic convolution equation of stellar statistics

$$A(m) = \int_{-\infty}^{+\infty} D(y) f(m-y) dy$$

where A(m), D(y), f(m-y) are the number of stars in a (m,m+dm) magnitude interval, the probability density of distance moduli and the luminosity function of stars, respectively.

The stars were binned into subsamples to study the occasional dependence of space distribution on spectral type. The range of spectral types defining one subsample were chosen to ensure sufficient number of stars in each bin and taking into account the sharpness of classificational criteria. For this reason we have defined the five following bins: B8-A1, A2-A3, A4-A7, A8-F2, F3-F7. The distribution of stars against the V measured magnitude in the given subgroups is shown in Fig. 2a-f.

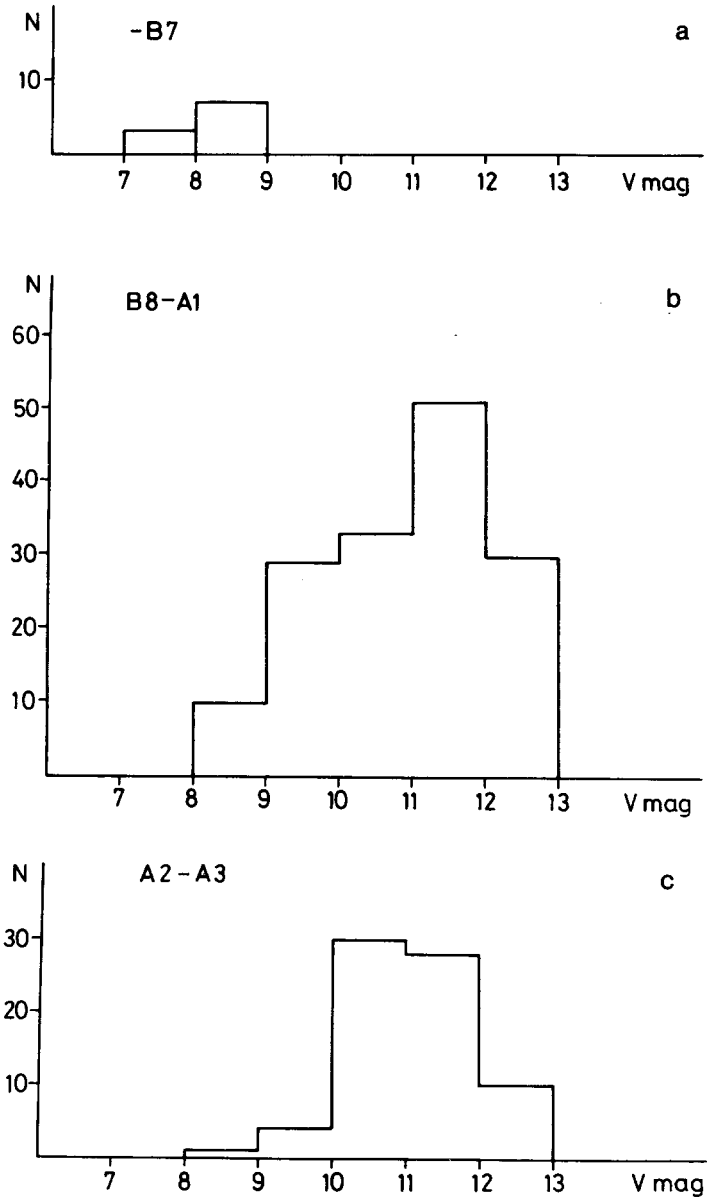

Fig.2a-c Distribution of stars against the V magnitude in different spectral ranges.

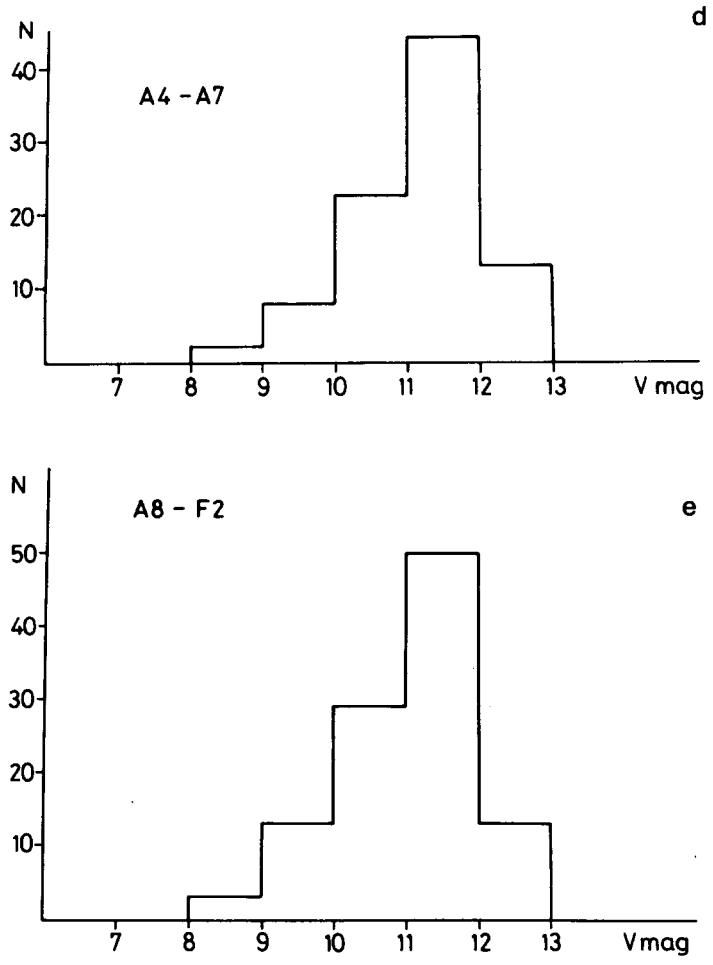

Fig.2d-e Distribution of stars against the V magnitude in different spectral ranges.

We assigned the mean absolute magnitude to each bin using the distributions of spectral types within them. The only exception was the B8-A1 group because of the lack of reliable classificational criteria of these stars on our small scale

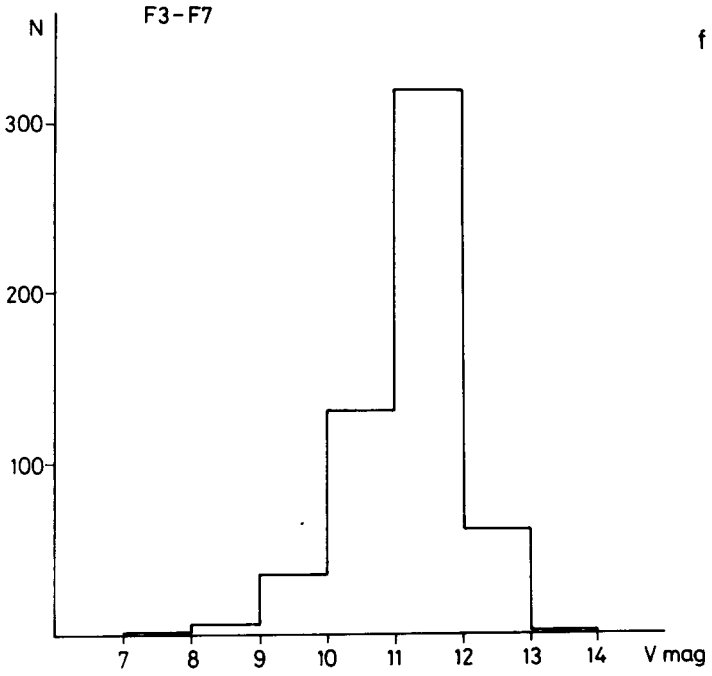

Fig.2f Distribution of stars against the V magnitude in F3-F7 spectral range.

spectra. To compute the mean absolute magnitudes of the corresponding subsamples we used the absolute magnitudes of *Allen (1973)* weighted with the distribution of spectral types observed.

To obtain the spatial densities in each spectral group defined above the convolution equation of stellar statistics was solved for them separately using the matrix method of *Dolan (1974)*. The luminosity function inside the spectral group was assumed to be Gaussian with a mean absolute magnitude equalling the mean absolute magnitude assigned to the subsample. The

standard deviation of the computed density values can be obtained from the formula yielding the densities.It is, however, obviously necessary to discuss in more detail the possible sources of bias inherent in this procedure.

The first source of bias is caused by the method itself. To solve the convolution equation we supposed that the form of the luminosity function is Gaussian, which is in fact true if one deals with a given spectral type (*McCuskey 1966*). In our case, however, we binned the data in a certain spectral range and used an average absolute magnitude to compute the densities. The distribution of absolute magnitudes could deviate significantly from the Gaussian depending on the distribution of spectral types inside the spectral range defined as one bin. We tried to eliminate this effect by grouping the stars into different spectral bins and comparing the densities obtained. No significant changes were observed in the case of A type stars. Eventually we binned the A type stars into groups A2-A3,A4-A7 and A8-F2. In these groups the ranges of absolute magnitudes are 0.2, 0.5 and 0.5, respectively. These variations are small compared with the about 1 magnitude standard deviations of absolute magnitudes for these spectral types. In groups B8-A1 and F3-F7, however, these figures are 1 and 0.8, respectively and if the distribution of spectral types has a significant skewness the distribution of absolute magnitudes cannot be described with one Gaussian in these subsamples and on solving the convolution equation assuming Gaussian distribution the bias could be inserted into the densities obtained.

Another possible source of bias comes from the uncertainties in the averaged absolute magnitude of stars assigned to the Gaussian-shaped luminosity function of a subsample. Its deviation from the true value causes changes in the distance scale and, consequently, in the spatial densities (0.5 mag. error in the absolute magnitudes results in a change of a factor of 2 in the densities). There is a significant difference between the calibrations made by different authors (e.g. for A0 stars *Alexander (1958)* reported 0.14, *Eggen (1962)* 0.85, *Perry (1969)* 0.71 *Hildich et al.* (1983) 1.2). Because we had no reliable

classificational criteria on our small scale spectra for B8-A1 stars we could not calculate the average absolute magnitude using the distribution of spectral types over this subsample. In view of this we assigned to this group an average absolute magnitude obtained from the spectral type distribution of stars near the Sun (data from *Allen(1973)*).

The third and probably the most serious bias in our determination of space densities was the truncation of our samples. The convolution model assumes that the measured quantity (in our case the apparent magnitude of stars) is a sum of two probability variates, i.e. the absolute magnitude and the distance modulus. Due to the limiting magnitude of the telescope utilized for the observations, we can observe only a part of the convolved sample for which the convolutional model holds exactly. If the truncated sample is used in our computations the result will be seriously biased because the sample does not fulfil the basic assumption of a convolution equation: the sample observed is generated by a convolution process. In the next paragraph we outline a way to overcome this difficulty and to separate a part of the computed spatial density curve that is only slightly biased.

Discussion of space densities:

Applying Dolan's method to the subsamples described in the previous paragraph we obtained the spatial density curves displayed in Fig.3a-e. A vertical dashed line indicates the estimated distance beyond which the densities are seriously biased due to the sample truncation. The estimation of this limit proceeded as follows: we visually inspected the distributions displayed in Fig.2; this revealed that all the subsamples contain only a few stars fainter than 12.5 magnitude. This value was adopted as the plate limit. We then computed the distance modulus using the plate limit and the absolute magnitude corresponding to the fainter edge of the spectral range of the subsample in question. Next we corrected this distance modulus for the absorption, and the distance obtained in this way was

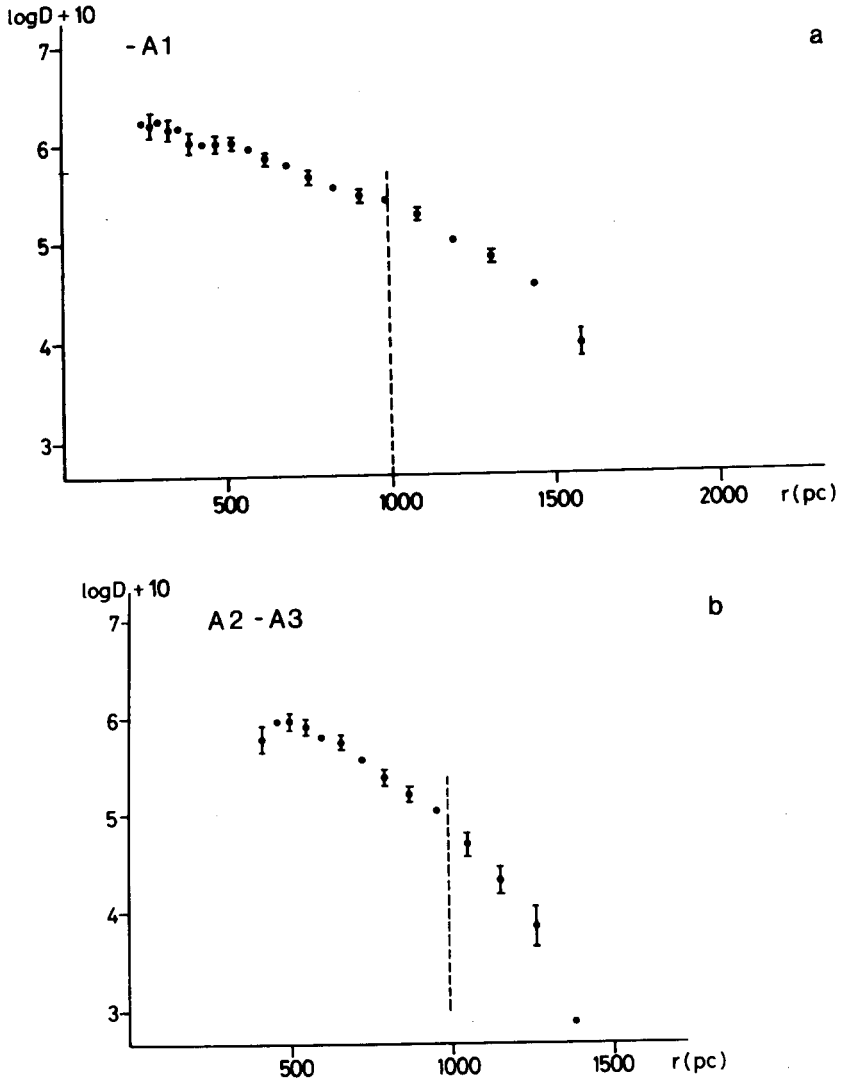

Fig.3a-b Space densities of stars in different spectral subgroups.
(The dashed line idicates the plate limit.)

adopted as the limit of the little-biased part of the density curves.

The most important remark to be made after inspecting the

density curves is to state that they do not display the inflexion feature described in the introductory paragraph of this paper. This inflexion feature was thought to be a consequence of the

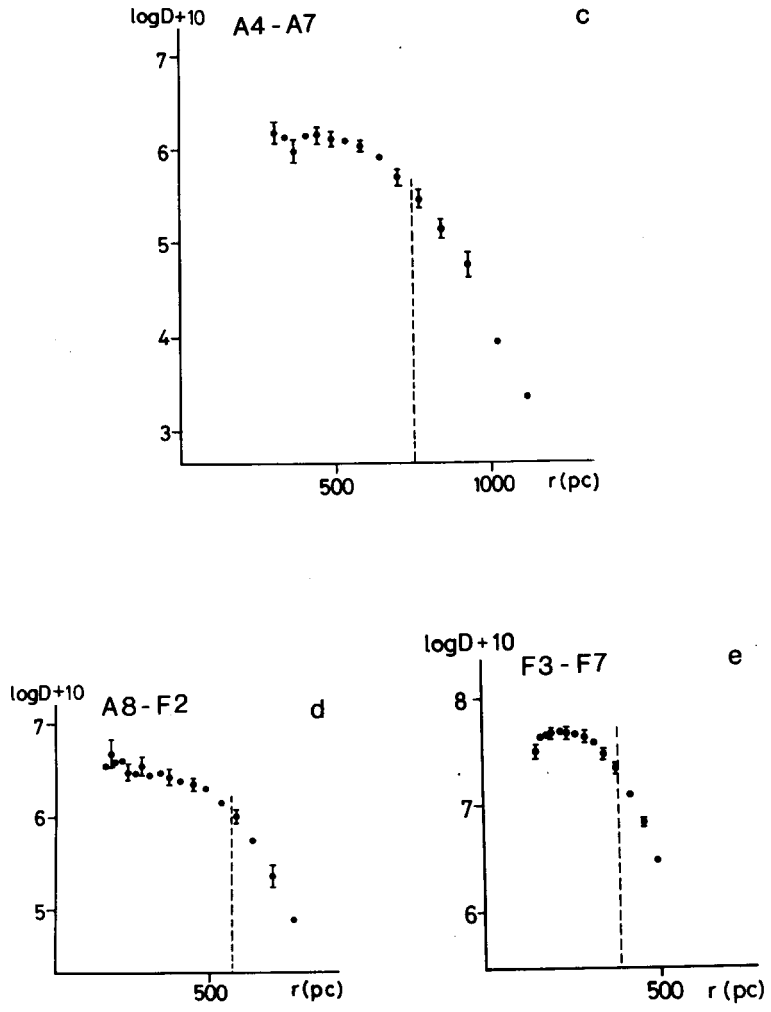

Fig.3c–e Space densities of stars in different spectral subgroups. (The dashed line indicates the plate limit.)

discontinuous star formation in the solar neighbourhood and of a subsequent dynamic evolution - as we pointed out in the introduction. *Oort(1932)*, *van Rhijn(1960)*, *Woolley and Stewart(1967)* accounted for the inflexion feature as being the superposition of subsystems having Gaussian (isothermal) velocity distribution of the velocity components perpendicular to the galactic plane but with different variances. The lack of inflexion on our curves may indicate that we could recognize only one isothermal component on the basis of our sample. This may be caused by the truncation due to the limiting magnitude of our observations. This means that the second isothermal component would have an influence beyond the bias-free part of the density curves. We shall discuss this assumption in more detail when comparing our empirical density curves with models.

Assuming that the density curves of A type stars represent essentially the different portions of the same density distribution we can construct a composite curve from the density curves of the A2-A3, A4-A7, A8-F2 subsamples. For constructing this we selected a common distance range on the little-biased parts of the density curves. This turned out to be at 500 pc. We normalized each curve by equalling the densities at this distance by shifting the curves vertically in the (log density; distance)

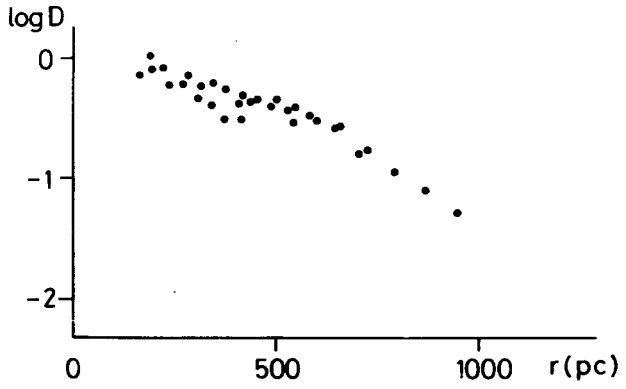

Fig.4 Composite space density curve of A type stars.

plane. The resulting curve obtained using this procedure is displayed in Fig.4.

We did not use the B8-A1 and F3-F7 stars in this procedure for different reasons. The density curve of B8-A1 is flatter than those of the A type stars in our sample. The flatness of the density curve may possibly be accounted for by assuming an about 0.5 magnitude systematic error in the absolute magnitude we used for determining the density distribution of this spectral range. We have already stressed above that the possible source of this systematic error was the lack of reliable classificational criteria on our small scale spectra in this spectral range. We have excluded the F3-F7 stars from these calculations because they did not have reliable density values near 500 pc.

Comparisons with models:

a. Exponential distribution

An exponential distribution is commonly used for describing the space distribution of stars perpendicular to the galactic plane. It was assumed also by *Bahcall and Soneira (1980)* for constructing their standard model of our Galaxy. It is so far the most detailed model of that type. Exponential models are represented by a straight line on the (log D, r) plane, where D is the spatial density and r is the distance in the line of sight. If our density plots of different spectral ranges are considered, it can be seen that the curves of B8-A1, A2-A3 and A8-F2 type stars can be represented by a sraight line in the 300-1000, 500-1000 and in the 200-500 pc distance range, respectively. Extrapolations of the densities to the galactic plane, however, yield in the case of A2-A3 stars about four-times higher values than observed whereas in A8-F2 range they are close to the values derived from the data of nearby stars *(Gliese,1969)*. With the A4-A7 stars the exponential fit is rather poor: the extrapolated density in the galactic plane, however, is close to the value of Gliese. Except for the A2-A3 group where the scale height is about 50 pc the scale heights are comparable

with those used by *Bahcall and Soneira (1980)*. The extrapolated density values in the galactic plane utilized by different models are listed in Table 1. The corresponding scale heights are summarized in Table 2. The composite density curve made up from the A-type stars (Fig.4) clearly shows a curvature and, correspondingly, an exponential model gives a poor fit to the data. The scale height of the best fitting exponential is about 70 pc in this case.

Table 1

Extrapolated densities in the galactic plane utilized by different models (log D(o)+10)

	A2-A3	A4-A7	A8-F2
Gliese catalog	6.25	6.66	6.89
Isothermal model	6.35	6.50	6.67
Exponential model	6.95	6.75	6.83

Table 2

Scale heights (pc) of the best fitting exponential models

	A2-A3	A4-A7	A8-F2
Exponential model	50	66	90
Standard model (Bahcall and Soneira 1980)	90	90	90

b. Camm's models

Camm (1950) studied self consistent solutions of the system consisting of a collisionless Boltzmann equation and the Poisson equation of the gravitational force field. He was looking for equilibrium configurations and found three particular solutions in the plane parallel case. His first solution corresponds to the isothermal case where the velocity dispersion is independent of the spatial coordinate. This result had actually already been found by *Spitzer(1942)*. The basic idea behind these calculations is that the stars obey the same distribution in the phase space independently of their spectral type. Comparing the distribution of A type stars with, for example, that of F type stars, this

assumption obviously does not hold. However, it is worth while to compare these models with our empirical density distributions. To facilitate comparison between the theoretical and empirical data we have displayed the empirical and model data on the (logD,logr) plane. The possible scale errors due to the systematic errors in absolute magnitudes appear as a shift along the log r axis. As to the isothermal model we shall return to its discussion later on in the context of the more advanced Bahcall model.

With regard to Camm's other two solutions, these models (Nos.II and III) were used more recently by *Hill, Hildich and Barnes (1979)* to explain the distributions of A and F type stars in the North Galactic Cap. The best fitting solution adopted by HHB was based on model No.II and it gives a reasonably good fit in the z < 200 pc distance range but deviates significantly from

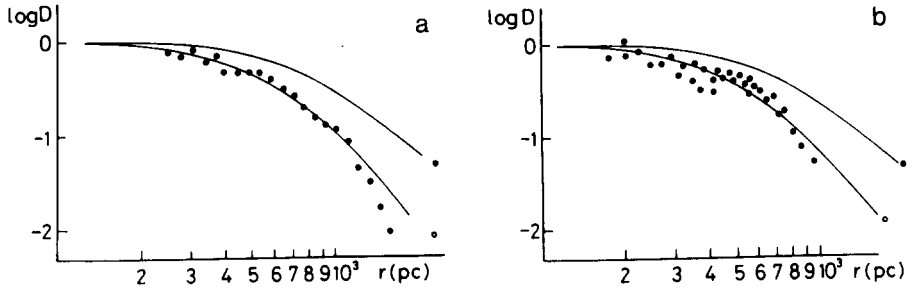

Fig.5 Comparison of space density distribution of B8-A1 stars (a) and of the composite density curve of A type stars (b) with the model of *Hill et al.(1979)*. (o HHB model for A type stars, ● HHB model for F type stars.)

the empirical plots of both the A and F type stars beyond this distance. Fig.5 shows a comparison between the B8-A1 stars (a) and our composite density curve of A type stars (b) with the HHB models after a suitable shift of the empirical curve in the log r direction to get the best fit with the model. As one can confirm from the figure the fit is satisfactory in case (a) and poorer in case (b) even in the distance range where the models give an excellent fit to the HHB data. As we shall discuss later

on, our data can be fitted quite well by an isothermal model and the discrepancy between our points and those of HHB might be accounted for by a systematic error inherent in deriving the space densities. One probable source of such a systematic error is the inaccurate deconvolution when determining the space densities from the magnitude data.

c. Bahcall's model

Bahcall attempted to find a self-consistent solution of the collisionless Boltzmann equation - Poisson equation pair assuming that the disc density can be written in the form of a sum of different isothermal components and a term representing the halo mass density. He made detailed calculations in the isothermal case. We have compared his model with our data in Fig.6 for

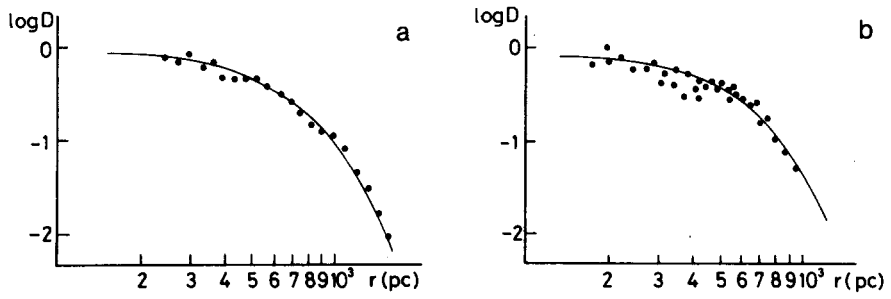

Fig.6 Comparisons of empirical space density curves with the *Bahcall*'s model (*1984*): a): B8-A1 b): composite density curve of A type stars.

B8-A1 stars (a) and for the composite distribution of our A type stars sample (b).

To get the closest fit we shifted the empirical plots along the log r axis corresponding to 1.45 and 1.8 times increase of the scales in the case of B8-A1 group and the composite curve

of A type stars, respectively. The scale differences might be accounted for not by the systematic errors of absolute magnitudes we used to derive the corresponding space densities but rather by the differences in the velocity dispersions assigned to the best fitting isothermal distribution for A and F type stars. The latter was used to fit the Bahcall model. The 1.24 times larger scale of B8-A1 stars in relation to the A type spectral group can be explained by a 0.5 magnitude systematic error in absolute magnitudes. The possibility of such an error was mentioned in paragraph 3.2 when we discussed the space densities of the sample stars.

Summarizing what has been said, our view is that the space distribution of B8-A1 and A type stars in our sample can be represented very well by Bahcall's isothermal model after appropriate scale transformation.

d. Two component model of Woolley and Stewart

Woolley and Stewart (1967) worked out a model superposing two isothermal components having a ratio of the velocity

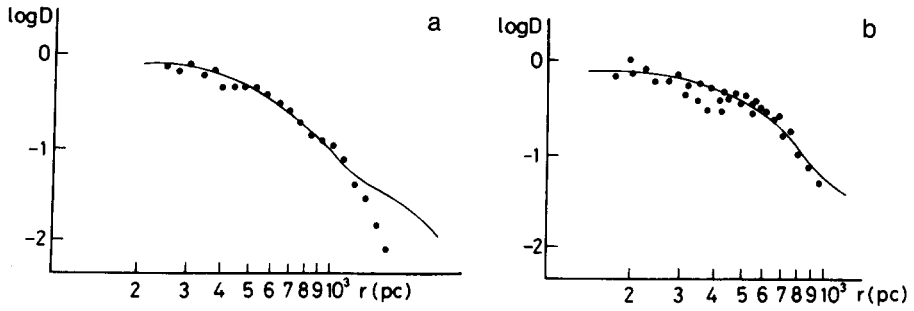

Fig.7 Fitting the empirical space densities by the model of *Woolley and Stewart (1967)*. a): B8-A1 stars b): A type stars. The model tends to deviate from the empirical curve beyond the limit of completeness of the empirical data. (We achieved the best fit with the WS model by shifting our experimental density plots by 0.04 and 0.13 along the log r direction for a) and b), respectively.)

dispersions of about 1:2. The aim of their model was to explain the inflexion feature inherent on the space density curve of A type stars perpendicular to the galactic plane. We have achieved the best fitting with the WS model by shifting our experimental density plots in the (log D,log r) plane by 0.04 and 0.13 along the log r direction in the case of B8-A1 and A type stars, respectively (see Fig. 7a and b). Below the inflexion the space distribution is dominated by one isothermal component and this part coincides well with the plots derived from our observations. The deviation from a simple isothermal model becomes significant beyond the limit of completeness of our sample so this limit does not enable us to study the possible presence of a secondary isothermal component in our data.

Mass density in the solar neighbourhood:

The total mass density could be determined knowing the gravitational potential by using the Poisson equation (see e.g. *Oort 1965*). In the case of isothermal distribution the logarithm of space density is proportional to the gravitational potential if we consider the plane parallel case:

$$\log D(z) - \log D(0) = -\frac{\varphi(z)}{\sigma_w^2}$$

where $D(z), \varphi(z), \sigma_w^2$ are the spatial density, gravitational potential and variance of velocities perpendicular to the galactic plane, respectively. Expanding $\varphi(z)$ into Taylor series and supposing that $\varphi(z)$ is symmetric to the galactic plane we have:

$$\varphi(z) \approx \varphi(0) + \frac{\varphi''(0)}{2} z^2 + \ldots$$

The log density could, therefore, be fitted by a simple parabola if z is sufficiently small for the higher order terms in this expansion to be neglected. Since the total mass density is connected with the potential by the Poisson equation the coefficient of the second order term in the expression of the log

density is given by

$$a = \frac{2\pi G\rho(0)}{\sigma_w^2}$$

where G, $\rho(0)$ are the gravitational constant and the total mass density in the plane of the Galaxy, respectively. Comparing our density curves with a suitably chosen parabola we can get an excellent fit to our B8-A1 and composite A type stars density curve (see Fig.8). We may conclude, therefore, that the parabola approximation is satisfactory in the $z<200$ pc range. Adopting $\sigma_w = 7.3\pm2$ km/sec (*Hill et al. 1979*) we get $\rho(0)=0.104\ M_\odot/pc^3$ and $\rho(0)=0.159\ M_\odot/pc^3$ in the case of B8-A1 and A type stars, respectively. Nevertheless, it is necessary to remark that the mass density derived from the B8-A1 sample is probably underestimated because of the possible scaling error of 1.24 (as pointed out in 3.2 paragraph). The total mass density of matter observed in the solar neighbourhood has an estimated value of $\rho(0)=0.108\ M_\odot/pc^3$ (*Hill et al.1979*). Taking into account the 2 km/sec standard deviation of velocity dispersion and computing $\rho(0)$ with $\sigma_w=5.3$ km/sec instead of 7.3 km/sec we get a mass density of $\rho(0)=0.084\ M_\odot/pc^3$. Thus the observed mass density is within the confidence interval of the derived mass density and there is no significant difference between the observed and

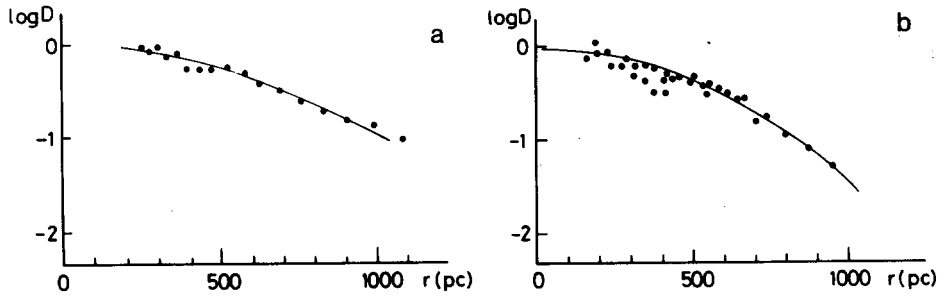

Fig.8 Parabola approximation of the empirical density curves: a): B8-A1 stars b): A type stars. The estimated values of the total local galactic mass density are 0.105 $M_\odot/pc^3$ and 0.159 $M_\odot/pc^3$ for a) and b), respectively.

computed local mass density. There are several papers, however, pointing towards the value of $\rho(0)=0.15\ M_{\odot}/pc^3$ thereby indicating the presence of a considerable amount of unseen matter near the Sun (*Oort 1965, Hill et al. 1979, Bahcall 1984*). Moreover the applicability of A type stars for determining the local mass density is also criticized (*King 1983, Bahcall 1984*) on the basis that they do not display a fully relaxed subsystem. We think, however, that the excellent fit given by a simple isothermal model to our empirical density curves of A type stars in our sample gives some support for the reliability of the procedure we applied to obtain the total mass density in our galactic neighbourhood.

CONCLUSIONS

We have studied the space distribution of interstellar matter and stars earlier than F7 in a 19.5 sq. degrees field centred on NGC 7686.

Using the spectral and colour data, we derived the interstellar absorption as $A_V=1.2$ mag.

After removing the effect of absorption we computed the spatial densities in the subsamples given by the spectral ranges of B8-A1, A2-A3, A4-A7, A8-F2, F3-F7. Normalizing the densities to the density at 500 pc we made a composite density curve for the A type stars.

The most significant remark to be made after inspecting the shape of the density curves obtained is that these curves do not display an inflexion indicating the possible presence of kinematically different subsystems as was found in our previous works and in the references listed therein.

We have compared our density curves with an exponential density distribution, with Camm's models, with Bahcall's model and with the two component model of Woolley and Stewart. We have found that the best fit is given by an isothermal model. Comparison with the WS model (yielding an inflexion by superposing two kinematically different isothermal components) indicated that the inflexion lies beyond the limit of

completeness of our sample. If the magnitude limit were to be extended by at least 1 mag. this could clear up whether this is in fact the case.

The best fitting isothermal model enabled us to compute the total mass density of matter near the Sun. We have obtained a value of 0.104 $M_\odot/pc^3$ for the B8-A1 group, and 0.159 $M_\odot/pc^3$ for the A type stars in our sample. The density obtained from the B8-A1 stars is probably underestimated because of a possible scale error of a factor of 1.24 due to the absolute magnitudes we used for this spectral group. Taking into account the uncertainties of velocity dispersions used in our computations the 0.108 $M_\odot/pc^3$ observed mass density does not differ on the one sigma level from the computed one. Results of other authors, however, point to a value of about 0.15 $M_\odot/pc^3$ indicating the presence of a considerable amount of dark matter near the Sun.

ACKNOWLEDGEMENTS

We are indebted to Dr. B. Szeidl for his advice on eliminating systematic errors from our colour data. The assistance of Mrs.I. Kalman in measuring the photographic UBV data is also acknowledged.

Budapest, December 16, 1985.

REFERENCES

Alexander, J.B., 1958, MNRAS, 118. 161.

Allen, C.W., 1973, Astrophysical Quantities 3rd.ed., Athlona Press London.

Bahcall, J.N., Soneira, R.M., 1980, Ap.J.Suppl.44.77.

Bahcall, J.N., 1984, Ap.J.276.169.

Balazs, L.G., 1975, Mitt. Sternwarte Ung.Ak.Wiss.No.68.(Paper I)

Balazs, L.G., 1977, The Cosmogonical Significance of the z Distribution of Stars in "Chemical and Dynamical Evolution of our Galaxy" IAU Coll. No.45.p.271.

Balazs, L.G., 1984, Statistics of A-Type Stars as Possible Indicator of Star Formation in "Astronomy with Schmidt-Type Telescopes" ed. M.Capaccioli, D.Reidel Publ.Co.p.269.

Camm, G.L., 1950, MNRAS 110.305.

Dolan, J.F., 1974,Astron. and Astrophys.35.5.

Eggen, O.J., 1962, R.Obs.Bull. No.42.

Gliese, W., 1969, Catalog of Nearby Stars (Veröff.Astr. Rechen-Inst. Heidelberg, Nr.22.)

Hildich, R.W., Hill, G., Barnes, J.V., 1983, MNRAS 204.241.

Hill, G. Hildich, R.W., Barnes, J.V., 1979, MNRAS 186.813.

Hoag, A.A., 1961, Publ.USNav.Obs. No.17.347.

King, I.R., 1983, On the Analysis of Motions Perpendicular to the Galactic Plane in "Kinematics, Dynamics and Structure of the Milky Way" ed. W.L.H. Shuter, D. Reidel Publ.Co.p.53.

Lacey, S.C., 1984, MNRAS 208.687.

McCuskey, S.W., 1966, Vistas in Astron. 7.141.

Oort, J.H., 1932, BAN 6.249.

Oort, J.H., 1965, Stellar Dynamics in "Galactic Structure", ed. A.Blauw and M.Schmidt, Univ. Chicago Press, p.455.

Palous, J., Piskunov, A.E., 1985, Astron. and Astrophys. 118.306.

Paparo, M., Balazs, L.G., 1982, Mitt. Sternwarte Ung.Ak.Wiss. No.82. (Paper II)

Perry, C.L., 1969, Astron.J. 74.139.

Spitzer, L., 1942, Ap.J. 95.239.

Spitzer, L., Schwarzschild, M., 1953, Ap.J. 118.306.

Svolopoulos, S.N., 1961, Ap.J. 134.612.
van Rhijn, P.J., 1960, Publ. Kapteyn Astr.Lab. Groningen No.61.
Villumsen, J.V., 1984, preprint (submitted to the Ap.J.)
Wielen, R., 1977, Astron. and Astrophys. 60.263.
Wielen, R., Fuchs, B., 1983, Velocity Distribution of Stars and Relaxation in the Galactic Disk in "Kinematics and Structure of the Milky Way" ed. W.L.H. Shuter, D. Reidel Publ.Co. p.81.
Woolley, R., Stewart, J.M., 1967, MNRAS 136.329.

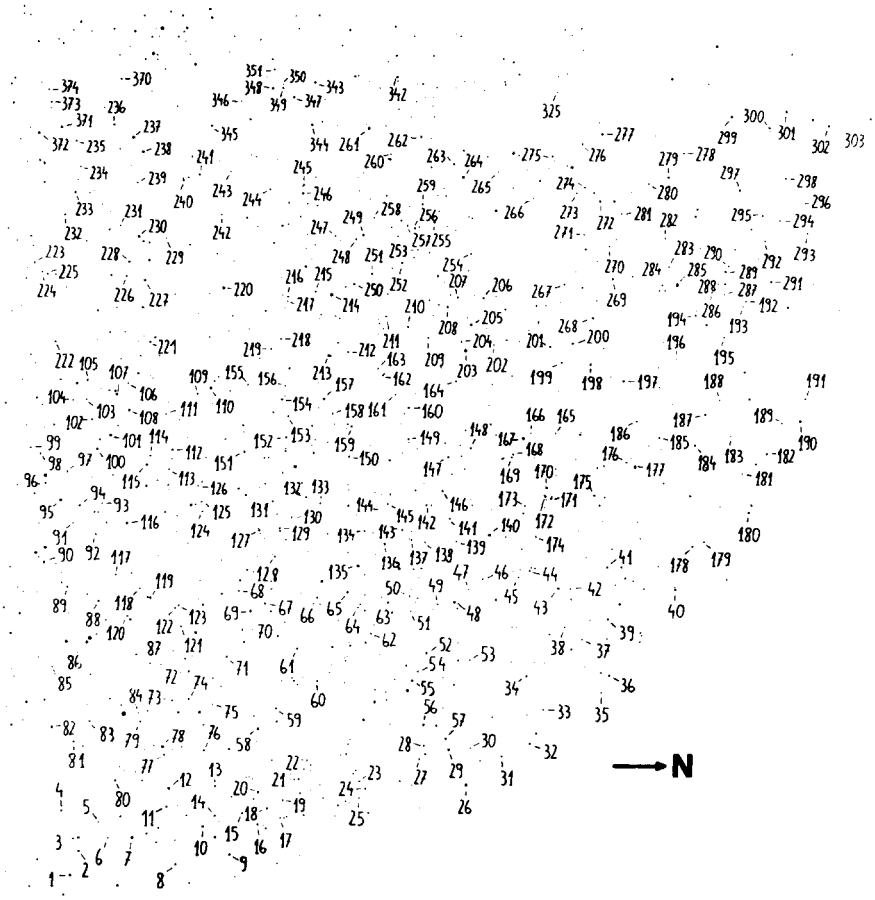

Finding chart of the survey stars

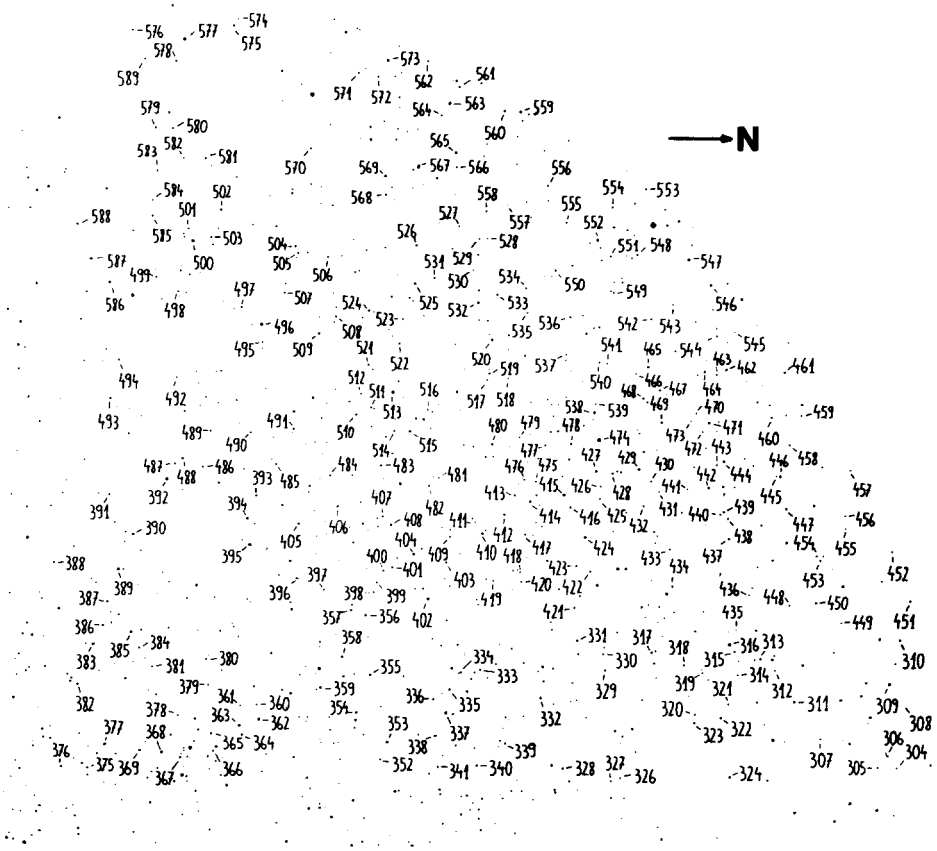

Finding chart of the survey stars

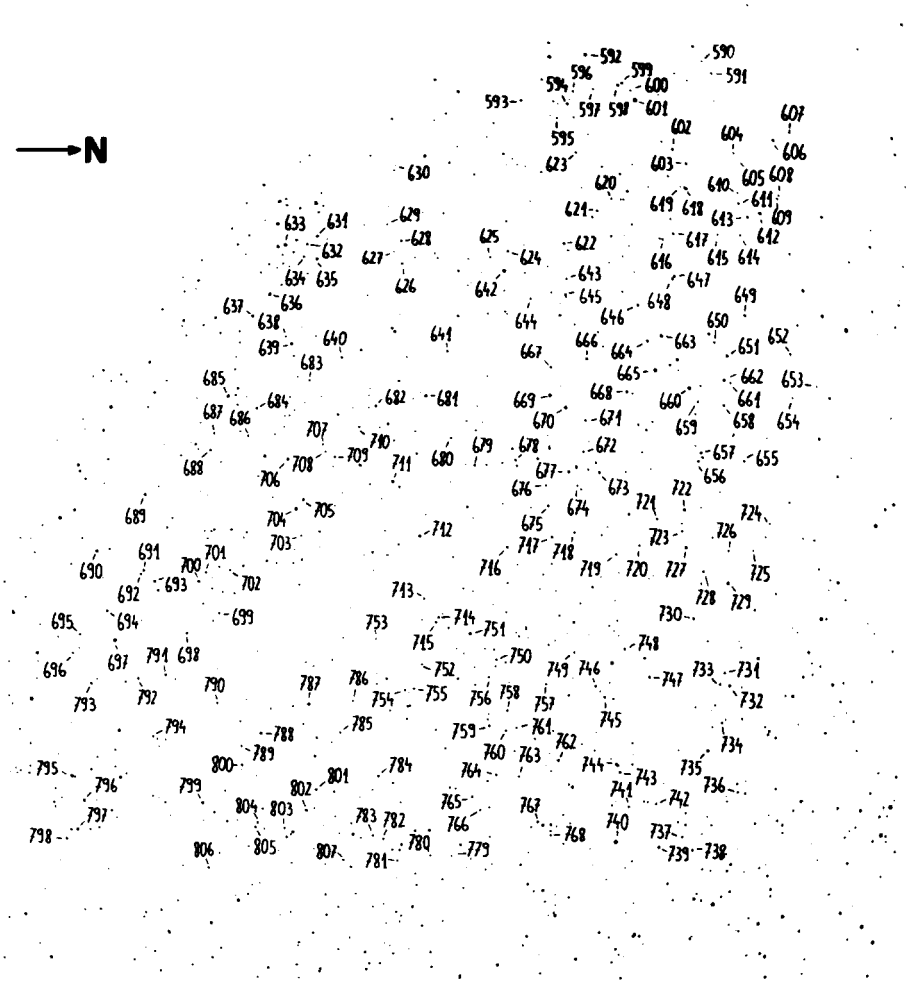

Finding chart of the survey stars

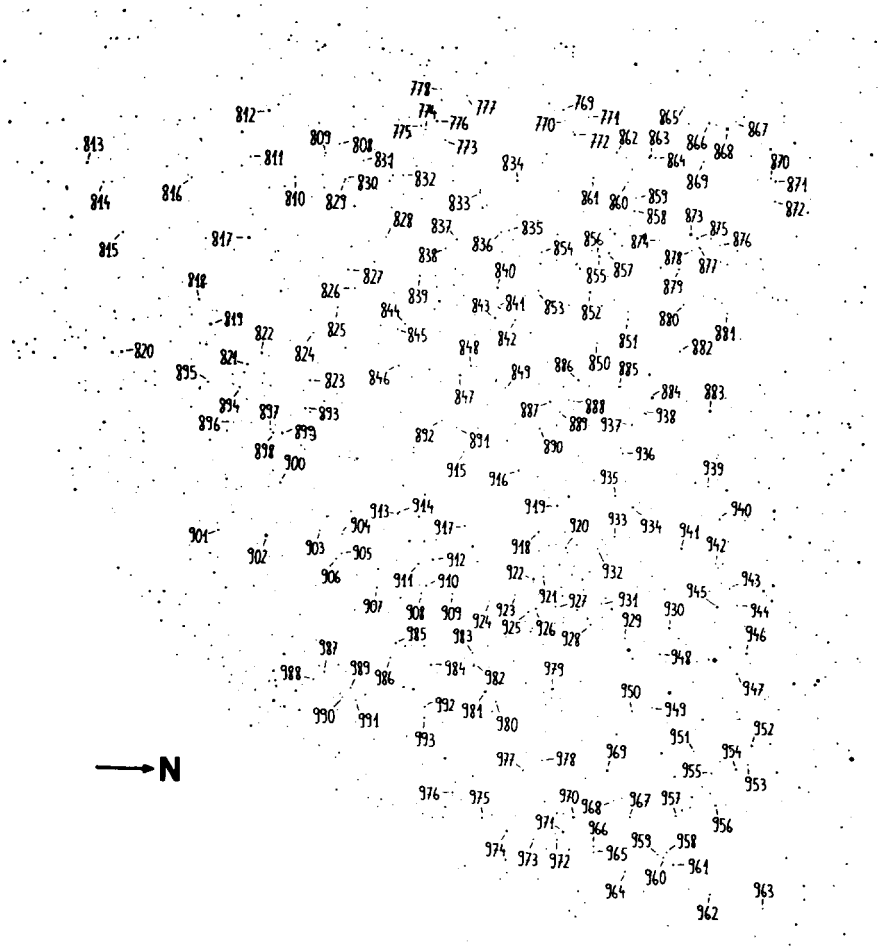

Finding chart of the survey stars

TABLE

Spectra and UBV data of survey stars

No.	Sp.	V	B-V	U-B	No.	Sp.	V	B-V	U-B
1	A9	9.58	0.51	0.19	51	A6	12.91	0.40	0.27
2	F7	10.39	0.84	0.16	52	F7	10.45	0.62	0.10
3	A2	10.77	0.34	-0.06	53	A0	12.47	0.36	0.03
4	A9	11.29	0.38	0.24	54	F6	11.63	0.47	0.11
5	A8	12.43	0.66	-0.02	55	F6	10.52	0.71	0.11
6	A2	12.12	0.37	0.13	56	F7	10.40	0.72	0.03
7	A0	9.38	0.30	-0.06	57	A2	10.24	0.28	0.30
8	A1	11.18	0.40	0.23	58	A2	10.00	0.30	0.18
9	F4	10.91	0.47	0.07	59	F7	11.09	0.50	0.12
10	F2	10.49	0.52	0.11	60	F6	11.57	0.58	0.18
11	F7	11.29	0.64	0.20	61	A1	11.58	0.26	0.12
12	F7	9.91	0.67	-0.02	62	F7	12.04	0.80	0.03
13	A7	11.75	0.51	0.33	63	F6	11.54	0.76	0.08
14	F7	11.16	0.73	0.00	64	B8	12.38	0.37	0.28
15	F0	11.80	0.60	-0.05	65	A1	11.15	0.13	-0.09
16	F7	11.28	0.79	0.09	66	A0	11.83	0.30	0.04
17	F7	11.84	0.90	0.13	67	F7	10.95	0.72	0.14
18	F7	11.42	0.69	-0.19	68	F7	11.85	0.64	0.19
19	F5	11.82	0.65	0.12	69	A1	9.98	0.17	0.13
20	F7	10.51	0.79	-0.11	70	F7	12.14	0.75	-0.04
21	F2	11.78	0.59	0.05	71	F5	11.37	0.53	0.14
22	A4	11.77	0.51	0.27	72	F7	11.08	0.68	0.16
23	A4	12.31	0.53	0.23	73	F0:	11.56	0.57	0.04
24	F7	11.59	0.81	0.05	74	F7	11.21	0.56	0.09
25	A1	12.22	0.56	0.12	75	A3	12.16	0.49	0.20
26	A1	8.97	0.32	0.19	76	F6	11.36	0.57	0.13
27	A7	11.77	0.59	0.00	77	F7	11.91	0.72	0.10
28	F7	11.15	0.92	0.25	78	A5	9.52	0.33	0.32
29	A2	10.60	0.31	0.08	79	F3	11.71	0.49	0.22
30	F7	11.92	0.77	0.01	80	F7	11.05	0.56	0.21
31	A2	11.22	0.59	0.06	81	F0	10.92	0.35	0.25
32	A5	10.82	0.46	0.18	82	F3	10.15	0.34	0.19
33	A4	11.76	0.48	0.32	83	F5	11.76	0.42	0.11
34	F2	10.84	0.49	0.22	84	F3	11.75	0.90	0.28
35	F6	11.26	0.61	0.22	85	F1	11.92	0.78	0.09
36	A5	10.83	0.51	0.21	86	A5	8.65	0.20	0.23
37	F7	11.74	0.61	0.26	87	F6	11.44	0.59	0.01
38	A0	11.58	0.36	0.19	88	F4	10.89	0.49	0.14
39	F0	11.32	0.40	0.33	89	F7	11.68	0.62	0.18
40	A3	10.46	0.32	0.45	90	A0	10.26	0.18	-0.04
41	A1	11.35	0.37	0.26	91	F4	12.22	0.66	-0.02
42	A5	11.86	0.38	0.37	92	F6	11.89	0.62	-0.08
43	F7	10.10	0.48	0.21	93	F7	12.54	0.44	0.05
44	A1	11.36	0.41	0.24	94	F6	10.67	0.61	-0.03
45	A0	12.26	0.36	0.19	95	A6	8.99	0.34	0.21
46	F7	11.17	0.64	0.15	96	F7	11.09	0.70	-0.12
47	A8	12.12	0.49	0.20	97	F7	11.72	0.67	-0.05
48	F5	11.04	0.47	0.27	98	F7	11.72	0.66	-0.09
49	F6	11.63	0.52	0.14	99	F7	11.68	0.71	-0.09
50	A3	12.09	0.29	0.36	100	F5	10.38	0.56	0.07

TABLE

No.	Sp.	V	B-V	U-B	No.	Sp.	V	B-V	U-B
101	A7	9.40	0.34	0.09	151	F6	10.75	0.50	-0.02
102	F7	11.86	0.75	-0.09	152	F6	10.91	0.66	-0.10
103	A3	11.79	0.42	0.17	153	F5	11.33	0.55	0.17
104	F7	12.02	0.60	-0.07	154	A2	11.01	0.20	0.03
105	F4	10.86	0.45	0.05	155	F0	12.27	0.30	0.12
106	A0	12.37	0.46	-0.02	156	F5	11.43	0.56	0.09
107	A1	10.52	0.19	-0.05	157	A5	10.25	0.38	0.11
108	F1:	10.49	0.34	0.16	158	F0	11.86	0.55	0.16
109	F7	11.45	0.78	0.02	159	A1	11.12	0.23	-0.09
110	A0	9.14	0.11	-0.04	160	F6	10.29	0.64	-0.17
111	A5:	11.86	0.38	0.32	161	F7	11.68	0.65	0.03
112	F6	10.34	0.54	-0.01	162	F5	11.63	0.67	-0.03
113	F4	11.54	0.64	-0.16	163	F7	11.67	0.69	-0.11
114	A1	11.61	0.30	0.20	164	F2:	11.11	0.52	0.15
115	A1	10.29	0.12	0.02	165	F7	11.68	0.78	0.05
116	A2	9.59	0.31	0.14	166	F7	12.06	0.64	0.00
117	F7	12.01	0.54	0.05	167	B8	8.45	0.04	-0.11
118	A7	12.37	0.34	0.06	168	F7	10.90	0.69	0.09
119	F6	9.94	0.56	0.04	169	A0	11.59	0.26	0.17
120	A0	11.68	0.30	0.12	170	F6	9.43	0.64	-0.06
121	A0	11.87	0.24	0.01	171	F7	11.00	0.53	0.12
122	F7	11.05	0.66	0.00	172	F5	10.96	0.63	0.05
123	F7	11.69	0.63	-0.26	173	F7	11.27	0.72	0.15
124	F5	11.91	0.61	-0.03	174	A1	11.42	0.44	0.24
125	A0	12.07	0.40	0.14	175	F7	10.90	0.68	0.28
126	A0	12.74	0.16	-0.42	176	A4:	11.39	0.26	0.25
127	F0:	10.43	0.52	-0.01	177	F1	10.29	0.52	0.57
128	A1	11.90	0.32	-0.09	178	F7	10.94	0.63	0.31
129	A6:	11.12	0.46	0.07	179	A8:	11.06	0.51	0.45
130	A0	12.34	0.25	0.09	180	A1	10.24	0.64	0.09
131	F6	11.57	0.57	-0.09	181	F7	11.06	0.78	0.24
132	F6	11.67	0.73	-0.04	182	A0	12.01	0.36	0.79
133	F7	11.59	0.71	-0.17	183	F7	11.26	1.15	-0.28
134	F6	11.52	0.68	0.01	184	A7	10.30	0.59	0.34
135	A0	8.86	0.01	-0.12	185	A1	11.09	0.42	0.61
136	A0	11.10	0.39	-0.04	186	F7	11.45	0.96	-0.07
137	A4	12.06	0.41	0.18	187	F1	9.51	0.57	0.33
138	F7	11.92	0.70	-0.03	188	A3	11.31	0.72	0.29
139	A6	12.09	0.41	0.18	189	F7	10.39	0.74	0.34
140	B9	9.28	0.04	-0.16	190	B7	8.83	0.24	0.04
141	F0	11.79	0.60	-0.01	191	F7	10.91	1.09	0.15
142	F7	11.53	0.71	-0.07	192	F3	11.30	0.71	0.20
143	A2	11.69	0.30	0.26	193	F3	11.25	0.81	0.19
144	A8	11.70	0.45	0.09	194	F4	10.68	0.80	-0.05
145	F7	11.48	0.79	0.26	195	A1	11.20	0.61	0.22
146	F4	11.39	0.60	-0.06	196	A0	11.93	0.47	0.24
147	F7	10.83	0.90	0.31	197	A3	10.24	0.31	0.17
148	F6	10.60	0.57	0.08	198	A3	10.52	0.26	0.26
149	A4	11.30	0.32	0.17	199	F6	10.88	0.61	0.11
150	F4	11.05	0.48	0.04	200	A3	10.32	0.34	0.09

TABLE

No.	Sp.	V	B-V	U-B	No.	Sp.	V	B-V	U-B
201	F4	10.18	0.68	-0.06	251	F7	10.55	0.71	0.01
202	A0	11.59	0.56	0.15	252	F6	10.45	0.61	-0.10
203	B6	7.93	-0.05	-0.23	253	F5	11.84	0.88	-0.02
204	F0	11.31	0.59	0.11	254	F2	11.65	0.65	0.11
205	A1	9.83	0.28	0.11	255	F4	11.17	0.71	0.32
206	A2	10.86	0.32	0.03	256	F7	11.21	0.75	0.12
207	F1:	11.41	0.51	-0.04	257	F7	11.51	0.71	-0.10
208	F7	10.40	0.88	-0.08	258	A3	12.16	0.36	0.06
209	A5	11.80	0.45	0.05	259	A2	11.07	0.43	0.13
210	A3	11.12	0.24	0.21	260	F7	11.53	0.62	0.01
211	F3	11.63	0.37	0.09	261	F5	9.28	0.46	-0.08
212	A2	11.88	0.55	-0.02	262	F5	10.94	0.55	-0.04
213	A1	10.48	0.24	-0.01	263	F0	10.94	0.41	0.07
214	B7	8.39	0.05	-0.06	264	A5	9.29	0.31	0.14
215	F5	10.87	0.57	0.18	265	A0	12.56	0.09	-0.06
216	F7:	11.79	0.72	0.02	266	A0	12.32	0.25	-0.12
217	F6	11.87	0.71	0.02	267	F7	10.87	0.73	0.03
218	F5	11.61	0.49	0.08	268	F7	11.47	0.60	0.01
219	A8:	11.48	0.55	-0.16	269	A0	10.79	0.26	-0.08
220	A0	8.66	0.17	-0.02	270	F4	11.49	0.74	-0.04
221	F7	10.64	0.67	-0.15	271	A8	11.91	0.45	0.08
222	F0:	10.54	0.45	0.00	272	F7	11.19	0.25	0.42
223	F7	11.49	0.65	-0.03	273	F4	11.97	0.66	-0.10
224	F7	12.01	0.57	-0.12	274	F7	11.48	0.67	-0.17
225	F6	11.35	0.52	0.08	275	F5	11.09	0.54	0.13
226	F3	11.01	0.56	-0.08	276	F7	11.22	0.62	-0.09
227	F5	10.14	0.58	-0.15	277	A6	10.72	0.28	0.11
228	A2	10.25	0.41	0.14	278	A9	11.26	0.53	0.14
229	A1	12.33	0.33	0.05	279	A0	10.31	0.52	-0.03
230	A2	9.40	0.32	0.13	280	A2	11.32	0.44	0.16
231	F7	11.41	0.78	-0.06	281	F7	11.57	0.71	-0.19
232	A6:	11.37	0.38	0.08	282	F7	11.41	0.74	-0.10
233	F5	10.68	0.48	-0.08	283	F7	11.25	0.59	0.13
234	F7	12.61	0.64	0.00	284	A7	11.11	0.48	0.21
235	F5	11.40	0.46	0.14	285	F6	10.49	0.68	-0.09
236	F7	10.56	0.63	0.01	286	A3	11.59	0.27	0.15
237	F2	8.95	0.47	0.18	287	A0	11.98	0.35	0.26
238	A1	9.46	0.12	-0.11	288	F7	10.55	0.78	0.13
239	A1	11.81	0.31	0.04	289	A1	10.53	0.54	0.18
240	A4	11.26	0.35	0.15	290	F7	11.18	0.78	0.20
241	F7	10.61	0.75	0.08	291	A0	10.27	0.41	0.20
242	F7	11.74	0.63	0.05	292	A2	11.06	0.66	0.06
243	F7	11.70	1.04	-0.05	293	F7	9.95	0.76	0.24
244	F7	10.77	0.65	-0.07	294	F6	10.95	0.90	0.04
245	A1	11.56	0.16	0.18	295	F7	10.18	1.01	0.02
246	A1	10.44	0.19	0.04	296	F7	10.68	0.79	0.27
247	F7	11.60	0.72	-0.02	297	A0	9.94	0.52	0.02
248	A2	11.84	0.35	0.08	298	A2	10.48	0.46	0.38
249	F5	10.28	0.51	0.28	299	A3	10.03	0.64	-0.06
250	A6	10.22	0.32	0.19	300	A2:	10.58	0.42	0.34

TABLE

No.	Sp.	V	B-V	U-B	No.	Sp.	V	B-V	U-B
301	F5	8.87	0.70	0.24	351	F7	11.95	0.40	0.10
302	A3	10.61	0.37	0.59	352	F7	11.72	0.60	-0.01
303	F7	10.47	0.51	0.49	353	F5	10.31	0.44	0.12
304	F7	11.16	0.58	0.69	354	F5	10.72	0.52	-0.09
305	F7	11.47	0.76	0.45	355	A7	11.08	0.26	0.09
306	F7	11.18	0.55	0.49	356	A6	10.98	0.26	0.19
307	F7	11.38	0.87	-0.11	357	F6	11.17	0.42	0.14
308	A0	11.32	-0.09	-0.14	358	F7	11.26	0.55	0.09
309	A0	8.91	0.08	0.39	359	F7	10.11	0.60	0.05
310	F6	10.12	0.41	0.57	360	F7	11.89	0.62	-0.22
311	F7	9.82	0.82	0.04	361	F7	12.23	0.82	-0.05
312	F0	11.39	0.55	0.20	362	B9	9.53	0.06	-0.04
313	F6	10.45	0.67	-0.13	363	A0	9.93	0.26	0.03
314	F7	11.41	0.65	0.12	364	A0	10.35	0.15	0.29
315	A8:	10.83	0.38	0.08	365	A8	11.18	0.38	0.10
316	B8	8.62	0.08	-0.13	366	F7	11.65	0.40	0.02
317	A1	11.01	0.28	0.03	367	F5	11.56	0.55	0.09
318	F6	11.22	0.62	0.17	368	F6	10.30	0.43	0.06
319	F7	11.97	0.69	-0.06	369	F7	11.29	0.43	0.16
320	F7	11.36	0.64	-0.28	370	A6	11.48	0.49	0.10
321	F3	11.46	0.57	0.08	371	A7	9.95	0.29	0.05
322	F6	10.51	0.60	-0.04	372	A2	10.21	0.48	-0.02
323	A2	10.77	0.48	0.08	373	A5	11.73	0.30	0.11
324	A0	10.29	0.34	-0.21	374	A0	12.58	0.30	0.12
325	A0	12.13	0.18	0.02	375	F4	11.98	0.44	0.01
326	F7	11.86	0.80	-0.08	376	A7	12.00	0.42	0.14
327	A4	12.06	0.44	0.15	377	A4	11.52	0.23	0.27
328	F7	10.81	0.58	0.05	378	A3:	12.52	0.18	-0.01
329	A4	11.03	0.34	0.04	379	A1	12.25	0.34	0.06
330	F2	11.61	0.57	0.02	380	F7	12.13	0.49	-0.20
331	F4	10.91	0.40	0.00	381	F7	12.19	0.65	0.37
332	F0	10.49	0.36	0.11	382	F7	11.27	0.58	-0.17
333	F7	11.44	0.46	0.00	383	A2	10.27	0.36	-0.06
334	F7	11.27	0.64	-0.18	384	F6	12.02	0.50	-0.07
335	A0	11.01	0.32	0.04	385	F6	10.07	0.54	0.01
336	F7	11.43	0.54	0.06	386	F6	11.41	0.50	0.10
337	B6	8.75	-0.06	-0.25	387	F4	10.74	0.49	0.09
338	F7	11.23	0.47	0.14	388	F5	11.14	0.45	0.17
339	F7	11.49	0.63	0.11	389	F5	9.10	0.39	-0.17
340	A0	11.39	0.25	0.10	390	A4:	10.46	0.10	0.15
341	F7	11.36	0.51	0.05	391	A5	11.77	0.16	0.17
342	F7	10.62	0.57	0.00	392	A0	9.17	-0.10	-0.20
343	A9	10.44	0.41	0.06	393	F7	11.31	0.49	-0.01
344	F7	9.83	0.74	0.00	394	F7	9.54	0.55	-0.04
345	A3	10.70	0.29	0.19	395	A4	9.56	0.91	0.46
346	A0	12.03	0.33	-0.07	396	A5:	12.10	0.13	0.16
347	F7	9.60	0.57	-0.05	397	F7	11.59	0.55	-0.16
348	A9	9.79	0.26	0.24	398	A9	12.17	0.49	-0.04
349	A4	11.07	0.14	0.20	399	A7:	12.16	0.46	-0.15
350	F7	11.97	0.72	0.23	400	F5	11.48	0.65	-0.13

TABLE

No.	Sp.	V	B-V	U-B	No.	Sp.	V	B-V	U-B
401	A2	11.76	0.29	0.19	451	A8	10.19	0.40	0.34
402	F4	9.45	0.50	-0.13	452	A0	11.35	-0.03	0.57
403	F4	11.45	0.51	-0.14	453	A0:	11.19	0.50	0.29
404	A1	10.58	0.13	-0.08	454	A4:	11.40	0.47	0.28
405	F7	10.41	0.53	-0.06	455	A0:	11.34	0.62	0.35
406	F7	10.95	0.61	-0.23	456	F7	11.24	0.50	0.23
407	F4	11.70	0.31	0.03	457	A0	11.45	0.12	0.46
408	F5	10.76	0.58	-0.08	458	A0	11.61	0.22	0.41
409	F5	11.99	0.57	0.25	459	F7	11.57	0.55	0.36
410	F5	9.86	0.63	-0.20	460	F7	11.08	0.40	0.20
411	A7	12.66	0.48	-0.16	461	F5	10.44	0.48	0.08
412	A7	10.86	0.33	0.05	462	A3:	11.59	0.15	0.18
413	F7	11.61	0.68	-0.16	463	F5	11.34	0.56	0.03
414	F6	10.13	0.57	-0.10	464	F1	10.93	0.36	-0.09
415	A1	9.35	0.05	-0.51	465	A0	10.69	0.14	-0.03
416	A0	10.78	0.26	0.00	466	A1	12.10	0.28	0.11
417	F7	11.52	0.61	-0.14	467	A8	11.27	0.39	0.18
418	F7	12.22	0.44	-0.01	468	F6	10.34	0.46	-0.01
419	F7	11.94	0.59	-0.20	469	A1	11.46	0.21	0.05
420	A3	12.23	0.38	0.00	470	F7	12.05	0.48	0.03
421	F7	11.41	0.63	-0.28	471	F7	10.67	0.47	0.14
422	F6	11.54	0.40	-0.02	472	F7	11.79	0.63	-0.08
423	F5	11.10	0.54	-0.19	473	F7	11.97	0.69	-0.03
424	A2	10.12	0.09	-0.14	474	B5	7.17	-0.18	0.18
425	A4:	11.64	0.51	-0.14	475	F7	11.39	0.54	0.06
426	F0:	11.69	0.38	-0.10	476	F5	11.73	0.51	-0.06
427	F5	10.10	0.54	-0.07	477	F3	11.94	0.47	0.04
428	F2	10.62	0.50	-0.21	478	A2	10.90	0.13	0.08
429	F6	9.81	0.43	-0.11	479	F7	12.04	0.56	0.00
430	F3:	12.23	0.45	-0.07	480	F0	10.41	0.29	0.11
431	F7	12.12	0.38	-0.03	481	F7	11.96	0.72	0.05
432	A0	12.03	0.10	0.01	482	F7	11.32	0.50	0.09
433	F7	11.54	0.65	-0.01	483	F7	10.97	0.60	-0.06
434	F6	10.64	0.40	-0.04	484	F7	11.48	0.54	0.10
435	F7	11.95	0.69	-0.21	485	F6	11.89	0.40	0.00
436	F2	11.68	0.61	0.04	486	F5	11.49	0.41	0.17
437	A7:	10.86	0.56	0.03	487	F7	10.93	0.66	-0.07
438	A5	11.59	0.43	-0.01	488	F6	10.87	0.43	-0.06
439	F2	11.15	0.31	0.04	489	F5	11.27	0.33	0.12
440	A5	11.75	0.50	-0.14	490	F7	11.70	0.44	0.26
441	F7	11.78	1.00	0.02	491	A5	11.47	0.28	0.16
442	F7	10.19	0.72	-0.06	492	F7	12.18	0.41	0.13
443	F7	11.56	0.61	0.03	493	F7	10.29	0.45	-0.09
444	A1	10.27	0.28	-0.02	494	F0	10.93	0.26	0.07
445	F7	12.92	0.78	-0.15	495	F7	11.73	0.41	0.13
446	F3	10.09	0.58	0.05	496	F6	8.16	0.27	-0.02
447	A3	10.67	0.49	-0.02	497	F5	11.55	0.43	0.13
448	F7	11.25	0.74	0.01	498	F5	11.70	0.25	0.07
449	A1	11.38	0.39	0.38	499	F4	11.13	0.32	-0.08
450	F2	10.46	0.65	0.04	500	F4	8.31	0.08	0.14

TABLE

No.	Sp.	V	B-V	U-B	No.	Sp.	V	B-V	U-B
501	F2	11.43	0.21	0.10	551	B9	11.92	0.36	0.18
502	F4	10.13	0.29	0.00	552	F1	10.66	0.06	0.55
503	F7	10.83	0.36	0.07	553	F7	11.31	0.29	-0.01
504	F7	10.77	0.49	0.09	554	F6	11.89	0.33	0.13
505	F7	11.44	0.40	0.19	555	F4	11.67	0.37	0.05
506	F5	12.03	0.27	0.23	556	F3	11.60	0.40	0.19
507	A1	12.10	0.06	0.22	557	F7	12.37	0.28	0.22
508	F1	11.39	0.26	0.15	558	A8:	11.70	0.30	0.17
509	A1	10.18	0.01	-0.33	559	A1	10.21	0.05	-0.10
510	F7	10.87	0.47	-0.06	560	F5	10.91	0.46	-0.16
511	A6	11.77	0.25	0.11	561	A7	11.55	0.21	0.26
512	F7	12.16	0.56	0.01	562	F7	11.68	0.09	-0.14
513	A3:	8.85	0.23	0.04	563	F2	9.97	0.46	-0.06
514	A1:	11.98	0.39	0.02	564	F6	11.69	0.45	-0.07
515	F7	10.69	0.00	-0.08	565	A0	9.61	0.10	-0.16
516	F3	11.91	0.32	0.13	566	F4	11.56	0.48	0.03
517	F7	12.18	0.41	0.15	567	F1	9.43	0.39	0.14
518	F6	12.15	0.54	-0.07	568	F7	11.38	0.58	0.18
519	F7	11.18	0.53	0.17	569	A7	9.52	0.36	0.06
520	F4	10.06	0.38	-0.04	570	A3	11.74	0.17	0.18
521	F4	11.31	0.36	-0.06	571	F3	11.13	0.59	0.10
522	A2	11.92	0.12	0.26	572	F7	11.38	0.50	0.05
523	F7	11.61	0.54	0.09	573	F5	8.96	0.41	-0.11
524	F7	10.94	0.39	0.05	574	A3	11.37	0.19	0.07
525	F1	9.99	0.34	0.17	575	A4	9.96	0.41	0.05
526	F1	11.50	0.34	-0.01	576	F6	9.77	0.63	-0.34
527	A0	12.24	-0.04	0.25	577	B5	8.00	-0.07	-0.15
528	F5	12.19	0.35	0.21	578	F6	11.37	0.48	-0.16
529	F7	11.95	0.46	0.06	579	A1	11.41	0.23	0.19
530	A6:	11.94	0.26	0.24	580	A8	9.98	0.31	-0.02
531	F7	11.64	0.46	0.01	581	F7	10.34	0.64	0.03
532	F7	9.82	0.48	-0.24	582	F5	11.12	0.36	-0.15
533	F6	11.07	0.36	0.14	583	F7	12.09	0.47	0.00
534	F7	11.95	0.23	0.16	584	F7	11.20	0.46	-0.04
535	F5	11.98	0.35	-0.08	585	A5	10.27	0.37	-0.04
536	F0	11.57	0.36	0.07	586	B9	9.06	0.01	0.05
537	F5	12.01	0.46	-0.04	587	A0	9.27	0.06	0.01
538	A1	9.53	0.19	0.12	588	F7	10.40	0.36	-0.04
539	F5:	11.97	0.41	-0.08	589	F3	11.01	0.30	-0.16
540	F5	12.23	0.35	0.24	590	F3	11.52	0.67	0.19
541	F2	11.66	0.39	0.09	591	F5	11.12	0.35	-0.17
542	F4	11.30	0.47	0.02	592	B8	9.34	-0.16	-0.02
543	F5	12.05	0.44	0.01	593	A3	11.27	-0.02	0.25
544	F7	11.65	0.55	0.19	594	A7	10.90	0.15	0.11
545	A0	12.66	0.04	0.26	595	F7	12.03	0.26	0.08
546	A3	10.51	0.09	0.22	596	F7	11.68	0.54	-0.19
547	A0	10.08	0.01	0.19	597	F7	11.65	0.39	-0.14
548	F4	11.40	0.39	0.05	598	A7	10.87	0.13	0.04
549	A0	11.73	0.39	0.17	599	A4	11.22	0.27	-0.04
550	A4	11.79	0.26	0.20	600	A7	12.11	0.13	0.13

TABLE

No.	Sp.	V	B-V	U-B	No.	Sp.	V	B-V	U-B
601	F3	8.03	0.34	-0.04	651	F7	9.40	0.50	-0.16
602	F5	10.22	0.45	-0.11	652	A5	11.06	0.20	0.06
603	A8	10.92	0.30	-0.01	653	F2	12.00	0.43	-0.18
604	F6	11.13	0.38	0.06	654	F7	11.54	0.86	0.21
605	F5	11.73	0.30	-0.15	655	F3	11.27	0.49	-0.02
606	F5	9.06	0.34	0.01	656	F7	11.18	0.52	-0.07
607	F0	11.66	0.39	-0.02	657	F5	10.86	0.47	-0.08
608	A8	10.92	0.21	0.23	658	A0	10.98	0.20	0.07
609	A2	10.76	0.18	0.20	659	F4	11.15	0.49	-0.04
610	F7	11.27	0.54	0.09	660	B7	8.58	-0.11	-0.37
611	A4	10.90	0.22	0.07	661	F2	11.49	0.69	-0.16
612	F5	9.07	0.18	0.06	662	F3	9.29	0.44	-0.20
613	F7	9.86	0.38	-0.02	663	A0	9.37	-0.21	-0.16
614	A3	11.24	0.33	0.30	664	F4	10.46	0.26	-0.03
615	F7	11.56	0.40	0.10	665	B9	8.39	-0.25	-0.04
616	F7	11.50	0.26	0.10	666	F6	10.47	0.49	-0.12
617	F7	10.94	0.37	0.07	667	A3	11.52	0.30	0.02
618	A0	9.38	0.07	0.02	668	F5	10.41	0.51	-0.14
619	F3	12.81	0.06	0.13	669	A0	8.95	0.25	-0.15
620	F7	12.06	0.39	0.03	670	F1	9.21	0.27	0.07
621	F0	11.48	0.28	0.02	671	F3	11.29	0.39	0.20
622	A9	11.08	0.18	0.29	672	A9:	11.75	0.29	0.13
623	F7	11.87	0.29	-0.07	673	A1	10.76	0.16	-0.18
624	F6	11.31	0.37	-0.03	674	F7	12.03	0.65	-0.01
625	F7	11.64	0.59	0.07	675	F7	11.58	0.47	-0.11
626	F6	10.93	0.30	-0.03	676	F5	11.88	0.34	0.12
627	F5	12.27	0.18	-0.01	677	A1	10.01	0.00	0.00
628	A5	11.01	0.17	0.17	678	A0	11.54	0.06	0.02
629	F7	13.26	0.50	-0.13	679	F7	11.12	0.46	0.03
630	F2	12.86	0.18	0.10	680	F7	11.55	0.57	0.52
631	A3	10.47	0.09	0.03	681	A0	9.63	0.04	0.08
632	A1	11.26	0.61	-0.42	682	F7	10.24	0.48	0.06
633	A0	9.51	-0.10	-0.03	683	F7	11.25	0.57	0.05
634	F5	10.98	0.30	0.14	684	F5	10.86	0.36	-0.05
635	F7	9.66	0.49	0.09	685	F7	9.53	0.26	0.18
636	A8	11.05	0.07	0.20	686	F7	11.88	0.30	-0.05
637	A0	9.95	-0.19	0.20	687	A3	11.73	0.15	0.35
638	F7	12.18	0.17	0.32	688	F6	11.08	0.34	0.07
639	A7	10.00	0.14	0.16	689	A0	10.54	-0.01	0.14
640	F4	10.79	0.07	0.36	690	A0	10.41	0.05	-0.08
641	A5	11.02	0.28	0.15	691	F0	10.59	0.34	0.04
642	B9	9.08	0.01	0.25	692	A0	11.69	0.37	0.04
643	F4	11.89	0.29	0.17	693	A3	10.92	0.03	-0.13
644	F5	11.56	0.40	0.24	694	F7	9.98	0.78	0.32
645	F3	11.03	0.36	0.06	695	F0	11.68	0.18	0.04
646	F7	10.38	0.75	0.16	696	F3	11.43	0.31	0.05
647	A6	11.10	0.24	0.09	697	F6	7.70	0.31	0.09
648	A0	10.74	0.21	0.22	698	A8	11.50	0.09	0.19
649	F6	9.59	0.47	-0.03	699	F7	11.61	0.26	0.24
650	F6	10.70	0.44	-0.10	700	F4	10.58	0.31	0.00

TABLE

No.	Sp.	V	B-V	U-B	No.	Sp.	V	B-V	U-B
701	F7	11.40	0.53	0.59	751	A0	9.67	0.02	-0.17
702	F2	11.51	0.51	0.13	752	F7	12.08	0.23	0.14
703	F5	12.02	0.48	-0.09	753	A0	12.33	0.41	0.12
704	F2	8.71	0.18	0.07	754	F4	11.29	0.26	0.20
705	A4	10.56	0.15	0.09	755	F6	11.00	0.41	-0.05
706	F5	9.92	0.34	-0.01	756	A4	12.16	0.15	0.40
707	F7	12.06	0.23	0.07	757	F6	11.75	0.48	0.11
708	F7	12.00	0.32	0.06	758	F6	11.18	0.39	-0.05
709	F6	11.54	0.32	0.06	759	F7	11.34	0.35	0.08
710	F3	11.76	0.32	0.04	760	A8:	11.80	0.37	0.20
711	B9	9.72	-0.07	0.07	761	F5	11.85	0.54	0.19
712	A1	9.89	0.10	0.08	762	F6	10.70	0.55	-0.09
713	F3	11.74	0.48	-0.01	763	A1	12.05	0.36	0.12
714	F6	11.46	0.29	0.29	764	A2	11.44	0.36	0.24
715	F7	11.45	0.53	0.05	765	F6	11.13	0.46	0.19
716	F7	10.96	0.54	0.14	766	F7	11.67	0.75	0.30
717	F6	10.22	0.50	-0.16	767	A9	11.16	0.37	-0.01
718	A3:	12.01	0.12	0.08	768	A0	12.26	0.03	-0.13
719	F5	11.58	0.33	0.02	769	A4	10.62	0.19	0.10
720	F2	11.62	0.39	-0.08	770	F7	12.22	0.64	0.01
721	A6	11.64	0.24	0.06	771	F2	11.92	0.34	0.07
722	F4	10.11	0.45	-0.25	772	A1	10.23	0.11	0.05
723	F5	12.06	0.27	0.07	773	F0	11.96	0.17	-0.11
724	F7	12.17	0.40	-0.01	774	A2	12.08	0.53	0.22
725	F7	11.85	0.36	0.02	775	A9	12.26	0.10	0.16
726	F7	11.79	0.40	-0.18	776	F2	10.58	0.33	0.10
727	A1	10.03	0.08	-0.04	777	F7	11.95	0.55	0.03
728	F7	11.26	0.59	-0.07	778	F7	12.05	0.40	0.32
729	F2	9.05	0.35	0.13	779	F7	12.12	0.46	0.00
730	F5	10.28	0.61	0.00	780	A3	12.46	0.32	0.09
731	A4	11.65	0.38	0.33	781	A5	12.61	0.15	0.08
732	A1	10.43	0.26	-0.22	782	F5	11.33	0.38	0.26
733	F7	11.13	0.58	0.03	783	F7	11.48	0.49	0.03
734	A2	11.82	0.32	0.07	784	A7	11.13	0.23	0.25
735	F5	10.25	0.46	-0.08	785	F7	11.93	0.45	0.12
736	F7	12.07	0.57	0.02	786	F7	12.14	0.38	0.13
737	F7	11.79	0.49	-0.04	787	A0	9.82	-0.07	0.24
738	F5	11.36	0.51	0.19	788	A6	10.00	0.15	0.38
739	F6	10.33	0.53	-0.03	789	F7	11.80	0.29	0.19
740	B6:	8.01	-0.11	-0.19	790	F7	11.93	0.41	0.20
741	F7	12.12	0.58	-0.26	791	A5	11.12	0.22	0.22
742	F2	12.01	0.26	0.13	792	F5	11.23	0.39	0.10
743	F1	11.52	0.48	-0.03	793	A9	11.00	0.25	0.08
744	A1	11.25	0.10	0.09	794	F7	11.04	0.53	0.37
745	F7	11.02	0.62	0.19	795	A3	9.28	0.00	0.06
746	F7	11.29	0.64	0.27	796	F2	9.23	0.31	0.24
747	F7	10.91	0.46	0.06	797	F2	9.80	0.39	0.07
748	F7	10.92	0.54	0.10	798	A6	10.87	0.21	0.17
749	F7	11.77	0.46	0.13	799	A7	9.90	0.15	0.26
750	F7	11.48	0.40	0.05	800	F5	11.01	0.23	0.11

TABLE

No.	Sp.	V	B-V	U-B	No.	Sp.	V	B-V	U-B
801	F5	11.00	0.20	0.13	851	A1	11.91	0.18	0.06
802	F7	10.20	0.34	0.14	852	F7	9.66	0.54	-0.20
803	F5	11.81	0.21	0.30	853	F7	11.53	0.75	0.20
804	A0	11.81	0.05	0.27	854	F3	11.63	0.31	0.06
805	F7	11.41	0.41	0.25	855	A5	11.17	0.34	0.04
806	F7	11.32	0.40	0.18	856	F7	13.03	0.75	-0.30
807	F4	11.84	0.31	0.11	857	A0	11.22	0.12	-0.17
808	F6	11.63	0.37	0.21	858	F7	11.11	0.54	-0.01
809	F6	11.44	0.50	0.14	859	F7	11.75	0.44	-0.04
810	F6	10.96	0.36	0.01	860	F7	12.07	0.48	-0.16
811	A5	11.53	0.15	0.20	861	A3	10.93	0.27	0.01
812	F7	9.25	0.23	0.08	862	F6	11.35	0.41	0.27
813	F7	9.37	0.50	0.08	863	F6	10.32	0.58	-0.12
814	F7	11.43	0.71	0.15	864	F7	11.31	0.33	-0.01
815	F7	10.95	0.59	0.11	865	F7	11.73	0.58	-0.22
816	F7	11.35	0.40	0.06	866	F0	10.38	0.51	-0.12
817	B8	8.11	0.11	0.21	867	F7	12.31	0.58	-0.14
818	A3	10.81	0.18	0.17	868	F3	8.09	0.41	-0.17
819	A1	9.21	-0.01	0.03	869	F7	11.59	0.54	-0.49
820	A1	9.78	0.05	0.29	870	F4	11.48	0.44	0.12
821	F6	10.01	0.48	-0.03	871	F7	10.75	0.64	-0.22
822	A2	10.66	0.14	0.13	872	F6	11.87	0.66	-0.16
823	F6	10.65	0.50	-0.04	873	A1	8.67	0.07	-0.05
824	F7	11.77	0.40	-0.09	874	A1	12.78	0.48	-0.17
825	F0	10.97	0.38	0.12	875	F6	9.52	0.58	-0.18
826	F1:	11.57	0.36	0.07	876	F7	12.02	0.49	-0.19
827	F4	11.14	0.37	0.11	877	F7	11.75	0.57	0.07
828	F7	11.64	0.75	0.38	878	F7	12.26	0.67	-0.39
829	F7	11.74	0.33	0.05	879	F7	10.69	0.62	-0.12
830	F6	11.23	0.40	0.02	880	F6	11.76	0.53	0.11
831	F7	12.05	0.46	0.11	881	F5	11.83	0.59	-0.18
832	F7	11.88	0.38	0.11	882	F5	11.03	0.39	-0.01
833	F7	11.80	0.29	0.07	883	F2	8.99	0.40	-0.16
834	F1	10.01	0.48	-0.12	884	B6	8.17	-0.07	0.07
835	F7	11.26	0.84	0.21	885	F7	11.50	0.47	-0.10
836	A8	12.00	0.21	-0.01	886	F5	10.73	0.18	-0.10
837	F6	10.61	0.43	-0.14	887	A6	10.71	0.22	0.13
838	F2	11.72	0.24	0.05	888	A1	12.52	0.32	0.06
839	A9	10.94	0.30	0.18	889	A3	12.31	0.20	0.13
840	F7	10.19	0.73	-0.09	890	A5	11.42	0.29	0.02
841	F4	11.69	0.40	-0.21	891	F7	11.81	0.53	0.18
842	F2	11.33	0.40	-0.02	892	F7	12.11	0.46	-0.20
843	A3	10.51	0.20	0.00	893	A3	10.97	0.07	0.13
844	A4	11.41	0.28	-0.03	894	F6	11.34	0.40	0.09
845	F7	11.78	0.36	0.07	895	F4	11.33	0.26	0.04
846	A1	11.17	0.07	-0.03	896	F7	12.71	0.31	0.13
847	F7	9.84	0.58	-0.05	897	F5	11.51	0.45	0.09
848	A1	11.21	0.12	0.08	898	A2	11.26	0.20	0.12
849	A1	12.12	0.20	0.15	899	A0	10.45	0.22	0.10
850	F5	11.57	0.39	-0.03	900	F6	10.91	0.41	0.10

TABLE

No.	Sp.	V	B-V	U-B	No.	Sp.	V	B-V	U-B
901	F7	11.24	0.54	-0.17	951	F7	11.86	0.80	-0.15
902	B7	8.32	-0.02	-0.07	952	A7	10.06	0.25	0.23
903	A1	12.26	0.26	0.19	953	A7	12.11	0.51	0.19
904	F7	11.95	0.54	-0.13	954	F6	9.88	0.73	0.02
905	F7	11.78	0.45	0.17	955	A4	11.48	0.32	0.16
906	F7	11.58	0.54	0.08	956	F2	10.52	0.43	0.02
907	F6	10.37	0.60	-0.04	957	F4	11.26	0.55	0.03
908	F4	11.67	0.47	0.05	958	F5	11.70	0.64	-0.03
909	F7	11.92	0.52	-0.01	959	A1	11.81	0.31	0.19
910	A6	10.75	0.23	0.71	960	F7	11.02	0.91	0.24
911	F3	10.56	0.44	-0.01	961	A1	11.30	0.13	-0.06
912	A1	10.00	0.24	-0.07	962	F6	11.24	0.61	-0.08
913	F3	11.59	0.31	-0.10	963	A2	11.64	0.43	0.15
914	A0	11.75	0.40	0.02	964	F7	10.98	0.75	0.03
915	F7	11.71	0.39	0.03	965	F7	11.79	0.50	-0.12
916	F6	10.92	0.55	0.01	966	F7	11.63	0.70	0.01
917	A2	11.76	0.11	0.09	967	A1	11.81	0.45	0.14
918	A3	10.96	0.12	0.27	968	F0	12.35	0.47	0.11
919	A1	10.76	0.18	-0.05	969	F0	9.23	0.32	0.08
920	F7	10.45	0.75	0.11	970	F7	9.81	0.75	0.29
921	F7	10.98	0.44	0.06	971	A7	10.23	0.37	0.08
922	F7	9.63	0.63	-0.17	972	A0	11.93	0.29	0.06
923	F6	11.60	0.67	-0.11	973	A9:	12.19	0.41	0.03
924	F7	12.14	0.80	-0.01	974	F6	9.73	0.63	-0.10
925	A2	11.08	0.26	-0.01	975	F7	11.06	0.56	0.00
926	F7	10.66	0.52	-0.01	976	A3:	11.25	0.38	0.00
927	F7	12.13	0.63	-0.19	977	F6	11.40	0.52	0.08
928	F6	11.01	0.48	0.13	978	A8	12.43	0.22	0.27
929	F7	11.59	0.70	0.03	979	F5	9.45	0.27	0.20
930	A7	10.76	0.45	0.01	980	F7	11.65	0.58	0.00
931	F7	11.72	0.76	-0.43	981	F0	9.52	0.35	0.14
932	F7	11.87	0.65	-0.19	982	F7	12.02	0.54	0.37
933	F2	12.01	0.51	-0.05	983	F7	11.89	0.67	0.21
934	F1	10.30	0.43	0.11	984	F7	10.78	0.68	0.07
935	F4	11.22	0.59	0.08	985	A8:	11.19	0.47	0.08
936	F7	11.79	0.58	0.05	986	F7	11.89	0.53	0.21
937	F6	11.24	0.25	-0.06	987	A0	10.76	0.22	0.10
938	F7	11.14	0.60	-0.12	988	F7	11.47	0.50	0.26
939	F3:	12.02	0.30	0.06	989	F6	11.57	0.59	0.18
940	F2	11.36	0.26	0.11	990	F7	12.61	0.42	0.14
941	A1	10.51	0.15	-0.09	991	A0:	12.18	0.33	0.38
942	A1	12.39	0.28	0.12	992	F7	11.00	0.54	0.23
943	F7	11.60	0.51	-0.05	993	F7	11.36	0.51	0.21
944	F7	11.88	0.59	-0.17					
945	A1	10.16	0.18	0.03					
946	F6	10.59	0.26	0.02					
947	A5	10.84	0.28	0.10					
948	F4	11.16	0.42	0.14					
949	F7	12.14	0.49	-0.10					
950	F7	11.67	0.57	-0.09					

COMMUNICATIONS
FROM THE
KONKOLY OBSERVATORY
OF THE
HUNGARIAN ACADEMY OF SCIENCES

MITTEILUNGEN
DER
STERNWARTE
DER UNGARISCHEN AKADEMIE
DER WISSENSCHAFTEN

BUDAPEST — SZABADSÁGHEGY

No. 86.

ERUPTIVE PHENOMENA IN STARS

EDITED
BY
L. SZABADOS

BUDAPEST, 1986

ISBN 963 8361 22 0
HU ISSN 0324 — 2234

Felelős kiadó: Szeidl Béla

Hozott anyagról sokszorosítva

8616412 MTA Sokszorosító, Budapest. F. v.: dr. Héczey Lászlóné

CONTENTS

LIST OF PARTICIPANTS

BULGARIA

Popova, M.D.
Tsvetkov, M.K.
Tsvetkova, A.G.

CZECHOSLOVAKIA

Chochol, D.
Harmanec, P.
Urban, Z.

G D R

Luthardt, R.
Richter, G.

HUNGARY

Jankovics, I.
Kelemen, J.
Olåh, K.
Szabados, L.
Szécsényi-Nagy, G.

POLAND

Schwarzenberg-Czerny, A.
Ziolkowski, J.

U S S R

Chavushian, H.S.
Denisov, A.A.
Dmitrienko, E.
Gasparian, K.G.
Gavrilov, V.V.
Gershberg, R.E.
Golovaty , V.V.
Goncharova, R.I.
Katsova, M.M.
Kimeridze, G.N.
Lozinskaya, T.A.
Merkulov, V.N.
Mirzoyan, L.V.
Natsvlishvili, R.S.
Pylskaya, O.P.
Romanov, Yu.S.
Sat, L.
Zalinjan, V.P.

INTRODUCTORY REMARKS

The Symposium "Eruptive Phenomena in Stars" was held at Konkoly Observatory, Budapest, from 10-12 September 1985. This biennial symposium of the multilateral co-operation "Stellar Physics and Evolution" was organized by Subcommission No. 3 ("Nonstationary stars") and the host institution.

Because one of the primary goals of these symposia is to gather as many astronomers taking part in the co-operative work as possible, the title of the conference was chosen so as to cover a very wide field. The eruptive variables themselves form a very diverse and inhomogeneous bunch of the variable stars. Recently, the fourth edition of the General Catalogue of the Variable Stars (Moscow, 1985) separated the cataclysmic variables from the eruptive (mostly young) ones. The realm of the variable stars, however, is not so simple that any sharp division of the main classes could successfully be applied. Eruptive phenomena do occur in other types of variables as well. The accompanying scheme clearly shows how the eruptive, cataclysmic, pulsating, rotating and eclipsing types of variability co-exist in real variable stars. This figure is the simplest example illustrating that the term "eruptive phenomena" embraces all types of variables in addition to the classical eruptive variables.

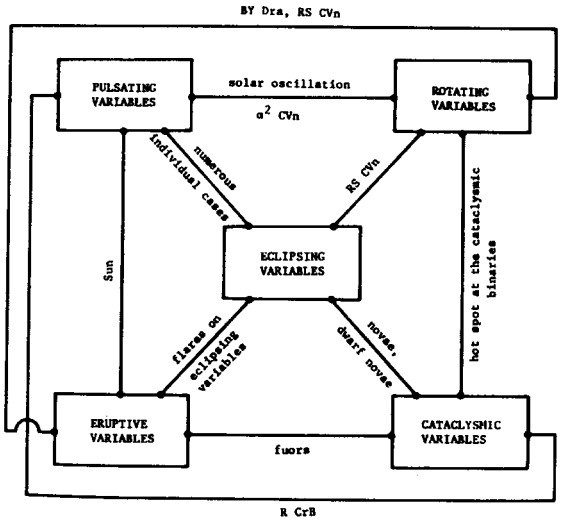

The 33 participants from six countries enjoyed five review lectures and 27 contributed papers. This volume contains a detailed version of the reviews and two-page abstracts of the contributions. The order is not strictly that in which they were presented.

I should like to thank all authors who submitted their manuscripts in camera-ready form at the beginning of the conference as requested thereby facilitating the editorial tasks. In particular, I express my gratitude to Mrs. É. Végvári and Mr. H. Shenker for their help in editing the proceedings. Our thanks go to the Hungarian Academy of Sciences for the financial support.

Budapest - Szabadsághegy, 6 February 1986

The Editor

"Eruptive Phenomena in Stars"
Comman. Konkoly Obs. Hung.
Acad. Sci., No.86, Budapest

THE NATURE OF DWARF NOVAE

Alex Schwarzenberg-Czerny

Warsaw University Observatory,
Warsaw, Poland.

0. Introduction.

In this paper only brief description of Dwarf Novae (DN) is given and interested reader is encouraged to look into reviews by Meyer (1985) and Smak (1984a) for more detailed account of theory and observations, respectively.

Reviews by Cordova and Mason (1982), King (1985), Pringle, (1981), Robinson (1976), Szkody, (1985) and Warner (1983) are on topics related to DN.

1. The Position of DN among Cataclysmic Binaries.

DN belong to Cataclysmic Variables. They all in fact are Cataclysmic Binaries (CBs) with short period consisting of a cool star (a red dwarf) filling its Roche Lobe and loosing mass, and a white dwarf. The stream of the gas from the cool star has excess angular momentum and it forms an accretion disk around a white dwarf, unless its magnetic field prevents it. Observations, discussed in detail by Robinson (1976), may be summed up as follows.

i/ The cool stars cause eclipses and their spectra are seen in the near infrared in some cases. Since their Roche Lobe is usually small, only red dwarfs may fit in. They have to fill it completely to transfer mass to their companions.

ii/ The disks are sources of blue and UV continuum and of emission lines with radial velocities varying in phase with the unseen star (the white dwarf). The lines are frequently doubled due to the Keplerian rotation of the disks and they show peculiar rotation shifts during eclipses, namely the low velocity cores are eclipsed first and the high velocity wings later. The collision region of the stream with the disk, called the hot spot, is a source of continuum and line emission variable in intensity and wavelength due to aspect and Doppler effects, respectively.

iii/ White Dwarfs are rarely seen directly, however their presence is inferred from the presence of high Keplerian velocities in the double lines from the orbits near the star's surface. In principle high velocities are permitted on orbits around neutron stars but gas crushing against their surface would emit too much soft X-rays to accommodate with observations.

The classification of CBs is based on their light curves with exception of systems with strong polarisation of light and, presumably, strong magnetic field called AM Her or Polar type stars (King, 1985).

DN have outbursts with amplitudes ranging from 2 to 6 magnitudes and which last several days and repeat on a time scale from weeks up to years (c.f. Fig. 1). Those outbursts are called normal outbursts. There are three subclasses of DN:

U Gem - type stars which suffer from normal outbursts alone.

Z Cam - type stars which after some outbursts fail to decline to the pre-outburst luminosity and remain in an intermediate state of brightness

for prolonged time intervals, called standstills. Eventually they complete the decline to quiescence and resume their normal outburst activity.

SU UMa stars apart from normal outbursts have superoutbursts lasting several times longer and with larger amplitude. The peak of superoutbursts is followed by a plateau.

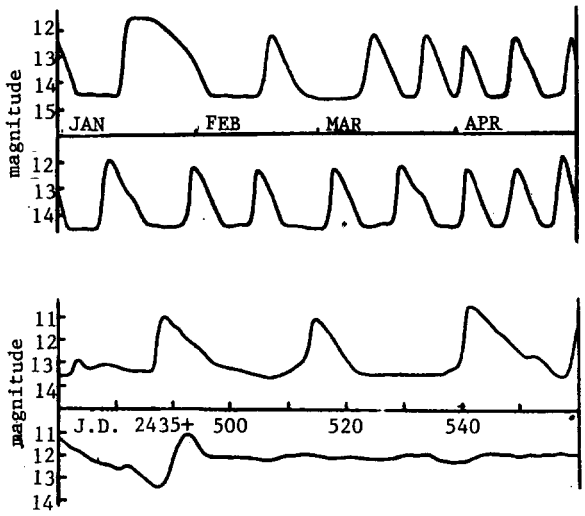

Fig. 1. The visual light curves of SU UMa (top) and Z Cam (bottom) (Glasby, 1968). Units are 30 and 10 days, respectively, and one magnitude.

Other CBs are Novae (N), which undergo violent outbursts, with amplitudes significantly exceeding 10 magnitudes, Recurrent Novae (RN) which multiple outbursts were observed and Nova-like stars (NL) which resemble old novae but were not seen in outburst. It is believed that outbursts of N and RN are thermonuclear explosions of white dwarf envelopes and we shall not concern with them any more in this paper.

2. $\dot{M}$ B P classification.

We shall demonstrate that three well defined theoretical parameters of the systems suffice to recover the same classification. The parameters, namely the accretion rate $\dot{M}$, the strength of magnetic field B and orbital period P, can be estimated from observations independently of the light curve.

The main source of energy in CV is gas falling down to the white dwarf, so time-averaged luminosity of CV is proportional to the accretion rate $\dot{M}$ and the visual rather than bolometric luminosity may be used since it is less sensitive to unknown mass of the white dwarf. Magnetic fields B are not measured directly but their presence is inferred in Polar stars unambigously from their light polarization.In the three dimensional space defined by the parameters $\dot{M}$ B P CB stars tend to group according to their variability class (see Fig. 2).

RN, N and NL stars are unresolved by the MBP classification, however, they all could have unobserved outbursts in the past and thus it is likely they are all the same but differ by the frequency of their outbursts. The Intermediate Polar (IP) and DQ Her (DQ) stars may be

just one subclass (King, 1985). CB's form a highly inhomogeneous class and it has to be kept in mind the segregation is not strict. Among one hundred of systems in Ritter's (1984) catalogue HT Cas, UU Aql, VW Vul, V2051 Oph, T Leo, TU Men, CP Lac and AM Her, 1E2003+225, EX Hya lay on the wrong side of period border while GK Per and VY Aqr are simultaneously members of N and U classes.

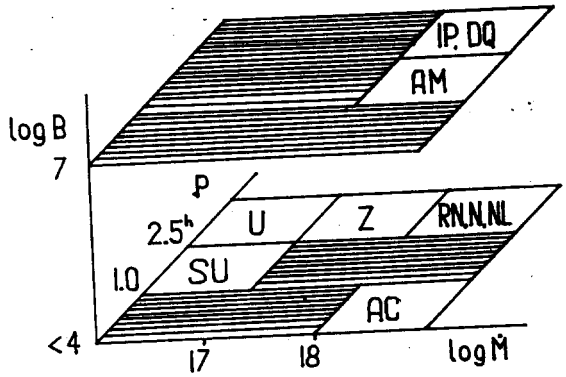

Fig. 2. The MBP classification of Cataclysmic Binaries. See text for details.

3. Stationary Accretion Disks.

In thin stationary disks radial gradients are smaller than those vertical by a ratio of thickness to radius $H/R \sim 1/30$ and may be neglected in the vertical structure equations. As in the stellar case there are four equations with the independent variable being fractional surface density rather than fractional mass. For our purpose suffice to use dimension relations:

$$
\begin{aligned}
&\Sigma \sim H\rho && \text{continuity}\\
&kT/\mu \equiv v_s^2 \sim v_k^2 (H/R)^2 && \text{hydrostatic equilibrium}\\
&\sigma T^4 \sim \Sigma \nu \omega^2 + \text{NTE} && \text{energy balance}\\
&T/T_e \sim (\Sigma\kappa)^{\beta/4} \qquad \beta = 1,\ \beta = 4\frac{\gamma-1}{\gamma} && \text{rad. transport, conv.}
\end{aligned}
\tag{1}
$$

where v_s and v_k are sound and Keplerian velocities and T and T_e are central plane and effective temperatures.

For lack of better theory we are forced to use α- prescription for viscosity: $\nu \sim \alpha v_s H$ where $\alpha \approx 0.2$ agrees with observations. Time scales and velocities of propagation of perturbations to the stationary disk are listed in Table 1.

Solution of the structure equations gives T - Σ relation (Hoshi, 1979), an analogue of the stellar mass - luminosity relation:

$$(\mu\sigma/k\omega)^{1/(\beta+1)} (T^3/\kappa^{\beta}\alpha)^{1/(\beta+1)} \sim \Sigma \tag{2}$$

In sufficiently high temperatures opacity κ, dominated by the electron scattering, is constant and Σ decreases with T. However, as temperature drops below 10000 K, hydrogen recombines and opacity

decreases so drastically that it overcompensates the decrease of the temperature and rises. At still lower temperatures opacity varies slower and decreases with T again. A complication caused by switching on the convective transport does change the exponent but does not change the general character of the T - Σ relation (Fig. 3). Since energy losses due to radiation are balanced by the gain due to viscosity, temperature increases as the local accretion rate increases and reverses.

Table 1.

time	velocity	type
$1/\omega$	$\omega R \equiv v_k \sim (GM/R)^{1/2}$	orbital
$1/\omega$	$v_k(H/R)$	vertical dynamic
$1/\omega\alpha$	$v_k(H/R)\,\alpha$	vertical thermal
$1/\omega\alpha\,(H/R)^{-1}$	$v_k(H/R)\,\alpha$	front propagation
$1/\omega\alpha\,(H/R)^{-2}$	$v_k(H/R)^2\,\alpha$	accretion.

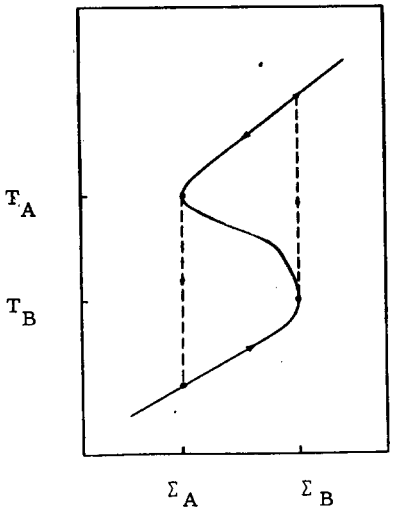

Fig. 3. Log Temperature - Log Surface Density plot for a given location in the disk.

4. Non-stationary Disks.

The stability of the disk depends on the fate of the perturbations with the thermal time scale. On one hand, the dynamical time scale is shorter than the thermal one so the hydrostatic equilibrium holds. On the other hand, the surface density remains practically constant during the thermal time scale. Out of the thermal equilibrium cooling is not compensated by heating and the NTE term in Eqtn. 1 does not vanish. Since they both enter in the same place in Eqtn. 1, the NTE term out of

the equilibrium has the same effect as the departure of the α-viscosity term in the equilibrium from its original value for α_o. Thus, the disk with the α_o-viscosity during cooling resembles the stationary disk with the α-viscosity, where $\alpha > \alpha_o$ (Smak, 1984). Such disk's place in Fig. 3 is to the left of the equilibrium line and it cools on the thermal time scale, at nearly constant surface density, moving vertically down in Fig. 3. By virtue of similar arguments disks to the right of the line heat up and move vertically up.

Stationary disks on the middle branch of $T - \Sigma$ relation are locally thermally unstable: if cooled a little bit, they would continue cooling till they reach the bottom stable branch or heated they would reach the top stable branch. Thus, for a range of accretion rates no stationary disk may exist. What happens, if mass is supplied at such rate? Let the disk be originally cool and it allows mass through at slower rate than it is supplied. The density in the disk rises and it evolves slowly, on the accretion time scale, up the equilibrium line. After some time the density reaches the maximum value on the stable branch, Σ_B, and the disk falls out of the thermal equilibrium, heating up on the thermal scale till the top stable branch is reached. However, now the local accretion rate in it is faster than the supply rate, surface density decreases down to Σ_A and and again the disk falls out of the thermal equilibrium and it lands back on the bottom cool branch. In such a way locally the disk follows a limit cycle. Its global behaviour depends on synchronisation of the local cycles.

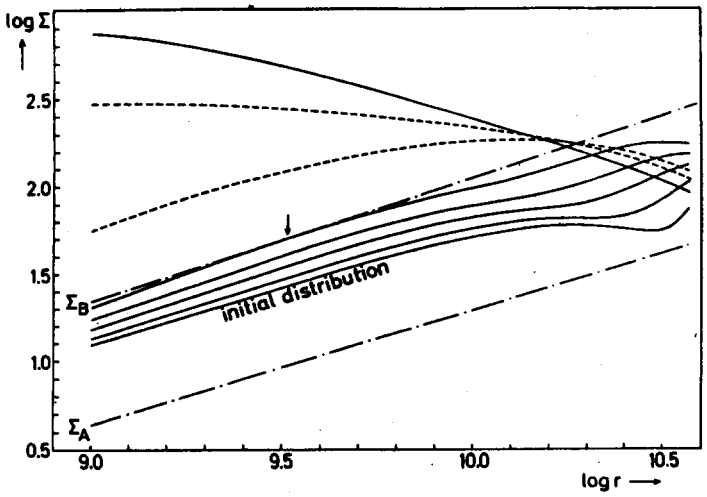

Fig. 4. Log Surface Density - Log Radius plot for the whole disk. It evolves from the bottom to top distribution of density. Start of outburst is marked with an arrow. Dot-dashed lines mark the instability region (Meyer and Meyer-Hoffmeister, 1984)

Generally, disks evolve on the accretion time scale R^2/ν, subjected to the mass and angular momentum conservation conditions. One

consequence of the conservation of momentum is that the accretion rate for a ring in the disk is proportional to the rate at which a net couple, resulting from non-equality of the viscous torques at inner and outer boundary, removes its angular momentum. The rate of the accumulation of mass in the ring is proportional to the gradient of the accretion rate (c.f. Lightman, 1974, for the rigorous diffusion equation):

(3) $\dot{M} \sim \partial(\Sigma\nu)/\partial r \qquad \partial\Sigma/\partial t \sim \partial^2(\Sigma\nu)/\partial r^2$

On the surface density - radius plot (Fig. 4) two lines delimit the instability region. Let us consider again a cool disk to which mass is supplied at the rate high enough to cause its accumulation. Surface density increases and the disk falls out of the equilibrium in the ring where first violation of the Σ_B limit occured. During the thermal time scale the ring reaches again equilibrium in the hot, high viscosity state. Small viscous torques from outside and inside the ring are not capable to balance its internal torques, so the ring expands in and out. Some mass gets into the adjacent rings, thus helping to start transition there. In effect transition fronts propagate from the initial ring inwards and outwards.

The fronts move faster than the accretion velocity since they are accelerated by steep gradients. On one hand the velocity of the front is the ratio of its thickness to the time of regaining equilibrium, the thermal time scale in our case, $v_f \sim l/\tau_t$. On the other hand, the accretion rate and so the velocity, are proportional to the rate of viscosity increase to the front thickness: $v_f \sim \nu/l$. Combining the two equations we get the answer given in Table 1. In a similar fashion the reverse transitions propagate. In effect, all limit cycles in the unstable part of the disk are synchronised within time shorter than the accretion time scale and longer than the thermal time scale (Meyer, 1984).

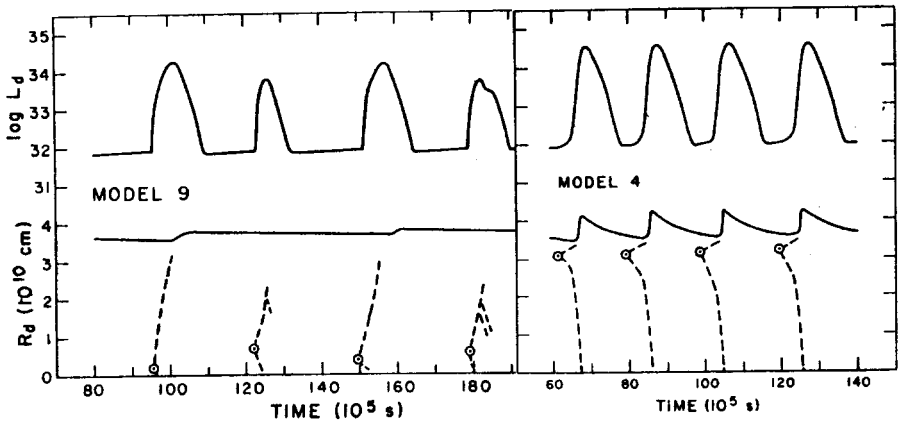

Fig. 5. Calculated bolometric light curves and location of transition fronts in type A (right) and type B (left) outbursts of DN (Smak, 1984b).

The detailed calculations of the evolution of accretion disks were conducted by Meyer and Meyer-Hoffmeister, (1984), Smak, (1984b) and also by Papaloizou et al. (1983) and Mineshige and Osaki (1983). In their models disks in DN in quiescence remain cool and accumulate mass on the

accretion time scale. Eventually, after accumulation of sufficient mass the transition starts and during the front propagation time scale the whole disk becomes hot at the beginning of an outburst. The outburst lasts for the accretion time, and eventually density decreases so that the reverse transition stops it.

The authors of calculations found two types of outbursts possible:

- type A which starts near the rim of the disk and propagates inwards, they tend to repeat periodically,
- type B which starts inside the disk and propagates outwards. The latter does not leave the disk in the original state, so alternate or irregular strength and frequency outbursts occur (see Fig. 5).

They were able to reproduce the observed ratio of the length of the outburst to the length of the whole cycle only with an arbitrary decrease of viscosity during quiescence. Meyer and Meyer-Hoffmeister (1984) gave some justification of this modification.

5. Evidence from Observations.

In a stationary flow both the spot and disk are powered by the accreted gas and in quiescence the ratio of their luminosities should be equal the ratio of the corresponding gravity potentials: $L_s/L_d \sim (R_d/R_{wd})^{-1}$. In fact the spot is too bright by a factor of 10 so that mass accreted by the spot during quiescence is accumulated in the disk and it is released during an outburst (Osaki, 1974). Indeed, the ratio of luminosities averaged over the outburst cycle is correct.

Paczynski and Schwarzenberg-Czerny (1980) strengthened the argument using more realistic models of the disk and spot to estimate the accretion rate. The estimates of the spot's luminosity from UV observations (Wu and Panek, 1982) and 2D hydrodynamic models of the flow in the spot (Rozyczka and Schwarzenberg-Czerny, 1986) lend further support to Osaki's hypothesis.

Osaki also noted that the cycle length - amplitude relation in DN is typical for a limit cycle proposed.

Smak (1984a) presented evidence that dwarf novae indeed occupy an instability strip of accretion rates as expected from the theory. We stress that GK Per is a true bilingual Rosetta stone in that its disk is cool enough to allow DN instability in its outer parts and at the same time it has accretion rate sufficient for a nova. It is worth of notice that no outbursts are observed in Polar stars where no disks exist but envelopes of the red stars should not be affected by companions magnetic field and where the accretion rate on occasions fall to the same level as in DN in quiescence.

Data for detailed comparison of outbursts are scarce. On one hand, theoretical models need further elaboration in order to give colours and spectra for outbursts of real DN. On the other hand, few outbursts were observed from the beginning to the end and with wide spectral coverage.

A complete outburst of VW Hyi was observed in the UV and visual bands simultaneously (Schwarzenberg-Czerny et al., 1985). Similarity of the observed light curves presented in Fig. 6b with those calculated for the type A outburst (Fig. 6a) suggests that outburst started near the disk's rim. At the very beginning, the UV flux and spectrum of the disk remained the same as in quiescence while the visual flux raised substantially (Fig. 7).

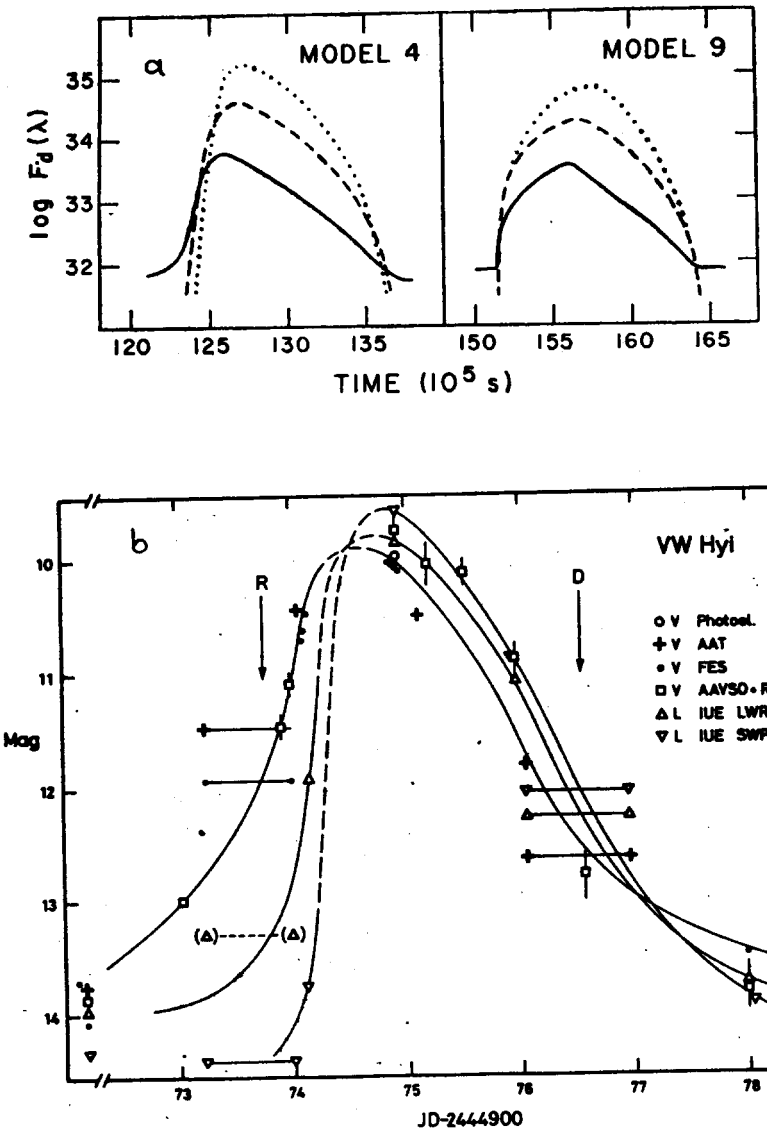

Fig. 6. Monochromatic light curves for 5500 Å (solid), 2500 Å (broken) and 1200 Å (dotted lines): a) calculated (Smak, 1984b), b) observed for VW Hyi (Schwarzenberg-Czerny et al., 1985). Note the delay of 1200 Å curve with respect to 5500 Å one.

The rise of the UV flux was delayed by a day and it took only several hours. Presumably in that time the transition front reached to the centre of the disk. Similar delay was observed in outbursts of RX And, SS Cyg and U Gem compiled by Szkody (1985). Widening of optical eclipses at the beginning of outbursts (Vogt, 1981a) is understandable for A type outbursts.

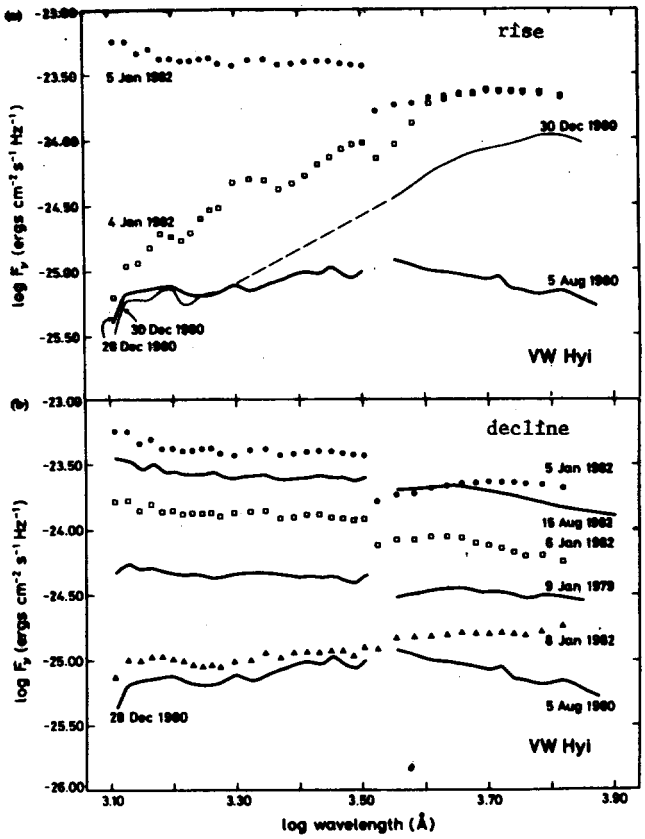

Fig. 7. Evolution of the continuous spectrum during the rise of the same outburst as on Fig. 7b (Schwarzenberg-Czerny et al., 1985).

No outburst observed in detail was of type B, but alternate type outbursts, known for long in SS Cyg and other DN, may be of that type.

6. Unresolved Problems and Future Prospects.

6.1 The SU UMa Syndrome.

Apart from superoutbursts SU UMa stars possess other distinct properties. Their periods (except for TU Men) are shorter than 2-3 hours period gap. The superoutburst light curves display modulation, called superhump, and with period by several percent longer than the orbital

period (Warner, 1983).

Observations of eclipsing systems indicate that it is the disk that becomes bright during the superoutbursts. They appear to be triggered by normal outbursts, but, since the accretion time scale may not be longer than the duration of normal outbursts, they are aided by the increased mass transfer. At least in one star, VW Hyi, there is a slight increase of mass transfer during the normal cycles preceding a superoutburst (Vogt, 1985) and correlations exist between the length of normal cycles and occurrence of superoutbursts (Smak 1985).

The amplitudes of superhumps do not depend on inclination and their peaks are too narrow for an aspect effect being responsible for them. Thus, they are the intrinsic variations of brightness.

The mechanism of superoutbursts is not clear. The red star instability model may enjoy here some success (Charles et al., 1985) although alternative explanations for superhumps and/or superoutbursts were proposed (Papaloizou and Pringle, 1979, Vogt, 1981b, Warner, 1983, Hensler, 1985).

6.2 Mass Supply.

The nature of CB's depends so much on the mass transfer that their ultimate explanation has to await clarification of the mechanism which supports the transfer. The latter requires angular momentum loss from the binary and/or expansion of the cool star.

One way of angular momentum loss, by the gravity radiation, is known to be efficient for short period systems only (Paczynski, 1967, Faulkner, 1971). However, there are plenty of long period systems with high accretion rate. Verbunt and Zwaan, (1981), Spruit and Ritter, (1983) reworked the magnetic braking model, involving a wind from the cool star, to explain both mass transfer and the period gap in CBs.

If the companion happens to be a giant, the nuclear time scale for expansion is short enough to ensure sufficient mass loss, as in case of GK Per. In the general case, however, the observed mass loss of cool stars is faster than expected by theorists. To decide whether evolution off the main sequence and/or departures from thermal equilibrium play role in the red stars more measurements of their radii are required (Wade, 1981).

Instability of the mass transfer on the time scale short in comparison to the stellar thermal time scale (not the envelope time scale) is observed in SU UMa stars (see Section 6.1) and in Polar and NL stars (so called antioutbursts).

References

Charles, P.A., Bath, G.T, Clarke, C.J., Whitehurst, R., and Bailey, J., 1985, in "Recent Results on Cataclysmic Variables", ESA workshop in Bamberg, ESA, Paris,

Cordova, F.A., and Mason, K.O., 1982, Cataclysmic variable stars from X-ray to IR wavelength: Recent results on continuum distribution, IAU Trans. Vol. XVIIIA,

Faulkner J., 1971, Astrophys. J., 170,99,

Glasby, J.S., 1968, Variable stars, Constable,London,

Hensler, G., 1985, Astron. Astrophys., 148,423,

Hoshi, R., 1979, Progr. Theor. Phys., 61,1307,

King, A., 1985, in "Recent Results on Cataclysmic Variables", ESA workshop in Bamberg, ESA, Paris,

Lightman, A.P., 1974, Astrophys. J., 194,429,

Meyer, F., 1984, Astron. Astrophys., 131,303,

Meyer, F., 1985, in "Recent Results on Cataclysmic Variables", ESA workshop in Bamberg, ESA, Paris,

Meyer, F., and Meyer-Hoffmeister, E., 1984, Astron. Astrophys., 132,143,

Mineshige, S. and Osaki, Y., 1983, P.A.S.J., 35,377,

Osaki, Y., 1974, P.A.S.J., 26,429,

Osaki, Y., 1985, Astron. Astrophys., 144,369,

Paczynski, B., 1967, Acta Astron., 17,287,

Paczynski, B. and Schwarzenberg-Czerny, A., 1980, Acta Astron., 30,127,

Papaloizou, J., Faulkner, J., and Lin, D.N.C., 1983, M.N.R.A.S., 208,721,

Papaloizou, J., and Pringle, J.E., 1979, M.N.R.A.S., 189,293,

Pringle, J.E., 1981, Ann. Rev. Astr. Astrophys., 19, 137,

Ritter, H., 1984, Astron. Astrophys. Suppl., 57,385,

Robinson, E.L., 1976, Ann. Rev. Astr. Astrophys., 14, 119,

Rozyczka, M., and Schwarzenberg-Czerny, A., 1986, in preparation,

Schwarzenberg-Czerny, A., Ward, M., Hanes, D.A., Jones, D.H.P., Pringle, J.E., Verbunt, F. and Wade, R.A., 1985, M.N.R.A.S., 212,645,

Smak, J., 1984a, P.A.S.P., 96,5,

Smak, J., 1984b, Acta Astron., 34,161,

Smak, J., 1985, submitted to Acta Astron.,

Spruit, H.C., and Ritter, H., 1983, Astron. Astrophys., 124.267,

Szkody, P., 1985, in "Recent Results on Cataclysmic Variables", ESA workshop in Bamberg, ESA, Paris,

Verbunt, F., and Zwaan, C., 1981, Astron. Astrophys., 100,L7,

Vogt, N., 1981a, habilitation thesis (in German), Bochum University,

Vogt, N., 1981b, Astrophys. J., 252,653,

Vogt, N., 1983, Astron. Astrophys., 118,95,

Wade, R.A., 1981, Astrophys. J., 246,215,

Warner, B., 1983, Interacting Binaries, NATO Advanced Studies Institute, Cambridge,

Wu, C.-C., and Panek, R.J., 1982, Astrophys. J., 262, 244.

"Eruptive Phenomena in Stars"
Comm. Konkoly Obs. Hung.
Acad. Sci., No. 84, Budapest

KUWANO-HONDA'S PECULIAR OBJECT (PU Vul) AND SOME PROBLEMS OF EXTREMELY SLOW NOVAE

R.E. Gershberg

Crimean Astrophysical Observatory
Crimea, Nauchny 334413, USSR

The results of many years' photometric, spectral, spectrometric and polarimetric observations of Kuwano-Honda's peculiar object (PU Vul) are briefly given. They permit this object to be attributed to anomalous slow novae of the RT Ser type and its observable properties to be connected with results of theoretical calculations of surface thermonuclear flares in binary systems containing accreting white dwarfs and with ideas on dust formation during nova explosions.

For six years a team of investigators of non-stationary stars from the Crimean Astrophysical Observatory (T.S. Belyakina, N.I. Bondar', K.K. Chuvaev, Yu.S. Efimov, R.E. Gershberg, V.I. Krasnobabtsev, E.P. Pavlenko, P.P. Petrov, I.S. Savanov, N.I. Shakhovskaya and N.M. Shakhovskoj) in cooperation with Dr. V. Piirola from the University of Helsinki and Dr. V.I. Shenavrin from the Sternberg Astronomical Institute, Moscow, carried out a study of Kuwano-Honda's peculiar object (PU Vul). This study covers the period of the brightness maximum in 1979, the episode of a deep minimum in 1980-81, the ascending stage from this minimum, and the last 4 years' duration of the brightness maximum. The PU Vul spectrograms obtained in 1979 at the Ondřejov observatory by Drs. D. Chochol, J. Grygar and L. Hric have been used as well.

In 1978 PU Vul flared from 14^m to 9^m, and in the maximum of 1979 it showed quasi-periodic brightness variations with an amplitude of about $0^m.2$ and 78^d quasi-period. In the maximum of 1982-85 quasi-periodic brightness variations disappeared but short-lived brightness decreases with unusual colour characteristics have taken place and then brightness increases with significant bluishing occurred. The deep optical range

minimum in 1980-81 was accompanied by IR brightness variations of small amplitude only.

Spectrometric observations have shown a close similarity in energy distributions within the optical range of spectra of the normal supergiant Alpha Per and of PU Vul in brightness maximum. Spectral features over a wide range of wavelengths were identified for spectrograms obtained during the phase of brightness increase in March-April 1981 and during the brightness maxima in 1979 and 1981. In spring 1981 the spectrum of PU Vul contained numerous emission lines of different elements and TiO absorption bands, and amongst the emission features we found many lines of La II, Sc II, Y II and Nd II but only a few Fe lines. In the brightness maximum periods the PU Vul absorption spectrum corresponded to the spectrum of a normal supergiant with no chemical anomalies.

Polarimetric observations have shown essential variations of intrinsic polarization parameters which were found to be closely correlated with variations of the photometric characteristics of PU Vul: during brightness decreases in 1979 and 1982, polarization with a "concave" dependence of a polarisation degree on wavelengths appeared, while after the deep minimum in 1980-81, $p(\lambda)$ increased monotonically towards the short wavelengths. A particular feature that was observed was a correlation between the angle of polarization and brightness variations in the second half of 1982.

Analysis of the observations leads to the following conclusions. PU Vul is a binary system consisting of a normal M giant and an exploded component with a maximum luminosity M_V of about $-6^m.3$. The system is located about 800 pc above the galactic plane and at a distance of about 5.3 kpc from the Sun. In 1979 and 1982 the exploded component was not different from a normal F supergiant in its absolute luminosity, the physical conditions in its atmosphere, or in its chemical abundances. Brightness variations of small amplitudes that had been observed in 1979 may be due to quasi-periodic pulsations of the extended atmosphere of the component. An effective temperature of the cool component of the PU Vul system is about 2400 K, such a temperature corresponds to an M 6.5 giant. The deep minimum in 1980-81 cannot be due to a usual eclipse in a binary system but is caused by the formation and consequent dissipation of a heavy dust structure within the PU Vul system. In the framework of the model of a non-stationary dust envelope that was formed around the exploded hot component

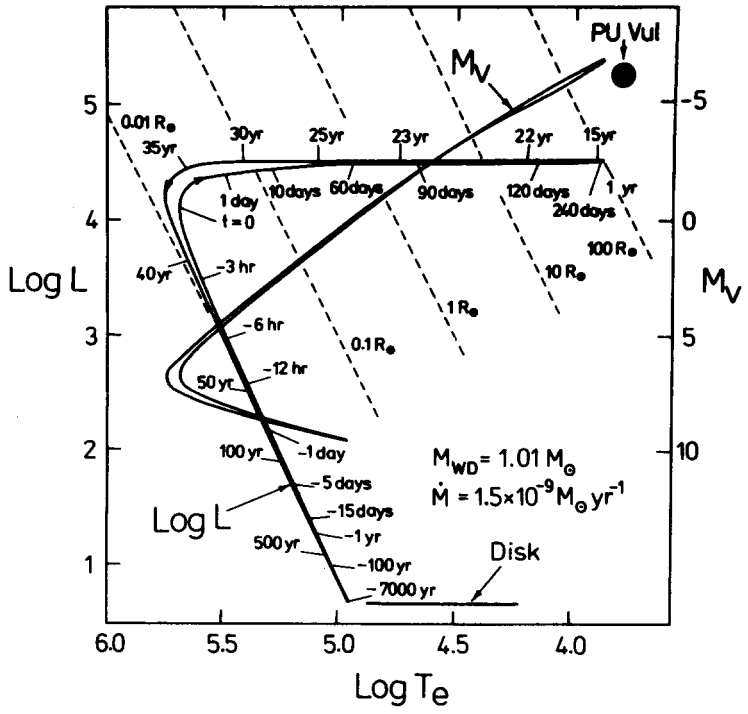

Fig. 1. The theoretical track of an accreting white dwarf computed by Iben (1982) and the position of PU Vul in the M_V, log T_e - plane

of the system, we found a reasonable explanation for the evolution of the polarization characteristics of Kuwano-Honda's object, for small indices B-V and U-B in the brightness minimum, for measured magnitudes of intensity jumps near molecular band heads and for the brightness of the system in the near infrared region during the deep minimum.

The study carried out permits us to attribute Kuwano-Honda's object to anomalous slow novae of the RT Ser type. Comparing the observed properties of the PU Vul system with the features of accreting white dwarfs in a "giant stage" calculated by I. Iben (Astrophys. J. v. 259, p. 244, 1982), one finds close similarities in effective temperatures and absolute luminosities in maximum, in the rate of brightness increase during a flare, and in the maximum phase duration. Further studies of Kuwano-Honda's object may throw light on problems relating to the non-linear pulsations of extended atmospheres of supergiants, dust formation during nova explosions, chemical

abundances of novae, the evolutionary status of high galactic latitude F supergiants, as well as on other problems.

Details of our investigations on PU Vul have been published in the following papers:

Belyakina et al., Astron. J. USSR v. 59, pp. 1-5, 1982;

Gershberg et al., Astron. J. USSR v. 59, pp. 6-14, 1982;

Belyakina et al., Astron. J. USSR v. 59, pp. 302-306, 1982;

Belyakina et al., Astron. Astrophys. v. 132, L12-14, 1984;

Belyakina et al., Izvestiya Crim. Astrophys. Obs. v. 72, 1985.

We are continuing to observe PU Vul, using Crimean telescopes, the 6 m reflector of the Special Astrophysical Observatory, and the Astrophysical Space Station "Astron".

"Eruptive Phenomena in Stars"
Commun. Konkoly Obs. Hung.
Acad. Sci., No.86, Budapest

PECULIAR SLOW NOVA-LIKE OBJECT PU Vul - FACTS AND INTERPRETATION

D. Chochol[1], J. Grygar[2]

[1]Astronomical Institute, Slovak Academy of Sciences,
CS - 059 60 Tatranská Lomnica, Czechoslovakia

[2]Institute of Physics, Czechoslovak Academy of Sciences,
CS - 250 68 Řež, Czechoslovakia

1. Light curve

PU Vul (Kuwano-Honda's object 1979) varied erratically between 16^m and $14^m.5$ in the years 1898-1977. Then a major flare-up occurred and within 1.5 years it brightened to 9^m. After reaching the maximum it displayed periodic variations with amplitude $0^m.25$ and period 78.1 days. The flat maximum lasted till January 1980 when a rather steep decline started ending in August 1980. After a short minimum at $13^m.65$ the object recovered until a new maximum ($8^m.6$) in August 1981. The whole episode lasted about 540 days. Since then its brightness has been increasing very slowly with occasional non-periodic fluctuations, particularly in 1982. In 1984 it reached $8^m.4$. Colour indices (B-V), (U-B), (V-R) and (V-I) exhibited strong variations during the decline and recovery in 1980-81, in the sense that the decline was steepest at the shortest wavelengths (see Kolotilov, 1983, 1984b; Chochol et al., 1984).

2. Spectrum

Continuum seems to be superimposed from two black-body curves of T_{eff} = 6300 K and T_{eff} = 2400 K. This corresponds well to the determined spectral classes of the components, F 8 Iab and M 6.5 III. The spectrum is normally in absorption, except for the 1980-81 episode when various emissions and during the minimum when nebular (forbidden) lines were also observed. P Cygni profiles of H_{alpha} are seen around the light maxima indicating the expansion velocity of the envelope of about 50 km/s (Iijima and Ortolani, 1984). Radial velocities determined from absorption as well as emission (em) lines are compiled in Fig. 1.

3. Interpretation

The light curve resembles that of very slow nova (RT Ser). The deep decline and more than complete recovery is more consistently interpreted as the formation and subsequent dilution of a dust envelope (see nova FH Ser). The absolute magnitude of the bursting component is $-6^m.3$. This corresponds to the F supergiant and to the Eddington luminosity for a stellar mass close to 1 $M_\odot$ (Belyakina et al. 1984). Thus we are strongly convinced that

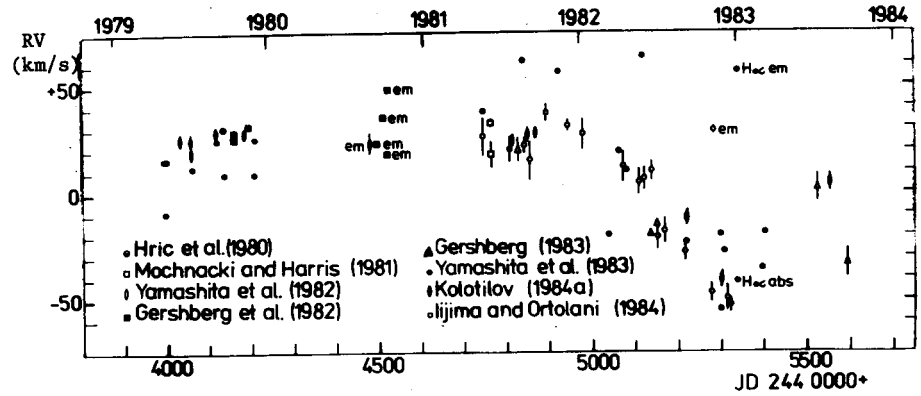

Fig. 1. Radial velocities of PU Vul

PU Vul is a close binary, consisting of an M giant and a hotter component that in the course of accretion expanded and flared-up to become a supergiant. According to Fadeyev (1984) the 78 day period of light variations is the consequence of nonlinear pulsations of the yellow supergiant (radius 154 $R_\odot$) that evolved from the original white dwarf (mass 1 $M_\odot$) via supercritical accretion of hydrogen-rich matter from the red giant. Assuming that the absorption lines originate in the atmosphere of the F supergiant we may infer from Fig. 1 that the changes of radial velocities reflect an orbital motion with a period of more than 5 years. If confirmed this would support the idea that the system resembles wide symbiotic binaries.

References:

Belyakina, T.S., Bondar, N.I., Chochol, D., Chuvaev, K.K., Efimov, Y.S., Gershberg, R.E., Grygar, J., Hric, L., Krasnobabtsev, V.I., Petrov, P.P., Piirola, V., Savanov, I.S., Shakhovskaya, N.I., Shakhovskoy, N.M., Shenavrin, V.I., 1984, Astron. Astrophys. 132, L 12.

Chochol, D., Hric, L., Skopal, A., Papoušek, J., 1984, Contr. Astron. Obs. Skalnaté Pleso 12, 261.

Fadeyev, Yu.A., 1984, Astrophys. Space Sci. 100, 329.

Gershberg, R.E., Krasnobabtsev, V.I., Petrov, P.P., Chuvaev, K.K., 1982, Astron. Zh. 59, 6.

Gershberg, R.E., 1983, personal commun.

Hric, L., Chochol, D., Grygar, J., 1980, Inform. Bull. Var. Stars No. 1835.

Iijima, T., Ortolani, S., 1984, Astron. Astrophys. 136, 1.

Kolotilov, E.A., 1983, Astron. Zh. 60, 746.

Kolotilov, E.A., 1984a, Pisma Astron. Zh. 10, 284.

Kolotilov, E.A., 1984b, Pisma Astron. Zh. 10, 609.

Mochnacki, S.W., Harris, H.C., 1981, IAU Circ. No. 3614.

Yamashita, Y., Maehara, H., Norimoto, Y., 1982, Publ. Astron. Soc. Japan, 34, 269.

Yamashita, Y., Norimoto, Y., Yoo, K.H., 1983, Publ. Astron. Soc. Japan, 35, 521.

"Eruptive Phenomena in Stars"
Commun. Konkoly Obs. Hung. Acad. Sci., No.86, Budapest

ANALYSIS OF LIGHT CURVES OF DQ HERCULIS BASED ON FIVE-COLOUR PHOTOMETRY IN 1982-1985

E.S. Dmitrienko

Crimean Astrophysical Observatory, Crimea, 334413, USSR

The light curves of DQ Her with a time resolution of 12-45 s in five broad band filters close to the standard UBVRI system using 1.25 m and 2.6 m reflectors were observed at the Crimean Astrophysical Observatory by Dmitrienko, Efimov, Shakhovskoy in 1982-1985. The photometer-polarimeter of Helsinki Observatory was used. The instrumentation and observations of 1982-1983 are available in the literature (Dmitrienko et al., 1985). The observations of 1984-1985 and an analysis of all available photometric data are due to be published elsewhere (Dmitrienko, 1986). Here we give some results of this analysis: (1) There is day-, month-, and year-scale variability. The out-of-eclipse light of DQ Her itself in 1982-83 became brighter compared with that in 1978 and was near the light level of 1954. In 1984-85 it decreased to the level of 1978. The mid-eclipse light level of DQ Her changed insignificantly. Hence, it is an eclipsed source which is variable: the primary, the side of the secondary which is turned to the primary and the gaseous stream. (2) The shape of the primary minima suggests the possibility of a total eclipse for several minutes. However, the mid-eclipse colours U-B, B-V indicate that a blue source is strong still. This may be due to the presence of a common gaseous envelope around the components. (3) Compared with 1954 (Walker, 1956) and 1975 (Nelson, Olson, 1976), in 1982-85 the greater shoulder is observed only at the ingress into eclipse. This implies the relative stabilization of the hot spot on the disk in 1982-85. (4) All light curves observed in 1982-85 can be classified into three types (see Fig. 1). Types 1-3 have the lowest, intermediate and greatest values of out-of-eclipse light level (L) at phases near 0.45 and it is different from the level at phases near 0.2. The relative height of the shoulder (ΔH) at phases near 0.89 is intermediate, greatest and lowest for types 1-3. Values of L, ΔH of 1978 (observations by Schneider and Greenstein, 1979) allow one to suppose type 1. The progressive change of DQ

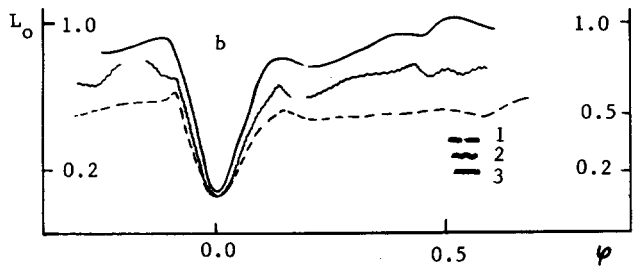

Fig. 1. Three types of schematic light curves in b-filter. The value of the light at phases near 0.45 of 20 July 1982 has been taken as unity

Her status corresponds to the evolution of light curves practically at the same time for all five colours from type 1 (1978) through type 2 (25-27 May to 18-19 July 1982) to type 3 (19-20 July 1982) and back through type 2 (13-15 Sep 1982, to 13-14 Aug 1983) to type 1 (28-29 Apr 1984 and 18-19 May, 18-22 May 1985). It is necessary to emphasize that observations can give us only the upper limit for the time-scale variability and the lowest limit for the light-scale one. The full transition "type 1 - type 3" indicates an increase of the brightness of the eclipsed source of about 70%. (5) The resemblance of the photometric behaviour of the old Nova DQ Her to that of the dwarf novae, e.g., Z Cha during its transition from normal - to superoutburst, as well as the correlation of mass exchange rates in both systems leads to the possibility of the following conclusion: After 50 years of nova-outburst DQ Her shows an activity in which

(a) the state with type 1 light curves corresponds to the state of dwarf nova in normal outburst;

(b) the transition "type 1 - type 3" corresponds to one of dwarf nova from normal - to superoutburst;

(c) the intermediate state with type 2 light curves, when the maximum value of ΔH was observed, indicates the possibility of the reduction of the disk size and/or the increase of the mass loss rate from the secondary before the rise of the brightness of the eclipsed source to its observed maximum value.

References:

Dmitrienko, E.S., Efimov, Y.S., Shakhovskoy, N.M., 1985, Astrofizika, 22, 31.
Dmitrienko, E.S., 1986, in preparation.
Nelson, M.R., Olson, E.C., 1976, Astrophys. J. 207, 195.
Schneider, D.R., Greenstein, J.L., 1979, Astrophys. J. 233, 935.
Walker, M.F., 1956, Astrophys. J. 123, 68.

"Eruptive Phenomena in Stars"
Commun. Konkoly Obs. Hung.
Acad. Sci., No.86, Budapest

ON THE NATURE OF THE RECURRENT NOVA T PYXIDIS

Zdeněk Urban

Astronomical Institute of the Slovak Academy of Sciences,
CS-059 60 Tatranská Lomnica, Czechoslovakia

The observed recurrent novae (hereafter RNs) form a small but very heterogeneous group (Webbink, 1982). Presumably all are white dwarf (WD), or blue star - cool star interacting binaries. However, some RNs contain red giants as the mass-losing components and are thus rather wide binaries, while the giant components are almost certainly excluded in the other members of the group. There are also further serious differences among the group members. Thus, RNs as a single group must be considered very cautiously. In general, all but one of the observed RNs differ to a relatively large extent from the ordinary classical novae when all the system and outburst properties (in addition to the multiple character of a RN outburst) are taken into account. The only exception is T Pyx (Urban, 1985a).

T Pyx has undergone five recorded outbursts to date: in 1890, 1902, 1920, 1944 and in 1966-1967. Concerning the outburst light curves, spectral development during the outbursts, photometry at minimum as well as the spectral energy distribution at minimum in the optical and in the UV - in all these aspects T Pyx strongly resembles ordinary slow novae. Moreover, there exists a well-developed ejected shell around T Pyx. The shell is ionized by UV radiation coming from the stellar nova remnant and has approximately solar heavy element abundances although there is probably some deficiency of He in relation to H. The absolute magnitude of T Pyx at minimum is probably about +1.5. This value is higher than the average value observed in old novae, although it is not unique (exact references to the observations of T Pyx are due to be given in a more detailed paper - Urban (1985b)). All this evidence brings T Pyx closer to the ordinary slow novae than to its co-RNs.

In order to understand the observed behaviour of T Pyx, we are carrying out a re-analysis of all the published observations of this nova in comparison with the ordinary slow novae (e.g. HR Del, RR Pic). The preliminary conclusion is that T Pyx is a quite normal nova but with an extraordinarily shortened outburst recurrence time, T (rec). This makes T Pyx of extreme interest for our understanding of the nova phenomenon (Duerbeck, 1984; Urban, 1985c). By analogy with the ordinary slow novae, we suggest a white dwarf (WD) - red dwarf (RD) interacting binary working model for T Pyx with an orbital period of a few hours. In fact, an orbital period as short as 2.2 hr has been suggested for T Pyx (Vogt, 1982), based on indirect evidence. Current thermonuclear runaway (TNR) nova theory allows for a relatively short T (rec) observed in RNs (tens of years) but at the price of rather limiting choices in the values of the main theory parameters - WD mass and luminosity, mass accretion rate, etc. (Truran, 1982). In a recent

important study (Starrfield et al., 1985) RN-like behaviour was achieved using an accretion of material of solar abundance on a very massive WD. Besides the high WD mass, the mass accretion rate was taken as higher than the average observed in nova binaries. Inasmuch as nothing is known about the WD mass in T Pyx, we adopt a value of about 1 $M_\odot$ suggested as a typical mean value in nova binaries (Truran, 1979 and MacDonald, 1983). In order to obtain a higher accretion rate (there is no giant donor which would ensure a high mass transfer rate like the situation in T CrB and related RNs - see Bath and Shaviv (1978)), we suggest the heating of the mass-losing component atmosphere by high energy radiation from the WD and an accretion disk. The WD component is in a thermally perturbed state of longer duration with the observed outbursts being only the peaks on the generally increased level of activity. This excited WD/accretion disk radiation together with the small system dimensions (Vogt, 1982) ensure the self-induced high mass transfer rate needed to replenish the hydrogen-rich envelope of the WD (necessary prerequisite for a TNR leading to the nova outburst) in a relatively short time. Moreover, there is a possibility that during a RN outburst only a fraction of the accreted envelope is really ejected. What is the possible cause of this thermally perturbed state in the WD component? It was pointed out (Webbink et al., (1978), Taam, (1980) see also Iben (1982) for a general analysis of quasi-static WD accretion) that *helium* TNR may play a significant role in the long-term evolution of nova activity (see also Urban, 1986). We suggest that perhaps some form of a mild He-TNR (Taam, 1980) may help T Pyx to have several *hydrogen* TNR during a relatively short time interval. A detailed discussion of the theoretical aspects as well as of the available observations of T Pyx is currently in preparation (Urban, 1985b).

In conclusion, necessary constraints on any theoretical picture of T Pyx must come from the observations. Unfortunately, our present knowledge of this exciting star is less than satisfactory. Detailed photometric and spectroscopic observations are highly desirable. In particular, radial velocity measurements allowing reliable estimates of the system dimensions and component masses are badly needed. Such observations would be of extreme importance for T Pyx may be well on its way to the next, in this case the sixth, observed outburst (Duerbeck, 1984).

References:

Bath, G.T., Shaviv, G., 1978, Mon. Not. R. astr. Soc. 183, 515.
Duerbeck, H.W., 1984, Ap. Space Sci. 99, 363.
Iben, I. Jr., 1982, Astrophys. J. 259, 244.
MacDonald, J., 1983, Astrophys. J. 267, 732.
Starrfield, S., Sparks, W.M., Truran, J.W., 1985, Astrophys. J. 291, 136.
Taam, R.E., 1980, Astrophys. J. 237, 142.
Truran, J.W., 1979, In: "White Dwarfs and Variable Degenerate Stars", IAU Coll. No.49, J.M. Van Horn and V. Weidemann (eds.), Rochester, p. 469.
Truran, J.W., 1982, In: "Essays in Nuclear Astrophysics", C.A. Barnes et al. (eds.), Cambridge Univ. Press, p. 467.
Urban, Z., 1985a, To be submitted to Ap. Space Sci.
Urban, Z., 1985b, In preparation.
Urban, Z., 1985c, In: "Recent Results on Cataclysmic Variables", Proc. ESA Workshop, ESA SP-236, p. 33.
Urban, Z., 1986, These proceedings, p.367.
Vogt, N., 1982, Mitt. Astr. Ges. 57, 79.
Webbink, R.F., 1982, In: "Pulsations in Classical and Cataclysmic Variables", J.P. Cox and C.J. Hansen (eds.), JILA, Boulder, CO, p. 1.
Webbink, R.F., Truran, J.W., Gallagher, J.S., 1978, Bull. AAS 10, 438.

"Eruptive Phenomena in Stars"
Commun. Konkoly Obs. Hung.
Acad. Sci., No.86, Budapest

THE AMPLITUDE - CYCLE LENGTH RELATION OF LONG-CYCLIC CATACLYSMIC BINARIES

G.A. Richter

Zentralinstitut für Astrophysik der Akademie der
Wissenschaften der DDR, Sternwarte Sonneberg

In 1934 Kukarkin and Parenago showed that there is a relationship between the amplitude A and the cycle length C of U Geminorum stars, that seemingly continues smoothly to the recurrent novae.

As the long cycles ($C \gtrsim 1^a$) given in the literature are affected by systematic errors, I have carried out a revision.

Two kinds of systematic errors can be found in the published material:

1. The mean interval between two eruptions is often equated with the cycle length C without an estimate of whether undiscovered eruptions exist or not.

2. Some objects occasionally show, after apparently long, quiet intervals, series of eruptions in relatively rapid succession. In such cases the common practice is to take the shortest interval as the cycle length.

Dr. W. Wenzel and I have taken the opportunity to use the numerous Sonneberg Sky Patrol plates for re-examining, in connection with the results of amateur organizations, the published cycle lengths and to make statistical statements concerning the most probable values of C. We have used three methods:

1. N photographic exposures may be distributed by chance over a certain period t. Because of the daylight gap we must replace the interval t by $T = t \cdot f$, where f is the fraction of the year during which observations are carried out. a_k stands for the observed number of eruptions recorded on a total of k plates. Taking the mean, each of the eruptions is present on $g = \sum_1^\infty k a_k / \sum_1^\infty a_k$ plates. On the other hand, one can show that $g = \lambda/(1-e^{-\lambda})$, where λ is the mean of the Poisson distribution. From this follows the cycle length ($\sum_1^\infty k a_k = n$):

$$C_1 = \lambda T/n \ . \qquad (1)$$

The advantage of this method is the fact that the duration L of the eruptions need not be known. Its disadvantage is the great demand on the homogeneity of the material.

2. It can be shown that $T/L = N/\lambda$. Substituting in (1) and by changing index 1 to 2 we obtain the formula

$$C_2 = L\,N/n \tag{2}$$

which has already been used several times by W. Wenzel. It has the advantage that the daylight gap is eliminated; the disadvantage is that errors in L are transferred to C_2.

3. By subdivision of the year into ν equal parts and plotting the number of observed eruptions over the season (e.g. monthly, $\nu = 12$), one can adjust the plots to a sinusoidal curve which has its maximum value ρ at about the season in which the upper culmination of the object is about midnight. We have then

$$C_3 = \frac{t}{\nu \cdot \rho} . \tag{3}$$

Strictly speaking, this value is an upper limit.

For 12 U Geminorum stars with $C > 240^d$ we obtained the relation

$$A = -3.4 + 3.35 \log C;$$

and for 5 recurrent novae,

$$A = -2.7 + 2.73 \log C.$$

The 3 recurrent X-ray novae are within the error limits in the neighbourhood of the recurrent novae, which may be pure chance.

U Sco is an outsider, also spectroscopically. It should have $C \approx 200$ years and not 39 years as is observed.

A more detailed discussion is being prepared for publication in Astron. Nachr.

"Eruptive Phenomena in Stars"
Commun. Konkoly Obs. Hung.
Acad. Sci., No.86, Budapest

MASS TRANSFER BURSTS IN THE SYMBIOTIC BINARY SYSTEM CH Cyg DURING THE MAXIMUM OF ITS ACTIVITY IN THE YEAR 1982

D. Chochol[1], A. Skopal[1], T.S. Galkina[2]

[1]Astronomical Institute, Slovak Academy of Sciences,
CS - 059 60 Tatranská Lomnica, Czechoslovakia

[2]Crimean Astrophysical Observatory, P/O Nauchny
334413 Crimea, USSR

The spectrum of CH Cygni usually looks like the spectrum of an M6 III star but during outbursts it resembles the spectra of symbiotic stars. Outbursts were observed in the periods: Sept. 63 - Aug. 65; June 67 - Sept. 70; May 77 - Dec. 84.

Mikolajewski and Biernikowicz (1985) investigated the radial velocities and intensities of the H_β profile as well as a drop of U,B,V brightness in August - December 1984 and came to the conclusion that the end of activity was caused by the eclipse of the hot component by the cool M giant in the binary system. This is in agreement with the epoch of eclipse predicted from a long period orbit of 5750 days, found by Yamashita and Maehara (1979).

CH Cygni reached the maximum brightness ($V = 5^m.5$) in 1982 (Chochol et al., 1984). The increase of brightness in 1981 was accompanied by spectroscopic changes: increase of intensity in blue continuum, in emission lines and in the velocity gradient of Balmer series (Skopal, 1985). The most interesting feature, well visible at high dispersion spectra (dispersion 6.5 Å/mm), was the splitting of shell lines of ionized metals Ti II, Cr II and Sc II into two components. Skopal explained the emergence of the red component of these lines by the sudden increase of mass flow from the M giant into the accretion disk of the hot component. The orientation of the binary system with respect to the observer was suitable to observe the projection of the receding gaseous stream onto the hot component.

Our spectroscopic material was obtained with the 1.22 m telescope of the Crimean Astrophysical Observatory and consists of 14 spectrograms with

dispersion 36 Å/mm taken during the maximum of activity of CH Cygni in the period Sept. 13 - Nov. 29, 1982. While at high dispersion spectra the main and additional absorption components of ionized metals are well separated ($\Delta \lambda \sim 0.7$ Å), at low dispersion spectra the emergence of red absorption causes only red shift of the centre of the main absorption line. Due to the long period orbit of CH Cygni the orientation of the binary system in the years 1981 and 1982 did not differ too much, so the sudden changes of radial velocities of absorption shell lines of ionized metals can be interpreted as an increase of mass transfer between the components. As is seen from Fig. 1, where the radial velocities of Ti II shell lines are plotted, the time scale of mass transfer bursts is about 20 days.

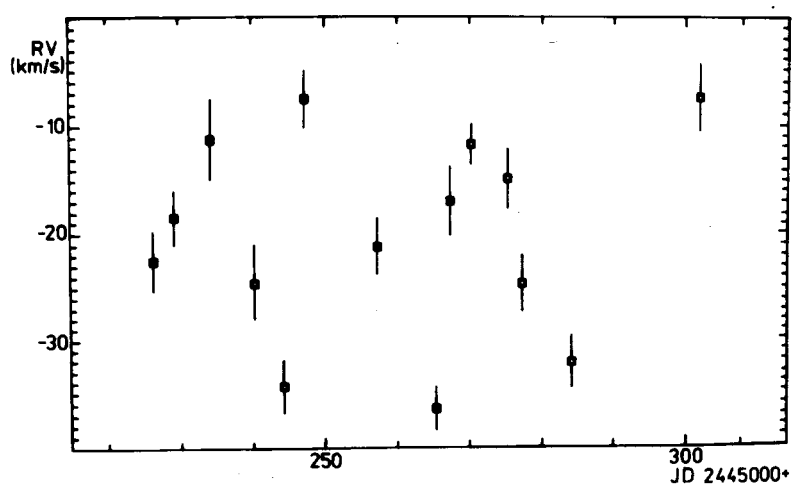

Fig. 1. Radial velocities of Ti II lines in CH Cyg

Our observations are in agreement with the theory of bursting mass transfer by the cool component in cataclysmic variable stars (Bath, 1984).

References:

Bath, G.T., 1984, Astrophys. Space Sci. 99, 127.
Chochol, D., Hric, L., Skopal, A., Papoušek, J., 1984, Contr. Astron. Obs. Skalnaté Pleso 12, 261.
Mikolajewski, M., Biernikowicz, R., 1985, Astron. Astrophys. (in press).
Skopal, A., 1985, Bull. Astron. Inst. Czechosl. (in press).
Yamashita, Y., Maehara, H., 1979, Publ. Astron. Soc. Japan 31, 307.

"Eruptive Phenomena in Stars"
Commun. Konkoly Obs. Hung.
Acad. Sci., No.86, Budapest

ON THE PERIOD OF THE SYMBIOTIC STAR AG PEGASI

R. Luthardt

Zentralinstitut für Astrophysik der Akademie
der Wissenschaften der DDR, Sternwarte Sonneberg

Two different periods of this symbiotic star have been published recently. This induced me to carry out a new photometric analysis.

AG Peg has shown a novalike light curve over the last 150 years. After a rapid brightening reaching 5th magnitude in 1855 the brightness has been decreasing. Now the star is near 9th magnitude again as before its outburst.

The spectrum of AG Peg has also shown significant variations. It is comparable to a typical nova spectrum - an emission spectrum with higher excitation features with decreasing magnitude (Merrill, 1958). An absorption spectrum of an M-giant also became increasingly more visible.

Measurements of radial velocities were carried out on highly resolved spectra taken between 1930 and 1970. The data could be best fitted by periods of about 790 to 840 days (Cowley et al., 1973; Hutchings et al., 1975). The material did not yield a better estimate.

Photoelectric measurements in U, B and V by Belyakina (1965) also showed magnitude variations with a period of about 800 days. Meinunger (1983) observed the light variations on plates of the Sonneberg Sky Patrol taken between 1930 and 1982. He found a period of 827 days. This period fits well into the radial velocity curve of the M-absorption lines which is a confirmation of its accuracy. Slovak (1982) published a period which differs considerably from that of Meinunger. He found 733 days. In order to find an explanation for this discrepancy I examined further observations: Visual estimations of the A.F.O.E.V. from 1970 to 1983, and photoelectric measurements with the Sonneberg 60 cm mirror II (Luthardt, 1984). I found two minima in addition to those detected by Meinunger. The differences $(O-C)_1$ derived from the elements of Meinunger are very large. The new elements calculated with the last 5 minima are: Min. = J.D. 244 2370+760$^d \cdot E_2$.

Table I

Min. J.D.	Author	E_1	$(O-C)_1$	E_2	$(O-C)_2$
244 2360	Meinunger	17	+ 51^d	0	-10^d
3150	Meinunger	18	+ 14	1	+20
3920	Meinunger	19	- 43	2	+30
4650	Luthardt	20	-140	3	0
5400	Luthardt	21	-217	4	-10

Table I shows these minima and differences $(O-C)_1$ (elements of Meinunger) and $(O-C)_2$ (elements of the author).

There is a systematic decrease of $(O-C)_1$, and the minima are well represented by the new elements.

The previous minima from $E_1 = 0$ to $E_1 = 16$ are well determined by the elements of Meinunger.

We may therefore suspect a change of period at about J.D. = 244 2000... ...3000.

Further observations, photoelectric measurements as well as radial velocities are necessary.

The point is whether the recently obtained radial velocity curve correlates with the old or with the new period.

Only in this way is a confirmation of the suspected period change possible. If this period change really exists, its cause would be of immense interest.

References:

Belyakina, T.S., 1965, Krim Isw., Tom. XXXIII, 226.
Bull. A.F.O.E.V., No. 8 to No. 26.
Cowley, A., Stencel, R., 1973, ApJ, 184, 687.
Hutchings, J.B., Cowley, A.P., and Redman, R.O., 1975, ApJ, 201, 404.
Luthardt, R., 1984, IBVS, No. 2495.
Meinunger, L., 1983, Mitt. Veränderl. Sterne, 9, 22.
Merrill, P.W., 1958, ApJ, 129, 44.
Slovak, M.H., 1982, Journal AAVSO, 11, No. 2, 67.

"Eruptive Phenomena in Stars"
Comm. Konkoly Obs. Hung.
Acad. Sci., No.86, Budapest

OUTBURST ACTIVITY IN CATACLYSMIC BINARIES: PARALLEL EVOLUTION OR ACTIVITY CYCLES?

Zdeněk Urban

Astronomical Institute of the Slovak Academy of Sciences,
CS-059 60 Tatranská Lomnica, Czechoslovakia

The possibility of finding very different modes of the outburst activity (classical and dwarf nova states, nova-like states) in otherwise structurally similar cataclysmic binaries (hereafter CBs) is one of the greatest puzzles related to these systems (Whyte and Eggleton, 1980). Nevertheless, all the observed differences between the various classes of CBs can be reduced to the differences in their accretion discs (Smak, 1984). The widely held opinion is that these differences reflect differences in the amount of mass coming into the disc, i.e. in the mass transfer rate (MTR) between the red dwarf (RD) and the white dwarf (WD) components of CBs (Patterson, 1984), although the heating of the accretion disc by the star inside it might confuse the story (Friedjung, 1985). It was suggested that MTR is correlated with the orbital period, P(orb), in CBs (Patterson, 1984). However, the spread in MTR at a given P(orb) may be up to three orders of magnitude (Szkody, 1985). It might be argued that different MTRs further reflect some deep-rooted systematic differences between the classes of CBs not sufficiently well recognized to date, say, in mass ratios (Smak, 1983). The simultaneous existence of a classical nova, a dwarf nova and a nova-like variable at approximately the same P(orb) would thus be explained by the parallel evolution of these systems on the secular evolution time-scale (see Ritter (1983) for a review), with different outburst behaviour conditioned by different MTR representing the natural spread in basic system parameters.

Another possibility is that MTR is not fixed but there can exist a modulation of it superimposed on the general decrease in MTR with P(orb) decreasing during the secular evolution. The classes of CBs may thus represent different phases of the more general outburst activity cycle which repeats many times during the secular evolution of these systems (see Urban (1985) for a general picture). We identify the main components of such a

cycle with the consecutive nova outbursts, for nova activity must recur many times during the secular evolution of a given CB characterized by more or less persistent WD accretion. Evolution towards and after the nova outburst leads to alternating phases of heating and cooling of the WD primaries and thus to variable RD atmosphere irradiation mediated variations in MTR with MTR being higher during the hotter states and lower during the cooler ones. We identify, following earlier suggestions by several authors, the hotter states with the observed old novae and nova-like stars and cooler ones with the dwarf novae.

In order to test the possibility of such a cycle, we are carrying out a comparative analysis of the published data on various classes of CBs to find possible sequences of objects representing different phases of our activity cycle in different short intervals of P(orb). Our efforts extend to those of Vogt (1982) who, in fact, first proposed a more detailed picture of such a cycle. We are also investigating possible changes in the character of the nova outburst during the secular evolution of a CB. The primary goal of all these efforts is to understand the observed behaviour of CBs within a unified evolutionary picture of the main modes of the outburst activity. Only preliminary conclusions can be made at present but it can be stated with a relatively high level of certainty that an extended form of Vogt's cycle is at least compatible with the present database of CBs.

However, the role (if any) of the magnetic CBs (polars and intermediate polars) in our scenario is unclear. Are these systems dormant perpetually with respect to the outburst activity? The question of the possible fate of the accreted matter on the surfaces of WD primaries in these systems is highly intriguing.

A detailed discussion of the results of comparative analysis of the observational data on CBs as well as of the theoretical aspects is currently in preparation.

I thank Dr. Paula Szkody for communicating me her results prior to publication.

References:

Friedjung, M., 1985, Astron. Astrophys. 146, 366.
Patterson, J., 1984, Astrophys. J. Suppl. Ser. 54, 443.
Ritter, H., 1983, Mitt. Astr. Ges. 60, 159.
Smak, J., 1983, Astrophys. J. 272, 234.
Smak, J., 1984, Publ. Astr. Soc. Pacif. 96, 5.
Szkody, P., 1985, Astron. J., in press.
Urban, Z., 1985, In: "Recent Results on Cataclysmic Variables", Proc. ESA Workshop, Bamberg, W. Germany, 17-19 April 1985, ESA SP-236, p. 33.
Vogt, N., 1982, Mitt. Astr. Ges. 57, 79.
Whyte, C.A., Eggleton, P.P., 1980, Mon. Not. R. astr. Soc. 190, 801.

"Eruptive Phenomena in Stars"
Comm. Konkoly Obs. Hung.
Acad. Sci., No.86, Budapest

INFLUENCE OF THE ACCRETION COLUMN'S ASYMMETRY ON THE ORBITAL VARIABILITY OF POLARS

I.L. Andronov

Odessa State University, T.G. Shevchenko Park 270014 Odessa, USSR

According to a standard model of AM Her-type stars, the plasma ejected from the atmosphere of the secondary through the inner Lagrangian point moves along the field lines to the magnetic pole of the white dwarf (Kruszewski, 1978). This cannot explain the observed asymmetry of orbital light curves in a wide spectral region from X-ray to IR, nor the phase curves of polarization and radial velocities. Thus the emitting region must be asymmetric (Stockman, 1977) for the following reasons:

1. the plasma does not fall vertically onto the magnetic pole, and the accretion column is inclined (Andronov, 1983);

2. the centres of the magnetic dipole and the white dwarf do not coincide (Kruszewski, 1978);

3. the plasma begins its motion along field lines not from the inner Lagrangian point but later, when it is sufficiently ionized by the hard emission;

4. in the vicinity of the compact star the field configuration essentially deviates from the dipole one (Mitrofanov et al., 1977);

5. the column is not axi-symmetrical.

If the accretion column is axi-symmetrical but inclined, the asymmetry may be observed only if the magnetized star saturates the column's base during orbital motion and the axis of the column, does not cross the rotational axis of the white dwarf (Andronov, 1983). The asymmetry increases with increasing contribution to the whole emission by the saturated regions of the column. If the column becomes higher, the light curves become more symmetrical and have one maximum if the column's axis during its rotation does not pass the plane of view otherwise two maxima are seen.

If the column's cross-section is not circular, then during the orbital period one may observe variability up to ten percent even if the angle Θ between the column's axis and the line of sight is constant - which may also cause the asymmetry.

In a real accretion column the density does not decrease abruptly with increasing distance from the column's axis but continuously (although rather rapidly). Thus the observed brightness and the value of the effective radius are not constant. They also depend on the wavelength we use for observation so the spectrum and polarization of the observed emission are essentially affected by this phenomenon (Andronov, 1983).

In the column self-oscillations may be excited (Langer et al., 1982) which may essentially change the emission characteristics usually investigated using stationary models. In the three-dimensional column, five additional types of instability may exist as well. The transfer of energy, generated due to accretion, becomes inefficient near the column's base, then the regions with low density and optical thickness appear, through which the energy is transferred from the inner parts of the column. The instability of the accretion flow causes the excitation of non-radial motions in the column. The column's asymmetry complicates the scenario much more.

The aim of this paper is not to interpret quantitatively the observations; it is planned to do this elsewhere. We have only briefly discussed the problems of magnetic close binary systems.

References:

Andronov, I.L., 1983, Dissertation, Univ. of Odessa.
Kruszewski, A., 1983, In: "Nonstationary Evolution of Close Binaries"; ed. A. Zytkow, Warszawa, p. 55.
Langer, S.H., Chanmugam, G., and Shaviv, G., 1982, Astrophys. J., 258, 285.
Mitrofanov, I.G., Pavlov, G.G., Gnedin, Yu.N., 1977, Pis'ma v Astron. Zhu., 3, 341.
Stockman, H.S., 1977, Astrophys. J., 218, L 57.

"Eruptive Phenomena in Stars"
Commun. Konkoly Obs. Hung.
Acad. Sci., No.86, Budapest

INFLUENCE OF THE MAGNETIC FIELD ON ACCRETION IN CLOSE BINARY SYSTEMS

I.L. Andronov

Odessa State University, T.G. Shevchenko Park 270014 Odessa, USSR

Magnetic close binary systems (MCBS) are objects with a secondary which fills its Roche lobe, and a white dwarf with a magnetic field which is sufficient to make the dimensions of the magnetosphere greater than the orbital separation (see Chiapetti et al. (1980) for a review). Accreting plasma in MCBS moves along the magnetic field lines. We now know 13 similar objects ("polars") in which a white dwarf rotates synchronously with the orbital motion.

Asynchronism of rotational and orbital motions leads to a change of the accretion scenario. Additional centrifugal force, in a direction from the white dwarf, appears and acts as an additional potential barrier. The dependence of the limit velocity, which is necessary to penetrate through this barrier, on the initial conditions (Andronov, 1982b) shows that plasma is ejected from asynchronous MCBS, moving outside the magnetosphere. This "propeller stage" is analogous to that of neutron stars investigated by Illarionov and Sunyaev (1975). During this period the white dwarf will be synchronized with the time $t_s \leq 10^3$ yr (Andronov, 1982b).

Systems at the "propeller stage" are unsuitable for observation because the plasma is ejected but not accreted. However, for the period of a white dwarf's rotation $P_{wd} \approx 1$ min. due to the excitation of MHD-waves, about 10^{33} erg/s (Lamb et al., 1983) is lost. The observed flux may change with a period P_{wd} (or $P_{wd}/2$). The deceleration of rotation leads to a reduction in the systemic luminosity and thus makes the discovery of such a system much more difficult. During this stage, the X-ray emission due to accretion is absent, but the plasma is still being ejected, the MHD-waves are being excited, the radioemission is appearing (Chanmugam and Dulk, 1983; Lamb et al., 1983). With the diminishing value of the parameter of asynchronism, the shape of the magnetosphere changes. The quantity of plasma

falling onto the white dwarf increases thereby causing a redistribution of the moments of forces.

If the angle Θ between the magnetic axis and the line of the centres is near 90°, the moment of forces - affecting the white dwarf - is zero. Near this equilibrium state the non-linear oscillations of orientation of the magnetic axis may be excited (Joss et al., 1979; Andronov, 1982c), causing cyclic variations of the orbital curves of polarization, radial velocities, and flux in different spectral regions from X-ray to IR. Similar variability of the photometric period with a 3-year cycle was discovered in AM Herculis (Andronov, 1982c). This value corresponds to the characteristic time of the changes, in the orientation of the dipole which is necessary to explain the observed radioemission (Lamb et al., 1983; Chanmugam and Dulk, 1983).

In MCBS one may observe a unique phenomenon for close binaries - the modulation of the accretion rate by the magnetic field of the white dwarf. The accretion rate is at maximum when $\Theta = 0^{\circ}$ and sharply decreases with increasing value of Θ. If $\Theta = 90^{\circ}$, the "magnetic valve" is fully closed, the magnetic field prevents the flow from the secondary. This mechanism explains the observed slow variations of the polar's luminosity (Andronov, 1982a, 1984).

Asynchronous MCBS (classified as III P (Lipunov, 1984)) are progenitors of polars (III M), but the "intermediate polars" (III A), in their evolutionary scenario, possibly do not have the "classical polar" stage because of the lack of a sufficiently high magnetic field.

The discovery of asynchronous MCBS, which discovery is difficult due to the above cited complexities, may allow us to fill another gap in the evolutionary scenario of the cataclysmic variables.

References:

Andronov, I.L., 1982a, Preprint VINITI, No. 5900-82 Dep., 20 pp.
Andronov, I.L., 1982b, Preprint VINITI, No. 5901-82 Dep., 29 pp.
Andronov, I.L., 1982c, Preprint VINITI, No. 5981-82 Dep., 23 pp.
Andronov, I.L., 1984, Astrofizika, 20, 165.
Chanmugam, G., and Dulk, G.A., 1983, In: "Cataclysmic Variables and Related Objects"; eds. M. Livio, G. Shaviv; Reidel, Dordrecht, p. 223.
Chiapetti, L., Tanzi, E.G., and Treves, A., 1980, Space Sci Rev., 27, 3.
Illarionov, A.F., and Sunyaev, R.A., 1975, Astron. Astrophys., 39, 185.
Joss, P.C., Katz, J.I., and Rappaport, S.A., 1979, Ap. J., 230, 176.
Lamb, F.K., Aly, J.J., Cook, M.C., and Lamb, D.Q., 1983, Ap. J., 274, L 71.
Lipunov, V.M., 1984, Adv. Space Res., 3, 323.

"Eruptive Phenomena in Stars"
Commun. Konkoly Obs. Hung.
Acad. Sci., No.86, Budapest

ADDITIONAL PHOTOMETRIC DATA FOR THE X-RAY SOURCE KR AURIGAE DURING 1971-1980

V.N. Popov, Z.T. Kraicheva, M.D. Popova

Department of Astronomy with National Astronomical Observatory
Bulgarian Academy of Sciences, Sofia, Bulgaria

In this communication some photometric data for the X-ray source KR Aur for the time interval 1971-1980 are presented. Popova's (1965) sequence was used for the magnitude estimation.

For the mentioned period only 31 values were known (Liller, 1980). We obtained 73 additional estimates: 47 from Sonneberg Sky Patrol plates (S), 15 based upon plates taken with the 40 cm astrograph in Sonneberg (A) and 11 made in Bulgaria (B). Fortunately, the 40 cm astrograph plates cover the fading of the brightness from Oct. 1971 till Apr. 1972 and fill the lack of observations during the minimum. In Table I the numerical values of the estimates are presented and the same data are presented with filled circles in Fig. 1. In the same figure Liller's data are also given with open circles.

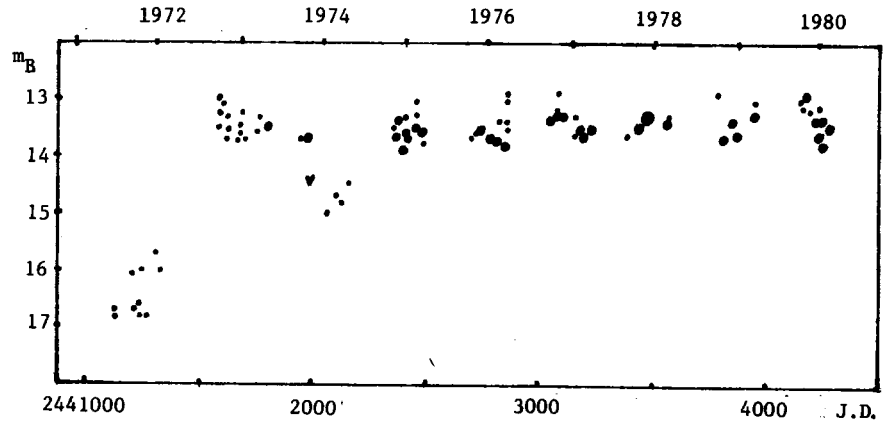

Fig. 1

Table I

J.D.	m_B	Obs.	J.D.	m_B	Obs.
244...			2359.453	13.5	S
1236.412	16.7	A	2395.409	13.4	S
1248.523	16.8	A	2449.282	13.3	S
1249.493	16.7	A	2449.347	13.0:	S
1300.543	16.1	A	2449.351	13.3	S
1322.396	16.7	A	2472.285	13.6	S
1333.506	16.6	A	2472.341	13.8	S
1334.460	16.8	A	2697.572	13.7	S
1350.294	16.0	A	2714.451	13.6	S
1356.260	(16	A	2717.519	13.7	S
1361.269	16.8	A	2831.425	13.5	B
1366.275	(16	A	2834.389	13.4	B
1390.300	15.7	A	2835.420	13.5	B
1394.297	16.5	A	2837.424	13.4	B
1421.402	16.0	A	2838.376	13.5	B
1592.494	14.0:	S	2839.325	13.1	S
1595.545	13.0	A	2839.444	13.5	S
1595.566	13.2	S	2841.344	13.0	S
1596.540	13.1	S	2858.306	13.2	S
1599.584	13.3	S	2866.369	12.9	S
1600.594	13.6	S	2867.392	13.3	B
1602.547	13.7	S	2868.403	13.5	B
1679.400	13.6:	S	2870.324	13.0	S
1680.445	13.7	S	3078.471	13.2	S
1681.382	13.7:	S	3078.519	12.9	S
1685.401	13.5	S	3157.340	13.3	S
1689.374	13.2	S	3162.417	13.3	S
1708.345	13.6	S	3400.576	13.6	S
1738.365	13.3	S	3482.543	13.3	S
1765.315	13.3	S	3483.449	13.3	S
1773.386	13.3	S	3575.395	13.3	S
1957.555	13.7	S	3789.511	12.9	S
1982.533	(14.4	S	3963.350	13.0	S
2068.367	15.0	B	4169.507	13.0	S
2091.369	14.7	B	4171.588	13.1	S
2118.335	14.8	B	4200.447	13.2	S
2151.320	14.5	B	4234.528	13.1	S

References:

Liller, M.H., 1980, Astron. J., 85, 1092.
Popova, M.D., 1965, Peremennye Zvezdy, 15, 534.

"Eruptive Phenomena in Stars"
Commun. Konkoly Obs. Hung.
Acad. Sci., No.86, Budapest

RECENT PHOTOMETRIC DATA FOR THE X-RAY SOURCE KR AURIGAE

A.P. Antov, V.N. Popov, M.D. Popova

Department of Astronomy with National Astronomical Observatory
of Bulgarian Academy of Sciences, Sofia

The interest in KR Aurigae is determined by its peculiar features. Photometric investigations after its discovery in 1960 (Popova, 1960) showed variability in all observed time intervals. The star spends more time in maximum varying between the 12th and 14th magnitudes but sometimes its brightness drops to between the 17th and 18th magnitude. This photometric behaviour has led to the suggestion that KR Aur belongs to a new type of variability - anti nova (Popova, 1974). On the basis of the spectral characteristics of the star a new class of nova-like variables known "anti-dwarf novae" was proposed by Bond (after Shafter, 1983). The spectra of these normally resemble dwarf nova at maximum. KR Aur was found to be a binary system (Shafter, 1983, Kraicheva et al., 1982) and a weak X-ray source (Mufson et al., 1980).

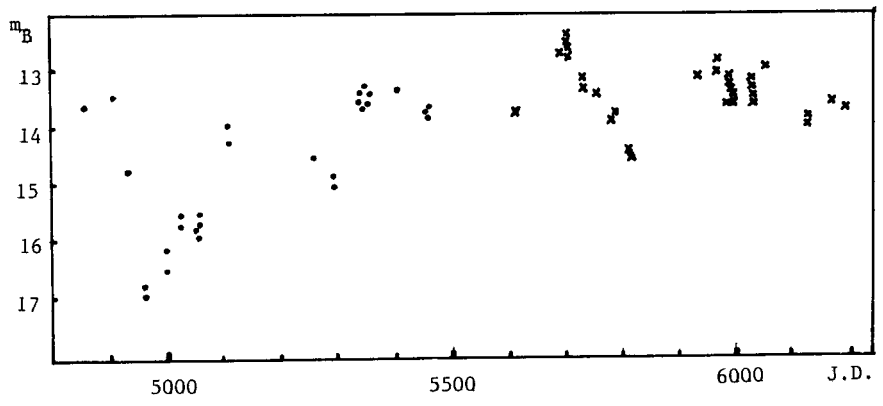

Figure 1

Further data on the light curve of KR Aur are of importance to clarify the nature of this remarkable variable. Systematic photometric observations are carried out with the 50/70 cm Schmidt, 60 cm Cassegrain and 2 m RC telescopes of the National Astronomical Observatory of the Bulgarian Academy of Sciences.

In this communication the estimates of the photographic magnitude of KR Aur are reported for the period J.D. 2445600-2446200. They are based on Popova's (1965) standard stars. The new data are shown by crosses in Fig. 1. In the same figure dots denote the known photometric data preceding the new observations.

References:

Kraicheva, Z.T., Popov, V.N., Popova, M.D., Antov, A.P., 1982, Publ. Symp. Relativistic Objects in Close Binary Systems of the Multilateral Co-operation on Stellar Physics and Evolution, Cluj-Napoca, Romania.
Mufson, S.L., Wisniewski, W.Z., and McMillan, R.S., 1980, IAU Circ. No. 3471.
Popova, M.D., 1960, Mitt. Ver. Sterne (Sonneberg), No. 463.
Popova, M.D., 1965, Peremennye Zvezdy, 15, 534.
Popova, M.D., 1974, In: "Late Stages of Stellar Evolution, ed. R.J. Tayler, p. 192.
Shafter, W.A., 1983, Astrophys. J., 267, 222.

"Eruptive Phenomena in Stars"
Comman. Konkoly Obs. Hung.
Acad. Sci., No.86, Budapest

ON THE LAST CYCLE OF OPTICAL VARIABILITY OF X-RAY SOURCE KR AURIGAE

Z.T. Kraicheva, V.N. Popov, M.D. Popova, A.P. Antov

Department of Astronomy with National Astronomical Observatory
of Bulgarian Academy of Sciences, Sofia

The photometric variations of the X-ray source KR Aurigae have been followed for a considerably long time interval - about 100 years. The observational material comes mainly from the plate collections of the Sonneberg and Harvard Observatories (Popova, 1975; Liller, 1980; Popov et al., 1986). In recent years the star was observed systematically by the National Astronomical Observatory of the Bulgarian Academy of Sciences and by Sonneberg and Harvard Observatories (Popov, 1982; Popova et al. 1984; Liller and Popova, 1984; Götz, 1982, 1984). All the magnitudes in these investigations are based on Popova's (1965) sequence and well complement each other.

We have used all this observational data to analyse the peculiarity of the long term photometric behaviour of KR Aurigae obtaining the mean semi-annual photographic magnitudes. The results for the years 1970-1985 are given in Fig. 1. The range of the magnitude variations is also presented.

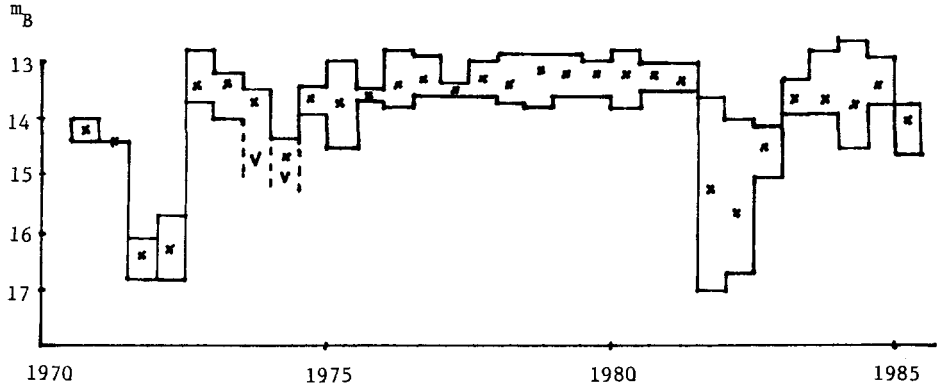

Figure 1

This latter cycle is unique in the sense of the number of observations taken with telescopes large enough to follow the lower part of the light curve. It is worth while to note the secondary minima in 1974 and 1984. If the character of the next cycle is similar to the last one, a deep minimum to 17-18 magnitude can be expected around 1990. It should be noted, however, that sometimes periods of irregular variations or some-years-long low stages occur between the cycles. It is interesting to study the possible relationship between the drop of the brightness of the variable and the decrease of the mass transfer from the secondary component (Shafter, 1983). Further photometric observations and spectrophotometry in different stages are needed.

References:

Götz, W., 1982, IAU Comm. 27 IBVS No. 2364.
Götz, W., 1984, IAU Comm. 27 IBVS No. 2540.
Liller, M.H., 1980, Astron. J., 85, 1092.
Liller, M.H., Popova, M.D., 1984, IAU Comm. 27 IBVS No. 2464.
Popov, V.N. 1982, IAU Comm. 27 IBVS No. 2095.
Popov, V.N., Kraicheva. Z.T., Popova. M.D., 1986, these Proceedings, p.373.
Popova, M.D., 1965, Peremennye Zvezdy, 15, 534.
Popova, M.D., 1975, Astrophys. Issled. (Sofia), 1, 68.
Popova, M., Popov, V., Antov, A., and Kraicheva, Z. 1984, Adv. Space Res., Vol. 3, No. 10-12, 55.
Shafter, W.A., 1983, Astrophys. J., 267, 222.

"Eruptive Phenomena in Stars"
Commun. Konkoly Obs. Hung.
Acad. Sci., No.86, Budapest

EJECTION OF MATTER BY MASSIVE STARS

Tatjana A. Lozinskaya

Sternberg State Astron. Inst., Moscow, USSR

Massive start ($M_{in} \gtrsim 10M_\odot$) lose matter in the following ways: 1. Stellar wind, 2. Ejection of a "slow" shell, 3. Supernova (SN) explosion. Previous investigations all concentrated on a single type of these ejecta. It is now clear that the problem should be investigated only when these separate threads combine into a unified picture. Real SN ejecta interact with pre-supernova wind and with a slow shell (if it exists), a slow shell may be accelerated by the wind, etc. Some items of the picture can be confronted with the following observations:

I. Recent UV, radio and IR observations indicate that early-type stars with $M_{init} > 10M_\odot$ always show evidence of a "fast wind" ($\dot{M} \simeq 10^{-7} - 10^{-6} M_\odot/yr$, $V_\infty \simeq 1000$-2000 km/s). A stronger fast wind ($\dot{M} \simeq 10^{-5}\ M_\odot/yr$, $V_\infty \simeq 2 \cdot 10^3$ km/s) is attributed to Of stars and to post-main-sequence WR stars; a "slow" wind ($\dot{M} \simeq 10^{-5}\ M_\odot/yr$, $V_\infty \simeq 10$ km/s) - to red supergiants being progenitor stars of type II SNe. Probably there is a very short "superwind" stage just before the SN explosion ($\dot{M} \simeq 10^{-3}\ M_\odot/yr$). The stellar winds disturb ambient ISM producing bubbles and shells with radii of the order of 1 to 20 pc and velocities 10-100 km/s (e.g. wind-blown bubbles around WR and Of: NGC 6888, NGC 2359, thin filamentary shell in NGC 6164-5).

II. Some WR- and Of- ring nebulae are generally ejected material rather than ISM swept up by stellar wind. The nebulae M1-67, RCW58, and the innermost shell of NGC 6164-5 are certainly slow shell ejecta with radii $\simeq 1$ pc, $M \simeq 1$-$5\ M_\odot$, velocities $\simeq 20$-100 km/s.

Both processes, slow ejecta and stellar wind, work in common. Expansion of an ejected shell takes place inside a bubble blown by the wind at the early "pre-ejecta" stage of the star evolution. A "post-ejecta" wing accelerates the ejected shell. Such a scenario is probably demonstrated by the system of four concentric shells NGC 6164-5.

III. When a massive star explodes as a supernova, the SN ejecta will interact mainly with stellar material (stellar wind and slow ejected shell). This is confirmed by:

a) Optical, radio-, UV-, IR- and X-ray light curves of the type II SN 1979c and 1980k (Chevalier, 1984).

b) Spectral line profiles with two absorption features P Cyg in SN 1984g (NGC 3169) are probably evidence of a "superwind" before the SN-explosion (Dopita et al., 1984).

c) Optical or X-ray halos around the Crab Nebula, Cas A, G292.0+1.8 and other young SNRs.

d) Ambient density ($n_0 \simeq 0.5\ cm^{-3}$ as required by X-ray observations of the SNRs Tycho and Kepler) is too large for ISM at $z \simeq 300$-400 pc. The most reasonable explanation seems to be the interaction of SN ejecta with the circumstellar material.

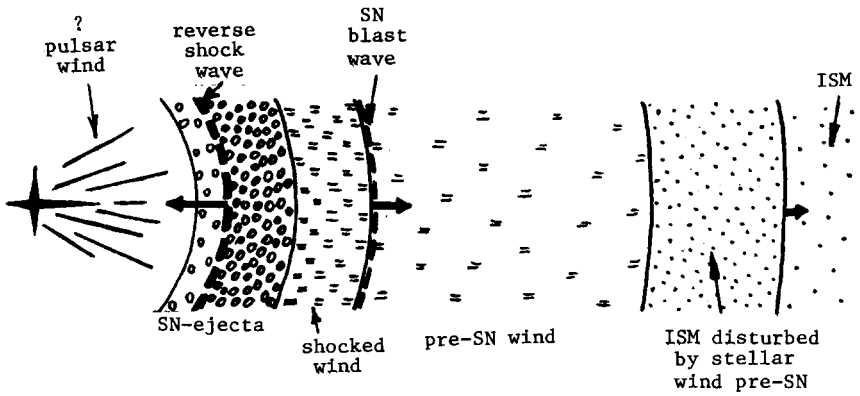

Fig. 1

e) A very thin radio "rim" surrounding the main radio shell of the Tycho SNR cannot be explained without a shell of matter - presumably a pre-SN planetary nebula - around the exploding white dwarf (Dickel, Jones, 1985).

f) In Cas A and Tycho SNRs X-ray emission of SN ejecta and of shocked progenitor's wind is resolved in space and corresponds to different T_e, n_e.

g) Optical and X-ray observations of Cas A show a two-component composition of the progenitor stellar wind (dense stationary optical condensations and diffuse X-ray shell) and two-component SN ejecta (fast optical filaments and diffuse X-ray shell). The X-ray image of Tycho's SNR (Seward et al., 1983) also shows diffuse and clumping SN ejecta.

h) A class of "O-rich" SNRs (Cas A, G292.0+1.8, N132D, 1E0102-7219) demonstrates non-spherical SN ejecta: an expanding torus plus a diffuse spherical shell, surrounded by a faint halo. Such a peculiar structure provides a model of a massive rotating (or with a compact companion) precursor with strong stellar wind, the most probable candidate being a WR star.

References:

Chevalier, R.A., 1984, 11. Texas Symp., Ann. N.Y.Acad.Sci., p. 215.
Dickel, J.R., Jones, E.M., 1985, Ap. J. Lett. v. 287, L69; Ap. J. v. 288, p. 707.
Dopita, M.A., Evans, R., Cohen, M., Schwartz, R.D., 1984, Ap. J. Lett. v. 287, L69.
Seward, F., Gorenstein, P., Tucker, W., 1983, Ap. J., v. 266, p. 287.

"Eruptive Phenomena in Stars"
Commun. Konkoly Obs. Hung.
Acad. Sci., No.86, Budapest

DISPERSION OF THE CHEMICAL ABUNDANCES IN CRAB NEBULA GAS FILAMENTS

V.V. Golovaty and V.I. Pronik

Lvov University Observatory and
Crimean Astrophysical Observatory, USSR

In a previous paper (Golovaty and Pronik, 1973) we presented qualitative arguments relating to the dispersion in the chemical abundances of Crab nebula filaments. However, this conclusion was based only on Woltjer's (1958) spectral observations of the filaments. There is now much more extensive information upon many individual condensations (Davidson, 1978 and 1979; Davidson et al., 1982; Fesen and Kirshner, 1982; Miller, 1978) and the present quantitative analysis was based on this information.

The complete set of spectral line intensities $I(\lambda)$ suitable for determining the chemical abundance of individual filaments has been observed, unfortunately, only for several bright condensations. To obtain the intensities $I(\lambda)$ which are missing from the observational data we studied the correlations between different $I(\lambda)$ using data on filaments for which these lines were observed.

As a result we were able to reveal all available relations between the intensities of different spectral lines: $[OIII]/H_\beta \hookrightarrow [OII]/H_\beta$; $[OIII]/H_\beta \hookrightarrow I(\lambda)/H_\beta$; and $[OIII]/H_\beta \hookrightarrow [OII]/I(\lambda)$. These relations were used to obtain a combined spectra of the filaments.. We consider three types of filament spectra (A,B,C) corresponding to the ratios of the intensities λ4959+5007 $[OIII]/H_\beta$ equal to 5, 16 and 40. These values correspond to minimum, average and maximum values of $[OIII]/H_\beta$ observed. In order to determine the abundances of the chemical elements we used the method based on the photoionization models of filaments (Golovaty and Novosiadly, 1985). The best agreement between calculated and observed spectra is achieved for the following chemical compositions:

	A	B	C
He/H	0.15	0.48	1.2
$N/H(10^{-4})$	0.92	0.33	0.28
$O/H(10^{-4})$	1.4	2.3	2.2
$Ne/H(10^{-4})$	0.78	0.86	0.80
$S/H(10^{-4})$	0.64	0.35	0.10

It is seen that the dispersion of abundances is real for He/H, N/H, S/H and possible for O/H. The chemical composition of the filaments of group A is near the normal one.

References:

Davidson, K., 1978, Astrophys. J., 220, 177.
Davidson, K., 1979, Astrophys. J., 228, 179.
Davidson, K., Gull, T.R., Maran, S.P., Stecher, T.P., Fesen, R.A., Parise, R.A., Harvel, C.A., Kafatos, M., and Trimble, V.L., 1982, Astrophys. J., 253, 696.
Fesen, R., and Kirshner, R., 1982, Astrophys. J., 258, 1.
Golovaty, V., and Novosiadly, B., 1985, Astrofizika, 22, (in press).
Golovaty, V., and Pronik, V., 1973, Astr. Zhu., 50, 1147.
Miller, J., 1978, Astrophys. J., 220, 490.
Woltjer, L., 1958, BAN, 14, No. 483, 39.

"Eruptive Phenomena in Stars"
Commun. Konkoly Obs. Hung.
Acad. Sci., No.86, Budapest

RUNAWAY INSTABILITY IN THE INNER COOLING REGION OF OPTICALLY THIN, BREMSSTRAHLUNG DISKS AROUND KERR BLACK HOLES

H.G. Paul

Zentralinstitut für Astrophysik der AdW der DDR,
Sternwarte Babelsberg. DDR-1502 Potsdam, Rosa-Luxemburg-Str. 17a

There is an inner rapidly cooling region in thin α-accretion disks (Fang, 1980; Zhang and Jiang, 1982) that is induced by gravity (Paul, 1985a) and shows non-singular inner boundary behaviour between the radii of marginally stable, r_{ms}, and marginally bound, r_{mb}, test particle orbits (Paul, 1985b). In the very short dynamic timescale t_φ of this region "catastrophic" mass overflow is found by taking into consideration the hole's change in the total mass-energy M and total angular momentum $a_* = a/M$. The hole evolution appearing during the change of its gravitational field is described by the differential equations $\delta M = E^+(r_{in})\delta M_o$ and $\delta a = [L^+(r_{in}) - aE^+(r_{in})]\frac{\delta M_o}{M}$ (Bardeen, 1970; Thorne, 1974). E^+ and L^+ are the specific energy and angular momentum, respectively, of the disk matter on the inner disk edge and these are carried into the hole by the accretion flow $\dot{M}_o$ through the free fall region ($\delta L^+ = 0$). Consequently, the cusp-like wall of the effective disk potential braking and supporting the disk matter in its innermost region, varies ($\delta r_o/r_o = K\delta M_o/M$) with the corresponding variation of the inner disk boundary ($\delta r_{in}/r_{in} = N\delta M_o/M$). For sufficiently high angular momenta of the Kerr hole ($1 > a_* \gtrsim 0.8$), runaway instability appears ($K > 0$, $K > N$) and operates on the dynamic timescale $t_\varphi = \frac{2\pi}{\Omega} = 2\pi \frac{r^{3/2}}{M^{1/2}}\left(1 + \frac{aM^{1/2}}{r^{3/2}}\right)$ of the inner cooling region. The instability condition $K > N$ is fulfilled while $\partial_r \ln T(r) > f(r)$ and $K > 0$. (T is the temperature profile and f(r) is an algebraic function determined by the Kerr space time.) This instability condition breaks down near the radius of the marginally stable test particle orbit, r_{ms}, being the inner boundary of the standard models. That means that the runaway instability acts in the inner cooling region only, $r_{mb} < r < r_{ms}$.

The runaway instability found in thick accretion disks in the slender torus approximation for the Schwarzschild hole (Abramowicz et al., 1983) does not exist for the thin α-disk models.

Very short aperiodic luminosity bursts could be connected with the instability, found here, because these act in the extremely short dynamic timescale t_φ of the disk matter moving in the immediate vicinity of the Kerr hole. For example, using the system parameter of Cyg X-1 and assuming an angular momentum $1 > a_* \gtrsim 0.8$ for the black hole candidate we get burst durations of $0.64\ \text{ms} > t_\varphi > 1.7\ \text{ms}$. ($a_* \simeq 0.8$ appears to be the best value with respect to the observation.) In the case of type II bursts of galactic bulge and cluster sources (Shapiro and Teukolsky, 1983) (t_φ is in the order of seconds to minutes) $M \simeq 10^6\ M_\odot$ and $1 > a_* \gtrsim 0.8$ must be imposed as the most convenient hole parameter. The typical history of the unstable inner cooling region repeating many times, could possibly be described by the filling up of the cooling region with the following emptying of the innermost disk region as a function of the time required for filling up.

References:

Abramowicz, M.A., Calvani, M., Nobili, L., 1983, Nature 302, 597.
Bardeen, J.M., 1970, Nature, 226, 64.
Fang, L., 1980, Scienta Sinica, 9, 867.
Paul, H.G., 1985a, Astron. Nachr. 306, 3.
Paul, H.G., 1985b, Astron. Nachr. in press.
Shapiro, S.L., Teukolsky, S.A., 1983, In: Black Holes, White Dwarfs, and Neutron Stars. John Wiley & Sons, New York.
Thorne, K.S., 1974, Ap. J. 191, 507.
Zhang, J., Jiang, S., 1982, Acta Astrophys. Sin., 2, 277.

"Eruptive Phenomena in Stars"
Commun. Konkoly Obs. Hung.
Acad. Sci., No.86, Budapest

SHELL PHENOMENON IN Be STARS

P. Harmanec

Astronomical Institute, Czechoslovak Academy of Sciences,
251 65 Ondřejov, Czechoslovakia

By definition, a Be star is a star of spectral type B which exhibited emission in at least one H I Balmer line on at least one occasion. Surprisingly enough, most of the objects meeting this purely descriptive definition show notable mutual similarities in their behaviour. Their basic properties are quite similar to those of normal main-sequence B stars.

Most bright Be stars cluster around the B2 spectral subclass with a secondary maximum near B8. One notable property of Be stars is the lack of very low $v \cdot \sin i$ values. The projected rotational velocities of most of these stars lie between 200 and 300 km/s.

Be stars are not rare. They represent at least 10 to 20 per cent of all B stars, perhaps even more because the time scales involved are long in many cases, and new (even bright) Be stars are being discovered almost every year.

A fascinating property of Be stars is their spectacular time variability. They are apparently the most variable objects in the upper main sequence. Spectral variations include line-profile variations, including a complete disappearance and re-appearance of the Balmer emission in some cases (most often on a time scale of years to decades), as well as radial-velocity and V/R variations of the double emission lines. Accompanying - or independent - light, colour and polarization variations have also been found for a number of Be stars. The time scales of these variations range from at least 0.5 days to decades, even for a particular star. (For a more detailed description of time variations of Be stars see, e.g., the reviews by McLaughlin 1961, Slettebak 1979 or Harmanec 1983b.) Although systematic work has led to discoveries of some periodic components in these variations, the future time behaviour of any real Be star appears unpredictable

at the moment. This fact may be either an essential property of Be stars or may reflect the fact that much longer series of observations (over several hundreds of years) are necessary to discover some regularity in the Be-star time behaviour.

In some Be stars, narrow absorption lines of hydrogen, metals, and (for early B stars) of He I are observed, superimposed on the photospheric and/or emission lines. These lines are usually called *shell lines*. Stars exhibiting shell lines have been called *shell stars*. Once, they were considered to form a distinct group of objects. Nowadays, the occurrence of a shell spectrum is understood as a certain phase in the time variability of Be stars which may or may not occur in particular objects (see Underhill and Doazan 1982, and references therein). It is preferable, then, to speak about the *shell phenomenon* rather than about shell stars.

In the classical picture, the hydrogen emission is assumed to originate in an extended envelope (shell, disk) around the star, and the shell lines in the parts of the envelope projected against the stellar disk. However, neither the nature of the Be and shell phenomenon nor the mere geometry of the envelopes is well understood. This is best illustrated by the fact that the number of hypotheses trying to explain the Be phenomenon is still increasing - obviously all of them have active proponents. In their historical order, they are as follows:

1. Rotational hypothesis by Struve (1931). This hypothesis assumes the formation of Be envelopes by the rotational instability of underlying stars, arguing with the observed correlation between the emission-line widths and $v \cdot \sin i$. This hypothesis, however, offers no clear explanation of the time variations observed. Extensive modelling of observable parameters has been carried out on the basis of the rotational hypothesis (see, e.g., Poeckert and Marlborough 1978, Křiž 1979, and references therein). A recent defence of the rotational model can be found in Dachs et al. (1984).

2. The hypothesis of a radial outflow of matter due to radiative pressure by Gerasimovič (1934, 1935) postulates cycles in which the increasing density of envelopes stops further outflow, thus explaining qualitatively the long-term variations of the envelopes.

3. Binary hypothesis by Křiž and Harmanec (1975) (see also Harmanec and Křiž, 1976 and Harmanec, 1982). This understands Be envelopes as accretion disks produced by mass transfer from a secondary (which is often unseen) in a binary system. Be stars are interpreted as close relatives of

Algol-type binaries, symbiotic binaries and similar objects. The binary model is potentially able to explain many of the time variations observed. Indeed, the number of known Be binaries (including the optical counterparts of the massive X-ray binaries) is still increasing, and the causal connection between binarity and the time variations observed in such objects appears well established. However, due to the negative results of the attempts to prove the binary nature of a number of well-known Be stars, most astronomers are reluctant to accept the binary hypothesis as a universal interpretation of Be stars.

4. *Variable spheroidal mass flux hypothesis* by Doazan and Thomas (see Chapter 13 in Underhill and Doazan, 1982, and references therein). In some respects this is reminiscent of Gerasimovič's model. It does not make any specific conclusions about the cause of the postulated mass flux. Mass flux, radiative energy flux, and non-radiative energy flux are considered as three independent parameters controlling the formation and the time variations of Be envelopes. The following - essentially radial - sequence of regions is postulated: photosphere, a hot region (chromosphere-corona) with large expansion velocities, and a cool Be envelope, with only small expansion velocities. A potential problem of this hypothesis in its present form is that the evidence of large mass outflows based on the observations of the UV resonance lines appears much less safe than believed so far (see Hubený et al., 1985). In some sense, however, the variable mass flux hypothesis represents an interesting attempt at unifying all other hypotheses as special cases of a more general one. The disadvantage of the present "empirical" approach is, however, that it does not offer any verifiable predictions other than "omnia mutant".

5. *The hypothesis of local magnetic fields* is being developed by Underhill and her collaborators (Underhill, 1982; Underhill and Fahey, 1984). It assumes the existence of local bipolar magnetic fields on the surface of Be stars, and connects the observed variations with them. Unfortunately, there is little hope of detecting such fields directly by means of available observational techniques. However, the mere existence of Be stars with strong global magnetic fields (Landstreet and Borra, 1978) makes this hypothesis worth developing further.

6. *Hypothesis of non-radial pulsations*. This hypothesis - originally proposed by Baade (1979, 1982), and further developed by Vogt and Penrod (1984) and Willson (1985) - assumes that Be stars are non-radial pulsators

and that their envelopes are formed when the amplitude of non-radial pulsations increases beyond a certain limit. Different investigators have different opinions, however, as to the relative role of pulsation, rotation, and stellar winds in the whole process. The main argument of the proponents of this hypothesis is that the line-profile variations, detected by signal-generating detectors, can usually be modelled successfully by (often high-order) non-radial pulsational modes.

Let us turn back to the observational evidence of the shell phenomenon. Recent studies have indicated that one has in fact to recognize the following distinct phenomena:

1. A particular phase of the long-term variations. Spectacular long-term spectral variations have been known for years for a number of Be stars. In extreme cases, transitions from the B to the Be phase and from the Be shell phase and back to the B phase have been observed. Until recently, there tended to be a lack of simultaneous photometric observations although as early as in 1928 Gerasimovič (1928) suspected a correlation between the light and the H I emission during the long-term variations of Mu Cen. After the pioneering systematic photoelectric observations of BU Tau by Sharov and Lyuty (1976 and references therein), Harmanec, Horn and Koubský (1980) organized an observing campaign on long-term photoelectric monitoring of all bright Be stars. At present, this campaign is supplemented by systematic H alpha profile monitoring of the same stars, initiated by Barker (1981). The first results obtained by this campaign as well as those obtained by other observers allowed Harmanec (1983a,b) to define two basic extreme cases of the long-term variations observed:

A) The positive correlation between the long-term light variations and the strength of the H I emission has been observed for most of the Be stars studied. The brightness of such objects increases during the transition from the B to the Be phase. In the U-B versus B-V diagram, such objects move from the main sequence to supergiants, essentially unchanging their photometric spectral type at the same time.

B) The inverse correlation between the long-term light and H I emission variations has been observed for several Be stars during the transition from the B to the Be phase. Such objects usually move along the main sequence towards later spectral subtypes in the U-B/B-V diagram, without changing their luminosity class.

A transition from Be to the Be shell phase is usually connected with a light decrease. Also, an increase in the degree of polarization usually accompanies the development of the envelope.

Harmanec (1983b) proposed that the above-mentioned types of behaviour can qualitatively be well understood as a geometrical effect of flattened Be envelopes that change their density and/or extent with time.

In a broader context, it is of interest that the light and spectral behaviour of long-term variations with the positive correlation is reminiscent of a very mild nova outburst (the full amplitude of the light changes of Be stars is usually less than 1^m, however) while the inverse correlation bears some resemblance to the variations of R CrB stars.

2. Recurrent shell episodes. The periodic or nearly periodic reappearance of a well-developed shell spectrum has been reported for several Be stars, for instance AX Mon ($P = 232^d.5$, Cowley, 1964), KX And ($P = 38^d.91$, Struve, 1944), and HR 2142 ($P = 80^d.86$, Peters, 1983). All such changes are now understood as phase-locked variations connected with the orbital motion of corresponding Be stars in binary orbits. The shell spectrum is observed when the gas stream between the components is projected against the disk of the Be component. A light minimum, observable in the U colour only, often accompanies such "shell" episodes.

3. Occasional occurrence of the blue-shifted shell lines. Doubling of the hydrogen shell lines, occurring at apparently irregular intervals, has been reported for several Be stars - particularly for known binaries with cool secondaries such as AX Mon, 17 Lep or KX And. The second system of shell lines is always blue-shifted, with velocities of about -100 to -300 km/s, and often of comparable intensity with respect to the basic system of the H I shell lines. The nature of this phenomenon is completely unclear at present.

4. Narrow blue-shifted components of the UV resonance lines. Such lines, with velocities ranging from -100 to -1500 km/s, have so far been observed in the resonance doublets of the C IV, N V, Si III, Si IV, etc., of about ten Be stars. The lines appear and disappear at apparently irregular intervals. Multiple components with several distinct velocities have been reported for a few stars. The same feature is quite common among the OB supergiants. Harmanec (1983b) called attention to the fact that these lines are observed only for Be stars of spectral type B2 and earlier. He also pointed out that the blue-shifted H I lines, seen in the optical

spectra, and these narrow components may in fact represent the same phenomenon.

Henrichs et al. (1983) developed a model of a radial outburst of a more dense material within a steady stellar wind to account for the existence of the narrow components, while Underhill and Fahey (1984) argue that the character of these lines indicates that the material is flowing from localized areas onto the stellar surface and they postulate the existence of local bipolar magnetic fields.

One may ask which of the observed phenomena are indicative of "eruptions" from Be stars. The answer to this question is not quite clear at present. Tentatively, one may consider the following phenomena:

i) Long-term variations, taking into account their similarity to novae eruptions.

ii) The narrow blue-shifted shell lines, keeping in mind, however, that they often persist for months or years.

iii) Photometric evidence: There is rather unconvincing work by Bakos (1969, 1970, 1984). He detected a 3^m flare of the B8e star HD 160202 occurring within several minutes. The trouble is that the flare was recorded with an experimental TV system. The image on the TV screen was regularly recorded on photographic plates. Subsequent photoelectric observations of the star over two observing seasons failed to detect any variations in excess of $0^m.01$. Page and Page (1970) found a flare-like brightening of 66 Oph for more than 1^m from their patrol photographs. Subsequent photoelectric photometry of the star by several groups of observers revealed only variations smaller than $0^m.1$, however.

iv) The following sequence of observations of Lambda Eri is worth mentioning: Lambda Eri is a Be star which was found to vary regularly in light and radial velocity, with a stable period of 0.7 days (Bolton, 1982; Percy, 1981). The amplitude of these variations changes with time, down to practically zero on some epochs. Penrod (1985) observed line-profile variations of this star and modelled them as non-radial pulsations. He recorded the following sequence of events:

1983 Aug 25, Sept 20	no Balmer emission	large "pulsational" amplitude (10–15 km/s)
Oct 10	emission present	amplitude still large
Nov 22	emission present	pulsations unseen
Dec 19	still emission	only small-amplitude variations
1984 Apr 12, Aug 17	no emission	pulsational variation returned.

One possible interpretation of this sequence of events, advocated by Penrod, is that the pulsational energy was temporarily spent on the release of a Be envelope. Harmanec (1984) advocates another interpretation, however. He pointed out that the rapid Be variables have usually double-wave light curves, and suggested that such Be stars may be spotted stars, similar to magnetic CP stars or RS CVn stars (see Olåh, page 393 in this volume). He mentioned three such cases but since then, other rapidly variable Be stars have been discovered and the number of Be stars with confirmed double-wave light curves now amounts to almost fifteen, including Lambda Eri itself. Practically all of them have periods between 0.5 and 2 days, i.e. in the range of expected rotational periods.

Concluding, I would like to stress the following two points:

i) The general importance of Be stars in a broader context lies, perhaps, in the fact that they may represent, after all, more simple examples of non-stationary phenomena such as are observed in violent form in novae, symbiotic or eruptive stars.

ii) Only new, systematically obtained observational data, and a careful critical analysis of existing observations along with continuing progress in theoretical modelling, could help in deciding between the various existing hypotheses of the Be phenomenon. It is of primary importance to find the ways how to decide whether non-radial pulsations or some geometrical (obscuration) effects are responsible for the rapid variations observed.

Acknowledgements

I am deeply obliged to Dr. John R. Percy for several discussions on the problem, and to Dr. Ivan Hubený for critically reading this manuscript.

References:

Baade, D., 1979 Thesis, Astron. Inst., Univ. Münster.
Baade, D., 1982, Astron. Astrophys., 105, 65, and 110, L15.
Bakos, G.A., 1969 in "Non-Periodic Phenomena in Variable Stars", ed. by L. Detre, Akadémiai Kiadó, Budapest, p. 159.
Bakos, G.A., 1970 Sky and Telescope 40, 214.
Bakos, G.A., 1984 in "The Origin of Nonradiative Heating / Momentum in hot Stars", ed. by A.B. Underhill and A.G. Michalitsianos, NASA CP 2358, p.62.

Barker, P.K., 1981 Be Newsletter 3, 14.
Bolton, C.T., 1982 IAU Symp. 98, 181.
Cowley, A.P., 1964 Astrophys. J. 139, 817.
Dachs, J., Hanuschik, R., Kaiser, D., 1984 Mitt. Astr. Gesell. No. 62.
Gerasimovič, B.P., 1928 Harvard Bull. 854, 3.
Gerasimovic, B.P., 1934 Mon. Not. R. astr. Soc. 94, 737.
Gerasimovic, B.P., 1935 Observatory 58, 115.
Harmanec, P., 1982, In: Proc. IAU Symp. No. 98; Eds. M. Jaschek and H.G. Groth, Reidel, Dordrecht, p. 279.
Harmanec, P., 1983a in "Advances in Photoelectric Photometry I", ed. by R.C. Wolpert and R.M. Genet, Fairborn, p. 42.
Harmanec, P., 1983b in "Workshop on Rapid Variability of Early-Type Stars", ed. by P. Harmanec and K. Pavlovski, Hvar Obs. Bull. 7, 55.
Harmanec, P., 1984 Bull. Astron. Inst. Czechosl. 35, 193.
Harmanec, P., Horn, J., Koubský, P., 1980 Be Newsletter 2, 3.
Harmanec, P., and Kříž, S., 1976, in "Be and Shell Stars", Proc. IAU Symp. No. 70, ed. A. Slettebak; Reidel, Dordrecht, p. 385.
Henrichs, H.F., Hammerschlag-Hensberge, G., Howarth, I.D., Barr, P., 1983 Astrophys. J. 268, 807.
Hubený, I., Štefl, S., Harmanec, P., 1985 Bull. Astron. Inst. Czechosl. 36, 214.
Kříž, S., 1979 Bull. Astron. Inst. Czechosl. 30, 83 and 95.
Kříž, S., Harmanec, P., 1975 Bull. Astron. Inst. Czechosl. 26, 65.
Landstreet, J.D., Borra, E.F., 1978 Astrophys. J. 224, L5.
McLaughlin, D.B., 1961 J. Roy. Astron. Soc. Canada 55, 13 and 73.
Page, A.A., Page, B., 1970 Proc. Astron. Soc. Australia 1, 324.
Penrod, G.D., 1985 Paper presented at a workshop on "Pulsation and Mass Loss in OB Stars", Univ. Colorado, Boulder, April 1985.
Percy, J.R., 1981 in "Workshop on Pulsating B Stars", ed. by G.E.V.O.N. and C. Sterken, Nice Obs., p. 227.
Peters, G.J., 1983 Publ. Astron. Soc. Pacific 95, 311.
Poeckert, R., Marlborough, J.M., 1978 Astrophys. J. Suppl. 38, 229.
Sharov, A.S., Lyuty, B.M., 1976 IAU Symp. 70, 105.
Slettebak, A., 1979 Space Sci. Rev. 23, 541.
Struve, O., 1931 Astrophys. J. 73, 94.
Struve, O., 1944 Astrophys. J., 99, 75.
Underhill, A.B. 1982 Be Newsletter 6, 21.
Underhill, A.B., Doazan, V., 1982 "B Stars with and without emission lines", NASA SP-456 Monograph.
Underhill, A.B., Fahey, R.P., 1984 Astrophys. J. 280, 712.
Vogt, S.S., Penrod, G.D., 1983 Astrophys. J. 275, 661.
Willson, A.L., 1985 Paper presented at a workshop on "Pulsation and Mass Loss in OB Stars", Univ. Colorado, Boulder, April 1985.

"Eruptive Phenomena in Stars"
Commun. Konkoly Obs. Hung.
Acad. Sci., No.86, Budapest

STARSPOT PROBLEMS

K. Olåh

Konkoly Observatory, Budapest, Hungary

"To the extent that there is an active relationship between spots and flares, spots should be viewed therefore not simply as cool areas which are dull, compared to the more interesting behaviour exhibited by flares: rather, spots should be viewed as engines which do the work of converting the energy of convective flows into flare-compatible form." Mullan, 1983.

It is, of course, common knowledge that starspots are general features on some kinds of late type stars. The class of spotted stars is large and contains the BY Dra stars, the RS CVn stars with short, medium and long periods, and some of the W UMa stars. It is a well known fact that the BY Dra variables are the most eruptive family of spotted stars but some of the others also exhibit flare activity, e.g. the short period RS CVn star SV Cam, as was shown by Patkós (1981).

The spots and flares are closely linked but whereas flares are transient phenomena, spots have a long lifetime and can be traced.

My intention, in this report, is to review our knowledge about starspots but since even this question is too large I should like to concentrate on two main tasks: problems related to the temperature of spots, and the differential rotation in stars.

I. Starspot temperatures

I should first like to summarize the history of starspot temperature determinations. The first estimate of a spot temperature was made by Hall (1972) for RS CVn itself. It has a sunspot-like activity on the cooler star's surface. Hall assumed a dark region extending $\pm 30^{o}$ from the equator

in latitude and 180° wide in longitude. A spot of this size would occupy ~60% of the fainter hemisphere. From the typical amplitude of the light curve he found that the cooler hemisphere should be 2/3 as bright as the other which implies ~1000 K difference between the cooler and the warmer side. In the case of assuming a completely dark spot, the latitude extent would be $\pm 15^{\circ}$ occupying 1/3 of the cooler disk.

Another method for calculating the spot sizes and temperatures of the spots was developed by Mullan (1974). He pointed out (Mullan, 1973) that the diameter of starspots should increase when the depth of the convective zone increases. The starspots would have the size of the "super" convective cells which are ~2-3 times the depth of the convective zone. He carried out numerical calculations for stars having masses > 0.4-0.5 $M_{\odot}$. In the case of YY Gem he found the convective zone to be 0.33 R_{*} and the upper limit for the spot extent of 50°. In the presence of a magnetic field as large as B = 20 kGauss, T_e (spot umbra) was found to be ~1600-1900 K.

The increasing number of multicolour observations of RS CVn and related stars called attention to the colour variations. This feature can be explained by different temperatures. However, Vogt (1975) tried to explain the (B-V) amplitudes (which should not exceed 0.015) for BY Dra in another way: colour variations of this order may be due to variable Balmer and CaII H and K emission.

Barnes et al. (1978) continued angular diameter measurements together with UBVRI and BVRI photometry and developed relationships between F_V (surface brightness parameter) and $(U-B)_o$, $(B-V)_o$, $(V-R)_o$ and $(R-I)_o$ colour indices. Their very important results gave a good possibility for the direct determination of the spot temperatures. A very good and tight relationship was found between F_V and $(V-R)_o$ over the whole sample including all luminosity classes and spectral types. Moreover, the form of the relation very much resembles the blackbody case. The colour amplitude actually indicates a difference in temperature between the disk at maximum and minimum light. It approximates the spot temperature fairly well if not too many spots are seen in maximum light.

A similar method was used by Eaton and Hall (1979). They obtained a reasonably good result for the spot temperature of SZ Psc which was found to be 1200 ± 400 K cooler than the surrounding surface. For RS CVn they got $\Delta T \geq 500$ K.

Bopp and Noah (1980) also used the blackbody approximation to calculate spot temperatures. They derived $\Delta T = 800$ K for λ And from two colour data. A very important conclusion of their paper was that no single ΔT can be appropriate for all stars. Moreover, a given star may exhibit variations in ΔT from season to season. (In their model the effect of the limb darkening was neglected.) The same conclusion was found for HK Lac by Ollåh (1983).

Dorren et al. (1981) obtained intermediate and narrow band observations of V711 Tau: from the data they determined the spot temperature of 3800 K. For the star's surface temperature they gave 5660 K, which was obtained from spectral classification. The temperature difference here, viz. $\Delta T = 1660$ K, is again close to the solar value.

Vogt (1981a) obtained low dispersion Reticon spectrophotometry of II Peg when the spots were least and most in view. The flux ratio of the spectrum with the spot in view was divided by the flux ratio of the spectrum with the spot out of view. From the resulting flux ratio the spectral type of the spot could be derived which gave some information about the spot temperature (T_{spot} ~3400 K).

Vogt (1981b) gave a unique, well determined solution for deriving spot temperatures using the Barnes-Evans relation. The crucial but, at the same time, weak point of this model is that it gives a good solution only in those cases when the spots pass completely out of view at some phase, and therefore the unspotted light level is precisely obtained.

His resulting temperature differences were: for II Peg, $\Delta T = 1200 \pm 100$; for BY Dra, $\Delta T = 600 \pm 450$; and for HK Lac, $T \geq 950 \pm 200$. (In the case of HK Lac a lower limit only of ΔT can be calculated because the unspotted light level was not well determined.)

Vogt (1983) in his review paper briefly discussed the temperature modelling for different stars. He gathered the results for several cases and arrived at the conclusion that the starspot temperature is 3600 ± 200 K regardless of spectral type.

Stauffer (1984) gave a statistical minimum for the ΔT values. He concluded that spotted stars are $\sim 0^{m}.04$ bluer in (B-V) relative to (V-I) than are normal stars. If the emitted light from the spotted stars is given as a sum of the emission from two normal stellar photospheres with different temperatures, this colour difference manifests itself at $\Delta T > 700$ K.

Jahn and Stepien (1984) carried out detailed modelling of magnetic starspots. They calculated the relation between the masses of the stars and ΔT for given mixing length parameters (which reflects the efficiency of the convection). They found that the difference between the temperature outside and inside the spots practically does not depend on the magnetic flux. To derive the $M_* - \Delta T$ relation they supposed (using observed ΔT values) that practically one and the same ΔT exists for each star.

Ramsey and Nations (1981) determined $\Delta T = 1100 \pm 450$ K for II Peg with the help of the Barnes-Evans relation using V and R data.

Eaton and Poe (1984) redetermined the Barnes-Evans relation which is still very useful for deriving spot temperatures. The same authors (Poe and Eaton, 1985) used their modified Barnes-Evans relation for computing ΔT for some RS CVn systems. Their results for II Peg for different years strengthened the conclusion of Bopp and Noah (1980) about the existence of different ΔT's in stars at different times. They found $\Delta T = 910^{\circ}$, 1020° and 730° for 1977.6, 1979.7 and 1980.7, respectively. They noted that the variation of the limb darkening value can produce great variations in the colour curves. We shall discuss this point later.

And finally I should like to draw attention to an important result of Maltby et al. (1983) for the Sun: "The umbral temperature appears to increase by ~300 K from the beginning to the end of each solar half-cycle" - which is evidence again for different ΔT values in the same star at different times.

Regular observations of the spotted stars date back only about 10-15 years (in some cases 20 years). This is a relatively short time interval in which to draw some sort of picture about the spot-cycles, the development of individual spots, etc. The situation is even worse when we collect only those observations which were made in the more powerful red regions for temperature calculations. At present, it is very fashionable to collect suitable colour data for spotted stars during 1-2 observing seasons and then derive the most correct values possible for the spot parameters for that short time. If we wish to obtain information from the old UBV data so that we can follow the long term variations we must carefully examine the reliability and accuracy of the results which can be derived from them. Unfortunately, single-colour observations cannot be used for this investigation.

The spot model used here for the calculations was developed by Budding (1977). The basic task of this model is to decrease the degree of freedom

of the process. In view of this we should derive as many parameters as we can, independently of the spot model process. Let us examine these parameters.

First, we need the inclination (i) of the star. Since most spotted stars are members of binary systems, in those cases - at least when we have double-lined binaries - i is more or less well determined. If the binary is single lined and only the mass function is known, we can give limits for i and choose an appropriate value (see Olåh et al., 1985). Regardless, i must be kept constant during the modelling (it very strongly affects the latitude (β) value).

Other very important parameters are the limb-darkening coefficients. Unfortunately there exist no well established model atmospheres for late-type dwarfs. For late-type giants the situation is better in that the tables of Manduca, Bell and Gustaffson (1977) are very useful. Nevertheless, it seems to me to be better to use some previously determined values for these coefficients rather than to consider them as variables since this increases the degree of freedom of the process. Poe and Eaton (1985) stated that when they used different limb darkening values in their model calculations they found great changes in the colour curves. They used a completely dark spot (T_{spot} = 0 K) with a radius of $33\overset{\circ}{.}6$ and the u_λ values were varied between 0.5 and 1.0 when u_V was fixed to 0.8.

We made model calculations to see how the (B-V) amplitude (A(B-V)) depends on the different limb darkening values. A realistic spot size ($\gamma = 30^\circ$), latitudes ($\beta = 10^\circ$, 40°, 70°) and temperature differences ($\Delta T = 1000^\circ$, 1500°) were assumed. Limb darkening coefficients were altered from 0.5 to 1.0 with a 0.1 difference between u_V and u_B. The resulting colour amplitudes versus different limb darkening values are displayed in Figs. 1 and 2. In the first case (Fig. 1) a surface temperature of an MOV star (T_{eff} = 4100 K), in the second case a surface temperature of a KOIII star (T_{eff} = 4800 K) was used to calculate the flux ratio with the help of Planck's function.

It is well illustrated in Figs. 1 and 2 that the different limb darkening values do not very much affect A(B-V). In the worst case (between the 0.5-0.6 and 0.9-1.0 pairs), the difference in A(B-V) is about 0.01 mag. which is similar to the usual observation error. The 0.1 difference between u_V and u_B is great with respect to the directly obtained values for dwarf stars so the real effect should be even less than displayed here.

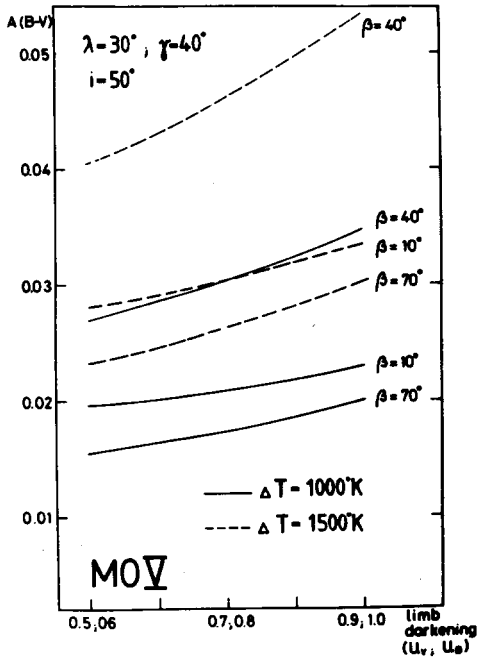

Figure 1. Amplitudes of B-V colour index vs. different limb darkening coefficients at different latitudes for an MOV star

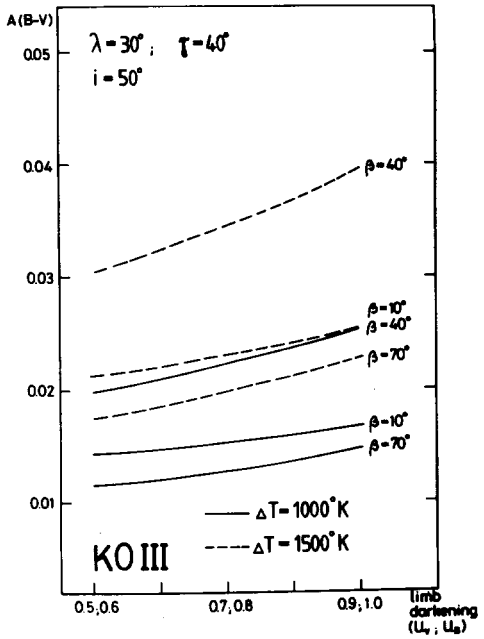

Figure 2. Amplitudes of B-V colour index vs. different limb darkening coefficients at different latitudes for a KOIII star

The question of the unspotted light level remains open; with the help of the literature some assumptions should be made.

A series of models was examined to study the dependence of the colour amplitude A(B-V) on ΔT. All the other parameters were fixed. In Table I the parameters used for the calculations are listed. Again, to obtain the flux ratio, Planck's function was used. The resulting curves are displayed in Figs. 3-11.

Table I

Spectral type	u_V	u_B	$\beta(^o)$	$\gamma(^o)$
MOV	0.78	0.82	10, 40, 70	30, 40
KOIII	0.75	0.85	10, 40, 70	30

It is not surprising that the greatest change in the colour amplitude is caused by the change in the spot area. Within the most probable ΔT interval (500-1500 K) the dependence of A(B-V) on orbital inclination i is not very strong in most cases. This means that the dependence of A(B-V) on the latitude of the spots is similar since i and β are closely related. (From this it follows that if the orbital inclination is well established with the use of a method other than spot modelling, the β value would be much better determined.)

We can now see that the most problematic point in spot modelling is to find suitable ΔT and γ values. One possibility exists to solve this problem, viz.: we must keep the parameters i, u_V, u_B and ΔT fixed during the process. Light curve models must be elaborated for the V and B light curves separately for a given ΔT value. Then, with different ΔT values, the procedure is repeated (with unchanged i, u_V and u_B values). The best solution that can be found is when the resulting spot parameters for the V and the B light curves are most similar to each other. An example of this method is given in Fig. 12, where the parameters for light curve modelling are given. The star which showed the light variation modelled here is BY Dra and the observations were carried out at Catania Observatory (Rodono, 1984). To solve the light curve, it was sufficient to assume one spot. In the modelling the unspotted light level was fixed very high, therefore no solu-

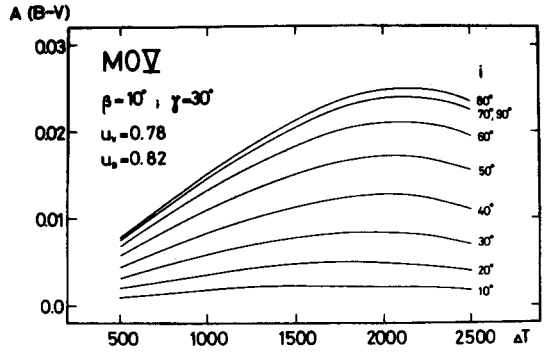

Figure 3

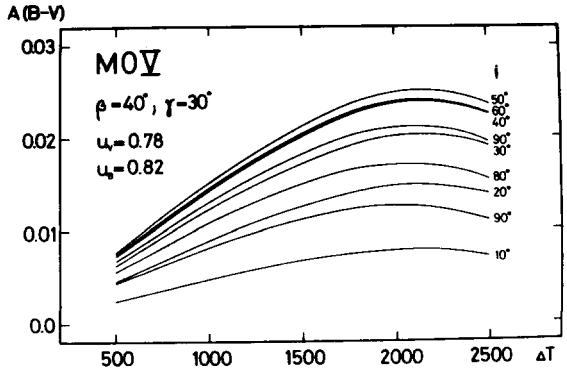

Figure 4

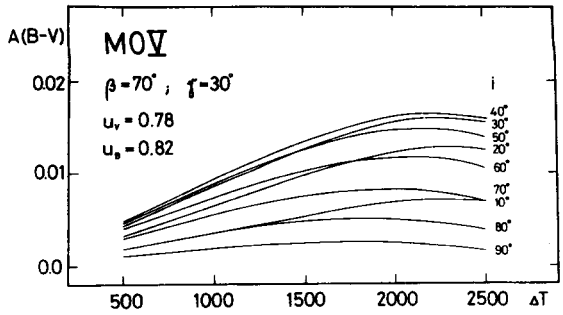

Figure 5

Figures 3-11. Amplitudes of B-V colour index vs. ΔT ($T_{star} - T_{spot}$) in case of different inclinations. β = spot latitude, γ = spot radius, u_V and u_B = limb darkening coefficients in V and B, respectively

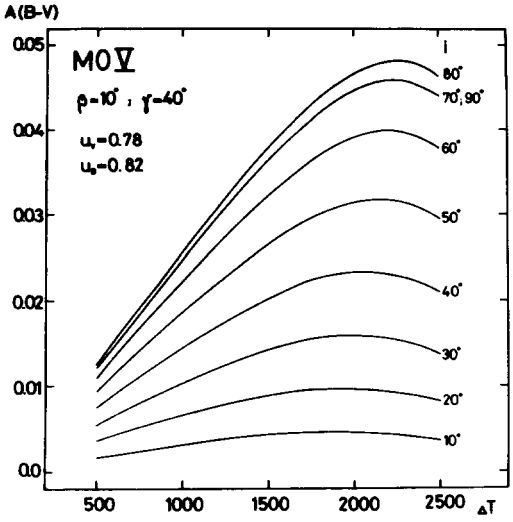

Figure 6

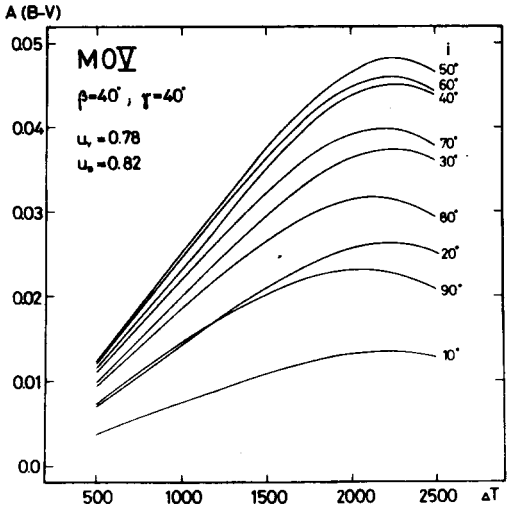

Figure 7

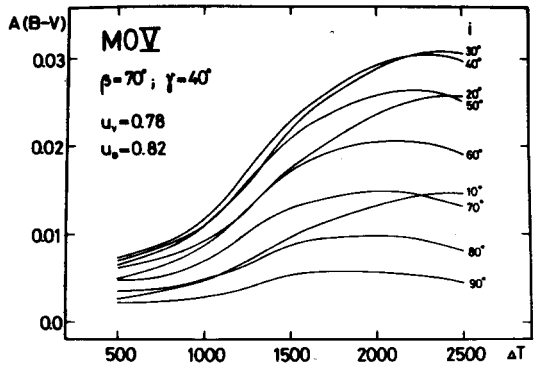

Figure 8

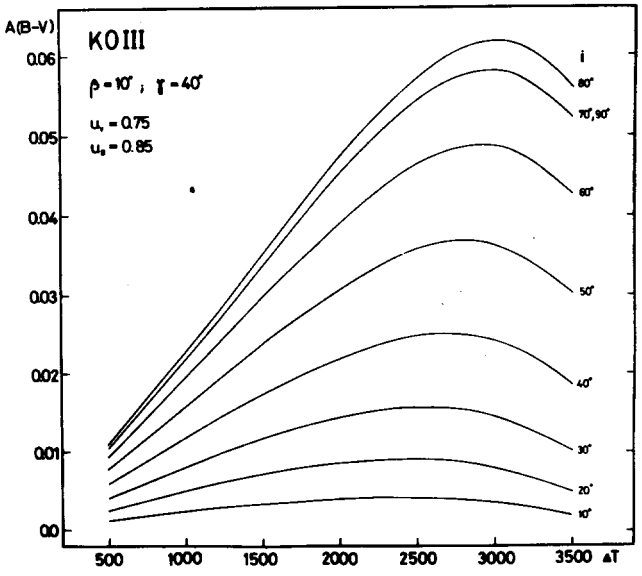

Figure 9

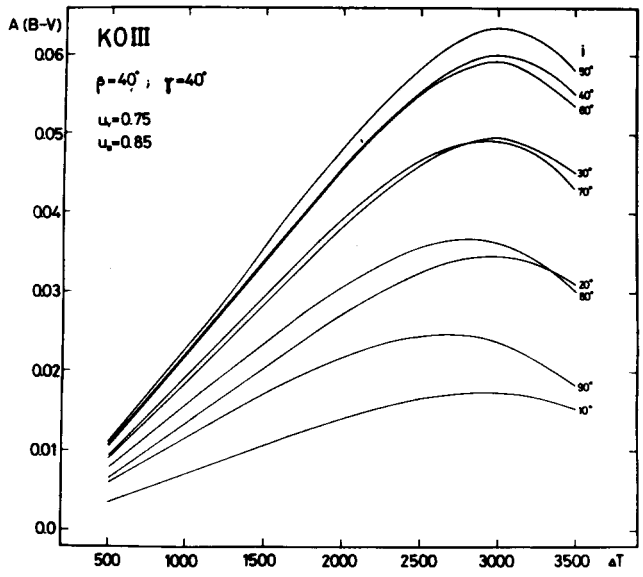

Figure 10

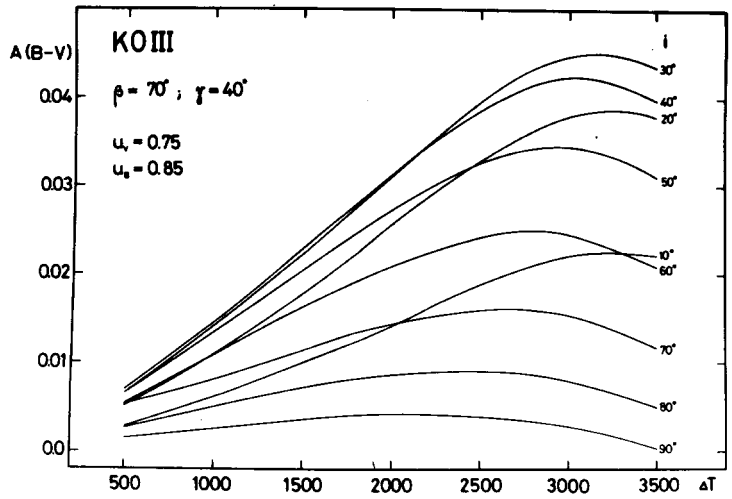

Figure 11

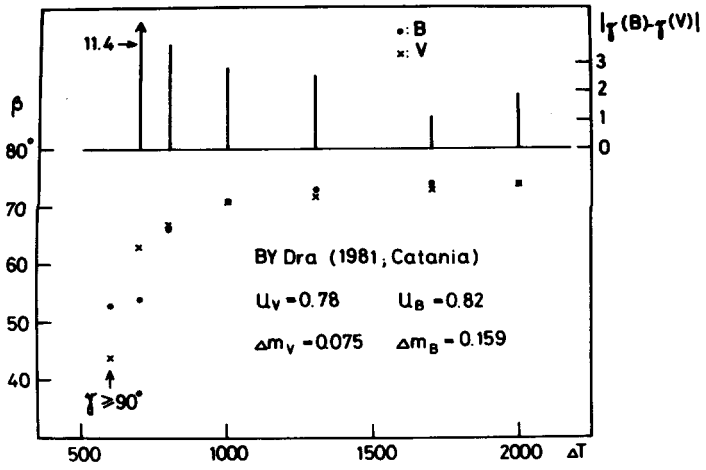

Figure 12. Latitudes and spot sizes' differences vs. ΔT ($T_{star} - T_{spot}$) using V and B light curves for modelling BY Dra.

tion exists for low temperatures. (The used value of the unspotted light level was chosen because at a given time the star was the brightest ever measured, and when it was observed, no light variation was found.)

In the upper part of the figure the differences between the resulting γ values (radius) for V and B colours are displayed. It is seen from the lower panel that the β coordinate of the spot soon became stable, and remained constant for a wide range of ΔT values. The λ (longitude) values were very stable during the whole modelling. The differences between the sizes of the spots have a minimum value around ΔT ~1500 K. Using the previously assumed and derived parameters with different methods this will provide the best solution for ΔT. The other parameters which were calculated by the model program enable the final solution of the spot coordinates to be obtained.

A similar method was used by Dorren et al. (1981) for V711 Tau. They determined the spot temperature from multicolour data and then that value was used in the course of the modelling.

II. Differential rotation

Since the very early period of starspot modelling researchers have been interested in the possibility of proving the existence of the differential rotation of the surface of spotted stars. The long-term behaviour of the spots on a star represents an excellent means of following the motions on the surface. However, this task needs more or less continuous observations of a given star for years. Here, I should like to stress the importance of the use of old UBV or even single colour observations. (Single colour observations can be used to determine the differential rotation since the great displacements - the coordinate changes - of the spots are not too much affected by the temperature differences between the spot and the surface.) The rotational and orbital periods, which we need to know for investigating the problem, are independent of the ΔT values. Determination of the differential rotation from the starspot motions needs no special procedure. Here we summarize some of the results obtained by different authors about different stars.

In one of the very first papers about RS CVn stars Hall (1972) discussed the light variation of RS CVn. By analysing the existing data he found that it was necessary to suppose the differential rotation which would produce the migration of the distortion wave. A co-rotating latitude at about 30° was estimated for the star. At that time no well defined starspot model existed so only indirect estimation of the spot coordinates was possible.

Chugainov (1973) found different periods for different epochs of BY Dra between 1965 and 1971 - doubtless these were caused by the differential rotation. This was theoretically discussed by Mullan (1974). Finally, using observations of BY Dra made between 1966 and 1977, Vogt (1981) determined a latitudinal shear for latitudes $40\text{-}80^{\circ}$; this was similar to the value given for the Sun in the same latitudes. In order to calculate this value, Vogt used well determined rotation periods and numerically derived spot coordinates using Budding's (1977) method.

Eaton and Hall (1979) found a link between the nonuniform rotation and the magnetic structure of the stars following the solar analogy.

Dorren et al. (1981) mentioned the possible existence of the differential rotation in V711 Tau.

Hall (1981) summarized our knowledge about the migration waves in different RS CVn systems and found them to be variable in most cases, as a

possible consequence of the latitude drifts of the spots in the 19 stars studied.

In spite of the fact that there was no possibility to derive accurate spot latitudes in λ And, Dorren and Guinan (1983) found direct evidence of the differential rotation. They found a spot cycle ~6 years long with corresponding period changes, which were thought to be caused by the relative displacements of the spots in differentially rotating latitudes (see Fig. 2 of their paper).

From the different migration rates of the maxima and minima of II Peg Rodono et al. (1983) found evidence of the differental rotation and gave a lower limit of the latitudinal shear in the star.

Based on solar analogy a method was developed by Busso et al. (1984) to determine the places of the co-rotating latitude, the spot forming region and the measure of the differential rotation. They used time series analysis for nonequally spaced data and they interpolated and reconstructed the light curves. With the help of the known value of the phase displacements of the migrating waves, Busso et al. (1984, 1985) calculated the parameters of the differential rotation for 5 systems (SV Cam, VV Mon, SS Boo, RU Cnc, CQ Aur).

Direct evidence (using a long series of V observations and the spot model) of the existence of the differential rotation was found by Olåh et al. (1985) for HK Lac. One of the spots rotated slightly faster and the other slightly slower than the orbital motion. Knowing the average latitudes of these spots we were able to estimate the co-rotating latitude of $25^{\circ} \pm 12^{\circ}$. The mean spot latitudes and the corresponding periods gave the other value of $31^{\circ} \pm 2^{\circ}$ for the co-rotating latitude.

Baliunas et al. (1985) carried out a survey on red dwarfs measuring the relative strength of the chromospheric CaII H and K emission cores during several seasons. From power spectra analysis of the data they found varying periodicities in 12 stars. For 10 stars significant peaks in the power spectrum at two different frequencies were found. These authors gave two possible explanations for this feature: either the two periods originate from two active areas at different latitudes (which are rotating differentially with respect to each other), or the active areas are born and subsequently decay at different longitudes. For 4 stars the differential rotation seemed to be the more likely explanation for the varying periodicities. For these stars the fractional differential rotation was found between 5% and 21%.

Both tasks mentioned here, viz. the ΔT problem and differential rotation, suffer from the lack of long series of observations. Nevertheless, some promising results are already available and it is to be hoped that within the next few years and with the help of better observational techniques, these questions can be answered in detail.

References:

Baliunas, S.L., Horne, J.H., Porter, A., Duncan, D.K., Frazier, J., Lanning, H., Misch, A., Mueller, J., Noyes, R.W., Soyumer, D., Vaughan, A.H., Woodard, L., 1985, Astrophys. J. 294, 310.

Barnes, T., Evans, D.S., Moffett, T.J., 1978, Mon. Not. Royal Astr. Soc. 183, 285.

Bopp, B.W., Noah, P.V., 1980, Publ. Astr. Soc. Pacific 92, 717.

Budding, E., 1977, Ap. Sp. Sci. 48, 207.

Busso, M., Scaltriti, F., Cellino, A., 1985, Astron. Astrophys. 148, 29.

Busso, M., Scaltriti, F., Blanco, C., Catalano, S., Marilli, E., Pazzani, V., Rodono, M., 1984, Astron. Astrophys. 135, 255.

Chugainov, P.F., 1973, Izv. Krymsk. Ap. Obs. 48, 3.

Dorren, J.D., Guinan, E.F., 1983, In: Cool Stars, Stellar Systems and the Sun, ed. by S. L. Baliunas and L. Hartmann, p. 259.

Dorren, J.D., Siah, M.J., Guinan, E.F., McCook, G.P., 1981, Astron. J. 86, 572.

Eaton, J.A., Hall, D.S., 1979, Astrophys. J. 227, 907.

Eaton, J.A., Poe, C.H., 1984, Acta Astronomica 34, 97.

Hall, D.S., 1972, Publ. Astr. Soc. Pacific 84, 323.

Hall, D.S., 1981, In: Solar Phenomena in Stars and Stellar Systems, ed. by R.M. Bonnet and A. Dupree, p. 431.

Jahn, K., Stepien, K., 1984, Acta Astronomica 34, 1.

Maltby, P., Albregtsen, F., Kjeldseth Moe, O., Kurucz, R., Avrett, E., 1983, In: Cool Stars, Stellar Systems and the Sun, ed. by S.L. Baliunas and L. Hartmann, p. 176.

Manduca, A., Bell, R.A., Gustaffson, B., 1977, Astron. Astrophys. 61, 809.

Mullan, D.J., 1973, Astrophys. J. 186, 1059.

Mullan, D.J., 1974, ibid. 192, 149.

Mullan, D.J., 1983, In: Activity in Red Dwarf Stars, IAU Coll. No. 71, ed. by P.B. Byrne and M. Rodono, p. 527.

Nations, H.A., Ramsey, L.W., 1981, Astron. J. 86, 433.

Olåh, K., 1983, In: Activity in Red Dwarf Stars, IAU Coll. No. 71, ed. by P.B. Byrne and M. Rodono, p. 403.

Olåh, K., Eaton, J.A., Hall, D.S., Henry, G.W., Burke, E.W., Chambliss, C.R., Fried, R.E., Landis, H.J., Louth, H., Renner, T.R., Stelzer, H.J., Wasatonic, R.P., 1985, Ap. Sp. Sci. 108, 137.

Patkós, L., 1981, Astrophys. Letters 22, 1.

Poe, C.H., Eaton, J.A., 1985, Astrophys. J. 289, 644.

Rodono, M., 1984, personal comm.

Rodono, M., Pazzani, V., Cutispoto, G., 1983, In: Activity in Red Dwarf Stars, IAU Coll. No. 71, ed. by P.B. Byrne and M. Rodono, p. 179.

Stauffer, J.R., 1984, Astrophys. J. 280, 189.

Vogt, S.S., 1975, Astrophys. J. 199, 418.

Vogt, S.S., 1981a, ibid. 247, 975.

Vogt, S.S., 1981b, ibid. 250, 327.

Vogt, S.S., 1983, In: Activity in Red Dwarf Stars, IAU Coll. No. 71, ed. by P.B. Byrne and M. Rodono, p. 137.

"Eruptive Phenomena in Stars"
Commun. Konkoly Obs. Hung.
Acad. Sci., No.86, Budapest

FLARE STARS - PHYSICS AND EVOLUTION

L.V. Mirzoyan

Byurakan Astrophysical Observatory, Armenia, USSR

Introduction

The most significant investigations on the study of flare stars and the phenomenon of stellar flares have been fulfilled during the last two decades. This work has resulted in a great deal of development and has helped to place the problem in one of the foremost positions in modern astrophysics.

Possibly the most important consequence of these investigations is the establishment of the flare activity stage in stellar evolution.

In the establishment of this important feature the following three results have played the decisive role:

1. Photographic observations of the Orion association region with wide-angle telescopes, leading to the discovery of some flare stars in this young system (Haro and Chavira, 1966).

2. The discovery of the first flare star HII 1306 in the Pleiades cluster (Johnson and Mitchell, 1958) thereby stimulating analogous photographic observations in this comparatively young system, owing to which some dozen flare stars were found in it.

3. The statistical estimation of the total number of flare stars in Pleiades (Ambartsumian, 1969) showing that almost all stars of low luminosity in this system are flare stars.

Highly significant results were obtained on the physical properties of stellar flares.

In this paper an attempt is made to present a state of the art report of the flare stars problem on the basis of flare star observations.*

---

*The fundamental tenets of the physical and evolutionary consideration of flare stars, on the basis of the observational data, were earlier given by Ambartsumian and the present author (1971, 1975) and in more detail by the present author (1981, 1984).

General Remarks

At the present time there is no doubt that the flare stars in star clusters and associations and the UV Ceti stars in the solar vicinity represent the same class of non-stable stars and the differences observed between them (luminosities, relation to nebula, etc.) are explained by the differences of their ages (see, for example, Mirzoyan, 1981).

Some apparent difference between them arises from the fact that the UV Ceti stars are studied, each individually, by methods possessing comparatively high time resolution (photoelectric photometry, slit spectroscopy, etc.) while the flare stars in systems are studied mostly by mass methods (photographic photometry, spectroscopy with objective prisms, etc.) having much lower time resolution.

Each of these approaches has its advantages and is suitable for the solution of different problems - the former of them related to physics and the latter to the evolution of flare stars.

At the same time, as expected, the most important results on stellar flares have been obtained by synchronous observations in different passbands.

The number of known UV Ceti stars in the solar vicinity has now reached 100 (a list of these stars is given in Gershberg's (1978) monograph). Apparently the majority of these stars are comparatively old stars which have already left the parent systems and have kept this activity until now owing to the longer duration for stars of very low luminosities (Mirzoyan, 1981) (see later).

Younger flare stars, possessing - on average - higher luminosities, are observed in star clusters and associations. By photographic observations with wide-angle cameras, carried out during about 7500 hours, approximately 1300 flare stars were found in the nearest systems.

Table I gives the distribution of flare stars in the comparatively better studied systems, according to Mirzoyan and Ohanian (1985). In it the total time of monitoring - τ, the number of known flare stars - n, the number of flare stars which showed only one flare-up during the whole time of photographic monitoring - n_1, and an estimation of the total number (low limit) - N of flare stars in the system, obtained by Ambartsumian's formula (Ambartsumian, 1969; Ambartsumian et al. 1970) are presented.

Table I. Flare Stars in Some Nearest Star Clusters and Associations

	τ (hours)	n	n_1	N
Pleiades	3175	546	287	994
Orion I	1406	482	380	1471
Taurus Dark Clouds	937	102	88	532
Cygnus (NGC 7000)	938	67	58	403
Praesepe	698	54	44	215
Monoceros I (NGC 2264)	105	42	40	442
around γ Cygni	324	16	15	129
T o t a l	7583	1309	912	4186

In Table I the striking fact is that the majority of known flare stars (about 70%) during the observations showed only one single flare-up. This can be explained by the too low mean frequency of flares in the majority. Really, as the distribution function of mean flare frequency for the stars of Pleiades cluster shows, the mean flare frequency for the majority of stars is very low in spite of the fact that there are great differences in these frequencies for different stars. This function was derived by Ambartsumian (1978) on the basis of the chronology of discoveries and the chronology of confirmations of flare stars. On the other hand, as a result of this, less than one third of all flare stars have been discovered up to now in the systems studied. If we take into account that the estimates of total number of flare stars in systems N, presented in Table I correspond to the lower limit of this magnitude (Ambartsumian et al., 1970), then it must be admitted that at present we know only a small part of all flare stars even in comparatively better studied systems like Pleiades and Orion.

Therefore, further photographic observations of regions of star clusters and associations with wide-angle telescopes are essential.

Evolutionary Stage of Flare Activity

Even before the determination of the evolutionary stage of flare activity the physical similarity between the emission of T Tauri type stars and the emission appearing during stellar flares, revealed by Ambartsumian (1954), suggested that the non-stable stars of these two classes are related.

Later, Haro and Chavira (1966), on the basis of the results of flare star photographic observations in associations and clusters, postulated that the stage of flare stars follows the stage of T Tau stars. A telling argument in favour of the evolutionary connection between these two stages was the discovery by Haro and Chavira (1966) and by Rosino (1969) of some T Tau type stars showing classical flare-ups in the Orion and the Monoceros associations.* This discovery has shown that the evolutionary stages of T Tau and UV Cet partly overlap in time. During the period of coverage the star is of the T Tau type and flare star, simultaneously.

Using the statistical data concerning the Orion association Ambartsumian (1970) has shown that the time of coexistence of these stages is equal to approximately one fourth of the duration of the T Tau stage. At the same time the observational data show that the duration of the flare star stage varies over wide limits.

Thus, the existence of flare stars in the Orion association (age of the order of 10^6 years (Allen, 1973)) gives us grounds to assume that the flare activity stage can begin very early. On the other hand, in this association there are stars of high enough luminosities which do not show flare activity or, at least, activity which is available for photographic observations. In the older systems, such as Pleiades (age of the order of 10^8 years (Allen, 1973)), and Hyades and Praesepe (age of the order higher than 10^8 years (Allen, 1973)), there are still some flare stars as well as the stars of high luminosities which have already ceased their flare activity. Finally, among stars of the solar vicinity there are flare stars whose age exceeds 10^9 years (Gershberg, 1978). Therefore, on the basis of the observational data, it can be concluded that the flare activity stage already begins when the age of stars is of the order of 10^6 years and even smaller and sometimes continues to more than 10^9 years.

It can be assumed that for an individual star the initial and ending phases of flare activity depend on the luminosity (mass) of the star: the higher the luminosity the earlier the flare activity begins and, correspondingly, ends.

In the case of the ending of flare activity phase this regularity is confirmed by the data related to the mean luminosities of flare stars in the system of different ages (Mirzoyan and Brutian, 1980). They show that

---

*Of about 90 flare stars, discovered by Hojaev (1985) recently in the Taurus Dark Clouds, 13 were found to be the known T Tau type stars.

the older the system (flare stars) the lower the mean luminosity of flare stars in it. This regularity can explain the fact that there are practically no flare stars of comparatively high luminosities in the general galactic field.

The inverse correlation between the mean luminosity of flare stars and the age of the system to which they belong, can be considered as direct observational evidence in favour of the idea that the evolution rates of stars depend directly on their luminosities (masses): stars possessing higher luminosity evolve more quickly than stars of lower luminosity (Mirzoyan, 1982).

Thus, the observational data allow one to outline the following evolutionary sequence of dwarf stars - T Tau stars - T Tau stars possessing flare activity - flare stars - stars of practically constant brightness.

Certainly, some questions connected with the presented evolutionary sequence have not yet been finally answered. For example, the transition from the T Tau stage to the flare star stage is apparently connected with the difficulty of solving the problem of masses.

The important question as to whether all stars, at least the dwarfs, pass through a flare activity stage, has not yet been solved. For example, the observations of flare stars in Pleiades testify that the positive answer to this question needs to assume that flare activity of stars has a cyclic nature: the periods of high flare activity alternate with the periods of comparatively low activity (Mirzoyan and Ohanian, 1977).

However, it is unlikely that new studies can lead to any essential change in the foregoing main evolutionary sequence.

Some Appearances of Flare Activity

The stellar flare is a rapid increase of the stellar brightness (usually during less than one minute) with its comparatively slower decrease to the former value. The course of the brightness variations during a flare can be given by its light-curve.

Investigations of light-curves of stellar flares have shown their large diversity (see, for example, the investigations of Oskanian (1969) and Moffett (1974)). It has turned out that to obtain an exact picture of the course of the brightness variations during a flare its observation with a sufficiently high time resolution is required.

Photoelectric observations of flares of the UV Cet type stars carried out with a time resolution of the order of 1 sec by Moffett (1974), Cristaldi and Rodono (1970), and by others has enabled flares to be recorded that have very complicated shapes of light-curves and that include the cases of superposition of a number of flares on each other. This fact led to the idea that the stellar flare is a complex phenomenon and, in general, it represents a multiple appearance of the additional energy released during the flare (Moffett, 1972; Mirzoyan, 1980).

It is necessary to note that the fine structure of light-curves of stellar flares can be studied only on the basis of observations possessing a sufficiently high time resolution. When time resolution is low, the shapes of light-curves are distorted. For example, very fast flares are usually lost and the complex shapes of flare light-curves obtained by the photographic multiexposure method are greatly distorted (see, for example, Mirzoyan, 1981).

For the study of fine details of flare light-curves, recorded by the photographic method in associations and clusters, the method of stellar tracks can be used successfully, as Chavushian (1985) has shown. In this method instead of a chain of images for each star its trace is recorded on the photographic plate.

With regard to the fine structure of flare light-curves the optical observations of flares of the UV Cet type stars carried out recently by Beskin et al. (1985) are valuable. The detailed analysis of some dozen light-curves of flares registered during these observations allowed them to affirm, in the author's opinion, that no major variation of their fine structure during the time of the order of 0.5 sec has been observed.

It should be noted that though the shape of the light-curve does not depend on the power of the flare (very powerful flares with spike-like light-curves and small flares with complex shape of light-curves have been observed (Moffett and Bopp, 1976)), however, there is some evidence that the more powerful a flare, on average, the higher the probability of observing a complex light-curve (Mirzoyan and Melikian, 1985).

A very essential property of stellar flares was discovered by Haro (1964). He divided all flares into two groups: "fast" and "slow", according to the flare rise time, using his multi-exposure photographic observations. Haro showed that for the majority of flares the rise time was short, that is 10-15 minutes ("fast"), whereas there are rare flares for which the

flare rise time reaches 20-30 minutes and more ("slow"). Haro also found that "fast" and "slow" flares differ from each other apparently by colours too ("slow" flares tend to be redder than the "fast" ones).

The difference between "fast" and "slow" flares can successfully be explained, if one assumes following Ambartsumian (1954), that the flare rise time is determined by the depth of the stellar atmospheric layers in which the flare takes place: the greater this depth the longer the flare rise time. Naturally, the flare rise time cannot be very long because if the depth is large enough then the flare will not be observable.

At present it can be said that Haro's classification, which was very fruitful, is actually a conditional one and is determined by the method of his observations. In reality the distribution of flare rise time durations is continuous: there is no sharp transition between "fast" and "slow" flares (Mirzoyan and Melikian, 1985). It is very probable that the flare rise time is indeed determined by the characteristics of those layers of stellar atmosphere in which the flare occurs. As evidence in favour of this idea the important fact can be considered that the majority of stars which have shown "slow" flares were also observed in "fast" flares (see, for example, Mirzoyan, 1981).

The fuor-like variations of star brightness (FU Ori phenomenon) can be considered as a remarkable manifestation of flare activity. After the brightening of V 1057 Cyg, before T Tau type spectrum, it has been revealed that such wonderful variations take place with some T Tau type stars (see, for example, Herbig, 1977). Ambartsumian (1971) - proceeding from the idea on the liberation of surplus flare energy in the surface layers of stars having different depths - has shown that a definite parallel exists between the differences in the emission of a prefuor and a postfuor, on the one hand, and the differences between the emission of "fast" and "slow" flares, on the other.

The results of Natsvlishvili's (1985) observations of the star Ab 24, on which Parsamian earlier found a flare, can be considered as some confirmation of this point of view. They show that fuor-like variations of star brightness in a smaller scale can occur in the flare activity stage. These observations give some reason to assume that the phenomena which occur during fuor-like variations of the stellar brightness and during "slow" flares have the same physical nature.

It can be added that fuor-like variations of star brightness are apparently connected with the throwing out of some noticeable quantity of

matter by a star leading to the formation of an envelope. Ambartsumian's (1971) interpretation of the fuor phenomenon is based on this assumption. There are indications of the appearance of a gas envelope around the star V 1057 Cyg after its brightening, see Chalonge et al. (1982), and of a dust envelope, see Kopatskaya (1984).

Optical Observations of Flare Emission

In order to reveal the nature of the emission originating during stellar flares it is important to obtain the spectral composition and its variations during the flare with high enough time resolution.

The optical spectrum of flare emission is unusual. According to the photoelectric observations of the flares of UV Cet type stars carried out with a time resolution of the order of 1 s the colour indices U-B and B-V of the flare radiations correspond to the different temperatures.

In the flare maximum they are, on average, equal to (see, for example, Moffett, 1974):

$$U - B \simeq - 1.0 , \qquad B - V \simeq + 0.3 .$$

These colour indices, however, differ for different flares and vary somewhat irregularly during a given flare (see, for example, Mirzoyan, 1981).

The colour indices U-B and B-V of flares in the star clusters and associations, determined from photographic observations with low resolution (~5 minutes) confirm this result (see, for example, Mirzoyan et al., 1981).

When considering the possible influence of emission lines on the colour indices U-B and B-V it is necessary to take into account that the maximum strengthening of emission lines follows after the maximum brightness and their extinction ends after the extinction of a flare (Moffett and Bopp, 1976; Kunkel, 1967).

The spectral observations of the UV Cet flare stars, which are very few, have also revealed the dominant role of the continuum emission, mainly at short wavelengths, and the sharp increase of brightness at the beginning of the flare, noted already in the pioneering paper by Joy and Humason (1949).

This significant result has been confirmed with special clarity by parallel spectral and photoelectric flare observations of the stars UV Cet, EV Lac, YY Gem, and EQ Peg, carried out by Bopp and Moffett (1973), and Moffett and Bopp (1976), with a high time resolution. These observations

allowed them to establish that the whole flare emission in the beginning - in "spike" phase - is conditioned by the continuous emission and only after - in the "slow" phase - does the line emission play an essential role. This result of Moffett and Bopp shows that the continuous emission is primary one at least when compared with the line emission.

These synchronous spectral and photometric observations (Bopp and Moffett, 1973; Moffett and Bopp, 1976) of flare emission also allowed a study to be carried out on its spectral variations in the later phases of flares.

A more detailed study of the flare emission spectrum should be based on the narrow-band photoelectric observations of stellar flares possessing higher time resolution. Unfortunately, such kind of observations have been carried out up to now only for a very limited number of flares by Chugainov (1972) and Kodaira et al. (1976).

For the problem of the nature of the flare phenomenon the following fact, found by Greenstein and Arp (1968) in the flare spectrum of Wolf 359, is of importance: all spectral lines were broadened and shifted to the ultraviolet.

Radio and X-Ray Observations of Flare Emission

The first observations of stellar flares in the radio-frequencies (see, for example, Lovell, 1964) already showed that in some cases the optical flares are accompanied by radioflares.

The problem of correlation between optical and radioflares has been considered in detail by Spangler and Moffett (1976) using the synchronous observations in both regions. They have shown that any strong correlation between the manifestations of stellar flare activity in optical and radio-frequencies is in fact absent. Some optical flares were accompanied by radioflares, but a number of optical flares do not have a radio counterpart. In some cases the radio counterparts of optical flares began earlier or later than the optical flares themselves. Finally this study gives a reason to assume that some radio flares occur which do not have their optical counterparts.

The recent synchronous optical and radio observations carried out with radio interferometers by Gibson et al. (see, for example, Gibson, 1983) testify to this significant conclusion. In addition, the radiointerferometric observations of flare stars has led to two unexpected results:

1. the discovery of the radioemission out of the flare - the *quiescent* radioemission of some UV Cet type stars; 2. the detection of circular polarization of flare radioemission, which can reach 100%, whereas linear polarization is completely absent.

It should also be noted that the data on the spectra of polarization and brightness temperature of radioflares have confirmed (Fisher and Gibson, 1981) the earlier result (Ambartsumian, 1954) concerning the non-thermal nature of flare emission.

The X-ray observations of stellar flares were begun later. X-ray flares were registered from some UV Cet stars. The synchronous optical and X-ray observations of flares showed the absence of any correlation between manifestations of flare phenomenon in the considered two spectral regions, too.

The quiescent X-ray emission from many flare stars was detected by the X-ray satellite "Einstein". Later on it was revealed that *all dwarf stars* of spectral classes F-M are *X-ray quiescent emission sources,* the intensity of this emission being determined by the stellar rotation velocity (Golub, 1983).

From this point of view note should be taken of the results of van Leeuwen's (1985) study, showing the rapid rotation of the brightest flare stars in the Pleiades.

Conclusion

The results of flare star investigations obtained during the last decades have turned out to be completely unexpected in terms of the existing theoretical stellar models.

This concerns, first of all, the conclusion that flare stars represent an evolutionary stage, this conclusion being obtained on the basis of their observations in star clusters and associations. No stellar evolution theory suspects this.

This concerns also the results obtained by studying the physical peculiarities of flare emission and, in general, the stellar flare phenomenon. The observational data in some cases contradict the theoretical calculations (for details, see Mirzoyan, 1981). The difficulties in this field increased essentially after the space observations of flare stars. This fact was taken into account by Rosner (1983) when, in his introductory paper presented at the IAU Colloquium "The Activity of Red Dwarf Stars", he

noted "...the recent new CaII, UV and X-ray observations have shown that *the behaviour of "activity" on stars is substantially more complex than hitherto suspected*".

Therefore, we have some grounds to hope that further studies in this branch of astrophysics can lead to essentially new consequences in the physics and evolution of stars.

In actuality, the hope of obtaining new significant results from the study of flare stars is based on two well founded regularities, viz. that flare activity is a feature of stars being in one of the early stages of evolution immediately following the earliest stage, represented by the T Tau type stars; that flare emission has a non-thermal nature and seems to be closely connected with the more general problem of stellar energy sources (Ambartsumian, 1954). In almost all suggested interpretations of flare emission solely the probable mechanism of the origin of flares is considered without paying special attention to the problem of the energy source. Obviously the presence or the appearance of the sources of energy in the star atmosphere which are necessary for flares must be considered.

The features mentioned above give some grounds to assume that the revealing of the sources of flare energies can contribute to the solution of the problems of stellar energy at least in the early stages of evolution.

It can be supposed that some of the problems connected with the study of flare activity and flare stars will be solved thanks to new investigations, including those which are planned at present using the coordinated synchronous ground-based and space observations of stellar flares and the quiescent emission of flare stars (Rodono, 1985). From this point of view essential results can be expected, in particular, from the realization of space observations of stars according to the program "Stellar Activity" suggested as "A Key Project" for the space telescope (Vaiana et al. 1985).

Thus, it seems to us that the flare star problem, being part of a more general problem of stellar activity in the initial stages of evolution, will remain for years as one of the most real astrophysical problems. Its final solution, of paramount significance for the ascertaining of the nature of stellar activity, will be obtained only when, on the basis of the observational data, we understand all the complex phenomena connected with the physics and evolution of this activity.

References:

Allen, C.W., 1973, Astrophysical Quantities, The Athlone Press, London.
Ambartsumian, V.A., 1954, Comm. Byurakan Obs., 13.
Ambartsumian, V.A., 1969, Stars, Nebulae, Galaxies; Ac. Sci. Armenian SSR, Yerevan, p. 283.
Ambartsumian, V.A., 1970, Astrofizika, 6, 31.
Ambartsumian, V.A., 1971, Astrofizika, 7, 557.
Ambartsumian, V.A., 1978, Astrofizika, 14, 367.
Ambartsumian, V.A., and Mirzoyan, L.V., 1971, In: Proc. IAU Coll. No.15, Bamberg Veröff., 9, No. 100, 98.
Ambartsumian, V.A., and Mirzoyan, L.V., 1975, In: Proc. IAU Symp. No. 67, eds. V. Sherwood, L. Plaut, Reidel, Dordrecht, p. 3.
Ambartsumian, V.A., Mirzoyan, L.V., Parsamian, E.S., Chavushian, H.S., and Erastova, L.K., 1970, Astrofizika, 6, 3.
Beskin, G.M., Neizvestnyi, S.I., Plachotnichenko, V.L., Pustilnik, L.A., Chekh, S.A., Shvartsman, V.F., and Gershberg, R.E., 1985, In: "Flare Stars and Related Objects", ed. L.V. Mirzoyan, Ac. Sci. Armenian SSR, Yerevan (in press).
Bopp, B.W., and Moffett, T.J., 1973, Astrophys. J., 285, 139.
Chalonge, D., Divan, L., and Mirzoyan, L.V., 1982, Astrofizika, 18, 263.
Chavushian, H.S., 1985, In: "Flare Stars and Related Objects", ed. L.V. Mirzoyan, Ac. Sci. Armenian SSR, Yerevan (in press).
Chugainov, P.F., 1972, Izv. Krim Obs., 44, 3.
Cristaldi, S., and Rodono, M., 1970, Astron. Astrophys. Suppl. Ser., 2, 223.
Fisher, P.L., and Gibson, D.M., 1981, In: "Cool Stars, Stellar Systems and the Sun", eds. M.S. Giampapa, L. Golub, Smithsonian Astrophys. Obs., Special Report 392, vol. 2, 109.
Gershberg, R.E., 1978, Flare Stars of Small Masses; Nauka, Moscow.
Gibson, D.N., 1983, In: Proc. IAU Coll. No. 71, eds. P.B. Byrne, M. Rodono, Reidel, Dordrecht, p. 273.
Golub, L., 1983, In: Proc. IAU Coll. No. 71, eds. P.B. Byrne, M. Rodono, Reidel, Dordrecht, p. 83.
Greenstein, J.L., and Arp, H.C., 1968, Astrophys. Letters, 3, 49.
Haro, G., 1964, In: "The Galaxy and the Magellanic Clouds", Proc. IAU-URSI Symp. No. 20, eds. F.J. Kerr, A.W. Rodgers, Australian Ac. Sci., Canberra, P. 30.
Haro, G., and Chavira, E., 1966, Vistas in Astronomy, 8, 89.
Herbig, G.H., 1977, Astrophys. J., 217, 693.
Hojaev, A.S., 1985, In: "Flare Stars and Related Objects", ed. L.V. Mirzoyan, Ac. Sci. Armenian SSR, Yerevan (in press).
Johnson, H.L., and Mitchell, R.I., 1958, Astrophys. J., 128, 31.
Joy, A.H., and Humason, M.L., 1949, Publ. Astron. Soc. Pacific, 61, 133.
Kodaira, K., Ichimura, K., and Nishimura, S., 1976, Publ. Astron. Soc. Japan, 28, 665.
Kopatskaya, E.N. 1984, Astrofizika, 20, 263.
Kunkel, W., 1967, An Optical Study of Stellar Flares; Texas University, Austin.
Lovell, B., 1964, Observatory, 84, 191.
Mirzoyan, L.V., 1980, "Flare Stars, Fuors and Herbig-Haro Objects", ed. L.V. Mirzoyan, Ac. Sci. Armenian SSR, Yerevan, p. 45.
Mirzoyan, L.V., 1981, "Stellar Instability and Evolution", Ac. Sci. Armenian SSR, Yerevan.
Mirzoyan, L.V., 1982, Publ. Astrophys. Obs. Potsdam, Nr. 110, 71.
Mirzoyan, L.V., 1984, Vistas in Astronomy, 27, 77.

Mirzoyan, L.V., and Brutian, G.A., 1980, Astrofizika, 16, 97.
Mirzoyan, L.V., Chavushian, H.S., Melikian, N.D., Natsvlishvili, R.Sh., Ohanian, G.B., Hambarian, V.V., and Garibjanian, A.T., 1981, Astrofizika, 17, 197.
Mirzoyan, L.V., and Melikian, N.D., 1985, In: "Flare Stars and Related Objects", ed. L.V.Mirzoyan, Ac. Sci. Armenian SSR, Yerevan (in press).
Mirzoyan, L.V., and Ohanian, G.B., 1977, Astrofizika, 13, 561.
Mirzoyan, L.V., and Ohanian, G.B., 1985, In: "Flare Stars and Related Objects", ed. L.V. Mirzoyan, Ac. Sci. Armenian SSR, Yerevan (in press).
Moffett, T.J., 1972, Nature, Phys. Sci., 240, 41.
Moffett, T.J., 1974, Astrophys. J., Suppl., 29, 1.
Moffett, T.J., and Bopp, B.W., 1976, Astrophys. J., Suppl., 31, 61.
Natsvlishvili, R.Sh., 1985, In: "Flare Stars and Related Objects", ed. L.V. Mirzoyan, Ac. Sci. Armenian SSR, Yerevan (in press).
Oskanian, V.S., 1969, In: "Non-Periodic Phenomena in Variable Stars", Proc. IAU Coll. No. 4, ed. L. Detre, Akadémiai Kiadó, Budapest, p. 131.
Rodono, M., 1985, In: "Flare Stars and Related Objects", ed. L.V. Mirzoyan, Ac. Sci. Armenian SSR, Yerevan, (in press).
Rosino, L., 1969, In: "Low Luminosity Stars", ed. S.S. Kumar, Gordon and Breach Science Publishers, New York - London - Paris, p. 18.
Rosner, R., 1983, In: "Activity in Red Dwarf Stars", IAU Coll. No. 71, eds. P.B. Byrne, M. Rodono, Reidel, Dordrecht- Boston- Lancaster, p. 5.
Spangler, S.R., and Moffett, T.J., 1976, Astrophys. J., 203, 497.
Vaiana, G.S., Praderie, F., and Rodono, M., 1985, Stellar Activity: a Key Project for the Space Telescope, preprint.
van Leeuwen, F., 1985, In: "Flare Stars and Related Objects", ed. L.V. Mirzoyan, Ac. Sci. Armenian SSR, Yerevan (in press).

"Eruptive Phenomena in Stars"
Commun. Konkoly Obs. Hung.
Acad. Sci., No.86, Budapest

PHOTOELECTRIC OBSERVATIONS OF EV Lac IN 1984: FAST FLARE ACTIVITY?

M.K. Tsvetkov, A.P. Antov, A.G. Tsvetkova

Department of Astronomy and National Astronomical Observatory,
Bulgarian Academy of Sciences, Bulgaria

Investigations of flare stars in the solar neighbourhood were carried out in the autumn of 1984 for a $15^h42^m.7$ monitoring of the flare star EV Lac. The observations were carried out using the 60 cm Cassegrain reflector of the Rozhen National Astronomical Observatory with an EF-1 single-channel photoelectric photometer in the U-colour. The accuracy of the observations carried out is within the limits of $\sigma_u \sim (0^m.04 - 0^m.09)$, the integration time being 1 second. During the period from 18 October to 10 November 1984 17 flares were observed and the mean magnitude of EV Lac in the instrumental UBV system was $v = 10^m.04 \pm 0^m.04$, $b = 11^m.42 \pm 0^m.05$, $u = 12^m.24 \pm 0^m.05$ (Tsvetkov et al., 1985). Along with the "classical" flares observed in EV Lac (Figs. 1, 2) we also observed 5 fast flares (Figs. 3, 4) of a duration of 1-2 seconds and an amplitude reaching $m_u = 1^m.77$. The nature of these peak-flares is still disputable which is due, above all, to their short duration, commensurable with the integration time of the instruments used. On the other

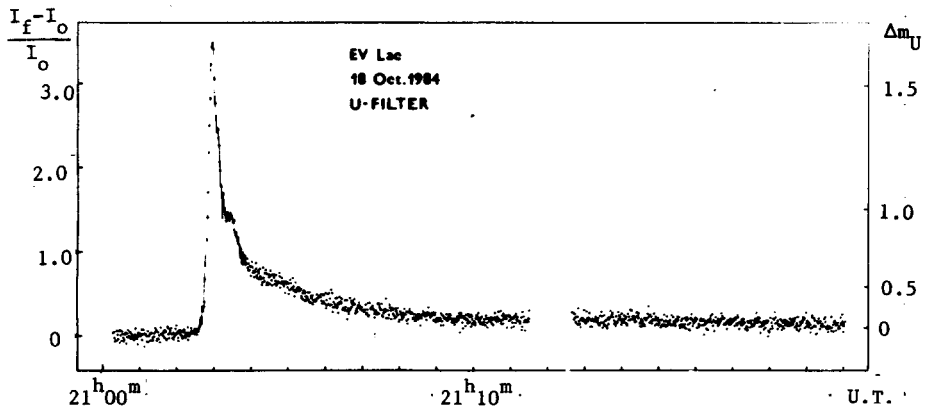

Figure 1

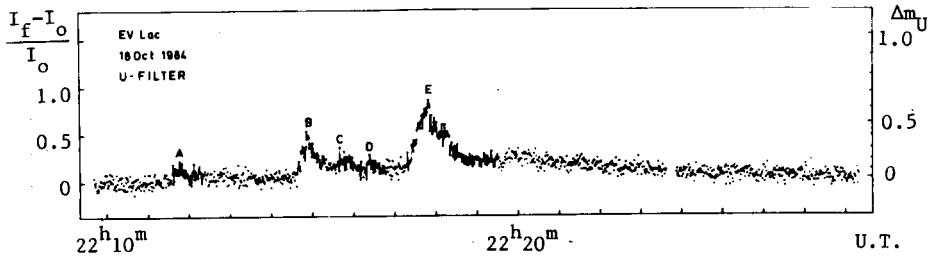

Figure 2

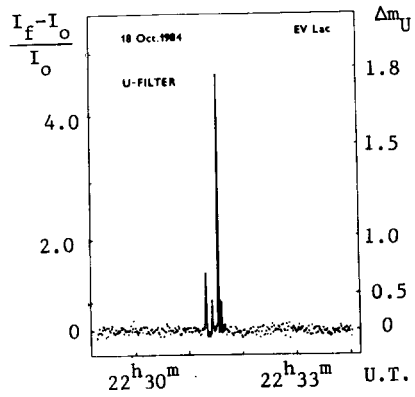

Figure 3

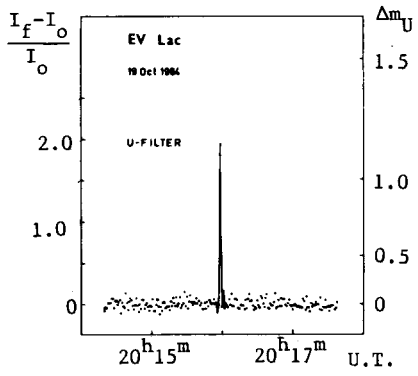

Figure 4

hand, fast flares were observed on only one telescope and in order to explain their nature it would be interesting to carry out parallel observations in the U-colour on different telescopes. In this sense, the case with a similar flare (Gershberg and Petrov, 1985) noticed during observations with the three-channel photometer of the Astron satellite is a significant example.

References:

Gershberg, R.F., Petrov, P.P., 1985, Proc. Symp. "Flare Stars and Related Objects", Byurakan, Ed. L.V. Mirzoyan.
Tsvetkov, M.K., Antov, A.P., Tsvetkova, A.G., 1985, (in preparation).

"Eruptive Phenomena in Stars"
Commun. Konkoly Obs. Hung.
Acad. Sci., No.86, Budapest

ON THE FLARE ACTIVITY VARIATIONS OF HII 2411

G. Szécsényi-Nagy

Department of Astronomy, L. Eötvös University, Budapest

Object number 2411 ($\alpha_{1900} = 3^h43^m44^s.8$, $\delta_{1900} = +24^o0'48''$, $m_{pg} = 15.52$) on Hertzsprung's second star-list of the Pleiades field (1947) is a Hyades member (Binnendijk, 1946). Its variability was discovered in 1963 and it was classified as a flare star (Hyades 1) by Haro and Chavira (1966). During 117^h50^m it showed 4 remarkable flare-ups ($\Delta m_U \geq 0.5$) and also small variations ($\Delta m_U \leq 0.3$).

Its spectral type was found to be M4e by Herbig (1962) and M2-M3 by McCarthy and Treanor (1964). High-speed photoelectric photometry of the star was initiated in 1972 by Rodono (1974). Measurements were only carried out in one colour near the B band. During 15 hours of observations 3 flare events were detected and the flare frequency of II Tau (= HII 2411) could be assumed to be almost the same or even higher than that of many UV Cet-type stars. The mean flare frequency for HII 2411 - determined by photoelectric methods - seemed to change from year to year. In the fall of 1972 it was found to be 0.25 h^{-1} but the next year Rodono (1975) observed a mean frequency of 1.56 h^{-1}.

Unfortunately systematic patrol observations of the object with high-speed photometers failed to materialize and we have only sporadic data about short-lived and low-energy flare-ups of II Tau. On the other hand a very long series of patrol observations of the Pleiades field has been carried out with fast (D:F ~ 1:3) photographic cameras. The effective duration of these observations totalled about 3200 hours in the period 1963--1983 (Szécsényi-Nagy, 1983, 1985). Albeit the average time-resolution reached by photographic methods is 5 minutes in the pg and 10 minutes in the U-band and consequently the majority of flare-ups (the very short ones and the low-amplitude flares) is indiscernible on the plates, 131 flare events of the object were discovered during that time. Regrettably 5 of them are only mentioned, without any particulars being given. This is the reason for limiting our statistical investigations to 126 occurrences.

In 108 cases the ultraviolet light of the flares was detected; in the remaining 18 measurements were performed in the B-band or in the pg-region only. In order to obtain a homogeneous sample the results of the latter were transformed into the U-band. The weakest 6 flares ($\Delta m_U = 0.4$) were discarded because most of the authors set a limit of detectability at $\Delta m_U = 0.5$. In such a way a mean flare frequency of 0.04 h^{-1} could be computed whereas Haro and Parsamian (1969) got a 2.25 times higher frequency for the same kind of flare-ups from the results of 551 hours of photographic patrol of the Pleiades field. It is strange that including further discoveries Rodono (1974) obtained a somewhat smaller frequency (0.07 h^{-1} as against 0.09 h^{-1}). All these pointed to a new possibility, namely the

determination of flare activity variations in the range of most energetic flares by photographic patrol of a star field.

With a view to having statistically meaningful samples, results of some consecutive observational periods had to be combined. Six "sections" were shaped as follows: A(1963/68), B(1968/70), C(1970/72), D(1972/73), E(1973/77) and F(1977/81). The calendar length of these ranges from 1 to 5 years, but they are almost equal if we compare the total effective time of observations carried out in different observatories during the given periods. Inequalities were removed by comparing the numbers of observed flare-ups of the star (n_f) in the different sections and the quantity (N_f) of all other flare events discovered on the same plates in the corresponding sections. A rarity index defined by the formula $R = N_f/n_f$ was used to classify the sections A, B, ... according to the actual average flare frequency of II Tau. The above procedure was performed at different Δm_U levels and the ranks (or placing numbers) of the sections were summarized. Subtotals of this sum were computed at each level and the sections were arranged as is done in figure skating championships.

In this way we could determine (irrespective of the actual Δm_U level) that the flare activity of the object peaked during section F and that the sequence continues in this manner: B, A, C, E, D. From this succession it is clear that HII 2411 was very active in the late seventies and also in the late sixties.

The significance of the result was checked by computing Kendall's coefficient of concordance and its amount ($w = 0.9263$) mathematically proves that the ranks alloted to the different sections are independent of the amplitude of flare-ups.

The conclusions of the study presented here are:

1. The activity variation is not a result of observational selection effects, it surely originates in physical processes taking place on or in the star.

2. The variation is relatively fast and if cyclic, its *cycle-length* (perhaps period?) *is in the range of 10-15 years!* (From the statistics of $\Delta m_U \geq 1$ flares a cycle-length of 10-12 years can be derived, while from that of all events with $\Delta m_U \geq 0.6$ 13 years and from the statistics of all published flare-ups of II Tau 13-15 years.)

3. When the star is very active it produces 2-4 times more high amplitude flare-ups than when it is quiet or least active.

References:

Binnendijk, L., 1946, Ann. Sterrew. Leiden 19, part 2.

Haro, G., Chavira E., 1966, in Vistas in Astronomy, Eds. A. Beer and K. Aa. Strand, Vol. 8, p. 89.

Haro, G., Parsamian, E., 1969, Bull. Obs. Tonantzintla Tacubaya 5, 41.

Herbig, G.H., 1962, Ap. J., 135, 736.

Hertzsprung, E., 1947, Ann. Sterrew. Leiden 19, part 1A.

McCarthy, M.F., Treanor, P.J., 1964, Richerche Astr. 6, 535.

Rodono, M., 1974, Astron. and Astrophys. 32, 337.

Rodono, M., 1975, in Variable Stars and Stellar Evolution, IAU Symposium No. 67, Eds. V.E. Sherwood and L. Plaut, Reidel, Dordrecht, p. 69.

Szécsényi-Nagy, G., 1983, Publ. Astr. Inst. Czech. Acad. Sci. No. 56, 219.

Szécsényi-Nagy, G., 1985, in Flare Stars and Related Objects, Ed. L.V. Mirzoyan, Yerevan (in press).

"Eruptive Phenomena in Stars"
Commun. Konkoly Obs. Hung.
Acad. Sci., No.86, Budapest

FLARE STARS' COUNT IN ORION

R.Sh. Natsvlishvili

Abastumani Observatory, Georgia, USSR

The total number of flare stars in Pleiades was estimated statistically by Ambartsumian (1969). We have applied another method to estimate the total number of flare stars for the Orion Nebula region in the field covered by a 70/100/210 cm Maksutov-type telescope with the centre in the Orion Trapezium comprising 306 hours' effective observational time; during that period 127 new flare stars were discovered. In all, 182 flare phenomena were recorded. To escape data inhomogeneities we took Abastumani observations (Kiladze, 1972; Kiladze and Natsvlishvili, 1980; Natsvlishvili, 1981, 1982a, 1982b, 1984; Natsvlishvili and Melikian, 1980) as a basis and used flare stars from other observations (Haro, 1968; Melikian, 1984; Parsamian et al., 1978; Rosino and Pigatto, 1969; Roslund, 1969; Tsvetkov and Tsvetkova, 1982, and references therein).

Flare stars may be divided into two groups: A and B according to the chronology of their discovery. Group A contains stars discovered in the initial observational time interval t_0t_1, the number of which is Q; all other unknown flare stars make group B. Let us assume that in the period t_1 to t, new flare stars from group B, denoted as Z, were revealed. At the same time during interval t_1t repeated flares occurred both in Q and Z, their total numbers designated as X and P correspondingly. Therefore, during the interval t_1t the number of flares that occurred in B will be Z+P. Assuming that flare phenomena are accidental in time, the mean flare frequency measure in A is X/Q, and in B it is P/Z.

Because flare stars in group A are known during the observational time t_1t, and B group stars are gradually revealed and are then being traced, to compare the mean frequencies of groups A and B one should know the number of repeated flares in A in the observational time t_0t_1, during which stars were discovered, their number designated as Z. If the total number of such repeated flares is K, then the mean frequency measure for group A will be K/Z.

If Z+P greatly exceeds X, then either the mean frequency of flares is more than B, or the number of stars is more, or else both conditions are fulfilled. But flare frequency of individual stars in B must be less as stars with less flare frequency are, on average, chronologically revealed later and eventually the least active stars remain undiscovered. So the frequency ratio $(K/Z)/(P/Z) = K/P$ is characterized by the degree to which the mean frequency in A is larger than in B. If $K/P > 1$, then $Z+P \gg X$ means that the number of flare stars in group B greatly exceeds that in A. At the same mean frequency the number of flare stars in B must be $Q\cdot(Z+P)/X$. Taking into account the frequency difference factor, their quantity will be $Q\cdot K\cdot(Z+P)/(X\cdot P)$, and the total number of flare stars N in the aggregate is:

$$N = Q + Q \cdot K \cdot \frac{Z+P}{P \cdot X} \qquad (1)$$

Using the correlation for the Orion aggregate and inserting corresponding values: Q = 358, Z+P = 138, X = 43, K/P = 1.3, we obtain that the total number of flare stars in Orion equals N = 1852. This represents the number of stars that are potentially capable of undergoing flares with amplitudes exceeding $0^m.5$.

The dependence (1) in individual cases gives a lower limit of true quantity in the sense that stars dimmer than a certain brightness are unobservable and it is possible that systems may contain objects of very low flare frequency.

Another factor might influence the result by increasing the number of flare stars in the systems: we originally thought that the flare activity of individual stars did not change, i.e. the mean frequency in groups remained unchanged, but if we assume that during the time of observations not all potentially flare stars with a cyclic activity showed flare activity (Mirzoyan and Ohanian, 1977), the number of flare stars will increase. However, if we do not know the duration of activity of individual groups and the interval between such cycles, it is impossible to determine statistically the number of undiscovered flare stars. Although flare activity in individual stars may be cyclic and there is also a group appearance of flare fluctuations of a star's brightness, for the numerous groups of such objects the sequence of flare phenomena is accidental in time.

References:

Ambartsumian, V.A., 1969, Stars, Nebulae, Galaxies, Yerevan.
Haro, G., 1968, In: "Stars and Stellar Systems", vol. 7, Chicago University Press, Chicago.
Kiladze, R.I., 1972, IBVS, No. 670.
Kiladze, R.I., Natsvlishvili, R.Sh., 1980, IBVS, No. 1725.
Melikian, N.D., 1984, IBVS, No. 2621.
Mirzoyan, L.V., and Ohanian, G.B., 1977, Astrofizika, 13, 561.
Natsvlishvili, R.Sh., 1981, IBVS, No. 1926.
Natsvlishvili, R.Sh., 1982a, IBVS, No. 2062.
Natsvlishvili, R.Sh., 1982b, IBVS, No. 2231.
Natsvlishvili, R.Sh., 1984, IBVS, No. 2565.
Natsvlishvili, R.Sh., and Melikian, N.D., 1980, IBVS, No. 1726.
Parsamian, E., Chavira, E., and Gonzalez, G., 1978, Bol. Obs. Tonantzintla, 2, No. 4.
Rosino, L., and Pigatto, L., 1969, Contr. Asiago Obs., No. 231.
Roslund, C., 1969, Uppsala Astr. Obs., Medd. No. 169.
Tsvetkov, M.K., and Tsvetkova, A.G., 1982, IBVS, No. 2132.

"Eruptive Phenomena in Stars"
Commun. Konkoly Obs. Hung.
Acad. Sci., No.86, Budapest

SEARCH FOR FLARE STARS WITH THE ESO GPO ASTROGRAPH IN LA SILLA

M.K. Tsvetkov[1], W.C. Seitter[2] and H. Duerbeck[2]

[1]Department of Astronomy and National Astronomical Observatory,
Bulgarian Academy of Sciences, Bulgaria

[2]Astronomical Institute of the University of Münster, FRG

An important role in the investigations of flare stars is given to programs that search for and study their properties with wide-angle telescopes. In this respect, surveys carried out with Schmidt-type telescopes are essential, the investigations being focused mainly on regions of stellar clusters and associations in the northern hemisphere.

Schmidt telescopes, which have recently been put into operation in the southern hemisphere, are engaged basically in programs to develop atlases, in fundamental surveys, etc.

In this respect, for the further development of surveys that study flare stars in southern regions, it is also necessary to make use of the possibilities offered by astrographs, thus widening the scope of the investigations carried out.

The aim of our program was to test the possibilities for flare star search by using the 40 cm GPO-astrograph of the European Southern Observatory in La Silla (Chile). For this purpose, observations for the search for and investigations of flare stars in relatively young aggregates (IC 2391, IC 2602 and Chamaeleontis T1) were carried out in January 1985. Control observations were done in the Orion aggregate M 42/43. During the processing of the material obtained in Orion with the GPO (Tsvetkov et al., 1985) nine flares have been discovered, seven of which were new flare stars, the effective time of monitoring being 26^h50^m. The comparison of these results with some of the first observations for the search for flare stars in Orion carried out with various Schmidt telescopes (Table I) shows that the effective use of the GPO astrograph is justified for the solving of such problems. If in the calculations of the relative frequency of

Table I. Data of surveys with different telescopes in the search for flare stars in the Orion Nebulae region (M42/43)

Observatory Type of telescope	Aperture (m)	Focal length (m)	Field (sq.deg.)	T_{eff} (h)	Number of observed flares	ν (flares/hour)	Light	References
Tonantzintla Schmidt	0.66/0.76	2.17	25	112.2	62	0.55	U,pg	1
Abastumani Meniscus	0.70/0.92	2.10	23	64.3	49	0.76	pg	2,3
Asiago Schmidt	0.67/0.92	2.15	25	114.4	48	0.42	pg	4
Mt. Stromlo Schmidt	0.50/0.65	1.73	13	39.6	15	0.38	B,U	5
Rozhen Schmidt	0.50/0.70	1.72	16	44.8	13	0.29	U	6,7
Byurakan Schmidt	1.00/1.30	2.13	16	32	9	0.28	U	8
La Silla Astrograph	0.40	4.00	4	26.8	9	0.34	pg	9

References: 1) Haro (1965); 2) Kiladze (1972); 3) Kiladze and Natsvlishvili (1980); 4) Rosino and Pigatto (1969); 5) Roslund (1969); 6) Tsvetkov et al. (1980); 7) Tsvetkov and Tsvetkova (1982); 8) Melikian (1981); 9) Tsvetkov et al. (1985)

flares the recording of the total number of flare stars in the area of $2^{o} \times 2^{o}$ investigated with the GPO astrograph was also taken into account, then the real frequency would be 0.56 flares/hour.

The authors thank the relevant authorities of the European Southern Observatory and the Department of Astronomy of the Bulgarian Academy of Sciences for the observing time provided by the ESO and the programs for completing this work.

References:

Haro, G., 1965, Stars and Stellar Systems VII, 141, Univ. Chicago Press.
Kiladze, R., 1972, IBVS, No. 670.
Kiladze, R., Natsvlishvili, R., 1980, IBVS, No. 1725.
Melikian, N.D., 1981, IBVS, No. 2018.
Rosino, L., Pigatto, L., 1969, Contrib. of Asiago Obs., No. 231.
Roslund, C., 1969, Arkiv för Astronomi, B 5, No. 22.
Tsvetkov, M.K., Tsvetkov, S.A., Tsvetkova, A.G., 1980, IBVS, No. 1889.
Tsvetkov, M.K., Tsvetkova, A.G., 1982, IBVS, No. 2132.
Tsvetkov, M.K., Duerbeck H., Seitter W., 1985 (in preparation).

"Eruptive Phenomena in Stars"
Commun. Konkoly Obs. Hung.
Acad. Sci., No.86, Budapest

PHOTOGRAPHIC PHOTOMETRY OF NEW FLARE STARS IN THE ORION NEBULA

A. Tsvetkova, S. Tsvetkov

Department of Astronomy and National Astronomical Observatory
Bulgarian Academy of Sciences
Sofia, Bulgaria

Monitoring photographic observations of flare stars in the Orion region (M 42-43) were carried out in 1980-1981. The plate-filter combination (ZU21-UG2) yielded U-magnitudes. A known multiexposure method was applied and each plate contained 6 exposures of a 10-minute duration. For a total effective observing time of 44^h50^m, 13 new flare stars were discovered (Tsvetkov et al., 1980, 1982, Tsvetkov, 1982). Photographic photometry was carried out by applying the method of Argue (Argue, 1960) using the Carl Zeiss Jena ASCORIS photometer of the NAO.

Table I contains the results of photographic photometry of all the flares and the mean moments of observations.

Figure 1 shows the light curves of some of the observed flares.

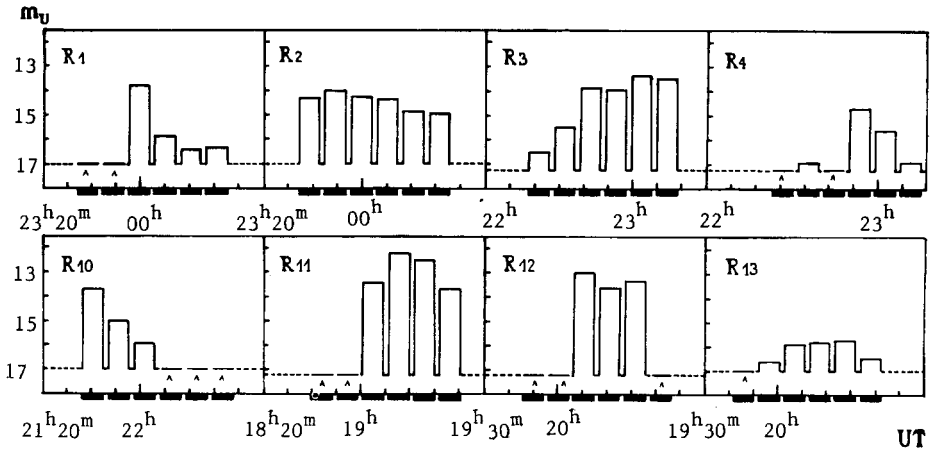

Fig. 1. Light curves of some of the observed flares in Orion

Table I. Photometric data for the observed flares in Orion

No.1 Umin = $18^m.5$	
UT	mu
1. 23^h33^m	(17^m
2. 23 43.5	(17
3. 23 54	13.75
4. 00 04.5	15.84
5. 00 15	16.40
6. 00 25.5	16.32

No.2 Umin = $18^m.3$	
UT	mu
1. 23^h33^m	$14^m.25$
2. 23 43.5	13.95
3. 23 54	14.20
4. 00 04.5	14.30
5. 00 15	14.82
6. 00 25.5	14.88

No.3 Umin = $16^m.1$	
UT	mu
1. 22^h16^m	$16^m.50$
2. 22 26.5	15.47
3. 22 37	13.85
4. 22 47.5	13.90
5. 22 58	13.37
6. 23 08.5	13.47

No.4 Umin = $17^m.1$	
UT	mu
1. 22^h16^m	($17^m.2$
2. 22 26.5	16.9:
3. 22 37	(17.2
4. 22 47.5	14.7
5. 22 58	15.6
6. 23 08.5	16.9

No.5 Umin = $15^m.8$	
UT	mu
1. 21^h53^m	$14^m.45$
2. 22 03.5	15.15
3. 22 14	14.75
4. 22 24.5	14.15
5. 22 35	14.07
6. 22 45.5	14.15

No.6 Umin = $18^m.1$	
UT	mu
1. 18^h14^m	$15^m.3$
2. 18 24.5	15
3. 18 35	14.93
4. 18 45.5	(17
5. 18 56	(17
6. 19 06.5	(17

No.7 Umin = $17^m.4$	
UT	mu
1. 00^h30^m	($17^m.2$
2. 00 40.5	(17.2
3. 00 51	(17.2
4. 01 01.5	(17.2
5. 01 11	15.37
6. 01 21.5	15.17

No.8 Umin = $16^m.2$	
UT	mu
1. 18^h04^m	(17^m
2. 18 14.5	(17
3. 18 25	(17
4. 18 35.5	(17
5. 18 46	15.97
6. 18 56.5	15.60

No.9 Umin = $18^m.5$	
UT	mu
1. 19^h40^m	(17^m
2. 19 50.5	16.95
3. 20 01	16.50
4. 20 11.5	16.47
5. 20 22	(17
6. 20 32.5	(17

No.10 Umin = $18^m.0$	
UT	mu
1. 21^h35^m	$13^m.7$
2. 21 45.5	15.0
3. 21 56	15.9
4. 22 06.5	(17
5. 22 17	(17
6. 22 27.5	(17

No.11 Umin = $20^m.2$	
UT	mu
1. 18^h38^m	($17^m.2$
2. 18 48.5	(17.2
3. 18 59	13.39
4. 19 09.5	12.17
5. 19 20	12.45
6. 19 30.5	13.65

No.12 Umin = 21^m:	
UT	mu
1. 19^h44^m	($17^m.2$
2. 19 54.5	(17.2
3. 20 05	12.95
4. 20 15.5	13.55
5. 20 26	13.27
6. 20 36.5	(17.2

No.13 Umin = $19^m.2$	
UT	mu
1. 19^h40^m	(17^m
2. 19 50.5	16.6
3. 20 01	15.9
4. 20 11.5	15.77
5. 20 22	15.72
6. 20 32.5	16.5

References:

Argue, A., 1960, Vistas in Astronomy, v. 3, ed. A. Beer, Pergamon Press, p. 184.

Tsvetkov, M., Tsvetkov, S., Tsvetkova, A., 1980, IBVS No. 1889.

Tsvetkov, M., Tsvetkova, A., Tsvetkov, S., 1982, IBVS No. 2132.

Tsvetkov, M., 1982, Communications from the Konkoly Observatory, No. 83, Budapest, p. 206.

"Eruptive Phenomena in Stars"
Commun. Konkoly Obs. Hung.
Acad. Sci., No.86, Budapest

PHOTOGRAPHIC PHOTOMETRY OF FLARE STARS IN PLEIADES

J. Kelemen

Konkoly Observatory
H-1525 Budapest, P.O.B. 67, Hungary

Some preliminary results are given of the photographic photometry of Pleiades flare stars. The measurements - on the multiexposure plate material between 1975 and 1983 - began in 1984.

The plates were obtained with the 60/90 cm Schmidt telescope of Konkoly Observatory. The observed material is homogeneous because all the exposures were made on KODAK 103aO plates +2 mm UG2 colour filter.

Flare searching was carried out by means of a blink-comparator. The flare-ups were measured by a Cuffey iris-type astrophotometer. The comparison stars were chosen from Johnson's photoelectric standards (Johnson, 1952).

Because there were six successive images of each star on the plates six individual photometric reductions were made. The results of the reductions show that the plate limit was, on average, between 17 and 18 mag. The mean error of the magnitude determinations for those stars brighter than 16 mag. was found to be less than 1 mag., but below 16 mag. the error increases very rapidly. The high error level is due to the following circumstances: the U band is very sensitive to atmospheric conditions; the long effective exposure time (1 hour) increases the veil level; the sky background in the Pleiades region is not uniform due to the bright circumstellar nebulosities.

The amplitude distribution of the 49 measured new flares is in good agreement with the amplitude distribution of the 519 known flares from the newest Haro catalog (Haro et al., 1982). However there is a strong selection effect on small amplitudes because the poor time resolution of the multiple exposure method smoothed out the flares and the high error level overwhelms the events.

The well-known Oskanyan exponential flare model (Oskanian, 1975) was used to compute theoretical light curves of the flare events. The numerical integration of the test curves shows that the measurable photographic amplitudes are only 1/2-2/3 of the true amplitudes. This means that these observational effects greatly influenced the usefulness of the common photographic, photoelectric flare amplitude statistics.

The relation between the number of the flare and the total observing time shows a flare frequency of about 1 flare-up/hour inside a 5 degree diameter circle around Alcyone.

References:

Haro, G., Chavira, E., and Gonzales, G., 1982, Bul. Inst. Tonantzintla, 3, No. 1.
Johnson, H.L., 1952, Ap. J., 116, 640.
Oskanian, V.S., 1975, In: "Nestatsionarnye Zvezdy", ed. M.A. Arakelyan, Yerevan.

"Eruptive Phenomena in Stars"
Commun. Konkoly Obs. Hung.
Acad. Sci., No.86, Budapest

A SYSTEM FOR RECORDING FAST VARIATIONS OF STELLAR BRIGHTNESS

V.P. Zalinian, H.M. Tovmassian

Byurakan Astrophysical Observatory, Armenia, USSR

In order to understand the nature of flare stars the study of the light curves of fast flares, especially of their very short-lasting rising parts, is very important. For detecting and recording such flares, observations with a time constant of 0.1 sec or less are needed. The event of a flare is a casual one and for its detection long patrolling is inevitable. For observations with small time constants a large amount of registration paper, paper tapes or magnetic tapes are needed.

We propose a method for registering light curves of flares with time constants of the order of 0.1-0.001 sec using microcomputers. The essence of the method is that the recording equipment operates only in the case of variations of the brightness of the observed star. During observations the output of the photoelectric photometer, operating in the photon counting mode, is connected with a computer which determines the mean value of the signal at a given time interval and the square root deflections from it. Then each subsequent count is compared with the value determined in the adjacent time interval. If the measured signal does not differ from the mean value by, say, 3 σ, nothing is being recorded in the computer memory. If the measured signal differs from the mean value by 3 σ all subsequent counts are automatically recorded in the computer's memory. This procedure stops when the output signal returns to its previous mean value.

The photoelectric photometer was tested in the laboratory and then in observations. During about 20 hours of operation with a dark photomultiplier nothing was recorded. Recording started immediately each time after flashing a lamp in front of the photomultiplier.

Observations were made with a 40 cm Cassegrain telescope. No flare was recorded during 50 hours of observations of standard stars. Similarly, no flare was recorded during 55 hours of observations of the flare stars AD Leo, Wolf 630, V 1258 Aql and BY Dra.

However, in the case of EV Lac, 3 flares were recorded during 22 hours of observation. Two of them happened within 40 minutes on 19 July 1985. The duration of both flares was about 3 seconds, the amplitudes of the flares were about $1^m.3$. These flares were recorded with a 1 sec time constant.

The duration of the third, larger flare of ~ $2^m.2$ was about 18 sec. It was recorded with a 0.1 sec time constant. The increase of brightness occurred during ~ 1 sec.

Thus, the proposed method permits short flares with very high time resolution to be recorded without wasting a large amount of recording paper and time for its analysis.

"Eruptive Phenomena in Stars"
Commun. Konkoly Obs. Hung. Acad. Sci., No.86, Budapest

THE COMMON NATURE OF FLARING PROCESSES ON THE SUN AND RED DWARFS

Maria M. Katsova* and M.A. Livshits**

*Sternberg State Astron. Inst., Univ. of Moscow, USSR

**IZMIRAN, Troizk, Moscow Region, USSR

A continuous transition is revealed from solar flares to other types of events, characteristic of late-type stars, i.e. to phenomena accompanied by the appearance of optical continuum radiation. It is shown that the value of the rate of increase of the flaring optical continuum intensity, following from the gas-dynamic model for the flare secondary processes, agrees well with the observations of impulse stellar flares, recently conducted using a 6 m telescope with extremely high time resolution.

We have compared the events in the hard (impulsive) phase of solar flares, which are only rarely accompanied by optical continuum emission, with the events on red dwarfs, when flare optical continuum is generated. The physics of both phenomena consists of sudden impulsive energy release in the upper chromosphere or low corona in the form of electron beams or heat fluxes and the subsequent development of the ensemble of secondary processes (Syrovatskii, 1972). The main secondary effects for the events considered are the peculiar "burn" of the lower dense atmospheric layers and the subsequent evaporation of the hot plasma into the upper part of magnetic tubes. Such a process for solar flares was first considered by Kostyuk and Pikel'ner (1974), but for conditions in the red dwarf atmosphere the numerical modelling of this process was given by Livshits et al. (1981), and Katsova et al. (1981). The low-temperature radiation in this model arises, in the main, behind the downward-moving shock wave front. The strong compression of the gas in the relaxation zone behind the front is connected with the radiative losses. Two possible regimes of the energy balance in the low-temperature source are revealed theoretically (Livshits, 1983): either the heating is compensated by the Balmer line emission or by recombination radiation of hydrogen for the most intense events. We show that the two above-mentioned possibilities are realized in solar and in stellar flares respectively.

1. The theory predicts that the distinctive peculiarity in these two possibilities of energy balance in the low-temperature source is the noticeable decrease of the X-ray-to-optical luminosity ratio L_x/L_{opt} by transition of one type of flares to the other. The consideration of the now available observational data on the solar and stellar flares indeed shows that the ratios L_x/L_{opt} decrease by approximately an order of magnitude by the transition from ordinary solar flares to the stellar ones with optical continuum. The characteristics of the emission source density $n \geq 10^{15}$ cm^{-3}, temperature $T \approx 8500$-12000 K and height extent 1-10 km satisfy the observations. This relates to both the colours of the flares and to their effective temperature: $T \approx 8500$ K according to Mochnacki and Zirin (1980); from

appearing now multichannel photometric data on the flares T ≈ 10000 K (Rodono, 1985).

2. The observational light curves of stellar flares agree with our gas-dynamic model better than with nonthermal models, where millisecond fluctuations are possible. Let us discuss in more detail the question about the steepness of the rising part of optical continuum bursts. At the arrival of the downward-moving perturbation - the source of the low-temperature radiation - to the rather dense layers, the conditions in the relaxation zone behind the shock front approach LTE. The kinetic energy of the wave is thereby spent on intense emission. The radiation at the optical-continuum frequencies lasts while the wave runs 1-2 scale heights in the chromosphere. From the numerical modelling, carried out for a weak stellar flare (Katsova et al. 1981), as well as from a previous estimate (Katsova and Livshits, 1985), it follows that the minimum rise time of the optical continuum intensity $\tau_I = v_s/M'g$ (v_s-the sound velocity in undisturbed chromosphere, $M' = v/v_s$-the Mach number for the motion of the gas behind the shock wave front, g-acceleration due to gravity on the star). From the energy of the flaring continuum it follows that $M' \approx 10\text{-}30$ and $\tau_I \gtrsim 0.7$ s.

The observations in the U-band for several tens of flares on FL Vir and V577 Mon were carried out recently using a 6 m telescope (Beskin et al. 1985). The value τ_I for some of these flares is 1s, for other ones 2-10s, typical for impulsive events. From these extremely high time resolution data, it follows that the millisecond features on the rising part of the light curve are undoubtedly absent. This can be considered as additional independent confirmation of the gas-dynamic model.

Thus, the general idea about the analogy of the solar and stellar flares (Gershberg, 1978) is supported here: the further development of the solar physics ideas allows us to explain naturally the origin of the optical continuum radiation by stellar flares.

References:

Beskin, G.M., Neizvestnyi, S.I., Plachotnichenko, V.L., Pustilnik, L.A., Chekh, S.A., Shvartsman, V.F., and Gershberg, R.E., 1985, In: "Flare Stars and Related Objects", ed. L.V. Mirzoyan, Ac. Sci. Armenian SSR, Yerevan (in press).

Gershberg, R.E., 1978, "Flare Stars of Low Masses", Nauka, Moscow.

Katsova, M.M., Kosovichev, A.G., and Livshits, M.A., 1981, Astrofizika, 17, 285.

Katsova, M.M., and Livshits, M.A., 1985, In: "Flare Stars and Related Objects", ed. L.V. Mirzoyan, Ac. Sci. Armenian SSR, Yerevan (in press).

Kostyuk, N.D., and Pikel'ner, S.B., 1974, Astron. Zhu., 51, 1002.

Livshits, M.A., 1983, Astron. Zhu., 60, 964.

Livshits, M.A., Badalyan, O.G., Kosovichev, A.G., and Katsova, M.M., 1981, Solar Physics, 73, 269.

Mochnacki, S.W., and Zirin, H., 1980, Astrophys. J., 239, L27.

Rodono, M., 1985, Osserv. Astrofis. Catania, Prepr. No. 1.

Syrovatskii, S.I., 1972, Solar-Terrestr. Phys., 3, 106.

"Eruptive Phenomena in Stars"
Commun. Konkoly Obs. Hung.
Acad. Sci., No.86, Budapest

SPACE DISTRIBUTION OF THE H_α AND FLARE STARS IN THE ORION OB1d ASSOCIATION

K.G. Gasparian

Byurakan Astrophysical Observatory, Armenia, USSR

The association Orion OB1d is concentrated around a multiple star - the Orion Trapezium. At present, the total number of known emission H_α stars in the association is 534 (Parsamian and Chavira, 1982) the number of flare stars is about 500. Until now the space distribution of these stars had been studied only by dividing the studied region into concentric rings with the Trapezium in the centre. Since this method is not sufficiently accurate, Mnatsakanian (1969) suggested, in the case of spherical symmetry, a more exact method for determining the space distribution of stars in poor globular clusters. Subsequently this method was utilized to determine the distribution of flare stars in Pleiades (Mirzoyan et al., 1971, 1980).

The aim of the present paper is to apply this method to determine the space distribution of flare and H_α-emission stars in the Orion OB1d association. For this purpose the apparent distribution of 420 flare and 495 H_α-stars was studied. As a first approach, spherically symmetric distribution of these stars in the association was supposed.

According to Mirzoyan et al. (1980) the function F(x), that is, the number of stars in the (-x, x) zone with the centre x = 0, is equal to

$$F(x) = N_o - \frac{2}{\pi} \sum_{\rho_i > x} \text{arc cos} \frac{x}{\rho_i} ,$$

where ρ_i is the plane projection of the distance of the i-th star from the centre of the association, N_o is the total number of stars in it.

N(x) was determined graphically as the crossover point of the tangent of function F(x) at the point x with the vertical axis. In fact N(x) gives the number of stars inside a sphere of radius x. In order to find the density of stars at a distance x from the centre, i.e. the space distribution of the stars, it is sufficient to find the number of stars in the spheres with radii $x-\Delta x$ and $x+\Delta x$. By dividing the difference of star numbers by the difference of the volumes of the spheres, we find the density of stars in the ring within the interval $x-\Delta x$ and $x+\Delta x$. In this case it is necessary to choose Δx so that the number of stars in the neighbourhood of point x be the optimum for calculating the star density.

By applying this method we obtained the dependence of the densities of flare and H_α-stars of the Orion OB1d association on the distance r from the centre (Fig. 1). The distance of the Orion OB1d association was assumed to be 500 pc. In Fig. 1 the distribution of stars with $r < 3$ pc is not given because the apparent distribution of stars in this region is strongly distorted by the light of the Great Orion Nebula.

It is interesting to note that the ratio n_f/n_α of the number of flare stars to that of H_α-stars (Fig. 2) shows that the number of flare stars in comparison with the number of H_α-stars increases continuously with the increase of the distance from the centre of the association. This is in agreement with results of Gurzadyan (1970) and Gasparian (1975) achieved by the method of "breaked up" rings using comparatively poorer observational material.

It is pleasure for the author to express his gratefulness to M.A. Mnatsakanian for valuable discussion.

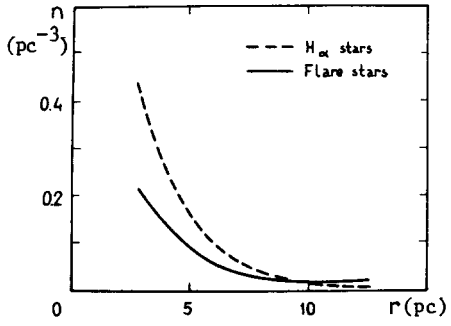

Figure 1

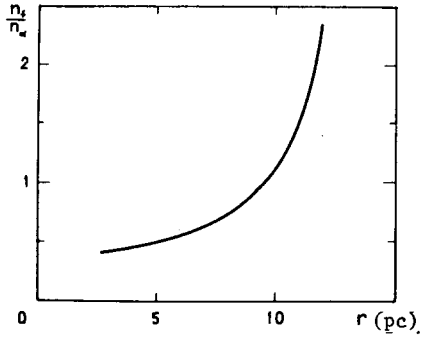

Figure 2

References:

Gasparian, K.G., 1975, Dissertation, 1975.
Gurzadyan, 1970, Bol. Obs. Tonantzintla, 35, 263.
Mirzoyan, L.V., and Mnatsakanian, M.A., 1971, IBVS, No. 528.
Mirzoyan, L.V., Mnatsakanian, M.A., and Oganian, G.B., 1980, In: "Flare Stars, Fuors and Herbig-Haro Objects", Ac. Sci. Armenian SSR, Erevan, p. 113.
Mnatsakanian, M.A., 1969, Dokl. A.N. Arm. SSR, 49, 33.
Parsamian, E.S., Chavira, E., 1982, Bol. Inst. Tonantzintla, 3, No. 1, 69.

"Eruptive Phenomena in Stars"
Commun. Konkoly Obs. Hung. Acad. Sci., No.86, Budapest

INTERPRETATION OF THE PHOTOMETRIC AND POLARIMETRIC OBSERVATIONS OF T TAURI STARS

N.P. Red'kina, K.V. Tarasov, N.N. Kiselev, G.P. Chernova

Institute of Astrophysics, Dushanbe, 734670, USSR

Simultaneous photometric (UBV and H_α) and polarimetric (V) observations of T Tau and RY Tau were obtained with the 0.7 m telescope at Gissar Astronomical Observatory during the 1979-1982 observing seasons. UBVR and i(7660 Å) photometry and UBVR polarimetry of T Tau and RY Tau were obtained during the 1984-1985 observing season with the 1 m telescope at Mount Sanglok Observatory.

T Tau has the greatest range of variability in U and smaller ranges at longer wavelengths. There is a flare (J.D. 2444142) in U ($\Delta U_{max} = 0^m.6$) and H_α($\Delta m_{max} = 0^m.3$). Variations at $F(H_\alpha)$ are correlated with U-B and polarization in V (Red'kina and Chernova, 1982). The wavelength dependence of polarization for T Tau is obtained.

RY Tau gets bluer in U-B and B-V when it is fainter during the local minima of 1979 (J.D. 2444165-196). It does the same in U-B and reddening in the other colours B-V, V-R and R-i during the local minima in 1984 (J.D. 2445959-6060). RY Tau shows a direct correlation of polarization in the V bandpass with brightness in V during the minima 1979.

Our interpretation is based on the hydromagnetic activity of T Tau stars. We have supposed that the variability of T Tau stars occurs due to the appearance and disappearance of spots. If the surface of the star has a global patchy structure (Gershberg, 1982) then a decrease in the strength of the magnetic field of a spot below the critical level will remove the magnetic inhibition of optical radiation and a normal bright photosphere (i.e. a hot spot) will appear. The other kind of variability is connected with the appearance of the new cool spots on the surface of the star if a normal photosphere prevails. Strong photospheric activity leads to the formation of external active areas like the solar one in the envelope and

chromosphere; a large variation of the flux in U and H_α will take place. The spot model (Torres and Ferraz-Mello, 1973) is used for the calculation and an envelope radiation according to Sobolev (1950) is added. T Tau has the following parameters: T_{eff}=4900 K; $T_{hot\ spot}$=6600 K; N_e=10^{10}-10^{11} cm^{-3}; T_e=10000-20000°. RY Tau: T_{eff}=4900 K; $T_{cool\ spot}$=3000 K; N_e=10^{10}-10^{11} cm^{-3}; T_e=7000-20000°.

The hypothesis of hydromagnetic activity can be proved by observational evidence showing the existence of both the global patchy structures and the strong magnetic fields on these stars. The direct demonstration of magnetic fields of the T Tau stars is a very hard task. The magnetic field of T Tau is determined from the wavelength dependence of linear polarization with the help of the method suggested by Gnedin and Silant'ev (1980). The magnitude of the field is estimated to be 100-400 gauss for a spherical envelope and 300-1200 gauss for an ellipsoidal envelope (Gnedin and Red'kina, 1984). The complicated motion of the polarization vector of RY Tau in the U-Q plane during a few days appears to be due to the interaction of the magnetic fields of starspots with the electron component of the star shell.

References:

Gershberg, R.E., 1982, Astron. Nachr., 303, No.4, 251.
Gnedin, Yu.N. and Silant'ev, N.A., 1980, Soviet Astron. J. Letters 6, 344.
Gnedin, Yu.N. and Red'kina, N.P., 1984, Soviet Astron. J. Letters 10, 613.
Red'kina, N.P. and Chernova, G.P., 1982, in Binary and Multiple Stars as Tracers of Stellar Evolution, D. Reidel Publ. Co., Dordrecht, Holland, p. 231.
Torres, G.A. and Ferraz-Mello, S., 1973, Astron. Astrophys., 27, 231.
Sobolev, V.V., 1950, Soviet Astron. J. 27, 81.

"Eruptive Phenomena in Stars"
Commun. Konkoly Obs. Hung.
Acad. Sci., No.86, Budapest

FLARE ACTIVITY OF ANTIFLARE STARS

G.U. Kovalchuck

Main Astronomical Observatory, Ukrainian
Academy of Sciences, Kiev, USSR

The results are presented of a study of the flare activity of antiflare stars (AFS). The objects investigated belong to the "Irregular variables, connected with diffuse nebulae, and rapid irregular" (GCVS).

Figures 1-6 show the light curves of the observed flares. The symbol "↓" indicates the moments of the maximum brightness during a flare in the U-band.

All the flares are connected with an active state of variable stars. (The active state of AFS is not only the minimum brightness state, but also the pre- and post-minimum -1^d -2^d -state.) "AS" (Figs 1-6) indicates the extent of activity of each variable star on the night of observation: "0" is the minimum brightness state; "+1" or "-1": 1^d after the minimum and 1^d before the minimum respectively. Δm is the deviation of the brightness from the normal brightness state (in V-band) in magnitude.

The variability of AFS is interpreted in the framework of an eruptive model (Pugach, 1983) according to which the global weakening of AFS brightness is due to the appearance of the absorbing matter near the variable star. The appearance of flares of the AFS in the minimum of brightness is caused, in our opinion, by the active processes in the chromosphere-like envelopes of AFS (Pugach, 1983; Kovalchuck, 1985).

References:

Kovalchuck, G.U., 1985, Kinematika i Fizika Nebesnich Tjel, 1, No. 3, p. 25-32.
Pugach, A.F., 1983, Astrometr. Astrofiz., Vyp. 49, p. 55-60.

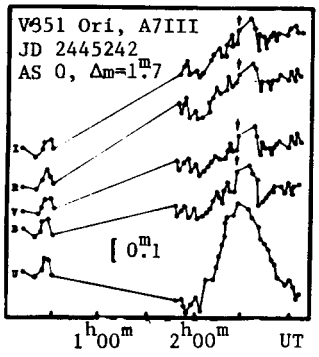

Figure 1

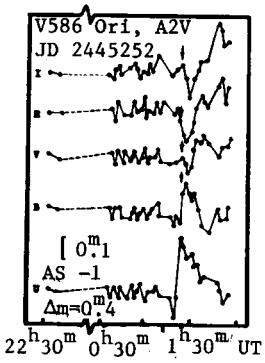

Figure 2

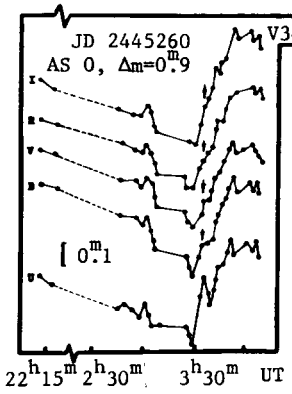

Figure 3

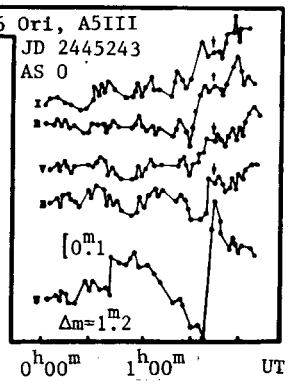

Figure 4

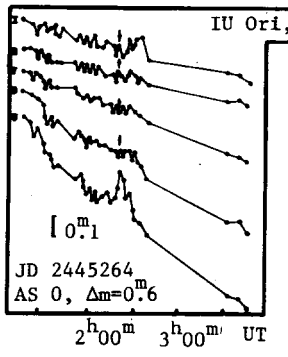

Figure 5

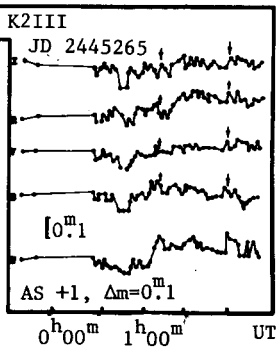

Figure 6

"Eruptive Phenomena in Stars"
Commun. Konkoly Obs. Hung.
Acad. Sci., No.86, Budapest

ANALYSIS OF R CORONAE BOREALIS VARIABILITY FROM PHOTOELECTRIC OBSERVATIONS

R.I. Goncharova

Main Astronomical Observatory, Ukrainian Academy of Sciences, USSR

RY Sgr, a star of R CrB type, clearly shows periodic pulsations. In this case it was found that the fading of stellar brightness takes place just at the moment of the pulsation peak (Pugach, 1977). An attempt has been made to find out the connection between pulsations and deep light fadings for R CrB by analogy with RY Sgr.

The oscillations of the maximum light of R CrB with a mean amplitude of about $\Delta m_v = 0\overset{m}{.}15$ were revealed by photoelectric magnitude estimates. In the paper by Goncharova et al. (1983) it was shown that R CrB had three pulsation periods: $P_1 = 27\overset{d}{.}36$, $P_2 = 39\overset{d}{.}96$, $P_3 = 53\overset{d}{.}64$. A comparison was made between the observed and computed moments of the maximum light pulsations before the beginning of deep light fadings. It was concluded that the brightness of the variable faded after the maximum of pulsational light variability with periods P_1 and P_2, in some cases the pulsation maxima (P_1 and P_2) and (P_1 and P_3) practically coincide before the light decline of the variable into the minimum from the normal state.

Figure 1 shows three starting moments of R CrB fading observed photoelectrically. The vertical line indicates the calculated moments of maximum with $P_1 = 27\overset{d}{.}36$.

Thus, R CrB seems to decrease its brightness after the maximum of pulsational light variability with any of three periods but after the maximum of $P_3 = 53\overset{d}{.}64$ the fading is less probable.

There is a suggestion that the R CrB phenomenon is triggered by the ejection of matter during a particularly large pulsation. From photometric observations during the maximum light we know that the star shows light fluctuations of about $0\overset{m}{.}1$ or $0\overset{m}{.}2$ with mean V-magnitudes of about $5\overset{m}{.}8$-$5\overset{m}{.}9$ (Fernie, 1982). Observations of R CrB near maximum light before the beginning of the light decline are shown in Fig. 1. It is clear that the 1983 minimum started after the light pulsation with the amplitude $\Delta m_v \approx 0\overset{m}{.}1$. The star reached $5\overset{m}{.}8$ in the V-filter at the maximum moment of this pulsation and for a month before the starting of the light fading the star showed mean light fluctuations of about $\Delta m_v \approx 0\overset{m}{.}15$. That is to say that when falling into the minimum the pulsation amplitude and the maximum value of the star's visible light had the mean values typical of the maximum light of this star.

On the other hand, near the maximum light the amplitude of R CrB light variations exceeds its mean values to a great extent from time to time. The pulsation with the maximum registered amplitude near maximum light - $\Delta m_v = 0\overset{m}{.}36$ was observed by Goncharova et al. (1983).

From the above it follows that pulsation amplitudes (neither accidental fluctuations nor superposition of several periods) do not affect the beginning of deep light fadings.

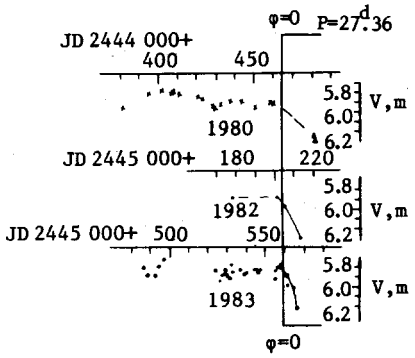

Fig. 1.

Starting moments of R CrB fading observed photoelectrically. Filled circles represent observations by the author, the other estimates were obtained from the literature

Table I. Comparison between the observed and computed moments of maximum light pulsation before the beginning of deep light fadings

Observed moments		Computed moments		
	J.D.	$P_1 = 27^d.36$	$P_2 = 39^d.96$	$P_3 = 53^d.64$
1938	2 429155	-	2 429152	-
1942	30632	-	30631	-
1962	37820:	2 437817	37823	-
1972	2 441(360:-380:)	41346	41380	-
1974	2 442029:	42030	42019	-
1975	42685:	42687	-	2 442689
1977	43180:	43179	43179	-
1983	45557	45559	-	-

References:

Fernie, J.D., 1982, Publ. Astron. Soc. Pacific., 94, No. 557, 172.
Goncharova, R.I., Kovalchuck, G.U., Pugach, A.F., 1983, Astrofizika, 19, 279.
Pugach, A.F., 1977, Inform. Bull. Variable Stars, No. 1277, 1.